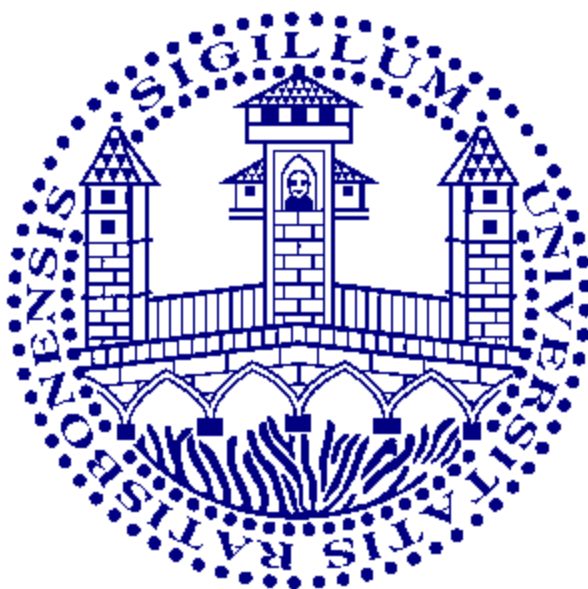


Contributions to the Chemistry of Phosphanylboranes



DISSERTATION
ZUR ERLANGUNG DES
DOKTORGRADES DER NATURWISSENSCHAFTEN
(DR. RER. NAT.)
DER FAKULTÄT FÜR CHEMIE UND PHARMAZIE
DER UNIVERSITÄT REGENSBURG

vorgelegt von

Oliver Niklas Hegen

aus Neuburg a. d. Donau

im Jahr 2018

Diese Arbeit wurde angeleitet von Prof. Dr. Manfred Scheer.

Promotionsgesuch eingereicht am: 20.07.2018

Tag der mündlichen Prüfung: 28.08.2018

Vorsitzender:	Prof. Dr. Arnd Vogler
Prüfungsausschuss:	Prof. Dr. Manfred Scheer
	Prof. Dr. Henri Brunner
	Prof. Dr. Frank-Michael Matysik



Universität Regensburg

Eidesstattliche Erklärung

Ich erkläre hiermit an Eides statt, dass ich die vorliegende Arbeit ohne unzulässige Hilfe Dritter und ohne Benutzung anderer als der angegebenen Hilfsmittel angefertigt habe; die aus anderen Quellen direkt oder indirekt übernommenen Daten und Konzepte sind unter Angabe des Literaturzitats gekennzeichnet.

Oliver Hegen

This thesis was elaborated within the period from October 2014 till July 2018 in the Institute of Inorganic Chemistry at the University of Regensburg, under the supervision of Prof. Dr. Manfred Scheer.

Parts of this work have already been published or submitted:

(* = Co-First Authorship: These authors contributed equally to this work.)

O. Hegen, C. Marquardt, A. Y. Timoshkin, M. Scheer, *Angew. Chem. Int. Ed.* **2017**, 56, 12783 –12787.

C. Marquardt*, O. Hegen*, A. Vogel, A. Stauber, M. Bodensteiner, A. Y. Timoshkin, M. Scheer, *Chem. Eur. J.* **2018**, 24, 360 – 363.

*"There's no easy way out
There's no shortcut home
There's no easy way out
Givin' in can't be wrong."*

Robert Tepper

*"Carry on my wayward son
There'll be peace when you are done."*

Kansas

"Don't stop believin'"

Journey

**For my family
my friends
my companions
my doubters
and**

for you

Preface

During the period of this thesis (October 2014 – July 2018) some results have already been published (*vide supra*). These thesis are also summarized in the present work, reprinted with permission of the respective scientific publisher. The associated license numbers are given at the end of the individual chapters.

At the beginning of each chapter a list of authors, who contributed to the particular part, is given. In addition, each chapter include the section 'author contributions', which accurately describes the extent of involvement of each author. If results from collaborations are in part also discussed in other theses, it is stated there.

To ensure a uniform design of this work, all chapters are subdivided into 'Introduction', 'Results and Discussion', 'Conclusion', 'References', 'Supporting Information' and 'Author Contributions'. Furthermore, all chapters have been uniformed in the text setting and the compound numeration begins anew. As different journals require different formatting, the presentation of figures for single crystal X-ray structures or the 'Supporting Information' may differ. In addition, a general introduction at the start, and a summary of all chapters is given at the end of this thesis.

Table of Contents

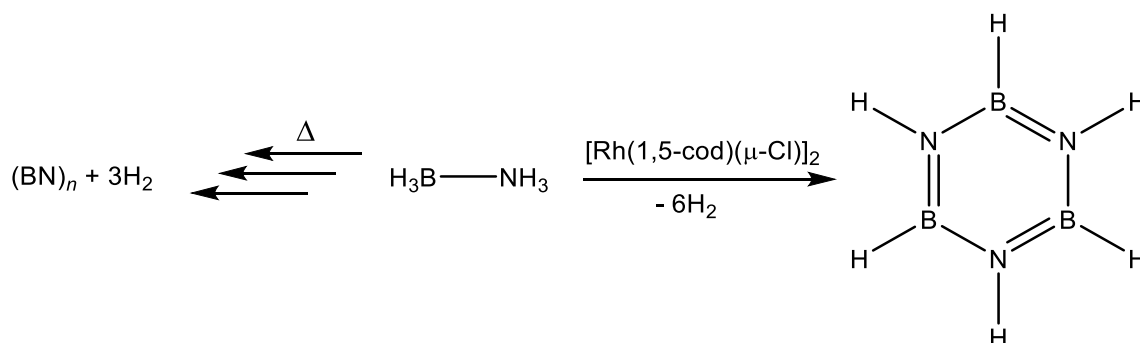
1. Introduction	1
1.1 Polymers consisting of alternating group 13/15 elements	2
1.2 Donor/acceptor stabilization of highly reactive small molecules	4
1.3 Frustrated Lewis Pairs (FLPs)	7
1.4 Literature	9
2. Research Objectives.....	12
3. A Convenient Route to Mixed Pnictogenylboranes.....	14
3.1 Introduction.....	15
3.2 Results and Discussion	17
3.3 Conclusion.....	21
3.4 References	22
3.5 Supporting Information	25
3.6 Author contributions	58
4. Depolymerization of Poly(phosphinoboranes): From Polymers to Lewis Base Stabilized Monomers	60
4.1 Introduction.....	61
4.2 Results and Discussion	62
4.3 Conclusion.....	66
4.4 References	66
4.5 Supporting Information	71
4.6 Author contributions	105
5 The Lewis base stabilized diphenylsubstituted Arsanylborane – A versatile building block for arsanylborane oligomers.....	107
5.1 Introduction.....	108
5.2 Results and Discussion	109
5.3 Conclusion.....	114
5.4 References	115

5.5 Supporting Information	118
5.6 Author contributions	150
6 Bidentate Phosphanyl- and Arsanylboranes.....	151
6.1 Introduction.....	152
6.2 Results and Discussion	153
6.3 Conclusion.....	160
6.4 References	161
6.5 Supporting Information	164
6.6 Author contributions	207
7 Thesis Treasury	208
7.1 Systematical Coordination of Pnictogenylboranes towards Transition Metal Lewis Acids	208
7.2 Synthesis of alkyl-substituted Lewis base stabilized phosphanylboranes	216
7.3 Synthesis of a LB stabilized Bismutylborane	234
7.4 Literature	237
8 Conclusion	238
9 Appendices	245
9.1 Alphabetic List of Abbreviations	245
9.2 Acknowledgments	247

1. Introduction

Materials consisting of group 13/15 elements have versatile applications, for instance as high temperature ceramics^[1], as micro-electronic devices,^[2a,b] or as flame retardants.^[2c,d] GaAs for example, has several applications in industry, due to its semiconducting properties. Small layers of GaAs are fabricated through MOCVD processes, in which a deposition of thin films is achieved by thermolysis of appropriate precursors.^[3] Another example is boron nitride (BN)_n, which occurs in three different modifications, hexagonal (α), cubic (β) and wurtzite (γ). As the layer structure of α-(BN)_n is analogue to graphite, it is used as high temperature lubricant.

Molecular units containing alternating group 13/15 atoms are isoelectronic to their carbon analogues. This leads to similar structural motifs, not only in the solid state as described above in the case of α-(BN)_n, but also in the structure of small molecules. For instance, Borazine (B₃N₃H₆), reported in 1926 by Pohland and Stock,^[4] shows a typical aromatic odor, is a colorless liquid at room temperature and exhibits similar characteristics as benzene. Although it is called “inorganic benzene”, the aromaticity is significantly lower due to the polar bonds between the group 13 and group 15 atoms. In case of ammonia borane H₃BNH₃, one takes advantage of the difference in electronegativity between B-N and the resulting polarity inside the molecule, as it exhibits protonic as well as hydridic hydrogen atoms. Therefore, and due to its high hydrogen content (up to 19.6 wt-%), it is in the current research focus as possible material for hydrogen storage.^[5] Dihydrogen can be either set free by thermolysis, which results in the highest hydrogen release, but also some recycling problems with the emerging, extraordinary stable (BN)_n, or by catalytical reactions (Scheme 1).



Scheme 1: Thermal and catalytic release of H₂ in H₃BNH₃ (1,5-cod = 1,5-cyclooctadiene).

The Manners group reported in 2001 on a transition metal catalyzed dehydrocoupling reaction. Using a dinuclear Rh(I)-complex, $[\text{Rh}(1,5\text{-cod})(\mu\text{-Cl})]_2$ (1,5-cod = 1,5-cyclooctadiene), they were able to dehydrocouple H_3NBH_3 to borazine as main product.^[6] Since then, a variety of early and late transition metal catalysts were discovered, which are able to catalyze dehydrocoupling reactions of ammonia borane adducts.^[7]

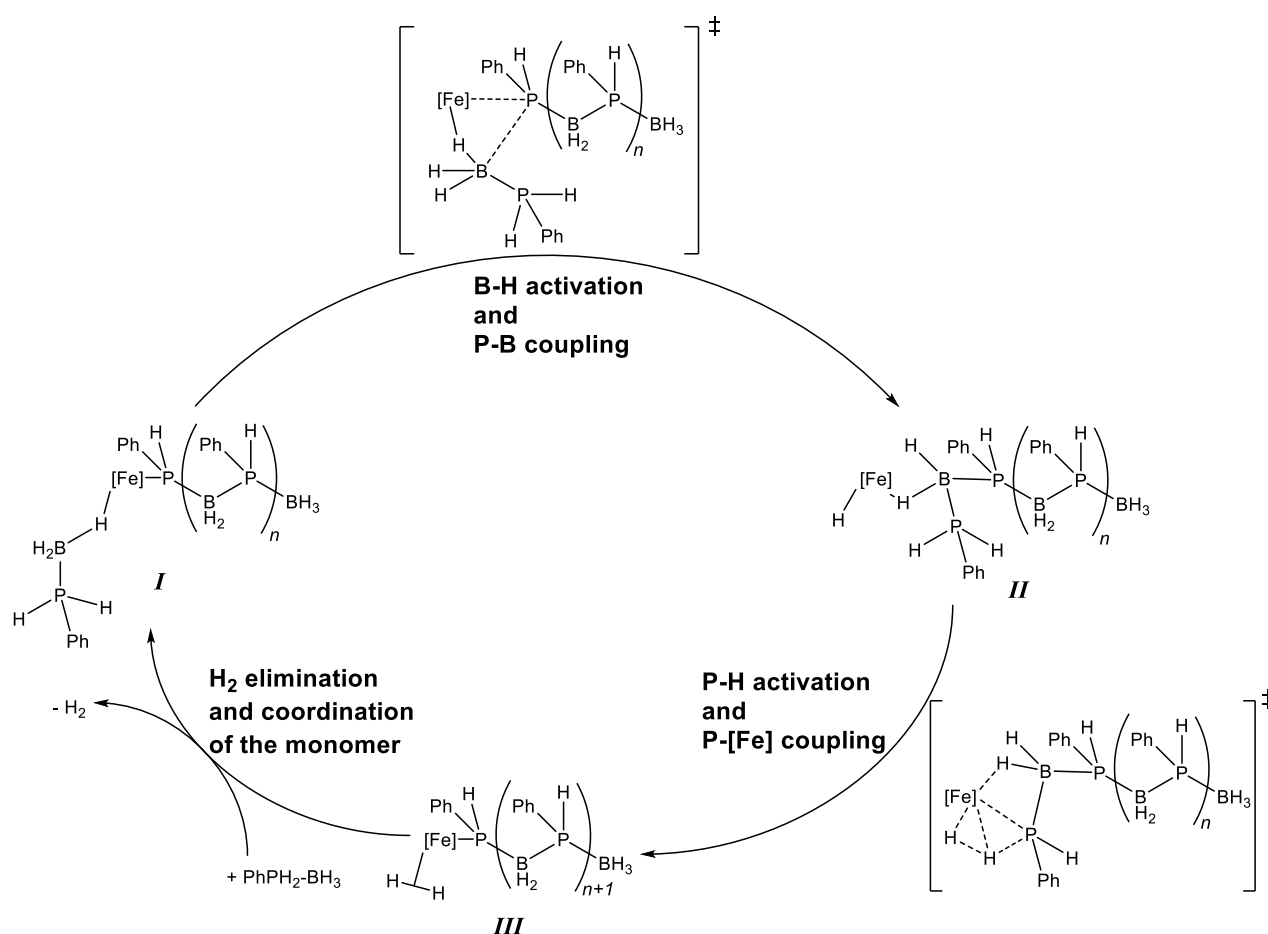
1.1 Polymers consisting of alternating group 13/15 elements

In 1977, Pusatcioglu reported on the synthesis of a boron-nitrogen polymer $[\text{F}_2\text{BNH}_2]_n$ with a molecular mass of 23.000 Da, measured by DLS (dynamic light scattering).^[8] A polymer containing hydrogen atoms bonded to boron was synthesized by the Manners group through a catalytic process.^[9] The GPC (gel permeation chromatography) and the DLS analysis results in a molecular mass up to 405.000 Da. This high molecular weight polymer, with partially over 4500 repeating units, is yielded by catalytical dehydrocoupling of RH_2NBH_3 ($\text{R} = \text{H}, \text{Me}, t\text{Bu}$) with Brookharts catalyst $[\text{IrH}_2(\mu_3\text{-}1,3\text{-(OP}t\text{Bu}_2)_2\text{C}_6\text{H}_3)]$.^[10]

In case of the heavier congener, phosphorus, poly(phosphinoborane)s were first reported by Manners et al. in 1999.^[11] Through dehydrocoupling of PhH_2PBH_3 with a Rh(I)-catalyst, a polymer with an average molecular mass of 31.000 Da, could be synthesized. Dennis and Gaumont showed, that transition metals are not absolutely necessary as catalysts, since the bubbling of PH_3 and B_2H_6 through a solution of $\text{B}(\text{C}_6\text{F}_5)_3$ yields $[\text{H}_2\text{PBH}_2]_n$.^[12] Applying Brookharts catalyst to aryl-substituted phosphine borane adducts RH_2PBH_3 ($\text{R} = \text{Ph}, p\text{Tol}, \text{Mes}$), the group of Radius^[13] was able to get access to similar polymers as described by the Manners group.^[11] However, the clarification of the catalytic process leads to completely different results. The stoichiometric reaction of the adduct and the catalyst results in the formation of $[(t\text{BuPOCOP})\text{Ir}(\text{H})_2(\text{BH}_3)]$ (POCOP = $(\text{OP}t\text{Bu}_2)_2\text{C}_6\text{H}_3$), the phosphine complex $[(t\text{BuPOCOP})\text{Ir}(\text{PH}_2\text{R})]$ and the iridium dihydrido phosphine complex $[(t\text{BuPOCOP})\text{Ir}(\text{H})_2(\text{PH}_2\text{R})]$, indicating a cleavage of the phosphine borane adduct throughout the catalytic process.

Recently, the first earth-abundant, iron-based (pre)catalyst for the synthesis of poly(phosphinoborane)s was described by Manners et al.^[14] In contrast to the iron-

catalyzed, heterogeneous dehydrocoupling of $\text{Me}_2\text{HN-BH}_3$,^[15] the catalytic process of $\text{PhH}_2\text{P-BH}_3$ with $[\text{Cp}(\text{CO})_2\text{Fe}(\text{OTf})]$ ($\text{OTf} = \text{OSO}_2\text{CF}_3$) appears to be homogenous in nature. Variation of catalyst loading at identical conditions assume a chain-growth polymerization, as higher catalyst loadings gave lower molecular weight polymers. Further, multinuclear NMR studies, as well as ESI-MS support a P-B bond forming and the formation of a metal-bond phosphine-borane dimer complex. Therefore, a chain-growth coordination-polymerization mechanism was postulated for this reaction (Scheme 2).



Scheme 2: Postulated catalytic cycle for the chain-growth coordination polymerization of $\text{PhH}_2\text{P-BH}_3$ by the iron catalyst derived from $[\text{Cp}(\text{CO})_2\text{Fe}(\text{PhPHBH}_3)]$ (scheme showing one insertion event; $[\text{Fe}] = \text{FeCp}(\text{CO})_2$).

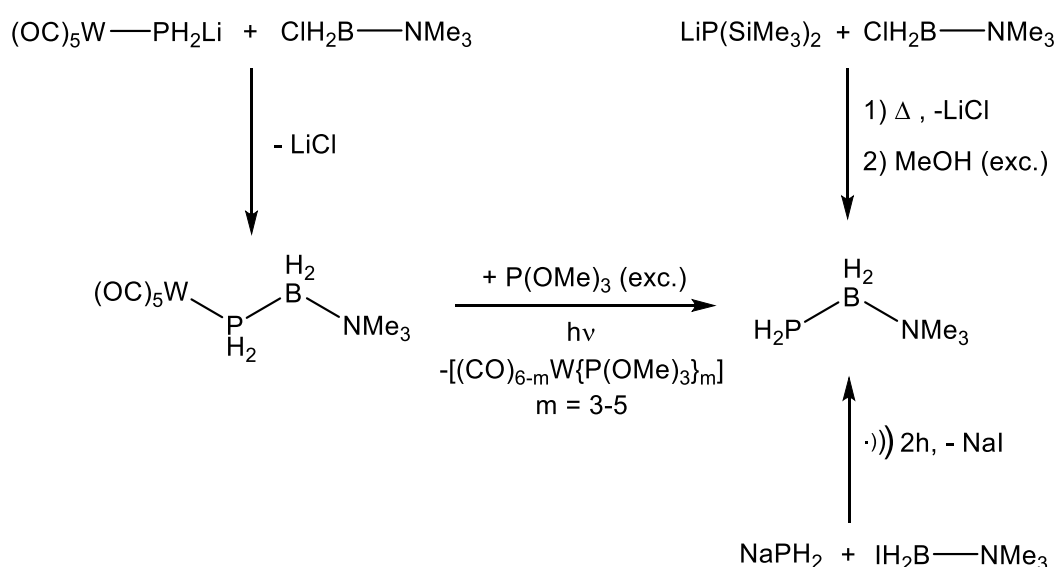
First attempts regarding copolymers consisting of different group 15 elements and boron were made by the Manners group in 2004.^[16] However, reactions of $\text{Me}_2\text{HN-BH}_2\text{-PPhH-BH}_3$ with a catalytic amount of $[\text{Rh}(1,5\text{-cod})(\mu\text{-Cl})_2]$ lead amongst other products to the dimeric $[\text{Me}_2\text{NBH}_2]_2$ and $\text{PhPH}_2\text{-BH}_3$ instead of the desired copolymer.

Thermal treatment (130°C) of the compound results also in a P-B bond cleavage and yield $[\text{Me}_2\text{NBH}_2]_2$ and $[\text{PhHP-BH}_2]_n$.

1.2 Donor/acceptor stabilization of highly reactive small molecules

To get greater insight into the polymerization reactions, it is inevitable to have a closer look onto the 13/15 building blocks $[\text{R}_2\text{E-E}'\text{R}'_2]$ ($\text{R}, \text{R}' = \text{H}, \text{alkyl}, \text{aryl}; \text{E} = \text{pnictogen}, \text{E}' = \text{triele}$). Monomeric compounds, like $t\text{Bu}_2\text{AsBMes}_2$, are stable at ambient conditions, due to the sterical hindrance.^[17] If the sterical demand is not sufficient enough, a head-to-tail polymerization/oligomerization would occur due to the empty p-orbital on the triele atom and the lone pair on the pnictogen atom. However, another way to stabilize such compounds with less sterical demand, like $[\text{R}_2\text{N-BH}_2]$, is in the coordination sphere of transition metals.^[18a] Even the highly reactive $[\text{H}_2\text{N-BH}_2]$, which has been isolated under cryogenic conditions,^[18b] can be stabilized in the coordination sphere of the complex $([\text{RuH}_2(\eta^2:\eta^2\text{-H}_2\text{BNH}_2)(\text{PCy}_3)_2])$.^[18c] Schulz et al. showed, that the addition of the strong Lewis base (LB) 4-Dimethylaminopyridine (DMAP) to cyclic oligomers $[\text{Me}_2\text{E-E}'(\text{SiMe}_3)_2]_n$ ($\text{E} = \text{Al}, \text{Ga}; \text{E}' = \text{P}, \text{As}; n = 2, 3$) leads to a bond cleavage and yields the monomeric LB stabilized compounds.^[19] Regarding only hydrogen substituted triele atoms, Cowley and Jones reported on a metathesis reaction resulting in LB stabilized phosphanyl- and arsanylanes $\text{Mes}_2\text{EAlH}_2\text{-NMe}_3$ ($\text{E} = \text{P}, \text{As}$).^[20] The use of a LB blocks the vacant p-orbital on the boron, therefore no oligomerization/polymerization can occur. First results in the field of monomeric phosphanylboranes were made in 2003 by our group. By applying a combination of Lewis acid (LA) /LB, we were able to stabilize the parent compound of phosphanylboranes and arsanylboranes.^[21] We showed that this electronical stabilization is also sufficient enough to work with the parent compounds of phosphanylanes and –galanes.^[22] It is noteworthy, that the synthesis of phosphanylanes and –galanes was achieved by H_2 elimination reactions, whereas the synthesis of phosphanylboranes and arsanylboranes was accomplished by salt metathesis (Scheme 3). DFT calculations indicated, that the additional stabilization by a LA is not absolutely necessary for pnictogenylboranes. The addition of P(OMe)_3 to $(\text{OC})_5\text{W-PH}_2\text{BH}_2\text{-NMe}_3$ and further irradiation with UV light leads to the elimination of $[(\text{OC})_{6-m}\text{W}\{\text{P(OMe)}_3\}_m]$ resulting in the LB stabilized phosphanylborane $\text{H}_2\text{PBH}_2\text{-NMe}_3$.^[23] The disadvantages of this pathway is the long

multistep synthesis and the isolation of $\text{H}_2\text{PBH}_2\text{-NMe}_3$ on a milligram scale. Further, the described reaction pathway is limited to phosphorus as pnictogen atom. Improvement has been made using silylated alkali metal phosphides $[(\text{Me}_3\text{Si})_2\text{PLi}\cdot 2\text{thf}]$ instead of $[(\text{OC})_5\text{W}]\text{PH}_2\text{Li}$.^[24] The reaction of $[(\text{Me}_3\text{Si})_2\text{PLi}\cdot 2\text{thf}]$ with $\text{ClBH}_2\text{-NMe}_3$ leads to $(\text{Me}_3\text{Si})_2\text{PBH}_2\text{-NMe}_3$, which is further reacted with MeOH to eliminate the SiMe_3 groups, resulting in high yields of $\text{H}_2\text{PBH}_2\text{-NMe}_3$ (Scheme 3). Further, this synthesis can be transferred to the heavier congener, arsenic, yielding the parent arsanylborane $\text{H}_2\text{AsBH}_2\text{-NMe}_3$. The usage of $\text{IBH}_2\text{-NMe}_3$ and NaPH_2 leads to a further shortening of the reaction time.^[25]



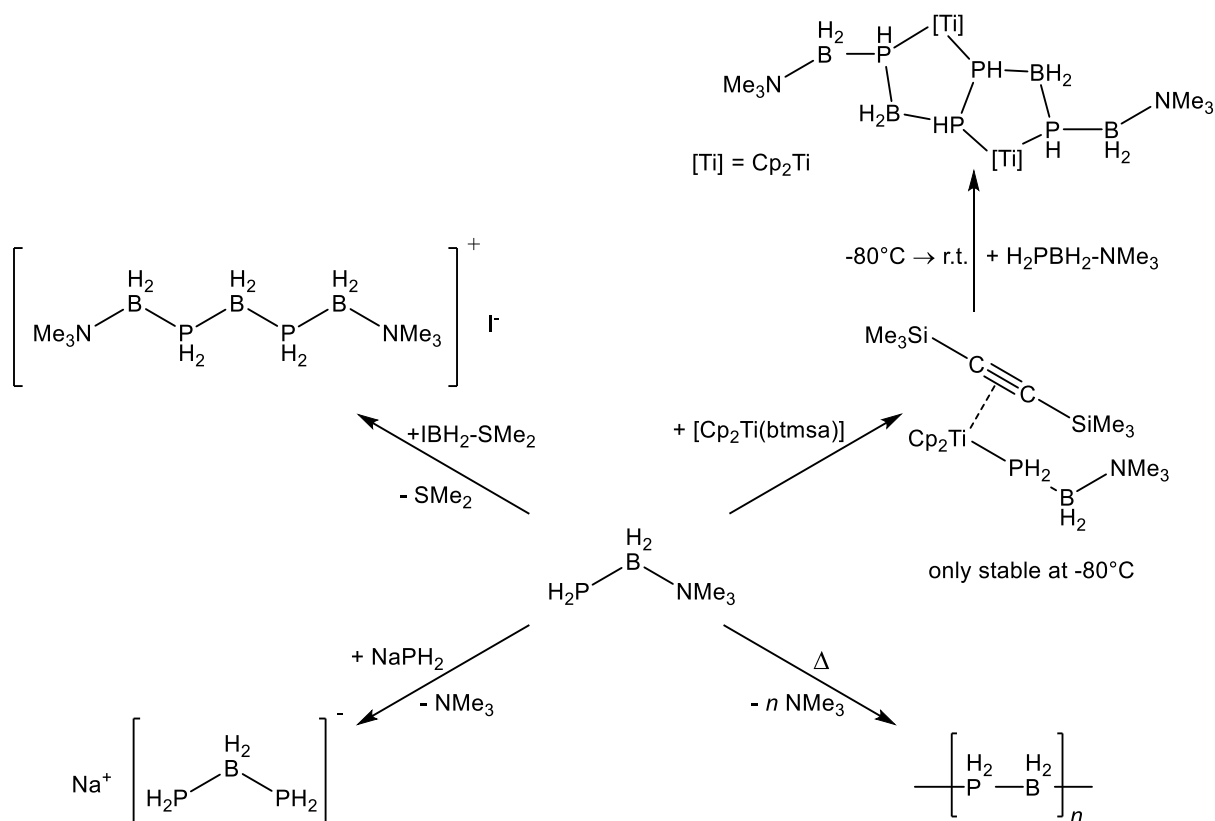
Scheme 3: Different synthetic pathways to $\text{H}_2\text{PBH}_2\text{-NMe}_3$.

Whereas a stabilization by a LB is sufficient to synthesize and isolate the parent compound of arsanylboranes and even the parent compound of stibanylboranes,^[26] all attempts to synthesize a LB stabilized azaborane $\text{H}_2\text{NBH}_2\text{-LB}$ failed. However, Rivard et al. succeeded in the preparation of a LA/LB stabilized azaborane.^[27] The addition of a strong LB (DMAP, $\text{NHC}^{\text{dipp}}\text{-CH}_2$, PCy_3 ; NHC = N-heterocyclic carbene, dipp = 2,6-diisopropylphenyl) to μ -aminodiborane $\text{H}_5\text{B}_2\text{NH}_2$ leads to the formation of $\text{H}_3\text{B-H}_2\text{NBH}_2\text{-LB}$. Interestingly, heating of $\text{H}_3\text{B-H}_2\text{NBH}_2\text{-DMAP}$ leads to a thermal dehydrocoupling reaction resulting in borazine and $\text{H}_3\text{B-DMAP}$. The same reaction behavior is observed by addition of catalytical amounts of CuBr or CuBr-SMe_2 .

The thermal treatment of NMe_3 stabilized phosphanylboranes leads to LB elimination.^[28] Due to the lone pair on the phosphorus atom and the free p-orbital of the boron atom of the resulting intermediate “ $\text{R}_2\text{P-BH}_2$ ”, a head-to-tail polymerization

takes place. Through variation of the substituents on the phosphorus atom different molecular weight polymers are accessible. Whereas thermal treatment of di-arylsubstituted phosphanylboranes, like $\text{Ph}_2\text{PBH}_2\text{NMe}_3$, results in oligomeric material, $[\text{Ph}_2\text{PBH}_2]_n$ ($n < 6$), the elimination of the LB in mono-alkylsubstituted phosphanylboranes, like $t\text{BuPHBH}_2\text{NMe}_3$, yields high molecular weight polymers $(t\text{BuPHBH}_2)_n$ ($n = 1900 - 2150$).^[28]

Besides a head-to-tail polymerization, LB stabilized phosphanylboranes are versatile building blocks to synthesize discrete oligomeric compounds. The reaction with $\text{IBH}_2\text{-LB}$ ($\text{LB} = \text{NMe}_3, \text{SMe}_2$) yields cationic compounds including either a $\text{H}_2\text{B-PH}_2\text{-BH}_2$ or a $\text{H}_2\text{B-PH}_2\text{-BH}_2\text{-PH}_2\text{-BH}_2$ chain (Scheme 4).^[29a] The synthetic pathway can be further transferred to substituted phosphanylboranes and even to the LB stabilized arsanylborane $\text{H}_2\text{AsBH}_2\text{-NMe}_3$.^[29a,b] Depending on the stoichiometry and the temperature, the coordination of $\text{H}_2\text{PBH}_2\text{-NMe}_3$ towards $[\text{Cp}_2\text{Ti}(\text{btmsa})]$ ($\text{btmsa} = \text{bis}(\text{trimethylsilyl})\text{acetylene}$) yields different transition metal bridged oligomers through a transition metal mediated dehydrooligomerization (Scheme 4).^[30] In addition, the replacement of NMe_3 , for example with phosphanides, is also possible resulting in unprecedented anionic compounds.^[31] The reaction of NaPH_2 with $\text{H}_2\text{PBH}_2\text{-NMe}_3$ results in $\text{Na}^+[\text{H}_2\text{PBH}_2\text{PH}_2]^-$ (Scheme 4). The linear $\text{H}_2\text{PBH}_2\text{PH}_2$ chain can be seen as anionic counterpart to the cationic $\text{Me}_3\text{N-H}_2\text{BPH}_2\text{BH}_2\text{-NMe}_3$. Variation of the substituents on the phosphanide yields, depending on the stoichiometry, to $\text{Na}^+[\text{H}_2\text{PBH}_2\text{PPh}_2]^-$ or to the five-membered $\text{Na}^+[\text{H}_2\text{PBH}_2\text{PPh}_2\text{BH}_2\text{PH}_2]^-$.



Scheme 4: Short overview on the reactivity of $\text{H}_2\text{PBH}_2\text{-NMe}_3$.

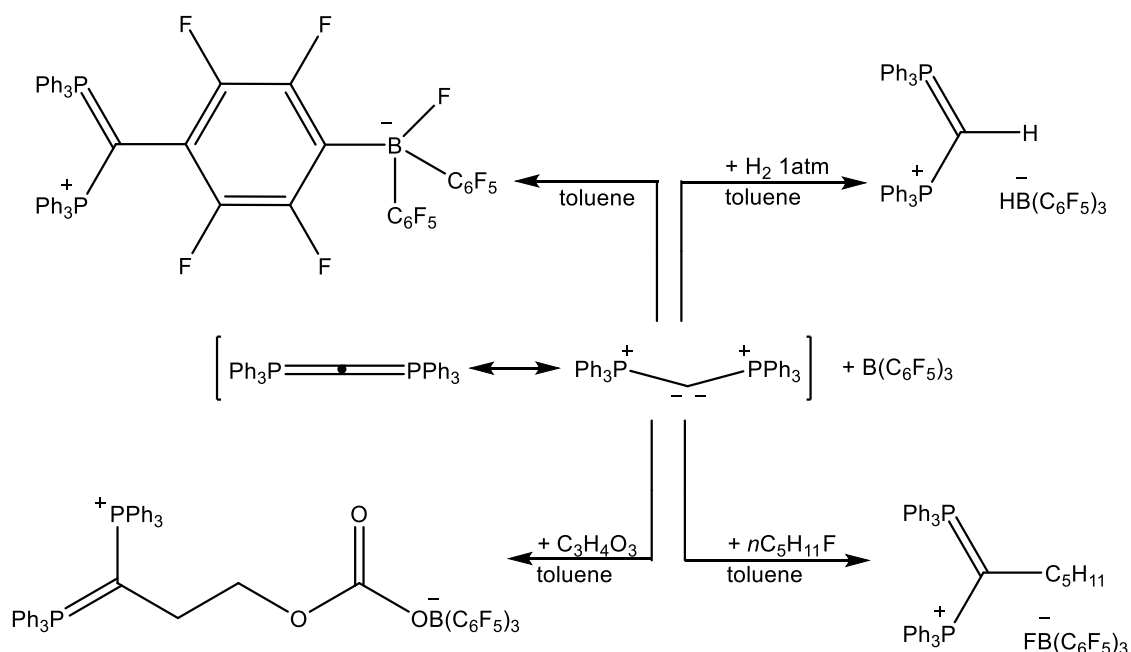
1.3 Frustrated Lewis Pairs (FLPs)

Besides many other properties, the use of a combination of group 13/15 elements as FLPs (Frustrated Lewis pairs) gained increased attention in the last 15 years. Usually, electron-rich Lewis bases and electron deficient Lewis acids form strong adducts,^[32] however, by using sterically demanding substituents, a formation of a dative bond between these Lewis pairs is precluded. Even if this behavior was observed over a long period of time,^[33] a systematic exploration took a while. In 2006, *Stephan* reported the famous FLP-system $(\text{Me}_3\text{C}_6\text{H}_2)_2\text{PC}_6\text{F}_4\text{B}(\text{C}_6\text{F}_5)_2$, which is able to cleave dihydrogen under ambient conditions yielding a zwitterionic phosphonium/hydridoborate and the release of H_2 upon thermal treatment.^[34]

Besides dihydrogen, FLP-systems have shown the ability to react with a large number of small molecules, including NO , CO , N_2O , CO_2 , SO_2 , olefins, alkynes and many more.^[35]

Inspired by the computational work of Tonner and Franking about carbodiphosphorane,^[36] Alcarazo et al. were able to build a FLP consisting of a carbon-

based LB and $B(C_6F_5)_3$.^[37] Besides the classic H-H, C-H, and C-O bond cleavages, this system is also able to activate alkyl fluorides and Si-H bonds (Scheme 5).



Scheme 5: Some reactions of the FLP $[(C(PPh_3)_2)(B(C_6F_5)_3)]$.

Apart from classic inter- and intramolecular FLPs, there are also so-called hidden FLPs, which feature a similar reactivity, but do not look like they are frustrated at first sight.^[38] In 2016, Styra et al. reported on a four-membered diphosphamethanide aluminium heterocycle with either alkyl or aryl substituents on the aluminium atom as hidden FLP.^[39] Apart from interesting properties concerning the structural environment around Al, the alkyl substituted cycle is able to cleave H_2 yielding the corresponding diphosphine and aluminiumhydride. DFT calculations suggest a possible reaction mechanism including a six-membered transition state, which might explain the reactivity of the alkyl-substituted species, in contrast to the aryl-substituted derivate. Inspired by the idea of a self-healing gel, based on small molecule interactions, Wang and Shaver designed a polymer, which contains complementary FLP donors and acceptors.^[40] First, they ensured that their chosen monomers, 4-styryl-diphenylborane and 4-styryl-dimesitylphosphine, did not form a classic LA-LB adduct. However, by adding the azo-bridged diethyl azodicarboxylate (DEAD) a rapid reaction occurs, forming a DEAD-bridged product of the monomers. By applying an addition-fragment-chain-transfer copolymerization with styrene the target polymers are formed.

1.4 Literature

- [1] A. F. Holleman, N. Wiberg, *Lehrbuch der Anorganischen Chemie* **102. Auflage**, 1111.
- [2] a) R. L. Wells, W. L. Gladfelter, *J. Cluster Sci.* **1997**, 8, 217–237; b) F. Maury, *Adv. Mater.* **1991**, 3, 542–548; c) Parshall, G. W. In *The Chemistry of Boron and its Compounds*; Muetterties, E. L., Ed.; Wiley: New York, **1967**; 617. d) Haiduc, I. *The Chemistry of Inorganic Ring Systems*; Wiley: New York, **1970**; 349.
- [3] H. M. Manasevit, *Appl. Phys. Lett.* **1968**, 12, 156–159.
- [4] A. Stock, E. Pohland, *Ber. Dtsch. Chem. Ges.* **1926**, 59, 2215–2223.
- [5] C. W. Hamilton, R. T. Baker, A. Staubitz, I. Manners, *Chem. Soc. Rev.* **2009**, 38, 279–293.
- [6] C. A. Jaska, K. Temple, A. J. Lough, I. Manners, *Chem. Comm.* **2001**, 962-963.
- [7] A. Staubitz, A. P. M. Robertson, M. E. Sloan, I. Manners, *Chem. Rev.* **2010**, 110, 4023-4078.
- [8] S. Y. Pusatcioglu, H. A. McGee, A. L. Fricke, J. C. Hassler, *Journal of Applied Polymer Science* **1977**, 21, 1561-1567.
- [9] A. Staubitz, A. Presa Soto, I. Manners, *Angew. Chem. Int. Ed.* **2008**, 47, 6212-6215.
- [10] M. C. Denney, V. Pons, T. J. Hebden, D. M. Heinekey, K. I. Goldberg, *J. Am. Chem. Soc.* **2006**, 128, 12048–12049.
- [11] H. Dorn, R. A. Singh, J. A. Massey, A. J. Lough, I. Manners, *Angew. Chem. Int. Ed.* **1999**, 38, 3321-3323; *Angew. Chem.* **1999**, 22, 3540-3543.
- [12] J.-M. Denis, H. Forintos, H. Szelke, L. Toupet, T.-N. Pham, P.-J. Madec, A.-C. Gaumont, *Chem. Commun.* **2003**, 54–55.
- [13] U. S. D. Paul, H. Braunschweig, U. Radius, *Chem. Commun.* **2016**, 52, 8573-8576.
- [14] a) A. Schäfer, T. Jurca, J. Turner, J. R. Vance, K. Lee, Van An Du, M. F. Haddow, G. R. Whittell, I. Manners, *Angew. Chem. Int. Ed.* **2015**, 54, 4836 – 4841; *Angew. Chem.* **2015**, 127, 4918-4923; b) J. R. Turner, D. A. Resendiz-Lara, T. Jurca, A. Schäfer, J. R. Vance, L. Beckett, G. R. Whittell, R. A. Musgrave, H. A. Sparkes, I. Manners, *Macromol. Chem. Phys.* **2017**, 218, 1700120.

- [15] J. R. Vance, A. Schäfer, A. P. M. Robertson, K. Lee, J. Turner, G. R. Whittell, I. Manners, *J. Am. Chem. Soc.* **2014**, *136*, 3048–3064.
- [16] C. A. Jaska, A. J. Lough, I. Manners, *Inorg. Chem.* **2004**, *43*, 1090-1099.
- [17] a) M. A. Petrie, M. M. Olmstead, H. Hope, R. A. Bartlett, P. P. Power, *J. Am. Chem. Soc.* **1993**, *115*, 3221-3226; b) M. A. Mardones, A. H. Rowley, L. Contreras, R. A. Jones, *J. Organomet. Chem.* **1993**, *455*, C1-C2; P. P. Power, *Chem. Rev.* **1999**, *99*, 3463-3503.
- [18] a) C. Y. Tang, A. L. Thompson, S. Aldridge, *Angew. Chem. Int. Ed.* **2010**, *49*, 921–925; *Angew. Chem.* **2010**, *122*, 933–937; b) C. T. Kwon, H. A. McGee, Jr., *Inorg. Chem.* **1970**, *9*, 2458–2461; c) G. Alcaraz, L. Vendier, E. Clot, S. Sabo-Etienne, *Angew. Chem. Int. Ed.* **2010**, *49*, 918–920; *Angew. Chem.* **2010**, *122*, 930–932.
- [19] F. Thomas, S. Schulz, M. Nieger, *Eur. J. Inorg. Chem.* **2001**, 161 - 166.
- [20] D. A. Atwood, L. Contreras, A. H. Cowley, R. A. Jones, M. A. Mardones, *Organometallics* **1993**, *12*, 17-18.
- [21] U. Vogel, P. Hoemensch, K.-C. Schwan, A. Y. Timoshkin, M. Scheer, *Chem. Eur. J.* **2003**, *9*, 515-520.
- [22] U. Vogel, A. Y. Timoshkin, M. Scheer, *Angew. Chem.* **2001**, *113*, 4541-4544; *Angew. Chem. Int. Ed.* **2001**, *40*, 4409-4412.
- [23] K.-C. Schwan, A. Y. Timoskin, M. Zabel, M. Scheer, *Chem. Eur. J.* **2006**, *12*, 4900–4908.
- [24] C. Marquardt, A. Adolf, A. Stauber, M. Bodensteiner, A. V. Virovets, A. Y. Timoshkin, M. Scheer, *Chem. Eur. J.* **2013**, *19*, 11887–11891.
- [25] C. Marquardt, *Dissertation*, Regensburg **2015**.
- [26] C. Marquardt, O. Hegen, M. Hautmann, G. Balázs, M. Bodensteiner, A. V. Virovets, A. Y. Timoshkin, M. Scheer, *Angew. Chem. Int. Ed.* **2015**, *54*, 13122–13125; *Angew. Chem.* **2015**, *127*, 13315–13318.
- [27] A. C. Malcolm, K. J. Sabourin, R. McDonald, M. J. Ferguson, E. Rivard, *Inorg. Chem.* **2012**, *51*, 12905–12916.
- [28] C. Marquardt, T. Jurca, K.-C. Schwan, A. Stauber, A. V. Virovets, G. R. Whittell, I. Manners, M. Scheer, *Angew. Chem. Int. Ed.* **2015**, *54*, 13782–13786; *Angew. Chem.* **2015**, *127*, 13986 – 13991.
- [29] a) C. Marquardt, C. Thoms, A. Stauber, G. Balázs, M. Bodensteiner, M. Scheer, *Angew. Chem. Int. Ed.* **2014**, *53*, 3727–3730; *Angew. Chem.* **2014**, *126*, 3801–

- 3804; b) C. Marquardt, G. Balázs, J. Baumann, A. V. Virovets, M. Scheer, *Chem. Eur. J.* **2017**, 23, 11423–11429.
- [30] C. Thoms, C. Marquardt, M. Bodensteiner, A. Y. Timoshkin, M. Scheer, *Angew. Chem. Int. Ed.* **2013**, 52, 5150–5154; *Angew. Chem.* **2013**, 125, 5254–5259.
- [31] C. Marquardt, T. Kahoun, A. Stauber, G. Balázs, M. Bodensteiner, A. Y. Timoshkin, M. Scheer, *Angew. Chem. Int. Ed.* **2016**, 55, 14828–14832; *Angew. Chem.* **2016**, 128, 15048–15052.
- [32] G. N. Lewis, *Valence and the Structure of Atoms and Molecules*, Chemical Catalogue Company, New York, **1923**.
- [33] a) G. Wittig, E. Benz, *Chem. Ber.* **1959**, 92, 1999–2013. b) W. Tochtermann, *Angew. Chem. Int. Ed.* **1966**, 5, 351–371; *Angew. Chem.* **1966**, 78, 355–375; c) H. C. Brown, H. I. Schlesinger, S. Z. Cardon, *J. Am. Chem. Soc.* **1942**, 64, 325–329. d) H. C. Brown, B. Kanner, *J. Am. Chem. Soc.* **1966**, 88, 986–992.
- [34] G. C. Welch, R. R. S. Juan, J. D. Masuda, D. W. Stephan, *Science* **2006**, 314, 1124–1126.
- [35] D. W. Stephan, *Science* **2016**, 354, 1248–1257.
- [36] a) R. Tonner, G. Frenking, *Chem. Eur. J.* **2008**, 14, 3273 – 3289; b) H. Schmidbaur, *Angew. Chem. Int. Ed.* **1983**, 22, 907 – 927; *Angew. Chem.* **1983**, 95, 980 – 1000; c) R. Tonner, G. Frenking, *Angew. Chem. Int. Ed.* **2007**, 46, 8695 – 8698; *Angew. Chem.* **2007**, 119, 8850 – 8853.
- [37] M. Alcarazo, C. Gomez, S. Holle, R. Goddard, *Angew. Chem. Int. Ed.* **2010**, 49, 5788 –5791; *Angew. Chem.* 2010, 122, 5924 –5927.
- [38] a) M. A. Dureen, D. W. Stephan, *J. Am. Chem. Soc.* **2010**, 132, 13559 –13568; b) B.-H. Xu, K. Bussmann, R. Fröhlich, C. G. Daniliuc, J. G. Brandenburg, S. Grimme, G. Kehr, G. Erker, *Organometallics* **2013**, 32, 6745 –6752.
- [39] S. Styra, M. Radius, E. Moos, A. Bihlmeier, F. Breher, *Chem. Eur. J.* **2016**, 22, 9508 – 9512.
- [40] M. Wang, F. Nudelman, R. R. Matthes, M. P. Shaver, *J. Am. Chem. Soc.* **2017**, 139, 14232–14236.

2. Research Objectives

In contrast to carbon-based polymers, the objective for copolymers based on alternating group 13/15 elements is still open. In order to get insight into the chemistry of possible inorganic copolymers, it is inevitable to take a closer look on the building blocks $\text{H}_2\text{E}-\text{BH}_2-\text{E}'\text{R}'_2-\text{BH}_2$ (E, E' = pnictogen). Due to the high sensitivity of these compounds, the following tasks arise:

- development of a suitable synthetic pathway to stabilize such highly reactive compounds under ambient conditions
- variation of one pnictogen atom to adjust the estimated properties
- variation of the substituents

As shown in the introduction, there are some examples for the cleavage of oligomeric or polymeric pnictogenyltrielanes with strong LBs. However, a systematic investigation of the cleavage of poly(phosphinoboranes) by different LBs has not been performed yet. Therefore, the following tasks arise:

- Investigation of different oligo-/poly(phosphanylboranes) to determine the influence of the substituents on the cleavage
- Variation of the LB to get insight into the donor strength needed for the cleavage
- Performance of the experiments under different conditions to optimize the cleavage process

As LB stabilized substituted phosphanylboranes $\text{RR}'\text{PBH}_2-\text{NMe}_3$ (R = R' = Ph; R = H, R' = *t*Bu) are versatile building blocks for oligomeric/polymeric material, the established pathways should be further extended to the heavier congener, arsenic. Thus, LB stabilized substituted arsanylboranes should be synthesized and characterized. The reactivity of these compounds should be further investigated towards:

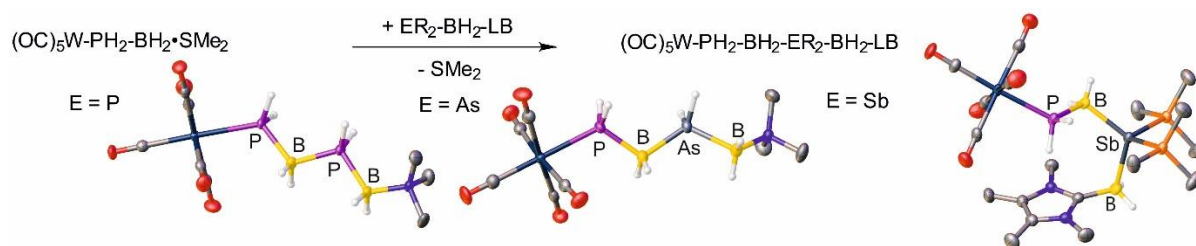
- main group LAs like BH_3 and BBr_3
- BH_2^+ building blocks to synthesize cationic compounds
- different chalcogens to yield the corresponding oxidated arsanylboranes
- the elimination of the LB through thermal activation to yield oligomeric/polymeric material

Due to only one phosphorus coordination site, the possibilities to build up discrete oligomeric units based on LB stabilized phosphanylboranes are limited. By application of bidentate LBs in order to stabilize phosphanylboranes instead of monodentate LBs like NMe_3 , the reactivity of these compounds should be further extended. However, there are several challenges to overcome:

- finding a suitable bidentate LB to stabilize phosphanylboranes
- transfer of established reaction strategies to yield different bidentate phosphanylboranes
- examine, if bidentate LBs are suitable to stabilize arsanylboranes

3. A Convenient Route to Mixed Pnictogenylboranes

Oliver Hegen, Christian Marquardt, Alexey Y. Timoshkin, and Manfred Scheer



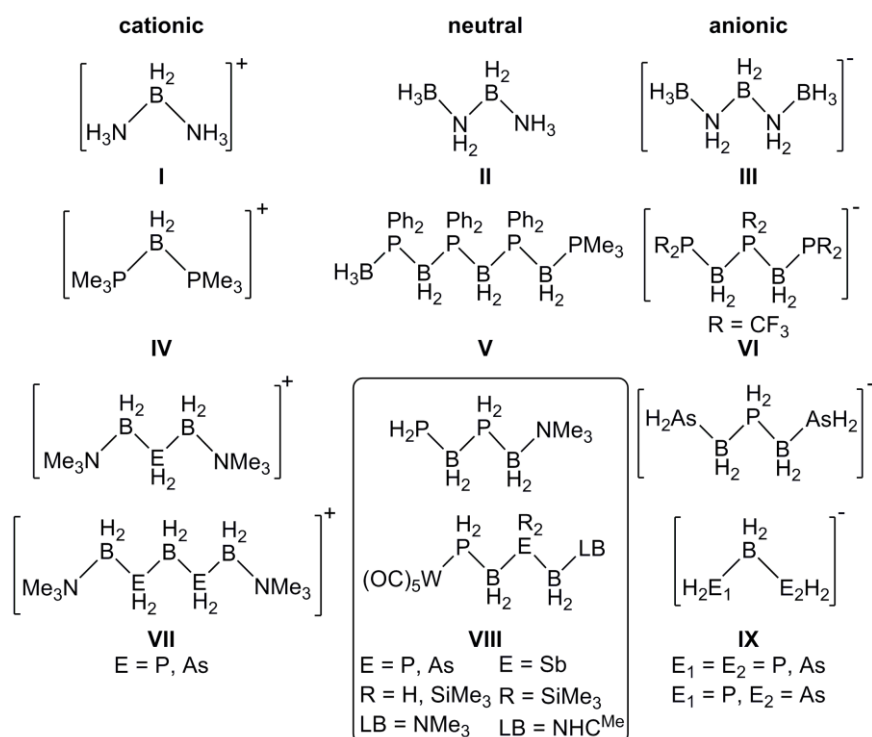
Abstract: We report on the synthesis and characterization of mixed pnictogenylboranes. The substitution of the Lewis base SMe_2 of $(OC)_5W-PH_2BH_2-SMe_2$ (**2**) by different pnictogenylboranes ER_2BH_2-LB ($E = P, As, Sb$) leads to the Lewis acid/base-stabilized, butane analogue molecules $(OC)_5W-PH_2BH_2ER_2BH_2-LB$ (**3a,b**: $E = P, R = H, SiMe_3, LB = NMe_3$; **4a,b**: $As, R = H, SiMe_3, LB = NMe_3$; **5**: $Sb, R = SiMe_3, LB = NHC^{Me}$). All these compounds were characterized by single crystal X-ray structure analysis, mass spectrometry, NMR and IR spectroscopy. In addition, the very unstable phosphanylborane chain $PH_2BH_2PH_2BH_2-NMe_3$ (**1**) was synthesized. DFT calculations provide insight into the thermodynamics of these reactions.

3.1 Introduction

Non-carbon-containing polymers based on main-group elements have versatile applications in the field of lithography, polyelectrolytes, optoelectronics, biomaterials or as precursors for ceramic materials.^[1,2] In particular, polymers with a backbone built on group 13/15 elements, which are isoelectronic to hydrocarbons, are of great interest. Owing to the polarity in the repeating unit, these polymers have different properties to C-C polymers.^[3] In particular, poly(phosphinoborane)s (RPH-BH_2)_n have received more attention in the last few years as high molecular weight polymers.^[4] These materials are prepared by transition-metal-catalyzed ($\text{Fe}^{[4b]}$, $\text{Ir}^{[4d]}$, $\text{Rh}^{[4a,4c]}$) dehydrocouplings of phosphine-borane adducts $\text{RPH}_2\text{-BH}_3$ ($\text{R} = \text{Ph}$, *t*Bu, *p*-*n*BuC₆H₄, *p*-C₁₂H₂₅C₆H₄). Recently, we reported a catalyst-free pathway as well as the synthesis of the first high-molecular-weight poly(alkylphosphinoborane).^[5] Thermal treatment of *t*BuPHBH₂-NMe₃ leads to the elimination of NMe₃ and the head-to-tail polymerization of the reactive intermediate [*t*BuPHBH₂], yielding [*t*BuPHBH₂]_n.

Similar highly reactive compounds such as $[\text{H}_2\text{N=BH}_2]$ have been isolated under cryogenic conditions.^[6] Under ambient conditions, however, stabilization is necessary, for example by trapping these compounds with transition-metal complexes ($[\text{RuH}_2(\eta^2:\eta^2\text{-H}_2\text{BNH}_2)(\text{PCy}_3)_2]$).^[7] The same $\eta^2:\eta^2$ coordination of $[\text{R}_2\text{N=BH}_2]$ was observed within an Ir complex.^[8] Another way to investigate these compounds at ambient conditions is either their protection with sterically demanding groups on the boron atom^[9] or donor-acceptor stabilization. In the latter case, the vacant p orbital on the boron atom is blocked by a Lewis base (LB), while the lone pair of the pnictogen atom coordinates to a Lewis acid (LA).^[10] Rivard and co-workers succeeded in the preparation of $\text{H}_3\text{B-H}_2\text{NBH}_2\text{-DMAP}$ (DMAP = dimethylaminopyridine) and its conversion into borazine.^[10a] In some cases, the stabilization induced by coordination of a Lewis base is sufficient for the isolation of such complexes. Using this strategy, our group was able to synthesize the parent compounds of the phosphanylboranes,^[11] the arsanylboranes^[12] and the stibanylboranes,^[13] which are stabilized by a Lewis base only. Evidence that the free, unstabilized phosphanylborane might exist was reported by Burg and co-workers with reference to the formation of H_2PBMe_2 .^[14,15b] In contrast to the matrix-characterized H_2NBH_2 ,^[6] the free parent phosphanylborane H_2PBH_2 has not yet been observed experimentally thus far, but has been studied computationally.^[15] As predicted by DFT computations and later shown by

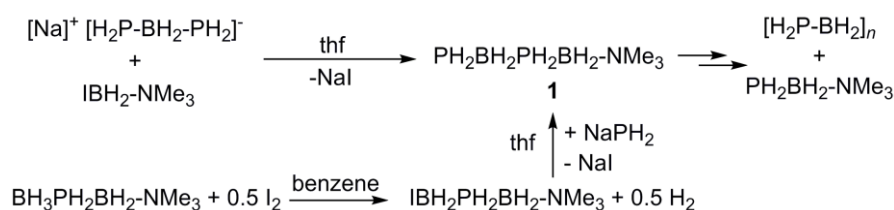
experiments,^[16] the Lewis base stabilized pnictogenylboranes $\text{H}_2\text{EBH}_2\text{-NMe}_3$ ($\text{E} = \text{P}, \text{As}$) can be handled easily under inert conditions and are available in good yields.^[11,12] Moreover, computations showed that a Lewis acid such as $\text{W}(\text{CO})_5$ is sufficient to prevent the polymerization of H_2PBH_2 .^[16] A phosphanylborane that is only stabilized by a Lewis acid would be an interesting compound as the empty p orbital on the boron atom renders it a versatile building block for extended Group 13/15 chains. Aside from different cationic (**I**^[17], **IV**)^[18], neutral (**II**^[19], **V**)^[20] and anionic (**III**^[21], **VI**)^[22] Group 13/15 chains, we could recently showed that Lewis base stabilized pnictogenylboranes are versatile starting materials for the synthesis of ionic extended group 13/15 compounds. Upon coordination of the pnictogen atom towards $\text{IBH}_2\text{-LB}$ ($\text{LB} = \text{NMe}_3, \text{SMe}_2$), it is possible to synthesize miscellaneous cationic chains (**VII**).^[23] The reactions with phosphanides and arsenides yield anionic chains of the type **IX**.^[24] Thus far, both pathways are restricted to phosphorus and arsenic as the pnictogen atom (Scheme 1).



Scheme 1: Overview of extended Group 13/15 compounds.

3.2 Results and Discussion

Herein, we report the longest X-ray-characterized parent phosphanylborane chain $\text{PH}_2\text{BH}_2\text{PH}_2\text{BH}_2\text{-NMe}_3$ (**1**) that is stabilized only by a Lewis base and the novel neutral Lewis acid/base stabilized pnictogenylboranes $(\text{OC})_5\text{W-PH}_2\text{BH}_2\text{ER}_2\text{BH}_2\text{-LB}$ (**VIII**; $\text{E} = \text{P, As, Sb}$; $\text{R} = \text{H or SiMe}_3$ and $\text{LB} = \text{NMe}_3, \text{NHC}^{\text{Me}} = 1,3,4,5\text{-Tetramethylimidazolyliidene}$), which are the first compounds that feature mixed Group 15 element sequences within the chain.



Scheme 2: Synthesis of compound **1**.

The metathesis reactions of either $[\text{Na}]^+[\text{PH}_2\text{BH}_2\text{PH}_2]^-$ with $\text{IBH}_2\text{-NMe}_3$ or NaPH_2 with $\text{IBH}_2\text{PH}_2\text{BH}_2\text{-NMe}_3$ gave $\text{PH}_2\text{BH}_2\text{PH}_2\text{BH}_2\text{-NMe}_3$ (**1**, Scheme 2). Compound **1** is not stable in solution and very prone to decompose to $\text{H}_2\text{PBH}_2\text{-NMe}_3$ and the polymer $[\text{H}_2\text{PBH}_2]_n$ (Scheme 2). DFT computations indicated that at room temperature the decomposition of **1** to $\text{H}_2\text{PBH}_2\text{-NMe}_3$ and $1/n[\text{H}_2\text{PBH}_2]_n$ is exergonic by 33 and 24 kJ mol^{-1} for $n = 3$ and 8, respectively. Nevertheless, we were able to isolate some crystals of **1** to study its solid state structure (Figure 1). Note that the subsequent stabilization of **1** by coordination to a Lewis acid such as $[(\text{OC})_5\text{W}(\text{thf})]$ failed.

On the other hand, DFT computations suggest that donor/acceptor stabilization is energetically sufficient to stabilize dimeric pnictogenylboranes of this type. Intrigued by the idea to study only hydrogen-containing dimeric pnictogenylboranes, we developed a reaction pathway with persistent Lewis acid/base stabilization. This not only enables the synthesis of longer neutral phosphanylboranes, but also paves the way to mixed pnictogenylboranes.

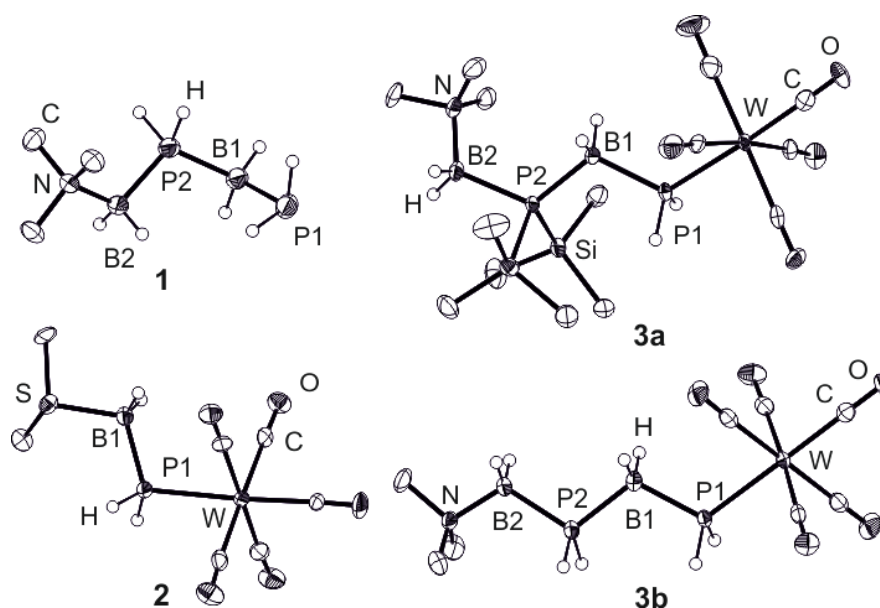
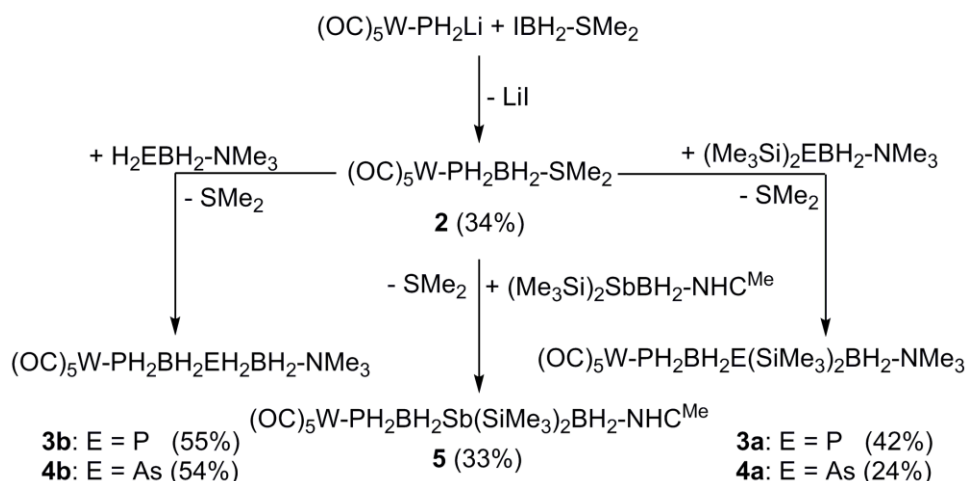


Figure 1: Molecular structure of **1**, **2**, **3a**, and **3b** in the solid state. Hydrogen atoms bonded to carbon are omitted for clarity. Thermal ellipsoids set at 50% probability.

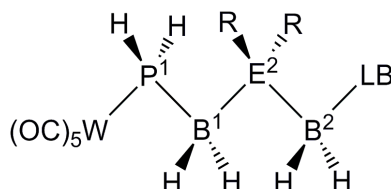
The reaction of $(OC)_5W-PH_2Li$ and IBH_2-SMe_2 leads to the Lewis acid/base stabilized phosphanylborane $(OC)_5W-PH_2-BH_2-SMe_2$ (**2**, Scheme 3). The molecular structure of **2** in the solid state is similar to the structure of $(OC)_5W-PH_2BH_2-NMe_3$ (Figure 1).^[16] The weak donor SMe_2 can be easily substituted by stronger Lewis bases, such as pnictogenylboranes, which results in pnictogenylborane backbones with a P-B-E-B-sequence (E = P, As, Sb; Scheme 3).



Scheme 3: Synthesis of compounds **2-5**. All reactions are performed in toluene for 18 h (**3a**, **3b**, **4a**) or 3h (**4b**, **5**). Yields are given in parentheses.

Therefore, the corresponding pnictogenylboranes ER_2BH_2-LB (E = P, As, Sb) were reacted with $(OC)_5W-PH_2BH_2-SMe_2$ (**2**) at room temperature. According to the ^{31}P NMR spectra of the crude reaction mixtures, all conversions proceeded with high

conversion (ca. 80-100%). However, the yields of isolated crystalline material are lower because of the used crystallization process and sometimes because of the similar solubility of the side products. The isolated products **3-5** (Scheme 4) are well soluble in toluene and slightly soluble in *n*-hexane. All products show the corresponding molecular ion peak in the mass spectra.



Scheme 4: The notation given above will be used for further discussion of compounds **3-5** (E = P, As, Sb).

The resonance of the P1 atom in the ^{31}P NMR spectra of compounds **3-5** is shifted downfield relative to that of the starting material **2**. Compared to the starting materials $\text{H}_2\text{PBH}_2\text{-NMe}_3$ ^[11] and $(\text{Me}_3\text{Si})_2\text{PBH}_2\text{-NMe}_3$,^[12] the P2 resonance of **3a** and **3b** undergoes a downfield shift upon coordination. In addition, the coordination to a second boron moiety leads to a substantial broadening of the resonance, which is consistent with former results and due to the quadrupole moment of the boron nuclei.^[11] In the ^{11}B NMR spectrum, the signals for the B1 and B2 atoms reveal an upfield shift (except for **5**) compared to the starting material.^[25]

The solid state structures of **1-5** were determined by single-crystal X-ray diffraction experiments (Figures 1 and 2). The replacement of SMe_2 by the pnictogenylboranes leads to a slight shortening of the E-B2-bond (Table 1). The length of the newly formed E-B1 bond (E = P, As, Sb) is comparable to that of an E-B single bond. The B2-P2 axis in **3a** shows a synclinal arrangement whereas the B1-P1 and P2-B1 axes adopt antiperiplanar conformations (Figure 1). Compound **3b** adopts a zigzag conformation, with all substituents being in an antiperiplanar arrangement (Figure 1). The molecular structure of **1** shows an antiperiplanar arrangement along the B1-P1 and the B2-P2 axes and, in contrast to **3b**, a synclinal configuration along the P2-B1 bond (Figure 1).

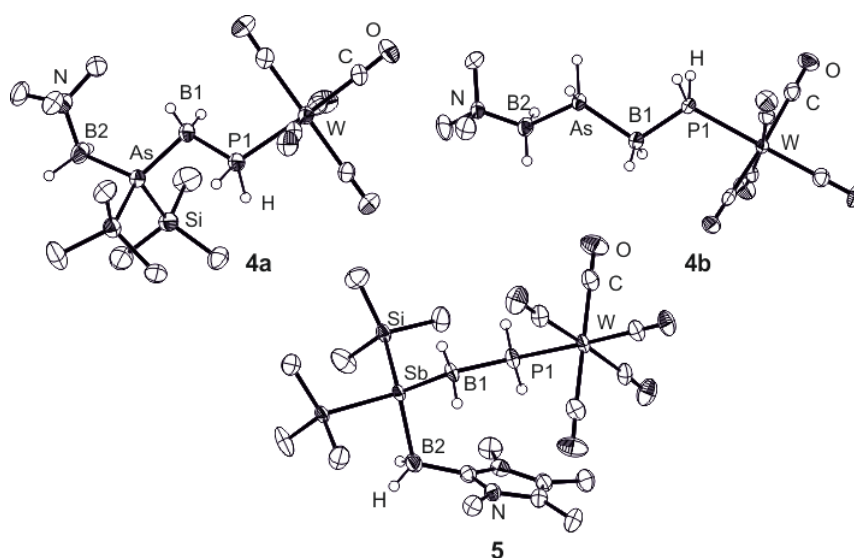


Figure 2: Molecular structure of **4a**, **4b** and **5** in the solid state. Hydrogen atoms bonded to carbon atoms are omitted for clarity. Thermal ellipsoids set at 50% probability.

Table 1: Selected bond lengths [Å] and angles [°] of compounds **2-5**.

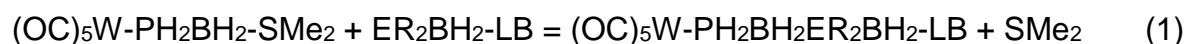
Compound	P1-B1	B1-E	E-B2-LB	W-P1-B1-E	B1-E-B2
2	1.942(11)	/	/	113.2(5)	/
3a	1.958(4)	1.981(4)	2.001(4)	114.4(2)	117.9(2)
3b	1.945(4)	1.939(5)	1.952(4)	114.3(2)	109.5(2)
4a	1.947(4)	2.094(4)	2.105(4)	113.2(2)	118.9(2)
4b	1.939(7)	2.059(6)	2.076(8)	111.6(3)	116.1(3)
5	1.945(4)	2.259(4)	2.301(4)	117.8(2)	114.6(2)

Compounds **4a** and **4b** (Figure 2) are the first neutral representatives of main-group chains possessing a P-B-As-B sequence, whereas previously only anionic chains containing As, P and B were known.^[24] The molecular structure of **4a** is similar to that of **3a**. Compared to the starting material (Me₃Si)₂AsBH₂-NMe₃^[12] (As-B = 2.112(7) Å), the As-B-bond lengths are similar (Table 1), and the Si-As-Si-angle is larger. The zigzag conformation in **4b** (Figure 2) is distorted, and the B1-As/ As-B2 bonds are comparable to those in the starting material H₂AsBH₂-NMe₃^[12] (2.071(4) Å). Compared to the anionic species [H₂As-BH₂-PH₂-BH₂-AsH₂]⁻ (2.081(3) Å), both As-B bonds are shorter.^[24]

Compound **5** is the first derivative containing a P-B-Sb-B sequence. It has an antiperiplanar configuration along the P-B2 bond, a synclinal arrangement along the Sb-B2 axis and a synperiplanar configuration along the Sb-B1 bond, which results in a

distorted U-shape arrangement. The newly formed Sb-B1 bond is slightly shorter than the Sb-B2 bond.

DFT computations showed that the energetics of the reaction for the synthesis of the mixed pnictogenylboranes [Eq. (1)] strongly depends on the element E, the group R,



and the Lewis base (Table 2). The exothermicity of the reaction increases in the order: Bi < Sb < As < P, H < SiMe₃, and Me₃N < NHC^{Me}. Thus the formation of heavier pnictogenylboranes remains exothermic only in the case of R = SiMe₃.^[26] Note that the nature of the Lewis base is also an important factor for the stabilization of the molecule: It was predicted that the stronger base NHC^{Me} is required to stabilize the antimony and bismuth derivatives.

Table 2: Standard enthalpies ΔH°_{298} , (kJ mol⁻¹) for the reaction shown in Eq. (1). Calculated at the B3LYP/def2-SVP level of theory. Data are given for the most stable isomers in the gas phase.

R	LB	E:	P	As	Sb	Bi
H	NMe ₃		-59.3	-27.3	5.7	40.0
H	NHC ^{Me}		-74.2	-37.7	0.4	40.0
SiMe ₃	NMe ₃		-39.2	-27.7	-12.2	13.0
SiMe ₃	NHC ^{Me}		-76.7	-58.5	-32.3	-2.3

3.3 Conclusion

In summary, we have presented the synthesis and characterization of the longest parent phosphanylborane chain **1** stabilized only by a Lewis base. Moreover, the newly synthesized phosphanylborane **2** stabilized by a strong Lewis acid ((OC)₅W) and a weak Lewis base (SMe₂) is a unique starting material for subsequent reactions. By substituting the weak Lewis base, unprecedented neutral molecules containing a P-B-P-B sequence (**3a**, **3b**) were obtained that are not stable without a Lewis acid.

As donor/acceptor stabilization is needed for the stabilization of longer neutral group 13/15 element chains, we successfully applied this general strategy by replacing the weaker base SMe₂ in **2** with Lewis base stabilized heavier pnictogenylboranes. By this way we were able to synthesize and characterize a series of previously unknown neutral pnictogenylboranes such as **4a** and **4b**, which contain an unprecedented P-B-

As-B chain, with **3b** and **4b** being the longest reported neutral parent pnictogenylborane chains thus far. Furthermore, the first neutral compound **5** containing a P-B-Sb-B unit was synthesized and fully characterized. The use of these mixed pnictogenylboranes as precursors for inorganic polymers or even longer Group 13/15 catena compounds is currently in the focus of our interest.

3.4 References

- [1] a) H. R. Allcock, *Chem. Mater.* **1994**, *6*, 1476-1491; b) F. Choffat, S. Käser, P. Wolfer, D. Schmid, R. Mezzenga, P. Smith, W. Caseri, *Macromolecules* **2007**, *40*, 7878-7889; c) G. Zhang, G. M. Palmer, M. W. Dewhirst, C. L. Fraser, *Nat. Mater.* **2009**, *8*, 747-751; d) A. Lorbach, M. Bolte, H. Li, H.-W. Lerner, M. C. Holthausen, F. Jäkle, M. Wagner, *Angew. Chem. Int. Ed.* **2009**, *48*, 4584-4588; *Angew. Chem.* **2009**, *121*, 4654-4658; e) H. Kuhtz, F. Cheng, S. Schwedler, L. Böhling, A. Brockhinke, L. Weber, K. Parab, F. Jäkle, *ACS Macro Lett.* **2012**, *1*, 555-559; f) F. Jäkle, *Chem. Rev.* **2010**, *110*, 3985-4022; g) Z. M. Hudson, D. J. Lunn, M. A. Winnik, I. Manners, *Nat. Commun.* **2014**, *5*, 3372-3379; h) R. D. Miller, J. Michl, *Chem. Rev.* **1989**, *89*, 1359-1410; i) X. He, T. Baumgartner, *RSC Adv.* **2013**, *3*, 11334-11350; j) J. Linshoeft, E. J. Baum, A. Hussain, P. J. Gates, C. Näther, A. Staubitz, *Angew. Chem. Int. Ed.* **2014**, *53*, 12916-12920; *Angew. Chem.* **2014**, *126*, 13130-13134; k) T. Imori, V. Lu, H. Cai, T. D. Tilley, *J. Am. Chem. Soc.* **1995**, *117*, 9931-9940; l) R. West, *J. Organomet. Chem.* **1986**, *300*, 327-346; m) W. Cao, Y. Gu, M. Meineck, T. Li, H. Xu, *J. Am. Chem. Soc.* **2014**, *136*, 5132-5137; n) A. M. Priegert, B. W. Rawe, S. C. Serin, D. P. Gates, *Chem. Soc. Rev.* **2016**, *45*, 922-953.
- [2] a) B. W. Rawe, C. P. Chun, D. P. Gates, *Chem. Sci.* **2014**, *5*, 4928-4938; b) R. De Jaeger, M. Gleria, *Prog. Polym. Sci.* **1998**, *23*, 179-276; c) M. Liang, I. Manners, *J. Am. Chem. Soc.* **1991**, *113*, 4044-4045; d) C. H. Honeyman, I. Manners, C. T. Morrissey, H. R. Allcock, *J. Am. Chem. Soc.* **1995**, *117*, 7035-7036; e) R. H. Neilson, P. Wisian-Neilson, *Chem. Rev.* **1988**, *88*, 541-562; f) S. Wilfert, H. Henke, W. Schoefberger, O. Brüggemann, I. Teasdale, *Macromol. Rapid Commun.* **2014**, *35*, 1135-1141.
- [3] a) A. Staubitz, M. E. Sloan, A. P. M. Robertson, A. Friedrich, S. Schneider, P. J. Gates, J. Schmedt auf der Günne, I. Manners, *J. Am. Chem. Soc.* **2010**, *132*,

- 13332-13345; b) A. Staubitz, A. P. Soto, I. Manners, *Angew. Chem. Int. Ed.* **2008**, *47*, 6212-6215; *Angew. Chem.* **2008**, *120*, 6308-6311; c) R. Dallanegra, A. P. M. Robertson, A. B. Chaplin, I. Manners, A. S. Weller, *Chem. Commun.* **2011**, *47*, 3763-3765; d) R. T. Baker, J. C. Gordon, C. W. Hamilton, N. J. Henson, P.-H. Lin, S. Maguire, M. Murugesu, B. L. Scott, N. C. Smythe *J. Am. Chem. Soc.* **2012**, *134*, 5598-5609; e) A. N. Marziale, A. Friedrich, I. Klopsch, M. Drees, V. R. Celinski, J. Schmedt auf der Gönne, S. Schneider, *J. Am. Chem. Soc.* **2013**, *135*, 13342-13355; f) M. E. Bluhm, M. G. Bradley, R. Butterick III, U. Kusari, L. G. Sneddon, *J. Am. Chem. Soc.* **2006**, *128*, 7748-7749; g) D. W. Himmelberger, C. W. Yoon, M. E. Bluhm, P. J. Carroll, L. G. Sneddon, *J. Am. Chem. Soc.* **2009**, *131*, 14101-14110; h) T. Wideman, P. J. Fazen, K. Su, E. E. Remsen, G. A. Zank, L. G. Sneddon, *Appl. Organomet. Chem.* **1998**, *12*, 681-693; i) A. Kumar, N. A. Beattie, S. D. Pike, S. A. Macgregor, A. S. Weller *Angew. Chem. Int. Ed.* **2016**, *55*, 6651-6656; *Angew. Chem.* **2016**, *128*, 6763-6768; j) H. C. Johnson, A. S. Weller *Angew. Chem. Int. Ed.* **2015**, *54*, 10173-10177; *Angew. Chem.* **2015**, *127*, 10311-10315.
- [4] a) H. Dorn, J. M. Rodezno, B. Brunnhöfer, E. Rivard, J. A. Massey, I. Manners *Macromolecules*, *36*, No. 2, **2003**, 291-297; b) A. Schäfer, T. Jurca, J. Turner, J. R. Vance, K. Lee, V. A. Du, M. F. Haddow, G. R. Whittell, I. Manners, *Angew. Chem. Int. Ed.* **2015**, *54*, 4836-4841; *Angew. Chem.* **2015**, *127*, 4918-4923; c) H. Dorn, R. A. Singh, J. A. Massey, A. J. Lough, I. Manners, *Angew. Chem. Int. Ed.* **1999**, *38*, 3321-3323; *Angew. Chem.* **1999**, *111*, 3540-3543; d) U. S. D. Paul, H. Braunschweig, U. Radius, *Chem. Commun.*, **2016**, *52*, 8573-8576; e) A. Staubitz, A. P. M. Robertson, M. E. Sloan, I. Manners, *Chem. Rev.* **2010**, *110*, 4023-4078; f) H. C. Johnson, T. N. Hooper, A. S. Weller, *Top. Organomet. Chem.* **2015**, *49*, 153-220.
- [5] a) C. Marquardt, T. Jurca, K.-C. Schwan, A. Stauber, A. V. Virovets, G. R. Whittell, I. Manners, M. Scheer, *Angew. Chem. Int. Ed.* **2015**, *54*, 13782-13787; *Angew. Chem.* **2015**, *127*, 13986-13991; b) A. Stauber, T. Jurca, C. Marquardt, M. Fleischmann, M. Seidl, G. R. Whittell, I. Manners, M. Scheer, *Eur. J. Inorg. Chem.* **2016**, 2684-2687.
- [6] C. T. Kwon, H. A. Jr. McGee, *Inorg. Chem.* **1970**, *9*, 2458-2461.
- [7] G. Alcaraz, L. Vendier, E. Clot, S. Sabo-Etienne, *Angew. Chem. Int. Ed.* **2010**, *49*, 918-920; *Angew. Chem.* **2010**, *122*, 930-932.

- [8] C. Y. Tang, A. L. Thompson, S. Aldridge, *Angew. Chem. Int. Ed.* **2010**, *49*, 921-925; *Angew. Chem.* **2010**, *122*, 933-937.
- [9] R. T. Paine, H. Nöth, *Chem. Rev.* **1995**, *95*, 343-379.
- [10] a) A. C. Malcolm, K. J. Sabourin, R. McDonald, M. J. Ferguson, E. Rivard, *Inorg. Chem.* **2012**, *51*, 12905-12916, b) K. J. Sabourin, A. C. Malcolm, R. McDonald, M. J. Ferguson, E. Rivard, *Dalton Trans.*, **2013**, *42*, 4625-4632; c) A. K. Swarnakar, Ch. Hering-Junghans, K. Nagata, M. J. Ferguson, R. McDonald, N. Tokitoh, E. Rivard, *Angew. Chem. Int. Ed.* **2015**, *54*, 10666-10669; *Angew. Chem.* **2015**, *127*, 10812-10816; d) Z. Mo, A. Rit, J. Campos, E. L. Kolychev, S. Aldridge, *J. Am. Chem. Soc.* **2016**, *138*, 3306-3309.
- [11] K.-C. Schwan, A. Y. Timoskin, M. Zabel, M. Scheer, *Chem. Eur. J.* **2006**, *12*, 4900-4908.
- [12] C. Marquardt, A. Adolf, A. Stauber, M. Bodensteiner, A. V. Virovets, A. Y. Timoshkin, M. Scheer, *Chem. Eur. J.* **2013**, *19*, 11887-11891.
- [13] C. Marquardt, O. Hegen, M. Hautmann, G. Balázs, M. Bodensteiner, A. V. Virovets, A. Y. Timoshkin, M. Scheer, *Angew. Chem. Int. Ed.* **2015**, *54*, 13122-13125; *Angew. Chem.* **2015**, *127*, 13315-13318.
- [14] A. B. Burg, R. I. Wagner, *J. Am. Chem. Soc.* **1953**, *75*, 3872-3877.
- [15] a) T. L. Allen, W. H. Fink, *Inorg. Chem.* **1992**, *31*, 1703-1705; b) T. L. Allen, A. C. Scheiner, H.F. Schaefer III, *Inorg. Chem.* **1990**, *29*, 1930-1936; c) M. B. Coolidge, W. T. Borden, *J. Am. Chem. Soc.* **1990**, *112*, 1704-1706.
- [16] U. Vogel, P. Hoemensch, K.-C. Schwan, A. Y. Timoshkin, M. Scheer, *Chem. Eur. J.* **2003**, *9*, 515-519.
- [17] M. Bowden, D. J. Heldebrant, A. Karkamkar, T. Proffen, G. K. Schenter, T. Autrey, *Chem. Commun.*, **2010**, *46*, 8564-8566.
- [18] H. Schmidbaur, T. Wimmer, G. Reber, G. Müller, *Angew. Chem. Int. Ed.* **1988**, *27*, *8*, 1071-1074; *Angew. Chem.* **1988**, *100*, *8*, 1135-1138.
- [19] X. Chen, J.-C. Zhao, S. G. Shore, *J. Am. Chem. Soc.* **2010**, *132*, 10658-10659.
- [20] T. Oshiki, T. Imamoto, *Bull. Chem. Soc. Jpn.* **1990**, *63*, 2846-2849.
- [21] R. Owarzany, K. J. Fijalkowski, T. Jaroń, P. J. Leszczyński, Ł. Dobrzycki, M. K. Cyrański, W. Grochala *Inorg. Chem.* **2016**, *55*, 37-45.
- [22] A. B. Burg, *Inorg. Chem.* **1978**, *17*, 593-599.
- [23] a) C. Marquardt, C. Thoms, A. Stauber, G. Balázs, M. Bodensteiner, M. Scheer, *Angew. Chem. Int. Ed.* **2014**, *53*, 3727-3730; *Angew. Chem.* **2014**, *126*, 3801-

- 3804; b) C. Marquardt, G. Balázs, J. Baumann, A. V. Virovets, M. Scheer, *Chem. Eur. J.* **2017**, 23, 11423-11429.
- [24] C. Marquardt, T. Kahoun, A. Stauber, G. Balázs, M. Bodensteiner, A. Y. Timoshkin, M. Scheer, *Angew. Chem. Int. Ed.* **2016**, 55, 14828-14832; *Angew. Chemie* **2016**, 128, 15048-15052.
- [25] See Supporting Information, Section 3.1
- [26] The formation of $(OC)_5W-PH_2BH_2SbH_2BH_2-NHC^{Me}$ was not observed in the reaction of $(OC)_5W-PH_2BH_2-SMe_2$ and $H_2SbBH_2-NHC^{Me}$, which is in accordance with computational predictions.

3.5 Supporting Information

Experimental Section: Synthetic Procedures

All manipulations were performed under an atmosphere of dry argon using standard glovebox and Schlenk techniques. All solvents are degassed and purified by standard procedures.

The compounds $R_2EBH_2 \cdot NMe_3$ ($E = P, As$; $R = H, SiMe_3$),^[1] $(OC)_5W \cdot PH_2Li$,^[2] $(Me_3Si)_2SbBH_2 \cdot NHC^{Me}$,^[3] $IH_2B \cdot SMe_2$,^[4] $IH_2B \cdot NMe_3$,^[4] $[Na]^+[H_2PBH_2PH_2]^-$,^[5] were prepared according to literature procedures.

The NMR spectra were recorded on either an Avance 400 spectrometer (1H : 400.13 MHz, ^{31}P : 161.976 MHz, ^{11}B : 128.378 MHz, $^{13}C\{^1H\}$: 100.623 MHz, ^{27}Al : 104.261 MHz) with δ [ppm] referenced to external $SiMe_4$ (1H , ^{13}C), H_3PO_4 (^{31}P), $BF_3 \cdot Et_2O$ (^{11}B), $CFCI_3$ (^{19}F) or $Al(NO_3)_3 \cdot 9 H_2O$ (^{27}Al).

IR spectra were measured on a DIGILAB (FTS 800) FT-IR spectrometer and on a Thermo Scientific Nicolet iS5. All mass spectra were recorded on a Finnigan MAT 95 (FDMS and EI-MS) and a Jeol AccuTOF GCX (LIFDI).

The C, H, N analyses were measured on an Elementar Vario EL III apparatus.

Synthesis of $IBH_2 \cdot H_2PBH_2 \cdot NMe_3$:

To a solution of 53 mg (0.50 mmol) $H_2PBH_2 \cdot NMe_3$ in 10 mL THF 0.5 mmol of $H_3B \cdot thf$ were added at r.t. and the mixture was stirred for 2 h. After removal of all volatiles under reduced pressure, the solid was dissolved in benzene and 63 mg (0.25 mmol) of I_2 were added. After stirring for 2 days all volatiles were removed under reduced

pressure and an orange oil was obtained.³¹P and ¹¹B NMR spectroscopy show a quantitative conversion to IBH₂·H₂PBH₂·NMe₃.

Spectroscopic data: ³¹P NMR (C₆D₆, 25 °C): δ = −108.7 (d, br, ¹J_{H,P} = 340 Hz). ³¹P{¹H} NMR (C₆D₆, 25 °C): δ = −108.7 (s, br). ¹¹B NMR (C₆D₆, 25 °C): δ = −36.11 (dt, ¹J_{B,P} = 63 Hz, ¹J_{B,H} = 125 Hz, BH₂l), −10.7 (dt, ¹J_{B,P} = 70 Hz, ¹J_{B,H} = 110 Hz, Me₃NBH₂). ¹¹B{¹H} NMR (C₆D₆, 25 °C): δ = −36.11 (d, ¹J_{B,P} = 63 Hz, BH₂l), −10.7 (d, ¹J_{B,P} = 70 Hz, Me₃NBH₂).

Synthesis of H₂PBH₂PH₂BH₂·NMe₃ (1):

A solution of 102 mg (0.25 mmol) [Na]⁺[H₂PBH₂PH₂][−] in 10 mL THF is added at −80°C to a solution of 22 mg (0.25 mmol) H₃B·thf and 50 mg (0.25 mmol) IH₂B·NMe₃ in THF and is stirred for 18 h. After removal of all volatiles under reduced pressure, the solid was extracted 3 times with 10 mL of *n*-hexane and filtrated over diatomaceous earth. The solution was concentrated under reduced pressure and stored at −80°C. A very small amount (~2 mg) of crystals of H₂PBH₂PH₂BH₂·NMe₃ was isolated.

Stoichiometric reaction:

To a solution of 112 mg (2mmol) NaPH₂ in 20 mL of thf 212 mg (2 mmol) H₂PBH₂·NMe₃ were added and the mixture was sonicated for 3h. The resulting [Na]⁺[H₂PBH₂PH₂][−] was added at −80°C to a solution of 400 mg (2.00 mmol) IH₂B·NMe₃ in THF and is stirred for 18 h. The ³¹P NMR spectrum of the reaction mixture showed only the decomposition products [H₂PBH₂]_{*n*} and PH₂BH₂·NMe₃.

Alternative route over IBH₂·H₂PBH₂·NMe₃:

To a solution of 28 mg (0.5 mmol) NaPH₂ in 20 mL of thf 61 mg (0.5 mmol) IBH₂·H₂PBH₂·NMe₃ were added and the mixture was stirred overnight. The ³¹P NMR spectrum of the reaction mixture showed besides small amounts of H₂PBH₂PH₂BH₂·NMe₃ mainly the decomposition products [H₂PBH₂]_{*n*} and PH₂BH₂·NMe₃.

Synthesis of (OC)₅W·PH₂BH₂·SMe₂ (2): A solution of 2.018 g (10 mmol) BH₂l·SMe₂ in 10 mL toluene is added to a suspension of 3.638 g (10 mmol) (OC)₅W·PH₂Li in 70 mL toluene dropwise under stirring at room temperature. After stirring the mixture for 3

days, the volume of the dark brown solution is reduced to a few mL. The remaining solution is filtrated into 100 mL of -80°C *n*-hexane. **2** precipitates as a brown solid. The remaining liquid is decanted off and the brown solid is dried under vacuum. **2** crystallizes as colorless blocks by storing a boiling *n*-hexane solution at 9°C .

Yield of **2**: 1.45g (34%). ^1H -NMR (C_6D_6 , 25°C): δ [ppm] = 1.01 (s, 6H, SMe_2), 2.18 (q, $^1J_{\text{H,B}} = 130$ Hz, 2H, BH_2), 2.69 (m, 2H, $^1J_{\text{H,P}} = 314$ Hz, PH_2). ^{11}B -NMR (C_6D_6 , 25°C): δ [ppm] = -17.88 (m, $^1J_{\text{H,B}} = 130$ Hz, $^1J_{\text{B,P}} = 61$ Hz, BH_2). $^{11}\text{B}\{^1\text{H}\}$ -NMR (C_6D_6 , 25°C): δ [ppm] = -17.88 (d, $^1J_{\text{B,P}} = 70$ Hz, BH_2). $^{13}\text{C}\{^1\text{H}\}$ -NMR (C_6D_6 , 25°C): δ [ppm] = 23.30 (d, $^3J_{\text{C,P}} = 5$ Hz, S-Me), 197.67 (td, $^2J_{\text{C,P}} = 6$ Hz, $^1J_{\text{C,W}} = 62$ Hz, CO_{cis}), 200.23 (m, $^2J_{\text{C,P}} = 18$ Hz, CO_{trans}). ^{31}P -NMR (C_6D_6 , 25°C): δ [ppm] = -186.1 (td, $^1J_{\text{P,H}} = 314$ Hz, $^1J_{\text{P,B}} = 70$ Hz, PH_2). $^{31}\text{P}\{^1\text{H}\}$ -NMR (C_6D_6 , 25°C): δ [ppm] = -186.1 (d, $^1J_{\text{P,B}} = 70$ Hz, PH_2). IR(KBr) : $\tilde{\nu}$ [cm^{-1}] = 2460 (w, BH), 2415 (w, BH), 2336 (w, PH), 2068 (vs, CO), 1915 (vs, CO), 1428 (m), 1332 (w), 1119 (m), 1089 (m), 1020 (m), 997 (m), 938 (vw), 772 (s), 655(vw), 595 (s), 569 (s). EI-MS (70eV): m/z = 432 (10%, $[\text{M}]^+$), 404 (5%, $[\text{M-CO}]^+$), 374 (5%, $[\text{M-2CO}]^+$), 359 (20%, $[\text{M-2CO-Me}]^+$), 344 (20%, $[\text{M-2CO-2Me}]^+$), 312 (20%, $[\text{M-2CO-SMe}_2]^+$), 300 (35%, $[(\text{CO})_3\text{W-PH}_2]^+$). Elemental analysis (%) calculated for $\text{C}_7\text{H}_{10}\text{BNO}_5\text{PSW}$ (**2**): C: 19.47, H: 2.33, S: 7.43; found: C: 19.47, H: 2.44, S: 7.40.

Synthesis of $(\text{OC})_5\text{W-PH}_2\text{BH}_2\text{P}(\text{SiMe}_3)_2\text{BH}_2\text{-NMe}_3$ (**3a**): A solution of 173 mg (0.4 mmol) of **2** in 6 mL toluene is added to a solution of 126 mg (0.5 mmol) $(\text{Me}_3\text{Si})_2\text{PBH}_2\text{-NMe}_3$ in 10 mL toluene. After stirring for 18 h, all volatiles are removed under reduced pressure. The product is extracted with 20 mL of boiling *n*-hexane. **3a** crystallizes by storing the solution at -27°C . Despite several recrystallization steps, it was not possible to obtain **3a** in analytical purity.

Yield of **3a**: 117mg (47% total; 86% purity according to ^{31}P -NMR: 105 mg, 42%). ^1H -NMR (C_6D_6 , 25°C): δ [ppm] = 0.18 (d, 18H, $^3J_{\text{H,P}} = 5$ Hz, $\text{P}(\text{SiMe}_3)_2$), 1.80 (s, 9H, NMe_3), 2.04 (m, 2H, $(\text{Me}_3\text{Si})_2\text{P-BH}_2\text{-NMe}_3$), 2.21 (m, 2H, $\text{H}_2\text{P-BH}_2\text{-P}(\text{SiMe}_3)_2$), 3.17 (m, 2H, $^1J_{\text{P,H}} = 299$ Hz, PH_2). ^{11}B -NMR (C_6D_6 , 25°C): δ [ppm] = -32.43 (m, br, $\text{PH}_2\text{-BH}_2\text{-P}(\text{SiMe}_3)_2$), -9.66 (m, $^1J_{\text{B,P}} = 56$ Hz, $(\text{Me}_3\text{Si})_2\text{P-BH}_2\text{-NMe}_3$). $^{11}\text{B}\{^1\text{H}\}$ -NMR (C_6D_6 , 25°C): δ [ppm] = -32.43 (s, br, $\text{PH}_2\text{-BH}_2\text{-P}(\text{SiMe}_3)_2$), -9.66 (d, $^1J_{\text{B,P}} = 56$ Hz, $(\text{Me}_3\text{Si})_2\text{P-BH}_2\text{-NMe}_3$). $^{13}\text{C}\{^1\text{H}\}$ -NMR (C_6D_6 , 25°C): δ [ppm] = 0.25 (d, $^2J_{\text{C,P}} = 6$ Hz, $\text{P}(\text{SiMe}_3)_2$), 52.97 (d, $^3J_{\text{C,P}} = 5$ Hz, N-Me), 198.51 (d, $^2J_{\text{C,P}} = 6$ Hz, CO_{cis}), 201.23 (d, $^2J_{\text{C,P}} = 16$ Hz,

CO_{trans}). ³¹P-NMR (C₆D₆, 25°C): δ [ppm] = -184.4 (s, br, P(SiMe₃)₂), -166.6 (t, br, ¹J_{P,H} = 299 Hz, PH₂). ³¹P{¹H}-NMR (C₆D₆, 25°C): δ [ppm] = -184.4 (s, br, P(SiMe₃)₂), -166.6 (s, br, PH₂). IR(KBr): $\tilde{\nu}$ [cm⁻¹] = 2957 (vw, CH), 2894 (vw, CH), 2432 (vw, BH), 2394 (vw, BH), 2358 (vw, PH), 2063 (m), 1970 (m, CO), 1907 (vs, CO), 1840 (m, CO), 1831 (w), 1717 (w), 1700 (w), 1684 (w), 1653 (w), 1635 (w), 1558 (w), 1540 (w), 1521 (w), 1506 (w), 1486 (w), 1465 (w), 1384 (w), 1250 (w), 1153 (vw), 1126 (w), 1083 (w), 1017 (vw), 988 (vw), 845 (m), 781 (m), 694 (vw), 598 (m), 579 (w). FD-MS (LIFDI-MS): *m/z* = 619 ([*M*]⁺). Elemental analysis (%) calculated for C₁₄H₃₃B₂NSi₂O₅P₂W (**3a**): C: 27.16, H: 5.37, N: 2.26; found: C: 26.39, H: 4.95, N: 1.62.

Synthesis of (OC)₅W·PH₂BH₂PH₂BH₂·NMe₃ (**3b**): A solution of 32 mg (0.3 mmol) H₂PBH₂·NMe₃ in 0.6 mL toluene is added to a solution of 108 mg (0.25 mmol) **2** in 15 mL toluene at room temperature. After stirring for 18 h, the volume of the dark brown solution is reduced to a few mL. The solution is added dropwise to 50 mL of *n*-hexane at -80°C. The liquid is decanted off and the precipitated solid is dried under vacuum. **3b** crystallizes as colorless needles by cooling a boiling *n*-hexane solution to room temperature.

Yield of **3b**: 65mg (55%). ¹H-NMR (C₆D₆, 25°C): δ [ppm] = 1.52 (s, 9H, NMe₃), 1.89 (m, 2H, H₂P-BH₂-PH₂), 1.99 (m, 2H, H₂P-BH₂-NMe₃), 2.99 (m, 2H, ¹J_{H,P} = 333 Hz, BH₂-PH₂-BH₂), 3.03 (m, 2H, ¹J_{H,P} = 300 Hz, (OC)₅W-PH₂-BH₂). ¹¹B-NMR (C₆D₆, 25°C): δ [ppm] = -35.58 (m, ¹J_{B,P} = 59 Hz, H₂P-BH₂-PH₂), -11.26 (m, ¹J_{B,P} = 68 Hz, H₂P-BH₂-NMe₃). ¹¹B{¹H}-NMR (C₆D₆, 25°C): δ [ppm] = -35.58 (t, ¹J_{B,P} = 59 Hz, H₂P-BH₂-PH₂), -11.26 (d, ¹J_{B,P} = 68 Hz, H₂P-BH₂-NMe₃). ¹³C{¹H}-NMR (C₆D₆, 25°C): δ [ppm] = 52.68 (d, ³J_{C,P} = 6 Hz, N-Me), 197.49 (d, ²J_{C,P} = 6 Hz, CO_{cis}), 201.04 (d, ²J_{C,P} = 16 Hz, CO_{trans}). ³¹P-NMR (C₆D₆, 25°C): δ [ppm] = -169.9 (td, br, ¹J_{P,B} = 59 Hz, ¹J_{P,H} = 300 Hz, (OC)₅W-PH₂-BH₂), -109.5 (t, br, ¹J_{P,H} = 333 Hz, H₂B-PH₂-BH₂). ³¹P{¹H}-NMR (C₆D₆, 25°C): δ [ppm] = -169.9 (m, br, ¹J_{P,B} = 59 Hz, (OC)₅W-PH₂-BH₂), -109.5 (m, br, H₂B-PH₂-BH₂). IR(KBr) : $\tilde{\nu}$ [cm⁻¹] = 2953 (vw, CH), 2428 (w, BH), 2394 (w, BH), 2346 (vw, PH), 2325 (vw, PH), 2064 (m), 1970 (s, CO), 1922 (vs, CO), 1895 (vs, CO), 1484 (w), 1467 (w), 1408 (vw), 1243 (vw), 1158 (vw), 1126 (w), 1087 (vw), 1067 (w), 1013 (vw), 977 (vw), 943 (vw), 866 (vw), 796 (vw), 754 (m), 717 (vw), 673 (vw), 631 (vw), 597 (m), 577 (m). FD-MS (70eV): *m/z* = 473 ([*M*]⁺). Elemental analysis (%) calculated for C₈H₁₇B₂NO₅P₂W (**3b**): C: 20.21, H: 3.61, N: 2.95; found: C: 20.21, H: 3.55, N: 2.88.

Synthesis of $(OC)_5W\cdot PH_2BH_2As(SiMe_3)_2BH_2\cdot NMe_3$ (**4a**): To a solution of 108 mg (0.25 mmol) of **2** in 5 mL toluene a solution of 73 mg (0.25 mmol) $(Me_3Si)_2AsBH_2\cdot NMe_3$ in 5 mL toluene is added at room temperature. After stirring the solution for 18 h, all volatiles are removed under reduced pressure. The remaining solid is dissolved in 35 mL of boiling *n*-hexane and filtrated over diatomaceous earth. **4a** crystallizes by storing the solution at $-27^\circ C$ overnight.

Yield of **4a**: 40 mg (24 %). 1H -NMR (C_6D_6 , $25^\circ C$): δ [ppm] = 0.22 (s, 18H, $SiMe_3$), 1.79 (s, 9H, NMe_3), 2.25 (m, 4H, BH_2), 3.24 (m, $^1J_{H,P}$ = 300 Hz, PH_2). ^{11}B -NMR (C_6D_6 , $25^\circ C$): δ [ppm] = -30.99 (s, br, $H_2P\text{-}\underline{B}H_2\text{-}As(SiMe_3)_2$), -8.66 (t, br, $^1J_{B,H}$ = 116 Hz, $(Me_3Si)_2As\text{-}\underline{B}H_2\text{-}NMe_3$). $^{11}B\{^1H\}$ -NMR (C_6D_6 , $25^\circ C$): δ [ppm] = -30.99 (s, br, $H_2P\text{-}\underline{B}H_2\text{-}As(SiMe_3)_2$), -8.66 (s, br, $(Me_3Si)_2As\text{-}\underline{B}H_2\text{-}NMe_3$). $^{13}C\{^1H\}$ -NMR (C_6D_6 , $25^\circ C$): δ [ppm] = 0.92 (s, $SiMe_3$), 53.15 (s, NMe_3), 198.79 (d, $^2J_{C,P}$ = 7 Hz, \underline{CO}_{cis}), 201.50 (d, $^2J_{C,P}$ = 16 Hz, CO_{trans}). ^{31}P -NMR (C_6D_6 , $25^\circ C$): δ [ppm] = -162.3 (t, br, $^1J_{P,H}$ = 300 Hz, $(OC)_5W\text{-}\underline{P}H_2\text{-}BH_2$). $^{31}P\{^1H\}$ -NMR (C_6D_6 , $25^\circ C$): δ [ppm] = -162.3 (s, br, $(OC)_5W\text{-}\underline{P}H_2\text{-}BH_2$). IR(KBr) : $\tilde{\nu}$ [cm^{-1}] = 3021 (vw), 3001 (vw), 2953 (w, CH), 2851 (vw), 2437 (w, BH), 2399 (w, BH), 2362 (w, PH), 2062 (m), 1972 (m), 1908 (vs, CO), 1485 (w), 1464 (m), 1450 (w), 1406 (vw), 1249 (w), 1163 (vw), 1119 (w), 1089 (vw), 1069 (m), 978 (w), 845 (m), 778 (m), 598 (m), 578 (w). FD-MS (LIFDI-MS): m/z = 663 ($[M]^+$). Elemental analysis (%) calculated for $C_{14}H_{33}AsB_2NO_5PSi_2W$ (**4a**): C: 25.36, H: 5.01, N: 2.11; found: C: 25.38, H: 4.99, N: 1.91.

Synthesis of $(OC)_5W\cdot PH_2BH_2AsH_2BH_2\cdot NMe_3$ (**4b**): To a solution of 216 mg (0.5 mmol) of **2** in 10 mL toluene a solution of 74 mg (0.5 mmol) $H_2AsBH_2\cdot NMe_3$ in 0.5 mL toluene is added at room temperature. After stirring the solution for 3 h, all volatiles are removed under reduced pressure. The remaining solid is suspended in 20 mL *n*-hexane. 2 to 3 mL CH_2Cl_2 are added dropwise, until a clear solution with a small amount of a brown solid is obtained (too much CH_2Cl_2 leads to the dissolving of the impurity). The solution is decanted off and stored at $-27^\circ C$ overnight. **4b** crystallizes as colorless blocks.

Yield of **4b**: 140 mg (54 %). 1H -NMR (C_6D_6 , $25^\circ C$): δ [ppm] = 1.56 (s, 9H, NMe_3), 2.07 (m, 2H, AsH_2), 2.21 (m, 4H, BH_2), 3.13 (m, $^1J_{H,P}$ = 303 Hz, PH_2). ^{11}B -NMR (C_6D_6 , $25^\circ C$):

δ [ppm] = -32.02 (m, br, $^1J_{B,P}$ = 76 Hz, $H_2P-BH_2-AsH_2$), -9.30 (t, br, $^1J_{B,H}$ = 115 Hz, $H_2As-BH_2-NMe_3$). $^{11}B\{^1H\}$ -NMR (C_6D_6 , 25°C): δ [ppm] = -32.02 (d, br, $^1J_{B,P}$ = 76 Hz, $H_2P-BH_2-AsH_2$), -9.30 (s, br, $H_2As-BH_2-NMe_3$). $^{13}C\{^1H\}$ -NMR (C_6D_6 , 25°C): δ [ppm] = 52.75 (s, NMe_3), 198.44 (td, $^1J_{C,W}$ = 63 Hz, $^2J_{C,P}$ = 7 Hz, \underline{CO}_{cis}), 201.19 (d, $^2J_{C,P}$ = 17 Hz, \underline{CO}_{trans}). ^{31}P -NMR (C_6D_6 , 25°C): δ [ppm] = -166.5 (td, br, $^1J_{P,H}$ = 303 Hz, $^1J_{P,B}$ = 76 Hz, $(OC)_5W-PH_2-BH_2$). $^{31}P\{^1H\}$ -NMR (C_6D_6 , 25°C): δ [ppm] = -166.5 (d, br, $^1J_{P,B}$ = 76 Hz, $(OC)_5W-PH_2-BH_2$). IR(KBr): $\tilde{\nu}$ [cm^{-1}] = 3003(vw), 2953 (vw, CH), 2927 (vw), 2469 (w, BH), 2435 (w, BH), 2361 (w, PH), 2338 (w, PH), 2180 (vw, AsH) 2064 (m), 1903 (vs, CO), 1473 (w), 1465 (w), 1407 (vw), 1241 (w), 1159 (w), 1123 (w), 1077 (m), 1004 (vw), 997 (vw), 986 (vw), 948 (vw), 862 (w), 785 (w), 724 (vw), 675 (m), 595 (m), 575 (m). FD-MS (70eV): m/z = 517 ($[M]^+$). Elemental analysis (%) calculated for $C_8H_{17}B_2NO_5PAsW$ (**4b**): C: 18.50, H: 3.30, N: 2.70; found: C: 18.66, H: 3.27, N: 2.64.

Synthesis of $(OC)_5W-PH_2BH_2Sb(SiMe_3)_2BH_2-NHC^{Me}$ (**5**): To a solution of 101 mg (0.25 mmol) $(Me_3Si)_2SbBH_2-NHC^{Me}$ in 7 mL toluene a solution of 108 mg (0.25 mmol) **2** in 7 mL toluene is added at room temperature. After stirring for 3 h, all volatiles are removed under reduced pressure. The remaining brown oil is suspended in 20 mL *n*-hexane. 2 to 3 mL CH_2Cl_2 are added dropwise, until a clear solution with less brown oil is obtained (too much CH_2Cl_2 leads to the dissolving of the impurity). The solution is decanted off and stored at -80°C overnight. Crystals of **5** are obtained as yellow plates.

Yield of **5**: 70 mg (33 %). 1H -NMR (C_6D_6 , 25°C): δ [ppm] = 0.37 (s, 18 H, $Sb(SiMe_3)_2$), 1.35 (s, 6H, C-CH₃), 2.17 (m, 4H, BH₂), 2.67 (m, $^1J_{H,P}$ = 302 Hz, PH₂), 2.93 (s, 6H, N-CH₃). ^{11}B -NMR (C_6D_6 , 25°C): δ [ppm] = -38.36 (m, br, $(Me_3Si)_2Sb-BH_2-NHC^{Me}$), -36.57 (m, br, $H_2P-BH_2-Sb(SiMe_3)_2$). $^{11}B\{^1H\}$ -NMR (C_6D_6 , 25°C): δ [ppm] = -38.36 (m, br, $(Me_3Si)_2Sb-BH_2-NHC^{Me}$), -36.57 (m, br, $H_2P-BH_2-Sb(SiMe_3)_2$). $^{13}C\{^1H\}$ -NMR (C_6D_6 , 25°C): δ [ppm] = 2.01 (s, $SiMe_3$), 7.98 (s, C-CH₃), 32.10 (s, N-CH₃), 124.70 (s, C=C), 198.95 (td, $^1J_{C,W}$ = 63 Hz, $^2J_{C,P}$ = 7 Hz, \underline{CO}_{cis}), 201.83 (d, $^2J_{C,P}$ = 16 Hz, \underline{CO}_{trans}). ^{31}P -NMR (C_6D_6 , 25°C): δ [ppm] = -158.4 (m, br, $^1J_{P,H}$ = 302 Hz, $(OC)_5W-PH_2-BH_2$). $^{31}P\{^1H\}$ -NMR (C_6D_6 , 25°C): δ [ppm] = -158.4 (s, br, $(OC)_5W-PH_2-BH_2$). IR(KBr) : $\tilde{\nu}$ [cm^{-1}] = 2957 (w, CH), 2897 (vw), 2424 (w, BH), 2403 (w, BH), 2317 (w, PH), 2062 (m), 1974 (s), 1910 (vs, CO), 1889 (vs, CO), 1652 (w), 1578 (vw), 1474 (w), 1441 (w), 1397 (vw), 1373 (vw), 1338 (vw), 1245 (w), 1164 (vw), 1081 (w), 1065 (vw), 1016 (vw), 979

(vw), 963 (vw), 935 (w), 884 (w), 839 (m), 775 (m), 697 (w), 6290 (w), 598 (m), 578 (m). LIFDI-MS: m/z = 774 ($[M]^+$). Elemental analysis (%) calculated for $C_{18}H_{36}B_2N_2O_5PSbSi_2W$ (**5**): C: 27.90, H: 4.69, N: 3.62; found: C: 27.83, H: 4.51, N: 3.58

Experimental Section: X-ray Diffraction analysis and details of the crystal structure solution and refinement

The X-ray diffraction experiments were performed on either an Agilent Gemini R Ultra diffractometer with Cu- $K\alpha$ radiation (λ = 1.54178 Å) (**3a**, **3b**, **4b**) and Mo radiation (λ = 0.71073 Å) (**2**) or a GV50 diffractometer with TitanS2 detector (**1c**, **4a**, **5**) from Rigaku Oxford Diffraction (formerly Agilent Technologies) applying Cu- $K\alpha$ radiation (λ = 1.54178 Å). The measurements were performed at 123 K. Crystallographic data together with the details of the experiments are given below. Absorption corrections were applied semi-empirically from equivalent reflections or analytically (SCALE3/ABSPACK algorithm implemented in CrysAlisPro software by Rigaku Oxford Diffraction).^[6]

All structures were solved using SIR97^[7], SHELXT^[8] and OLEX.^[9] Least square refinements against F^2 in anisotropic approximation were done using SHELXL.^[8]

The hydrogen positions of the methyl groups were located geometrically and refined riding on the carbon atoms. Hydrogen atoms belonging to BH₂, PH₂ and AsH₂ groups were located from the difference Fourier map and refined without constraints (**1**, **3a**, **3b**, **4a**, **4b**, **5**) or with restrained E–H distances (**2**). All crystals of **2** showed twinning, they were refined applying hklf5 refinement.

CCDC reference numbers 1563260 (**1**), 1563261 (**2**), 1563262 (**3a**), 1563263 (**3b**), 1563264 (**4a**), 1563265 (**4b**), and 1563266 (**5**) contain the supplementary crystallographic data, which can be obtained free of charge at www.ccdc.cam.ac.uk/conts/retrieving.html or from the Cambridge Crystallographic Data Center, 12 Union Road, Cambridge CB2 1EZ, UK; Fax: (internat.) + 44-1223-336-033; E-mail: deposit@ccdc.cam.ac.uk

Crystal Structures

H₂PBH₂PH₂BH₂·NMe₃: **1** crystallizes from a concentrated *n*-hexane solution at -80°C in the monoclinic space group *P*2₁/*n*. Figure S1 shows the structure of **1** in the solid state.

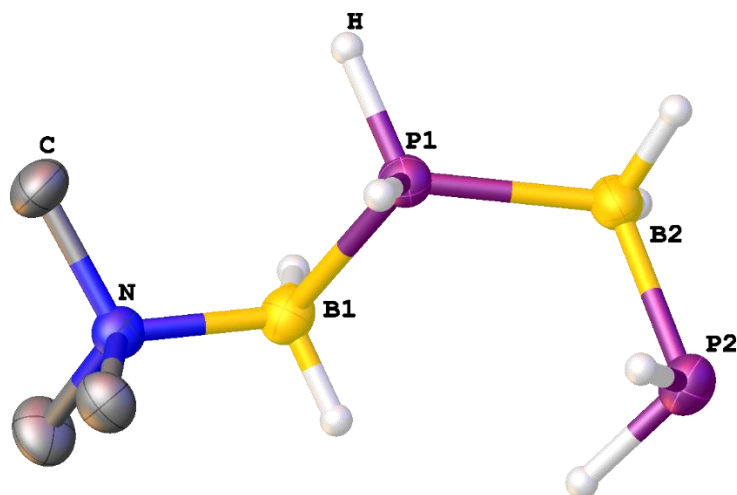


Figure S1: Molecular structure of **1** in the solid state. Hydrogen atoms bonded to carbon are omitted for clarity. Thermal ellipsoids are drawn with 50% probability. Selected bond lengths [Å] and angles [°]: P1–B1 1.954(2), P1–B2 1.947(2), P2–B2 1.967(3), N1–B1 1.601(3), B2–P1–B1 112.84(10), N1–B1–P1 115.39(13), P1–B2–P2 109.85(12).

(OC)₅W·PH₂BH₂·SMe₂: **2** crystallizes from cooling a boiling *n*-hexane solution to 6°C as colorless blocks in the monoclinic space group *P*2₁/*c*. Figure S2 shows the structure of **2** in the solid state.

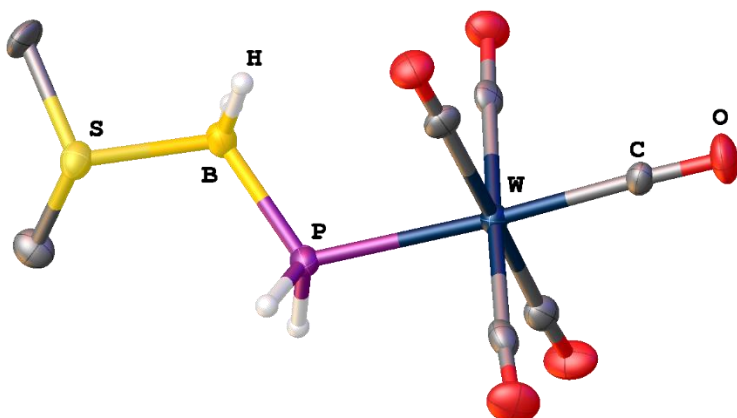


Figure S2: Molecular structure of **2** in the solid state. Hydrogen atoms bonded to carbon are omitted for clarity. Thermal ellipsoids are drawn with 50% probability. Selected bond lengths [Å] and angles [°]: W–P 2.541(3), P–B 1.942(11), B–S 1.920(12), B–P–W 113.3(4), P–B–S 113.2(5).

(OC)₅W·PH₂BH₂P(SiMe₃)₂BH₂·NMe₃: **3a** crystallizes from cooling a boiling *n*-hexane solution to -27°C as colorless blocks in the triclinic space group $P\bar{1}$. Figure S4 shows the structure of **3a** in the solid state.

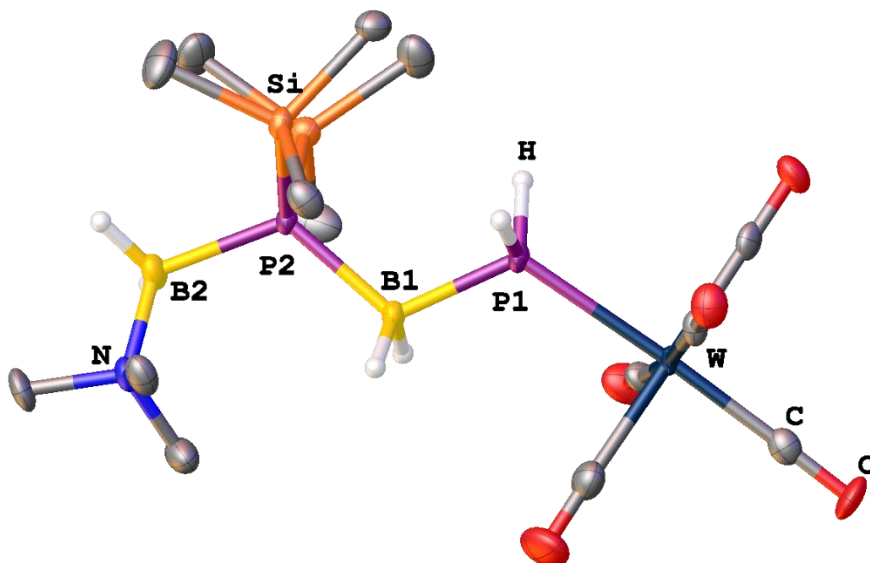


Figure S3: Molecular structure of **3a** in the solid state. Hydrogen atoms bonded to carbon are omitted for clarity. Thermal ellipsoids are drawn with 50% probability. Selected bond lengths [Å] and angles [°]: W-P1 2.532(1), P1-B1 1.958(4), B1-P2 1.981(4), P2-B2 2.001(4), B2-N 1.606(5), W-P1-B1 119.6(1), P1-B1-P2 114.4(2), B1-P2-B2 117.9 (2).

(OC)₅W·PH₂BH₂PH₂BH₂·NMe₃: **3b** crystallizes as colorless needles by cooling a boiling *n*-hexane solution to room temperature in the monoclinic space group $P2_1/n$. Figure S3 shows the structure of **3b** in the solid state.

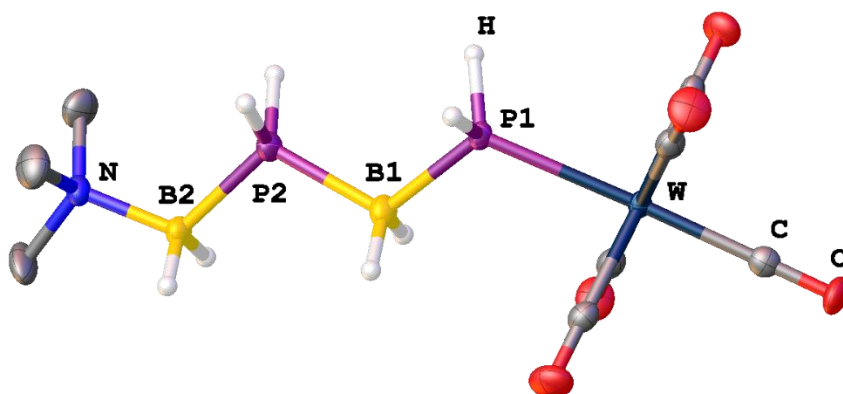


Figure S4: Molecular structure of **3b** in the solid state. Hydrogen atoms bonded to carbon are omitted for clarity. Thermal ellipsoids are drawn with 50% probability. Selected bond lengths [Å] and angles [°]: W-P1 2.534(1), P1-B1 1.945(4), B1-P2 1.939(5), P2-B2 1.952(4), B2-N 1.595(5), B1-P1-W 115.9(1), P2-B1-P1 114.3(2), B2-P2-B1 109.5(2), N-B2-P2 115.8(3).

(OC)₅W·PH₂BH₂As(SiMe₃)₂BH₂·NMe₃: **4a** crystallizes by cooling a boiling *n*-hexane solution to -27°C as colorless needles in the triclinic space group $P\bar{1}$. Figure S5 shows the structure of **4a** in the solid state.

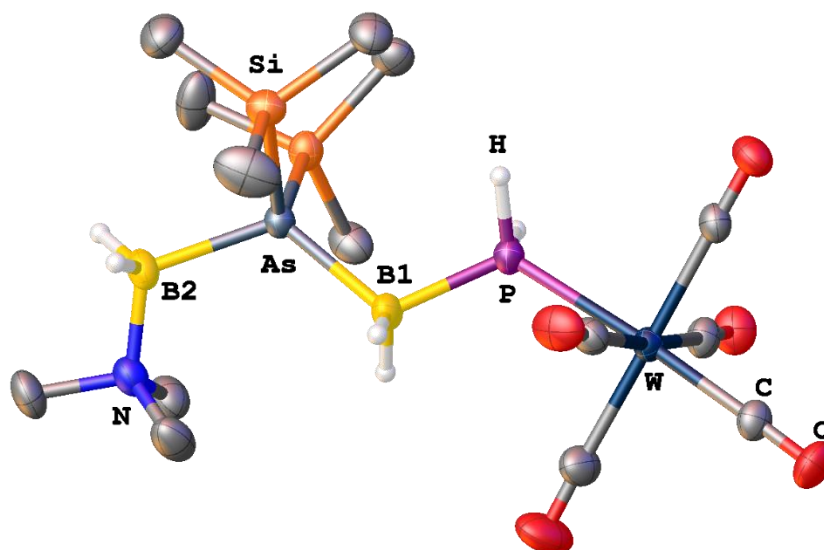


Figure S5: Molecular structure of **4a** in the solid state. Hydrogen atoms bonded to carbon are omitted for clarity. Thermal ellipsoids are drawn with 50% probability. Selected bond lengths [Å] and angles [°]: P-B1 1.947(4), B1-As 2.094(4), As-B2 2.105(4), B1-P-W 118.9(1), As-B1-P 113.2(2), B2-As-B1 118.9(2).

(OC)₅W·PH₂BH₂AsH₂BH₂·NMe₃: **4b** crystallizes from a solution of *n*-hexane and CH₂Cl₂ at -28°C as colorless blocks in the orthorhombic space group $P2_12_12_1$. Figure S6 shows the molecular structure of **4b** in the solid state.

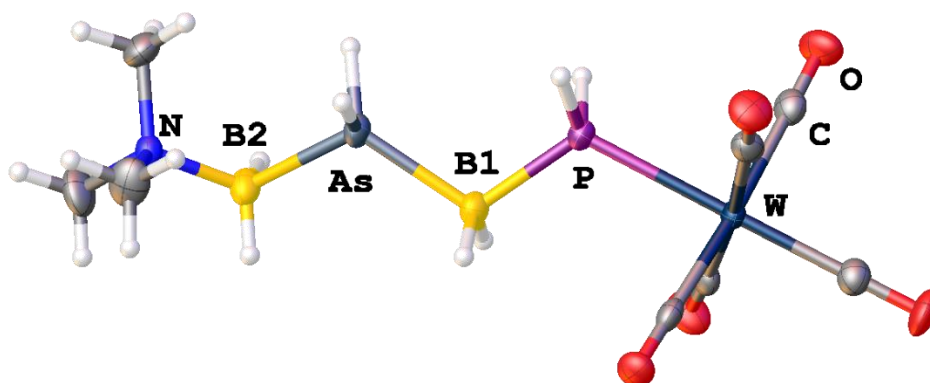


Figure S6: Molecular structure of **4b** in the solid state. Hydrogen atoms bonded to carbon are omitted for clarity. Thermal ellipsoids are drawn with 50% probability. Selected bond lengths [Å] and angles [°]: P-B2 1.939(7), B2-As 2.059(6), As-B1 2.076(8), B1-P-W 118.6(2), As-B1-P 111.6(3), B2-As-B1 116.1(3).

$(OC)_5W \cdot PH_2BH_2Sb(SiMe_3)_2BH_2 \cdot NHC^{Me}$: **5** crystallizes from a solution of *n*-hexane and CH_2Cl_2 at $-80^\circ C$ as yellow plates in the triclinic space group $P\bar{1}$. Figure S7 shows the molecular structure of **5** in the solid state.

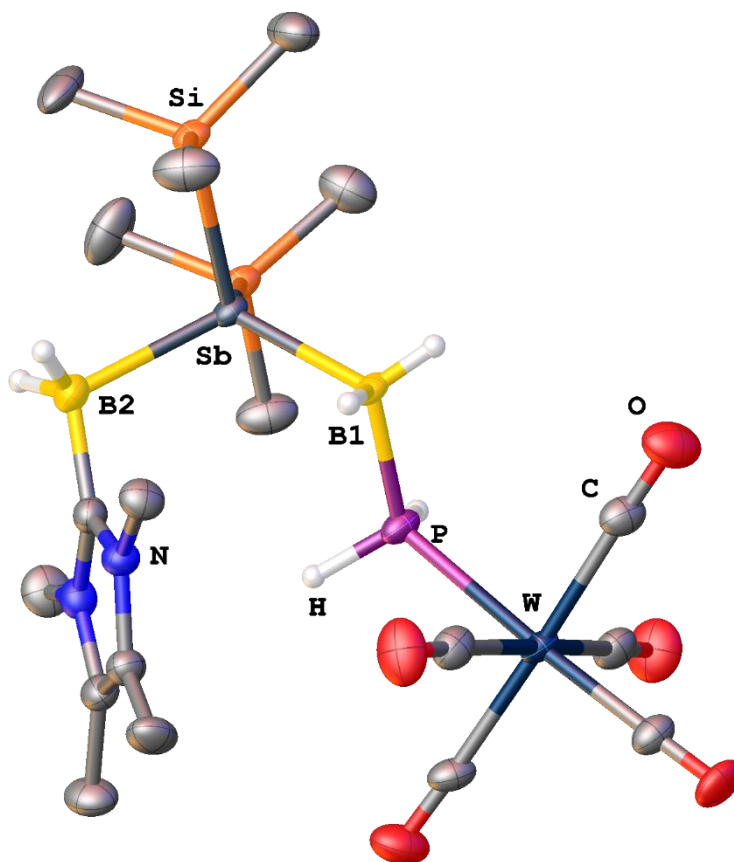


Figure S7: Molecular structure of **5** in the solid state. Hydrogen atoms bonded to carbon are omitted for clarity. Thermal ellipsoids are drawn with 50% probability. Selected bond lengths [Å] and angles [°]: P-B1 1.945(4), B1-Sb 2.259(4), Sb-B2 2.301(4), B1-P-W 120.5(1), Sb-B1-P 117.8(2), B2-Sb-B1 114.6(2).

Crystallographic Information:**Table S1:** Crystallographic data for compounds **1** and **2**

	1	2
Empirical formula	C ₃ H ₁₇ B ₂ NP ₂	C ₇ H ₁₀ BO ₅ PSW
Formula weight	150.73	431.84
Crystal	colourless plate	colourless blocks
Crystal size/mm ³	0.16 × 0.07 × 0.05	0.3072 × 0.1473 × 0.1336
Temperature/K	123.00(14)	123.00(14)
Crystal system	monoclinic	monoclinic
Space group	P2 ₁ /n	P2 ₁ /c
Unit cell dimensions	<i>a</i> = 10.2429(4) Å <i>b</i> = 9.2237(3) Å <i>c</i> = 11.0740(5) Å α = 90° β = 113.455(5)° γ = 90°	<i>a</i> = 9.3344(7) Å <i>b</i> = 12.2815(16) Å <i>c</i> = 11.7623(13) Å α = 90° β = 92.935(8)° γ = 90°
Volume <i>V</i>	959.79(7) Å ³	1346.7(3) Å ³
Formula units <i>Z</i>	4	4
Absorption coefficient μ	3.458 mm ⁻¹	8.851 mm ⁻¹
Density ρ_{calc}	1.043 g/cm ³	2.130 g/cm ³
<i>F</i> (000)	328.0	808.0
Theta range $\theta_{\text{min}}/\theta_{\text{max}}$	9.958°/146.818°	6.61°/58.36°
Absorption correction	analytical	gaussian
Index ranges	-11 ≤ <i>h</i> ≤ 12 -10 ≤ <i>k</i> ≤ 11 -13 ≤ <i>l</i> ≤ 5	-12 ≤ <i>h</i> ≤ 12 -16 ≤ <i>k</i> ≤ 16 -15 ≤ <i>l</i> ≤ 13
Reflections collected	3230	5214
Independent reflections	1851 [<i>R</i> _{sigma} = 0.0396]	5214 [<i>R</i> _{sigma} = 0.0525]
Completeness to full θ	0.998	0.997
Transmission <i>T</i> _{min} / <i>T</i> _{max}	0.712 / 0.849	0.228/0.307
Data/restraints/parameters	1851/0/108	5214/4/157
Goodness-of-fit on <i>F</i> ²	1.068	1.008
Final <i>R</i> -values [<i>I</i> ≥ 2σ (<i>I</i>)]	<i>R</i> ₁ = 0.0453, <i>wR</i> ₂ = 0.1234	<i>R</i> ₁ = 0.0474, <i>wR</i> ₂ = 0.1314
Final <i>R</i> -values [all data]	<i>R</i> ₁ = 0.0509, <i>wR</i> ₂ = 0.1327	<i>R</i> ₁ = 0.0579, <i>wR</i> ₂ = 0.1343
Largest difference hole and peak $\Delta\rho$	-0.35, 0.53 e Å ⁻³	-2.24, 2.26 e Å ⁻³

Table S2: Crystallographic data for compounds **3a** and **3b**

	3a	3b
Empirical formula	C ₁₄ H ₃₃ B ₂ NO ₅ P ₂ Si ₂ W	C ₈ H ₁₇ B ₂ NO ₅ P ₂ W
Formula weight	619.00	474.63
Crystal	colourless blocks	colourless needles
Crystal size/mm ³	0.462 × 0.24 × 0.113	0.2106 × 0.1749 × 0.0979
Temperature/K	123.00(14)	123.05(10)
Crystal system	triclinic	monoclinic
Space group	P-1	P2 ₁ /n
Unit cell dimensions	<i>a</i> = 9.7353(4) <i>b</i> = 12.0520(7) <i>c</i> = 12.5967(6) α = 77.571(5) β = 68.712(4) γ = 86.662(4)	<i>a</i> = 6.45587(10) Å <i>b</i> = 26.5981(4) Å <i>c</i> = 9.82438(16) Å α = 90° β = 94.5064(15)° γ = 90°
Volume <i>V</i>	1344.52(12)	1681.77(5) Å ³
Formula units <i>Z</i>	2	4
Absorption coefficient μ	10.124 mm ⁻¹	14.643 mm ⁻¹
Density ρ_{calc}	1.529 g/cm ³	1.875 g/cm ³
<i>F</i> (000)	612.0	904.0
Theta range $\theta_{\text{min}}/\theta_{\text{max}}$	7.514°/132.896°	9.624°/133.426°
Absorption correction	analytical	gaussian
Index ranges	-11 ≤ <i>h</i> ≤ 11 -14 ≤ <i>k</i> ≤ 13 -14 ≤ <i>l</i> ≤ 14	-6 ≤ <i>h</i> ≤ 7 -28 ≤ <i>k</i> ≤ 31 -11 ≤ <i>l</i> ≤ 11
Reflections collected	28384	9099
Independent reflections	4697 [<i>R</i> _{int} = 0.0768]	2982 [<i>R</i> _{int} = 0.0308]
Completeness to full θ	0.993	0.991
Transmission <i>T</i> _{min} / <i>T</i> _{max}	0.103/0.319	0.150/0.391
Data/restraints/parameters	4697/0/277	2982/0/207
Goodness-of-fit on <i>F</i> ²	1.105	1.172
Final <i>R</i> -values [<i>I</i> ≥ 2σ (<i>I</i>)]	<i>R</i> ₁ = 0.0285 <i>wR</i> ₂ = 0.0708	<i>R</i> ₁ = 0.0215 <i>wR</i> ₂ = 0.0569
Final <i>R</i> -values [all data]	<i>R</i> ₁ = 0.0288 <i>wR</i> ₂ = 0.0711	<i>R</i> ₁ = 0.0236 <i>wR</i> ₂ = 0.0579
Largest difference hole and peak $\Delta\rho$	-1.55, 1.14 e Å ⁻³	-0.81, 0.52 e Å ⁻³

Table S3: Crystallographic data for compounds **4a** and **4b**

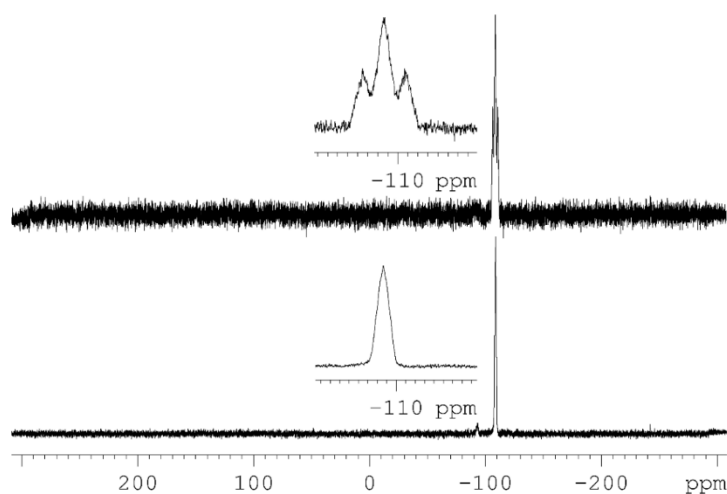
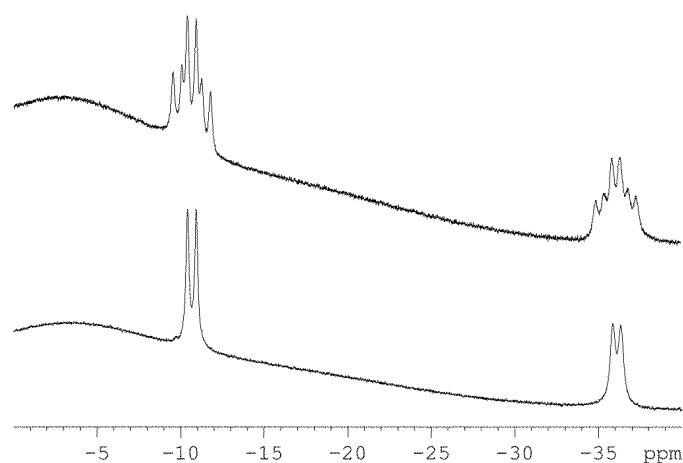
	4a	4b
Empirical formula	C ₁₄ H ₃₃ AsB ₂ NO ₅ PSi ₂ W	C ₈ H ₁₇ AsB ₂ NO ₅ PW
Formula weight	662.95	518.58
Crystal	colourless needles	colourless blocks
Crystal size/mm ³	0.332 × 0.049 × 0.03	0.082 × 0.079 × 0.052
Temperature/K	123.00(10)	122.8(6)
Crystal system	triclinic	orthorhombic
Space group	P-1	P2 ₁ 2 ₁ 2 ₁
Unit cell dimensions	<i>a</i> = 9.7841(5) Å <i>b</i> = 12.1362(4) Å <i>c</i> = 12.6935(5) Å α = 77.366(3)° β = 68.592(4)° γ = 86.189(4)°	<i>a</i> = 10.0490(2) Å <i>b</i> = 10.78818(19) Å <i>c</i> = 15.6134(3) Å α = 90° β = 90° γ = 90°
Volume <i>V</i>	1369.13(11) Å ³	1692.66(5) Å ³
Formula units <i>Z</i>	2	4
Absorption coefficient μ	10.732 mm ⁻¹	15.827 mm ⁻¹
Density ρ_{calc}	1.608 g/cm ³	2.035 g/cm ³
<i>F</i> (000)	648.0	976.0
Theta range $\theta_{\text{min}}/\theta_{\text{max}}$	7.466°/148.338°	9.966°/133.24°
Absorption correction	multi-scan	gaussian
Index ranges	-11 ≤ <i>h</i> ≤ 12 -14 ≤ <i>k</i> ≤ 15 -15 ≤ <i>l</i> ≤ 15	-11 ≤ <i>h</i> ≤ 11 -12 ≤ <i>k</i> ≤ 11 -18 ≤ <i>l</i> ≤ 18
Reflections collected	21586	14040
Independent reflections	5425 [<i>R</i> _{int} = 0.0391]	2964 [<i>R</i> _{int} = 0.0314]
Completeness to full θ	0.999	0.999
Transmission <i>T</i> _{min} / <i>T</i> _{max}	0.393/1.000	0.391/0.541
Data/restraints/parameters	5425/0/277	2964/0/207
Goodness-of-fit on <i>F</i> ²	1.075	0.990
Final <i>R</i> -values [<i>I</i> ≥ 2σ (<i>I</i>)]	<i>R</i> ₁ = 0.0270, <i>wR</i> ₂ = 0.0722	<i>R</i> ₁ = 0.0190, <i>wR</i> ₂ = 0.0434
Final <i>R</i> -values [all data]	<i>R</i> ₁ = 0.0281, <i>wR</i> ₂ = 0.0731	<i>R</i> ₁ = 0.0204, <i>wR</i> ₂ = 0.0437
Largest difference hole and peak $\Delta\rho$	-1.26 1.02 e Å ⁻³	-0.40 1.56 e Å ⁻³

Table S4: Crystallographic data for compound **5**

5	
Empirical formula	C ₁₈ H ₃₆ B ₂ N ₂ O ₅ PSbSi ₂ W
Formula weight	774.86
Crystal	yellow plates
Crystal size/mm ³	0.293 × 0.187 × 0.093
Temperature/K	123.2(6)
Crystal system	triclinic
Space group	P-1
Unit cell dimensions	<i>a</i> = 11.9817(4) <i>b</i> = 12.6685(2) <i>c</i> = 12.8127(3) α = 107.8051(18) β = 113.066(3) γ = 105.879(2)
Volume <i>V</i>	1522.17(7) Å ³
Formula units <i>Z</i>	2
Absorption coefficient μ	15.401 mm ⁻¹
Density ρ_{calc}	1.691 g/cm ³
<i>F</i> (000)	752.0
Theta range $\theta_{\text{min}}/\theta_{\text{max}}$	8.204°/148.556°
Absorption correction	analytical
Index ranges	-13 ≤ <i>h</i> ≤ 14 -15 ≤ <i>k</i> ≤ 14 -12 ≤ <i>l</i> ≤ 15
Reflections collected	12491
Independent reflections	5889 [<i>R</i> _{int} = 0.0336]
Completeness to full θ	0.988
Transmission <i>T</i> _{min} / <i>T</i> _{max}	0.115/0.437
Data/restraints/parameters	5889/0/323
Goodness-of-fit on <i>F</i> ²	1.056
Final <i>R</i> -values [<i>I</i> ≥ 2σ (<i>I</i>)]	<i>R</i> ₁ = 0.0325, <i>wR</i> ₂ = 0.0854
Final <i>R</i> -values [all data]	<i>R</i> ₁ = 0.0333, <i>wR</i> ₂ = 0.0864
Largest difference hole and peak $\Delta\rho$	-2.40 1.43 e Å ⁻³

NMR spectroscopy:**Table S5:** NMR parameters of compounds **2-5**

Compound	^{31}P [ppm] (OC) $_5$ W-PH $_2$	^{11}B [ppm] BH $_2$	^{31}P [ppm] ER $_2$	^{11}B [ppm] H $_2$ B-LB
2	-186.1	-17.9	/	/
3a	-166.6	-32.4	-184.4	-9.7
3b	-169.9	-35.6	-109.5	-11.3
4a	-162.3	-31.0	/	-8.7
4b	-166.5	-32.0	/	-9.3
5	-158.4	-36.6	/	-38.4

IH $_2$ B·PH $_2$ BH $_2$ ·NMe $_3$:**Figure S8:** ^{31}P (top) and $^{31}\text{P}\{^1\text{H}\}$ NMR spectrum (bottom) of IH $_2$ B·PH $_2$ BH $_2$ ·NMe $_3$ in C $_6$ D $_6$.**Figure S9:** ^{11}B NMR (top) and $^{11}\text{B}\{^1\text{H}\}$ spectrum (bottom) of IH $_2$ B·PH $_2$ BH $_2$ ·NMe $_3$ in C $_6$ D $_6$.

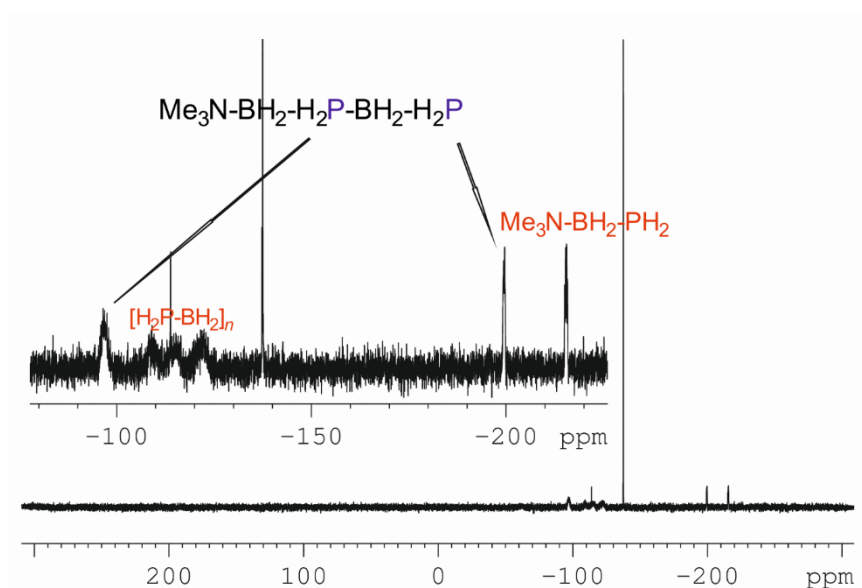
H₂PBH₂PH₂BH₂·NMe₃ (1):

Figure S10: $^{31}\text{P}\{^1\text{H}\}$ NMR of $\text{H}_2\text{PBH}_2\text{PH}_2\text{BH}_2\cdot\text{NMe}_3$ in C_6D_6 at 300K. The signals at $\delta = -215$ ppm and at $\delta = -107$ - -125 ppm, respectively are attributed to the decomposition products $\text{H}_2\text{PBH}_2\cdot\text{NMe}_3$ and polymeric $[\text{BH}_2\text{PH}_2]_n$. The signal at $\delta = -200$ ppm is tentatively assigned to the terminal PH_2 group and the one at $\delta = -97$ ppm to the Me_3NBH_2 -bond PH_2 group.

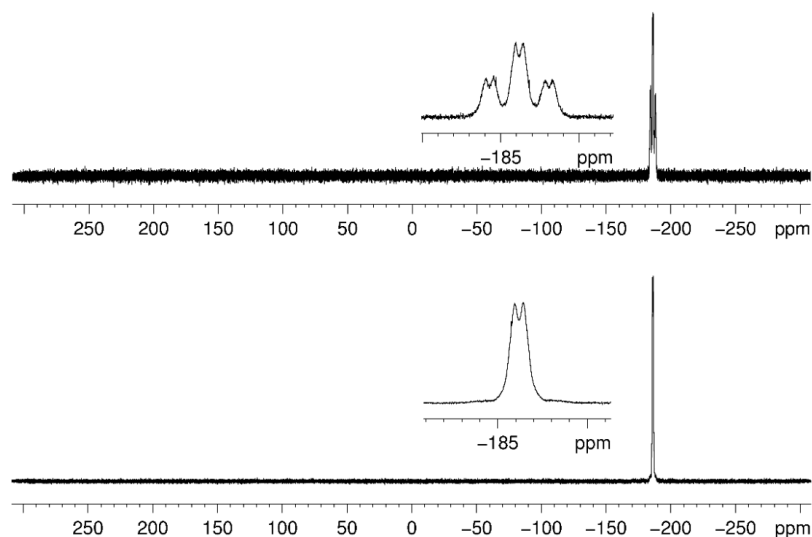
(OC)₅W·PH₂BH₂·SMe₂ (2):

Figure S11: ^{31}P (top) and $^{31}\text{P}\{^1\text{H}\}$ NMR spectrum (bottom) of **2** in C_6D_6

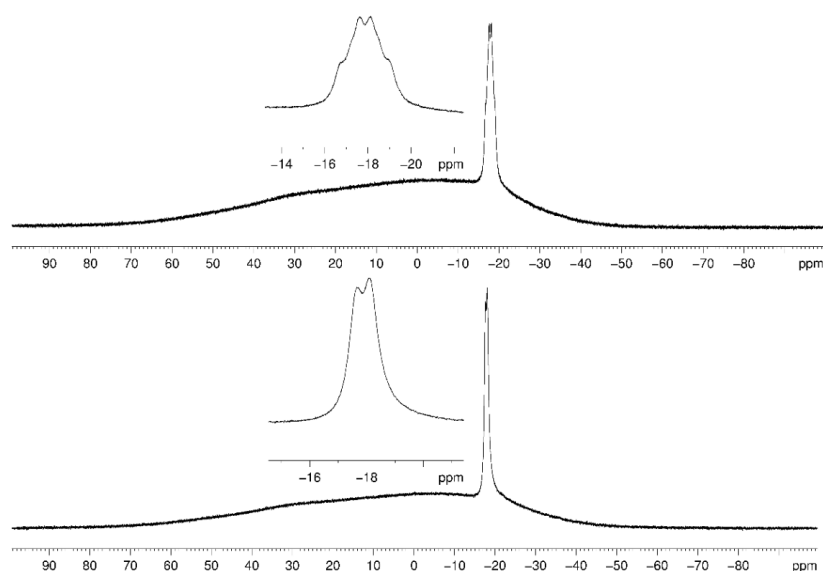


Figure S12: $^{11}\text{B}\{^1\text{H}\}$ (top) and ^{11}B NMR spectrum (bottom) of **2** in C_6D_6

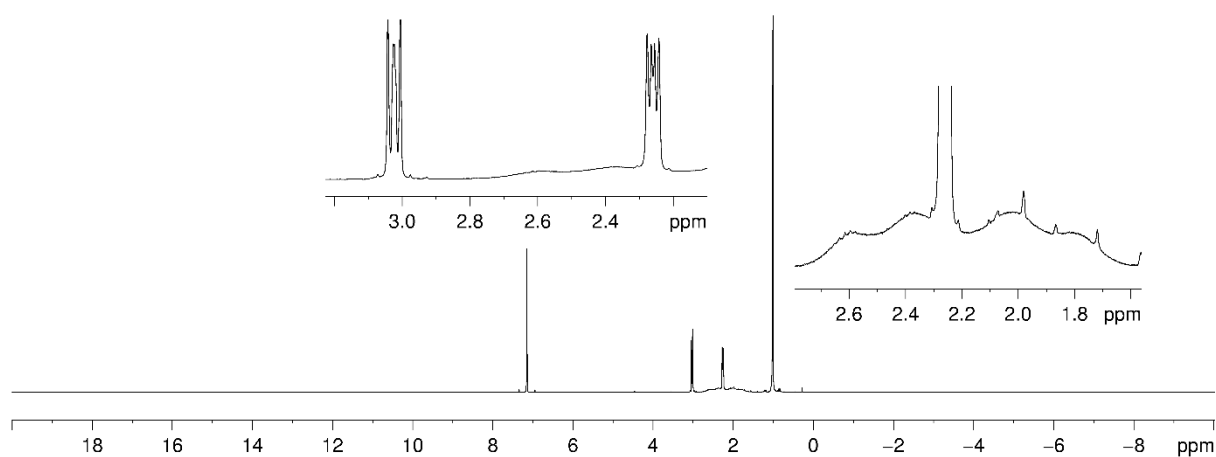


Figure S13: ^1H NMR spectrum of **2** in C_6D_6

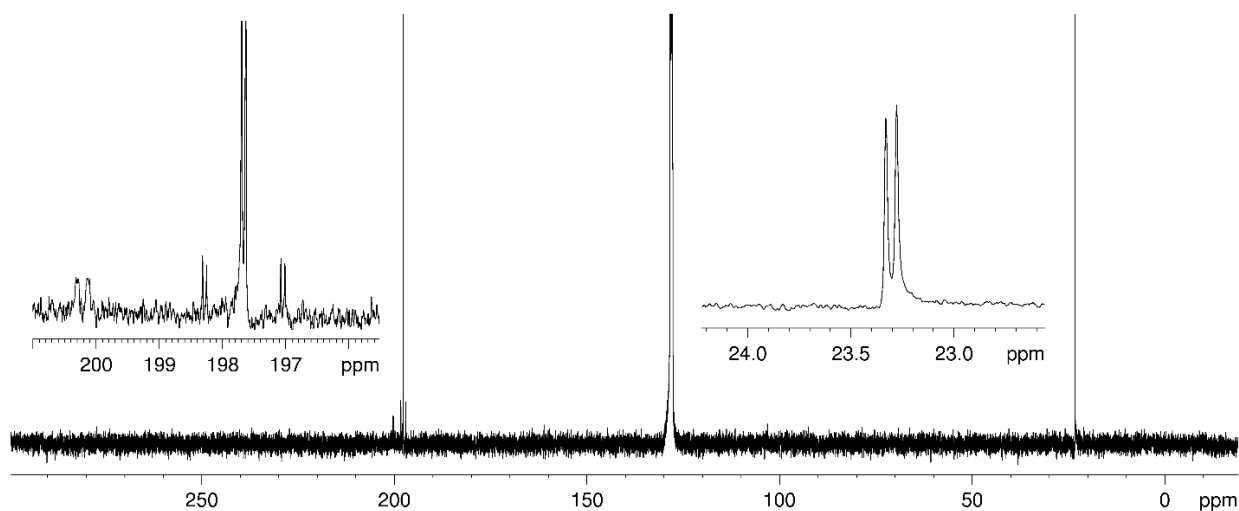


Figure S14: $^{13}\text{C}\{^1\text{H}\}$ NMR spectrum of **2** in C_6D_6

$(\text{OC})_5\text{W}\cdot\text{PH}_2\text{BH}_2\text{P}(\text{SiMe}_3)_2\text{BH}_2\cdot\text{NMe}_3$ (**3a**):

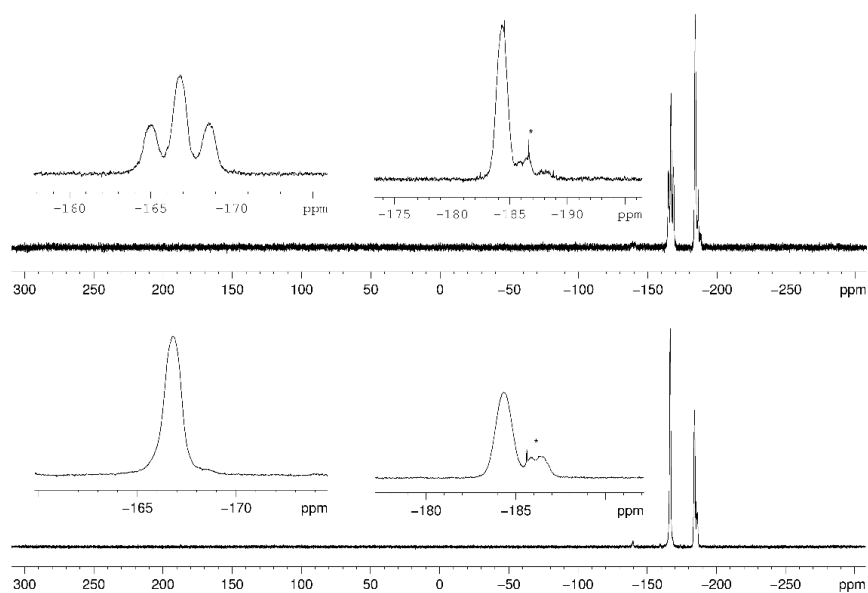


Figure S15: ^{31}P (top) and $^{31}\text{P}\{^1\text{H}\}$ NMR spectrum (bottom) of **3a** in C_6D_6 (* = 1).

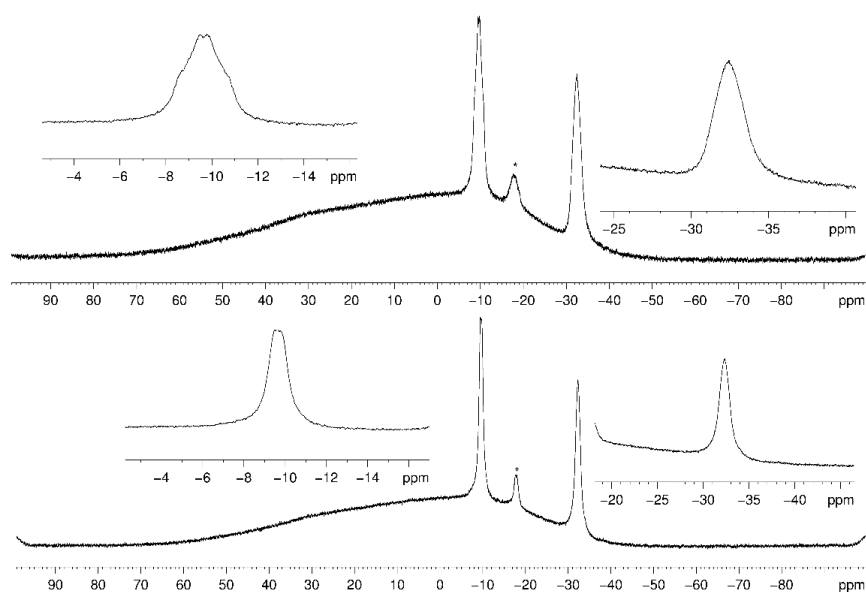


Figure S16: ^{11}B (top) and $^{11}B\{^1H\}$ NMR spectrum (bottom) of **3a** in C_6D_6 (* = 1).

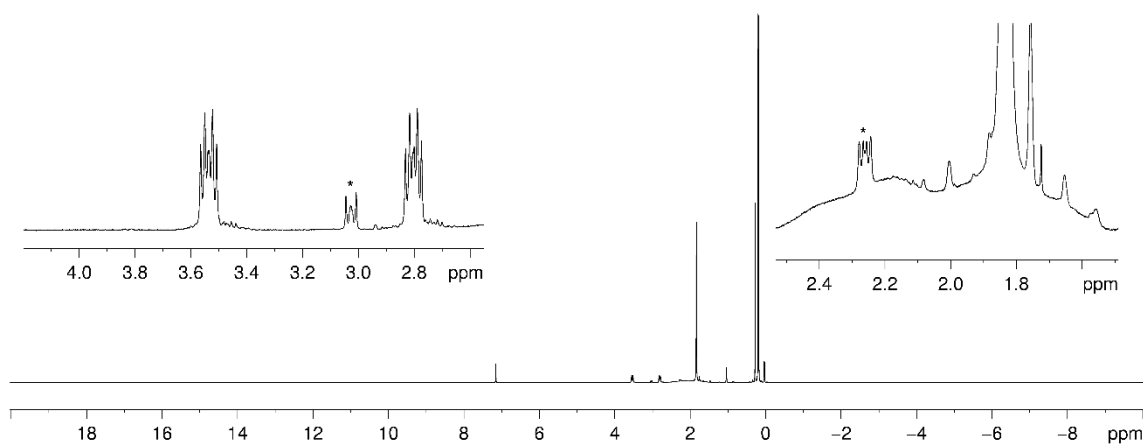


Figure S17: 1H NMR spectrum of **3a** in C_6D_6 (* = 1).

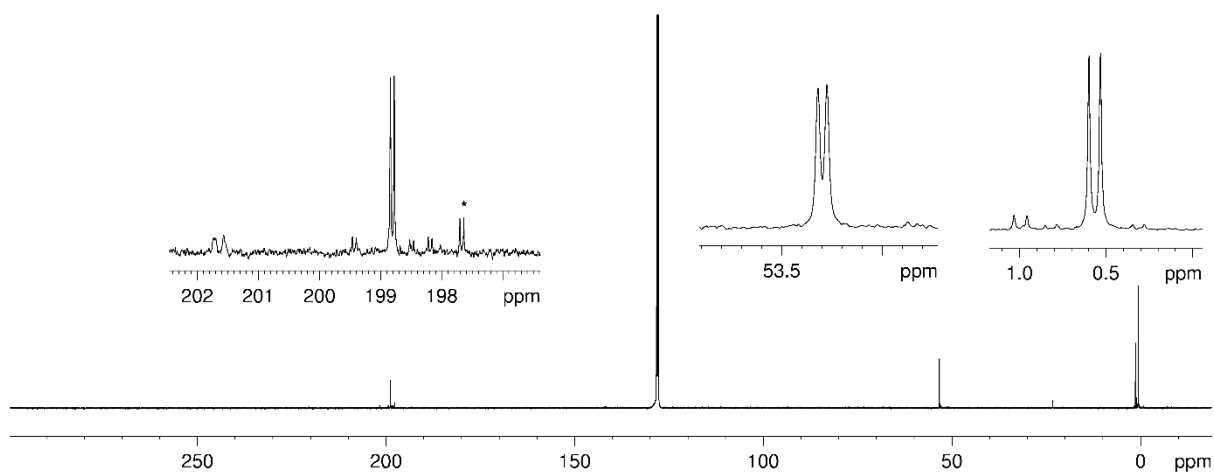


Figure S18: $^{13}\text{C}\{^1\text{H}\}$ NMR spectrum of **3a** in C_6D_6 (* = 1).

$(\text{OC})_5\text{W}\cdot\text{PH}_2\text{BH}_2\text{PH}_2\text{BH}_2\cdot\text{NMe}_3$ (**3b**):

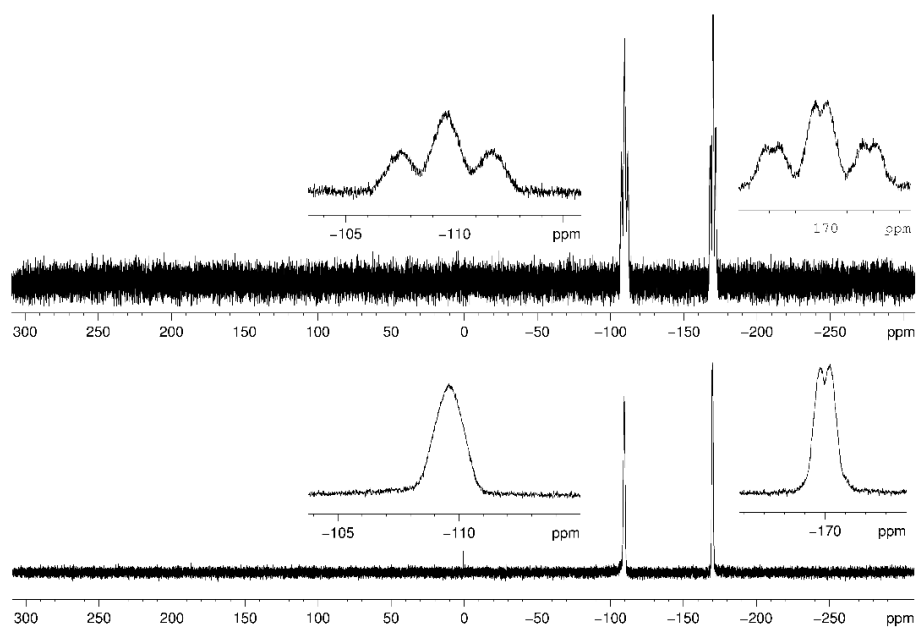


Figure S19: ^{31}P (top) and $^{31}\text{P}\{^1\text{H}\}$ NMR spectrum (bottom) of **3b** in C_6D_6

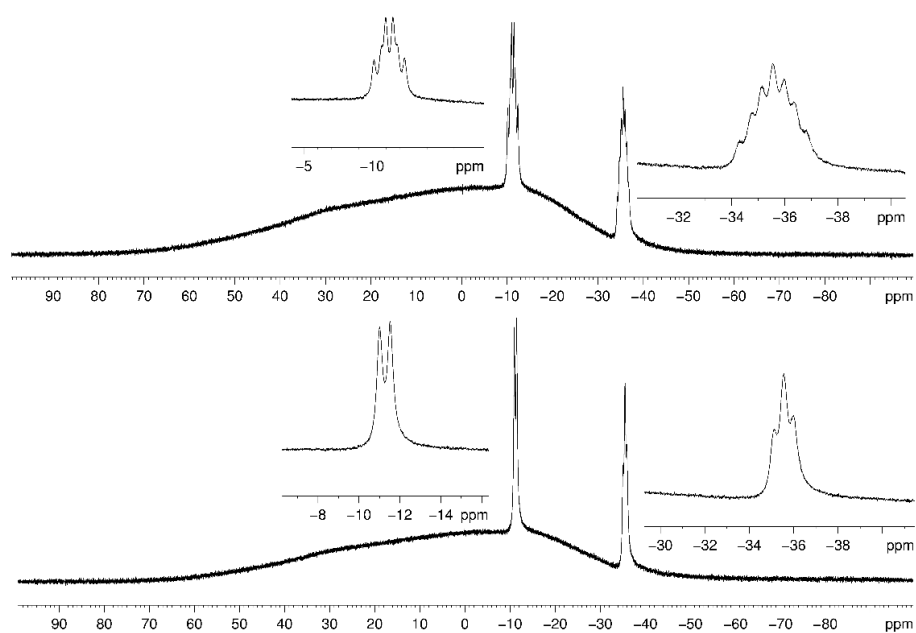


Figure S20: ^{11}B (top) and $^{11}B\{^1H\}$ NMR spectrum (bottom) of **3b** in C_6D_6

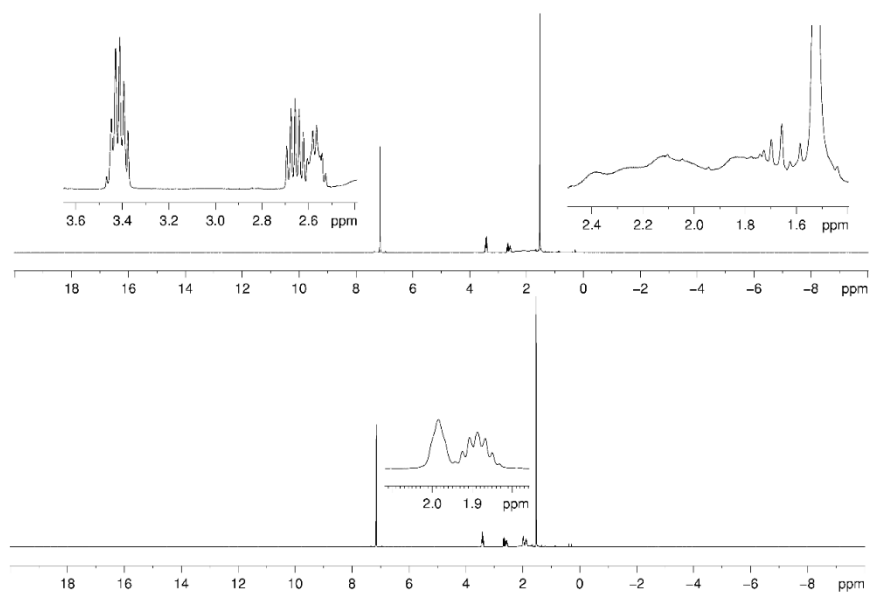


Figure S21: 1H (top) and $^1H\{^{11}B\}$ NMR spectrum of **3b** in C_6D_6

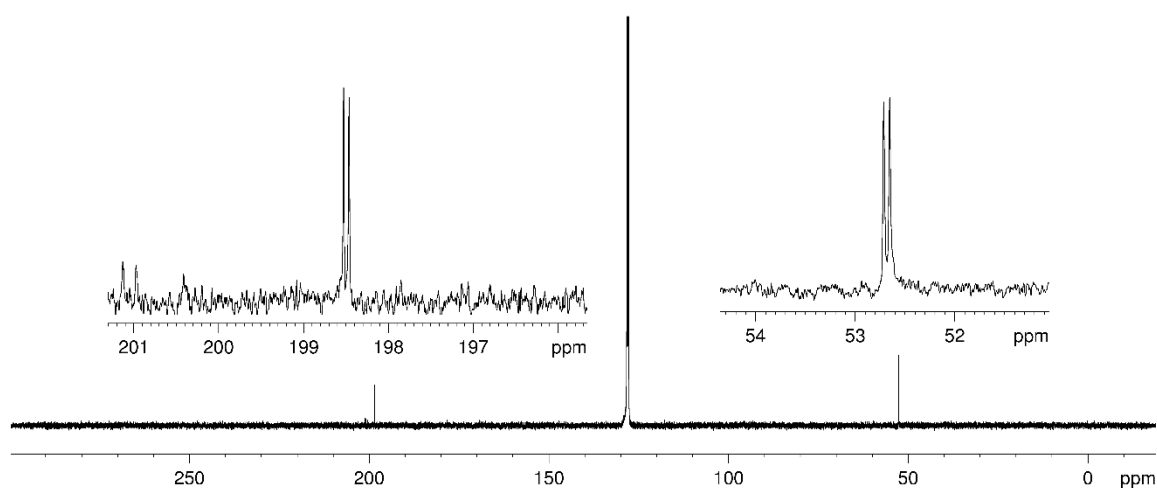


Figure S22: $^{13}\text{C}\{^1\text{H}\}$ NMR spectrum of **3b** in C_6D_6

$(\text{OC})_5\text{W}\cdot\text{PH}_2\text{BH}_2\text{As}(\text{SiMe}_3)_2\text{BH}_2\cdot\text{NMe}_3$ (**4a**):

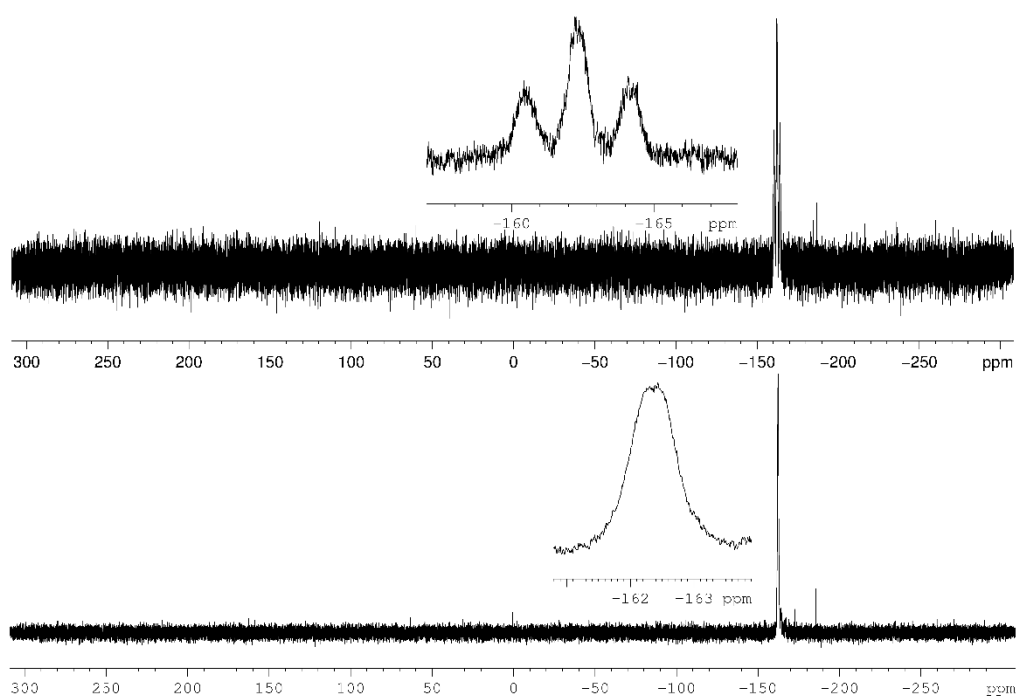


Figure S23: ^{31}P (top) and $^{31}\text{P}\{^1\text{H}\}$ NMR spectrum (bottom) of **4a** in C_6D_6 .

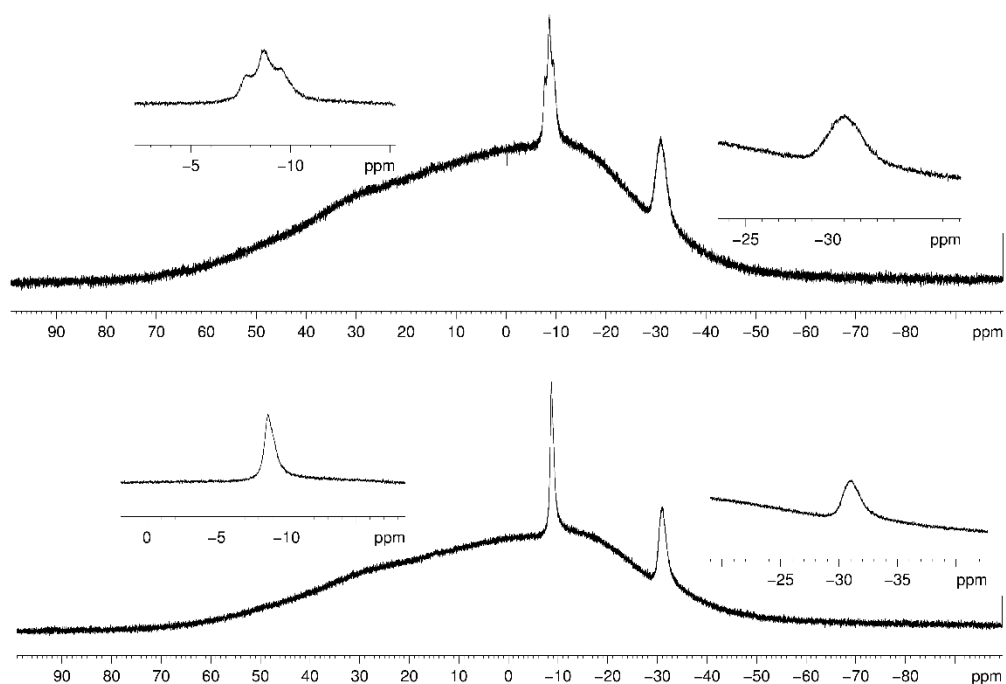


Figure S24: ^{11}B (top) and $^{11}B\{^1H\}$ NMR spectrum of **4a** in C_6D_6 .

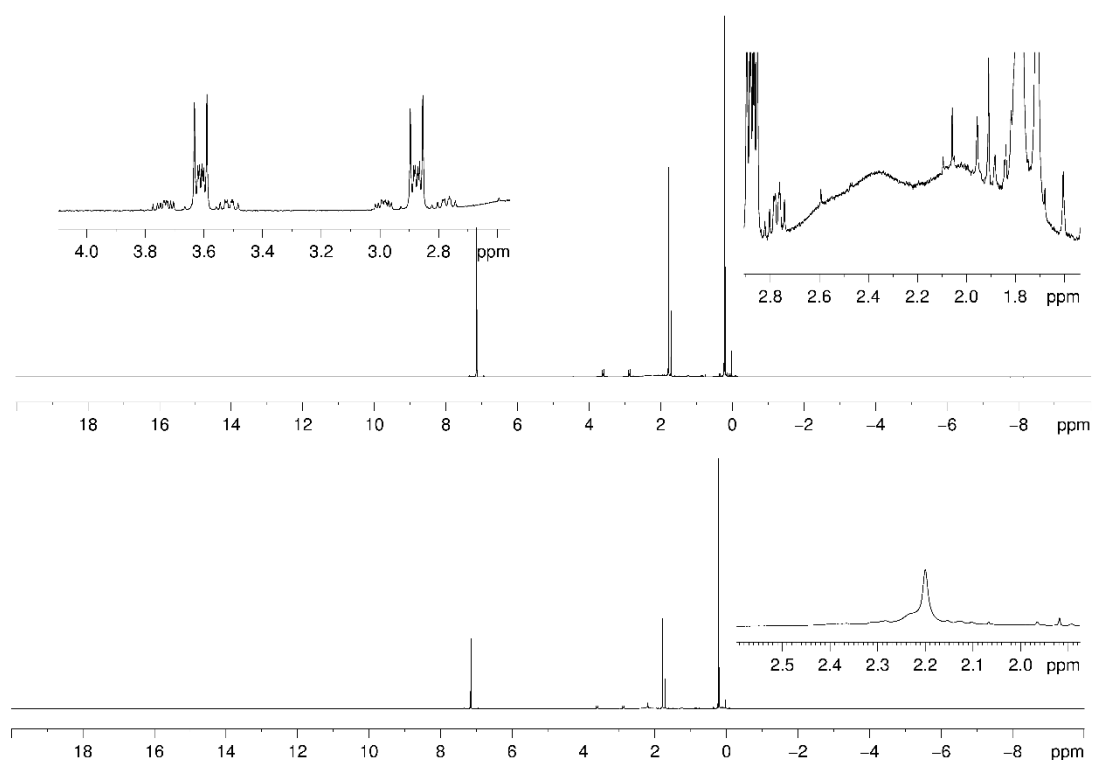


Figure S25: 1H (top) and $^1H\{^{11}B\}$ NMR spectrum (bottom) of **4a** in C_6D_6

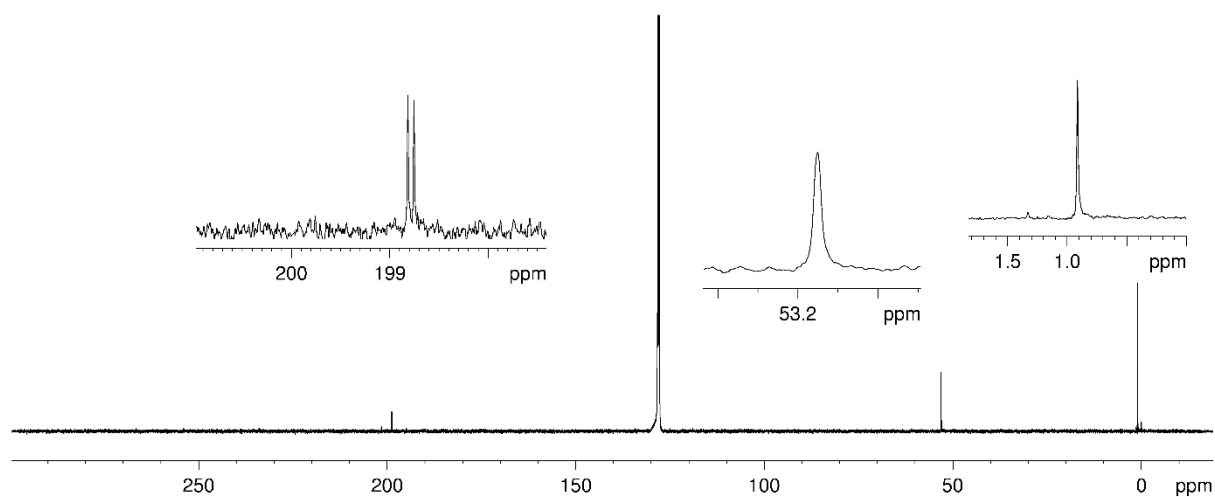


Figure S26: $^{13}\text{C}\{^1\text{H}\}$ NMR spectrum of **4a** in C_6D_6

$(\text{OC})_5\text{W}\cdot\text{PH}_2\text{BH}_2\text{AsH}_2\text{BH}_2\cdot\text{NMe}_3$ (**4b**):

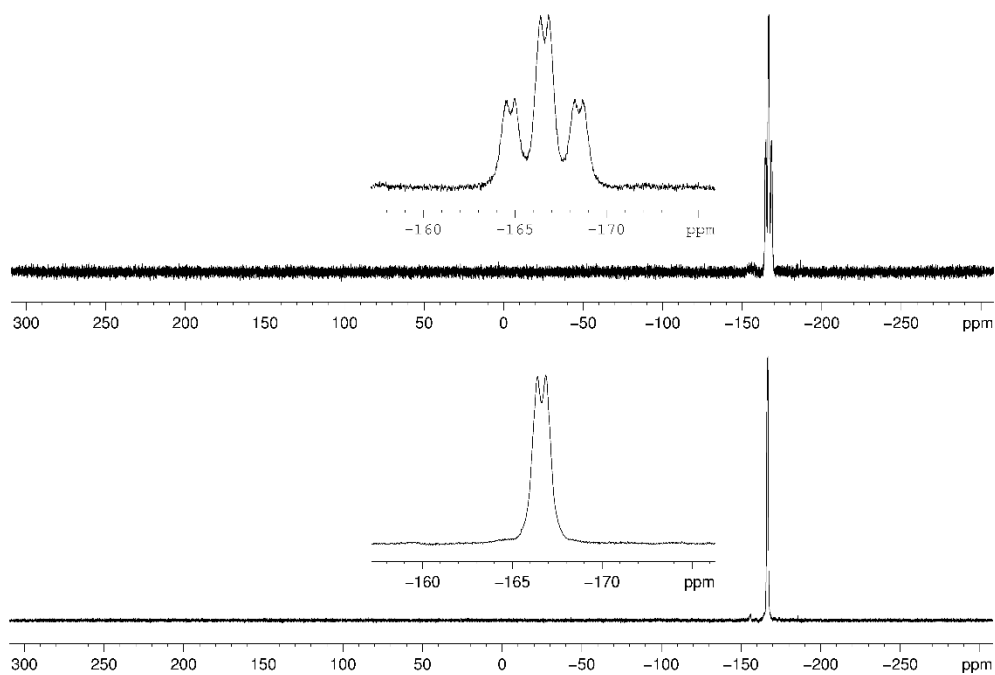


Figure S27: ^{31}P (top) and $^{31}\text{P}\{^1\text{H}\}$ NMR spectrum (bottom) of **4b** in C_6D_6

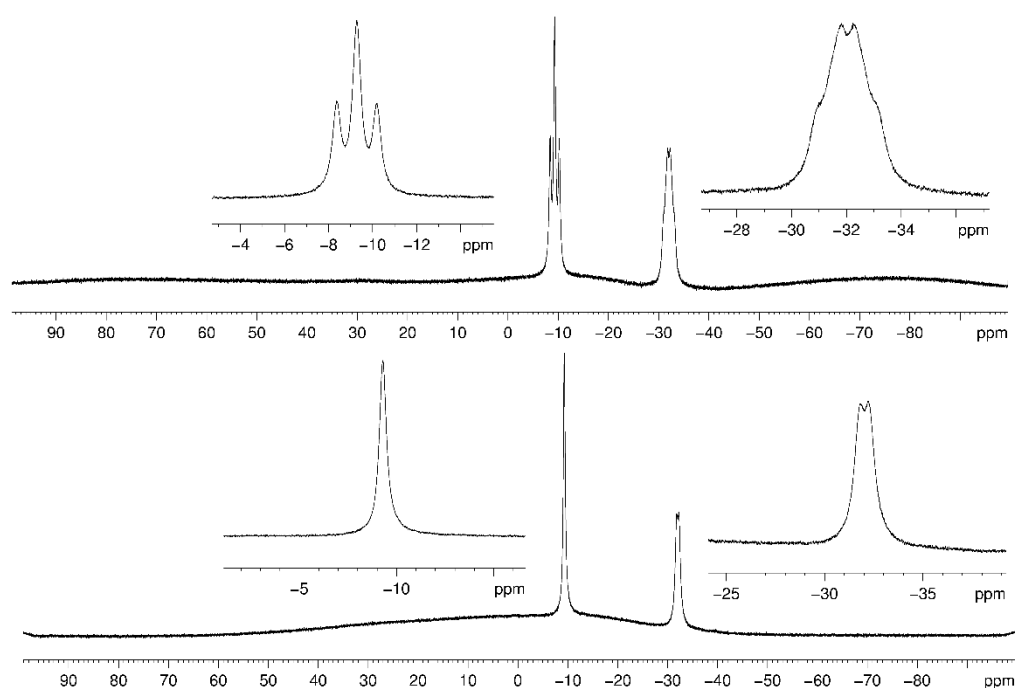


Figure S28: ^{11}B (top) and $^{11}\text{B}\{^1\text{H}\}$ NMR spectrum of **4b** in C_6D_6

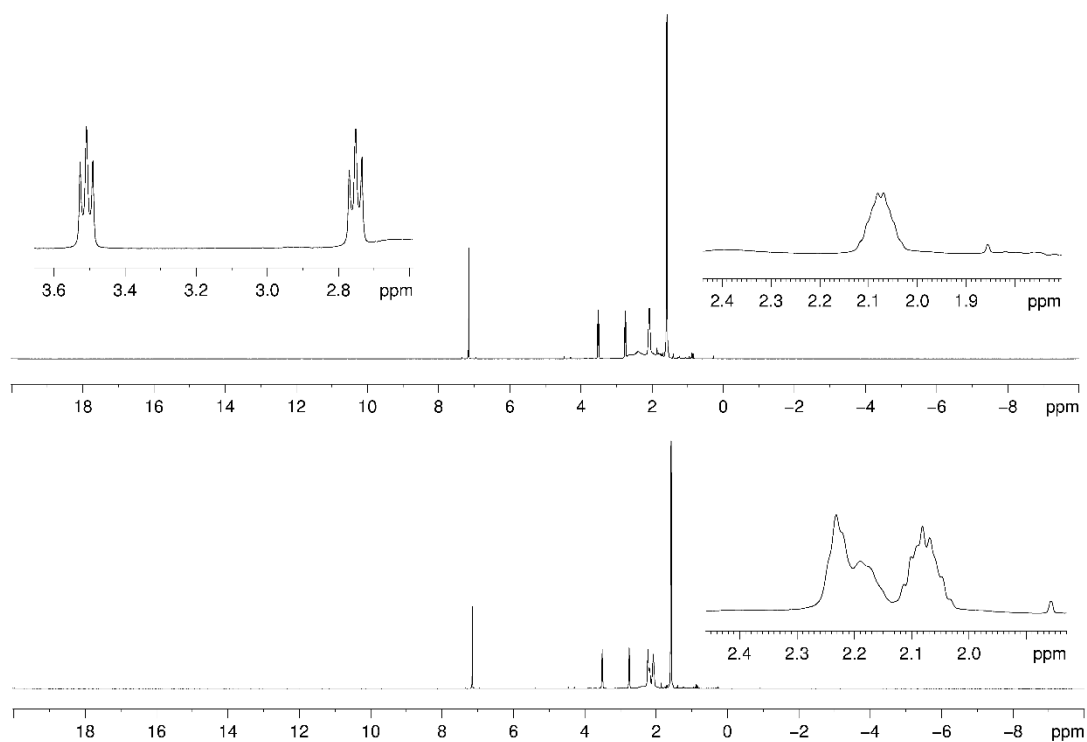


Figure S29: ^1H (top) and $^1\text{H}\{^{11}\text{B}\}$ NMR spectrum of **4b** in C_6D_6

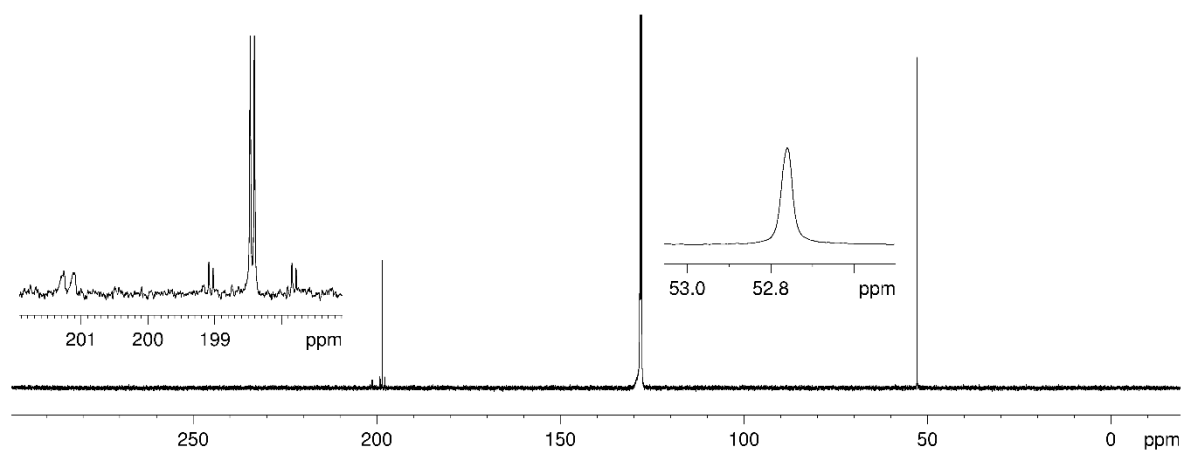


Figure S30: $^{13}\text{C}\{^1\text{H}\}$ NMR spectrum of **4b** in C_6D_6

$(\text{OC})_5\text{W}\cdot\text{PH}_2\text{BH}_2\text{Sb}(\text{SiMe}_3)_2\text{BH}_2\cdot\text{NHC}^{\text{Me}}$ (**5**):

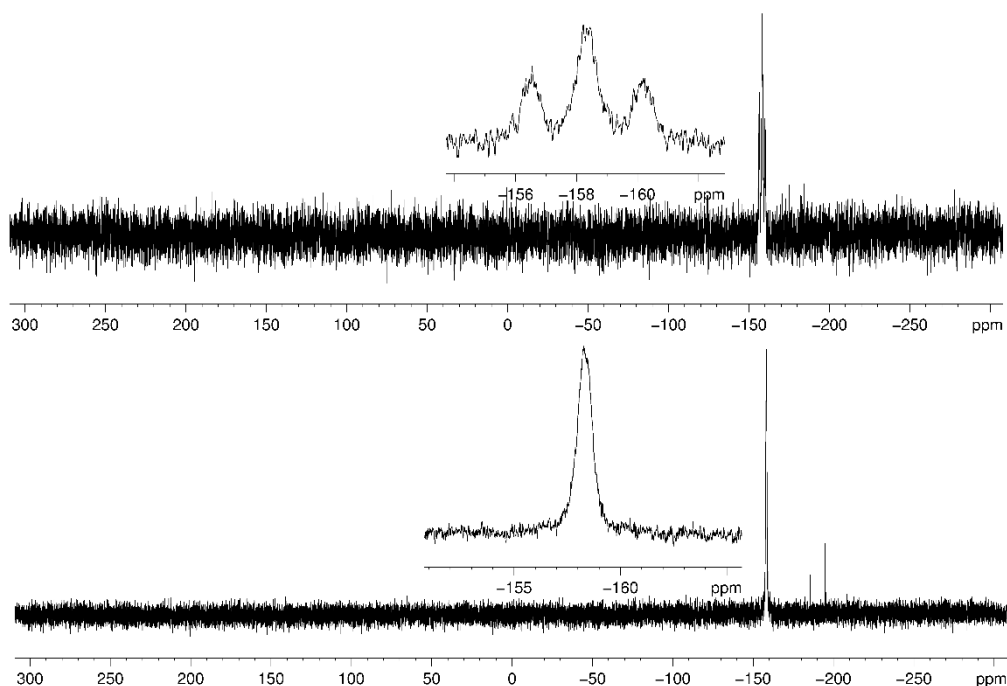


Figure S31: ^{31}P (top) and $^{31}\text{P}\{^1\text{H}\}$ NMR spectrum (bottom) of **5** in C_6D_6

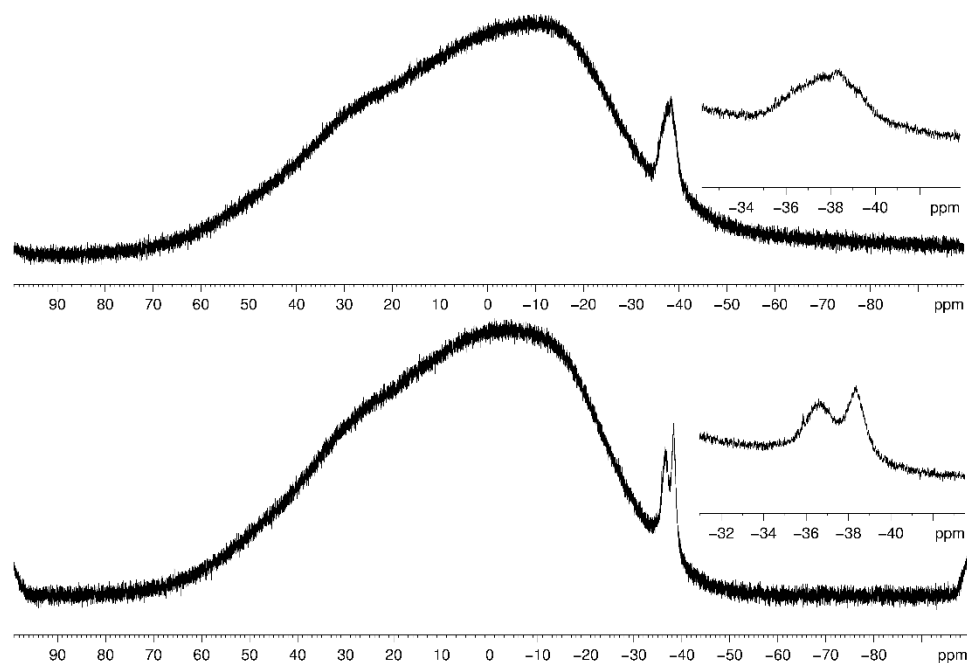


Figure S32: ^{11}B (top) and $^{11}\text{B}\{^1\text{H}\}$ NMR spectrum of **5** in C_6D_6

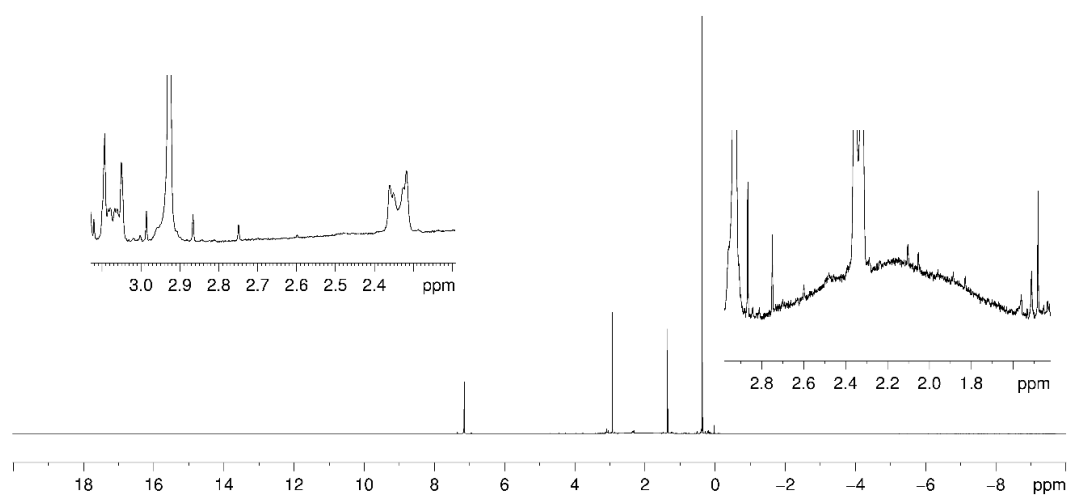


Figure S33: ^1H NMR spectrum of **5** in C_6D_6

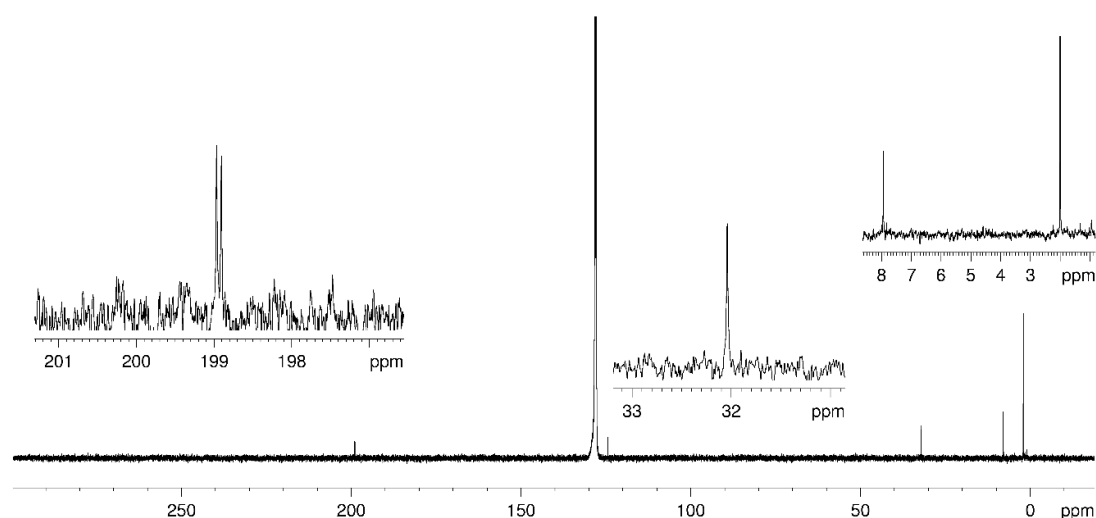
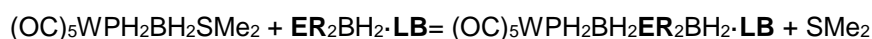


Figure S34: $^{13}\text{C}\{^1\text{H}\}$ NMR spectrum of **5** in C_6D_6

Computational Details

The geometries of the compounds have been fully optimized with gradient-corrected density functional theory (DFT) in form of Becke's three-parameter hybrid method B3LYP^[10] with def2-SVP all electron basis set (ECP for Sb, Bi, W).^[11] Gaussian 09 program package^[12] was used throughout. All structures correspond to minima on their respective potential energy surfaces. Basis sets were obtained from the EMSL basis set exchange database.^[13]

Table S6: Standard enthalpies ΔH°_{298} , (kJ mol^{-1}) for reaction



B3LYP/def2-SVP level of theory. Data are given for the most stable isomers in the gas phase.

R	LB	P	E		
			As	Sb	Bi
H	NMe ₃	-59.3	-27.3	5.7	40.0
H	NHC ^{Me}	-74.2	-37.7	0.4	40.0
SiMe ₃	NMe ₃	-39.2	-27.7	-12.2	13.0
SiMe ₃	NHC ^{Me}	-76.7	-58.5	-32.3	-2.3

Exothermicity of the reaction decreases from P to Bi; for E=Bi, reaction is endothermic or almost thermoneutral. Reactions with NHC^{Me} as Lewis base are in general more exothermic (less endothermic). Substitution of H by SiMe₃ groups in general increase reaction exothermicity, with the exception of $\text{PH}_2\text{BH}_2 \cdot \text{NMe}_3$.

Table S7: Reaction energies ΔE°_0 , standard enthalpies ΔH°_{298} , Gibbs energies ΔG°_{298} (kJ mol⁻¹) and standard entropies ΔS°_{298} (J mol⁻¹ K⁻¹) for the considered gas phase processes. B3LYP/def2-SVP level of theory. Data are given for the most stable isomers in the gas phase.

Process	ΔE°_0	ΔH°_{298}	ΔS°_{298}	ΔG°_{298}
<hr/>				
$\text{W(CO)}_5\text{PH}_2\text{BH}_2\text{SMe}_2 + \text{PH}_2\text{BH}_2\text{NMe}_3 =$				
$\text{W(CO)}_5\text{PH}_2\text{BH}_2\text{PH}_2\text{BH}_2\text{NMe}_3 + \text{SMe}_2$	-62.0	-59.3	-11.6	-55.8
$\text{W(CO)}_5\text{PH}_2\text{BH}_2\text{SMe}_2 + \text{AsH}_2\text{BH}_2\text{NMe}_3 =$				
$\text{W(CO)}_5\text{PH}_2\text{BH}_2\text{AsH}_2\text{BH}_2\text{NMe}_3 + \text{SMe}_2$	-28.9	-27.3	-21.0	-21.0
$\text{W(CO)}_5\text{PH}_2\text{BH}_2\text{SMe}_2 + \text{SbH}_2\text{BH}_2\text{NMe}_3 =$				
$\text{W(CO)}_5\text{PH}_2\text{BH}_2\text{SbH}_2\text{BH}_2\text{NMe}_3 + \text{SMe}_2$	5.4	5.7	-8.7	8.3
$\text{W(CO)}_5\text{PH}_2\text{BH}_2\text{SMe}_2 + \text{BiH}_2\text{BH}_2\text{NMe}_3 =$				
$\text{W(CO)}_5\text{PH}_2\text{BH}_2\text{BiH}_2\text{BH}_2\text{NMe}_3 + \text{SMe}_2$	41.0	40.0	-2.8	40.8
<hr/>				
$\text{W(CO)}_5\text{PH}_2\text{BH}_2\text{SMe}_2 + \text{PH}_2\text{BH}_2\text{NHC}^{\text{Me}} =$				
$\text{W(CO)}_5\text{PH}_2\text{BH}_2\text{PH}_2\text{BH}_2\text{NHC}^{\text{Me}} + \text{SMe}_2$	-76.9	-74.2	-7.4	-72.0
$\text{W(CO)}_5\text{PH}_2\text{BH}_2\text{SMe}_2 + \text{AsH}_2\text{BH}_2\text{NHC}^{\text{Me}} =$				
$\text{W(CO)}_5\text{PH}_2\text{BH}_2\text{AsH}_2\text{BH}_2\text{NHC}^{\text{Me}} + \text{SMe}_2$	-38.9	-37.7	-12.9	-33.8
$\text{W(CO)}_5\text{PH}_2\text{BH}_2\text{SMe}_2 + \text{SbH}_2\text{BH}_2\text{NHC}^{\text{Me}} =$				
$\text{W(CO)}_5\text{PH}_2\text{BH}_2\text{SbH}_2\text{BH}_2\text{NHC}^{\text{Me}} + \text{SMe}_2$	0.7	0.4	0.6	0.2
$\text{W(CO)}_5\text{PH}_2\text{BH}_2\text{SMe}_2 + \text{BiH}_2\text{BH}_2\text{NHC}^{\text{Me}} =$				
$\text{W(CO)}_5\text{PH}_2\text{BH}_2\text{BiH}_2\text{BH}_2\text{NHC}^{\text{Me}} + \text{SMe}_2$	41.0	40.0	11.8	36.5
<hr/>				
$\text{W(CO)}_5\text{PH}_2\text{BH}_2\text{SMe}_2 + \text{P(SiMe}_3)_2\text{BH}_2\text{NMe}_3 =$				
$\text{W(CO)}_5\text{PH}_2\text{BH}_2\text{P(SiMe}_3)_2\text{BH}_2\text{NMe}_3 + \text{SMe}_2$	-41.2	-39.2	-24.2	-32.0
$\text{W(CO)}_5\text{PH}_2\text{BH}_2\text{SMe}_2 + \text{As(SiMe}_3)_2\text{BH}_2\text{NMe}_3 =$				
$\text{W(CO)}_5\text{PH}_2\text{BH}_2\text{As(SiMe}_3)_2\text{BH}_2\text{NMe}_3 + \text{SMe}_2$	-28.1	-27.7	7.6	-29.9
$\text{W(CO)}_5\text{PH}_2\text{BH}_2\text{SMe}_2 + \text{Sb(SiMe}_3)_2\text{BH}_2\text{NMe}_3 =$				
$\text{W(CO)}_5\text{PH}_2\text{BH}_2\text{Sb(SiMe}_3)_2\text{BH}_2\text{NMe}_3 + \text{SMe}_2$	-10.8	-12.2	4.6	-13.6
$\text{W(CO)}_5\text{PH}_2\text{BH}_2\text{SMe}_2 + \text{Bi(SiMe}_3)_2\text{BH}_2\text{NMe}_3 =$				
$\text{W(CO)}_5\text{PH}_2\text{BH}_2\text{Bi(SiMe}_3)_2\text{BH}_2\text{NMe}_3 + \text{SMe}_2$	14.8	13.0	23.5	6.0
<hr/>				
$\text{W(CO)}_5\text{PH}_2\text{BH}_2\text{SMe}_2 + \text{P(SiMe}_3)_2\text{BH}_2\text{NHC}^{\text{Me}} =$				
$\text{W(CO)}_5\text{PH}_2\text{BH}_2\text{P(SiMe}_3)_2\text{BH}_2\text{NHC}^{\text{Me}} + \text{SMe}_2$	-77.8	-76.7	-28.5	-68.2
$\text{W(CO)}_5\text{PH}_2\text{BH}_2\text{SMe}_2 + \text{As(SiMe}_3)_2\text{BH}_2\text{NHC}^{\text{Me}} =$				
$\text{W(CO)}_5\text{PH}_2\text{BH}_2\text{As(SiMe}_3)_2\text{BH}_2\text{NHC}^{\text{Me}} + \text{SMe}_2$	-59.0	-58.5	-30.8	-49.3
$\text{W(CO)}_5\text{PH}_2\text{BH}_2\text{SMe}_2 + \text{Sb(SiMe}_3)_2\text{BH}_2\text{NHC}^{\text{Me}} =$				
$\text{W(CO)}_5\text{PH}_2\text{BH}_2\text{Sb(SiMe}_3)_2\text{BH}_2\text{NHC}^{\text{Me}} + \text{SMe}_2$	-30.9	-32.3	-0.2	-32.2

$W(CO)_5PH_2BH_2Sb(SiMe_3)_2BH_2NHC^{Me} + SMe_2$				
$W(CO)_5PH_2BH_2SMe_2 + Bi(SiMe_3)_2BH_2NHC^{Me} =$				
$W(CO)_5PH_2BH_2Bi(SiMe_3)_2BH_2NHC^{Me} + SMe_2$	-1.0	-2.3	-10.9	1.0
$W(CO)_5THF + PH_2BH_2PH_2BH_2NMe_3 =$	-85.0	-82.4	-33.1	-72.6
$W(CO)_5PH_2BH_2PH_2BH_2NMe_3 + THF$				
$PH_2BH_2PH_2BH_2NMe_3 =$	-24.9	-26.4	23.3	-33.3
$\frac{1}{3} (PH_2BH_2)_3 + PH_2BH_2NMe_3$				
$PH_2BH_2PH_2BH_2NMe_3 =$	-23.7	-24.0	-0.6	-23.8
$\frac{1}{8} (PH_2BH_2)_3 + PH_2BH_2NMe_3$				

A Convenient Route to Mixed Pnictogenylboranes

Table S8: Total energies E^0 , sum of electronic and thermal enthalpies H^0_{298} (Hartree) and standard entropies S^0_{298} (cal mol⁻¹K⁻¹). B3LYP/def2-SVP level of theory.

Compound	Point group	E^0	H^0_{298}	S^0_{298}
SMe ₂	C _{2v}	-477.8445747	-477.763668	67.882
THF	C _s	-232.278684	-232.156585	69.941
W(CO) ₅ THF	C ₂	-865.7468615	-865.567974	146.213
cis_W(CO) ₅ PH ₂ BH ₂ SMe ₂	C ₁	-1479.8327099	-1479.649258	163.853
PH ₂ BH ₂ NMe ₃	C _s	-542.8627187	-542.689354	88.461
AsH ₂ BH ₂ NMe ₃	C _s	-2437.2394131	-2437.067688	93.546
SbH ₂ BH ₂ NMe ₃	C _s	-441.9144850	-441.744913	95.353
BiH ₂ BH ₂ NMe ₃	C _s	-416.2822950	-416.113645	98.42
PH ₂ BH ₂ NHC ^{Me}	C _s	-751.7185165	-751.479272	115.731
AsH ₂ BH ₂ NHC ^{Me}	C _s	-2646.0978687	-2645.860207	120.001
SbH ₂ BH ₂ NHC ^{Me}	C _s	-650.7767781	-650.541328	122.619
BiH ₂ BH ₂ NHC ^{Me}	C _s	-625.1466082	-624.912024	127.304
P(SiMe ₃) ₂ BH ₂ NMe ₃	C ₁	-1359.9118257	-1359.516004	163.201
As(SiMe ₃) ₂ BH ₂ NMe ₃	C ₁	-3254.2916974	-3253.896492	166.358
Sb(SiMe ₃) ₂ BH ₂ NMe ₃	C _s	-1258.9663545	-1258.571462	172.603
Bi(SiMe ₃) ₂ BH ₂ NMe ₃	C _s	-1233.3350633	-1232.940599	176.400
P(SiMe ₃) ₂ BH ₂ NHC ^{Me}	C ₁	-1568.7637298	-1568.301954	188.542
As(SiMe ₃) ₂ BH ₂ NHC ^{Me}	C ₁	-3463.1459395	-3462.684889	195.104
Sb(SiMe ₃) ₂ BH ₂ NHC ^{Me}	C ₁	-1467.8256701	-1467.365015	198.105
Bi(SiMe ₃) ₂ BH ₂ NHC ^{Me}	C ₁	-1442.1973268	-1441.737045	202.041
W(CO) ₅ PH ₂ BH ₂ PH ₂ BH ₂ NMe ₃	C ₁	-1544.8744620	-1544.597532	181.656
W(CO) ₅ PH ₂ BH ₂ AsH ₂ BH ₂ NMe ₃	C ₁	-3439.2385539	-3438.963661	184.488
W(CO) ₅ PH ₂ BH ₂ SbH ₂ BH ₂ NMe ₃	C ₁	-1443.9005622	-1443.628332	189.245
W(CO) ₅ PH ₂ BH ₂ BiH ₂ BH ₂ NMe ₃	C ₁	-1418.2548314	-1417.984010	193.726
W(CO) ₅ PH ₂ BH ₂ PH ₂ BH ₂ NHC ^{Me}	C ₁	-1753.7359266	-1753.393140	209.924
W(CO) ₅ PH ₂ BH ₂ AsH ₂ BH ₂ NHC ^{Me}	C ₁	-3648.1008272	-3647.760139	212.89
W(CO) ₅ PH ₂ BH ₂ SbH ₂ BH ₂ NHC ^{Me}	C ₁	-1652.7646528	-1652.426757	218.741
W(CO) ₅ PH ₂ BH ₂ BiH ₂ BH ₂ NHC ^{Me}	C ₁	-1627.1191267	-1626.782382	226.091
W(CO) ₅ PH ₂ BH ₂ P(SiMe ₃) ₂ BH ₂ NMe ₃	C ₁	-2361.9156705	-2361.416537	253.389
W(CO) ₅ PH ₂ BH ₂ As(SiMe ₃) ₂ BH ₂ NMe ₃	C ₁	-4256.2905228	-4255.792624	264.136

W(CO) ₅ PH ₂ BH ₂ Sb(SiMe ₃) ₂ BH ₂ NMe ₃	C ₁	-2260.9586130	-2260.461707	269.676
W(CO) ₅ PH ₂ BH ₂ Bi(SiMe ₃) ₂ BH ₂ NMe ₃	C ₁	-2235.3175572	-2234.821220	277.989
W(CO) ₅ PH ₂ BH ₂ P(SiMe ₃) ₂ BH ₂ NHC ^{Me}	C ₁	-2570.7814970	-2570.216754	277.698
W(CO) ₅ PH ₂ BH ₂ As(SiMe ₃) ₂ BH ₂ NHC ^{Me}	C ₁	-4465.1565431	-4464.592752	283.704
W(CO) ₅ PH ₂ BH ₂ Sb(SiMe ₃) ₂ BH ₂ NHC ^{Me}	C ₁	-2469.8255904	-2469.262901	294.019
W(CO) ₅ PH ₂ BH ₂ Bi(SiMe ₃) ₂ BH ₂ NHC ^{Me}	C ₁	-2444.1858418	-2443.623501	295.404
PH ₂ BH ₂ PH ₂ BH ₂ NMe ₃	C _s	-911.3739179	-911.154747	113.296
(PH ₂ BH ₂) ₃	C ₃	-1105.562019	-1105.426301	91.206
(PH ₂ BH ₂) ₈	C ₁	-2948.161857	-2947.796221	197.532

Cartesian coordinates of the optimized geometry can be obtained from:

<https://doi.org/10.1002/anie.201707436>

or from the provided DVD.

References:

- [1] C. Marquardt, A. Adolf, A. Stauber, M. Bodensteiner, A. V. Virovets, A. Y. Timoshkin, M. Scheer, *Chem. Eur. J.* **2013**, 19, 11887 – 11891.
- [2] F. Nief, F. Mercier, F. Mathey, *J. Organomet. Chem.* **1987**, 328, 349-355.
- [3] C. Marquardt, O. Hegen, M. Hautmann, G. Balázs, M. Bodensteiner, A. V. Virovets, A. Y. Timoshkin, M. Scheer, *Angew. Chem. Int. Ed.* **2015**, 54, 13122–13125.
- [4] C. Marquardt, C. Thoms, A. Stauber, G. Balazs, M. Bodensteiner, M. Scheer, *Angew. Chem. Int. Ed.* **2014**, 53, 3727–3730.
- [5] C. Marquardt, T. Kahoun, A. Stauber, G. Balázs, M. Bodensteiner, A. Y. Timoshkin, M. Scheer *Angew. Chem.* **2016**, 128, 15048 –15052.
- [6] Agilent Technologies **2006-2011**, CrysAlisPro Software system, different versions, Agilent Technologies UK Ltd, Oxford, UK.
- [7] A. Altomare, M. C. Burla, M. Camalli, G. L. Cascarano, C. Giacovazzo, A. Guagliardi, A. G. Moliterni, G. Polidori, R. Spagna, *J. Appl. Cryst.* (1999) 32, 115-119.
- [8] G. M. Sheldrick, *Acta Cryst.* **2008**, A64, 112–122.

- [9] O.V. Dolomanov, L. J. Bourhis, R. J. Gildea, J. A. K. Howard, H. Puschmann, OLEX2: A complete structure solution, refinement and analysis program, **2009**. *J. Appl. Cryst.*, **42**, 339-341.
- [10] a) A.D. Becke, *J. Chem. Phys.* **1993**, *98*, 5648. b) C. Lee, W. Yang, R.G. Parr, *Phys. Rev. B* **1988**, *37*, 785.
- [11] a) F. Weigend, R. Ahlrichs, *Phys. Chem. Chem. Phys.*, **2005**, *7*, 3297-3305. b) D. Andrae, U. Haeussermann, M. Dolg, H. Stoll, H. Preuss, *Theor. Chim. Acta*, **1990**, *77*, 123-141.
- [12] M. J. Frisch, G. W. Trucks, H. B. Schlegel, G. E. Scuseria, M. A. Robb, J. R. Cheeseman, G. Scalmani, V. Barone, B. Mennucci, G. A. Petersson, H. Nakatsuji, M. Caricato, X. Li, H. P. Hratchian, A. F. Izmaylov, J. Bloino, G. Zheng, J. L. Sonnenberg, M. Hada, M. Ehara, K. Toyota, R. Fukuda, J. Hasegawa, M. Ishida, T. Nakajima, Y. Honda, O. Kitao, H. Nakai, T. Vreven, J. A. Montgomery, Jr., J. E. Peralta, F. Ogliaro, M. Bearpark, J. J. Heyd, E. Brothers, K. N. Kudin, V. N. Staroverov, T. Keith, R. Kobayashi, J. Normand, K. Raghavachari, A. Rendell, J. C. Burant, S. S. Iyengar, J. Tomasi, M. Cossi, N. Rega, J. M. Millam, M. Klene, J. E. Knox, J. B. Cross, V. Bakken, C. Adamo, J. Jaramillo, R. Gomperts, R. E. Stratmann, O. Yazyev, A. J. Austin, R. Cammi, C. Pomelli, J. W. Ochterski, R. L. Martin, K. Morokuma, V. G. Zakrzewski, G. A. Voth, P. Salvador, J. J. Dannenberg, S. Dapprich, A. D. Daniels, O. Farkas, J. B. Foresman, J. V. Ortiz, J. Cioslowski, and D. J. Fox, Gaussian 09, Revision E.01, Gaussian, Inc., Wallingford CT, 2013.
- [13] (a) D. Feller, *J. Comp. Chem.* **1996**, *17*, 1571-1586; (b) K. L. Schuchardt, B. T. Didier, T. Elsethagen, L. Sun, V. Gurumoorthi, J. Chase, J. Li, T. L. Windus, *J. Chem. Inf. Model.* **2007**, *47*, 1045-1052.

3.6 Author contributions

The synthesis and characterization of $\text{IBH}_2\cdot\text{PH}_2\text{BH}_2\cdot\text{NMe}_3$ and **1** were performed by Dr. Christian Marquardt (reported in his PhD-thesis, Regensburg **2015**).

2 was first synthesized by Dr. Christian Marquardt and further characterized by Oliver Hegen

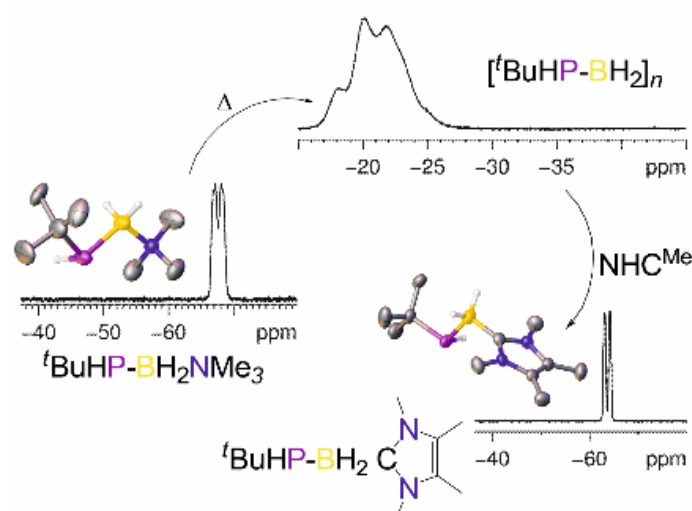
Compounds **3a**, **3b**, **4a**, **4b** and **5** were synthesized and characterized by Oliver Hegen. All DFT-calculations were performed by Prof. Dr. A. Y. Timoshkin.

The manuscript (including supporting information, figures, schemes and graphical abstract) was written by Oliver Hegen.

This chapter was reprinted with slight modifications with permission of “John Wiley and Sons”, License Number: 4332410563039

4. Depolymerization of Poly(phosphinoboranes): From Polymers to Lewis Base Stabilized Monomers

Christian Marquardt, Oliver Hegen, Ariane Vogel, Andreas Stauber, Michael Bodensteiner, Alexey Y. Timoshkin, and Manfred Scheer

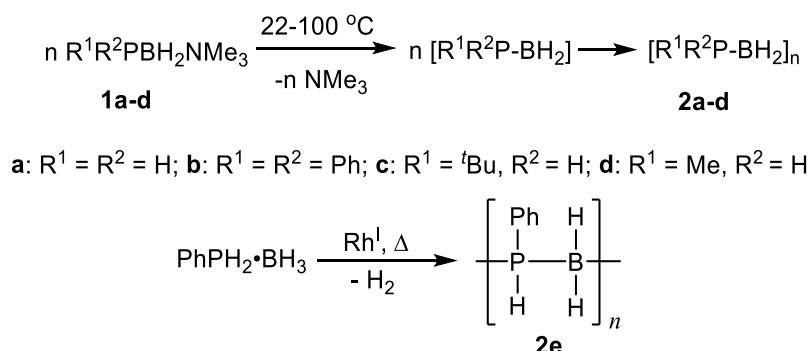


Abstract: We report on depolymerization reactions of poly(phosphinoboranes). The cleavage of the polymers $[\text{H}_2\text{PBH}_2]_n$ (**2a**), $[\text{tBuHPBH}_2]_n$ (**2c**), $[\text{PhHPBH}_2]_n$ (**2e**) and the oligomer $[\text{Ph}_2\text{PBH}_2]_n$ (**2b**), with strong Lewis bases (LBs), in particular with NHCs, leads to the corresponding monomeric phosphanylboranes $\text{R}^1\text{R}^2\text{PBH}_2\text{LB}$. It is observed that the depolymerization depends on the strength and stability of the LBs as well as on the substitution pattern of the poly(phosphinoboranes). The solid state structures of the monomeric phosphinoboranes $\text{H}_2\text{PBH}_2\text{NHC}^{\text{Me}}$ (NHC = N-heterocyclic carbene) (**4a**), $\text{H}_2\text{PBH}_2\text{NHC}^{\text{dipp}}$ (**5a**) and $t\text{BuHPBH}_2\text{NHC}^{\text{Me}}$ (**4c**) were determined. DFT calculations support the experimentally observed reaction behaviour.

4.1 Introduction

Polymers based on main-group elements other than carbon are in the focus of current research as a result of their versatile potential applications for elastomers, lithographic resists, or as ceramic precursors.^[1,2] Main-group macromolecules can be accessed by different polymerization pathways.^[3] Metal-catalyzed polycondensation routes and, in particular, dehydrocoupling processes attracted a lot of attention and were successfully used for the preparation of poly(aminoboranes) $[\text{RHNBH}_2]_n$ ($\text{R} = \text{alkyl, H}$)^[4,5] and poly(phosphinoboranes) $[\text{RHPBH}_2]_n$ ($\text{R} = \text{aryl}$).^[6] Those polymers exhibit backbones of alternating Group 13 and Group 15 elements and are formally isoelectronic to polyolefins. However, due to the difference in electronegativity and their thus resulting polar bonds, they possess significantly different physical and chemical properties,^[7] leading to the synthesis of a large variety of polymeric BN analogues.^[8] Poly(phosphinoboranes) with reasonably high molar masses were prepared by the Rh- and Fe-catalyzed dehydrogenation of primary phosphine-boranes RPH_2BH_3 .^[6,9,10] Studies of the coordination chemistry of phosphine-borane ligands at the metal centers allowed to elucidate the P-B bond formation processes leading to dehydrogenative oligomerization and polymerization.^[10,11] With nearly non-polar P-H bonds, the catalytic dehydrocoupling routes depend on the electron withdrawing properties of the aryl groups on the phosphorus atoms to facilitate the reaction, resulting in a limited substrate range. The only examples of poly(alkylphosphinoboranes) of modest molar mass were achieved by Rh-catalyzed dehydrocoupling of RPH_2BH_3 ($\text{R} = t\text{Bu, FcCH}_2$) in reactions that generally lead to chain branching and crosslinking.^[6b,d] Recently, a new way for the generation of poly(phosphinoboranes) was presented, circumventing the disadvantages of metal-catalyzed dehydropolymerization^[9] and giving access to high molecular weight poly(alkylphosphinoboranes),^[12] based on the use of pnictogenylboranes $\text{R}_2\text{EBH}_2\text{NMe}_3$ ($\text{R} = \text{alkyl, aryl, H}$), which are easily accessible at gram scale^[12,13] and are valuable starting materials for the formation of ionic oligomeric ($\text{E} = \text{As, P}$)^[13b,14] and polymeric materials (Scheme 1, $\text{E} = \text{P}$).^[12] Thermal treatment of the phosphanylboranes $\text{R}_2\text{PBH}_2\text{NMe}_3$ ($\text{R} = \text{H, alkyl, aryl}$, Scheme 1, **1a - d**) either in solution or in the absence of a solvent leads to the elimination of NMe_3 and subsequent polymerization yielding oligo- and poly(phosphinoboranes) $[\text{R}^1\text{R}^2\text{P}-\text{BH}_2]_n$ (Scheme 1, **2a-d**). In particular, the gentle thermolysis (22–40 °C) of $t\text{BuPHBH}_2\text{NMe}_3$ (Scheme 1, **1c**) afforded the poly(alkylphosphinoborane) $[t\text{BuPHBH}_2]_n$ (Scheme 1, **2c**) with a high

molar mass and a reasonably low polydispersity index, which is characteristic of a mainly linear material (Scheme 1).



Scheme 1: Polymerization of phosphanylboranes by either LB elimination for **2a-d**^[12,13] and dehydrocoupling for **2e**^[9] ($\text{Rh}^I = [\text{Rh}(\mu\text{-Cl})(1,5\text{-cod})]_2$).

Although many examples of polymerization reactions are known, the opposite process, namely depolymerization reactions, are quite scarce. Schulz et al. presented the cleavage of the cyclic oligomeric phosphino- and arsinoalanes by DMAP (4-(dimethylamino)-pyridine) as a convenient way for the synthesis of monomeric group 13/15 compounds.^[15] Hänisch et al. also succeeded in the cleavage of a series of cyclic phosphino- and arsinogallanes with Lewis bases such as DMAP and N-heterocyclic carbenes (NHCs).^[16] Based on NMR investigations, the *Manners* group has recently found that poly(aminoboranes) $[\text{RHNBH}_2]_n$ ($\text{R} = \text{alkyl}, \text{H}$) can be transformed into monomeric compounds by cleaving with NHCs.^[17] The importance of NHCs in the stabilization of reactive main group compounds was already demonstrated by our group^[18] and also by the groups of Rivard^[19] and Robinson.^[20] However, systematic investigation of cleavage of inorganic polymers in general and poly(phosphinoboranes) in particular by very different Lewis bases has not been performed yet.

4.2 Results and Discussion

Herein we report on an alternative approach to the monomeric phosphinoboranes by the depolymerization of poly(phosphinoboranes) with strong Lewis bases and, in particular, NHCs. For those studies, we chose the parent compound of the poly(phosphinoboranes) **2a** and the substituted derivatives **2b** and **2c** as well as the well-known poly(phenylphosphinoborane) $[\text{PhHPBH}_2]_n$ (**2e**). DFT computations revealed that among the $[\text{H}_2\text{PBH}_2]_m$ ($m = 1 - 8$) oligomers, the cyclic trimer $[\text{H}_2\text{PBH}_2]_3$

is the most energetically stable one. Therefore, the model reaction (1) was used for the computation of the energetics of the first step of a non-cross-linked polymer cleavage:



in which LB = Lewis base. The data in Table 1 indicate that energetics strongly depends both on the nature of the Lewis base and the substituents R on the phosphorus atom. The favorability of the reaction (1) expectedly increases with the increase of the basicity of LB in the order of $\text{NMe}_3 < \text{DMAP} < \text{NHC}^{\text{Dipp}} < \text{NHC}^{\text{Me}}$. The cleavage of all polymers by NHC^{Me} (1,3,4,5-tetramethylimidazolyliene) is exothermic, while NHC^{Dipp} (1,3-bis(2,6-diisopropylphenyl)imidazolin-2-ylidene) is predicted to exothermically cleave only H,H and H,Ph derivatives.

Table 1: Standard enthalpies for the gas phase reaction (1); [kJ mol⁻¹]. B3LYP/def2-SVP level of theory.

LB \ R ¹ , R ²	H, H	Ph, Ph	H, ^t Bu	H, Ph
NMe ₃	56	120	124	57
DMAP ^[a]	10	66	68	11
NHC ^{Me} ^[b]	-76	-19	-5	-76
NHC ^{dipp} ^[c]	-56	41	29	-43

[a] DMAP = 4-dimethylaminopyridine, [b] NHC^{Me} = 1,3,4,5-tetramethyl-imidazolyliene, [c] NHC^{dipp} = 1,3-bis(2,6-diisopropylphenyl)imidazolin-2-ylidene

According to DFT computations (see the Supporting Information), the cleavage of trimers by NMe₃ is endergonic, which indicates the thermodynamic instability of R¹R²PBH₂NMe₃ with respect to its polymerization. Interestingly, while the phosphinoboranes **1a-d** can be obtained in gram scale, the isolation of HPhPBH₂NMe₃ (**1e**) in large amounts has failed so far despite many attempts being made (see the Supporting Information). For the stronger Lewis base DMAP, computational data indicate that the cleavage process is much less endergonic. Interestingly, no cleavage was observed experimentally with DMAP for **2a**, **2b** and **2c** for 72 h in boiling toluene. Only for the polymer **2e** a partial (ca. 25% based on ³¹P NMR spectroscopy) conversion was observed, when an excess of DMAP was used (18 h at 110 °C in boiling toluene;

see the Supporting Information). An excess of DMAP presumably shifts the equilibrium to the formation of **3e**.

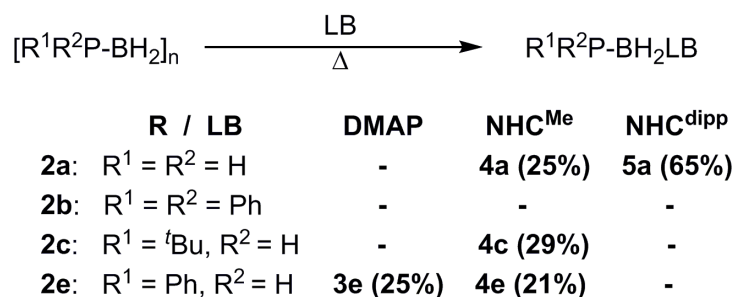
The stronger donor NHC^{Me} is predicted to exergonically cleave all considered polymers. In the reaction of $[\text{H}_2\text{PBH}_2]_n$ (**2a**) with NHC^{Me} , only a 5% conversion to $\text{H}_2\text{PBH}_2\text{NHC}^{\text{Me}}$ (**4a**) was observed (24 h in boiling toluene). The addition of an excess of NHC^{Me} or elongated reaction times do not lead to a higher conversion rate. To ensure a correct assignment of the NMR signals, compound **4a** was obtained using an alternative synthetic route (see the Supporting Information).

The reaction of $[\text{PhHPBH}_2]_n$ **2e** with NHC^{Me} in boiling THF (65 °C) leads to the cleavage of over 70% of the polymeric material after 30 min. $\text{PhHPBH}_2\text{NHC}^{\text{Me}}$ (**4e**) is obtained in about 40% yield (based on ^{31}P NMR spectroscopy)^[21] as a white solid, which readily crystallizes from *n*-hexane. Unfortunately, single crystals suitable for X-ray structure analysis could not be obtained. However, **4e** could unambiguously be identified by NMR spectroscopy and mass spectrometry experiments.

The addition of an equimolar amount of NHC^{Me} to $[\text{tBuHPBH}_2]_n$ (**2c**) smoothly cleaves **2c** (72 h at 45 °C in toluene) yielding the monomeric phosphanylborane $\text{tBuHPBH}_2\text{NHC}^{\text{Me}}$ (**4c**) in about 80% yield (determined by ^{31}P NMR spectroscopy). Further addition of NHC^{Me} does not lead to higher yields due to the contents of crosslinked/low molecular weight polymers.^[22] **4c** can be extracted with *n*-hexane, however, unassigned side products and $[\text{tBuHPBH}_2]_n$ are also soluble, and thus several recrystallization steps are necessary to obtain analytically pure **4c**, leading to a low crystalline yield of 29%. In contrast, the di-substituted oligomer **2b** could not be cleaved at all, which we attribute to a steric shielding of the two substituents at the P-atom.

Computational data indicate that the process of interaction of polymers with NHC^{dipp} with the formation of $\text{R}^1\text{R}^2\text{PBH}_2\text{NHC}^{\text{dipp}}$ is exergonic. However, when the initial stage, modelled by the reaction (1), is considered, NHC^{dipp} exothermically cleaves only the parent compound (**2a**) and the monophenyl-derivative (**2e**), while the cleavage of **2b** and **2c** is endothermic. In agreement with these computational predictions, no monomeric phosphinoboranes can be found in the reaction of NHC^{dipp} with **2b** and **2c** (Scheme 2). The parent poly(phosphinoborane) **2a** is cleaved (72 h in boiling toluene) resulting in the formation of $\text{H}_2\text{PBH}_2\text{NHC}^{\text{dipp}}$ (**5a**). According to the ^{31}P NMR, **5a** is formed in a 65 % yield, along with two other compounds, which could not be separated or identified. Alternatively, **5a** can be synthesized by a LB exchange adding NHC^{dipp} to

H₂PBH₂NMe₃ in boiling toluene (see the Supporting Information). Some cleavage of the polymer **2e** by NHC^{dipp} is detected (72 h in boiling toluene), but no monomeric phosphinoborane is formed.



Scheme 2: Depolymerization of poly(phosphinoboranes) (yield in parentheses).

The experiments revealed that for the cleavage of polymeric materials strong Lewis bases are needed. The strong NHC^{Me} is able to cleave monosubstituted polymers [R¹HPBH₂]_n (R₁ = ^tBu (**2c**), Ph (**2e**)) and the parent compound [H₂PBH₂]_n (**2a**). However, due to the insolubility of **2a**, its cleavage requires higher temperatures and prolonged reaction times. Since NHC^{Me} is thermally unstable,^[23] the prolonged heating results in its partial thermal destruction and low yield of **4a** (5%). In this case, the thermally stable NHC^{dipp} performs much better (65% conversion of **2a** to **5a**).

In contrast to the report of *Manners et al.*,^[17] where the products RHNH₂·NHC were characterized in solution but not isolated in the solid state, we were able to isolate and characterize several NHC-stabilized phosphanylboranes.^[24] The X-ray crystallographic determination of the solid-state structures revealed that all compounds possess P-B single bonds (**4a**: 1.993(2) Å, **4c**: 1.988(2) Å, **5a**: 1.990(2) Å) and C-B single bonds (**4a**: 1.597(3) Å, **4c**: 1.599(3) Å, **5a**: 1.593(2) Å) (Figure 1).

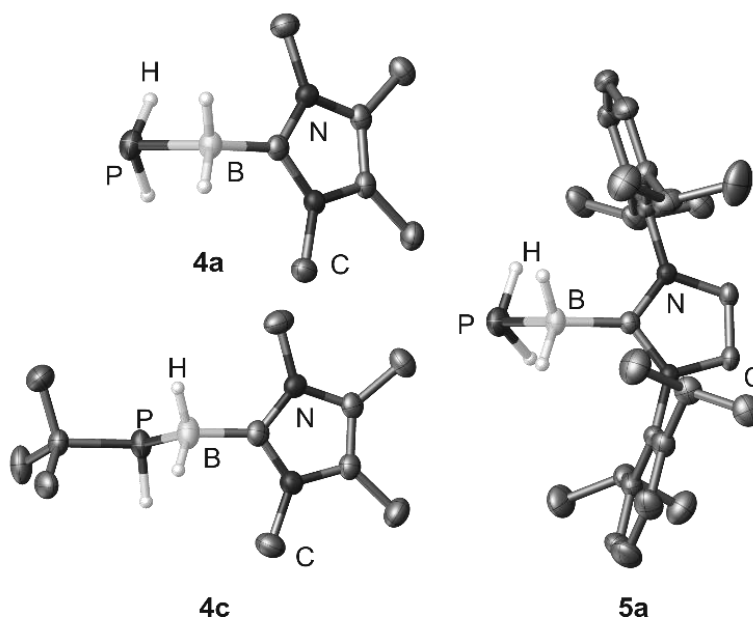


Figure 1: Molecular structures of $\text{H}_2\text{PBH}_2\text{NHC}^{\text{Me}}$ (**4a**), $t\text{BuHPBH}_2\text{NHC}^{\text{Me}}$ (**4c**) and, $\text{H}_2\text{PBH}_2\text{NHC}^{\text{dipp}}$ (**5a**) in the solid state. Thermal ellipsoids are drawn with 50% probability. Hydrogen atoms bonding to carbon are omitted for clarity. Selected bond lengths [Å] and angles [°]: **4a**: P–B 1.993(2), B–C 1.597(3), C–B–P 109.66(12); **4c**: P–B 1.988(2), B–C 1.599(3), C–B–P 106.31(9), **5a**: P–B 1.990(2), B–C 1.593(2), C–B–P 111.94(12).

4.3 Conclusion

In summary, it was shown that linear poly(phosphinoboranes) can be cleaved by strong LBs to form the corresponding monomeric phosphanylboranes. However, the depolymerization reaction depends not only on the basicity of the LB but also on its thermal stability. The solubility and stability of the poly(phosphinoboranes), influenced by the substitution patterns, also play an important role. Computations predict that other thermally stable NHCs, such as 1,3-bis-*tert*-butylimidazol-2-ylidene (NHC^{tBu}) and 1,3-bis[2,6-bis(diphenylmethyl)-4-methylphenyl]imidazole-2-ylidene ($\text{NHC}^{\text{Ph*}}$), should also exothermically cleave **2a** and **2e**.^[25] The expansion of the new recycling strategies for other polymers will be explored in the future.

4.4 References

- [1] a) M. Liang, I. Manners, *J. Am. Chem. Soc.* **1991**, *113*, 4044–4045; b) H. R. Allcock, *Chem. Mater.* **1994**, *6*, 1476–1491; c) C. H. Honeyman, I. Manners, C. T. Morrissey, H. R. Allcock, *J. Am. Chem. Soc.* **1995**, *117*, 7035–7036; d) R. D.

- Archer, *Inorganic and Organometallic Polymers*, Wiley-VCH, New York, **2001**;
- e) I. Manners, *Angew. Chem. Int. Ed. Engl.* **1996**, *35*, 1602–1621; *Angew. Chem.* **1996**, *108*, 1712–1731; f) S. J. S. Clarson, J. A. Semlyen, *Siloxane Polymers*, Prentice Hall, Englewood Cliffs, **1993**; g) R. H. Neilson, P. Wisian-Neilson, *Chem. Rev.* **1988**, *88*, 541–562; h) R. D. Miller, J. Michl, *Chem. Rev.* **1989**, *89*, 1359–1410; i) R. De Jaeger, M. Gleria, *Prog. Polym. Sci.* **1998**, *23*, 179–276; j) R. West, *J. Organomet. Chem.* **1986**, *300*, 327–346; k) T. Imori, V. Lu, H. Cai, T. D. Tilley, *J. Am. Chem. Soc.* **1995**, *117*, 9931–9940; l) X. He, T. Baumgartner, *RSC Adv.* **2013**, *3*, 11334–11350; m) S. Wilfert, H. Henke, W. Schoefberger, O. Brüggemann, I. Teasdale, *Macromol. Rapid Commun.* **2014**, *35*, 1135–1141; n) W. Cao, Y. Gu, M. Meineck, T. Li, H. Xu, *J. Am. Chem. Soc.* **2014**, *136*, 5132–5137; o) F. Choffat, S. Käser, P. Wolfer, D. Schmid, R. Mezzenga, P. Smith, W. Caseri, *Macromolecules* **2007**, *40*, 7878–7889; p) J. Linshoeft, E. J. Baum, A. Hussain, P. J. Gates, C. Näther, A. Staubitz, *Angew. Chem. Int. Ed.* **2014**, *53*, 12916–12920; *Angew. Chem.* **2014**, *126*, 13130–13134; q) B. W. Rawe, C. P. Chun, D. P. Gates, *Chem. Sci.* **2014**, *5*, 4928–4938; v) A. M. Priegert, B. W. Rawe, S. C. Serin, D. P. Gates, *Chem. Soc. Rev.*, **2016**, *45*, 922–953.
- [2] a) P. J. Fazen, J. S. Beck, A. T. Lynch, E. E. Remsen, L. G. Sneddon, *Chem. Mater.* **1990**, *2*, 96–97; b) F. Jäkle, *Chem. Rev.* **2010**, *110*, 3985–4022; c) H. Kuhtz, F. Cheng, S. Schwedler, L. Böhling, A. Brockhinke, L. Weber, K. Parab, F. Jäkle, *ACS Macro Lett.* **2012**, *1*, 555–559; d) Z. M. Hudson, D. J. Lunn, M. A. Winnik, I. Manners, *Nat. Commun.* **2014**, *5*, 3372; e) A. Lorbach, M. Bolte, H. Li, H.-W. Lerner, M. C. Holthausen, F. Jäkle, M. Wagner, *Angew. Chem. Int. Ed.* **2009**, *48*, 4584–4588; *Angew. Chem.* **2009**, *121*, 4654–4658; f) A. Hübner, Z.-W. Qu, U. Englert, M. Bolte, H.-W. Lerner, M. C. Holthausen, M. Wagner, *J. Am. Chem. Soc.* **2011**, *133*, 4596–4609; g) G. Zhang, G. M. Palmer, M.W. Dewhirst, C. L. Fraser, *Nat. Mater.* **2009**, *8*, 747–751.
- [3] a) E. M. Leitao, T. Jurca, I. Manners, *Nat. Chem.* **2013**, *5*, 817–829; b) G. He, L. Kang, W. T. Delgado, O. Shynkaruk, M. J. Ferguson, R. McDonald, E. Rivard, *J. Am. Chem. Soc.* **2013**, *135*, 5360–5363.
- [4] See, for example: a) A. Staubitz, A. Presa Soto, I. Manners, *Angew. Chem. Int. Ed.* **2008**, *47*, 6212–6215; *Angew. Chem.* **2008**, *120*, 6308–6311; b) A. Staubitz, M. E. Sloan, A. P. M. Robertson, A. Friedrich, S. Schneider, P. J. Gates, J.

- Schmedt auf der G nne, I. Manners, *J. Am. Chem. Soc.* **2010**, *132*, 13332–13345; c) A. N. Marziale, A. Friedrich, I. Klopsch, M. Drees, V. R. Celinski, J. Schmedt auf der G nne, S. Schneider, *J. Am. Chem. Soc.* **2013**, *135*, 13342–13355; d) H. C. Johnson, E. M. Leita, G. R. Whittell, I. Manners, G. C. Lloyd-Jones, A. S. Weller, *J. Am. Chem. Soc.* **2014**, *136*, 9078–9093; e) J. R. Vance, A. P. M. Robertson, K. Lee, I. Manners, *Chem. Eur. J.* **2011**, *17*, 4099–4103; f) R. Dallanegra, A. P. M. Robertson, A. B. Chaplin, I. Manners, A. S. Weller, *Chem. Commun.* **2011**, *47*, 3763–3765; g) H. C. Johnson, A. S. Weller, *Angew. Chem. Int. Ed.* **2015**, *54*, 10173–10177; *Angew. Chem.* **2015**, *127*, 10311–10315.
- [5] a) M. E. Bluhm, M. G. Bradley, R. Butterick III, U. Kusari, L. G. Sneddon, *J. Am. Chem. Soc.* **2006**, *128*, 7748–7749; b) D. W. Himmelberger, C. W. Yoon, M. E. Bluhm, P. J. Carroll, L. G. Sneddon, *J. Am. Chem. Soc.* **2009**, *131*, 14101–14110; c) L. G. Sneddon, M. G. L. Mirabelli, A. T. Lynch, P. J. Fazen, K. Su, J. S. Beck, *Pure & Appl. Chem.* **1991**, *63*, 407–410; d) T. Wideman, P. J. Fazen, K. Su, E. E. Remsen, G. A. Zank, L. G. Sneddon, *Appl. Organometal. Chem.* **1998**, *12*, 681–693.
- [6] See, for example: a) H. Dorn, R. A. Singh, J. A. Massey, J. M. Nelson, C. A. Jaska, A. J. Lough, I. Manners, *J. Am. Chem. Soc.* **2000**, *122*, 6669–6678; b) H. Dorn, J. M. Rodezno, B. Brunnhofer, E. Rivard, J. A. Massey, I. Manners, *Macromolecules* **2003**, *36*, 291–297; c) T. J. Clark, J. M. Rodezno, S. B. Clendenning, S. Aouba, P. M. Brodersen, A. J. Lough, H. E. Ruda, I. Manners, *Chem. Eur. J.* **2005**, *11*, 4526–4534; d) S. Pandey, P. L nnecke, E. Hey-Hawkins, *Eur. J. Inorg. Chem.* **2014**, 2456–2465; e) D. Jacquemin, C. Lambert, E. A. Perpete, *Macromolecules* **2004**, *37*, 1009–1015; f) A. Sch fer, T. Jurca, J. R. Vance, K. Lee, V. A. Du, M. F. Haddow, G. R. Whittell, I. Manners, *Angew. Chem. Int. Ed.* **2015**, *54*, 4836–4841; *Angew. Chem.* **2015**, *127*, 4918–4923; g) J.-M. Denis, H. Forintos, H. Szelke, L. Toupet, T.-N. Pham, P.-J. Madec, A.-C. Gaumont, *Chem. Commun.* **2003**, 54–55.
- [7] a) Electronegativities on the Pauling scale, B = 2.04, N = 3.04, P = 2.19; W. M. Haynes, ed., *CRC Handbook of Chemistry and Physics, 95th Edition (Internet Version 2015)*, CRC Press/Taylor and Francis, Boca Raton, FL, **2015**; b) Z. Liu, T. B. Marder, *Angew. Chem. Int. Ed.* **2008**, *47*, 242–244; *Angew. Chem.* **2007**,

- 120, 248-250; c) A. Staubitz, A. P. M. Robertson, M. E. Sloan, I. Manners, *Chem. Rev.* **2010**, *110*, 4023-4078.
- [8] a) A. Ledoux, P. Larini, Ch. Boisson, V. Monteil, J. Raynaud, E. Lacote, *Angew. Chem. Int. Ed.* **2015**, *54*, 15744–15749; *Angew. Chem.* **2015**, *127*, 15970–15975; b) M. J. D. Bosdet, W. E. Piers, T. S. Sorensen, M. Parvez, *Angew. Chem. Int. Ed.* **2007**, *46*, 4940-4943; *Angew. Chem.* **2007**, *119*, 5028-5031; c) M. Terrones, J. M. Romo-Herrera, E. Cruz-Silva, F. Lopez-Urias, E. Munoz-Sandoval, J. J. Velazquez-Salazar, H. Terrones, Y. Bando, D. Goldberg, *Mater. Today*, **2007**, *10*, 30-38; d) X. Wang, Y. Xie, Q. Guo, *Chem. Commun.* **2003**, 2688-2689; e) T. Lorenz, M. Crumbach, T. Eckert, A. Lik, H. Helten, *Angew. Chem. Int. Ed.* **2017**, *56*, 2780-2784; *Angew. Chem.* **2017**, *129*, 2824-2828; f) O. Ayhan, T. Eckert, F. A. Plamper, H. Helten, *Angew. Chem. Int. Ed.* **2016**, *55*, 13321-13325; *Angew. Chem.* **2016**, *128*, 13515-13519 g) A. W. Baggett, F. Guo, B. Li, S.-Y. Liu, F. Jäkle, *Angew. Chem. Int. Ed.* **2015**, *54*, 11191-11195; *Angew. Chem.* **2015**, *127*, 11343-11347.
- [9] H. Dorn, R. A. Singh, J. A. Massey, A. J. Lough, I. Manners, *Angew. Chem. Int. Ed.* **1999**, *38*, 3321 – 3323; *Angew. Chem.* **1999**, *111*, 3540–3543.
- [10] a) M. A. Huertos, A. S. Weller, *Chem. Commun.* **2012**, *48*, 7185–7187; b) M. A. Huertos, A. S. Weller, *Chem. Sci.* **2013**, *4*, 1881–1888; c) T. N. Hooper, M. A. Huertos, T. Jurca, S. D. Pike, A. S. Weller, I. Manners, *Inorg. Chem.* **2014**, *53*, 3716–3729; d) H. C. Johnson, T. N. Hooper, A. S. Weller, *Top. Organomet. Chem.* **2015**, *49*, 153–220.
- [11] C. Thoms, C. Marquardt, A. Y. Timoshkin, M. Bodensteiner, M. Scheer, *Angew. Chem. Int. Ed.* **2013**, *52*, 5150-5154; *Angew. Chem.* **2013**, *125*, 5254-5259.
- [12] a) C. Marquardt, T. Jurca, K.-C. Schwan, A. Stauber, A. V. Virovets, G. R. Whittell, I. Manners, M. Scheer, *Angew. Chem. Int. Ed.* **2015**, *54*, 13782–13786; *Angew. Chem.* **2015**, *127*, 13986–13991; b) A. Stauber, T. Jurca, C. Marquardt, M. Fleischmann, M. Seidl, G. R. Whittell, I. Manners, M. Scheer, *Eur. J. Inorg. Chem.* **2016**, 2684–2687.
- [13] a) K. Schwan, A. Timoshkin, M. Zabel, M. Scheer, *Chem. Eur. J.* **2006**, *12*, 4900–4908; b) C. Marquardt, A. Adolf, A. Stauber, M. Bodensteiner, A. V. Virovets, A.Y. Timoshkin, M. Scheer, *Chem. Eur. J.* **2013**, *19*, 11887–11891.
- [14] a) C. Marquardt, C. Thoms, A. Stauber, G. Balazs, M. Bodensteiner, M. Scheer, *Angew. Chem. Int. Ed.* **2014**, *53*, 3727–3730; *Angew. Chem.* **2014**, *126*, 3801–

- 3804; b) C. Marquardt, T. Kahoun, A. Stauber, G. Balázs, M. Bodensteiner, A. Y. Timoshkin, M. Scheer, *Angew. Chem. Int. Ed.* **2016**, *55*, 14828–14832; *Angew. Chem. Int. Ed.* **2016**, *55*, 14828–14832; c) C. Marquardt, G. Balázs, J. Baumann, A. V. Virovets, M. Scheer, *Chem. Eur. J.* **2017**, *23*, 11423–11429.
- [15] a) F. Thomas, S. Schulz, M. Nieger, *Eur. J. Inorg. Chem.* 2001, 161–166, b) S. Schulz, M. Nieger, *J. Chem. Crystallogr.* **2011**, *41*, 349–352.
- [16] a) M. Kapitein, M. Balmer, C. von Hänisch, *Z. Anorg. Allg. Chem.* **2016**, *22*, 1275–1281, b) M. Kapitein, M. Balmer, C. von Hänisch, *Phosphorus Sulfur Silicon Relat. Elem.* **2016**, *191*, 641–644.
- [17] N. E. Stubbs, T. Jurca, E. M. Leitao, C. H. Woodall, I. Manners, *Chem. Commun.* **2013**, 49, 9098–9100.
- [18] C. Marquardt, O. Hegen, M. Hautmann, G. Balázs, M. Bodensteiner, A. V. Virovets, A. Y. Timoshkin, M. Scheer, *Angew. Chem. Int. Ed.* **2015**, *54*, 13122–13125; *Angew. Chem.* **2015**, *127*, 13315–13318.
- [19] a) A. K. Swarnakar, M. J. Ferguson, R. McDonald, E. Rivard, *Dalton Trans.* **2017**, 46, 1406–1412; b) A. K. Swarnakar, C. Hering-Junghans, M. J. Ferguson, R. McDonald, E. Rivard, *Chem. Sci.* **2017**, *8*, 2337–2343; c) A. K. Swarnakar, C. Hering-Junghans, K. Nagata, M. J. Ferguson, R. McDonald, N. Tokitoh, E. Rivard, *Angew. Chem. Int. Ed.* **2015**, *54*, 10666–10669; *Angew. Chem.* **2015**, *127*, 10812–10816; d) M. R. Momeni, L. Shulman, E. Rivard, A. Brown, *Phys. Chem. Chem. Phys.* **2015**, *17*, 16525–16535; e) P. Lummis, M. R. Momeni, M. W. Lui, R. McDonald, M. J. Ferguson, M. Miskolzie, A. Brown, E. Rivard, *Angew. Chem. Int. Ed.* **2014**, *53*, 9347–9351; *Angew. Chem.* **2014**, *126*, 9501–9505; f) E. Rivard, *Dalton Trans.* **2014**, 43, 8577–8586; g) S. M. I. Al-Rafia, A. C. Malcolm, R. McDonald, M. J. Ferguson, E. Rivard, *Chem. Comm* **2012**, 48, 1308–1310; h) S. M. I. Al-Rafia, A. C. Malcolm, M. J. Ferguson, R. McDonald, E. Rivard, *Angew. Chem. Int. Ed.* **2011**, *50*, 8354–8357; *Angew. Chem.* **2011**, *123*, 8504–8507; i) S. M. I. Al-Rafia, A. C. Malcolm, S. K. Liew, E. Rivard, *J. Am. Chem. Soc.* **2011**, *133*, 777–779; j) K. Thimer, I. Al-Rafia, M. J. Ferguson, R. McDonald, E. Rivard, *Chem. Commun.* **2009**, 7119–7122.
- [20] a) Y. Wang, G. H. Robinson, *Inorg. Chem.* **2014**, *53*, 11815–11832; b) Y. Wang, G. H. Robinson, *Dalton Trans.* **2012**, 41, 337–345; c) Y. Wang, G. H. Robinson, *Inorg. Chem.* **2011**, *50*, 12326–12337; d) R. C. Fischer, P. P. Power, *Chem.*

- Rev.* **2010**, *110*, 3877–3923; e) Y. Wang, M. Chen, Y. Xie, P. Wei, H. F. Schaefer III, P. von R. Schleyer, G. H. Robinson, *Nat. Chem.* **2015**, *7*, 509–513.
- [21] In all our experiments, we used the high molecular weight polymer $[\text{PhHPBH}_2]_n$ in mixture with crosslinked/low molecular weight $[\text{PhHPBH}_2]_n$ as it is obtained as the product of the polymerization process (see ref. [6a]). While the signal for the first one disappears completely during the depolymerization reactions, the signal for the higher aggregated/crosslinked polymer retains, indicating that it is stable against the reaction with NHC^{Me} .
- [22] In agreement with the results reported in ref. [12a], **2c** is obtained as a mixture of the high molecular weight polymer $[\text{tBuHPBH}_2]_n$ (~80%) with the crosslinked/low molecular weight polymer $[\text{tBuHPBH}_2]_n$ (circa 20%). The crosslinked polymer is obviously stable against the reaction with NHC^{Me} .
- [23] See Supporting Information section 1.4.
- [24] Sometimes alternative approaches were used, cf. Supporting Information.
- [25] See the Supporting Information section 3.

4.5 Supporting Information

Experimental Section: Synthetic Procedures

General Techniques: All manipulations were performed under an atmosphere of dry nitrogen or argon using standard Glovebox and Schlenk techniques. Solvents are degassed and purified by standard procedures. The compounds NHC^{Me} ,^[1] NHCdipp ,^[2] IBH_2NMe_3 ,^[3] $\text{PhP}(\text{SiMe}_3)_2$,^[4] $[\text{PPhH-BH}_2]_n$,^[5] $(\text{C}_6\text{F}_5)_3\text{GaEt}_2\text{O}$,^[6] $[\text{H}_2\text{PBH}_2]_n$, $[\text{Ph}_2\text{PBH}_2]_n$, $[\text{tBuHPBH}_2]_n$,^[7] $(\text{C}_6\text{F}_5)_3\text{EPhHP-BH}_2\text{NMe}_3$ (E = B, Ga),^[9] and $\text{H}_2\text{PBH}_2\text{NMe}_3$ ^[11] were prepared according to the literature procedures. $[\text{LiPPh}(\text{SiMe}_3)\text{tmeda}]_2$ was synthesized based on a slightly modified procedure.^[8] DMAP and $n\text{BuLi}$ was used as received. MeOH was dried over molecular sieve, tmeda over CaH_2 and distilled.

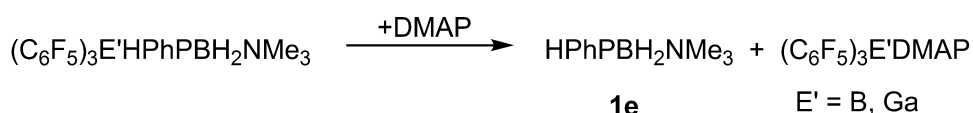
The NMR spectra are recorded on either a Avance 300 (^1H : 300.132 MHz, ^{31}P : 121.468 MHz, ^{19}F : 282.404 MHz) or Avance 400 spectrometer (^1H : 400.13 MHz, ^{31}P : 161.976 MHz, ^{11}B : 128.378 MHz, $^{13}\text{C}\{^1\text{H}\}$: 100.623 MHz) with δ [ppm] referenced to external SiMe_4 (^1H , ^{13}C), H_3PO_4 (^{31}P) or $\text{BF}_3\cdot\text{Et}_2\text{O}$ (^{11}B). IR spectra are measured on a DIGILAB (FTS 800) FT-IR spectrometer. All mass spectra are recorded on a

ThermoQuest Finnigan TSQ 7000 (ESI-MS) or a Finnigan MAT 95 (FD-MS and EI-MS). The C, H, N analyses are measured on an Elementar Vario EL III apparatus.

1. Syntheses of LB stabilized phosphanylboranes and thermal instability of NHC^{Me} in solution

1.1 Syntheses of HPhPBH₂NMe₃ (1e) and polymerization by thermolysis to [HPhPBH₂]_n (2e)

First attempts involved the cleavage of the LA from the LA/LB-stabilized compounds (C₆F₅)₃E'PhHPBH₂NMe₃ (E' = B, Ga).^[9] While the reaction of (C₆F₅)₃BPhHPBH₂NMe₃ with DMAP (4-dimethylaminopyridine, Scheme SI1), even with a large excess, did not lead to a full conversion, a complete elimination of the LA was achieved in the reaction of (C₆F₅)₃GaPhHPBH₂NMe₃ with a stoichiometric amount of DMAP. The phosphanylborane HPhPBH₂NMe₃ (**1e**) and (C₆F₅)₃GaDMAP are obtained as reaction products (Scheme 2). Unfortunately **1e** could not be separated from (C₆F₅)₃GaDMAP ((C₆F₅)₃GaDMAP, was also synthesized selectively to ensure a correct assignment of the signals of the reaction products) and be isolated as a pure product due to similar solubility. EI mass spectrometry and NMR spectroscopy studies clearly indicate the formation of HPhPBH₂NMe₃ (**1e**).



Scheme SI1: Generation of **1e** via displacement of the LA.

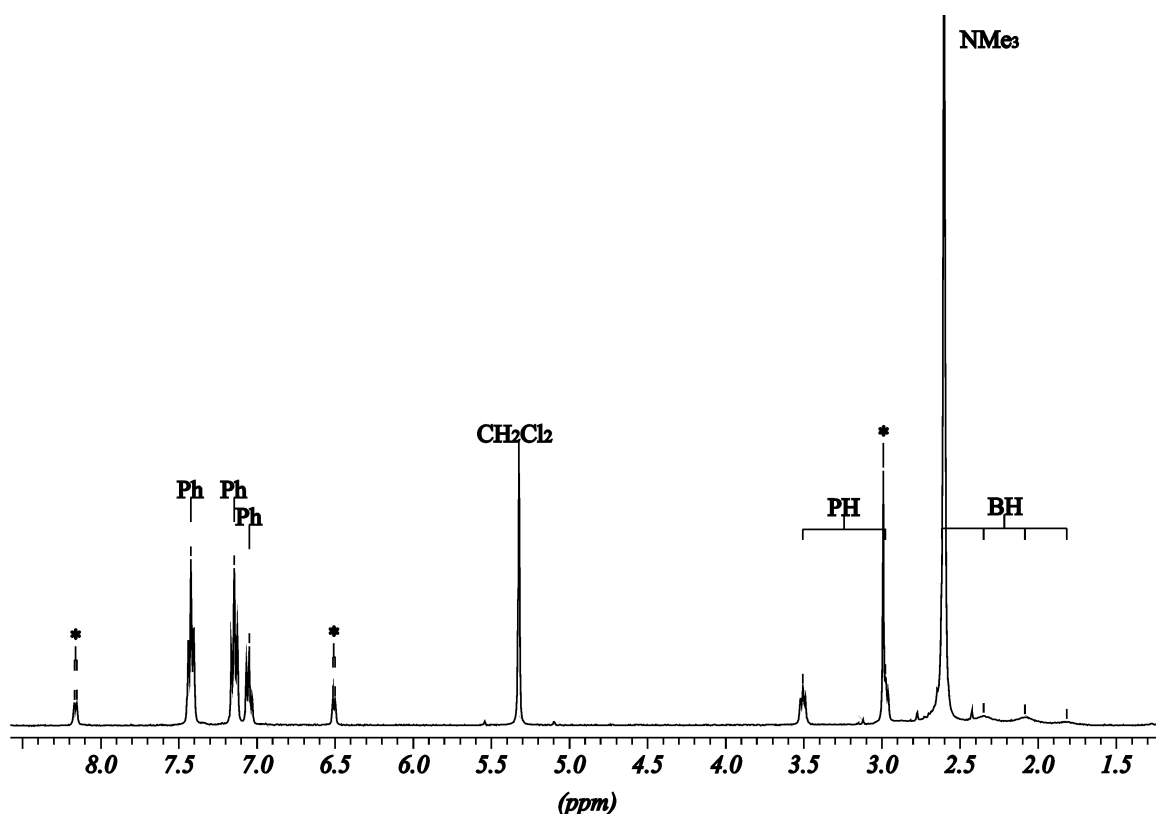
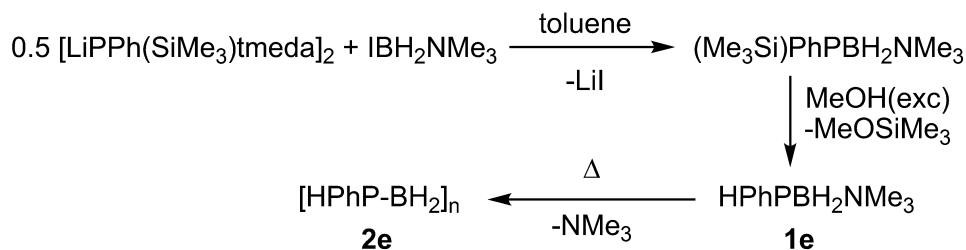


Figure S11: ^1H NMR spectrum of **1e** and $(\text{C}_6\text{F}_5)_3\text{GaDMP}$ in CD_2Cl_2 . All signals marked with * are assigned to $(\text{C}_6\text{F}_5)_3\text{GaDMP}$ (the signals are shifted about 0.1 to 0.2 ppm in comparison to the pure substance).

For a selective generation of **1e** a metathesis route by the reaction of $[\text{LiPPh}(\text{SiMe}_3)\text{tmeda}]_2$ (tmeda = N,N,N,N-Tetramethylethane-1,2-diamine, $\text{C}_6\text{H}_{16}\text{N}_2$) with IBH_2NMe_3 proved to be the best procedure (Scheme S12). During the synthesis and isolation of **1e** the stabilizing NMe_3 seems to be too loosely attached to the boron atom, because partly elimination and subsequent polymerization occurs yielding $[\text{HPhPBH}_2\text{B}]_n$ (**2e**, Scheme S12).



Scheme S12: Synthesis of **1e** and subsequent polymerization to $[\text{HPhPBH}_2]_n$ (**3e**).

However, a small amount of crystals could be isolated and the proposed structure of **1e** was confirmed by single crystal X-ray structure analysis and ^1H , ^{11}B and ^{31}P NMR

spectroscopy. The best yield of **1e** was obtained if the reaction is done in toluene as a solvent and at low temperatures (Scheme SI2).

Single crystals are obtained by storing a solution of **1e** in *n*-hexane at -28°C . In the solid state the P–B distance is 1.955(2) Å, corresponding to a P–B single bond (Figure SI3).

Heating a solution of HPhPBH₂NMe₃ (**1e**) in toluene to 100°C affords a product, which shows overlapping signals in the ³¹P NMR spectrum (Figure SI2), similar to those reported for the thermolytic, uncatalyzed dehydrocoupling of H₂PhPBH₃.^[10] Generation of the free phosphine H₂PhP is also observed. Poorly resolved peaks in the ³¹P NMR spectrum suggest a mixture of low molecular weight polymers; therefore the reaction mixture was not characterized any further.

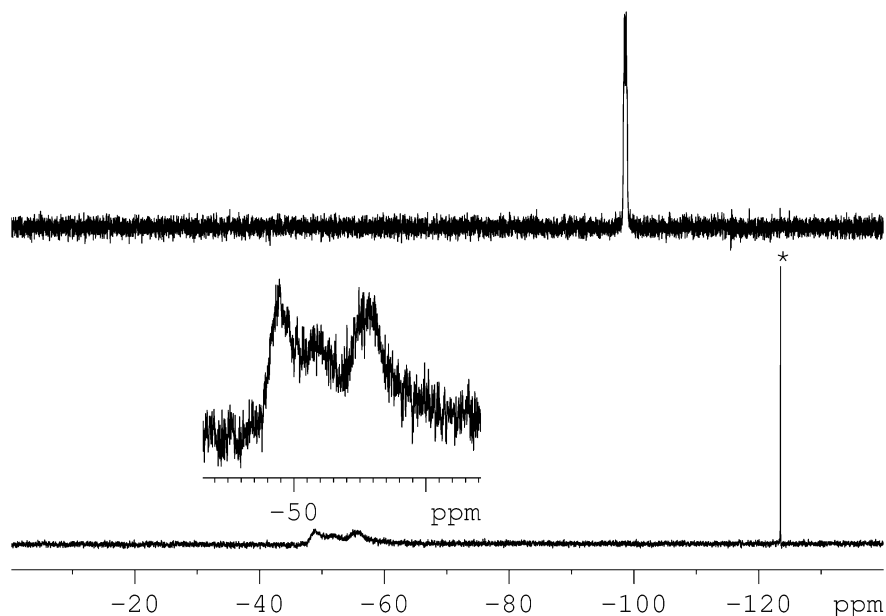


Figure SI2: ³¹P{¹H} NMR spectra of HPhPBH₂·NMe₃ (top) and [HPhPBH₂]_n (bottom) in C₆D₆ at r.t. * = PhPH₂.

1.2 Alternative syntheses of H₂PBH₂NHC (NHC = NHC^{Me}, NHC^{dipp})

Heating a solution of H₂PBH₂NMe₃ (**1a**) and NHC^{Me} in toluene to 110°C yields the monomeric phosphanylborane H₂PBH₂NHC^{Me} (**4a**). After 2h no H₂PBH₂NMe₃ (**1a**) can be observed in the ³¹P-NMR-spectrum of the reaction mixture. H₂PBH₂NHC^{Me} (**4a**) is with 97% the main product. The unidentified side product is precipitated by addition of *n*-hexane. Crystals of **4a** are obtained by slow evaporation of a 2:1-mixture of *n*-hexane/toluene as colorless blocks (Figure SI5).

Heating a solution of $\text{H}_2\text{PBH}_2\text{NMe}_3$ (**1a**) and NHC^{dipp} in toluene to 110°C yields the monomeric phosphanylborane $\text{H}_2\text{PBH}_2\text{NHC}^{\text{dipp}}$ (**5a**). After 1h no $\text{H}_2\text{PBH}_2\text{NMe}_3$ (**1a**) can be observed in the ^{31}P -NMR-spectrum of the reaction mixture. $\text{H}_2\text{PBH}_2\text{NHC}^{\text{dipp}}$ (**5a**) is with 90% the main product. **5a** crystallizes by storing a saturated benzene solution at r.t. as colorless blocks (Figure S17).

1.3 Thermal instability of NHC^{Me} at prolonged heating in solution

15 mg of fresh sublimed NHC^{Me} were dissolved in toluene- d^8 and heated in a NMR tube at 100°C . At the beginning, after 24h, after 48h and after 72h a ^1H -NMR-spectrum was measured. In addition, a second NMR tube with fresh sublimed NHC^{Me} in toluene- d^8 was measured after 6d stirring at r.t.

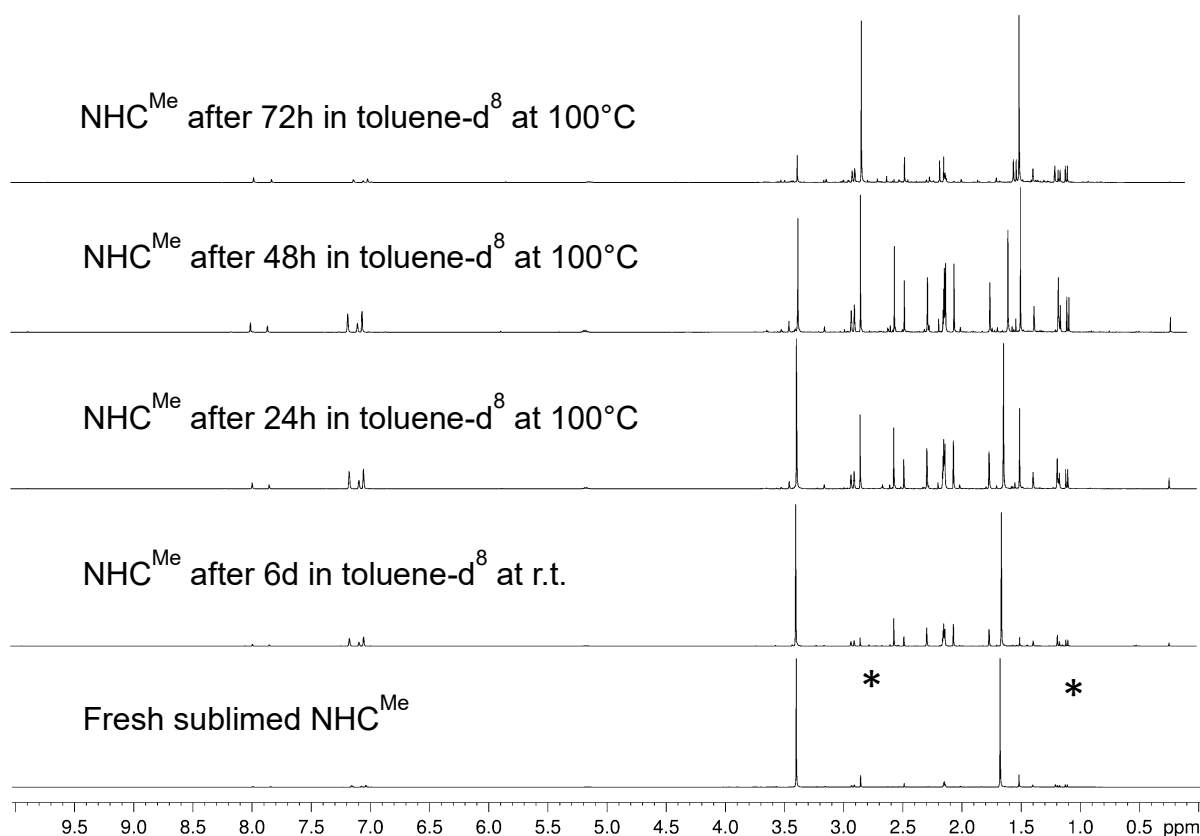


Figure S13: ^1H -NMR spectra of NHC^{Me} in toluene- d^8 after 24h, 48h and after 72h at 100°C (Signals generated by the methyl groups of NHC^{Me} are marked with *). For comparison the ^1H -NMR spectra of fresh sublimed NHC^{Me} and after 6d in toluene- d^8 are also pictured.

The signals produced by decomposition products increase at prolonged heating compared to the signals generated by the methyl groups of NHC^{Me} . This shows the thermal instability of NHC^{Me} in solution.

1.4 Synthesis of $(\text{C}_6\text{F}_5)_3\text{GaDMP}$ and $\text{PhHPBH}_2\text{NMe}_3$

Direct synthesis of $(\text{C}_6\text{F}_5)_3\text{GaDMP}$: $(\text{C}_6\text{F}_5)_3\text{GaEt}_2\text{O}$ (300 mg, 0.465 mmol) and DMAP (57 mg, 0.467 mmol) were dissolved in 15 mL of toluene. The reaction mixture was stirred overnight (18 h) at room temperature. The solution was concentrated under reduced pressure to about 2 – 3 mL and stored at 4°C. After one day $(\text{C}_6\text{F}_5)_3\text{GaDMP}$ crystallizes as colourless prisms. The crystals were filtered off the solution and washed with *n*-hexanes (3 × 7 mL). Yield: 302 mg (94 %).

^1H NMR (CD_2Cl_2 , 25°C): δ = 3.12 (s, 6H, NMe_2), 6.64 (d, $^3J_{\text{H,H}}$ = 8 Hz, 2H, H-C(2)), 7.97 (d, $^3J_{\text{H,H}}$ = 7 Hz, 2H, H-C(3)).

^{19}F NMR (CD_2Cl_2 , 25°C): δ = -123.3 (m, *o*-F, 6F, $\text{Ga}(\text{C}_6\text{F}_5)_3$), -154.5 (t, $^3J_{\text{F,F}}$ = 19 Hz, *p*-F, 3F, $\text{Ga}(\text{C}_6\text{F}_5)_3$), -162.2 (m, *m*-F, 6F, $\text{Ga}(\text{C}_6\text{F}_5)_3$).

ESI-MS (MeCN): m/z = 692 (11 %, $[\text{M}]^+$), 570 (8 %, $[(\text{C}_6\text{F}_5)_3\text{Ga}]^+$), 525 (17 %, $[\text{M}-\text{C}_6\text{F}_5]^+$), 403 (24 %, $[\text{Ga}(\text{C}_6\text{F}_5)_2]^+$), 168 (35 %, $[\text{C}_6\text{F}_5\text{H}]^+$), 122 (100 %, $[\text{DMAP}]^+$).

Synthesis of $\text{PhHPBH}_2\text{NMe}_3$ (1e)

Route via elimination of LA

$(\text{C}_6\text{F}_5)_3\text{GaPhHPBH}_2\text{NMe}_3$ (300 mg, 0.4 mmol) was dissolved in 10 mL CH_2Cl_2 and then DMAP (49 mg, 0.4 mmol) was added. The solution was stirred overnight (18 h) at room temperature and the solvent was removed under reduced pressure. $\text{PhHPBH}_2\text{NMe}_3$ (**1e**) and $(\text{C}_6\text{F}_5)_3\text{GaDMP}$ was obtained in equal quantities. Attempts to purify and isolate **1e** from $(\text{C}_6\text{F}_5)_3\text{GaDMP}$ failed.

^1H NMR (CD_2Cl_2 , 25°C): δ = 2.21 (q, br, $^1J_{\text{B,H}}$ = 107 Hz, 2H, BH), 2.60 (s, 9H, NMe_3), 3.24 (dt, $^1J_{\text{P,H}}$ = 212 Hz, $^3J_{\text{H,H}}$ = 6.4 Hz, 1H, PH), 7.05 (t, $^3J_{\text{H,H}}$ = 7 Hz, *p*-Ph, 1H), 7.14 (t, $^3J_{\text{H,H}}$ = 7 Hz, *m*-Ph, 2H), 7.42 (m, *o*-Ph, 2H).

^{31}P NMR (CD_2Cl_2 , 25°C): δ = -99.7 (d, $^1J_{\text{P,H}}$ = 212 Hz, PH).

$^{31}\text{P}\{^1\text{H}\}$ NMR (CD_2Cl_2 , 25°C): δ = -99.7 (s, PH,).

^{11}B NMR (CD_2Cl_2 , 25°C): δ = -4.7 (td, $^1J_{\text{B,H}}$ = 107 Hz, $^1J_{\text{B,P}}$ = 32 Hz, BH_2).

$^{11}\text{B}\{^1\text{H}\}$ NMR (CD_2Cl_2 , 25°C): δ = -4.7 (d, $^1J_{\text{B,P}}$ = 32 Hz, BH_2).

$^{13}\text{C}\{^1\text{H}\}$ NMR (CD_2Cl_2 , 25°C): δ = 53.3 (d, $^2J_{\text{C,P}}$ = 6 Hz, NMe_3), 125.3 (s, *m*-C, Ph), 128.2 (d, $^3J_{\text{C,P}}$ = 5 Hz, *p*-C, Ph), 132.8 (d, $^2J_{\text{C,P}}$ = 12.5 Hz, *o*-C, Ph).

EI-MS (70 eV, toluene): m/z = 181 (4 %, $[\text{M}]^+$).

Metathesis route

Alternative synthesis of [LiPPh(SiMe₃)tmeda]₂: 13.7 g (53.9 mmol) PhP(SiMe₃)₂ and 11 mL tmeda are dissolved in 60 mL of THF. Under vigorous stirring 34.25 mL of a 1.6 M (54.8 mmol) solution of *n*BuLi in *n*-hexane are added dropwise and the solution is stirred for 12h. After removal of all volatiles under reduced pressure the resulting [LiPPh(SiMe₃)tmeda]₂ is washed 2 times with 10 mL of toluene and 2 times with 10 mL of *n*-hexane. The solid is dried under reduced pressure.

Yield of [LiPPh(SiMe₃)tmeda]₂: 14.6 g (89%). All analytical data are in accordance with the previously published values.

Synthesis of (Me₃Si)PhPBH₂NMe₃: A solution of 199 mg (1.0 mmol) IBH₂NMe₃ in 10 mL of toluene is added to a solution of 304 mg (0.5 mmol) [LiPPh(SiMe₃)tmeda]₂ in 10 mL toluene at –40°C. The reaction mixture is stirred for 18 h upon slow warming to r.t.. The solution is filtrated through diatomaceous earth and all volatiles are removed under reduced pressure and a white wax is obtained.

³¹P NMR (C₆D₆, 25 °C): δ = –129.5 (m, br).

³¹P{¹H} NMR (C₆D₆, 25 °C): δ = –129.5 (m, br).

¹¹B NMR (C₆D₆, 25 °C): δ = –3.5 (m).

¹¹B{¹H} NMR (C₆D₆, 25 °C): δ = –3.5 (m).

Synthesis of PhHPBH₂NMe₃ (1e): A solution of 199 mg (1.0 mmol) IBH₂NMe₃ in 10 mL of toluene is added to a suspension of 304 mg (0.5 mmol) [LiPPh(SiMe₃)tmeda]₂ in 10 mL toluene at –40°C. After stirring the reaction mixture for 18 h at r.t. the solution is filtered through diatomaceous earth and is cooled to –40°C. 0.5 mL of methanol are added and the mixture is stirred for further 18 h. All volatiles are removed under reduced pressure and the remaining solid is extracted with *n*-hexane (3 x 50 mL) and filtered through diatomaceous earth. The solution is concentrated under reduced pressure. Storing the solution at 3°C affords a small amount of crystals as colourless needles.

¹H NMR (C₆D₆, 25 °C): δ = 1.80 (s, NMe₃), 2.61 (m, BH₂), 3.66 (dt, ¹J_{H,P} = 210 Hz, ³J_{H,H} = 6 Hz, PH), 7.02 (m, 1H, *p*-Ph), 7.15 (m, 2H, *m*-Ph), 7.73 (m, 2H, *o*-Ph).

³¹P NMR (C₆D₆, 25 °C): δ = –98.5 (dm, br, ¹J_{H,P} = 210 Hz).

³¹P{¹H} NMR (C₆D₆, 25 °C): δ = –98.5 (m).

^{11}B NMR (C_6D_6 , 25 °C): $\delta = -4.0$ (dt, $^1J_{\text{B,P}} = 35$ Hz, $^1J_{\text{B,H}} = 107$ Hz).

$^{11}\text{B}\{^1\text{H}\}$ NMR (C_6D_6 , 25 °C): $\delta = -4.0$ (d, $^1J_{\text{B,P}} = 35$ Hz).

FTIR (KBr): $\tilde{\nu} = 3065$ (w, CH), 3059 (w, CH), 2994 (w, CH), 2942 (w, CH), 2916 (w, CH), 2383 (s, B-H), 2296 (sh), 2264 (m, P-H), 1951 (w), 1584 (m), 1480 (vs), 1463 (s), 1447 (m), 1431 (m), 1404 (m), 1385 (w), 1251 (s), 1158 (m), 1123 (s), 1074 (s), 1062 (s), 1030 (m), 1011 (m), 980 (m), 952 (w), 907 (w), 887 (m), 851 (s), 745 (s), 738 (s), 696 (s), 575 (w), 551 (w), 480 (w), 462 (w).

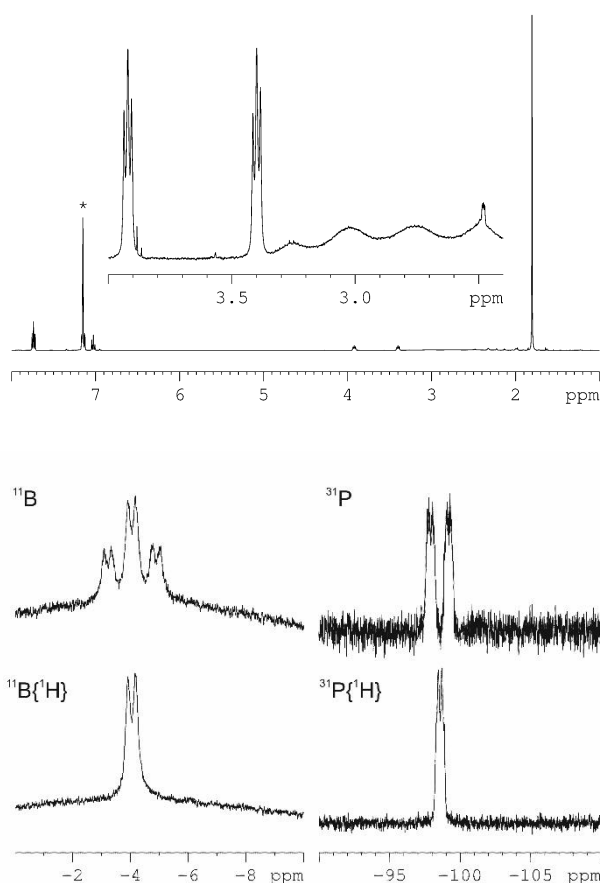


Figure S14: (left) ^1H NMR spectrum of **1e** in C_6D_6 at r.t., (right) ^{11}B and ^{31}P NMR spectra of **1e** in C_6D_6 at r.t. * = solvent C_6D_6 .

1.5 Synthesis of 4a and 5a by LB exchange

Synthesis of $\text{H}_2\text{PBH}_2\text{NHC}^{\text{Me}}$ (4a): To a solution of 110 mg (1.05 mmol) $\text{H}_2\text{PBH}_2\text{NMe}_3^{[11]}$ in 20 mL toluene 194 mg (1.56 mmol) NHC^{Me} is added in portions at 0°C. The reaction mixture was refluxed for 2 h, and the still hot solution was filtered through diatomaceous earth. The reaction mixture is layered with *n*-hexane. The mother liquor containing 4a is decanted. All volatiles including NHC^{Me} are removed

under reduced pressure. The remaining solid is washed with *n*-hexane and dried under reduced pressure. **4a** is obtained as colorless powder. The product is not given in analytical purity. Yield: 42 mg (25%)

^1H NMR (CD_2Cl_2 , 25°C): δ = 0.85 (dt, $^1J_{\text{P,H}} = 178$ Hz, $^3J_{\text{H,H}} = 7$ Hz, 2H, PH), 1.56 (q, $^1J_{\text{B,H}} = 94$ Hz, 2H, BH), 2.11 (s, CCH_3 , 6H, NHC^{Me}), 3.57 (s, NCH_3 , 6H, NHC^{Me}).

^{31}P NMR (CD_2Cl_2 , 25°C): δ = -211.7 (tq, $^1J_{\text{B,P}} = 24$ Hz, $^1J_{\text{P,H}} = 178$ Hz, PH).

$^{31}\text{P}\{^1\text{H}\}$ NMR (CD_2Cl_2 , 25°C): δ = -211.7 (q, $^1J_{\text{B,P}} = 24$ Hz).

^{11}B NMR (CD_2Cl_2 , 25°C): δ = -34.9 (dt, $^1J_{\text{B,P}} = 24$ Hz, $^1J_{\text{B,H}} = 94$ Hz).

$^{11}\text{B}\{^1\text{H}\}$ NMR (CD_2Cl_2 , 25°C): δ = -34.9 (d, $^1J_{\text{B,P}} = 24$ Hz).

$^{13}\text{C}\{^1\text{H}\}$ NMR (CD_2Cl_2 , 25°C): δ = 8.8 (s, CCH_3 , NHC^{Me}), 32.4 (NCH_3 , NHC^{Me}), 123.9 (s, $\text{C}=\text{C}$, NHC^{Me}).

FTIR (KBr): $\tilde{\nu}$ = 2943 (m, CH), 2923 (w, CH), 2863 (w, CH), 2365 (vs, br, 2 sh, BH), 2308 (m, PH), 2274 (s), 2259 (vs), 1659 (m), 1477 (m), 1455 (w), 1438 (m), 1398 (m), 1369 (w), 1261 (w), 1230 (w), 1207 (w), 1167 (m), 1115 (m, br), 1077 (m), 1007 (s, sh), 967 (m), 808 (w, br), 740 (w), 673 (m), 584 (w), 485 (w), 466 (w) cm^{-1} .

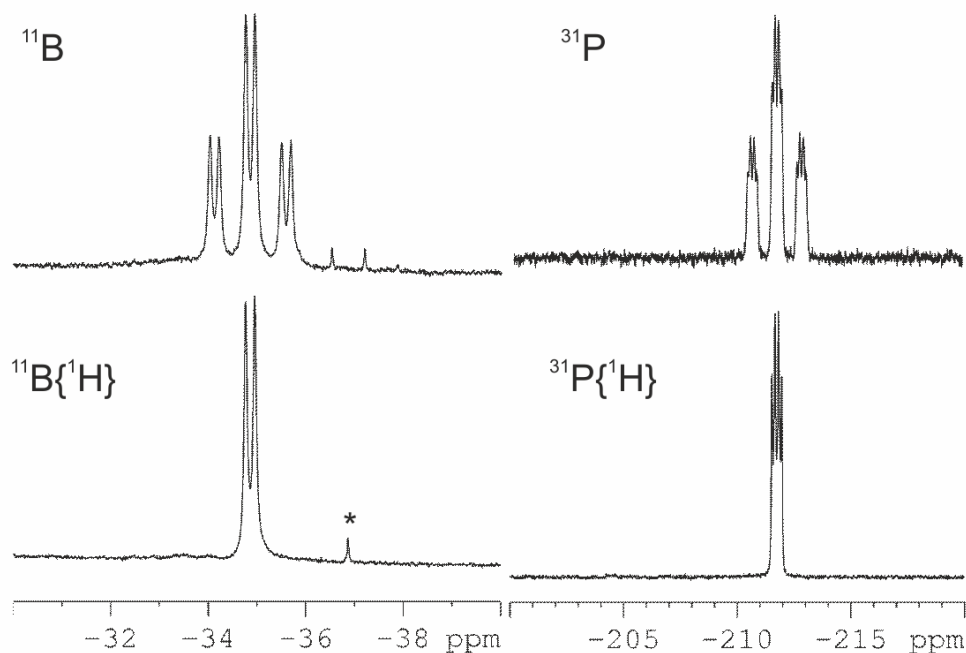


Figure S15: ^{11}B and ^{31}P NMR spectra of **4a** in C_6D_6 at r.t. * = $\text{H}_3\text{BNHC}^{\text{Me}}$ [12]

Synthesis of $\text{H}_2\text{PBH}_2\text{NHC}^{\text{dipp}}$ (5a**):** To a solution of 118 mg (1.12 mmol) $\text{H}_2\text{PBH}_2\text{NMe}_3$ in 50 mL toluene 436 mg (1.12 mmol) NHC^{dipp} is added in portions at 0°C . The reaction mixture was refluxed for 1 h. After cooling down the solution was filtered through

diatomaceous earth. All volatiles are removed under reduced pressure and the remaining solid is washed with *n*-hexane and dried under reduced pressure. **5a** is obtained as colorless powder. The product is contaminated by $\text{H}_3\text{BNHC}^{\text{dipp}}$.

Yield: 317 mg (65%)

^1H NMR (C_6D_6 , 25°C): δ = 1.02 (d, $^3J_{\text{HH}} = 7$ Hz, 12H; CH-**Me**), 1.24 (br d, $^1J_{\text{PH}} = 177$ Hz, 2H; PH_2), 1.37 (d, $^3J_{\text{HH}} = 7$ Hz, 12H; CH-**Me**), 1.87 (br q, $^1J_{\text{BH}} = 96$ Hz, 2H; BH_2), 2.77 (sept, $^3J_{\text{HH}} = 7$ Hz, 4H; CH-**Me**), 6.41 (s, 2H; CH=CH), 7.09 (m, 4H; *m*-Ph), 7.22 (m, 2H; *p*-Ph).

^{31}P NMR (C_6D_6 , 25°C): δ = -212.7 (br t, $^1J_{\text{P,H}} = 177$ Hz, PH).

$^{31}\text{P}\{^1\text{H}\}$ NMR (C_6D_6 , 25°C): δ = -212.7 (br s).

^{11}B NMR (C_6D_6 , 25°C): δ = -34.1 (br t, $^1J_{\text{B,H}} = 92$ Hz).

$^{11}\text{B}\{^1\text{H}\}$ NMR (C_6D_6 , 25°C): δ = -34.1 (br, s).

FD-MS (toluene): m/z = 434.4 (100 %, $[\text{M}]^+$).

FTIR (KBr): $\tilde{\nu}$ = 3154 (w, CH), 3070 (w, CH), 3033 (w, CH), 2946 (vs, CH), 2930 (s, CH), 2870 (s, CH), 2761 (w), 2732 (w), 2381 (m br, BH), 2285 (w br, PH), 1681 (w), 1597 (m), 1535 (m), 1468 (s), 1422 (w), 1387 (w), 1366 (w), 1331 (m), 1302 (w), 1269 (m), 1208 (w), 1182 (w), 1163 (w br), 1163 (m), 1062 (s br), 1023 (w), 983 (w), 953 (w), 937 (w), 805 (s), 757 (s), 686 (m) cm^{-1} .

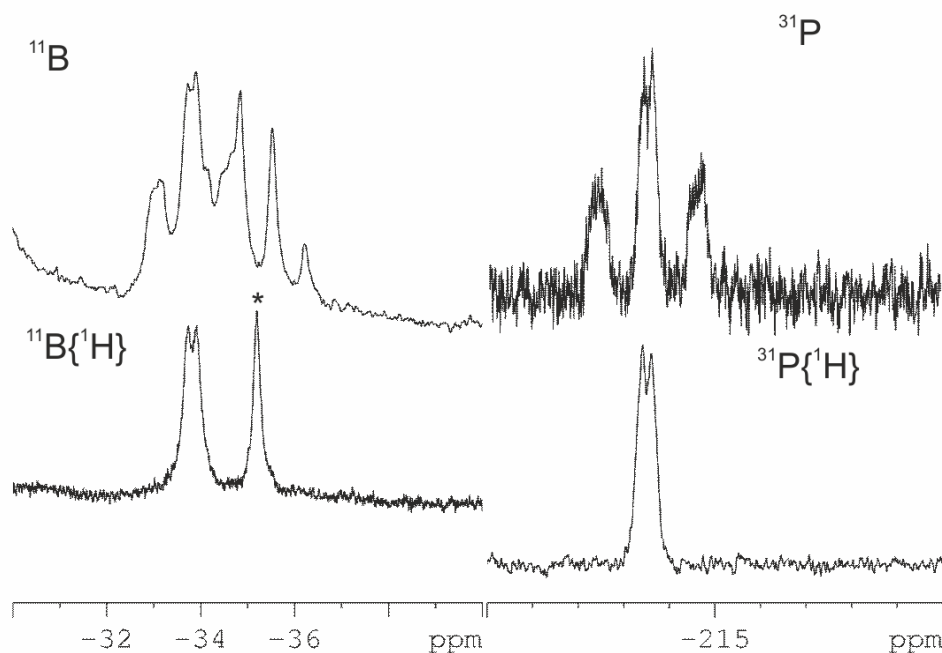


Figure SI6: ^{11}B and ^{31}P NMR spectra of **5a** in C_6D_6 at r.t. * = $\text{H}_3\text{BNHC}^{\text{dipp}}$ [13]

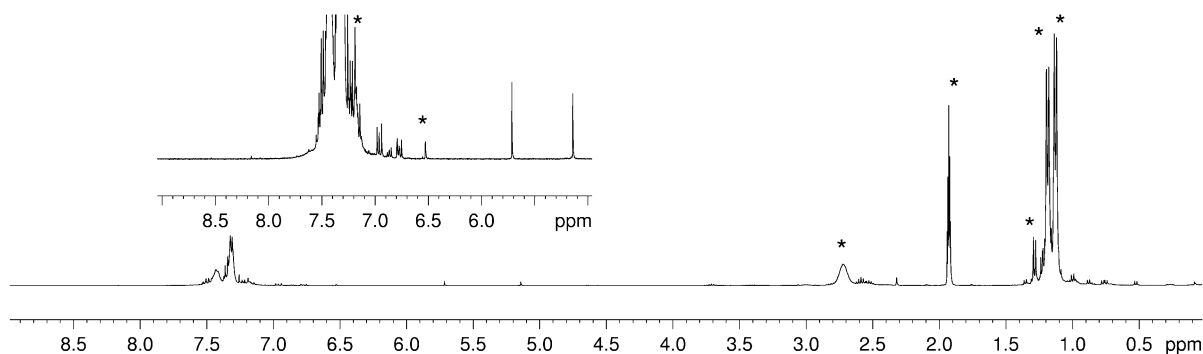


Figure S17: ^1H NMR spectrum of **5a** in C_6D_6 at r.t. * = **5a**

1.6 Depolymerization reactions

Synthesis of PhHPBH₂DMAP (**3e**)

[PhHPBH₂]_n (**2e**, 209 mg, 1.7 mmol) and DMAP (866 mg, 7.1 mmol) were dissolved in 30 mL toluene. The mixture was refluxed for 18 h (spectroscopic yield approximately 25% by ^{31}P NMR) and then filtrated. The NMR shows a mixture of [PhHPBH₂]_n, DMAP and the cleavage product PhHPBH₂DMAP (**3e**). Further purification or separation from DMAP by sublimation, crystallisation or extraction with different solvents failed.

^{31}P NMR (C_6D_6 , 25°C): $\delta = -71.7$ (d, $^1J_{\text{P,H}} = 193$ Hz, PH).

$^{31}\text{P}\{^1\text{H}\}$ NMR (C_6D_6 , 25°C): $\delta = -71.7$ (s, PH).

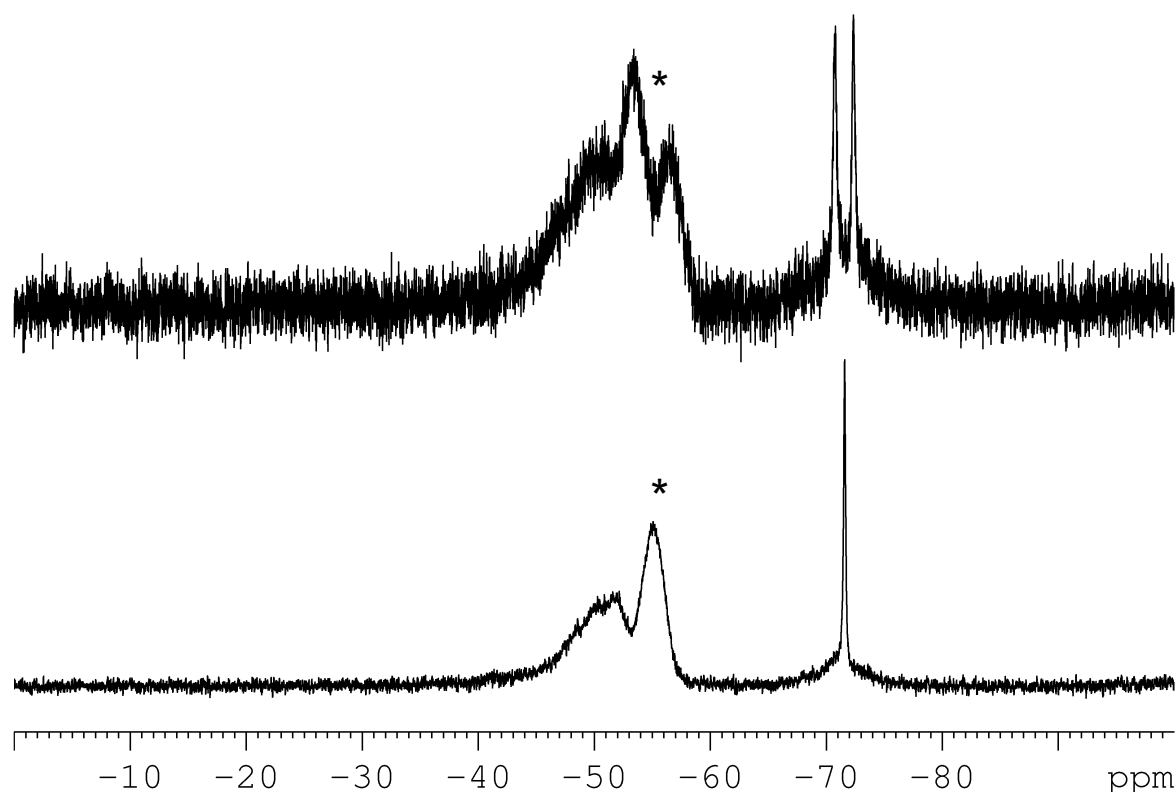


Figure S18: ^{31}P NMR spectra of reaction mixture **1e** and **3e** in C_6D_6 at r.t. * = **2e**

Synthesis of $^t\text{BuHPBH}_2\text{NHC}^{\text{Me}}$ (4c**):** A solution of 161 mg (1.00 mmol) $^t\text{BuHP-BH}_2\text{NMe}_3$ in 5 mL toluene is stirred at 45°C for 3 days. The completeness of the reaction was confirmed by ^{31}P NMR. The resulting solution of $[\text{}^t\text{BuHP-BH}_2]_n$ (**2c**) is added to 124 mg (1.00 mmol) freshly sublimed solid NHC^{Me} . After refluxing the mixture for 3 days (spectroscopic yield approximately 80% by ^{31}P NMR), all volatiles are removed under reduced pressure. $^t\text{BuHPBH}_2\text{NHC}^{\text{Me}}$ (**4c**) is dissolved in 10 mL of *n*-hexane and filtrated. The solution is concentrated under reduced pressure. $^t\text{BuHPBH}_2\text{NHC}^{\text{Me}}$ (**4c**) crystallises at -28°C as colourless needles. After decanting of the supernatant the crystals are dissolved in a minimum of *n*-hexane and recrystallized for 2 more times. The crystals are separated and washed with cold *n*-hexane (-80°C , 3×5 mL). Yield: 65 mg (29 %).

^1H NMR (C_6D_6 , 25°C): $\delta = 1.14$ (s, 6H, C-Me), 1.70 (d, $^3J_{\text{H,P}} = 10$ Hz, 9H, ^tBu), 2.37 (m, BH_2), 2.55 (dm, $^1J_{\text{H,P}} = 173$ Hz, 1H, PH), 3.15 (s, 6H, N-Me).

^{31}P NMR (C_6D_6 , 25°C): $\delta = -63.7$ (d, $^1J_{\text{H,P}} = 173$ Hz, br).

$^{31}\text{P}\{^1\text{H}\}$ NMR (C_6D_6 , 25°C): $\delta = -63.7$ (q, $^1J_{\text{B,P}} = 28$ Hz).

^{11}B NMR (C_6D_6 , 25°C): $\delta = -32.5$ (td, $^1J_{\text{B,H}} = 95$ Hz, $^1J_{\text{B,P}} = 28$ Hz).

$^{11}\text{B}\{^1\text{H}\}$ NMR (C_6D_6 , 25°C): $\delta = -32.5$ (d, $^1J_{\text{B,P}} = 28$ Hz).

$^{13}\text{C}\{^1\text{H}\}$ NMR (C_6D_6 , 25 °C): δ = 7.8 (s, C-Me), 26.6 (d, $^1J_{\text{C,P}}$ = 11 Hz, CMe₃), 32.0 (N-Me), 33.4 (d, $^1J_{\text{C,P}}$ = 6 Hz, C-Me₃), 122.8 (s, C=C), 169.6 (q, $^1J_{\text{C,B}}$ = 52 Hz, CB).

FTIR (KBr): $\tilde{\nu}$ = 2946 (vs, CH), 2929 (vs, CH), 2887 (s, CH), 2850 (s, CH), 2358 (vs, br, BH), 2300 (s, BH), 2245 (s, PH), 2233 (s, PH), 1656 (m), 1471 (s), 1455 (s), 1431 (s), 1441 (s), 1396 (s), 1355 (m), 1231 (w), 1167 (m), 1111 (w), 1016 (m), 997 (m), 953 (m), 873 (m), 820 (m), 780 (w), 715 (w), 604 (w).

EI-MS (toluene): m/z = 57 (9%, [^tBu]⁺), 137 (100%, [BH₂· NHC^{Me}]⁺), 226 (15 %, [M]⁺).

Elemental analysis (%) calculated for C₁₁H₂₄BN₂P: C: 58.36, H: 10.69, N: 12.38; found: C: 58.29, H: 10.65, N: 12.25.

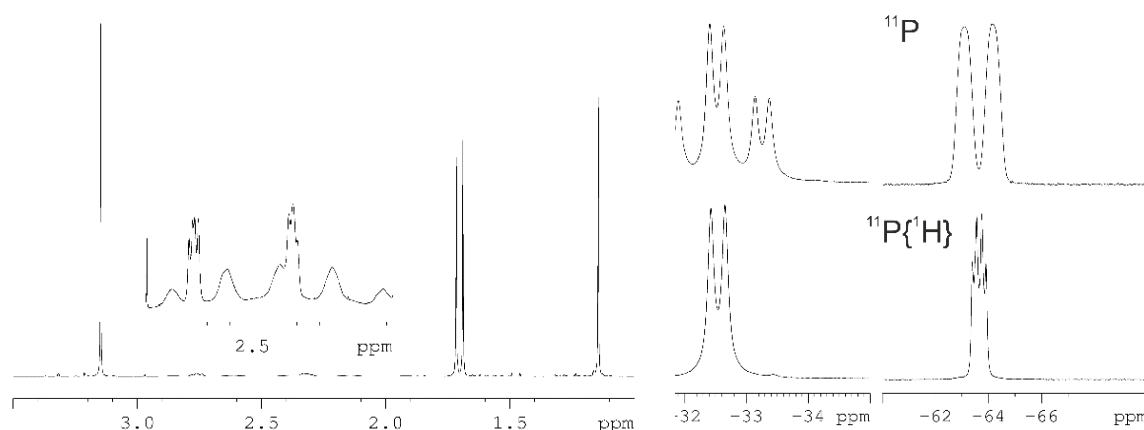


Figure SI9: (left) ^1H NMR spectrum of **4c** in C_6D_6 at r.t., (right) ^{11}B and ^{31}P NMR spectra of **4c** in C_6D_6 at r.t.* = solvent C_6D_6 .

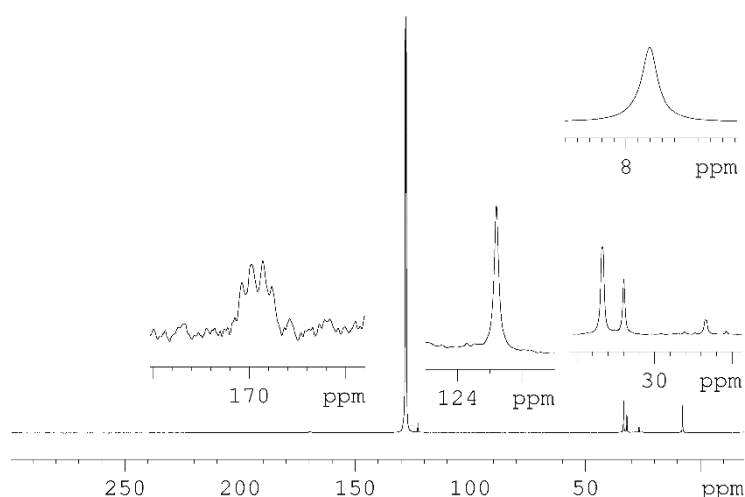


Figure SI10: $^{13}\text{C}\{^1\text{H}\}$ NMR spectrum of **4c** in C_6D_6 at r.t.

Synthesis of PhHPBH₂NHC^{Me} (4e): [PhHP–BH₂]_n (**2e**, 200 mg, 1.6 mmol) was dissolved in 10 mL THF and 1,3,4,5-Tetramethylimidazol-2-yliden (NHC^{Me}) (203 mg, 1.6 mmol) was added. The mixture was refluxed for 1.5 h (spectroscopic yield approximately 40% by ³¹P NMR) and then concentrated under reduced pressure. For purification of **4e** the remaining unreacted polymer was precipitated from vigorously stirred *n*-hexane. **4e** was extracted from hot *n*-hexane and filtered off the precipitated polymer. By cooling the *n*-hexanes solution of **4e** featherlike crystals of **4e** were obtained, which could not be characterised by X-ray diffraction. The product is not obtained analytically pure. Yield: 83 mg (21 %).

¹H NMR (C₆D₆, 25°C): δ = 1.12 (s, CCH₃, 6H, NHC^{Me}), 2.77 (s, NCH₃, 6H, NHC^{Me}), 3.52 (dt, ¹J_{P,H} = 187 Hz, ³J_{H,H} = 7 Hz, 1H, PH), 6.9 – 7.0 (m, 3H, Ph), 7.4 – 7.5 (m, 2H, Ph).

³¹P NMR (C₆D₆, 25°C): δ = –87.8 (d, ¹J_{P,H} = 187 Hz, PH).

³¹P{¹H} NMR (C₆D₆, 25°C): δ = –87.8 (s, PH).

¹¹B NMR (C₆D₆, 25°C): δ = –29.3 (t, ¹J_{B,H} = 98 Hz, BH₂).

¹¹B{¹H} NMR (C₆D₆, 25°C): δ = –29.3 (s, BH₂).

¹³C{¹H} NMR (C₆D₆, 25°C): δ = 8.8 (s, CCH₃, NHC^{Me}), 35.0 (NCH₃, NHC^{Me}), 122.8 (s, C=C, NHC^{Me}), 124.8 (s, *m*-C, Ph), 127.5 (d, ³J_{C,P} = 6 Hz, *p*-C, Ph), 133.7 (d, ²J_{C,P} = 14 Hz, *o*-C, Ph), 167.3 (s, br, BC, NHC^{Me}).

EI-MS (70 eV, toluene): *m/z* = 246 (7 %, [M]⁺), 137 (100 %, [BH₂NHC^{Me}]⁺).

FTIR (C₆D₆): $\tilde{\nu}$ = 2395 (m, BH), 2371 (m, br, BH), 2303 (m, br), 2279 (s, PH), 2249 (m, br), 1942 (w, br), 1739 (m), 1677 (vs), 1576 (m), 1458 (s), 1440 (s), 1421 (s), 1397 (s), 1365 (vs), 1309 (w), 1261 (vs), 813 (s, br), 740 (m), 697 (m), 603 (w), 624 (m), 567 (w), 536 (m) cm^{–1}.

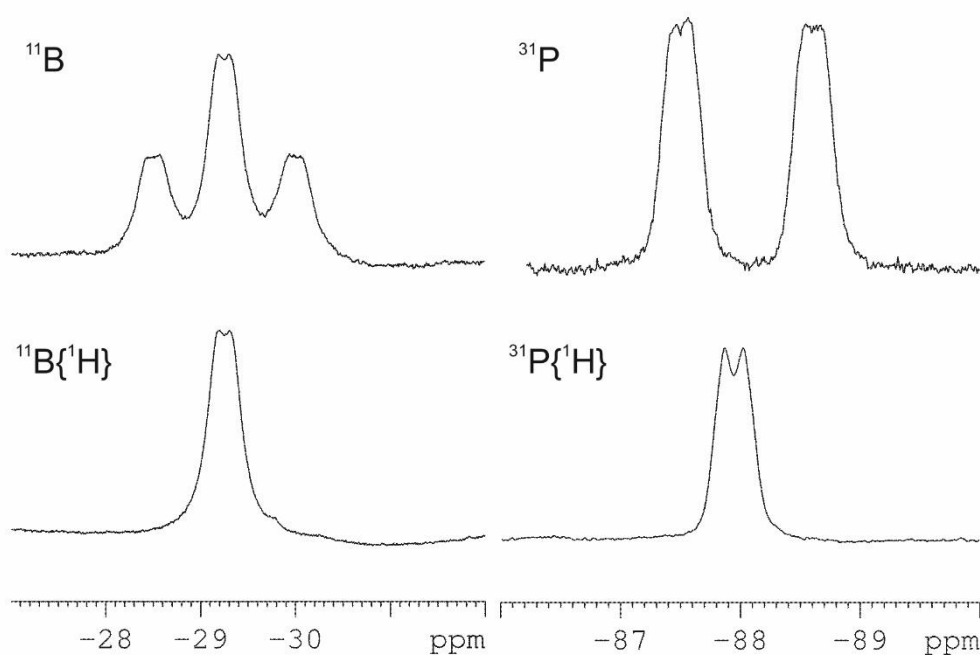


Figure SI11: ^{11}B and ^{31}P NMR spectra of **4e** in C_6D_6 at r.t.

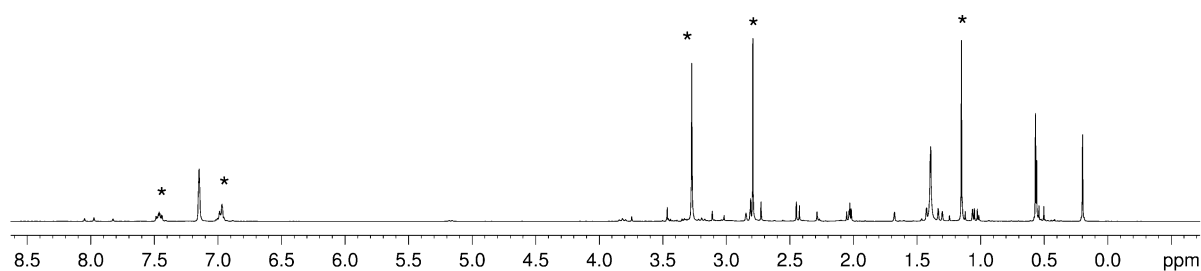


Figure SI12: ^1H NMR spectrum of **4e** in C_6D_6 at r.t. * = **4e**

Depolymerization of $[\text{H}_2\text{PBH}_2]_n$ (**2a**):

A solution of 1.00 mmol **2a** was combined with 1.00 mmol of DMAP in refluxing toluene for 48 h. No conversion was observed, even after addition of excess DMAP and prolonged reaction times.

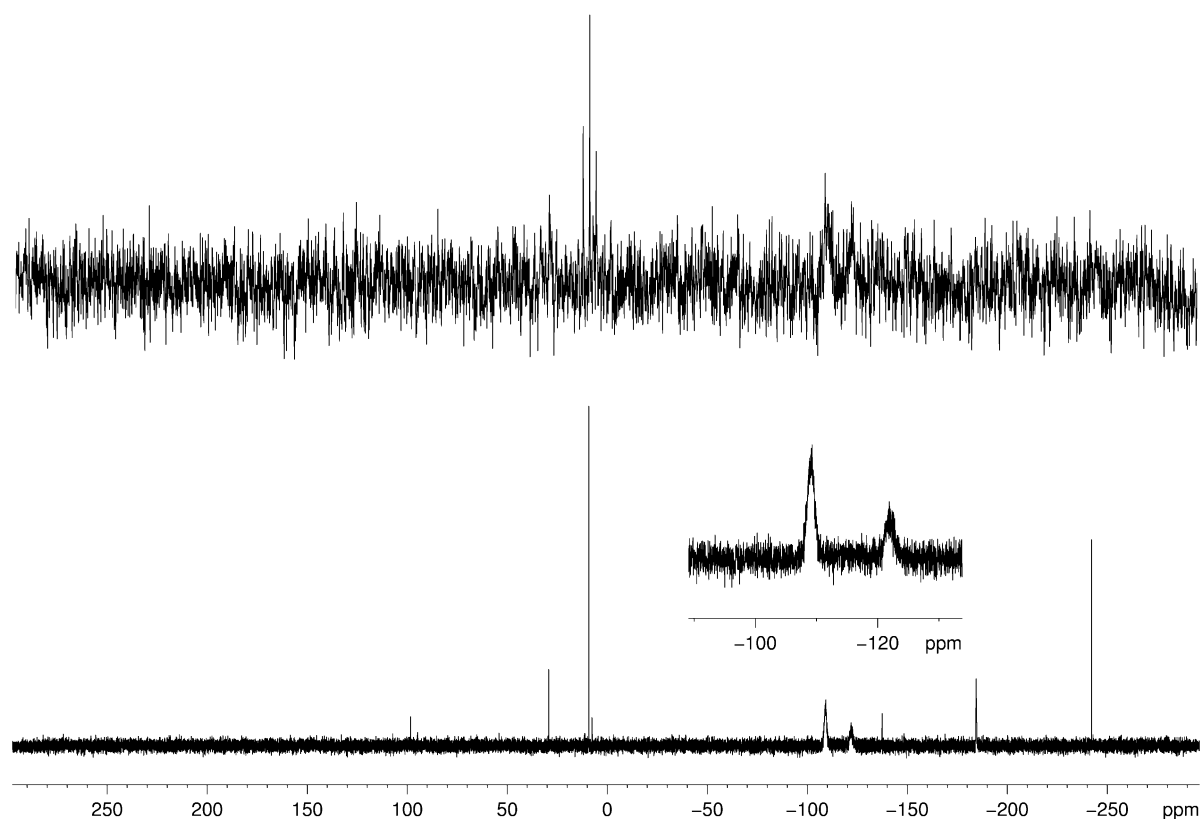


Figure SI13: $^{31}\text{P}\{^1\text{H}\}$ NMR spectrum of **2a** with one equivalent DMAP after 48h in boiling toluene (bottom) and with an excess of DMAP (top) in C_6D_6 at r.t.

A solution of 1.00 mmol **2a** in toluene was reacted with 1.00 mmol of NHC^{Me} in refluxing for 24 h. Addition of excess NHC^{Me} and prolonged reaction times do not lead to higher conversion. According to ^{31}P NMR a reaction occurs (see Figure SI14), but no clean cleavage to **4a** is observed. If the reaction is performed in THF at lower temperatures no conversion is observed.

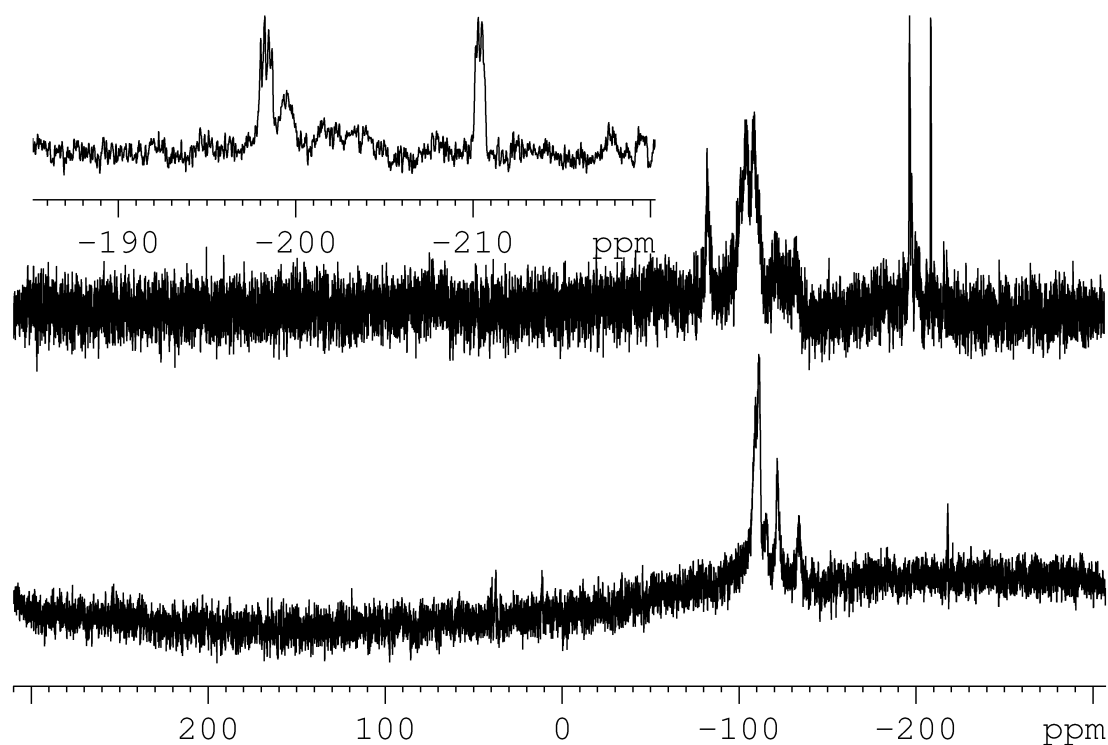


Figure SI14: $^{31}\text{P}\{^1\text{H}\}$ NMR spectrum of **2a** (bottom) and after reaction with NHC^{Me} (top) in C_6D_6 at r.t.

A solution of 0.5 mmol **2a** in DME was reacted with 0.5 mmol NHC^{Me} at 80°C . According to ^{11}B NMR spectroscopy about 15% $\text{H}_2\text{PBH}_2\text{NHC}^{\text{Me}}$ (**4a**) was obtained along with unreacted **2a**.

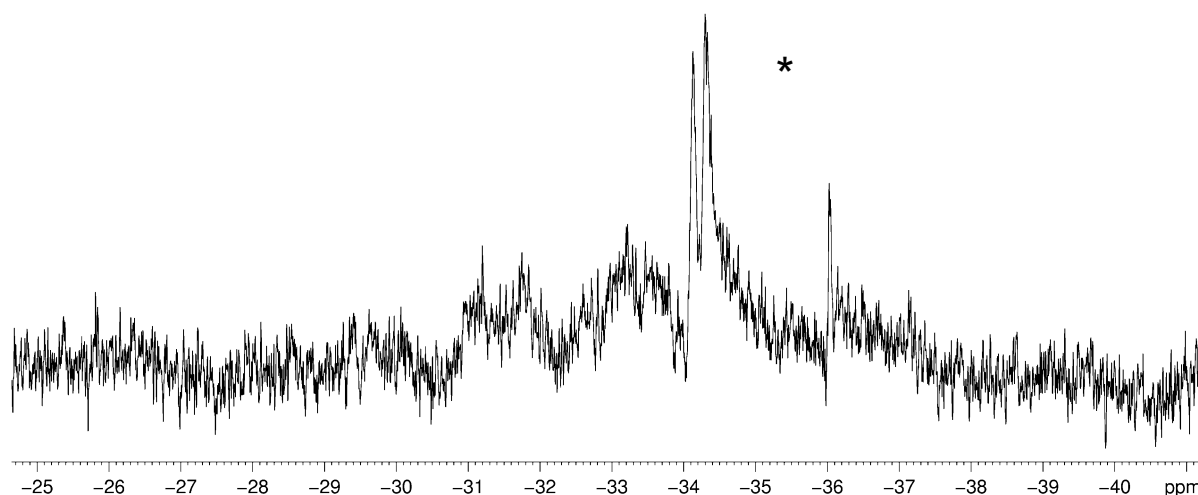


Figure SI15: $^{11}\text{B}\{^1\text{H}\}$ NMR spectrum (C_6D_6 at r. t.) of **2a** after the reaction with NHC^{Me} in DME (* = **4a**)

A solution of 1.00 mmol **2a** in refluxing toluene was reacted with 1.00 mmol of NHC^{dipp} for 96 h. According to ^{31}P NMR spectroscopy 65% $\text{H}_2\text{PBH}_2\text{NHC}^{\text{dipp}}$ (**5a**) was obtained along with unassigned side products. No **2a** could be observed in the ^{31}P NMR spectrum.

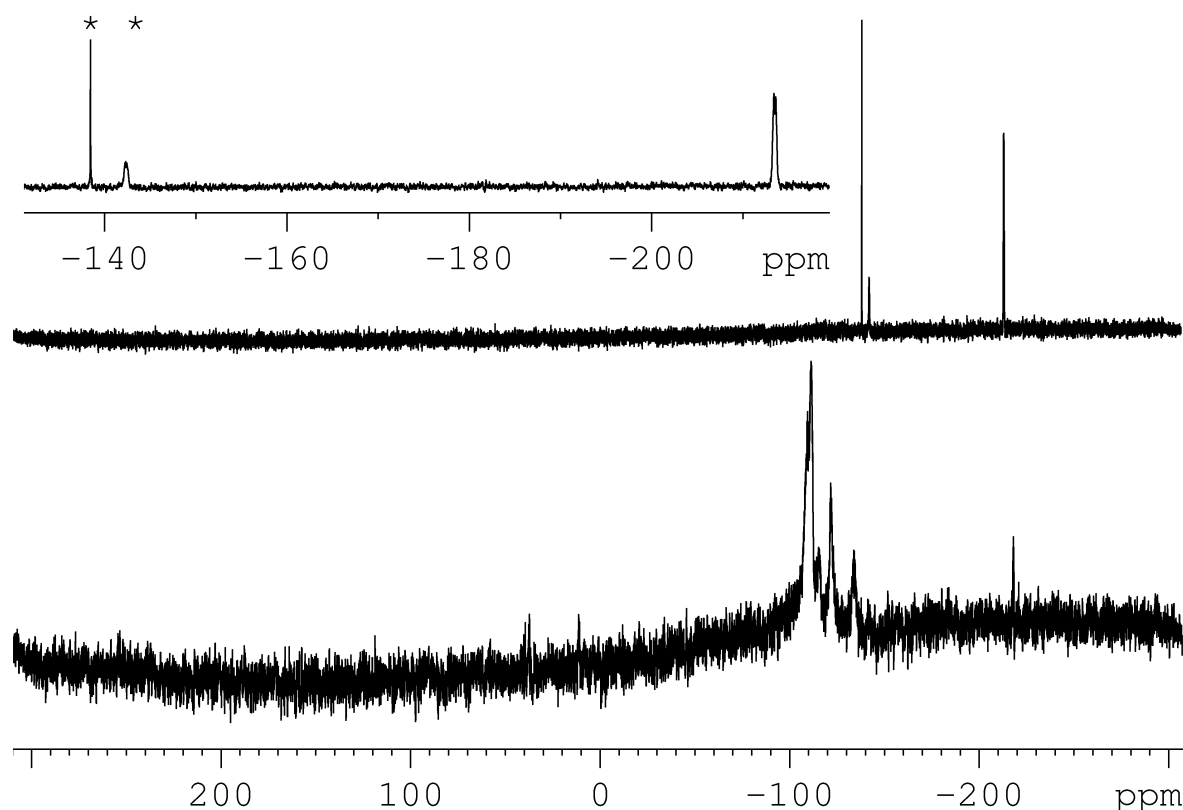


Figure SI16: $^{31}\text{P}\{^1\text{H}\}$ NMR spectrum of **2a** (bottom) and after reaction with NHC^{dipp} (top) in C_6D_6 at r.t.

* = unassigned side products

Depolymerization of $[\text{Ph}_2\text{PBH}_2]_n$ (**2b**):

A solution of 1.00 mmol **2b** was combined with 1.00 mmol of DMAP, NHC^{Me} or NHC^{dipp} , respectively in refluxing toluene for 72 h. No conversion was observed.

Depolymerization of $[\text{'BuHPBH}_2]_n$ (**2c**):

A solution of 1.00 mmol **2c** was combined with 1.00 mmol of DMAP or NHC^{dipp} respectively in refluxing toluene for 72 h. No conversion was observed.

A solution of 1.00 mmol **2c** was reacted with 1.00 mmol of NHC^{Me} in toluene for 72 h. About 80% conversion is observed according to ^{31}P NMR spectroscopy.

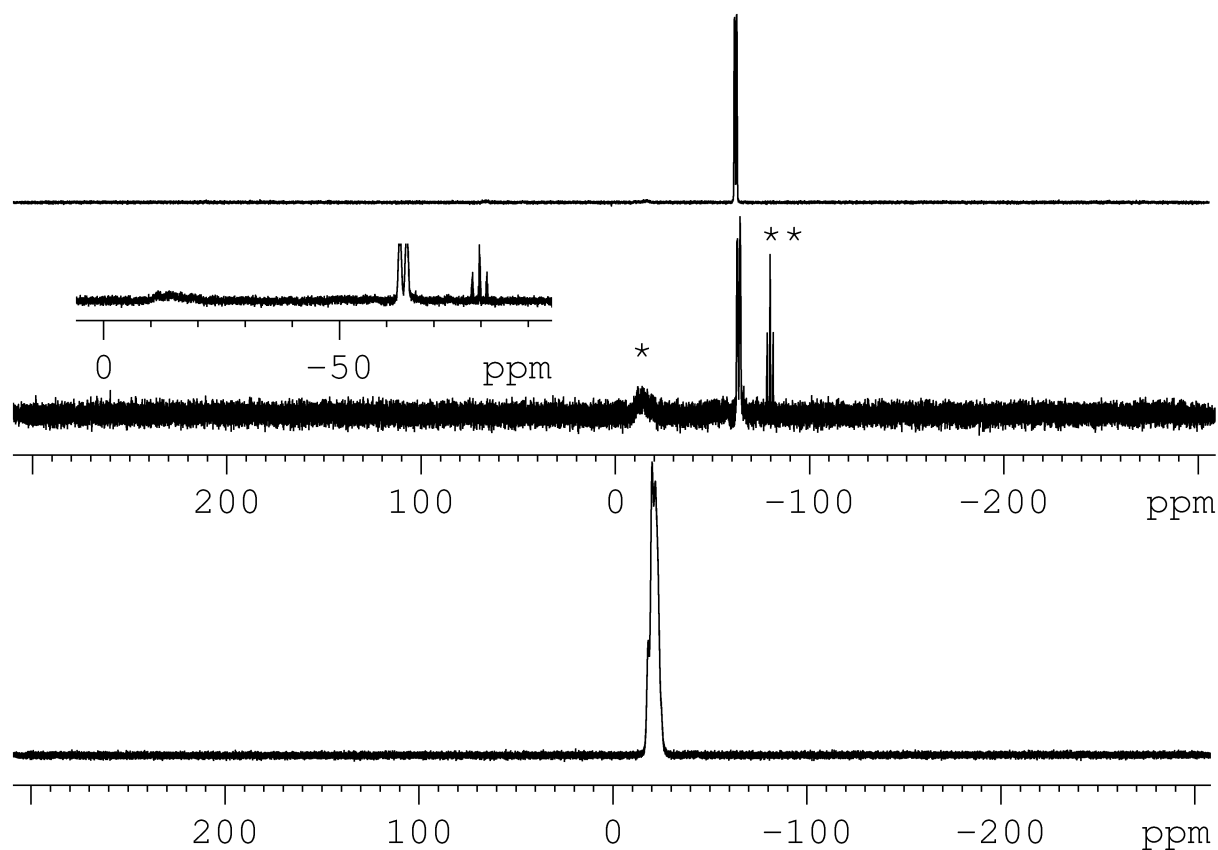


Figure SI17: ^{31}P -NMR spectrum of **2c** (bottom), after reaction with NHC^{Me} (middle), and **4c** after crystallization (top) in C_6D_6 at r.t. * = **2c**, ** = $t\text{-BuPH}_2$

Depolymerization of $[\text{PhHPBH}_2]_n$ (**2e**):

$[\text{PhHPBH}_2]_n$ (**2e**, 209 mg, 1.7 mmol) and DMAP (866 mg, 7.1 mmol) were dissolved in 30 mL toluene. The mixture was refluxed for 18 h (spectroscopic yield approximately 25% by ^{31}P NMR) and then filtrated. The NMR shows a mixture of $[\text{PhHPBH}_2]_n$, DMAP and the cleavage product **3e**. Further purification or separation failed.

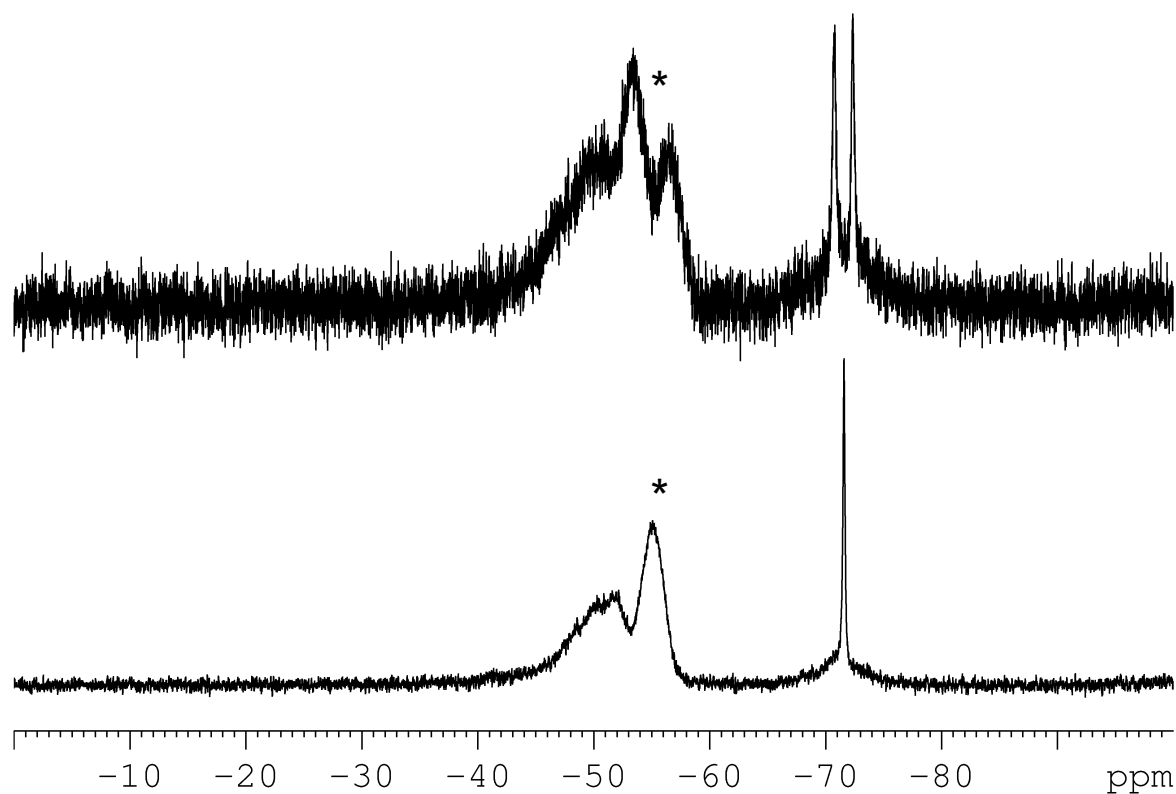


Figure S118: ^{31}P NMR spectra of reaction mixture **1e** and **3e** in C_6D_6 at r.t. * = **2e**

A solution of 1.00 mmol **2e** was reacted with 1.00 mmol of NHC^{dipp} respectively in refluxing toluene for 72 h. Some cleavage of polymer **2e** by NHC^{dipp} is observed, but monomeric phosphinoborane is not formed.

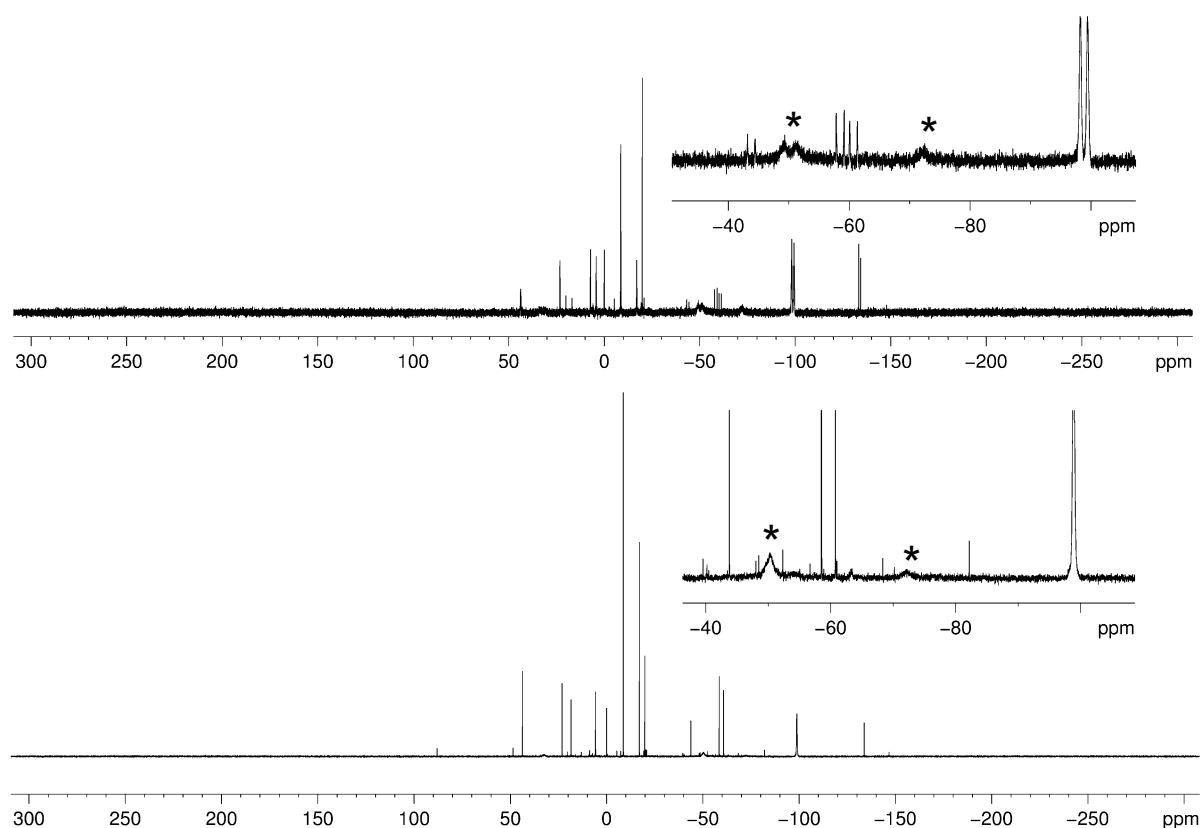


Figure SI19: ^{31}P -NMR spectra of **2e** with NHC^{dipp} after 72h in boiling toluene in C_6D_6 at r.t. * = oligomer/polymer

A solution of 1.6 mmol **2e** was reacted with 1.6 mmol NHC^{Me} in refluxing THF for 1.5 h (spectroscopic yield approximately 40% by ^{31}P NMR). Neither addition of NHC^{Me} nor prolonged reaction times lead to a higher conversion.

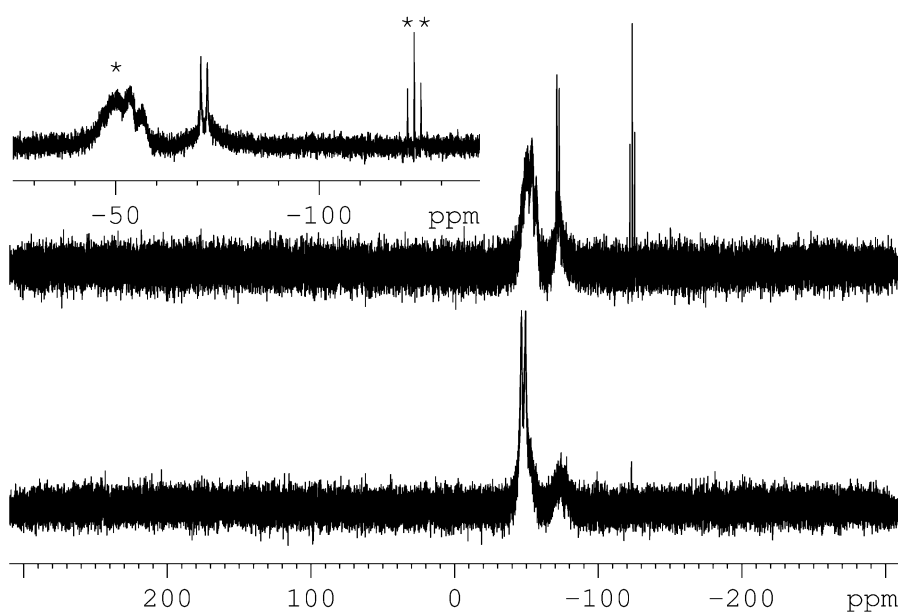


Figure SI20: ^{31}P NMR spectrum of **2e** (bottom), after reaction with NHC^{Me} (top) in C_6D_6 at r.t. * = **2e**, ** = PhPH_2

2. Single crystal X-Ray diffraction experiments

The single crystal X-Ray diffraction experiments were performed on either a Gemini R Ultra CCD diffractometer (**1e**, (C₆F₅)₃GaDMAP, **4a**), a SuperNova A CCD diffractometer (**5a**) or a GV50 diffractometer (**4c**) from Agilent Technologies (formerly Oxford Diffraction) applying Cu- K_{α} radiation ($\lambda = 1.54178 \text{ \AA}$). All measurements were performed at 123 K. Crystallographic data together with the details of the experiments are given below. Absorption corrections were applied semi-empirically from equivalent reflections or analytically (SCALE3/ABSPACK algorithm implemented in CrysAlis PRO software by Agilent Technologies Ltd).^[14] All structures were solved using SIR97,^[15] SHELXT, SHELXS^[16] and OLEX 2.^[17] Refinements against F^2 in anisotropic approximation were done using SHELXL.^[16] The hydrogen positions of the methyl groups were located geometrically and refined riding on the carbon atoms. Hydrogen atoms belonging to BH₂ and PH₂ groups were located from the difference Fourier map and refined without constraints (**1e**, (C₆F₅)₃GaDMAP, **4a**, **5a**) or with restrained P–H distances (**4c**). A disordered toluene molecule in **5b** and a disordered P–B unit in **7** were refined using the SADI command. Figures were created with OLEX 2.^[17] CIF files are deposited in Cambridge Crystallographic Data Center under the deposition codes CCDC 1578187 (**1e**), 1578188 (**4a**), 1578189 (**4c**), 1578190 (**5a**) and 1578191 ((C₆F₅)₃GaDMAP).

Table 1S Crystallographic data.

compound	1e	(C ₆ F ₅) ₃ GaDMAP	4a	4c	5a
empirical formula	C ₉ H ₁₇ BNP	C ₅₇ H ₂₈ F ₃₀ Ga ₂ N ₄	C ₇ H ₁₆ BN ₂ P	C ₁₁ H ₂₄ BN ₂ P	C ₂₇ H ₄₀ BN ₂ P
formula weight	181.01	1478.27	170.00	226.10	434.39
temperature [K]	123(1)	123(1)	123(1)	123(1)	123(1)
crystal system	monoclinic	triclinic	monoclinic	monoclinic	monoclinic
space group	<i>Pn</i>	<i>P</i> -1	<i>P</i> 2 ₁ / <i>c</i>	<i>P</i> 2 ₁ / <i>c</i>	<i>P</i> 2 ₁ / <i>n</i>
<i>a</i> [Å]	6.26140(16)	11.157(3)	6.1020(5)	20.4072(4)	11.39804(19)
<i>b</i> [Å]	8.4380(2)	11.352(2)	16.3278(12)	12.16809(19)	13.5524(2)
<i>c</i> [Å]	10.2943(3)	12.914(2)	10.7138(11)	11.9600(2)	17.6287(3)
α [°]	90	88.168(15)	90	90	90
β [°]	94.756(3)	69.571(18)	109.823(7)	106.177(2)	92.6737(16)
γ [°]	90	65.81(2)	90	90	90
Volume [Å ³]	542.01(3)	1386.3(6)	1004.19(16)	2852.27(9)	2720.14(8)
<i>Z</i>	2	1	4	8	4
ρ_{calc} /cm ³	1.109	1.771	1.124	1.053	1.061
μ /mm ⁻¹	1.814	2.536	1.955	1.479	0.998
<i>F</i> (000)	196.0	730.0	368.0	992.0	944.0
crystal size [mm ³]	0.38 × 0.08 × 0.06	0.12 × 0.08 × 0.06	0.36 × 0.15 × 0.10	0.29 × 0.12 × 0.08	0.24 × 0.13 × 0.12
absorption correction	analytical	multi-scan	multi-scan	multi-scan	Gaussian
<i>T</i> _{min} / <i>T</i> _{max}	0.746 / 0.918	0.652 / 1.000	0.682 / 1.000	0.608 / 1.000	0.852 / 0.909
2 θ range [°]	10.484 to 133.096	7.368 to 124.288	10.314 to 133.162	8.554 to 147.73	8.232 to 145.632
completeness	0.993	0.989	0.998	0.996	0.996
index ranges	-7 ≤ <i>h</i> ≤ 7	-12 ≤ <i>h</i> ≤ 12	-6 ≤ <i>h</i> ≤ 7	-25 ≤ <i>h</i> ≤ 25	-13 ≤ <i>h</i> ≤ 12
	-10 ≤ <i>k</i> ≤ 9	-12 ≤ <i>k</i> ≤ 12	-11 ≤ <i>k</i> ≤ 19	-15 ≤ <i>k</i> ≤ 14	-16 ≤ <i>k</i> ≤ 11
	-12 ≤ <i>l</i> ≤ 8	-11 ≤ <i>l</i> ≤ 14	-11 ≤ <i>l</i> ≤ 12	-10 ≤ <i>l</i> ≤ 14	-21 ≤ <i>l</i> ≤ 14
reflections collected	3759	19827	3468	15424	10796
	1425	4319	1772	5573	5268
independent reflections	[<i>R</i> _{int} = 0.0355, <i>R</i> _{sigma} = 0.0384]	[<i>R</i> _{int} = 0.0294, <i>R</i> _{sigma} = 0.0220]	[<i>R</i> _{int} = 0.0350, <i>R</i> _{sigma} = 0.0448]	[<i>R</i> _{int} = 0.0420, <i>R</i> _{sigma} = 0.0360]	[<i>R</i> _{int} = 0.0381, <i>R</i> _{sigma} = 0.0474]
data/restraints/parameters	1425/3/124	4319/15/419	1772/0/164	5573/4/321	5268/0/304
GOF on <i>F</i> ²	1.025	1.116	0.957	1.023	1.034
final <i>R</i> indexes [<i>I</i> ≥ 2 σ (<i>I</i>)]	<i>R</i> ₁ = 0.0412	<i>R</i> ₁ = 0.0367	<i>R</i> ₁ = 0.0372	<i>R</i> ₁ = 0.0506	<i>R</i> ₁ = 0.0553
	<i>wR</i> ₂ = 0.1051	<i>wR</i> ₂ = 0.1011	<i>wR</i> ₂ = 0.0895	<i>wR</i> ₂ = 0.1338	<i>wR</i> ₂ = 0.1530
final <i>R</i> indexes [all data]	<i>R</i> ₁ = 0.0418	<i>R</i> ₁ = 0.0430	<i>R</i> ₁ = 0.0487	<i>R</i> ₁ = 0.0551	<i>R</i> ₁ = 0.0647
	<i>wR</i> ₂ = 0.1062	<i>wR</i> ₂ = 0.1047	<i>wR</i> ₂ = 0.0934	<i>wR</i> ₂ = 0.1394	<i>wR</i> ₂ = 0.1646
max/min $\Delta\rho$ [e·Å ⁻³]	0.24/-0.17	0.95/-0.39	0.21/-0.24	0.43/-0.31	0.83/-0.29
flack parameter	-0.04(4)	-	-	-	-

2.1 $\text{HPhBH}_2\text{NMe}_3$ (**1e**)

$\text{HPhBH}_2\text{NMe}_3$ (**1e**) crystallizes at 3° C out of a saturated *n*-hexane solution as colorless needles in the monoclinic space group *Pn*.

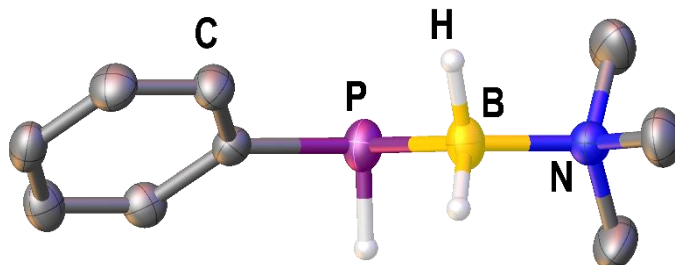


Figure SI21: Molecular structure of **1e** in the solid state. Thermal ellipsoids are drawn with 50% probability. Hydrogen atoms bond to carbon are omitted for clarity. Selected bond lengths [Å] and angles [°]: P–B 1.955(2), N–B–P 116.47(12).

2.2 $(\text{C}_6\text{F}_5)_3\text{GaDMP}$

$(\text{C}_6\text{F}_5)_3\text{GaDMP}$ crystallizes at 4° C out of a saturated toluene solution as colorless prisms in the triclinic space group *P*-1.

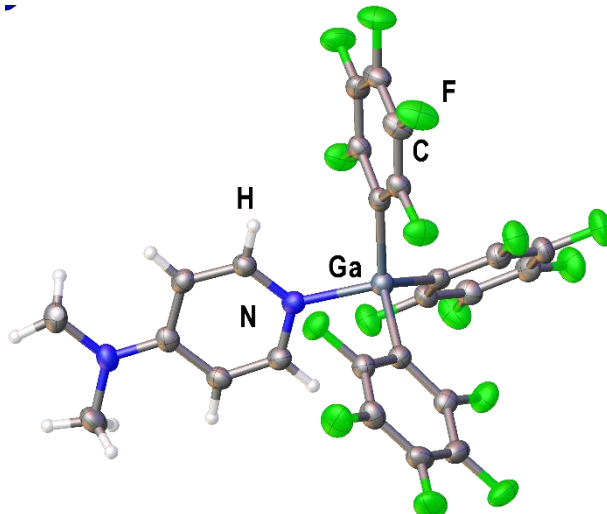


Figure SI22: Molecular structure of $(\text{C}_6\text{F}_5)_3\text{GaDMP}$ in the solid state. Thermal ellipsoids are drawn with 50% probability. Selected bond lengths [Å] and angles [°]: Ga–N 1.996(2).

2.3 $\text{H}_2\text{PBH}_2\text{NHC}^{\text{Me}}$ (**4a**)

$\text{H}_2\text{PBH}_2\text{NHC}^{\text{Me}}$ (**4a**) crystallizes by slow evaporation of a 2:1-mixture of *n*-hexane/toluene as colorless blocks in the monoclinic space group *P*2₁/*c*.

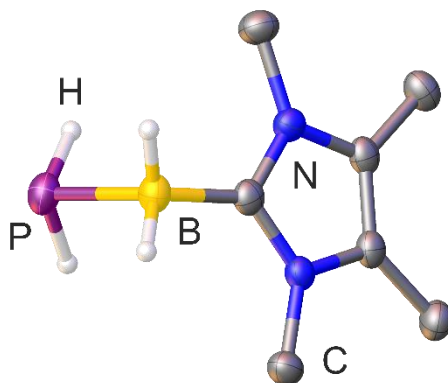


Figure SI23: Molecular structure of **4a** in the solid state. Thermal ellipsoids are drawn with 50% probability. Hydrogen atoms bond to carbon are omitted for clarity. Selected bond lengths [Å] and angles [°]: P–B 1.993(2), B–C 1.597(3), C–B–P 109.66(12).

2.4 *t*BuHPBH₂NMe₃ (**4c**)

*t*BuHPBH₂NMe₃ (**4c**) crystallizes at -28° C out of a saturated *n*-hexane solution as colorless needles in the monoclinic space group *P*2₁/*c*.

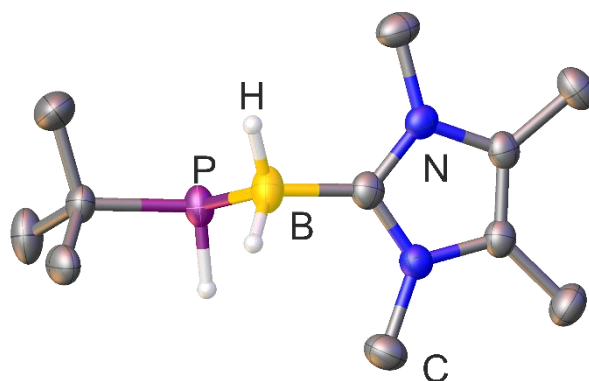


Figure SI24: Molecular structure of **4c** in the solid state. Thermal ellipsoids are drawn with 50% probability. Hydrogen atoms bond to carbon are omitted for clarity. Selected bond lengths [Å] and angles [°]: P–B 1.988(2), B–C 1.599(3), C–B–P 106.31(9).

2.5 H₂PBH₂NHC^{dipp} (**5a**)

H₂PBH₂NHC^{dipp} (**5a**) crystallizes by storing a saturated solution in benzene at r.t. as colorless blocks in the monoclinic space group *P*2₁/*n*.

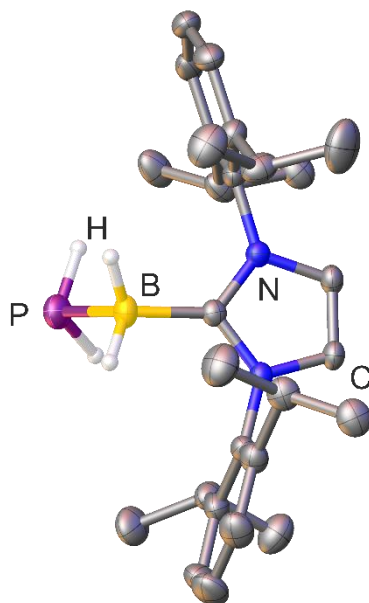


Figure SI25: Molecular structure of **5a** in the solid state. Thermal ellipsoids are drawn with 50% probability. Hydrogen atoms bond to carbon are omitted for clarity. Selected bond lengths [Å] and angles [°]: P–B 1.990(2), B–C 1.593(2), C–B–P 111.94(12).

3. Computational details

Gaussian 09 program package^[18] was used throughout. Density functional theory (DFT) in form of Becke's three-parameter hybrid functional B3LYP^[19] with def2-SVP all electron basis set^[20] was employed. Basis sets were obtained from the EMSL basis set exchange database.^[21] The geometries of the compounds have been fully optimized and verified to be true minima on their respective potential energy surfaces (PES).

For the $(\text{H}_2\text{PBH}_2)_n$ cyclic oligomers, structures possessing the main axis of the order n were found to be high level stationary points on the PES in case of $n \geq 4$. Optimization starting from these geometries without the symmetry constraints resulted in the structures presented in Table 3S. The $(\text{H}_2\text{PBH}_2)_3$ cyclic trimers are the most energetically favorable among the considered oligomers and therefore were chosen as a model compounds for the cleavage of the first P–B bond in polymers by interaction with Lewis bases.

Depolymerization of Poly(phosphinoboranes)

Table 2S. Optimized geometries of $ring(PR^1R^2BH_2)_3$ and respective LB stabilized $chain(PR^1R^2BH_2)_3$

LB	R ¹ ,R ²			
	H,H	H,Ph	H, ^t Bu	Ph,Ph
-				
NMe ₃				
dmap				
NHC ^{Me}				
NHC ^{Dipp}				
NHC ^{tBu}				
NHC ^{Ph*}				

Depolymerization of Poly(phosphinoboranes)

Table 3S. Optimized geometries of $(\text{PH}_2\text{BH}_2)_n$ and respective LB stabilized $(\text{PH}_2\text{BH}_2)_n\text{-LB}$.

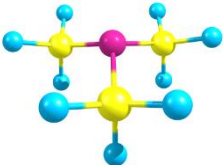
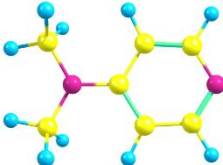

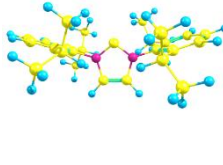
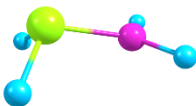
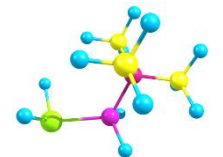
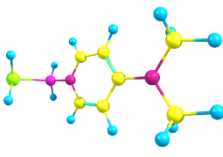
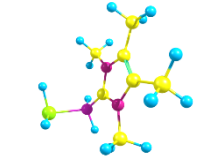
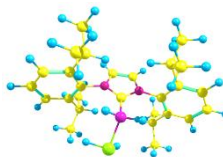
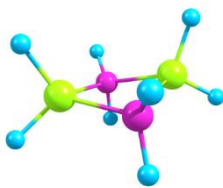
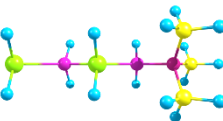
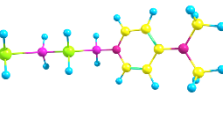
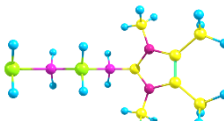

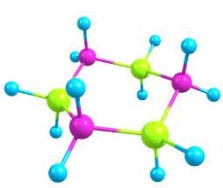
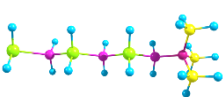
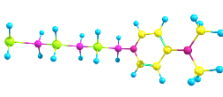
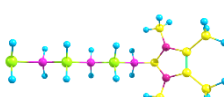
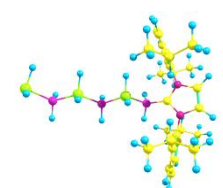
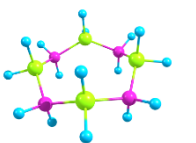
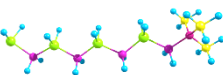
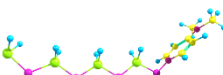
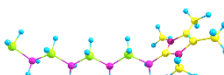
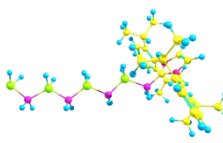

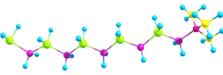
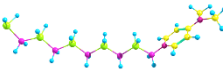
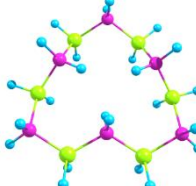

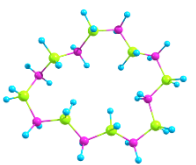
n		LB			
		NMe ₃	dmap	NHC ^{Me}	NHC ^{Dipp}
-	-				
1					
2					
3					
4					
5				-	-
6		-	-	-	-
7		-	-	-	-
8		-	-	-	-

Table 4S. Reaction energies ΔE°_0 , standard enthalpies ΔH°_{298} , Gibbs energies ΔG°_{298} (kJ mol⁻¹) and standard entropies ΔS°_{298} (J mol⁻¹ K⁻¹) for the considered gas phase processes. B3LYP/def2-SVP level of theory.

Process	ΔE°_0	ΔH°_{298}	ΔS°_{298}	ΔG°_{298}
$\text{PH}_2\text{BH}_2 = \frac{1}{2} (\text{PH}_2\text{BH}_2)_2$	-78.0	-72.3	-95.9	-43.7
$\text{PH}_2\text{BH}_2 = \frac{1}{3} (\text{PH}_2\text{BH}_2)_3$	-121.5	-113.4	-127.7	-75.3
$\text{PH}_2\text{BH}_2 = \frac{1}{4} (\text{PH}_2\text{BH}_2)_4$	-118.3	-109.5	-138.2	-68.3
$\text{PH}_2\text{BH}_2 = \frac{1}{5} (\text{PH}_2\text{BH}_2)_5$	-117.4	-108.3	-144.9	-65.1
$\text{PH}_2\text{BH}_2 = \frac{1}{6} (\text{PH}_2\text{BH}_2)_6$	-118.7	-109.5	-147.5	-65.5
$\text{PH}_2\text{BH}_2 = \frac{1}{7} (\text{PH}_2\text{BH}_2)_7$	-120.4	-111.3	-149.4	-66.8
$\text{PH}_2\text{BH}_2 = \frac{1}{8} (\text{PH}_2\text{BH}_2)_8$	-120.4	-111.0	-151.6	-65.8
$\text{PH}_2\text{BH}_2 + \text{NMe}_3 = \text{PH}_2\text{BH}_2\text{NMe}_3$	-111.5	-97.4	-172.9	-45.9
$(\text{PH}_2\text{BH}_2)_2 + \text{NMe}_3 = (\text{PH}_2\text{BH}_2)_2\text{NMe}_3$	-52.2	-40.0	-132.1	-0.6
$(\text{PH}_2\text{BH}_2)_3 + \text{NMe}_3 = (\text{PH}_2\text{BH}_2)_3\text{NMe}_3$	47.6	56.0	-98.2	85.3
$(\text{PH}_2\text{BH}_2)_4 + \text{NMe}_3 = (\text{PH}_2\text{BH}_2)_4\text{NMe}_3$	42.2	50.1	-87.8	76.3
$(\text{PH}_2\text{BH}_2)_5 + \text{NMe}_3 = (\text{PH}_2\text{BH}_2)_5\text{NMe}_3$	38.8	45.8	-73.0	67.6
$\text{PH}_2\text{BH}_2 + \text{dmap} = \text{PH}_2\text{BH}_2\text{dmap}$	-137.8	-126.9	-164.8	-77.8
$(\text{PH}_2\text{BH}_2)_2 + \text{dmap} = (\text{PH}_2\text{BH}_2)_2\text{dmap}$	-90.3	-81.1	-131.8	-41.8
$(\text{PH}_2\text{BH}_2)_3 + \text{dmap} = (\text{PH}_2\text{BH}_2)_3\text{dmap}$	4.2	10.1	-97.6	39.2
$(\text{PH}_2\text{BH}_2)_4 + \text{dmap} = (\text{PH}_2\text{BH}_2)_4\text{dmap}$	-4.1	0.7	-90.5	27.7
$(\text{PH}_2\text{BH}_2)_5 + \text{dmap} = (\text{PH}_2\text{BH}_2)_5\text{dmap}$	-9.4	-5.0	-79.8	18.8
$\text{PH}_2\text{BH}_2 + \text{NHC}^{\text{Me}} = \text{PH}_2\text{BH}_2\text{NHC}^{\text{Me}}$	-224.4	-212.7	-165.2	-163.4
$(\text{PH}_2\text{BH}_2)_2 + \text{NHC}^{\text{Me}} = (\text{PH}_2\text{BH}_2)_2\text{NHC}^{\text{Me}}$	-178.2	-168.5	-126.1	-130.9
$(\text{PH}_2\text{BH}_2)_3 + \text{NHC}^{\text{Me}} = (\text{PH}_2\text{BH}_2)_3\text{NHC}^{\text{Me}}$	-82.7	-76.4	-85.4	-51.0
$(\text{PH}_2\text{BH}_2)_4 + \text{NHC}^{\text{Me}} = (\text{PH}_2\text{BH}_2)_4\text{NHC}^{\text{Me}}$	-90.5	-85.2	-80.2	-61.3
$\text{PH}_2\text{BH}_2 + \text{NHC}^{\text{Dipp}} = \text{PH}_2\text{BH}_2\text{NHC}^{\text{Dipp}}$	-198.0	-186.9	-199.7	-127.3
$(\text{PH}_2\text{BH}_2)_2 + \text{NHC}^{\text{Dipp}} = (\text{PH}_2\text{BH}_2)_2\text{NHC}^{\text{Dipp}}$	-156.1	-146.5	-168.3	-96.4
$(\text{PH}_2\text{BH}_2)_3 + \text{NHC}^{\text{Dipp}} = (\text{PH}_2\text{BH}_2)_3\text{NHC}^{\text{Dipp}}$	-62.4	-55.9	-130.0	-17.2
$(\text{PH}_2\text{BH}_2)_4 + \text{NHC}^{\text{Dipp}} = (\text{PH}_2\text{BH}_2)_4\text{NHC}^{\text{Dipp}}$	-71.5	-66.4	-123.9	-29.5
$\text{PH}_2\text{BH}_2 + \text{NHC}^{\text{tBu}} = \text{PH}_2\text{BH}_2\text{NHC}^{\text{tBu}}$	-163.6	-149.4	-198.1	-90.4
$(\text{PH}_2\text{BH}_2)_3 + \text{NHC}^{\text{tBu}} = (\text{PH}_2\text{BH}_2)_3\text{NHC}^{\text{tBu}}$	-27.3	-18.4	-135.4	21.9
$\text{PH}_2\text{BH}_2 + \text{NHC}^{\text{Ph}^*} = \text{PH}_2\text{BH}_2\text{NHC}^{\text{Ph}^*}$	-186.0	-174.7	-181.5	-120.6
$(\text{PH}_2\text{BH}_2)_3 + \text{NHC}^{\text{Ph}^*} = (\text{PH}_2\text{BH}_2)_3\text{NHC}^{\text{Ph}^*}$	-60.9	-54.7	-122.0	-18.3

Depolymerization of Poly(phosphinoboranes)

$\text{P(Ph)HBH}_2 + \text{NMe}_3 = \text{P(Ph)HBH}_2\text{NMe}_3$	-106.7	-92.6	-171.4	-41.5
$[\text{P(Ph)HBH}_2]_3 + \text{NMe}_3 = [\text{P(Ph)HBH}_2]_3\text{NMe}_3$	47.5	57.4	-129.3	96.0
$\text{P(Ph)HBH}_2 + \text{dmap} = \text{P(Ph)HBH}_2\text{dmap}$	-143.1	-132.1	-173.6	-80.3
$[\text{P(Ph)HBH}_2]_3 + \text{dmap} = [\text{P(Ph)HBH}_2]_3\text{dmap}$	3.8	10.8	-122.0	47.2
$\text{P(Ph)HBH}_2 + \text{NHC}^{\text{Me}} = \text{P(Ph)HBH}_2\text{NHC}^{\text{Me}}$	-223.7	-211.5	-176.9	-158.8
$[\text{P(Ph)HBH}_2]_3 + \text{NHC}^{\text{Me}} = [\text{P(Ph)HBH}_2]_3\text{NHC}^{\text{Me}}$	-83.2	-75.5	-126.8	-37.7
$\text{P(Ph)HBH}_2 + \text{NHC}^{\text{Dipp}} = \text{P(Ph)HBH}_2\text{NHC}^{\text{Dipp}}$	-197.9	-186.3	-206.6	-124.7
$[\text{P(Ph)HBH}_2]_3 + \text{NHC}^{\text{Dipp}} = [\text{P(Ph)HBH}_2]_3\text{NHC}^{\text{Dipp}}$	-50.0	-42.7	-190.9	14.2
$\text{P(Ph)HBH}_2 + \text{NHC}^{\text{tBu}} = \text{P(Ph)HBH}_2\text{NHC}^{\text{tBu}}$	-161.2	-146.9	-207.8	-85.0
$[\text{P(Ph)HBH}_2]_3 + \text{NHC}^{\text{tBu}} = [\text{P(Ph)HBH}_2]_3\text{NHC}^{\text{tBu}}$	-15.3	-4.8	-167.8	45.3
$\text{P(Ph)HBH}_2 + \text{NHC}^{\text{Ph}^*} = \text{P(Ph)HBH}_2\text{NHC}^{\text{Ph}^*}$	-198.1	-186.1	-205.4	-124.8
$[\text{P(Ph)HBH}_2]_3 + \text{NHC}^{\text{Ph}^*} = [\text{P(Ph)HBH}_2]_3\text{NHC}^{\text{Ph}^*}$	-32.0	-24.2	-161.3	23.9
$\text{P}^{\text{(tBu)}}\text{HBH}_2 + \text{NMe}_3 = \text{P}^{\text{(tBu)}}\text{HBH}_2\text{NMe}_3$	-101.7	-88.0	-177.0	-35.2
$[\text{P}^{\text{(tBu)}}\text{HBH}_2]_3 + \text{NMe}_3 = [\text{P}^{\text{(tBu)}}\text{HBH}_2]_3\text{NMe}_3$	114.0	123.7	-143.5	166.5
$\text{P}^{\text{(tBu)}}\text{HBH}_2 + \text{dmap} = \text{P}^{\text{(tBu)}}\text{HBH}_2\text{dmap}$	-123.3	-112.5	-169.9	-61.8
$[\text{P}^{\text{(tBu)}}\text{HBH}_2]_3 + \text{dmap} = [\text{P}^{\text{(tBu)}}\text{HBH}_2]_3\text{dmap}$	60.6	67.7	-147.1	111.6
$\text{P}^{\text{(tBu)}}\text{HBH}_2 + \text{NHC}^{\text{Me}} = \text{P}^{\text{(tBu)}}\text{HBH}_2\text{NHC}^{\text{Me}}$	-210.3	-198.9	-162.6	-150.4
$[\text{P}^{\text{(tBu)}}\text{HBH}_2]_3 + \text{NHC}^{\text{Me}} = [\text{P}^{\text{(tBu)}}\text{HBH}_2]_3\text{NHC}^{\text{Me}}$	-12.9	-5.4	-157.5	41.5
$\text{P}^{\text{(tBu)}}\text{HBH}_2 + \text{NHC}^{\text{Dipp}} = \text{P}^{\text{(tBu)}}\text{HBH}_2\text{NHC}^{\text{Dipp}}$	-191.1	-179.8	-216.7	-115.2
$[\text{P}^{\text{(tBu)}}\text{HBH}_2]_3 + \text{NHC}^{\text{Dipp}} = [\text{P}^{\text{(tBu)}}\text{HBH}_2]_3\text{NHC}^{\text{Dipp}}$	22.5	29.3	-202.2	89.6
$\text{P}^{\text{(tBu)}}\text{HBH}_2 + \text{NHC}^{\text{tBu}} = \text{P}^{\text{(tBu)}}\text{HBH}_2\text{NHC}^{\text{tBu}}$	-122.2	-108.7	-212.1	-45.5
$[\text{P}^{\text{(tBu)}}\text{HBH}_2]_3 + \text{NHC}^{\text{tBu}} = [\text{P}^{\text{(tBu)}}\text{HBH}_2]_3\text{NHC}^{\text{tBu}}$	31.5	41.8	-179.9	95.5
$\text{P}^{\text{(tBu)}}\text{HBH}_2 + \text{NHC}^{\text{Ph}^*} = \text{P}^{\text{(tBu)}}\text{HBH}_2\text{NHC}^{\text{Ph}^*}$	-183.4	-172.3	-200.4	-112.6
$[\text{P}^{\text{(tBu)}}\text{HBH}_2]_3 + \text{NHC}^{\text{Ph}^*} = [\text{P}^{\text{(tBu)}}\text{HBH}_2]_3\text{NHC}^{\text{Ph}^*}$	21.8	28.1	-250.7	102.9
$\text{PPh}_2\text{BH}_2 + \text{NMe}_3 = \text{PPh}_2\text{BH}_2\text{NMe}_3$	-98.9	-85.5	-171.8	-34.3
$[\text{PPh}_2\text{BH}_2]_3 + \text{NMe}_3 = [\text{PPh}_2\text{BH}_2]_3\text{NMe}_3$	109.1	119.7	-162.9	168.3
$\text{PPh}_2\text{BH}_2 + \text{dmap} = \text{PPh}_2\text{BH}_2\text{dmap}$	-133.6	-123.1	-190.6	-66.3
$[\text{PPh}_2\text{BH}_2]_3 + \text{dmap} = [\text{PPh}_2\text{BH}_2]_3\text{dmap}$	58.7	66.0	-145.9	109.5
$\text{PPh}_2\text{BH}_2 + \text{NHC}^{\text{Me}} = \text{PPh}_2\text{BH}_2\text{NHC}^{\text{Me}}$	-220.7	-209.7	-177.7	-156.7
$[\text{PPh}_2\text{BH}_2]_3 + \text{NHC}^{\text{Me}} = [\text{PPh}_2\text{BH}_2]_3\text{NHC}^{\text{Me}}$	-26.9	-19.2	-150.2	25.6
$\text{PPh}_2\text{BH}_2 + \text{NHC}^{\text{Dipp}} = \text{PPh}_2\text{BH}_2\text{NHC}^{\text{Dipp}}$	-178.6	-176.6	-224.2	-109.8
$[\text{PPh}_2\text{BH}_2]_3 + \text{NHC}^{\text{Dipp}} = [\text{PPh}_2\text{BH}_2]_3\text{NHC}^{\text{Dipp}}$	32.7	41.2	-232.1	110.4
$\text{PPh}_2\text{BH}_2 + \text{NHC}^{\text{tBu}} = \text{PPh}_2\text{BH}_2\text{NHC}^{\text{tBu}}$	-140.7	-127.9	-224.4	-61.0
$[\text{PPh}_2\text{BH}_2]_3 + \text{NHC}^{\text{tBu}} = [\text{PPh}_2\text{BH}_2]_3\text{NHC}^{\text{tBu}}$	47.0	58.0	-197.6	116.9
$\text{PPh}_2\text{BH}_2 + \text{NHC}^{\text{Ph}^*} = \text{PPh}_2\text{BH}_2\text{NHC}^{\text{Ph}^*}$	-133.5	-122.4	-264.7	-43.5
$[\text{PPh}_2\text{BH}_2]_3 + \text{NHC}^{\text{Ph}^*} = [\text{PPh}_2\text{BH}_2]_3\text{NHC}^{\text{Ph}^*}$	55.7	63.3	-237.9	134.3
$\frac{1}{3} [\text{PH}_2\text{BH}_2]_3 + \text{NMe}_3 = \text{PH}_2\text{BH}_2\text{NMe}_3$	10.1	15.9	-45.2	29.4
$\frac{1}{3} [\text{P(Ph)HBH}_2]_3 + \text{NMe}_3 = \text{P(Ph)HBH}_2\text{NMe}_3$	21.2	28.0	-40.2	40.0

Depolymerization of Poly(phosphinoboranes)

$\frac{1}{3} [\text{P}(\text{tBu})\text{HBH}_2]_3 + \text{NMe}_3 = \text{P}(\text{tBu})\text{HBH}_2\text{NMe}_3$	32.8	39.0	-48.2	53.4
$\frac{1}{3} [\text{PPh}_2\text{BH}_2]_3 + \text{NMe}_3 = \text{PPh}_2\text{BH}_2\text{NMe}_3$	29.8	36.9	-23.8	44.0
$\frac{1}{3} [\text{PH}_2\text{BH}_2]_3 + \text{dmap} = \text{PH}_2\text{BH}_2\text{dmap}$	-16.2	-13.5	-37.1	-2.5
$\frac{1}{3} [\text{P}(\text{Ph})\text{HBH}_2]_3 + \text{dmap} = \text{P}(\text{Ph})\text{HBH}_2\text{dmap}$	-15.1	-11.5	-42.4	1.2
$\frac{1}{3} [\text{P}(\text{tBu})\text{HBH}_2]_3 + \text{dmap} = \text{P}(\text{tBu})\text{HBH}_2\text{dmap}$	11.2	14.5	-41.1	26.8
$\frac{1}{3} [\text{PPh}_2\text{BH}_2]_3 + \text{dmap} = \text{PPh}_2\text{BH}_2\text{dmap}$	-4.9	-0.7	-42.7	12.0
$\frac{1}{3} [\text{PH}_2\text{BH}_2]_3 + \text{NHC}^{\text{Me}} = \text{PH}_2\text{BH}_2\text{NHC}^{\text{Me}}$	-102.9	-99.3	-37.5	-88.1
$\frac{1}{3} [\text{P}(\text{Ph})\text{HBH}_2]_3 + \text{NHC}^{\text{Me}} = \text{P}(\text{Ph})\text{HBH}_2\text{NHC}^{\text{Me}}$	-95.8	-90.9	-45.7	-77.3
$\frac{1}{3} [\text{P}(\text{tBu})\text{HBH}_2]_3 + \text{NHC}^{\text{Me}} = \text{P}(\text{tBu})\text{HBH}_2\text{NHC}^{\text{Me}}$	-75.8	-71.9	-33.7	-61.8
$\frac{1}{3} [\text{PPh}_2\text{BH}_2]_3 + \text{NHC}^{\text{Me}} = \text{PPh}_2\text{BH}_2\text{NHC}^{\text{Me}}$	-92.0	-87.2	-29.7	-78.4
$\frac{1}{3} [\text{PH}_2\text{BH}_2]_3 + \text{NHC}^{\text{Dipp}} = \text{PH}_2\text{BH}_2\text{NHC}^{\text{Dipp}}$	-76.5	-73.5	-72.1	-52.0
$\frac{1}{3} [\text{P}(\text{Ph})\text{HBH}_2]_3 + \text{NHC}^{\text{Dipp}} = \text{P}(\text{Ph})\text{HBH}_2\text{NHC}^{\text{Dipp}}$	-70.0	-65.7	-75.4	-43.2
$\frac{1}{3} [\text{P}(\text{tBu})\text{HBH}_2]_3 + \text{NHC}^{\text{Dipp}} = \text{P}(\text{tBu})\text{HBH}_2\text{NHC}^{\text{Dipp}}$	-56.6	-52.8	-87.9	-26.6
$\frac{1}{3} [\text{PPh}_2\text{BH}_2]_3 + \text{NHC}^{\text{Dipp}} = \text{PPh}_2\text{BH}_2\text{NHC}^{\text{Dipp}}$	-49.9	-54.2	-76.3	-31.4
$\frac{1}{3} [\text{PH}_2\text{BH}_2]_3 + \text{NHC}^{\text{tBu}} = \text{PH}_2\text{BH}_2\text{NHC}^{\text{tBu}}$	-42.1	-36.1	-70.4	-15.1
$\frac{1}{3} [\text{P}(\text{Ph})\text{HBH}_2]_3 + \text{NHC}^{\text{tBu}} = \text{P}(\text{Ph})\text{HBH}_2\text{NHC}^{\text{tBu}}$	-33.3	-26.3	-76.6	-3.5
$\frac{1}{3} [\text{P}(\text{tBu})\text{HBH}_2]_3 + \text{NHC}^{\text{tBu}} = \text{P}(\text{tBu})\text{HBH}_2\text{NHC}^{\text{tBu}}$	12.3	18.3	-83.3	43.1
$\frac{1}{3} [\text{PPh}_2\text{BH}_2]_3 + \text{NHC}^{\text{tBu}} = \text{PPh}_2\text{BH}_2\text{NHC}^{\text{tBu}}$	-12.0	-5.5	-76.5	17.3
$\frac{1}{3} [\text{PH}_2\text{BH}_2]_3 + \text{NHC}^{\text{Ph}^*} = \text{PH}_2\text{BH}_2\text{NHC}^{\text{Ph}^*}$	-64.5	-61.4	-53.8	-45.3
$\frac{1}{3} [\text{P}(\text{Ph})\text{HBH}_2]_3 + \text{NHC}^{\text{Ph}^*} = \text{P}(\text{Ph})\text{HBH}_2\text{NHC}^{\text{Ph}^*}$	-70.1	-65.5	-74.2	-43.4
$\frac{1}{3} [\text{P}(\text{tBu})\text{HBH}_2]_3 + \text{NHC}^{\text{Ph}^*} = \text{P}(\text{tBu})\text{HBH}_2\text{NHC}^{\text{Ph}^*}$	-48.9	-45.3	-71.6	-24.0
$\frac{1}{3} [\text{PPh}_2\text{BH}_2]_3 + \text{NHC}^{\text{Ph}^*} = \text{PPh}_2\text{BH}_2\text{NHC}^{\text{Ph}^*}$	-4.8	0.0	-116.7	34.8

Table 5S. Total energies E^0 , sum of electronic and thermal enthalpies H^0_{298} (Hartree) and standard entropies S^0_{298} (cal mol⁻¹K⁻¹). B3LYP/def2-SVP level of theory.

Compound	Point group	E^0	H^0_{298}	S^0_{298}
NMe ₃	C _{3v}	-174.3458754	-174.219985	68.868
dmap	C _{2v}	-381.9816942	-381.810708	90.336
NHC ^{Me}	C _{2v}	-383.1586677	-382.966025	94.309
NHC ^{Dipp}	C ₁	-1159.2022092	-1158.603433	200.965
NHC ^{tBu}	C _{2v}	-540.2940193	-539.984816	117.812
NHC ^{Ph*}	C ₂	-2770.570623	-2769.462903	348.043
PH ₂ BH ₂	C _s	-368.4743914	-368.432251	60.918
(PH ₂ BH ₂) ₂	C _{2v}	-737.0081737	-736.919542	76.001
(PH ₂ BH ₂) ₃	C _{3v}	-1105.562019	-1105.426301	91.206
(PH ₂ BH ₂) ₄	C _{2v}	-1474.077814	-1473.895832	111.587
(PH ₂ BH ₂) ₅	C ₁	-1842.59554	-1842.367478	131.471
(PH ₂ BH ₂) ₆	C ₁	-2211.117501	-2210.843728	154.014
(PH ₂ BH ₂) ₇	C ₁	-2579.641879	-2579.322474	176.536
(PH ₂ BH ₂) ₈	C ₁	-2948.161857	-2947.796221	197.532
PH ₂ BH ₂ NMe ₃	C _s	-542.8627187	-542.689354	88.461
PH ₂ BH ₂ dmap	C _s	-750.5085519	-750.291295	111.874
PH ₂ BH ₂ NHC ^{Me}	C _s	-751.7185165	-751.479272	115.731
PH ₂ BH ₂ NHC ^{Dipp}	C ₁	-1527.7520218	-1527.106859	214.146
PH ₂ BH ₂ NHC ^{tBu}	C ₁	-908.8307292	-908.473983	131.379
PH ₂ BH ₂ NHC ^{Ph*}	C ₁	-3139.115871	-3137.961707	365.575
(PH ₂ BH ₂) ₂ NMe ₃	C _s	-911.3739179	-911.154747	113.296
(PH ₂ BH ₂) ₂ dmap	C _s	-1119.024261	-1118.76114	134.827
(PH ₂ BH ₂) ₂ NHC ^{Me}	C _s	-1120.234721	-1119.949736	140.178
(PH ₂ BH ₂) ₂ NHC ^{Dipp}	C ₁	-1527.7520218	-1527.106859	214.146
(PH ₂ BH ₂) ₃ NMe ₃	C _s	-1279.889756	-1279.624938	136.612
(PH ₂ BH ₂) ₃ dmap	C _s	-1487.542115	-1487.23317	158.225
(PH ₂ BH ₂) ₃ NHC ^{Me}	C _s	-1488.752189	-1488.42144	165.102
(PH ₂ BH ₂) ₃ NHC ^{Dipp}	C ₁	-2264.787992	-2264.05103	261.103
(PH ₂ BH ₂) ₃ NHC ^{tBu}	C ₁	-1645.86642	-1645.418132	176.663
(PH ₂ BH ₂) ₃ NHC ^{Ph*}	C ₁	-3876.155818	-3874.910042	410.086
(PH ₂ BH ₂) ₄ NMe ₃	C _s	-1648.407621	-1648.096729	159.479
(PH ₂ BH ₂) ₄ dmap	C _s	-1856.061063	-1855.706262	180.304
(PH ₂ BH ₂) ₄ NHC ^{Me}	C _s	-1857.270957	-1856.894318	186.735
(PH ₂ BH ₂) ₄ NHC ^{Dipp}	C ₁	-2633.307247	-2632.524549	282.948
(PH ₂ BH ₂) ₅ NMe ₃	C _s	-2016.926629	-2016.57002	182.889
(PH ₂ BH ₂) ₅ dmap	C _s	-2224.580798	-2224.1801	202.726
P(Ph)HBH ₂	C ₁	-599.3621491	-599.232305	89.018
[P(Ph)HBH ₂] ₃	C ₃	-1798.232649	-1797.834707	172.987

Depolymerization of Poly(phosphinoboranes)

P(^t Bu)HBH ₂	C ₁	-525.6159113	-525.454729	89.43
[P(Ph)HBH ₂] ₃	C ₃	-1577.00142	-1576.509311	175.928
PPh ₂ BH ₂	C ₁	-830.2506517	-830.033009	115.121
[PPh ₂ BH ₂] ₃	C ₃	-2490.898983	-2490.238928	239.299
P(Ph)HBH ₂ NMe ₃	C ₁	-773.7486821	-773.487563	116.915
P(Ph)HBH ₂ dmap	C ₁	-981.3983453	-981.093309	137.871
P(Ph)HBH ₂ NHC ^{Me}	C ₁	-982.6060360	-982.27889	141.048
P(Ph)HBH ₂ NHC ^{Dipp}	C ₁	-1758.6397514	-1757.906707	240.598
P(Ph)HBH ₂ NHC ^{tBu}	C ₁	-1139.717568	-1139.273084	157.155
P(Ph)HBH ₂ NHC ^{Ph*}	C ₁	-3370.008212	-3368.766081	387.967
P(^t Bu)HBH ₂ NMe ₃	C ₁	-700.0005237	-699.708233	115.999
P(^t Bu)HBH ₂ dmap	C ₁	-907.6445658	-907.308289	139.155
P(^t Bu)HBH ₂ NHC ^{Me}	C ₁	-908.8546870	-908.496505	144.888
P(^t Bu)HBH ₂ NHC ^{Dipp}	C ₁	-1684.8909255	-1684.126641	238.603
P(^t Bu)HBH ₂ NHC ^{tBu}	C ₁	-1065.956489	-1065.480959	156.545
P(^t Bu)HBH ₂ NHC ^{Ph*}	C ₁	-3296.256391	-3294.983265	389.572
PPh ₂ BH ₂ NMe ₃	C ₁	-1004.6341923	-1004.285577	142.939
PPh ₂ BH ₂ dmap	C ₁	-1212.2832229	-1211.890615	159.903
PPh ₂ BH ₂ NHC ^{Me}	C ₁	-1213.4933796	-1213.078892	166.97
PPh ₂ BH ₂ NHC ^{Dipp}	C ₁	-1989.520874	-1988.703705	262.502
PPh ₂ BH ₂ NHC ^{tBu}	C ₁	-1370.598255	-1370.066541	179.302
PPh ₂ BH ₂ NHC ^{Ph*}	C ₁	-3600.872103	-3599.542532	399.908
[P(Ph)HBH ₂] ₃ NMe ₃	C ₁	-1972.560418	-1972.03283	210.946
[P(Ph)HBH ₂] ₃ dmap	C ₁	-2180.212886	-2179.641297	234.154
[P(Ph)HBH ₂] ₃ NHC ^{Me}	C ₁	-2181.423011	-2180.82949	237.000
[P(Ph)HBH ₂] ₃ NHC ^{Dipp}	C ₁	-2957.453914	-2956.454406	328.319
[P(Ph)HBH ₂] ₃ NHC ^{tBu}	C ₁	-2338.532505	-2337.821348	250.682
[P(Ph)HBH ₂] ₃ NHC ^{Ph*}	C ₁	-4568.815448	-4567.306826	482.48
[P(^t Bu)HBH ₂] ₃ NMe ₃	C ₁	-1751.30386	-1750.682172	210.504
[P(^t Bu)HBH ₂] ₃ dmap	C ₁	-1958.960019	-1958.294232	231.107
[P(^t Bu)HBH ₂] ₃ NHC ^{Me}	C ₁	-1960.164986	-1959.477407	232.591
[P(^t Bu)HBH ₂] ₃ NHC ^{Dipp}	C ₁	-2736.195077	-2735.101566	328.557
[P(^t Bu)HBH ₂] ₃ NHC ^{tBu}	C ₁	-2117.283459	-2116.478197	250.733
[P(^t Bu)HBH ₂] ₃ NHC ^{Ph*}	C ₁	-4347.563749	-4345.961509	464.042
[PPh ₂ BH ₂] ₃ NMe ₃	C ₁	-2665.203317	-2664.413311	269.236
[PPh ₂ BH ₂] ₃ dmap	C ₁	-2872.858329	-2872.024486	294.753
[PPh ₂ BH ₂] ₃ NHC ^{Me}	C ₁	-2874.067889	-2873.212265	297.709
[PPh ₂ BH ₂] ₃ NHC ^{Dipp}	C ₁	-3650.088752	-3648.826659	384.801
[PPh ₂ BH ₂] ₃ NHC ^{tBu}	C ₁	-3031.175117	-3030.201662	309.890
[PPh ₂ BH ₂] ₃ NHC ^{Ph*}	C ₁	-5261.44838	-5259.677706	530.478

Cartesian coordinates of the optimized geometry can be obtained from:

<https://doi.org/10.1002/chem.201705510>

or from the provided DVD.

4. References

- [1] N. Kuhn, T. Kratz, *Synthesis* **1993**, 561.
- [2] L. Hintermann, *Beilstein J. Org. Chem.* **2007**, 3, No.22.
- [3] C. Marquardt, C. Thoms, A. Stauber, G. Balazs, M. Bodensteiner, M. Scheer, *Angew. Chem. Int. Ed.* **2014**, 53, 3727 – 3730; *Angew. Chem.* **2014**, 126, 3801–3804.
- [4] W. Uhlig, A. Tzschach, *Z. anorg. allg. Chem.* **1989**, 576, 281-283.
- [5] H. Dorn, R. A. Singh, J. A. Massey, J. M. Nelson, C. A. Jaska, A. J. Lough, I. Manners, *J. Am. Chem. Soc.* **2000**, 122, 6669–6678.
- [6] J. L. W. Pohlmann, F. E. Brinckmann, *Z. Naturforsch. Teil B*, **1965**, 20, 5.
- [7] C. Marquardt, T. Jurca, K.-C. Schwan, A. Stauber, A. V. Virovets, G. R. Whittell, I. Manners, M. Scheer, *Angew. Chem. Int. Ed.* **2015**, 54, 13782–13786; *Angew. Chem.* **2015**, 127, 13986–13991.
- [8] E. Hey, C. L. Raston, B. W. Skelton, A. H. White, *J. Organomet. Chem.* **1989**, 362, 1-10.
- [9] A. Adolf, M. Zabel, M. Scheer, *Eur. J. Inorg. Chem.* **2007**, 2136–2143.
- [10] H. Dorn, R. A. Singh, J. A. Massey, A. J. Lough, I. Manners, *Angew. Chem. Int. Ed.* **1999**, 38, 3321 – 3323; *Angew. Chem.* **1999**, 111, 3540–3543.
- [11] C. Marquardt, A. Adolf, A. Stauber, M. Bodensteiner, A. V. Virovets, A.Y. Timoshkin, M. Scheer, *Chem. Eur. J.* **2013**, 19, 11887–11891.
- [12] N. Kuhn, G. Henkel, T. Kratz, J. Kreutzberg, R. Boese, A. H. Maulitz, *Chem. Ber.* **1993**, 126, 2041-2045.
- [13] Y. Wang, B. Quillian, P. Wei, C. S. Wannere, Y. Xie, R. B. King, H. F. Schaefer, P. v. R. Schleyer, G. H. Robinson, *J. Am. Chem. Soc.* **2007**, 129, 12412-12413.
- [14] Agilent Technologies **2006-2015**, CrysAlisPro Software system, different versions, Agilent Technologies UK Ltd, Oxford, UK.
- [15] A. Altomare, M. C. Burla, M. Camalli, G. L. Cascarano, C. Giacovazzo, A. Guagliardi, A.G. G. Moliterni, G. Polidori, R. Spagna, *J. Appl. Cryst.* (1999) 32, 115-119.

- [16] G. M. Sheldrick, *Acta Cryst.* **2008**, A64, 112–122.
- [17] O.V. Dolomanov, L.J. Bourhis, R.J. Gildea, J.A.K. Howard, H. Puschmann, OLEX2: A complete structure solution, refinement and analysis program, **2009**. *J. Appl. Cryst.*, 42, 339-341.
- [18] M. J. Frisch, G. W. Trucks, H. B. Schlegel, G. E. Scuseria, M. A. Robb, J. R. Cheeseman, G. Scalmani, V. Barone, B. Mennucci, G. A. Petersson, H. Nakatsuji, M. Caricato, X. Li, H. P. Hratchian, A. F. Izmaylov, J. Bloino, G. Zheng, J. L. Sonnenberg, M. Hada, M. Ehara, K. Toyota, R. Fukuda, J. Hasegawa, M. Ishida, T. Nakajima, Y. Honda, O. Kitao, H. Nakai, T. Vreven, J. A. Montgomery, Jr., J. E. Peralta, F. Ogliaro, M. Bearpark, J. J. Heyd, E. Brothers, K. N. Kudin, V. N. Staroverov, T. Keith, R. Kobayashi, J. Normand, K. Raghavachari, A. Rendell, J. C. Burant, S. S. Iyengar, J. Tomasi, M. Cossi, N. Rega, J. M. Millam, M. Klene, J. E. Knox, J. B. Cross, V. Bakken, C. Adamo, J. Jaramillo, R. Gomperts, R. E. Stratmann, O. Yazyev, A. J. Austin, R. Cammi, C. Pomelli, J. W. Ochterski, R. L. Martin, K. Morokuma, V. G. Zakrzewski, G. A. Voth, P. Salvador, J. J. Dannenberg, S. Dapprich, A. D. Daniels, O. Farkas, J. B. Foresman, J. V. Ortiz, J. Cioslowski, and D. J. Fox, Gaussian 09, Revision E.01, Gaussian, Inc., Wallingford CT, 2013.
- [19] a) A.D. Becke, *J. Chem. Phys.* **1993**, 98, 5648. b) C. Lee, W. Yang, R.G. Parr, *Phys. Rev. B.* **1988**, 37, 785.
- [20] a) F. Weigend, R. Ahlrichs, *Phys.Chem.Chem.Phys.*, **2005**, 7, 3297-3305. b) D. Andrae, U. Haeussermann, M. Dolg, H. Stoll, H. Preuss, *Theor.Chim.Acta*, **1990**, 77, 123-141.
- [21] a) D. Feller, *J. Comp. Chem.* 1996, 17, 1571-1586; b) K. L. Schuchardt, B. T. Didier, T. Elsethagen, L. Sun, V. Gurumoorthi, J. Chase, J. Li, T. L. Windus, *J. Chem. Inf. Model.* **2007**, 47, 1045-1052.

4.6 Author contributions

Dr. Ariane Vogel performed the following reactions (reported in her PhD-thesis, Regensburg 2007):

- Synthesis and characterization of (F₅C₆)₃GaDMAP
- Synthesis of **1e** by elimination of (F₅C₆)₃Ga with DMAP
- Cleavage of [PhHPBH₂]_n with DMAP to yield **3e** and NHC^{Me} to yield **4e**

Dr. Andreas Stauber performed the following reactions (reported in his PhD-thesis, Regensburg 2014):

- Synthesis and characterization of **4a** and **5a** by LB exchange
- Cleavage of $[\text{H}_2\text{PBH}_2]_n$ with NHC^{Me} and NHC^{dipp}

Dr. Christian Marquardt performed the following reactions (reported in his PhD-thesis, Regensburg 2015):

- Synthesis and characterization of $[\text{LiPPh}(\text{SiMe}_3)\text{tmeda}]_2$
- Synthesis and characterization of $(\text{Me}_3\text{Si})\text{PPhBH}_2\text{NMe}_3$ by metathesis reaction
- Synthesis and characterization of **1e** by metathesis reaction
- Thermolysis of **1e**
- Synthesis and characterization of **4c** through cleavage of $(t\text{BuPHBH}_2)_n$ with NHC^{Me}
- Combining $(\text{Ph}_2\text{PBH}_2)_n$ with DMAP and NHC^{Me}

Oliver Hegen performed the following reactions:

- Thermal instability of NHC^{Me}
- Combination of $(\text{Ph}_2\text{PBH}_2)_n$ with NHC^{dipp}
- Combination of $(\text{PhHPBH}_2)_n$ with NHC^{dipp}
- Combination of $(\text{H}_2\text{PBH}_2)_n$ with DMAP
- Combination of $(t\text{BuPHBH}_2)_n$ with DMAP and NHC^{dipp}

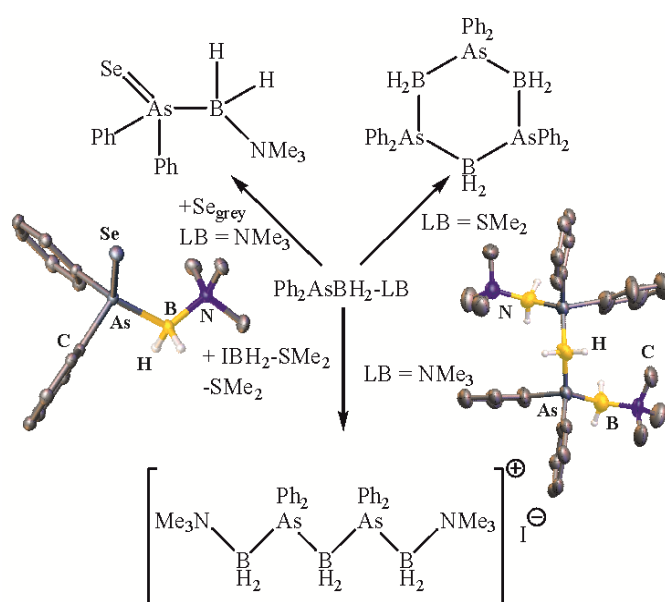
All DFT-calculations were performed by Prof. Dr. A. Y. Timoshkin.

The manuscript (including supporting information, figures, schemes and graphical abstract) was written by Dr. Christian Marquardt and Oliver Hegen in equal contribution.

This chapter was reprinted with slight modifications with permission of “John Wiley and Sons”, License Number: 4332411053152

5 The Lewis base stabilized diphenylsubstituted Arsanylborane – A versatile building block for arsanylborane oligomers

Oliver Hegen, Alexander V. Virovets, Alexey Y. Timoshkin and Manfred Scheer



Abstract: The synthesis and properties of the Lewis base stabilized diphenylsubstituted arsanylborane $\text{Ph}_2\text{AsBH}_2\text{SMe}_2$ (**1**) and $\text{Ph}_2\text{AsBH}_2\text{NMe}_3$ (**2**) are reported. These compounds were obtained by the reaction of KAsPh_2 with $\text{IBH}_2\text{-LB}$ ($\text{LB} = \text{SMe}_2$, NMe_3). Compounds **1** and **2** can be used as starting material for oligomeric/polymeric arsinoboranes. The neutral species, $\text{H}_3\text{B-Ph}_2\text{AsBH}_2\text{NMe}_3$ (**3**) and $\text{Br}_3\text{B-Ph}_2\text{AsBH}_2\text{NMe}_3$ (**4**), are synthesized by the reaction with either H_3B or Br_3B . Through reaction with $\text{IBH}_2\text{-LB}$ ($\text{LB} = \text{SMe}_2$, NMe_3) the cationic oligomeric group 13/15 compounds $[(\text{Me}_3\text{NBH}_2\text{Ph}_2\text{AsBH}_2\text{NMe}_3)]_n^+$ (**5**) and $[\{\text{H}_2\text{B}(\text{Ph}_2\text{AsBH}_2\text{NMe}_3)_2\}]_n$ (**6**) were synthesized. All compounds were completely characterized. In addition, we studied the oxidation of $\text{Ph}_2\text{AsBH}_2\text{NMe}_3$ with chalcogenes. Whereas both sulfur $\text{Ph}_2\text{As}(\text{S})\text{BH}_2\text{NMe}_3$ (**7b**) and selenium $\text{Ph}_2\text{As}(\text{Se})\text{BH}_2\text{NMe}_3$ (**7c**) oxidation products could be isolated and fully characterized, the bis(trimethylsilyl)peroxide oxidated arsinoborane $\text{Ph}_2\text{As}(\text{O})\text{BH}_2\text{NMe}_3$ (**7a**) is not stable enough and could only be characterized in solution. DFT computations support the decomposition pathway of this compound.

5.1 Introduction

Inorganic polymers based on main-group elements other than carbon are in the focus of current research, because of their versatile applications.^[1,2,3] Polymers consisting of alternating group 13 and group 15 elements are accessible by metal-catalyzed polycondensation reactions and dehydrocoupling processes. Both pathways are established for poly(aminoboranes) $[\text{RHNBH}_2]_n$ ($\text{R} = \text{alkyl, H}$) and poly(phosphinoboranes) $[\text{RHPBH}_2]_n$ ($\text{R} = \text{aryl}$). In the case of poly(phosphinoboranes), a third, catalyst-free pathway was recently developed.^[4] The thermal elimination of the Lewis base (LB) in $t\text{BuHPBH}_2\text{NMe}_3$ leads to a head-to-tail polymerization of the formed highly reactive intermediate $[t\text{BuHPBH}_2]$ and enables the access to the first high molecular weight poly(alkylphosphinoborane). With regard to the heavier pnictogen homologue, the quest for poly(arsinoboranes) is still open. Only a few arsinoboranes and cyclic oligo(arsinoboranes) are known (Figure 1).^[5] Protected with big substituents on both atoms, B and As, neutral rings (I)^[5b] and monomeric arsanylboranes (II)^[5b,d] were achievable. Applying less steric protection, there is only one example known of a cyclic arsinoborane containing hydrogen substituents on the B atom, $(\text{Me}_2\text{AsBH}_2)_3$ (III),^[5c] which reveals the high tendency for oligomerisation/polymerization of these highly reactive monomers. Another possibility is to use a LB for stabilization, as our group reported on the synthesis of the parent compound of arsanylboranes $\text{H}_2\text{AsBH}_2\text{NMe}_3$ (IV).^[6] As the goal for achieving poly(arsinoboranes) is still open, we tried to transfer our polymerization strategy of LB stabilized phosphanylboranes^[4] to arsanylboranes. Unfortunately, all attempts for thermal elimination of the LB in IV to force a head-to-tail polymerization failed and resulted in the cleavage of the labile As-B bond. Therefore, we targeted the synthesis of a partly sterically protected arsanylborane (V) as model compound. Substituting As with phenyl-groups will lead to less electron density on the pnictogen atom and stabilize the As-B bond.

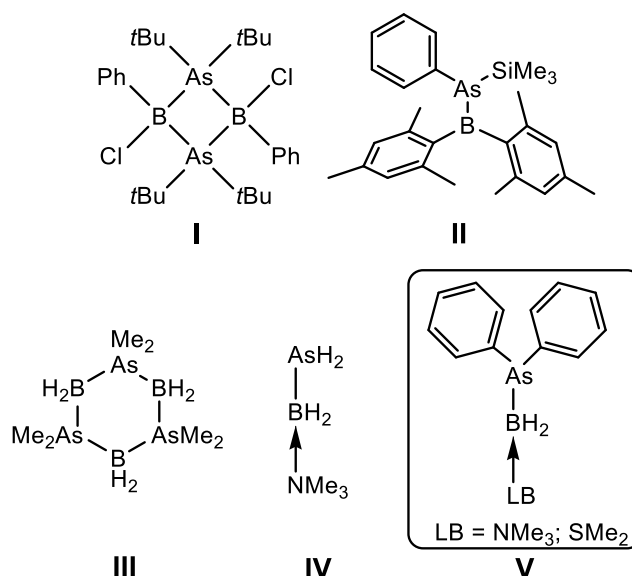


Figure 1: Selection of annular and monomeric arsinoboranes.

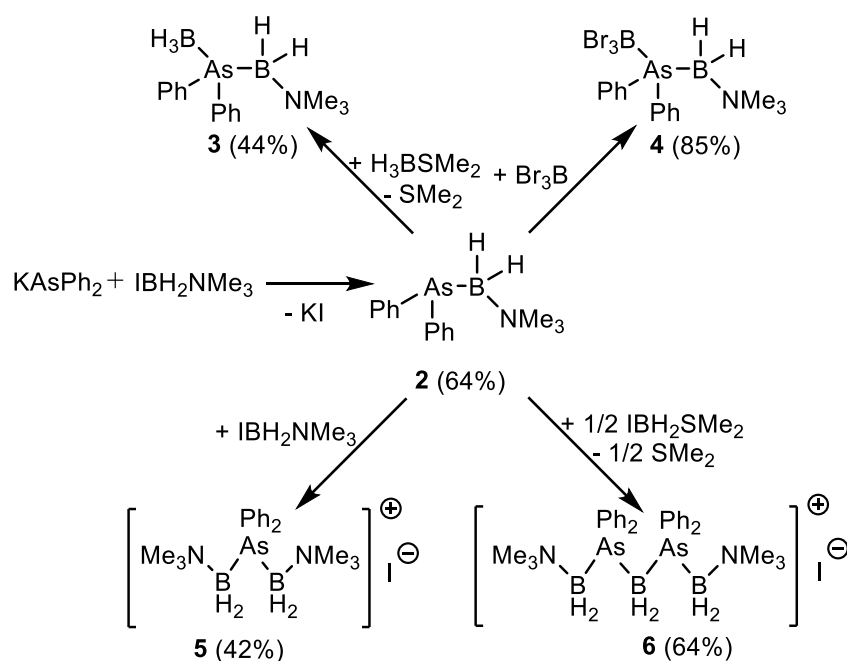
5.2 Results and Discussion

Herein, we present a one-pot synthesis for the LB stabilized arsanylborane $\text{Ph}_2\text{AsBH}_2\text{LB}$ in high yields. This reaction route enables the study of the reactivity of this new compound and open the way to neutral and cationic oligomeric group 13/15 compounds. Furthermore, we were able to synthesize the first oxidized arsanylboranes $\text{Ph}_2\text{As}(\text{Q})\text{BH}_2\text{NMe}_3$ ($\text{Q} = \text{O}, \text{S}, \text{Se}$).

The reaction of IBH_2SMe_2 with KAsPh_2 in thf leads to the LB stabilized arsanylborane $\text{Ph}_2\text{AsBH}_2\text{SMe}_2$ (**1**). According to NMR investigations, the conversion proceeds nearly quantitatively and is accompanied by a color change from red to colorless.^[7] All attempts to isolate **1** even at low temperatures or to stabilize the compound by coordination with a LA failed. However, as free SMe_2 is already detected by ^1H NMR spectroscopy of the reaction mixture at low temperatures, an elimination of the LB in **1** can be assumed. After allowing the reaction mixture to reach room temperature, a white solid is received in moderate yields, which is well soluble in solvents like toluene and thf. In the $^{11}\text{B}\{^1\text{H}\}$ NMR spectrum, a broad signal at $\delta = -31.04$ ppm is observed, which shows further broadening in the ^{11}B NMR spectrum. The signal lies in the range of the oligomer $[\text{Ph}_2\text{PBH}_2]_n$.^[4b] Furthermore, in the EI-MS fragment ion patterns of $[(\text{Ph}_2\text{AsBH}_2)_2\text{BH}_2]^+$ and $[(\text{Ph}_2\text{AsBH}_2)_3\text{BH}_2]^+$ are observed. Similar ion patterns are observed for $(\text{Me}_2\text{AsBH}_2)_3$ in the EI-MS.^[5c] Therefore, the decomposition of **1** and

formation of the trimer $(\text{Ph}_2\text{AsBH}_2)_3$ can be proposed. Unfortunately, it was not possible to obtain single crystals of the reaction products suitable for X-ray diffraction analysis. As polymerization processes depend decisively on controlled conditions and the purity of the starting materials, which is not given under the synthetic conditions for **1**, we targeted the synthesis of an arsanylborane stabilized by a stronger LB.

The salt metathesis reaction of KAsPh_2 with IBH_2NMe_3 in thf leads to $\text{Ph}_2\text{AsBH}_2\text{NMe}_3$ (**2**) in good yields (Scheme 1).^[8] In the ^{11}B NMR spectrum, the product shows a triplet at $\delta = -0.91$ ppm with a typical coupling constant $^1J_{\text{B,H}} = 115$ Hz. The absorptions of the B-H valence stretches in the IR spectra appear between 2376 cm^{-1} and 2360 cm^{-1} . Whereas thermal treatment of $\text{Ph}_2\text{PBH}_2\text{NMe}_3$ leads to the elimination of NMe_3 inducing a head-to-tail oligomerization,^[4b] by applying similar thermal polymerization conditions for **2** only the cleavage of the As-B bond instead of the B-N bond was observed. Therefore, only decomposition products like As_2Ph_4 could be detected. Interestingly, **2** shows a much higher thermal stability than $\text{Ph}_2\text{PBH}_2\text{NMe}_3$. It can be still detected by ^{11}B NMR spectroscopy after heating for 5 days at 100°C in toluene.^[9] However, above 100°C , decomposition occurs.



Scheme 1: Synthesis of compounds **2-6** (isolated yields in parentheses).

To determine if the donor strength of the As atom in a diphenylsubstituted arsanylborane is sufficient to build oligomeric chain compounds, we investigated the coordination chemistry of **2** with respect to the formation of longer neutral and cationic

13/15 chains. The reactions with Lewis acids (LA = H_3B , Br_3B) yields the corresponding LA-LB stabilized diphenylarsanylborane $\text{H}_3\text{BAsPh}_2\text{BH}_2\text{NMe}_3$ (**3**) and $\text{Br}_3\text{BAsPh}_2\text{BH}_2\text{NMe}_3$ (**4**; Scheme 1). Both reactions proceed smooth and nearly quantitative according to the ^{11}B NMR spectroscopy of the reaction mixtures.^[8] The signal of the BH_3 moiety in **3** is observed at $\delta = -33.51$ ppm, and for the BBr_3 moiety in **4** at $\delta = -13.40$ ppm in the ^{11}B NMR spectra. As expected, the ^{11}B resonance of the BH_2 moiety shifts highfield in **3** and **4**. The same tendency is observed in the $^{13}\text{C}\{^1\text{H}\}$ NMR spectra for the signals of the *ipso*-carbons.

The reaction of **2** with IBH_2LB (LB = NMe_3 , SMe_2) yields selectively compounds containing cationic oligomeric chains of different length. Depending on the donor strength of the LB, either the formation of the shorter chain $[\text{Me}_3\text{NBH}_2\text{AsPh}_2\text{BH}_2\text{NMe}_3]^+ \text{I}^-$ (**5**; LB = NMe_3), or the longer chain $[\text{Me}_3\text{NBH}_2\text{AsPh}_2\text{BH}_2\text{AsPh}_2\text{BH}_2\text{NMe}_3]^+ \text{I}^-$ (**6**; LB = SMe_2) can be observed (Scheme 1). Both conversations proceed with a yield up to 70% according to ^{11}B NMR spectroscopy.^[10] **5** and **6** are the first examples, that contain cationic chains derived from substituted arsanylboranes.

As expected, the signals of the Me_3N bonded BH_2 units of **5** and **6** in the ^{11}B NMR spectra shift highfield. In accordance to previous results,^[12] the BH_2 moiety between the two AsPh_2 groups in **6** shows broadening and a highfield shift at $\delta = -28.38$ ppm.

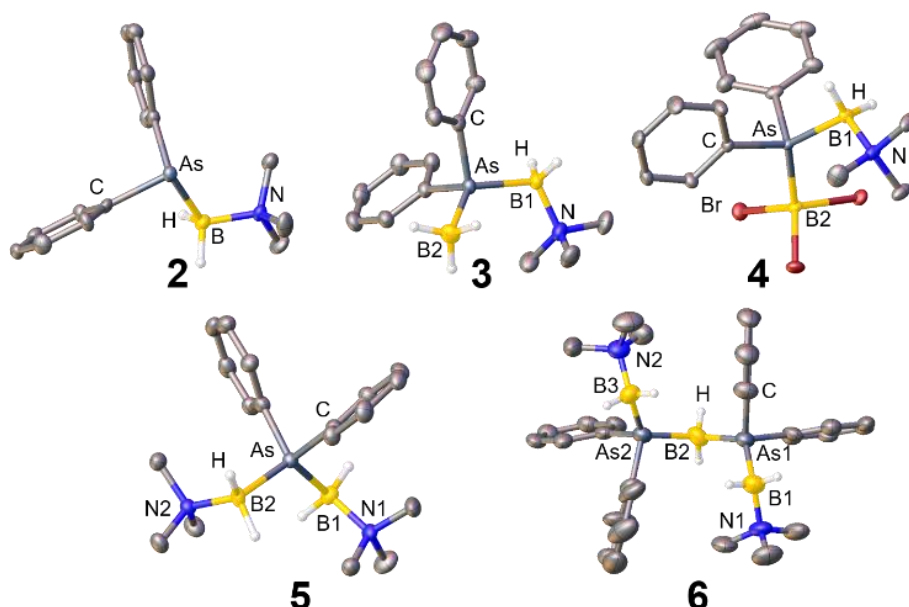


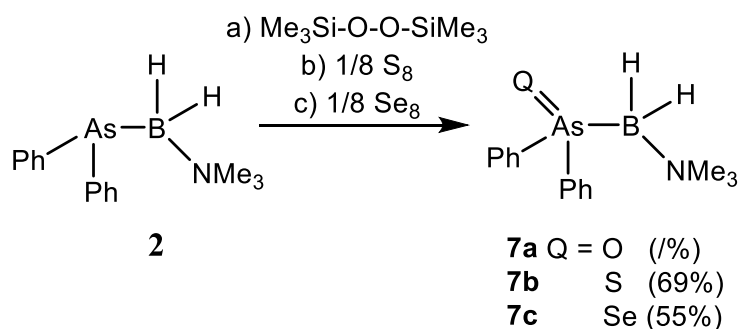
Figure 2: Molecular structure of compounds **2-6** in solid state. Hydrogen atoms bonded to carbon atoms and counterions are omitted for clarity. Thermal ellipsoids set at 50% probability. Selected bond lengths [Å] and angles [°]: **2**: As-B 2.098(8), N-B-As 111.2(5); **3**: As-B 2.058(3)-2.073(3), N-B-As 112.84(17)-112.91(16), B-As-B 123.13(12)-124.29(13); **4**: As-B 2.071(3)-2.090(4), N-B-As 116.6(2), B-As-B 122.48(14); **5**: As-B 2.083(3)-2.100(3), N-B-As 114.06(18)-114.68(19), B-As-B 121.74(13); **6**: As-B 2.052(11)-2.107(10), N-B-As 114.2(7)-116.4(7), B-As-B 127.3(4)-129.3(4).

The solid state structures of **2-6** were determined by single crystal X-ray diffraction (Figure 2). All bond lengths are in the range of single bonds. Compound **2** adopts an anticlinal arrangement along the As-B bond. The B atom presents a nearly tetrahedral arrangement. Similar to the environment of the P atom in $\text{Ph}_2\text{PBH}_2\text{NMe}_3$,^[4b] the As atom in **2** adopts a distorted tetrahedral arrangement.

In the solid state, the B-N and the As-B bonds of **3** and **4** are slightly shortened compared to **2**. Depending on the steric demand of the coordinated LA, the N-B-As angle is widened. Both compounds adopt a similar anticlinal arrangement along the As-B1-axis as **2**. Compound **3** and **4** exhibit certain structural analogies to the phosphorus homologues.^[11] Compounds **5** and **6** are the first examples of cationic substituted arsanylboranes (Figure 2), whereas cationic substituted phosphanylboranes are already known.^[12] Both, **5** and **6**, reveal a staggered conformation along the B-As chain. The two As-B axis in **5** adopt a synclinal arrangement, whereby an anticlinal environment is observed at the three As-B bonds in **6**.

The B-N as well as the As-B bond lengths do not change essentially compared to the starting material **2**. However, it was found that the N-B-As angle in **5** and **6** is widened. Interestingly, presumably resulting from packing effects, the B-As-B angles in **6** differ between 5° - 7° compared to **5**.

In contrast to $\text{H}_2\text{PBH}_2\text{NMe}_3$, where a selective oxidation to the boranylphosphine chalcogenides $\text{H}_2\text{P}(\text{Q})\text{BH}_2\text{NMe}_3$ (Q = S, Se) occurs,^[13] all attempts to oxidize $\text{H}_2\text{AsBH}_2\text{NMe}_3$ failed due to decomposition. Interestingly, arsine oxides^[14] are well investigated, but there are only few examples for arsine sulfides^[15] and only one structurally characterized arsine selenide.^[16] To get further insight into the stability of the As-B bond, we targeted for the oxidation of $\text{Ph}_2\text{AsBH}_2\text{NMe}_3$ (**2**).



Scheme 2: Synthesis of compounds **7a-c** (isolated yields in parentheses).

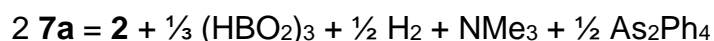
The reactions of **2** with bis(trimethylsilyl)peroxide, sulfur or grey selenium in CH₂Cl₂ yields the corresponding boranylarsine chalcogenides Ph₂As(Q)BH₂NMe₃ (**7a-c**). All reactions proceed smooth and in quantitative yields according to the ¹¹B NMR spectroscopy of the reaction mixtures.^[17] This reminds on the oxidation of substituted phosphanylboranes R₂PBH₂NMe₃ (R = Ph; R = *t*Bu and H).^[18] In contrast to the Ph₂PBH₂NMe₃, it was not possible to get access to the tellurium derivative, which is in accordance with the CV data of **2**, showing an irreversible oxidation at E = 1.65 V.^[19] However, **7a-c** represent the first oxidized arsanylboranes.

Whereas the sulfur (**7b**) and selenium derivative (**7c**) can be isolated as crystalline solids and fully characterized, all attempts to isolate the oxygen derivative Ph₂As(O)BH₂NMe₃ (**7a**) analytically pure failed due to the stability of the compound at ambient conditions. However, **7a** could be unambiguously identified by ESI-MS, IR and NMR spectroscopy.

DFT computations at B3LYP/def2-SVP level of theory (see SI, section 4.2) reveal that in the gas phase the formation of **7a-c** by the oxidation of **2** with O₂, S₈ and Se₈ is exothermic and exergonic at room temperature. Therefore, their spontaneous decomposition due to the reverse reaction



is thermodynamically forbidden. However, computational data predict the existence of several alternative decomposition pathways of **7a**, which are exergonic at room temperature. Among these reactions, the process



yields the starting material **2** as one of the detected decomposition products. An intermolecular mechanism for this reaction could be assumed, with the transfer of the oxygen atom from the first molecule of **7a** to the boron atom of a second molecule of **7a**, yielding **2**, polymeric metaboric acid (HBO)_n, trimethylamine, molecular hydrogen and AsPh₂ radicals, which are expected to dimerize to form As₂Ph₄. A long term (28 days) NMR study confirms the decomposition of **7a** with formation of **2**, in accord with the postulated decomposition pathway.^[20] Furthermore, the identification of the diarsine As₂Ph₄ gives further evidence of the discussed pathway.^[21]

In the ¹¹B NMR spectra of **7a-c**, triplets arise, shifted more strongly highfield with rising electronegativity of the chalcogen substituent Q compared to the starting material **2**.^[22] In the ESI-MS (**7a**) and the LIFDI-MS (**7b**, **7c**), respectively, the molecular ion peaks are detected. The IR spectra of **7a-c** show clearly a shift to higher wavenumbers for

the absorptions of the B-H valence stretches compared to the starting material **2**. The broad band of the As-O valence stretches in **7a** ($\tilde{\nu}(\text{As}=\text{O}) = 846 \text{ cm}^{-1}$) is similar to those in triphenylarsine oxide ($\tilde{\nu}(\text{As}=\text{O}) = 877, 885 \text{ cm}^{-1}$).^[23]

Single crystals suitable for X-ray structure analysis were obtained by layering a solution of CH_2Cl_2 with *n*-hexane (**7b**) or by slow evaporation of CH_2Cl_2 (**7c**). Both molecules adopt a synclinal arrangement along the B-As axis in solid state (Figure 3). The B-As bond length is slightly shorter as in the starting material. Compared to triphenylarsine sulfide ($\text{As-S} = 2.090 \text{ \AA}$),^[15b] the influence of the boron moiety H_2BNMe_3 leads to a slight elongation of the As-S bond in **7b** ($\text{As-S} = 2.1136(7) \text{ \AA}$). The same tendency can be observed for **7c**, where the As-Se bond ($\text{As-Se} = 2.2553(4) \text{ \AA}$) is elongated in comparison to triethylarsine selenide ($\text{As-Se} = 2.234 \text{ \AA}$)^[16b] due to the influence of the boron moiety.

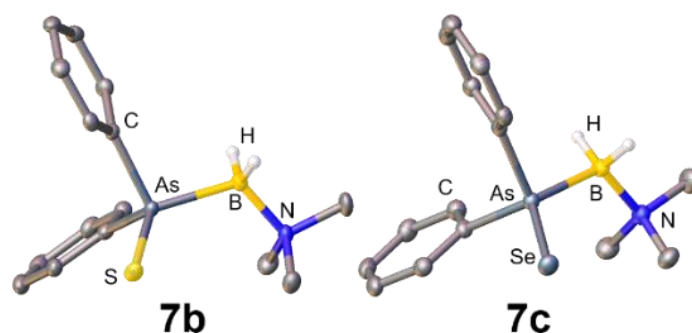


Figure 3: Molecular structure of **7b** and **7c** in solid state. Hydrogen atoms bonded to carbon atoms are omitted for clarity. Thermal ellipsoids set at 50% probability.

5.3 Conclusion

In summary, we showed a one-pot synthesis as an elegant way to access a new class of LB stabilized organo-substituted arsanylboranes. Whereas $\text{Ph}_2\text{AsBH}_2\text{SMe}_2$ (**1**) can only be characterized in solution, due to its thermal instability, $\text{Ph}_2\text{AsBH}_2\text{NMe}_3$ (**2**) can be isolated in good yields and shows a high thermal stability. By reaction with different moieties novel compounds are accessible containing neutral (**3**, **4**) and cationic (**5**, **6**) arsanylborane chains, with alternating group 13 and 15 group elements. Furthermore, we were able to synthesize the first oxidized arsanylboranes (**7a-c**). Besides the highly sensitive oxygen derivative $\text{Ph}_2\text{As}(\text{O})\text{BH}_2\text{NMe}_3$ (**7a**), which could unambiguously be characterized in solution, the sulfur (**7b**) and the selenium derivative (**7c**) have been

characterized also in solid state. **7a-c** are the first compounds containing a Q=As-B fragment (Q = O, S, Se). We proved, that the donor strength of the As moiety, as well as the stability of the As-B bond has significant influence on a possible head-to-tail polymerization. To enable this, the As-B bond must be stronger than the LB-B bond to achieve an elimination of the LB. All attempts to thermally eliminate NMe₃ in **2** failed due to decomposition of the As-B bond, whereas SMe₂ in **1** is already eliminated at lower temperatures, presumably forming the trimeric arsinoborane (Ph₂AsBH₂)₃. To optimize both influencing factors and to get further access to poly(arsinoborane)s, reactions with alkyl-substituted arsinoboranes, stabilized with primary and secondary amines as LB are under current investigation.

5.4 References

- [1] a) M. Liang, I. Manners, *J. Am. Chem. Soc.* **1991**, *113*, 4044-4045; b) H. R. Allcock, *Chem. Mater.* **1994**, *6*, 1476-1491; c) R. D. Archer, *Inorganic and Organometallic Polymers*, Wiley-VCH, New York, **2001**; d) I. Manners, *Angew. Chem. Int. Ed. Engl.* **1996**, *35*, 1602-1621; *Angew. Chem.* **1996**, *108*, 1712-1731; e) R. H. Neilson, P. Wisian-Neilson, *Chem. Rev.* **1988**, *88*, 541-562; f) S. J. S. Clarson, J. A. Semlyen, *Siloxane Polymers*, Prentice Hall, Englewood Cliffs, **1993**; g) F. Choffat, S. Käser, P. Wolfer, D. Schmid, R. Mezzenga, P. Smith, W. Caseri, *Macromolecules* **2007**, *40*, 7878-7889; h) R. D. Miller, J. Michl, *Chem. Rev.* **1989**, *89*, 1359-1410; i) R. De Jaeger, M. Gleria, *Prog. Polym. Sci.* **1998**, *23*, 179-276; j) X. He, T. Baumgartner, *RSC Adv.* **2013**, *3*, 11334-11350; k) A. M. Priegert, B. W. Rawe, S. C. Serin, D. P. Gates, *Chem. Soc. Rev.*, **2016**, *45*, 922-953; l) J. Linshoeft, E. J. Baum, A. Hussain, P. J. Gates, C. Näther, A. Staubitz, *Angew. Chem. Int. Ed.* **2014**, *53*, 12916-12920; *Angew. Chem.* **2014**, *126*, 13130-13134; m) B. W. Rawe, C. P. Chun, D. P. Gates, *Chem. Sci.* **2014**, *5*, 4928-4938; n) G. Zhang, G. M. Palmer, M. W. Dewhirst, C. L. Fraser, *Nat. Mater.* **2009**, *8*, 747-751; o) Z. M. Hudson, D. J. Lunn, M. A. Winnik, I. Manners, *Nat. Commun.* **2014**, *5*, 3372; p) A. Hübner, Z.-W. Qu, U. Englert, M. Bolte, H.-W. Lerner, M. C. Holthausen, M. Wagner, *J. Am. Chem. Soc.* **2011**, *133*, 4596-4609; q) P. J. Fazen, J. S. Beck, A. T. Lynch, E.

- E. Remsen, L. G. Sneddon, *Chem. Mater.* **1990**, *2*, 96-97; r) F. Jäkle, *Chem. Rev.* **2010**, *110*, 3985-4022.
- [2] See, for example: a) A. Staubitz, M. E. Sloan, A. P. M. Robertson, A. Friedrich, S. Schneider, P. J. Gates, J. Schmedt auf der Günne, I. Manners, *J. Am. Chem. Soc.* **2010**, *132*, 13332-13345; b) H. C. Johnson, E. M. Leita, G. R. Whittell, I. Manners, G. C. Lloyd-Jones, A. S. Weller, *J. Am. Chem. Soc.* **2014**, *136*, 9078-9093; c) A. N. Marziale, A. Friedrich, I. Klopsch, M. Drees, V. R. Celinski, J. Schmedt auf der Günne, S. Schneider, *J. Am. Chem. Soc.* **2013**, *135*, 13342-13355; d) H. C. Johnson, A. S. Weller, *Angew. Chem. Int. Ed.* **2015**, *54*, 10173-10177; *Angew. Chem.* **2015**, *127*, 10311-10315; e) T. Wideman, P. J. Fazen, K. Su, E. E. Remsen, G. A. Zank, L. G. Sneddon, *Appl. Organometal. Chem.* **1998**, *12*, 681-693; f) R. Dallanegra, A. P. M. Robertson, A. B. Chaplin, I. Manners, A. S. Weller, *Chem. Commun.* **2011**, *47*, 3763-3765; g) A. Staubitz, A. P. M. Robertson, M. E. Sloan, I. Manners, *Chem. Rev.* **2010**, *110*, 4023-4078.
- [3] a) S. Pandey, P. Lönnecke, E. Hey-Hawkins, *Eur. J. Inorg. Chem.* **2014**, 2456-2465; b) H. Dorn, R. A. Singh, J. A. Massey, J. M. Nelson, C. A. Jaska, A. J. Lough, I. Manners, *J. Am. Chem. Soc.* **2000**, *122*, 6669-6678; c) H. Dorn, J. M. Rodezno, B. Brunnhofer, E. Rivard, J. A. Massey, I. Manners, *Macromolecules* **2003**, *36*, 291-297; d) J.-M. Denis, H. Forintos, H. Szelke, L. Toupet, T.-N. Pham, P.-J. Madec, A.-C. Gaumont, *Chem. Commun.* **2003**, 54-55; e) D. Jacquemin, C. Lambert, E. A. Perpete, *Macromolecules* **2004**, *37*, 1009-1015; f) A. Kumar, N. A. Beattie, S. D. Pike, S. A. Macgregor, A. S. Weller, *Angew. Chem. Int. Ed.* **2016**, *55*, 6651-6656; *Angew. Chem.* **2016**, *128*, 6763-6768; g) A. N. Marziale, A. Friedrich, I. Klopsch, M. Drees, V. R. Celinski, J. Schmedt auf der Günne, S. Schneider, *J. Am. Chem. Soc.* **2013**, *135*, 13342-13355; h) R. T. Baker, J. C. Gordon, C. W. Hamilton, N. J. Henson, P.-H. Lin, S. Maguire, M. Murugesu, B. L. Scott, N. C. Smythe, *J. Am. Chem. Soc.* **2012**, *134*, 5598-5609.
- [4] a) A. Stauber, T. Jurca, C. Marquardt, M. Fleischmann, M. Seidl, G. R. Whittell, I. Manners, M. Scheer, *Eur. J. Inorg. Chem.* **2016**, 2684-2687; b) C. Marquardt, T. Jurca, K.-C. Schwan, A. Stauber, A. V. Virovets, G. R. Whittell, I. Manners, M. Scheer, *Angew. Chem. Int. Ed.* **2015**, *54*, 13782-13786; *Angew. Chem.* **2015**, *127*, 13986-13991.

- [5] a) J. Burt, J. W. Emsley, W. Levason, G. Reid, I. S. Tinkler, *Inorg. Chem.* **2016**, *55*, 8852–8864; b) M. A. Petrie, M. M. Olmstead, H. Hope, R. A. Bartlett, P. P. Power, *J. Am. Chem. Soc.* **1993**, *115*, 3221–3226; c) R. Goetze, H. Nöth, *Z. Naturforsch.* **1975**, *30b*, 875–882; d) M. A. Mardones, A. H. Rowley, L. Contreras, R. A. Jones, *J. Organomet. Chem.* **1993**, *455*, C1–C2.
- [6] a) C. Marquardt, A. Adolf, A. Stauber, M. Bodensteiner, A. V. Virovets, A. Y. Timoshkin, M. Scheer, *Chem. Eur. J.* **2013**, *19*, 11887–11891; b) U. Vogel, P. Hoemensch, K.-C. Schwan, A. Y. Timoshkin, M. Scheer, *Chem. Eur. J.* **2003**, *9*, 515–519.
- [7] See Supporting Information: Formation of Ph₂AsBH₂SMe₂.
- [8] The reactions proceeds nearly quantitative according to ¹¹B NMR spectroscopy. **4** can be isolated as a powder, whereas for **2** and **3** crystallization is necessary, to ensure the analytical purity, which lowers the overall yield.
- [9] See Supporting Information: NMR spectra of oligomerization/polymerization attempts.
- [10] To ensure the analytical purity of **5** and **6**, several washing steps are necessary, lowering the overall yield.
- [11] C. Marquardt, T. Kahoun, J. Baumann, M. Scheer, *Z. Anorg. Allg. Chem.* **2017**, *643*, 1326–1330.
- [12] C. Marquardt, G. Balász, J. Baumann, A. V. Virovets, M. Scheer, *Chem. Eur. J.* **2017**, *23*, 11423–11429.
- [13] K.-C. Schwan, A. Y. Timoshkin, M. Zabel, M. Scheer, *Chem. Eur. J.* **2006**, *12*, 4900–4908.
- [14] a) A. Michaelis, U. Paetow, *Liebigs Ann. Chem.* **1886**, 60–92; b) R. F. Ketelaere, F. T. Delbeke, G. P. van der Kelen, *J. Organomet. Chem.* **1971**, *28*, 217–223; c) A. Merijanian, R. A. Zingaro, *Inorg. Chem.* **1966**, *5*, 187–191; d) V. Krishnan, A. Datta, S. V. L. Narayana, *Inorg. Nucl. Chem. Letters* **1977**, *13*, 517–522.
- [15] a) G. Sakane, T. Shibahara, *Transition Met. Chem.* **1996**, *21*, 398–400; b) S. V. L. Narayana, H. N. Shrivastava, *Acta Cryst.* **1981**, *B37*, 1189–1193; c) D. H. Brown, A. F. Cameron, R. J. Cross, M. McLaren, *J. Chem. Soc., Dalton Trans.*, **1981**, 1459–1462.
- [16] a) E. Krzywanska, *Acta Physica Polonica*, **1985**, *A68*, 75–78; b) V.E.Zavodnik, B.E.Abalonin, V.K.Bel'skii, *Metalloorgisheskaya Khimiia*, **1992**, *5*, 210.

- [17] To ensure analytical purity of **7b** and **7c** a washing step is necessary, which lowers the overall yield.
- [18] C. Marquardt, O. Hegen, T. Kahoun, M. Scheer, *Chem. Eur. J.* **2017**, 23, 4397–4404.
- [19] See Supporting Information: Cyclovoltamogram of Ph₂AsBH₂NMe₃.
- [20] See Supporting Information: Long term NMR spectra.
- [21] Crystalline As₂Ph₄ was obtained reproducibly in this reaction procedure.
- [22] See Supporting Information: Comparison of ¹¹B NMR data of **2**, **7a**, **7b** and **7c**.
- [23] G. B. Deacon, J. H. S. Green, *Spectrochim. Acta* **1969**, 25A, 355–364.

5.5 Supporting Information

Experimental Section

Synthetic procedures

All manipulations were performed under an atmosphere of dry argon using standard glovebox and Schlenk techniques. All solvents are degassed and purified by standard procedures.

The compounds IBH₂·NMe₃^[1], IBH₂·SMe₂^[1] and KAsPh₂^[2] were prepared according literature procedures. Other chemicals were obtained from Sigma-Aldrich (S₈, H₃B·SMe₂, Br₃B, Segrey) and Fluorochem (Me₃Si-O-O-SiMe₃).

The NMR spectra were recorded on either an Avance 400 spectrometer (¹H: 400.13 MHz, ³¹P: 161.976 MHz, ¹¹B: 128.378 MHz, ¹³C{¹H}: 100.623 MHz, ²⁷Al: 104.261 MHz) with δ [ppm] referenced to external SiMe₄ (¹H, ¹³C), H₃PO₄ (³¹P), BF₃·Et₂O (¹¹B), CFC₃ (¹⁹F) or Al(NO₃)₃·9 H₂O (²⁷Al).

IR spectra were measured on a DIGILAB (FTS 800) FT-IR spectrometer and on a Thermo Scientific Nicolet iS5. All mass spectra were recorded on a Finnigan MAT 95 (FDMS and EI-MS) and a Jeol AccuTOF GCX (LIFDI).

The C, H, N analyses were measured on an Elementar Vario EL III apparatus.

Synthesis of Ph₂AsBH₂SMe₂ (**1**)

To a solution of 16.3 mg (0.05 mmol) KAsPh₂ 0.65 dioxane in 1 mL thf-d⁸ 0.05 mL (0.05 mmol) of a solution of IBH₂SMe₂ in toluene is added at -80°C in a NMR tube. The color of the solution changed within seconds after the addition from red to colorless. The formation of Ph₂AsBH₂SMe₂ is observed by VT NMR experiments. **9** decomposes

over -20°C and under reduced pressure. All attempts to isolate or quench the product failed.

Analytical Data of 1: ^{11}B -NMR (thf- d^8 , -60°C): δ [ppm] = -14.11 (s, br, BH_2).

Attempts to synthesize $[\text{Ph}_2\text{As-BH}_2]_n$

a) A solution of 150 mg (0.5 mmol) $\text{Ph}_2\text{AsBH}_2\text{NMe}_3$ in 10 mL toluene is heated at 100°C for five days. The color of the clear solution turned red-orange after about 10 h. Proper signals, which indicate oligomeric/polymeric material are not observed.

b) To a solution of 712 mg (2 mmol) KAsPh_2 dioxane in 10 mL thf 2 mL of a 1M solution $\text{IBH}_2\cdot\text{SMe}_2$ is added at -80°C. The solution is stirred for 18 h and allowed to reach room temperature. The deep red solution is bleached. All volatiles are removed via vacuum. The remaining solid is suspended in 25 mL toluene and filtrated. After removal of all volatiles, the received oil is suspended in 35 mL *n*-pentane and the solvent is decanted after stirring for 18 h. The sustained white solid is dried via vacuum.

Yield: 182 mg; ^{11}B -NMR (C_6D_6 , 25°C): δ [ppm] = -31.04 (m, br, BH_2); $^{11}\text{B}\{^1\text{H}\}$ -NMR (C_6D_6 , 25°C): δ [ppm] = -31.04 (m, br, BH_2); EI-MS: m/z = 497 [$\{\text{BH}_2(\text{AsPh}_2\text{BH}_2)_2\}^+$], 739 [$\{\text{AsPh}_2(\text{BH}_2\text{AsPh}_2\text{BH}_2)_2\}^+$].

Synthesis of $\text{Ph}_2\text{AsBH}_2\text{NMe}_3$ (**2**):

A solution of 2.948 g (11 mmol) KAsPh_2 in 30 mL thf is added to a solution of 1.988 g (10 mmol) $\text{IBH}_2\cdot\text{NMe}_3$ in 35 mL thf at -80°C. The solution is allowed to reach room temperature overnight and the color changes from red to colorless. All volatiles are removed under reduced pressure. The product is extracted with 50 mL toluene and filtrated over diatomaceous earth. The solution was concentrated *in vacuo* until the first crystals appear and stored at -28°C. **2** crystallizes as colorless prisms.

Yield of 2: 1.950 g (64%, crystalline). ^1H -NMR (C_6D_6 , 25°C): δ [ppm] = 1.86 (s, 9H, NMe_3), 2.92 (q, 2H, $^1J_{\text{H,B}} = 115$ Hz, BH_2), 7.09 (m, 2H, *p*- C_6H_5), 7.20 (m, 4H, *m*- C_6H_5), 7.94 (m, 4H, *o*- C_6H_5); ^{11}B -NMR (C_6D_6 , 25°C): δ [ppm] = -0.91 (t, $^1J_{\text{B,H}} = 115$ Hz, BH_2); $^{11}\text{B}\{^1\text{H}\}$ -NMR (C_6D_6 , 25°C): δ [ppm] = -0.91 (s, BH_2); ^{11}B -NMR (CDCl_3 , 25°C): δ [ppm] = -1.13 (t, $^1J_{\text{B,H}} = 115$ Hz, BH_2); $^{11}\text{B}\{^1\text{H}\}$ -NMR (CDCl_3 , 25°C): δ [ppm] = -1.13 (s, BH_2);

^{13}C -NMR (C_6D_6 , 25°C): δ [ppm] = 53.11 (s, NMe_3), 126.60 (s, $p\text{-C}_6\text{H}_5$), 128.12 (s, $m\text{-C}_6\text{H}_5$), 135.29 (s, $o\text{-C}_6\text{H}_5$), 144.05 (s, $i\text{-C}_6\text{H}_5$). IR(KBr): $\tilde{\nu}$ [cm^{-1}] = 3057 (vw, $\text{C}_{\text{Ph}}\text{-H}$), 3003 (vw, $\text{C}_{\text{Ph}}\text{-H}$), 2941 (vw, $\text{C}_{\text{Me}}\text{-H}$), 2376 (m, BH), 2360 (m, BH), 2290 (vw), 1894 (vw), 1575 (vw), 1477 (s), 1459 (s), 1430 (s), 1404 (w), 1303 (vw), 1263 (vw), 1251 (w), 1154 (m), 1116 (s), 1076 (w), 1045 (vs), 1022 (m), 1006 (vw), 979 (vw), 852 (s), 741 (s), 696 (s), 584 (w), 486 (m). LIFDI-MS: m/z = 373 ($[\text{M}^+]$). Elemental analysis (%) calculated for $\text{C}_{15}\text{H}_{21}\text{NBAs}$ (**1**): C: 59.84, H: 7.03, N: 4.65; found: C: 59.64, H: 7.05, N: 4.65.

Synthesis of $\text{H}_3\text{B-Ph}_2\text{AsBH}_2\text{NMe}_3$ (**3**):

0.04 mL (0.4 mmol) H_3BSMe_2 is added to 50 mg (0.16 mmol) $\text{Ph}_2\text{AsBH}_2\text{NMe}_3$ in 5 mL thf. After stirring overnight all volatiles are removed *in vacuo*. The remaining white solid is washed with 10 mL *n*-hexane and dissolved in 10 mL toluene. The solution is stored at -28°C to obtain **3** as colorless plates.

Yield of **3**: 22 mg (44%, crystalline). ^1H -NMR (C_6D_6 , 25°C): δ [ppm] = 1.91 (s, 9H, NMe_3), 2.23 (m, 3H, BH_3), 2.82 (m, 2H, BH_2), 7.04 (m, 2H, $p\text{-C}_6\text{H}_5$), 7.12 (m, 4H, $m\text{-C}_6\text{H}_5$), 8.05 (m, 4H, $o\text{-C}_6\text{H}_5$); ^{11}B -NMR (C_6D_6 , 25°C): δ [ppm] = -5.72 (t, $^1J_{\text{B,H}} = 116$ Hz, BH_2), -33.51 (q, $^1J_{\text{B,H}} = 103$ Hz, BH_3); $^{11}\text{B}\{^1\text{H}\}$ -NMR (C_6D_6 , 25°C): δ [ppm] = -5.72 (s, BH_2), -33.51 (s, BH_3); ^{13}C -NMR (C_6D_6 , 25°C): δ [ppm] = 53.47 (s, NMe_3), 128.82 (s, $p\text{-C}_6\text{H}_5$), 128.63 (s, $m\text{-C}_6\text{H}_5$), 133.36 (s, $o\text{-C}_6\text{H}_5$), 136.82 (s, $i\text{-C}_6\text{H}_5$). IR(KBr): $\tilde{\nu}$ [cm^{-1}] = 3048 (vw, $\text{C}_{\text{Ph}}\text{-H}$), 2948 (vw, $\text{C}_{\text{Me}}\text{-H}$), 2918 (vw, $\text{C}_{\text{Me}}\text{-H}$), 2451 (m, B-H), 2389 (s, B-H), 2369 (s, B-H), 2281 (w), 2267 (w), 1481 (m), 1467 (m), 1435 (m), 1410 (vw), 1245 (w), 1157 (w), 1145 (w), 1119 (m), 1070 (m), 1045 (vs), 974 (w), 864 (m), 755 (m), 745 (m), 698 (m), 590 (vw), 487 (w). LIFDI-MS: m/z = 373 [$\{(\text{Me}_3\text{N})_2\text{BH}(\text{AsPh}_2\text{BH}_3)\}^+$], 615 [$\{(\text{Me}_3\text{N})_2\text{B}(\text{AsPh}_2\text{BH}_3)_2\}^+$]. Elemental analysis (%) calculated for $\text{C}_{15}\text{H}_{24}\text{AsB}_2\text{N}$ (**2**): C: 57.12, H: 7.68, N: 4.45; found: C: 56.97, H: 7.33, N: 4.28.

Synthesis of $\text{Br}_3\text{B-Ph}_2\text{AsBH}_2\text{NMe}_3$ (**4**):

0.05 mL (0.5 mmol) BBr_3 is added to a solution of 150 mg (0.5 mmol) $\text{Ph}_2\text{AsBH}_2\text{NMe}_3$ in 15 mL toluene at -80°C . The clear solution is allowed to reach room temperature. A white precipitate is observed. All volatiles are removed *in vacuo*, the solid is washed 2 times with 5 mL *n*-hexane and dried *in vacuo*. **4** crystallizes by storing a saturated CH_3CN -solution at -28°C as colorless cubes.

Yield of 4: 235 mg (85%, powder). ^1H -NMR (CD_3CN , 25°C): δ [ppm] = 2.84(s, 9H, NMe_3), 2.95 (m, 2H, BH_2), 7.43 (m, 4H, *m*- C_6H_5), 7.49 (m, 2H, *p*- C_6H_5), 7.75 (m, 4H, *o*- C_6H_5); ^{11}B -NMR (CD_3CN , 25°C): δ [ppm] = -6.05 (t, $^1J_{\text{B,H}} = 115$ Hz, BH_2), -13.40 (s, BBr_3); $^{11}\text{B}\{^1\text{H}\}$ -NMR (CD_3CN , 25°C): δ [ppm] = -6.05 (s, BH_2), -13.40 (s, BBr_3); ^{13}C -NMR (CD_3CN , 25°C): δ [ppm] = 55.48 (s, NMe_3), 129.73 (s, *p*- C_6H_5), 131.13 (s, *m*- C_6H_5), 134.94 (s, *o*- C_6H_5), 131.57 (s, *i*- C_6H_5). IR(KBr): $\tilde{\nu}$ [cm^{-1}] = 3058 (w, $\text{C}_{\text{Ph}}\text{-H}$), 2992 ($\text{C}_{\text{Me}}\text{-H}$), 2946 (w), 2484 (m, B-H), 2428 (m, B-H), 2359 (vw), 2319 (vw), 1954 (vw), 1888 (vw), 1812 (vw), 1683 (vw), 1653 (vw), 1581 (vw), 1558 (vw), 1481 (vs), 1463 (vs), 1436 (m), 1410 (w), 1384 (vw), 1250 (m), 1239 (m), 1188 (m), 1163 (m), 1118 (vs), 1085 (s), 1063 (vs), 1025 (m), 1014 (m), 999 (m), 971 (w), 867 (s), 740 (vs), 692 (vs), 677 (s), 647 (m), 610 (vs), 610 (vs), 594 (s), 478 (m), 459 (m). LIFDI-MS: $m/z = 472$ [(M-Br) $^+$], 301 [(M- BBr_3) $^+$]. Elemental analysis (%) calculated for $\text{C}_{15}\text{H}_{21}\text{AsB}_2\text{Br}_3\text{N}$ (**3**): C: 32.66, H: 3.84, N: 2.54; found: C: 32.95, H: 4.01, N: 2.48.

Synthesis of $(\text{Me}_3\text{NH}_2\text{B-Ph}_2\text{AsBH}_2\text{NMe}_3)^+\text{I}^-$ (**5**):

A solution of 150 mg (0.5 mmol) $\text{Ph}_2\text{AsBH}_2\text{NMe}_3$ in 5 mL CH_2Cl_2 is mixed with a solution of 100 mg (0.5 mmol) IBH_2NMe_3 in 5 mL CH_2Cl_2 at -80°C . After stirring for six days, all volatiles are removed *in vacuo*. The remaining white solid is washed two times with 5 mL toluene. **5** crystallizes by layering a saturated CH_2Cl_2 solution with *n*-hexane.

Yield of 5: 105 mg (42%, powder). ^1H -NMR (CDCl_3 , 25°C): δ [ppm] = 2.75 (s, 18H, NMe_3), 2.87(m, 4H, BH_2), 7.42 (m, 2H, *p*- C_6H_5), 7.43 (m, 4H, *m*- C_6H_5), 7.53 (m, 4H, *o*- C_6H_5); ^{11}B -NMR (CDCl_3 , 25°C): δ [ppm] = -6.41(s, br, BH_2); $^{11}\text{B}\{^1\text{H}\}$ -NMR (CDCl_3 , 25°C): δ [ppm] = -6.41(s, br, BH_2); ^{13}C -NMR (CDCl_3 , 25°C): δ [ppm] = 55.09 (s, NMe_3), 129.75 (s, *m*- C_6H_5), 130.38 (s, *p*- C_6H_5), 130.69 (s, *i*- C_6H_5), 133.01 (s, *o*- C_6H_5). IR(KBr): $\tilde{\nu}$ [cm^{-1}] = 3043 (vw, $\text{C}_{\text{Ph}}\text{-H}$), 3005 (vw, $\text{C}_{\text{Ph}}\text{-H}$), 2946 (vw, $\text{C}_{\text{Me}}\text{-H}$), 2738 (vw), 2457 (m, B-H), 2402 (m, B-H), 1771 (vw), 1733 (vw), 1716 (vw), 1699 (vw), 1683 (vw), 1652 (vw), 1635 (vw), 1575 (vw), 1558 (vw), 1539 (vw), 1520 (vw), 1506 (vw), 1482 (m), 1472 (m), 1434 (w), 1393 (w), 1237 (w), 1172 (w), 1115 (m), 1051 (s), 1013 (w), 961 (vw), 867 (m), 740 (w), 720 (w), 692 (w), 486 (w). ES-MS (cation): $m/z = 373$ (M^+). Elemental analysis (%) calculated for $\text{C}_{15}\text{H}_{21}\text{AsBNS}$ (**4**): C: 43.25, H:6.45, N:5.60; found: C:40.90, H:6.42, N:5.57.

Synthesis of (Me₃NBH₂Ph₂As-H₂B-Ph₂AsBH₂NMe₃)⁺I⁻ (**6**):

To a solution of Ph₂AsBH₂NMe₃ (0.5 mmol) in 10 mL CH₂Cl₂ a solution of 1M IBH₂SMe₂ (0.25 mmol) in toluene is added at -80°C. The reaction solution is allowed to reach room temperature overnight. All volatiles are removed *in vacuo*. The remaining white solid is washed two times with 5 mL toluene and dried *in vacuo*. **6** crystallizes as colorless plates by slow evaporation of the solvent of a saturated CH₂Cl₂ solution.

Yield of **6**: 118 mg (64%, powder). ¹H-NMR (CDCl₃, 25°C): δ [ppm] = 2.54 (s, 18H, NMe₃), 2.61 (m, 6H, BH₂), 7.28 (m, 4H, *m*-C₆H₅), 7.35 (m, 2H, *p*-C₆H₅), 7.37 (m, 4H, *o*-C₆H₅); ¹¹B-NMR (CDCl₃, 25°C): δ [ppm] = -6.19 (s, br, BH₂-NMe₃), -28.38 (s, br, AsPh₂-BH₂-AsPh₂); ¹¹B{¹H}-NMR (CDCl₃, 25°C): δ [ppm] = -6.19 (s, BH₂-NMe₃), -28.38 (s, AsPh₂-BH₂-AsPh₂); ¹³C-NMR (CDCl₃, 25°C): δ [ppm] = 54.68 (s, NMe₃), 129.01 (s, *p*-C₆H₅), 129.88 (s, *m*-C₆H₅), 132.14 (s, *o*-C₆H₅), 133.09 (s, *i*-C₆H₅). IR(KBr): $\tilde{\nu}$ [cm⁻¹] = 3042 (s, C_{Ph}-H), 2975 (m, C_{Me}-H), 2809 (vw), 2730 (vw), 2458 (m, B-H), 2417 (m, B-H), 2362 (m), 1733 (vw), 1699 (vw), 1683 (vw), 1652 (vw), 1635 (vw), 1558 (vw), 1540 (vw), 1506 (vw), 1480 (s), 1434 (s), 1305 (vw), 1261 (w), 1160 (w), 1120 (m), 1062 (vs), 1013 (m), 957 (m), 866 (m), 802 (w), 764 (w), 743 (s), 695 (vs), 668 (vw), 640 (w), 483 (w), 458 (m). ES-MS (cation): *m/z* = 615 [M⁺]. Elemental analysis (%) calculated for C₃₀H₄₄As₂B₃IN₂ (**5**): C: 48.50, H: 5.97, N: 3.77; found: C: 47.70, H: 5.96, N: 3.62.

Synthesis of Ph₂As(O)BH₂NMe₃ (**7a**):

To a solution of 301 mg (1 mmol) Ph₂AsBH₂NMe₃ in 10 mL CH₂Cl₂ 0.25 mL (1.13 mmol) Bis-trimethylsilylperoxide at -80°C is added. According to ¹H-NMR and ¹¹B-NMR-spectra the product yields in 100%. Due to decomposition isolation by removing the solvent or precipitation was not successful.

Analytical data of **7a**: ¹H-NMR (CD₂Cl₂): δ [ppm] = δ [ppm] = 2.66 (m, 2H, BH₂), 2.89 (s, 9H, NMe₃), 7.38 (m, 4H, *m*-C₆H₅), 7.39 (m, 2H, *p*-C₆H₅), 7.73 (m, 4H, *o*-C₆H₅); ¹¹B-NMR (CD₂Cl₂, 25°C): δ [ppm] = -7.91 (t, ¹J_{B,H} = 112 Hz, BH₂); ¹¹B{¹H}-NMR (CD₂Cl₂, 25°C): δ [ppm] = -7.91 (s, BH₂). IR(KBr vessel, CH₂Cl₂): $\tilde{\nu}$ [cm⁻¹] = 3054 (m, C_{Ph}-H), 2986 (vw, C_{Me}-H), 2958 (w, C_{Me}-H), 2451 (w, B-H), 2407 (w, B-H), 2348 (vw), 1484 (vw), 1422 (vw), 1290 (vw), 1270 (vs), 1158 (vw), 1120 (vw), 1061 (w), 895 (w), 846

(m, As=O), 778 (vw), 758 (m), 700 (vs). ESI-MS (CH₂Cl₂): Kation: m/z = 318 [{M}⁺], 635 [{M₂}⁺].

Synthesis of Ph₂As(S)BH₂NMe₃ (**7b**):

150 mg (0.5 mmol) Ph₂AsBH₂NMe₃ and 16 mg (0.5 mmol) S₈ are put together as solid. The solids are dissolved in 10 mL CH₂Cl₂ to receive a clear yellow solution. After stirring for 18 h, all volatiles of the colorless solution are removed *in vacuo* and the remaining solid is washed with 5 mL toluene and dried *in vacuo*. **7b** crystallizes by layering a saturated CH₂Cl₂ solution with *n*-hexane at -28°C.

Yield of **7b**: 115 mg (69%, powder). ¹H-NMR (CDCl₃, 25°C): δ [ppm] = 2.85(m, 2H, BH₂), 2.91 (s, 9H, NMe₃), 7.34 (m, 4H, *m*-C₆H₅), 7.35 (m, 2H, *p*-C₆H₅), 7.89 (m, 4H, *o*-C₆H₅); ¹¹B-NMR (CDCl₃, 25°C): δ [ppm] = -6.44(t, ¹J_{B,H} = 115 Hz, BH₂); ¹¹B{¹H}-NMR (CDCl₃, 25°C): δ [ppm] = -6.44(s, BH₂); ¹³C-NMR (CDCl₃, 25°C): δ [ppm] = 54.09 (s, NMe₃), 128.44 (s, *m*-C₆H₅), 129.49 (s, *p*-C₆H₅), 130.69 (s, *o*-C₆H₅), 138.31 (s, *i*-C₆H₅). IR(KBr): $\tilde{\nu}$ [cm⁻¹] = 3017 (w, C_{Ph}-H), 2998 (w, C_{Me}-H), 2945 (vw), 2462 (m, B-H), 2423 (m, B-H), 2360 (w, P-H), 1843 (vw), 1771 (vw), 1733 (vw), 1716 (vw), 1699 (vw), 1683 (vw), 1652 (vw), 1635 (vw), 1616 (vw), 1576 (vw), 1539 (w), 1506 (w), 1478 (s), 1464 (s), 1435 (m), 1404 (vw), 1305 (w), 1243 (w), 1154 (w), 1114 (m), 1079 (w), 1053 (s), 1019 (vw), 1004 (w), 970 (w), 869 (m), 751 (s), 698 (s), 485 (s), 467 (m).

LIFDI-MS: m/z = 333 [{M}⁺], 405 [{Me₃NBH₂AsPh₂S-BH₂NMe₃}⁺], 666 [{M}⁺].

Elemental analysis (%) calculated for C₁₅H₂₁AsBNS (**7**): C: 54.08, H: 6.35, N: 4.20; found: C: 53.96, H: 6.31, N: 3.98.

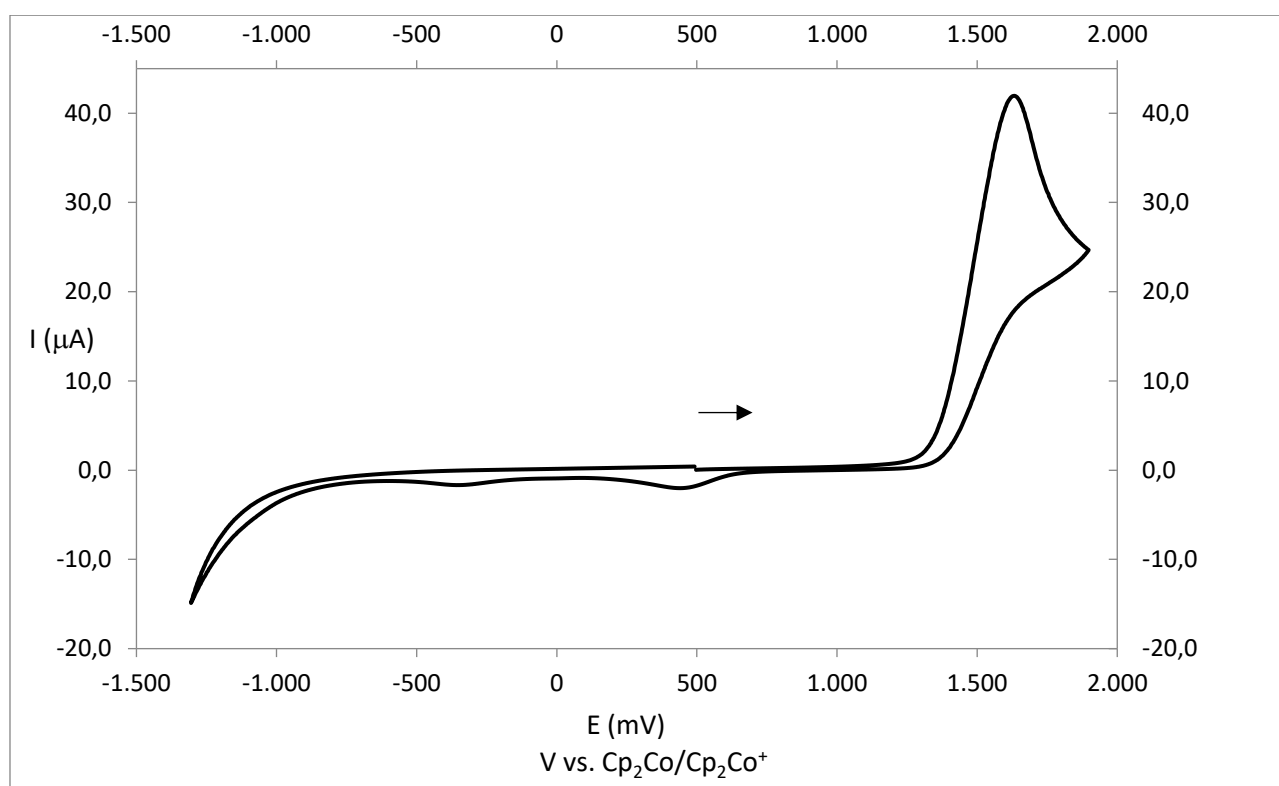
Synthesis of Ph₂As(Se)BH₂NMe₃ (**7c**):

150 mg (0.5 mmol) Ph₂AsBH₂NMe₃ and 39 mg (0.5 mmol) Se_{grey} are put together as solid. The solids are dissolved in 10 mL CH₂Cl₂ to receive a clear gray solution. After stirring for 18 h, all volatiles of the colorless solution are removed *in vacuo* and the remaining solid is washed with 5 mL toluene and dried *in vacuo*. **7c** crystallizes by evaporation of a saturated CH₂Cl₂ solution at room temperature.

Yield of **7c**: 105 mg (55%, powder). ¹H-NMR (CDCl₃, 25°C): δ [ppm] = 2.90 (m, 2H, BH₂), 2.92 (s, 9H, NMe₃), 7.32 (m, 4H, *m*-C₆H₅), 7.35 (m, 2H, *p*-C₆H₅), 7.89 (m, 4H, *o*-C₆H₅); ¹¹B-NMR (CDCl₃, 25°C): δ [ppm] = -6.15 (t, ¹J_{B,H} = 106 Hz, BH₂); ¹¹B{¹H}-NMR (CDCl₃, 25°C): δ [ppm] = -6.15 (s, BH₂); ¹³C-NMR (CDCl₃, 25°C): δ [ppm] = 54.22 (s,

NMe₃), 128.42 (s, *m*-C₆H₅), 129.49 (s, *p*-C₆H₅), 131.35 (s, *o*-C₆H₅), 136.28 (s, *i*-C₆H₅). IR(KBr): $\tilde{\nu}$ [cm⁻¹] = 3060 (vw), 3040 (vw), 3015 (vw, C_{Ph}-H), 2946 (vw, C_{Me}-H), 2460 (m, B-H), 2422 (m, B-H), 2362 (vw, P-H), 1980 (vw), 1576 (w), 1478 (s), 1467 (m), 1450 (m), 1434 (s), 1411 (vw), 1403 (vw), 1305 (w), 1242 (w), 1174 (w), 1154 (m), 1114 (s), 1077 (m), 1051 (s), 1020 (m), 1003 (m), 970 (w), 869 (m), 759 (m), 750 (s), 733 (w), 696 (s), 668 (w), 574 (w), 483 (m), 454 (w). LIFDI-MS: m/z = 381 [$\{M\}^+$], 453 [$\{Me_3BH_2AsPh_2Se-BH_2NMe_3\}^+$]. Elemental analysis (%) calculated for C₁₅H₂₁AsBNSe (**8**): C: 47.41, H: 5.57, N: 3.69; found: C: 47.04, H: 5.49, N: 3.44.

Cyclovoltamogram of Ph₂AsBH₂NMe₃



Compound **2** shows an irreversible oxidation, with no reversibility at either lower or higher feed rates. The CV was measured in CH₂Cl₂ with [Cp₂Co][PF₆] / Cp₂Co as reference.

X-Ray diffraction analysis

The X-ray diffraction experiments were performed on either on Rigaku Oxford Diffraction SuperNova diffractometer (**2-5**, **7b**, **7c**, T=123K, Cu-*K* α microsource, λ = 1.54178 Å, TitanS2 CCD detector) or on P11 beamline at DESY, Hamburg^[3] (**6**, T=80K, synchrotron radiation, λ = 0.6199 Å, 1-cycle diffractometer with horizontal ϕ -axis,

PILATUS 6M pixel detector). Crystallographic data together with the details of the experiments are given below. Integration of frames, data finalization and absorption corrections for all compounds, including **5**, was done using Rigaku Oxford Diffraction CrysAlisPro software.^[4]

Details of structure refinement and solution

All structures were solved using SIR97^[5], SHELXT^[6] and OLEX.^[7] Least square refinements against F^2 in anisotropic approximation were done using SHELXL.^[8]

The hydrogen positions of the methyl groups were located geometrically and refined riding on the carbon atoms. Hydrogen atoms belonging to BH₂ groups were located from the difference Fourier map and refined without constraints. All crystals of **2** and **6c** showed twinning, they were refined applying hklf5 refinement.

Crystal structures

Ph₂AsBH₂NMe₃ (**2**)

2 crystallizes from a solution of toluene at -28°C as colorless prisms in the monoclinic space group Cc. Figure S1 shows the molecular structure of **2** in solid state.

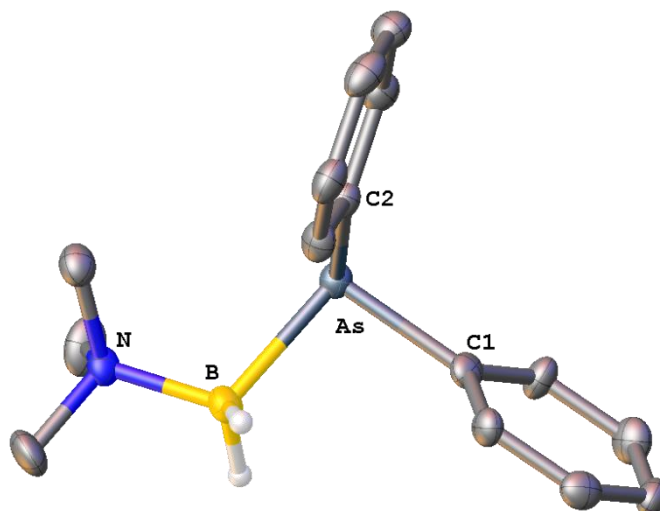


Figure S1: Molecular structure of **2** in the solid state. Hydrogen atoms bonded to carbon are omitted for clarity. Thermal ellipsoids are drawn with 50% probability. Selected bond lengths [Å] and angles [°]: N-B 1.612(10), B-As 2.098(8), As-C1 1.971(6), As-C2 1.979(7), C1-As-C2 98.4(3), N-B-As 111.2(5).

H₃B-Ph₂AsBH₂NMe₃ (3)

Compound **3** crystallizes from a solution of toluene at -28°C as colorless plates in the triclinic space group $P\bar{1}$ with one molecule toluene in the unit cell. All crystals showed twinning. Figure S2 shows the molecular structure of **3** in solid state.

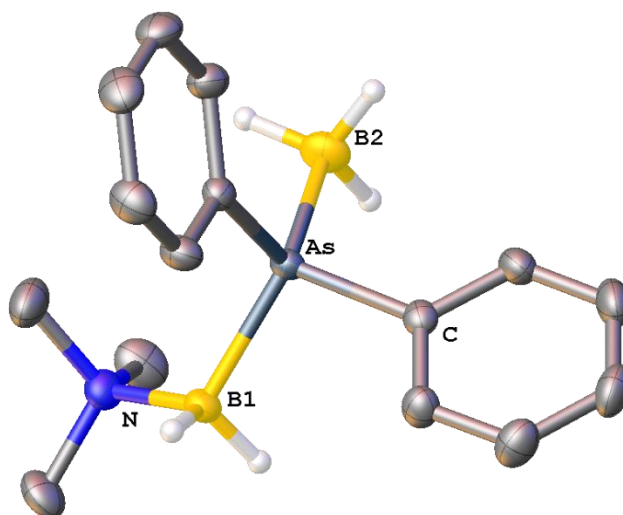


Figure S2: Molecular structure of **3** in the solid state. Hydrogen atoms bonded to carbon are omitted for clarity. Thermal ellipsoids are drawn with 50% probability. Selected bond lengths [Å] and angles [°]: N-B1 1.595(2), B1-As 2.0702(19), As-B2 2.056(2), N-B1-As 112.74(11), B1-As-B2 123.27(9).

Br₃B-Ph₂AsBH₂NMe₃ (4)

Compound **4** crystallizes from a solution of MeCN at -28°C as colorless cubes in the orthorhombic space group $Pbca$. Figure S3 shows the molecular structure of **4** in solid state.

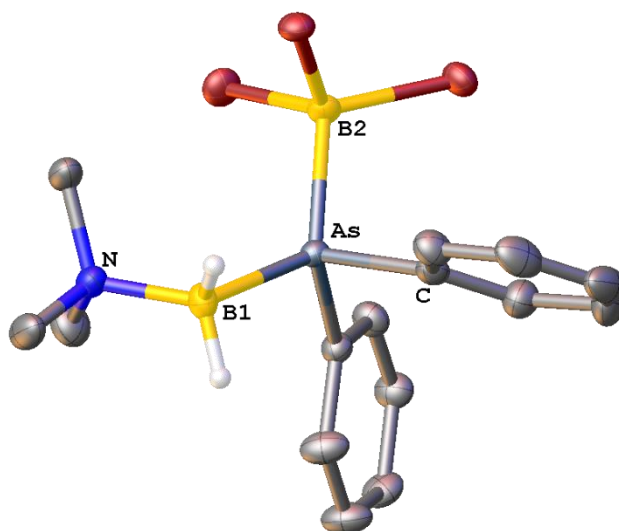


Figure S3: Molecular structure of **4** in the solid state. Hydrogen atoms bonded to carbon are omitted for clarity. Thermal ellipsoids are drawn with 50% probability. Selected bond lengths [Å] and angles [°]: N1-B1 1.598(5), B1-As1 2.093(4), As1-B2 2.077(4), N1-B1-As1 116.5(3), B1-As1-B2 122.59(18).

(Me₃NH₂B-Ph₂AsBH₂NMe₃)⁺t⁻ (5**)**

Compound **5** crystallizes from a solution of CH₂Cl₂ layered with *n*-hexane at -28°C as colorless plate with one molecule CH₂Cl₂ in the unit cell in the triclinic space group *P* $\bar{1}$. Figure S4 shows the molecular structure of **5** in solid state.

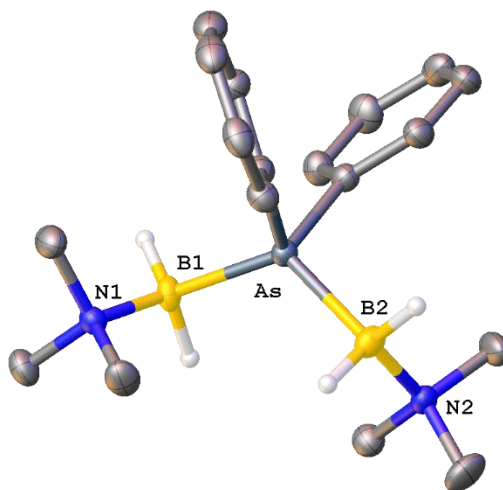


Figure S4: Molecular structure of **5** in the solid state. Hydrogen atoms bonded to carbon and counterions are omitted for clarity. Thermal ellipsoids are drawn with 50% probability. Selected bond lengths [Å] and angles [°]: N1-B1 1.600(3), N2-B2 1.593(4), B1-As 2.100(3), B2-As 2.083(4), N1-B1-As 114.03(17), N2-B2-As 114.74(18), B2-As-B1 121.71(13).

(Me₃NBH₂Ph₂As-H₂B-Ph₂AsBH₂NMe₃)⁺I⁻ (6)

Compound **6** crystallizes through evaporation of the solvent of a saturated CH₂Cl₂ solution as colorless plates in the triclinic space group $P\bar{1}$. There are two independent molecules of the compound with two molecules toluene and one molecule CH₂Cl₂ inside the unit cell. Figure S5 shows the molecular structure of **6** in solid state.

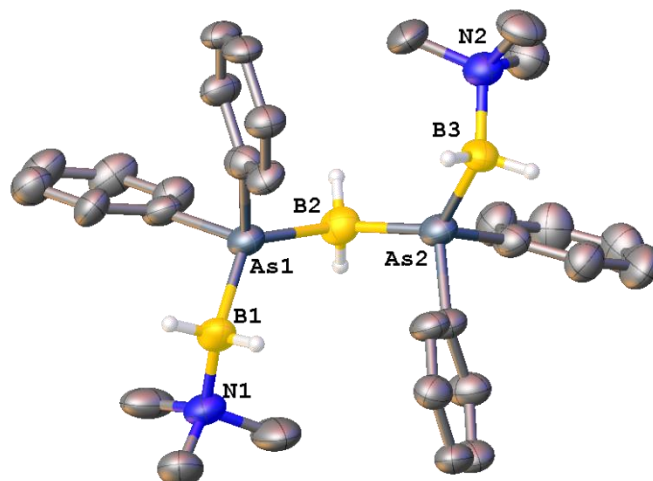


Figure S5: Molecular structure of **6** in the solid state. Hydrogen atoms bonded to carbon and counterions are omitted for clarity. Thermal ellipsoids are drawn with 50% probability. Selected bond lengths [Å] and angles [°]: N-B 1.577(13)-1.612(12), B-As 2.052(11)-2.107(10), N-B-As 114.2(7)-116.4(7), B-As-B 127.3(4)-129.3(4).

Ph₂As(S)BH₂NMe₃ (7b)

Compound **7b** crystallizes from a solution of CH₂Cl₂ layered with *n*-hexane at -28°C as colorless blocks in the orthorhombic space group $P2_12_12_1$. Figure S6 shows the molecular structure of **7b** in solid state.

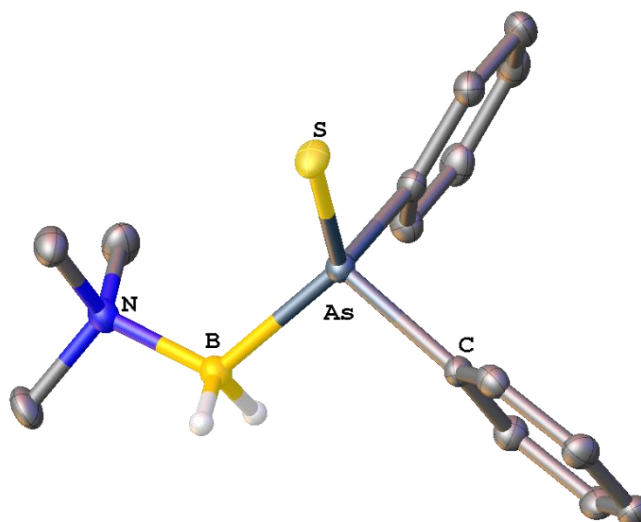


Figure S6: Molecular structure of **7b** in the solid state. Hydrogen atoms bonded to carbon are omitted for clarity. Thermal ellipsoids are drawn with 50% probability. Selected bond lengths [Å] and angles [°]: N-B 1.596(5), B-As 2.070(4), As-S 2.1133(8), N-B-As 116.6(2), B-As-S 120.50(11).

Ph₂As(Se)BH₂NMe₃ (7c)

Compound **7c** crystallizes by evaporation of a saturated solution of CH₂Cl₂ at room temperature as colorless block in the monoclinic space group *P*2₁/*c*. All crystals showed twinning. Figure S7 shows the molecular structure of **7c** in solid state.

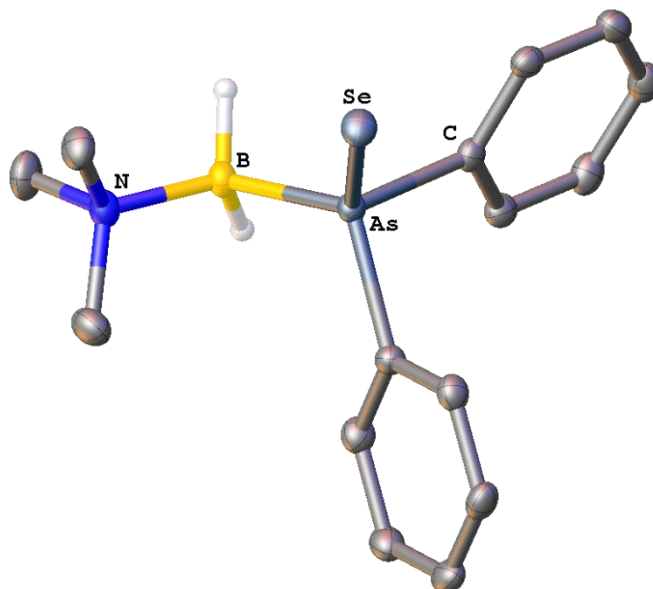


Figure S7: Molecular structure of **7c** in the solid state. Hydrogen atoms bonded to carbon are omitted for clarity. Thermal ellipsoids are drawn with 50% probability. Selected bond lengths [Å] and angles [°]: N-B 1.593(6), B-As 2.071(5), As-Se 2.2555(6), N-B-As 117.2(3), B-As-Se 120.78(15).

Crystallographic information**Table S1:** Crystallographic data for compounds **2** and **3**

	2	3
Empirical formula	C ₁₅ H ₂₁ AsBN	C ₃₇ H ₅₆ As ₂ B ₄ N ₂
Formula weight	301.06	360.96
Crystal	colorless prism	colorless plates
Crystal size/mm ³	0.04 × 0.069 × 0.187	0.259 × 0.037 × 0.034
Temperature/K	123.2(6)	123
Crystal system	monoclinic	triclinic
Space group	Cc	<i>P</i> $\bar{1}$
Unit cell dimensions	<i>a</i> = 14.3237(4) <i>b</i> = 9.0552(2) <i>c</i> = 11.3772(3) α = 90 β = 95.362(3) γ = 90	<i>a</i> = 8.4744(2) <i>b</i> = 13.1709(5) <i>c</i> = 19.1051(6) α = 71.232(3) β = 79.836(2) γ = 74.431(3)
Volume <i>V</i>	1469.21(7) Å ³	1935.44(12)
Formula units <i>Z</i>	4	4
Absorption coefficient μ	2.959 mm ⁻¹	2.320
Density ρ_{calc}	1.361 g/cm ³	1.239
<i>F</i> (000)	624.0	756.0
Theta range $\theta_{\text{min}}/\theta_{\text{max}}$	11.576°/148.424°	4.91/148.73
Absorption correction	gaussian	gaussian
Index ranges	-17 ≤ <i>h</i> ≤ 17 -8 ≤ <i>k</i> ≤ 11 -13 ≤ <i>l</i> ≤ 14	-7 ≤ <i>h</i> ≤ 10 -15 ≤ <i>k</i> ≤ 16 -23 ≤ <i>l</i> ≤ 23
Reflections collected	8013	13750
Independent reflections	2871 [<i>R</i> _{int} = 0.0371]	13750 [<i>R</i> _{int} = 0.0406]
Completeness to full θ	0.988	0.964
Transmission <i>T</i> _{min} / <i>T</i> _{max}	0.743/0.910	0.639/0.912
Data/restraints/parameters	2871/2/174	13750/0/454
Goodness-of-fit on <i>F</i> ²	1.186	1.050
Final <i>R</i> -values [<i>I</i> ≥ 2σ (<i>I</i>)]	<i>R</i> ₁ = 0.0362, <i>wR</i> ₂ = 0.1064	<i>R</i> ₁ = 0.0360, <i>wR</i> ₂ = 0.1064
Final <i>R</i> -values [all data]	<i>R</i> ₁ = 0.0378, <i>wR</i> ₂ = 0.1090	<i>R</i> ₁ = 0.0420, <i>wR</i> ₂ = 0.1091
Largest difference hole and peak $\Delta\rho$	-0.47 1.18 e Å ⁻³	-0.58, 0.49

Table S2: Crystallographic data for compounds **4** and **5**

	4	5
Empirical formula	C ₁₅ H ₂₁ AsB ₂ Br ₃ N	C ₁₉ H ₃₄ AsB ₂ Cl ₂ IN ₂
Formula weight	551.60	584.82
Crystal	colorless cubes	colorless plate
Crystal size/mm ³	0.359 × 0.228 × 0.174	0.68 × 0.122 × 0.074
Temperature/K	123	123
Crystal system	orthorhombic	triclinic
Space group	<i>Pbca</i>	<i>P</i> $\bar{1}$
Unit cell dimensions	a = 14.02470(19) b = 14.63913(18) c = 19.4863(2) α = 90 β = 90 γ = 90	a = 9.35198(20) b = 10.7164(2) c = 13.3184(3) α = 84.4330(17) β = 75.6426(18) γ = 84.0876(16)
Volume V	4000.72(9)	1282.66(5)
Formula units Z	8	2
Absorption coefficient μ	9.260	13.195
Density ρ_{calc}	1.832	1.514
F(000)	2128.0	584.0
Theta range $\theta_{\text{min}}/\theta_{\text{max}}$	9.076/147.286	6.87/147.9
Absorption correction	analytical	analytical
Index ranges	-11 ≤ h ≤ 17 -17 ≤ k ≤ 17 -16 ≤ l ≤ 23	-11 ≤ h ≤ 11 -13 ≤ k ≤ 13 -16 ≤ l ≤ 16
Reflections collected	8686	19124
Independent reflections	3909 [R_{int} = 0.0209]	5101 [R_{int} = 0.0505]
Completeness to full θ	0.968	0.979
Transmission $T_{\text{min}}/T_{\text{max}}$	0.210/0.395	0.040/0.508
Data/restraints/parameters	3909/0/210	5101/0/266
Goodness-of-fit on F^2	1.255	1.071
Final R-values [$I \geq 2\sigma(I)$]	R_1 = 0.0301, wR_2 = 0.0763	R_1 = 0.0306 wR_2 = 0.0824
Final R-values [all data]	R_1 = 0.0328, wR_2 = 0.0777	R_1 = 0.0318 wR_2 = 0.0832
Largest difference hole and peak $\Delta\rho$	-0.77, 0.46	-1.02 1.33

Table S3: Crystallographic data for compounds **6** and **7b**

	6	7b
Empirical formula	C _{37.1} H _{52.1} As ₂ B ₃ Cl _{0.1} IN ₂	C ₁₅ H ₂₁ AsBNS
Formula weight	840.35	333.12
Crystal	colorless plates	colorless block
Crystal size/mm ³	0.170 × 0.060 × 0.020	0.236 × 0.223 × 0.145
Temperature/K	80K	123
Crystal system	triclinic	orthorhombic
Space group	<i>P</i> $\bar{1}$	<i>P</i> 2 ₁ 2 ₁ 2 ₁
Unit cell dimensions	a = 16.1345(2) b = 16.9253(3) c = 18.2864(3) α = 99.4540(14) β = 115.4079(14) γ = 92.5597(12)	a = 8.9777(2) b = 10.1495(2) c = 17.4837(4) α = 90 β = 90 γ = 90
Volume V	4412.09(13)	1593.10(6)
Formula units Z	4	4
Absorption coefficient μ	1.561	3.977
Density ρ_{calc}	1.265	1.389
F(000)	1701.0	688
Theta range $\theta_{\text{min}}/\theta_{\text{max}}$	3.352/43.856	10.078/148.202
Absorption correction	multi-scan	gaussian
Index ranges	-19 ≤ h ≤ 19 -20 ≤ k ≤ 20 -22 ≤ l ≤ 22	-11 ≤ h ≤ 8 -12 ≤ k ≤ 8 -21 ≤ l ≤ 17
Reflections collected	53642	5520
Independent reflections	[R _{int} =]	2969 [R _{int} = 0.0278]
Completeness to full θ	0.952	1.59/0.92
Transmission $T_{\text{min}}/T_{\text{max}}$	0.972/1.000	0.560/0.761
Data/restraints/parameters	15374/147/863	2969/0/183
Goodness-of-fit on F ²	0.881	1.046
Final R-values [$I \geq 2\sigma(I)$]	R ₁ = 0.0704, wR ₂ = 0.1881	R ₁ = 0.0229, wR ₂ = 0.0580
Final R-values [all data]	R ₁ = 0.1247 wR ₂ = 0.2019	R ₁ = 0.0240, wR ₂ = 0.0586
Largest difference hole and peak $\Delta\rho$	-0.91, 1.63	-0.60 0.33

Table S4: Crystallographic data for compounds **7c**

	7c
Empirical formula	C ₁₅ H ₂₁ AsBNSe
Formula weight	380.02
Crystal	colorless block
Crystal size/mm ³	0.311 × 0.218 × 0.167
Temperature/K	123
Crystal system	monoclinic
Space group	<i>P</i> 2 ₁ / <i>c</i>
Unit cell dimensions	<i>a</i> = 10.1667(3) <i>b</i> = 9.1322(3) <i>c</i> = 17.6684(4) α = 90 β = 99.025(2) γ = 90
Volume <i>V</i>	1620.10(8)
Formula units <i>Z</i>	4
Absorption coefficient μ	4.030
Density ρ_{calc}	1.558
<i>F</i> (000)	760.0
Theta range $\theta_{\text{min}}/\theta_{\text{max}}$	7.95/120.308
Absorption correction	analytical
Index ranges	$-12 \leq h \leq 12$ $-11 \leq k \leq 11$ $-21 \leq l \leq 21$
Reflections collected	4425
Independent reflections	5944 [<i>R</i> _{sigma} = 0.0212]
Completeness to full θ	1.350
Transmission <i>T</i> _{min} / <i>T</i> _{max}	0.454/0.640
Data/restraints/parameters	4425/0/184
Goodness-of-fit on <i>F</i> ²	1.086
Final <i>R</i> -values [$ I \geq 2\sigma(I)$]	<i>R</i> ₁ = 0.0347, <i>wR</i> ₂ = 0.0933
Final <i>R</i> -values [all data]	<i>R</i> ₁ = 0.0379, <i>wR</i> ₂ = 0.0961
Largest difference hole and peak $\Delta\rho$	-0.43, 0.75

NMR spectroscopy

The Formation of $\text{Ph}_2\text{AsBH}_2\text{SMe}_2$

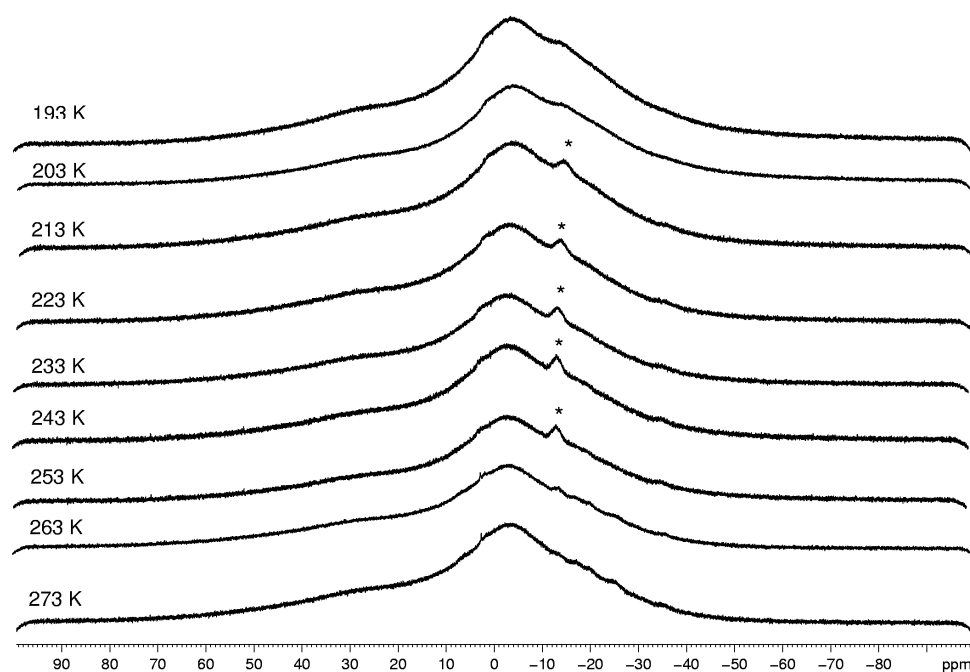


Figure S8: ^{11}B VT NMR spectra of the reaction of KAsPh_2 with IBH_2SMe_2 at different temperatures (* = $\text{Ph}_2\text{AsBH}_2\text{SMe}_2$) in thf-d^8 .

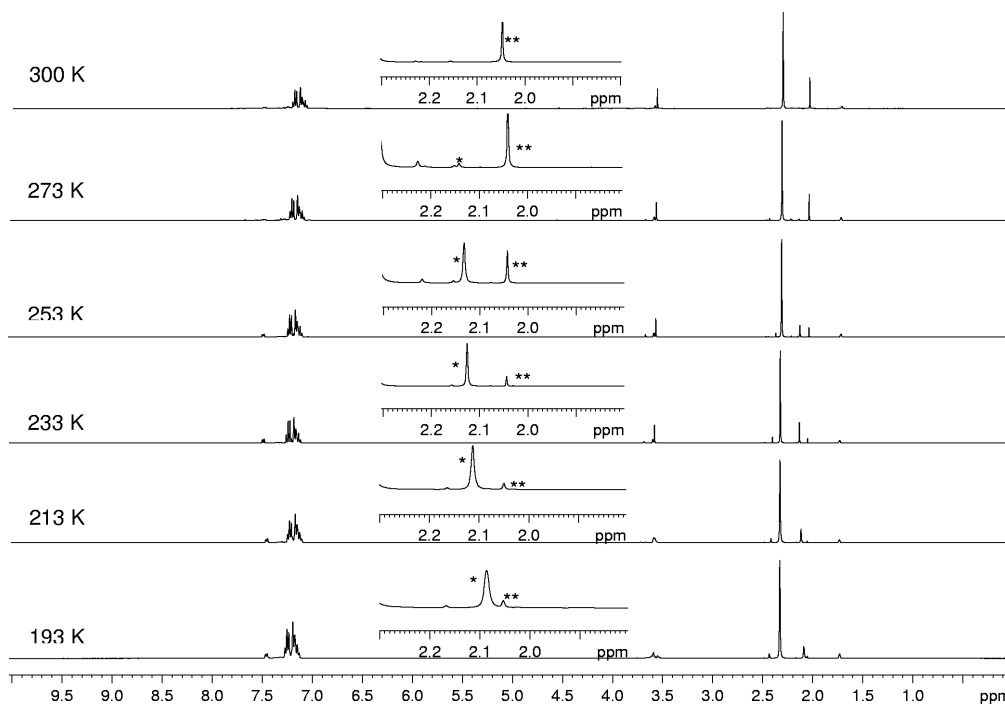


Figure S9: ^1H VT NMR spectra of the reaction of KAsPh_2 with IBH_2SMe_2 at different temperatures (* = SMe_2 of $\text{Ph}_2\text{AsBH}_2\text{SMe}_2$; ** = free SMe_2) in thf-d^8 .

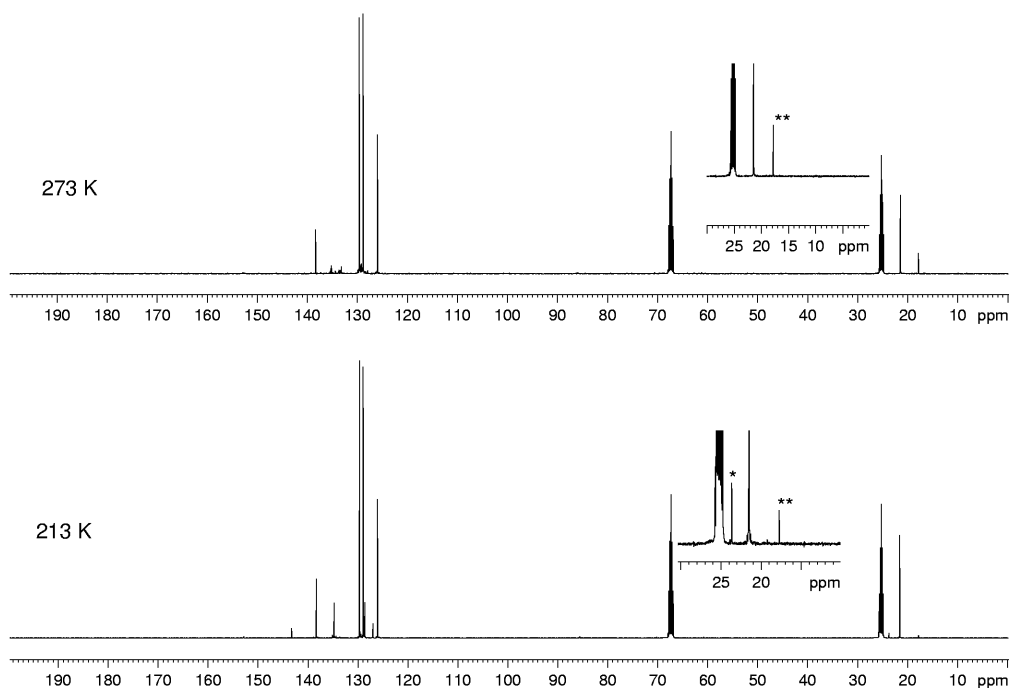


Figure S10: ^{13}C VT NMR spectra of the reaction of KAsPh_2 with IBH_2SMe_2 at different temperatures (* = SMe_2 of $\text{Ph}_2\text{AsBH}_2\text{SMe}_2$; ** = free SMe_2) in thf-d^8 .

NMR spectra of the oligomerization/polymerization attempts

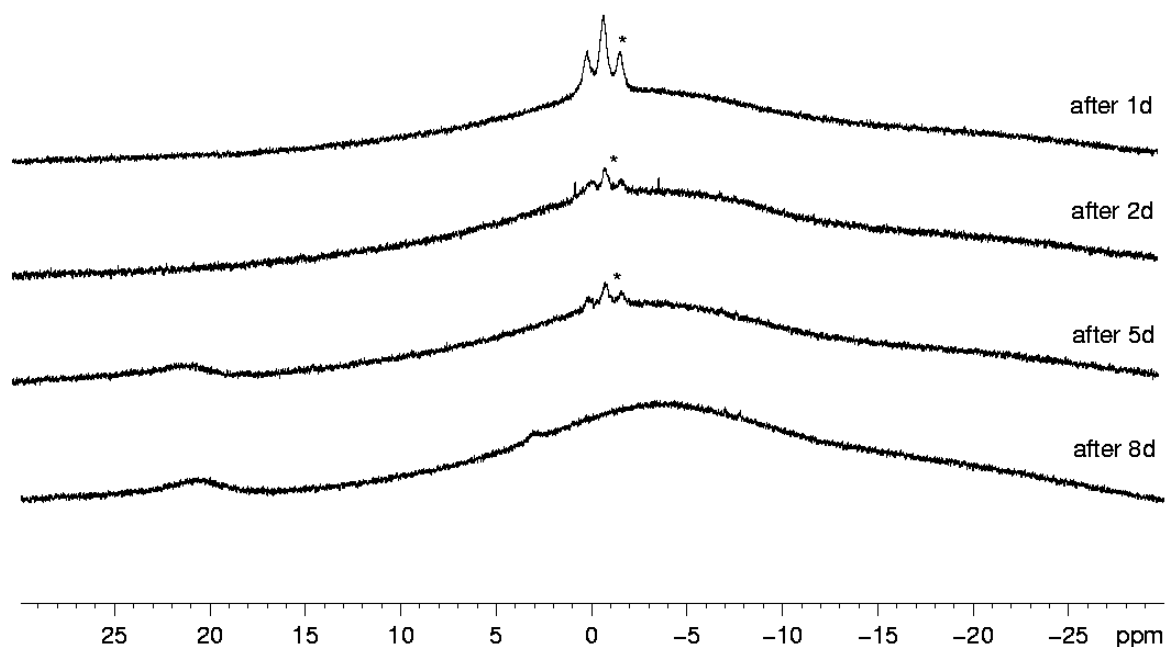


Figure S11: ^{11}B NMR spectra of the thermal treatment of $\text{Ph}_2\text{AsBH}_2\text{NMe}_3$ (=*) in toluene with C_6D_6 capillary.

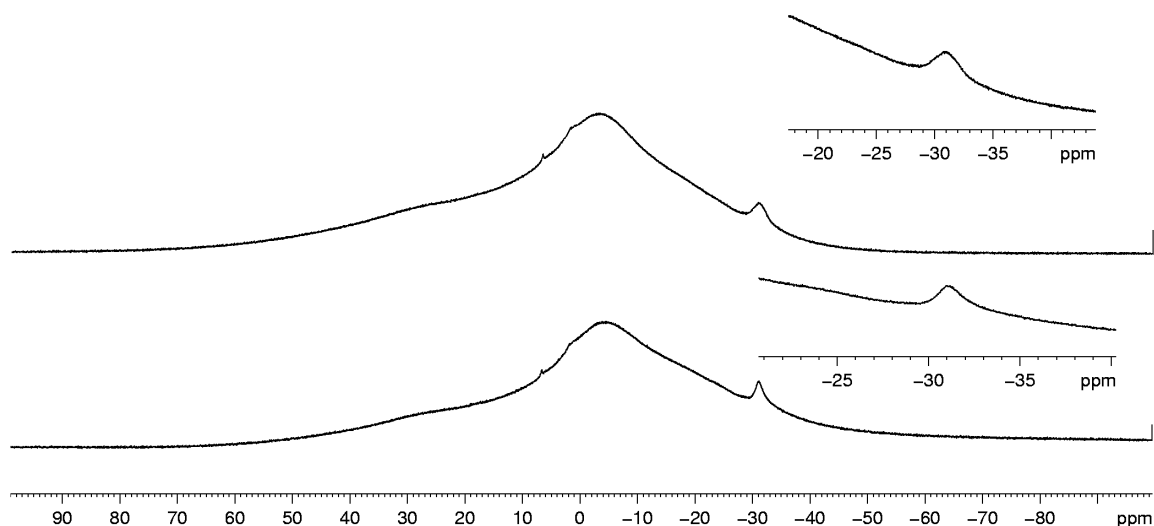


Figure S12: ^{11}B (top) and $^{11}\text{B}\{^1\text{H}\}$ NMR spectrum of the isolated solid of the reaction of KAsPh_2 with IBH_2SMe_2 in C_6D_6 .

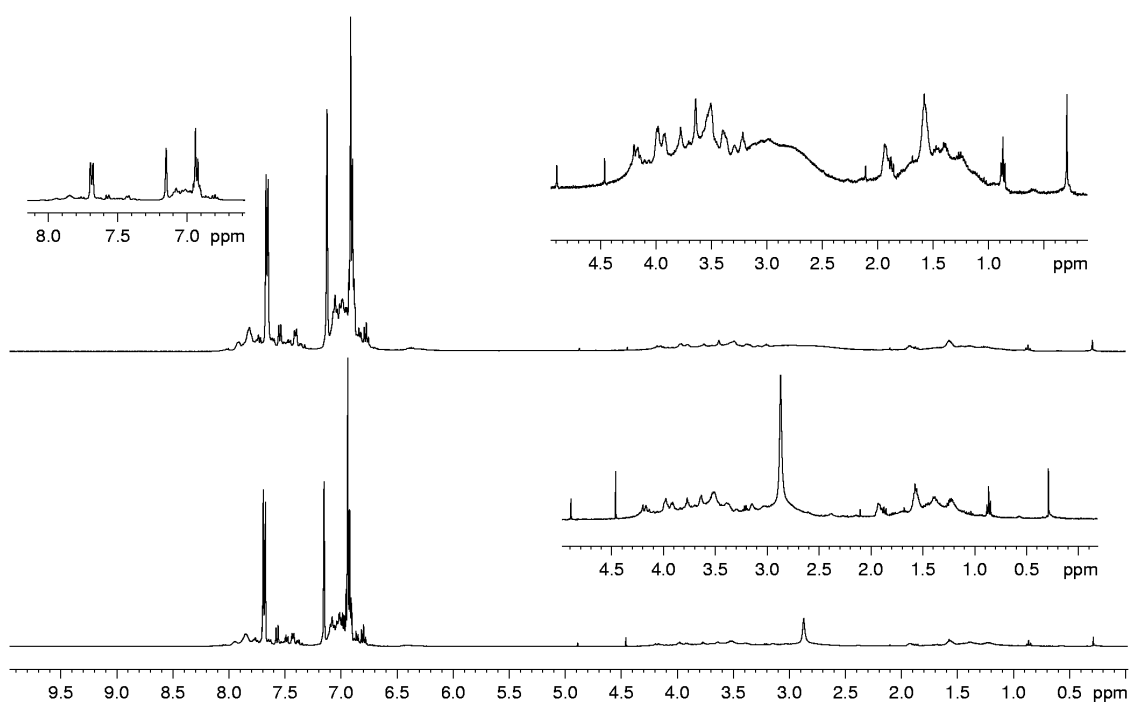


Figure S13: ^1H (top) and $^1\text{H}\{^{11}\text{B}\}$ NMR spectrum of the isolated solid of the reaction of KAsPh_2 with IBH_2SMe_2 in C_6D_6 .

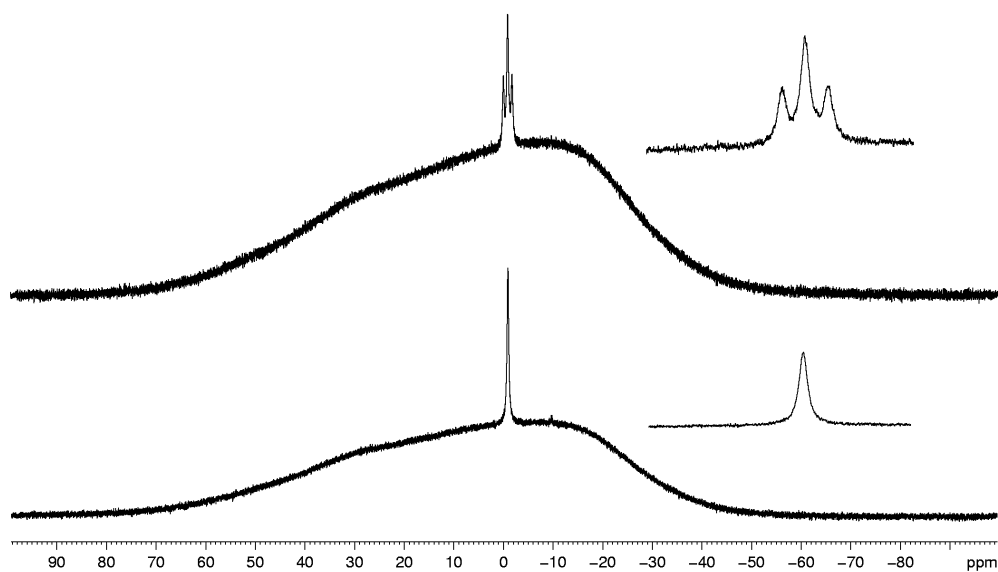


Figure S14: ^{11}B (top) and $^{11}\text{B}\{^1\text{H}\}$ NMR spectrum of **2** in C_6D_6 .

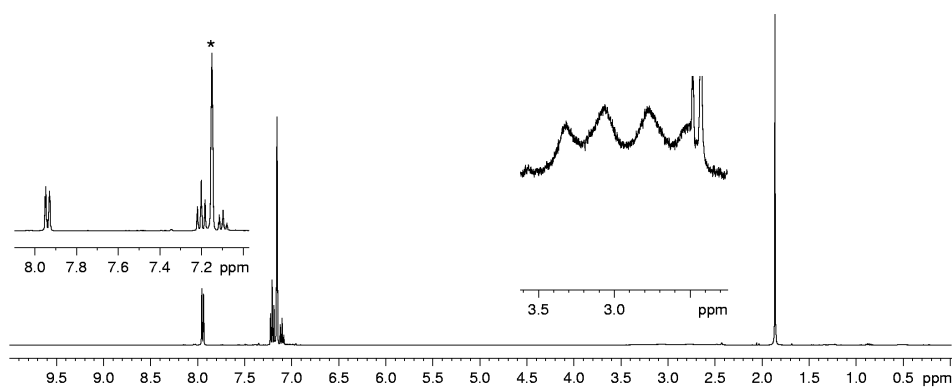


Figure S15: ^1H NMR spectrum of **2** in C_6D_6 (=*).

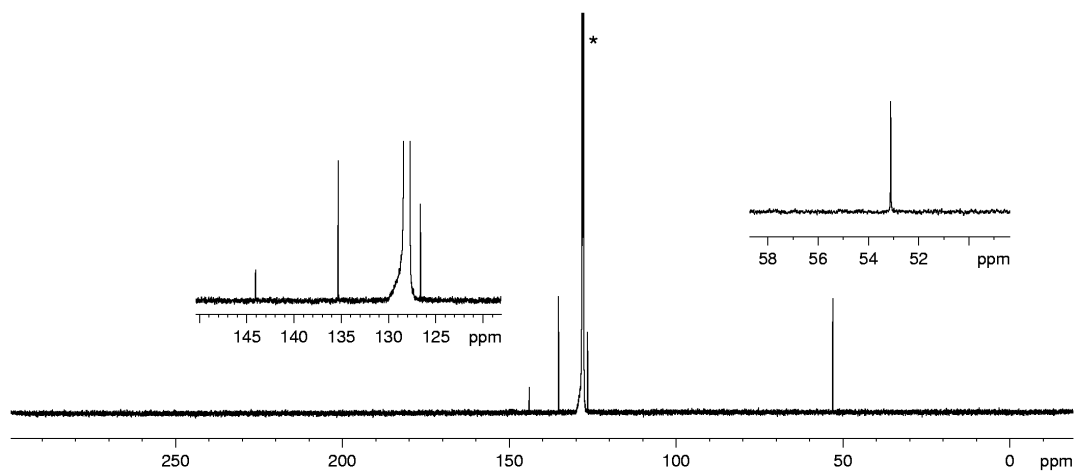


Figure S16: ^{13}C NMR spectrum of **2** in C_6D_6 (=*).

$H_3B-Ph_2AsBH_2NMe_3$

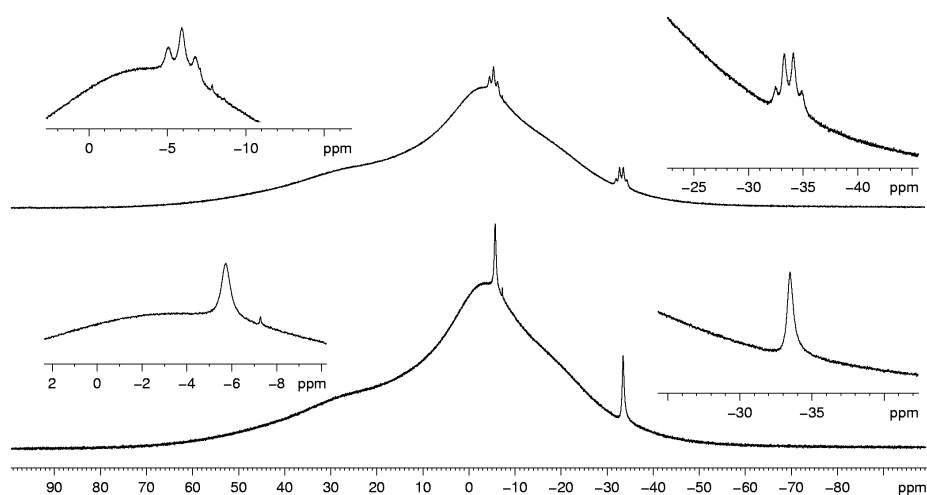


Figure S17: ^{11}B (top) and $^{11}B\{^1H\}$ (bottom) NMR spectrum of **3** in C_6D_6 .

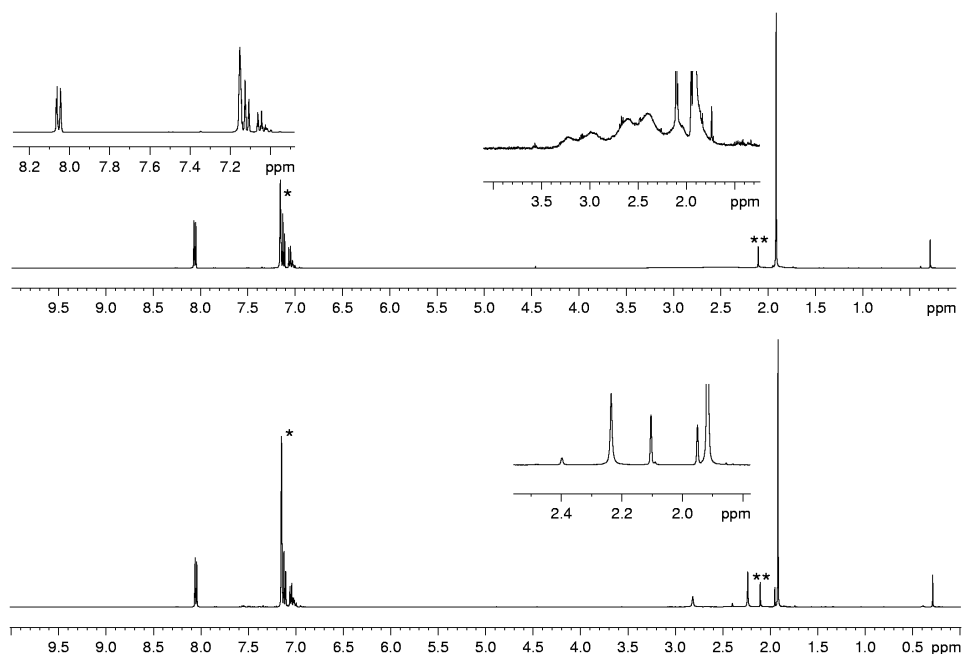


Figure S18: 1H (top) and $^1H\{^{11}B\}$ (bottom) NMR spectrum of **3** in C_6D_6 (=*) (impurity = **).

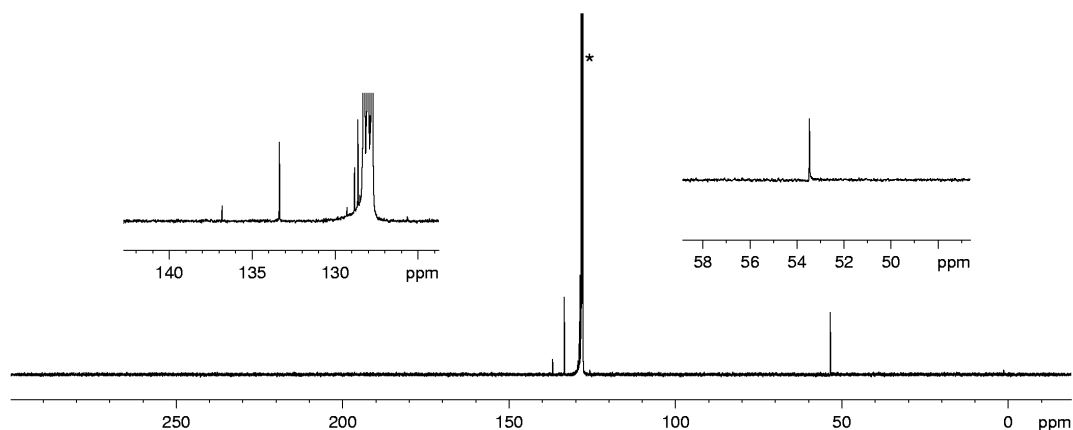


Figure S19: ^{13}C NMR spectrum of **3** in C_6D_6 (=*).

$\text{Br}_3\text{B-Ph}_2\text{AsBH}_2\text{NMe}_3$

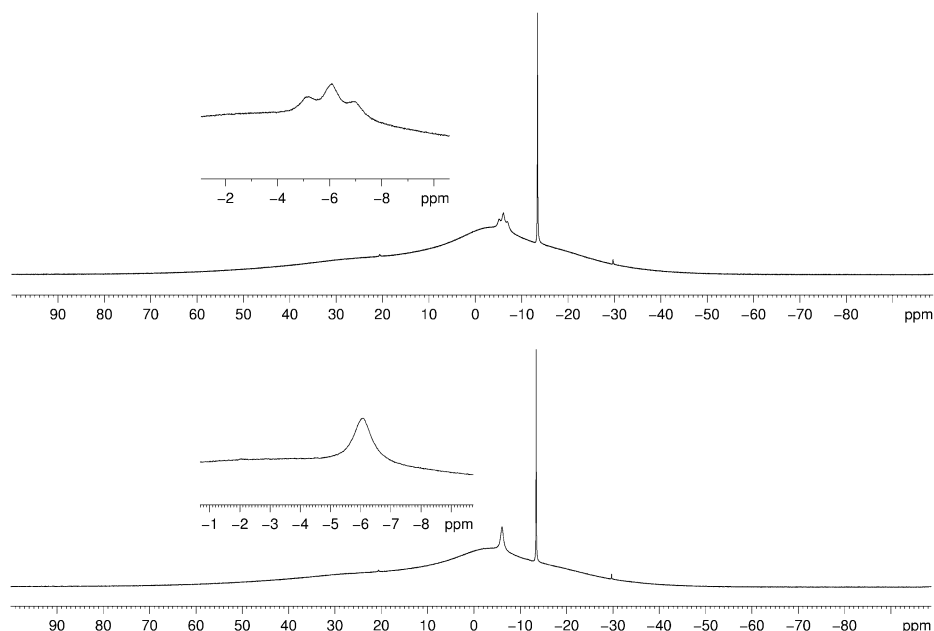


Figure S20: ^{11}B (top) and $^{11}\text{B}\{^1\text{H}\}$ NMR spectrum of **4** in CD_3CN .

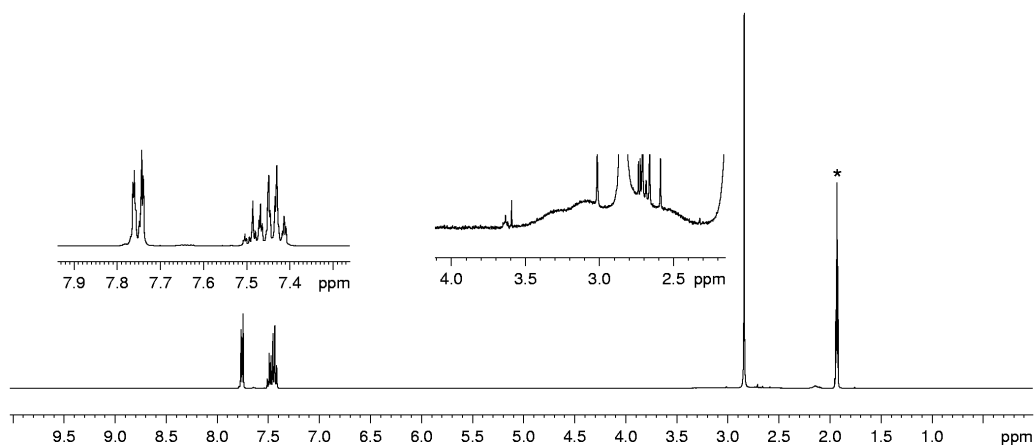


Figure S21: ^1H NMR spectrum of **4** in CD_3CN (=*).

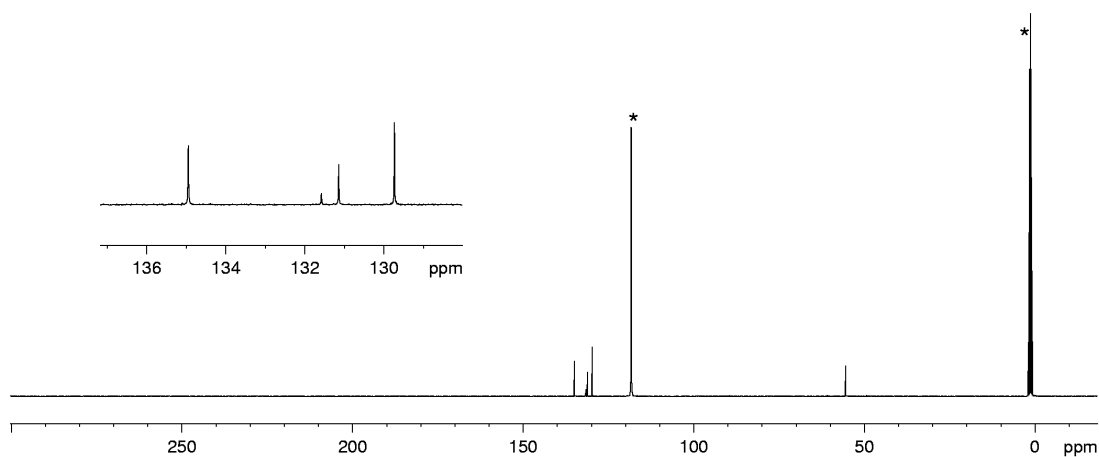


Figure S22: ^{13}C NMR spectrum of **4** in CD_3CN (= *).

(Me₃NH₂B-AsPh₂BH₂NMe₃)⁺ I⁻

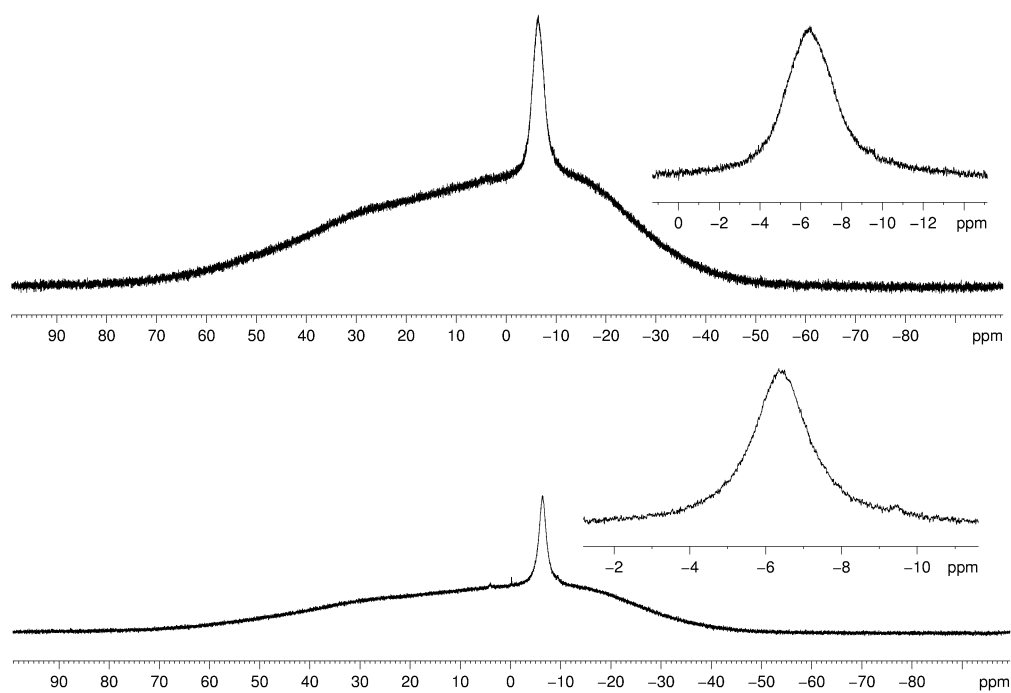


Figure S23: ^{11}B (top) and $^{11}\text{B}\{^1\text{H}\}$ NMR spectrum of **5** in CDCl_3

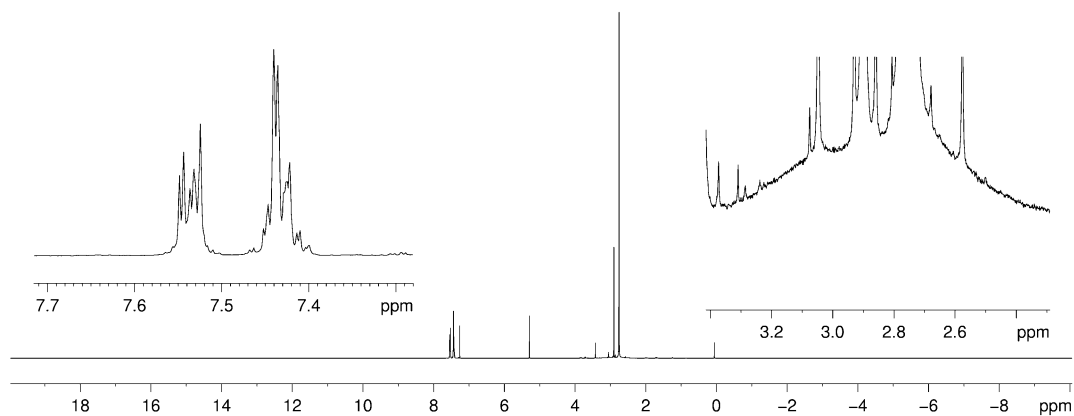


Figure S24: ^1H NMR spectrum of **5** in CDCl_3

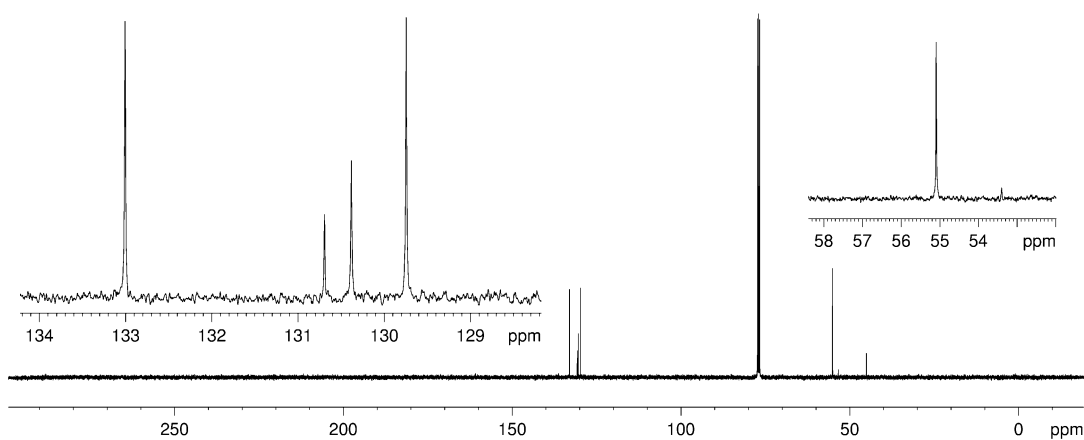


Figure S25: $^{13}\text{C}\{^1\text{H}\}$ NMR spectrum of **5** in CDCl_3

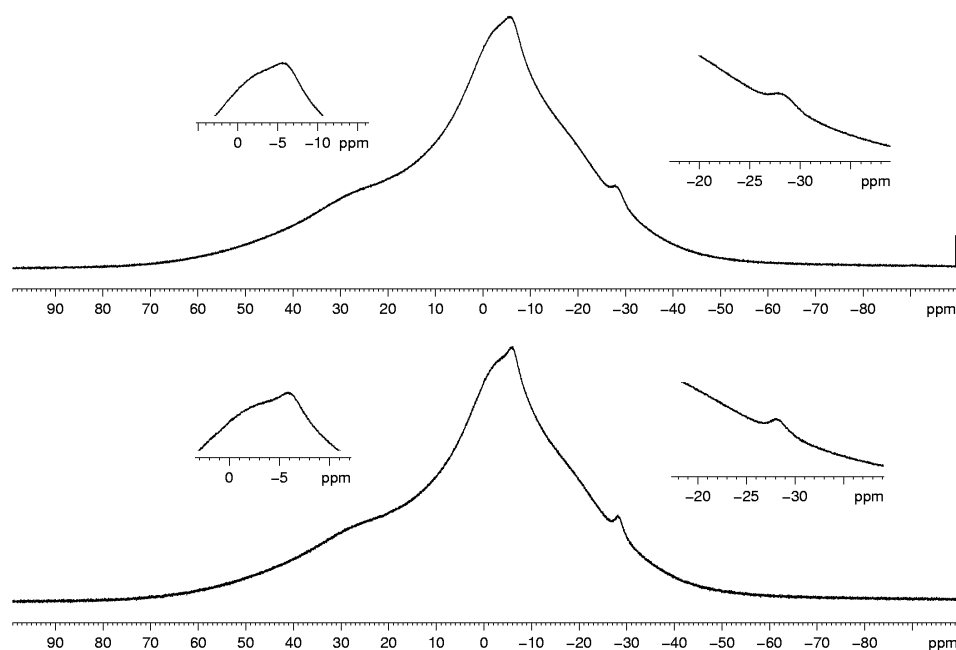
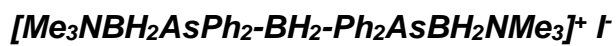


Figure S26: ^{11}B (top) and $^{11}\text{B}\{^1\text{H}\}$ NMR spectrum of **6** in CDCl_3 .

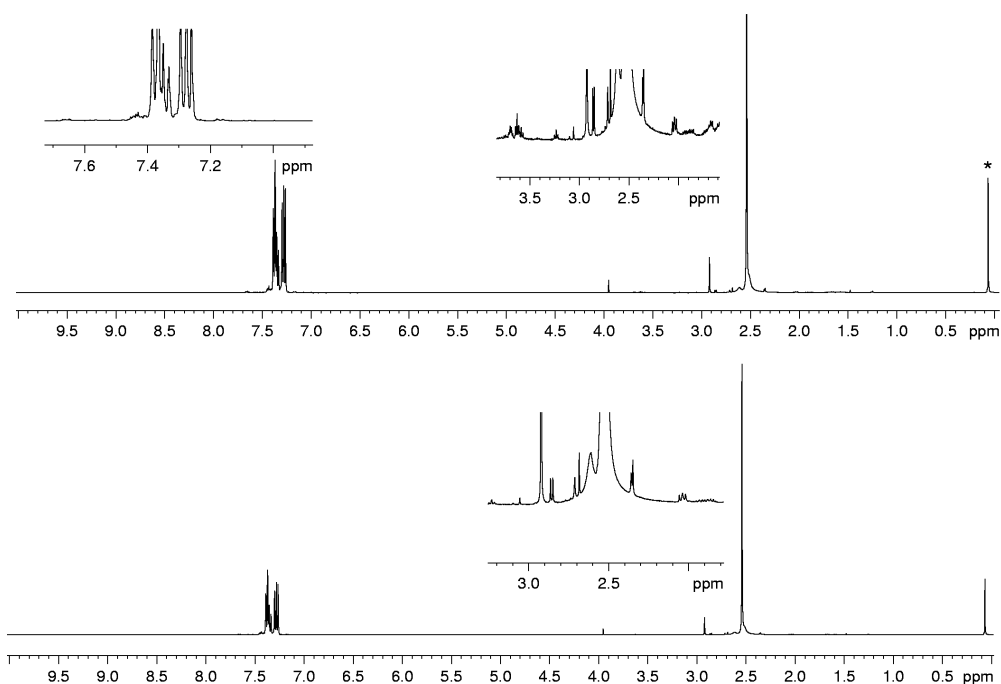


Figure S27: ^1H (top) and $^1\text{H}\{^{11}\text{B}\}$ NMR spectrum of **6** in CDCl_3 (*=silicon grease).

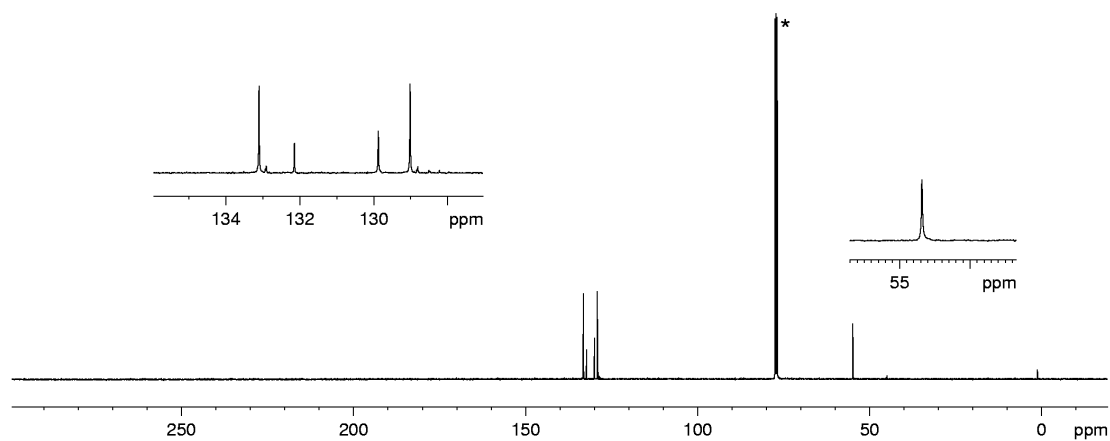


Figure S28: ^{13}C NMR spectrum of **6** in CDCl_3 (=*).

$\text{Ph}_2\text{As}(\text{O})\text{BH}_2\text{NMe}_3$

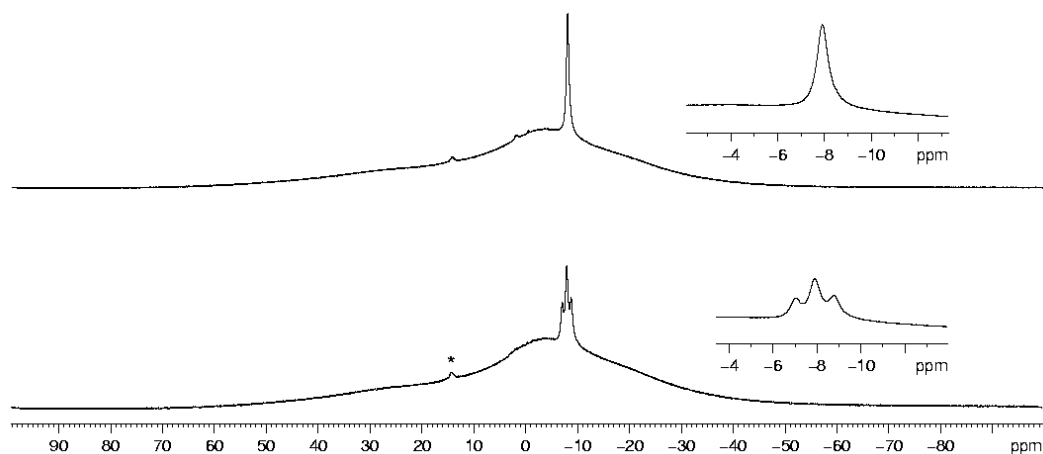


Figure S29: $^{11}\text{B}\{^1\text{H}\}$ (top) and ^{11}B (bottom) NMR spectra of a reaction mixture of Bis-trimethylsilylperoxide and $\text{Ph}_2\text{AsBH}_2\text{NMe}_3$ in CD_2Cl_2 (*= $(\text{HBO}_2)_3$).

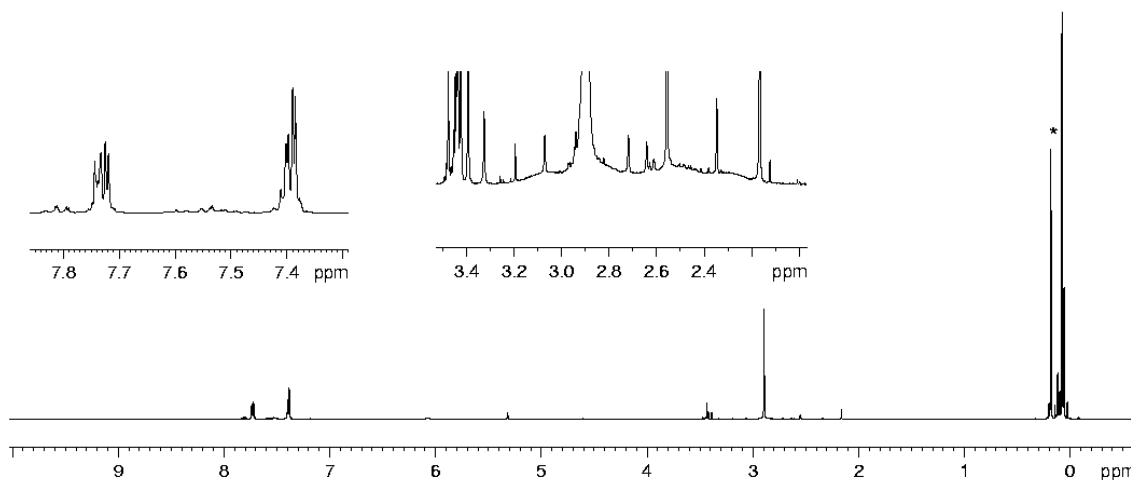


Figure S30: ^1H NMR spectrum of a reaction mixture of Bis-trimethylsilylperoxide and $\text{Ph}_2\text{AsBH}_2\text{NMe}_3$ in CD_2Cl_2 (* = $(\text{Me}_3\text{Si})_2\text{O}$).

$\text{Ph}_2\text{As}(\text{S})\text{BH}_2\text{NMe}_3$

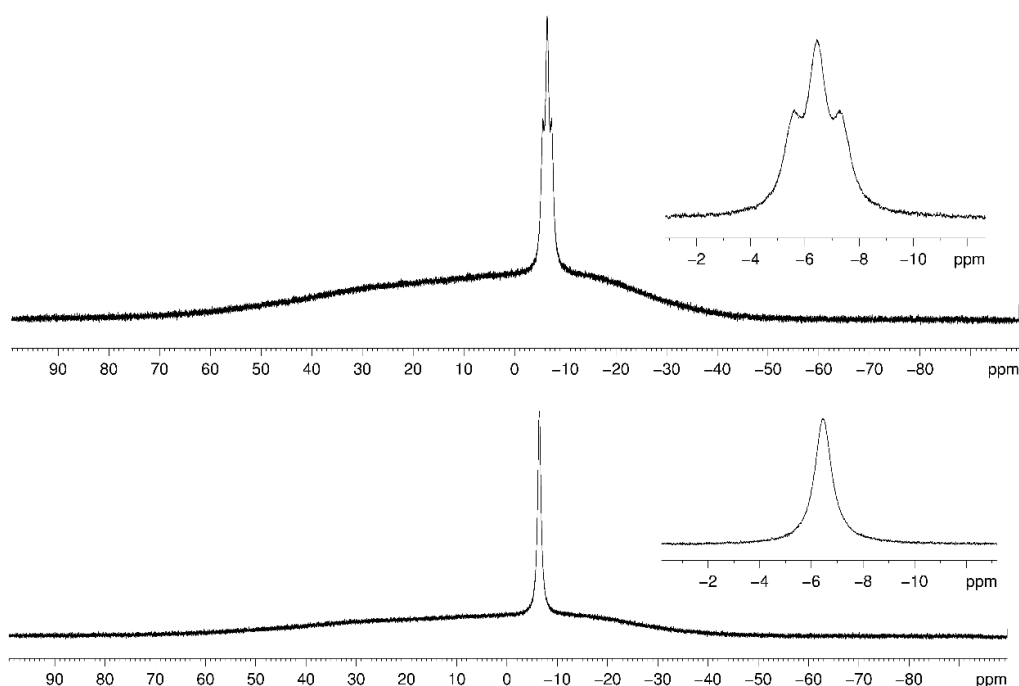


Figure S31: ^{11}B (top) and $^{11}\text{B}\{^1\text{H}\}$ NMR spectrum of **7b** in CDCl_3 .

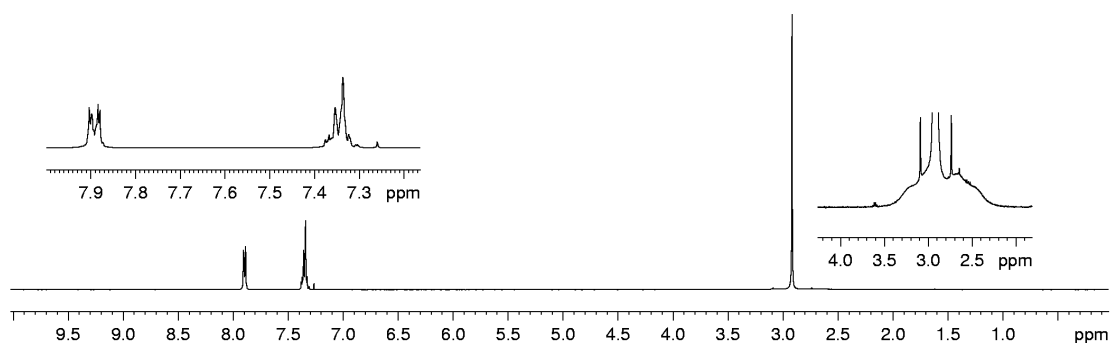


Figure S32: ¹H NMR spectrum of **7b** in CDCl₃.

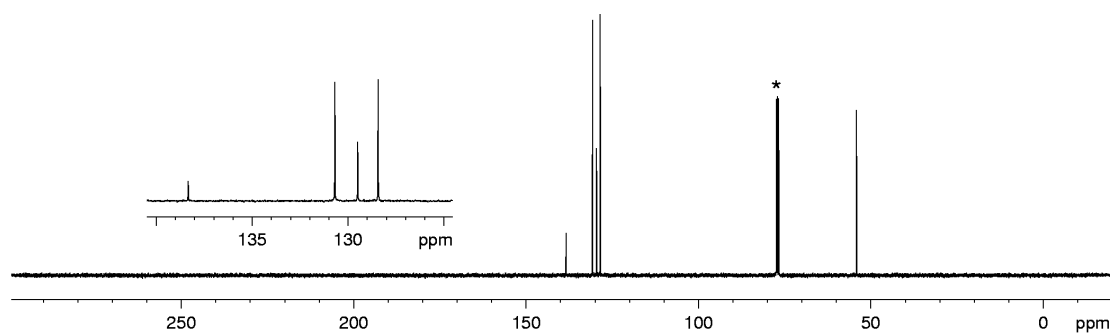


Figure S33: ¹³C{¹H} NMR spectrum of **7b** in CDCl₃ (=*).

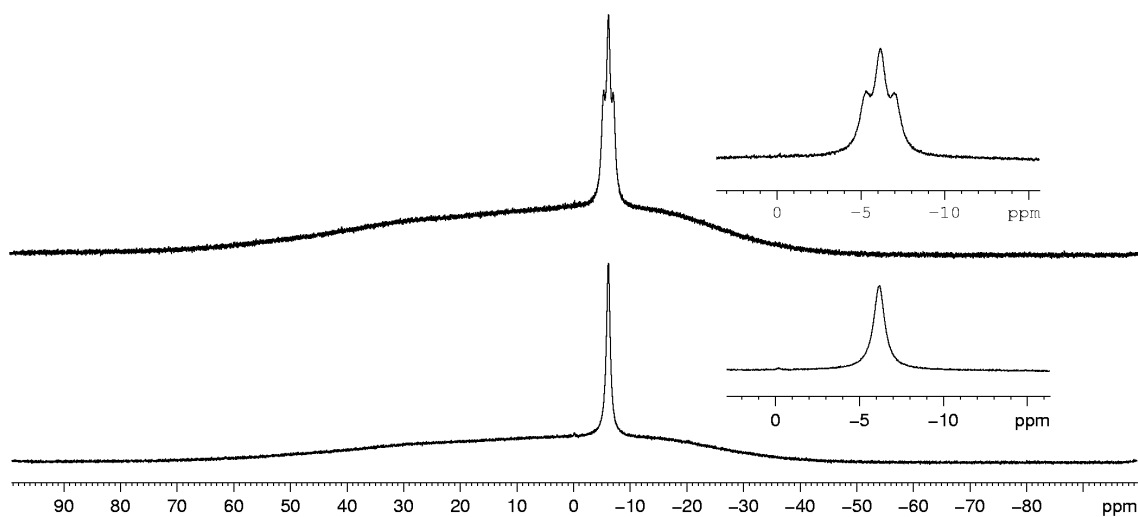


Figure S34: ¹¹B (top) and ¹¹B{¹H} NMR spectrum of **7c** in CDCl₃

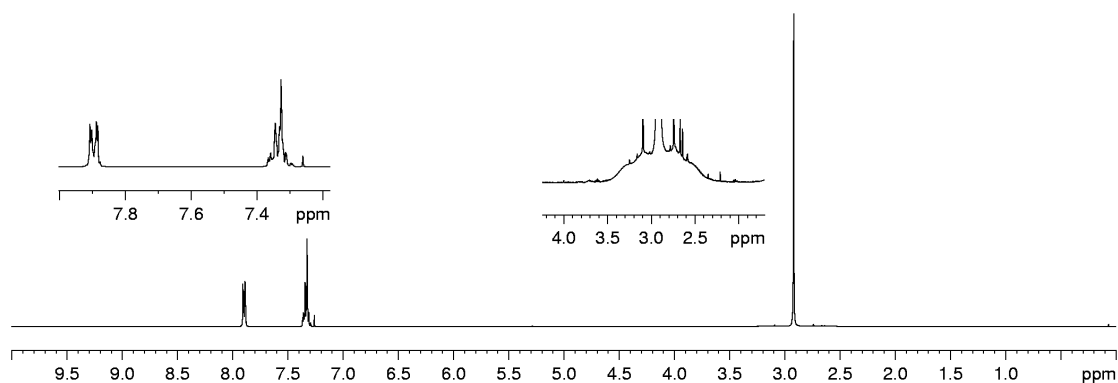


Figure S35: ^1H NMR spectrum of **7c** in CDCl_3

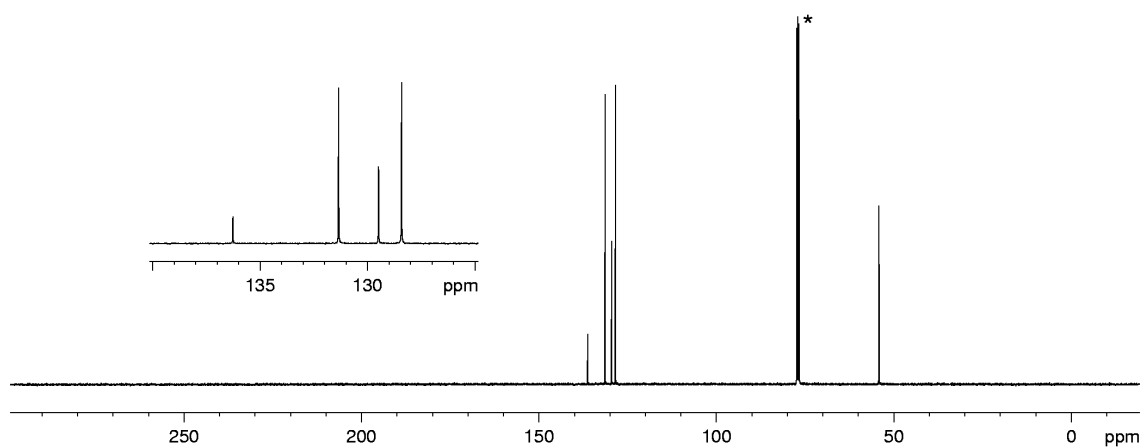


Figure S36: $^{13}\text{C}\{^1\text{H}\}$ NMR spectrum of **7c** in CDCl_3 (= *).

Comparison of the ^{11}B NMR data of compounds **2, **7a**, **7b** and **7c****

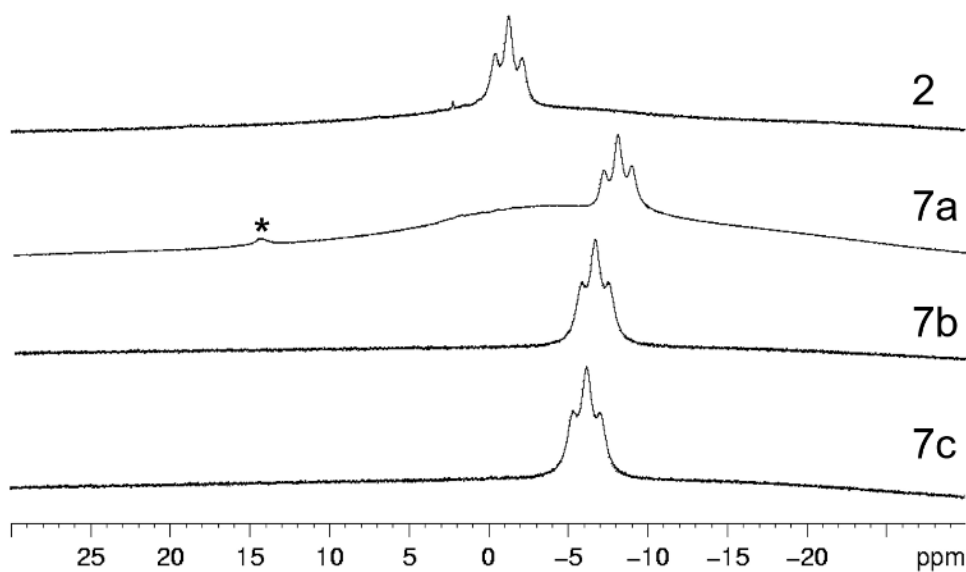


Figure S37: ^{11}B NMR spectra of **2** (CDCl_3), **7a** (CD_2Cl_2 ; * = assumedly traces of $(\text{HBO}_2)_3$ ^[9]), **7b** (CDCl_3) and **7c** (CDCl_3).

Instability of $\text{Ph}_2\text{As}(\text{O})\text{BH}_2\text{NMe}_3$

Long term NMR spectra

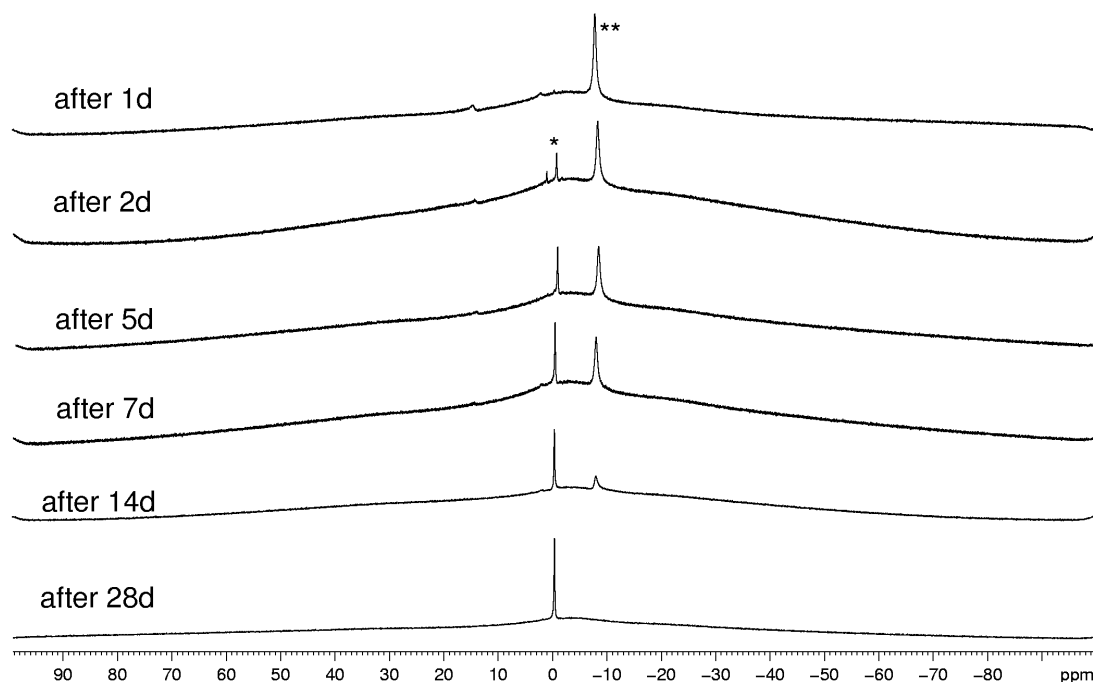


Figure S38: $^{11}\text{B}\{^1\text{H}\}$ NMR spectra of the reaction mixture of Bis-trimethylsilylperoxide and $\text{Ph}_2\text{AsBH}_2\text{NMe}_3$ in CH_2Cl_2 with C_6D_6 capillary after 1d, 2d, 5d, 7d, 14d and 28d (* = $\text{Ph}_2\text{AsBH}_2\text{NMe}_3$; ** = $\text{Ph}_2\text{As}(\text{O})\text{BH}_2\text{NMe}_3$).

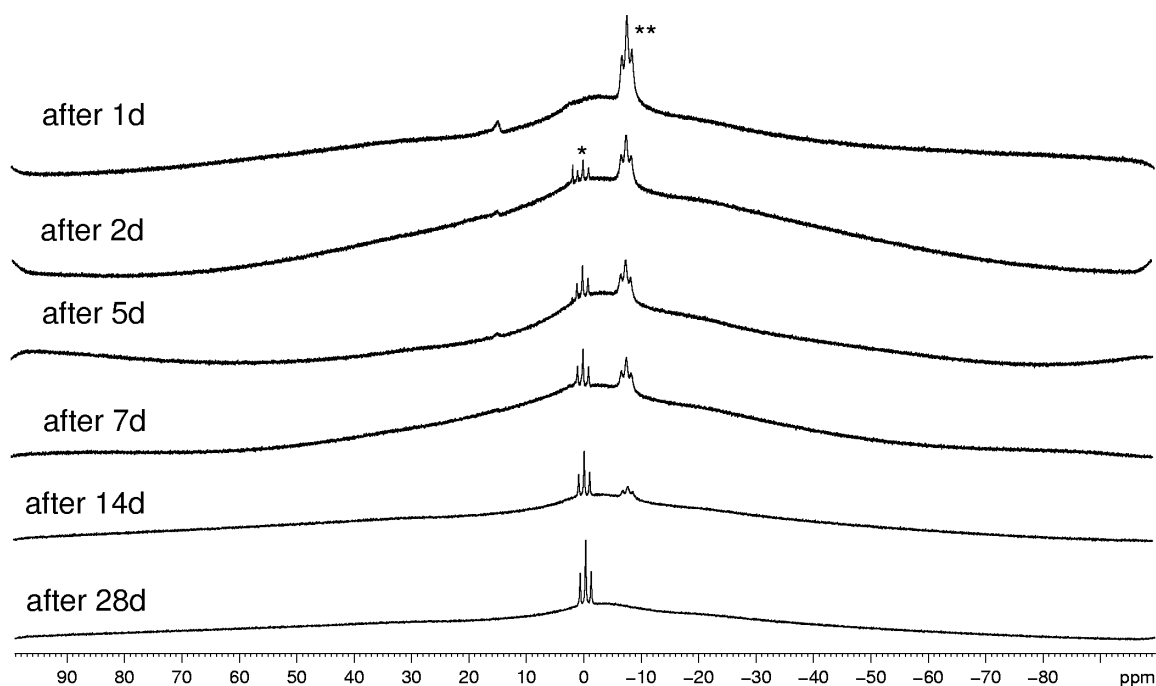


Figure S39: ^{11}B NMR spectra of the reaction mixture of Bis-trimethylsilylperoxide and $\text{Ph}_2\text{AsBH}_2\text{NMe}_3$ in CH_2Cl_2 with C_6D_6 capillary after 1d, 2d, 5d, 7d, 14d and 28d (* = $\text{Ph}_2\text{AsBH}_2\text{NMe}_3$; ** = $\text{Ph}_2\text{As}(\text{O})\text{BH}_2\text{NMe}_3$).

Computational Data

The geometries of the compounds have been fully optimized with gradient-corrected density functional theory (DFT) in form of Becke's three-parameter hybrid method B3LYP^[10] with all electron def2-SVP basis set.^[11] Gaussian 09 program package^[12] was used throughout. All structures correspond to minima on their respective potential energy surfaces. Basis sets were obtained from the EMSL basis set exchange database.^[13]

Table S5: Reaction energies ΔE°_0 , standard enthalpies ΔH°_{298} , Gibbs energies ΔG°_{298} (kJ mol⁻¹) and standard entropies ΔS°_{298} (J mol⁻¹ K⁻¹) for the considered gas phase processes. B3LYP/def2-SVP level of theory.

N	Process	ΔE°_0	ΔH°_{298}	ΔS°_{298}	ΔG°_{298}
1	2 Ph ₂ As(O)BH ₂ NMe ₃ → AsPh ₂ BH ₂ NMe ₃ + $\frac{1}{3}$ (HBO ₂) ₃ + $\frac{1}{2}$ H ₂ + NMe ₃ + $\frac{1}{2}$ As ₂ Ph ₄	-404.3	-412.9	210.8	-475.8
2	2 Ph ₂ As(S)BH ₂ NMe ₃ → AsPh ₂ BH ₂ NMe ₃ + $\frac{1}{3}$ (HBS ₂) ₃ + $\frac{1}{2}$ H ₂ + NMe ₃ + $\frac{1}{2}$ As ₂ Ph ₄	-34.3	-57.5	219.4	-122.9
3	2 Ph ₂ As(Se)BH ₂ NMe ₃ → AsPh ₂ BH ₂ NMe ₃ + $\frac{1}{3}$ (HBSe ₂) ₃ + $\frac{1}{2}$ H ₂ + NMe ₃ + $\frac{1}{2}$ As ₂ Ph ₄	41.5	15.3	221.7	-50.8
4	Ph ₂ As(O)BH ₂ NMe ₃ → AsPh ₂ BH ₂ NMe ₃ + $\frac{1}{2}$ O ₂	150.6	146.7	88.5	120.3
5	Ph ₂ As(S)BH ₂ NMe ₃ → AsPh ₂ BH ₂ NMe ₃ + $\frac{1}{8}$ S ₈	56.5	53.3	28.7	44.7
6	Ph ₂ As(Se)BH ₂ NMe ₃ → AsPh ₂ BH ₂ NMe ₃ + $\frac{1}{8}$ Se ₈	32.2	29.4	30.1	20.4
7	Ph ₂ As(O)BH ₂ NMe ₃ → HBO·NMe ₃ + $\frac{1}{2}$ H ₂ + $\frac{1}{2}$ As ₂ Ph ₄	-88.8	-101.2	175.2	-153.4
8	Ph ₂ As(O)BH ₂ NMe ₃ → NMe ₃ + $\frac{1}{3}$ (HBO) ₃ + $\frac{1}{2}$ H ₂ + $\frac{1}{2}$ As ₂ Ph ₄	-203.6	-218.4	202.7	-278.9

As expected, reactions of a direct loss of O, S, Se from E=AsPh₂BH₂NMe₃ to AsPh₂BH₂NMe₃ (reactions 4-6, Table S5) are endothermic and endergonic, making compounds stable towards this decomposition pathway and allowing their synthesis using the reverse reactions.

However, alternative pathways of decomposition exist which are exothermic. For example, reaction of formation of trimeric ring (HBO₂)₃ is highly exothermic and supposedly a driving force for the experimentally observed reaction (Table S5, reaction 1). For the sulfur derivative analogous reaction 2 is still exothermic (could proceed at

elevated temperatures, however (HBS)₃ rings should be prone to oxidation), but for Se analog the reaction 3 is endothermic.

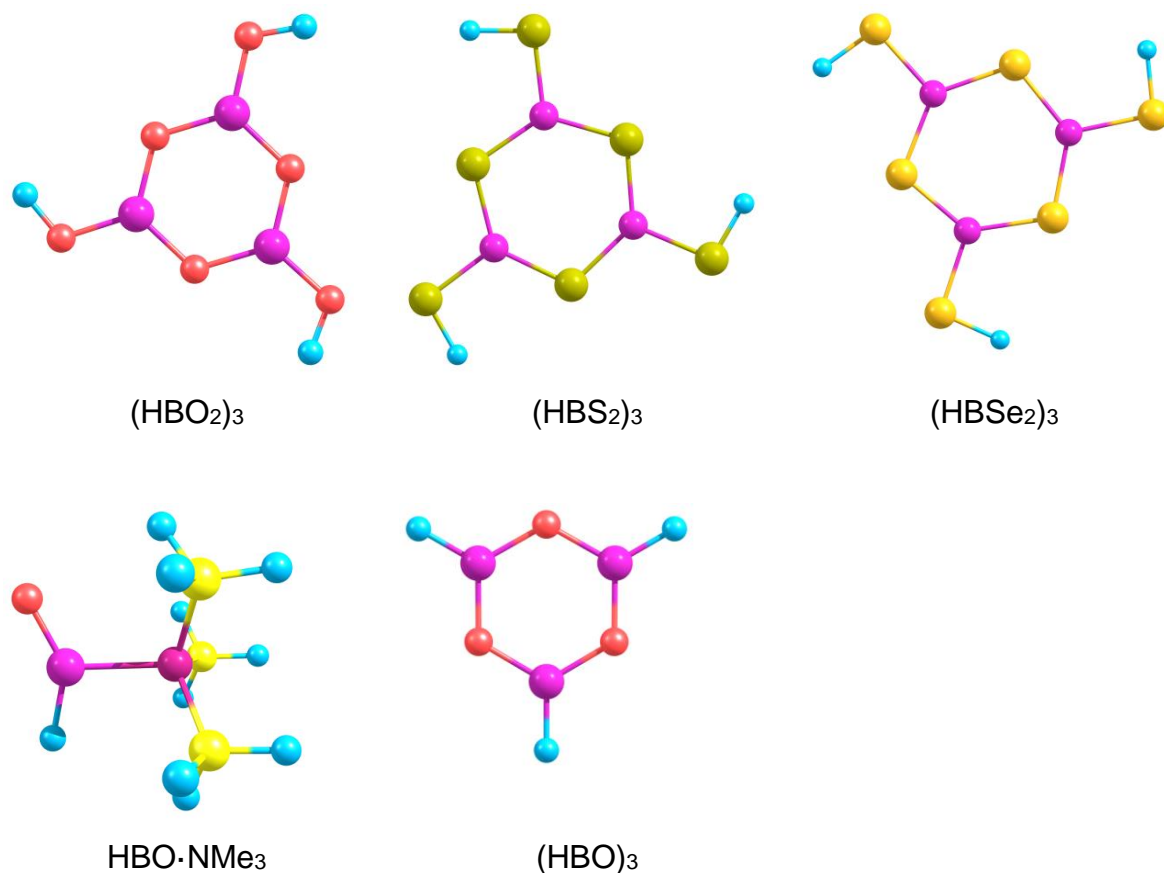
Since reactions 7,8 in Table S5 are also very favorable energetically (and should lead to the full conversion of the starting compound to the reaction products), it is assumed that the reaction path is not intramolecular.

Intermolecular mechanism for the reaction 1 could be assumed, with the O=As group from the first O=AsPh₂BH₂NMe₃ molecule attacking the B-H bond of the second molecule. The first molecule loses O and converges to AsPh₂BH₂NMe₃, the second completely disintegrates with B-As bond breaking, transfer of O atom from As to B, leading to AsPh₂ radicals which will dimerize to form As₂Ph₄. NMe₃, polymeric metaboric acid (HOB(O))_n and molecular hydrogen are expected as by-products.

Table S6: Total energies E⁰, sum of electronic and thermal enthalpies H⁰₂₉₈ (Hartree) and standard entropies S⁰₂₉₈ (cal mol⁻¹K⁻¹). B3LYP/def2-SVP level of theory.

Compound	Point group	E ⁰	H ⁰ ₂₉₈	S ⁰ ₂₉₈
H ₂	D _{∞h}	-1.1737901	-1.160528	31.227
O ₂	D _{∞h}	-150.2047989	-150.197625	48.961
S ₈	D _{4d}	-3184.691874	-3184.668126	103.978
Se ₈	D _{4d}	-19210.50315	-19210.48134	129.865
NMe ₃	C _{3v}	-174.3458754	-174.219985	68.868
(HBO ₂) ₃	C _{3h}	-527.8057542	-527.722544	85.547
(HBS ₂) ₃	C _{3h}	-2465.072405	-2465.011281	108.478
(HBSe ₂) ₃	C _{3h}	-14484.28879	-14484.23327	127.682
As ₂ Ph ₄	C ₁	-5397.225697	-5396.837119	175.563
AsPh ₂ BH ₂ NMe ₃	C ₁	-2899.007385	-2898.659688	143.735
Ph ₂ As(O)BH ₂ NMe ₃	C _s	-2974.167129	-2973.814368	147.062
Ph ₂ As(S)BH ₂ NMe ₃	C ₁	-3297.115379	-3296.76351	149.861
Ph ₂ As(Se)BH ₂ NMe ₃	C ₁	-5300.332541	-5299.981037	152.786
HBO·NMe ₃	C ₁	-275.0012146	-274.854095	85.537
1/3 (HBO) ₃	D _{3h}	-302.0972164	-302.036273	69.703

Figure S40: Optimized geometries of model reaction products. B3LYP/def2-SVP level of theory.



Cartesian coordinates of the optimized geometry can be obtained from the provided DVD.

References:

- [1] C. Marquardt, C. Thoms, A. Stauber, G. Balazs, M. Bodensteiner, M. Scheer, *Angew. Chem. Int. Ed.* **2014**, 53, 3727–3730; *Angew. Chem.* **2014**, 126, 3801–3804.
- [2] A. Tzschach, W. Lange, *Chem. Ber.* **1962**, 95, 1360-1366.
- [3] A. Burkhardt et al. *Eur. Phys. J. Plus* **2016**, 131:56
- [4] Agilent Technologies **2006-2011**, CrysAlisPro Software system, different versions, Agilent Technologies UK Ltd, Oxford, UK.
- [5] A. Altomare, M. C. Burla, M. Camalli, G. L. Cascarano, C. Giacovazzo, A. Guagliardi, A. G. G. Moliterni, G. Polidori, R. Spagna, *J. Appl. Cryst.* (1999) 32, 115-119.
- [6] G. M. Sheldrick, *Acta Cryst.* **2008**, A64, 112–122.

- [7] O.V. Dolomanov, L. J. Bourhis, R. J. Gildea, J. A. K. Howard, H. Puschmann, OLEX2: A complete structure solution, refinement and analysis program, **2009**. *J. Appl. Cryst.*, 42, 339-341.
- [8] G. M. Sheldrick, *Acta Cryst.* **2008**, A64, 112–122.
- [9] H. C. Brown, T. P. Stocky, *J. Am. Chem. Soc.* **1977**, 99, 8218-8226.
- [10] a) A.D. Becke, *J. Chem. Phys.* **1993**, 98, 5648. b) C. Lee, W. Yang, R.G. Parr, *Phys. Rev. B* **1988**, 37, 785.
- [11] F. Weigend, R. Ahlrichs, *Phys.Chem.Chem.Phys.*, **2005**, 7, 3297-3305;
- [12] M. J. Frisch, G. W. Trucks, H. B. Schlegel, G. E. Scuseria, M. A. Robb, J. R. Cheeseman, G. Scalmani, V. Barone, B. Mennucci, G. A. Petersson, H. Nakatsuji, M. Caricato, X. Li, H. P. Hratchian, A. F. Izmaylov, J. Bloino, G. Zheng, J. L. Sonnenberg, M. Hada, M. Ehara, K. Toyota, R. Fukuda, J. Hasegawa, M. Ishida, T. Nakajima, Y. Honda, O. Kitao, H. Nakai, T. Vreven, J. A. Montgomery, Jr., J. E. Peralta, F. Ogliaro, M. Bearpark, J. J. Heyd, E. Brothers, K. N. Kudin, V. N. Staroverov, T. Keith, R. Kobayashi, J. Normand, K. Raghavachari, A. Rendell, J. C. Burant, S. S. Iyengar, J. Tomasi, M. Cossi, N. Rega, J. M. Millam, M. Klene, J. E. Knox, J. B. Cross, V. Bakken, C. Adamo, J. Jaramillo, R. Gomperts, R. E. Stratmann, O. Yazyev, A. J. Austin, R. Cammi, C. Pomelli, J. W. Ochterski, R. L. Martin, K. Morokuma, V. G. Zakrzewski, G. A. Voth, P. Salvador, J. J. Dannenberg, S. Dapprich, A. D. Daniels, O. Farkas, J. B. Foresman, J. V. Ortiz, J. Cioslowski, and D. J. Fox, Gaussian 09, Revision E.01, Gaussian, Inc., Wallingford CT, 2013.
- [13] a) D. Feller, *J. Comp. Chem.* 1996, 17, 1571-1586; b) K. L. Schuchardt, B. T. Didier, T. Elsethagen, L. Sun, V. Gurumoorthi, J. Chase, J. Li, T. L. Windus, *J. Chem. Inf. Model.* 2007, 47, 1045-1052.

5.6 Author contributions

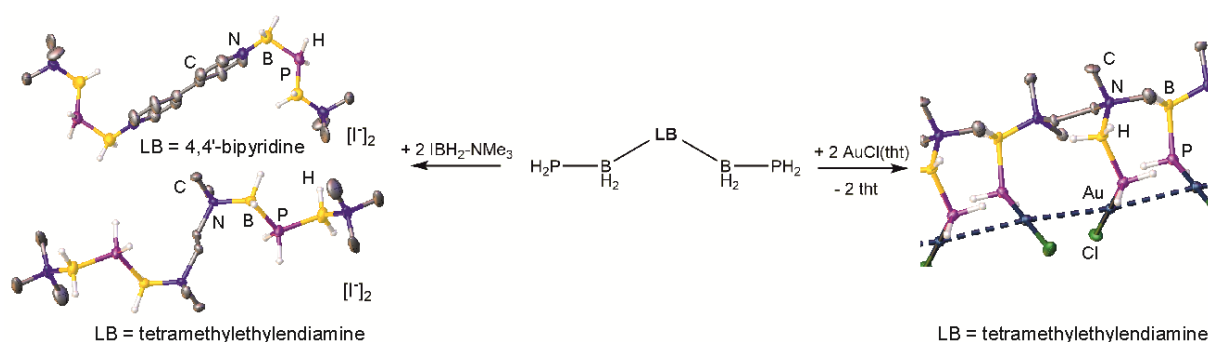
All compounds were synthesized and characterized by Oliver Hegen, except the X-ray diffraction analysis of compound **6**, which was performed and solved by Dr. A. V. Virovets.

All DFT-calculations were performed by Prof. A. Y. Timoshkin.

The manuscript (including supporting information, figures, schemes and graphical abstract) was written by Oliver Hegen.

6 Bidentate Phosphanyl- and Arsanylboranes

Oliver Hegen, Jens Braese, Alexey Y. Timoshkin and Manfred Scheer*



Abstract: A new class of neutral bidentate ligands with pnictogenyl-functional sites have been obtained. Reaction of $\text{tmeda} \cdot (\text{BH}_2\text{I})_2$ (**1**, tmeda = tetramethylethylenediamine) with different phosphanides yield the corresponding bidentate phosphanylboranes $\text{tmeda} \cdot (\text{BH}_2\text{PH}_2)_2$ (**2a**), $\text{tmeda} \cdot (\text{BH}_2\text{PPh}_2)_2$ (**2b**) and $\text{tmeda} \cdot (\text{BH}_2\text{tBuPH}_2)_2$ (**2c**). This reaction strategy could be further extended to synthesize the first bidentate arsanylborane $\text{tmeda} \cdot (\text{BH}_2\text{AsPh}_2)_2$ (**3**). Depending on the substituents on the phosphorus, these compounds form different Au(I) complexes, to build either polymeric, $\text{tmeda} \cdot (\text{BH}_2\text{PH}_2\text{AuCl})_2$ (**4a**), and monomeric $\text{tmeda} \cdot (\text{BH}_2\text{PPh}_2\text{AuCl})_2$ (**4b**) products. These compounds form neutral oligomeric group 13/15 chain-like molecules by coordination to a boron moiety like $\text{tmeda} \cdot (\text{BH}_2\text{PH}_2\text{BH}_3)_2$ (**5a**) and $\text{tmeda} \cdot (\text{BH}_2\text{AsPh}_2\text{BH}_3)_2$ (**5b**). In addition, the reaction of the iodinated boranes $\text{tmeda} \cdot (\text{BH}_2\text{I})_2$ (**1**) and 4,4'-bpy $\cdot (\text{BH}_2\text{I})_2$ (**7**) with $\text{Me}_3\text{N} \cdot \text{BH}_2\text{PH}_2$ yields the dicationic chain compounds $[(\text{tmeda} \cdot (\text{BH}_2\text{PH}_2\text{BH}_2 \cdot \text{NMe}_3)_2) [I^+]_2$ (**6**) and $[(4,4'\text{-bpy} \cdot (\text{BH}_2\text{PH}_2\text{BH}_2 \cdot \text{NMe}_3)_2) [I^+]_2$ (**8**, bpy = bipyridine). DFT calculations provide insight into the differences between the syntheses of mono- or bidentate pnictogenylboranes.

6.1 Introduction

Bidentate ligands are often used compounds in coordination, supramolecular and organometallic chemistry.^[1,2] Usually, these ligands have two pnictogen coordination sites. Whereas ligands containing nitrogen donor atoms, like 4,4'-bipyridene and its derivatives, are most common as building blocks e.g. for the construction of 3D MOFs,^[3] ligands with phosphorus coordination sites, like dppe (=1,2-Bis(diphenylphosphino)ethane, **I**) and dppm (=Bis(diphenylphosphino)methane),^[4] are more used in catalysis, in the formation of 1D-coordination polymers and luminescent materials. E. g. *Nozaki et al.* demonstrated, that rhodium(I) complexes including chiral phosphine-phosphite ligands (**II**) are highly efficient catalysts for asymmetric hydroformylations of a wide range of olefins.^[5] Whereas cyclic ligands like the four-membered 1,3-diphosphacyclobutadiene-diide (**III**) are only stable in the coordination sphere of transition metals,^[6] five-membered cyclopentadienyl-analogues like 1,3-diphospholyl rings (**IV**) can be isolated as potassium salts.^[7] Complexes of these ligands reveal an interesting coordination chemistry towards unsaturated metal fragments, to build up either higher aggregates^[6] and polymers.^[7b] Using gold (I) complexes supported by phosphine ligands, versatile properties as luminescent materials can be observed.^[8]

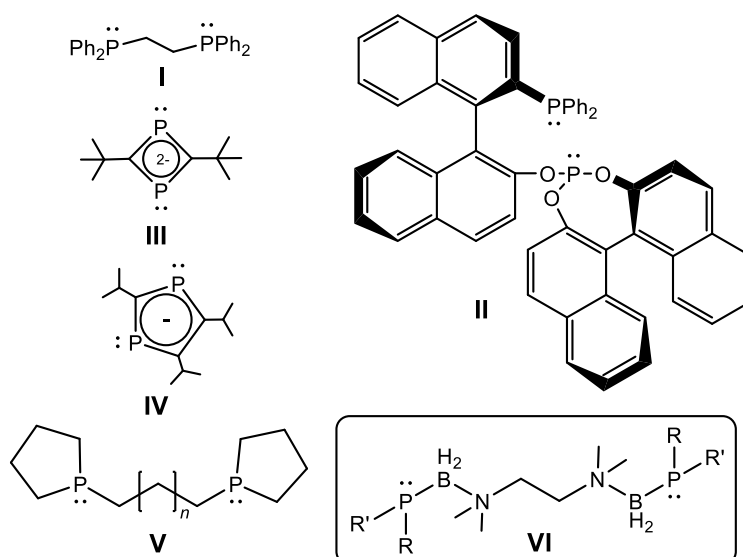


Figure 1: Selected examples of bidentate ligands containing phosphorus coordination sites.

Applying bridged phosphine ligands, the distance between the gold centers can be further reduced, leading to tuned luminescent properties.^[9,10] Moreover, *Hey-Hawkins*

et al. demonstrated the influence of the carbon backbone of bis-phospholanes (**V**) towards gold(I) to synthesize selectively macrocycles or chains and nanotubes, respectively.^[11]

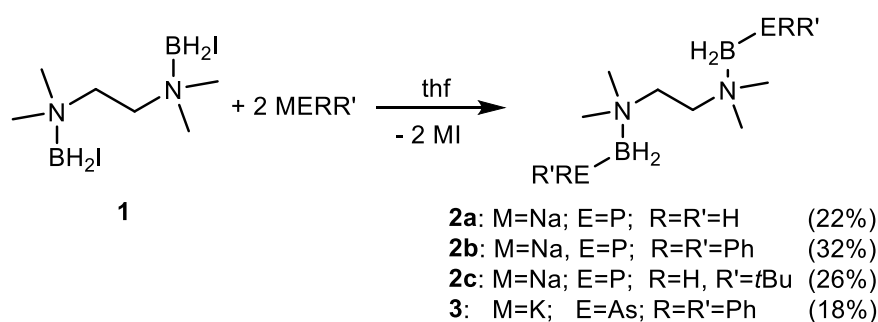
Our group showed, that Lewis base (LB) stabilized pnictogenylboranes are excellent building blocks for the synthesis of extended neutral and ionic mixed group 13/15 compounds.^[12] At least an electronic stabilization induced by the coordination of a LB, like Me₃N, is necessary, to prevent head-to-tail polymerization.^[13] However, as a result of only one pnictogen atom as a donor, the possibilities to build up longer chains or even frameworks based on main group elements without a possible polymerization are limited. Therefore the introduction of a second pnictogen donor site into the system of LB stabilized pnictogenylboranes should give access to organic phosphorus boron based oligomers and networks. Furthermore, by exploiting the isolobal relation between an ethyl-moiety and a boranyl group linked to a phosphorus moiety, the bond polarity inside the molecule is further extended which should lead to different features as potential ligands (**VI**).

By coordination to transition metal complexes, pnictogenylboranes show a manifold chemistry to establish higher aggregates.^[14] For example, the coordination of pnictogenylboranes towards Au(I) gives either monomeric, dimeric or polymeric compounds depending on the pnictogen atom and the substituents revealing interesting luminescent properties.^[15] Intrigued by the idea of connecting metal centers with a pnictogenylborane-linker, to evoke intra- as well as intermolecular interactions, we developed a pathway for the synthesis of bidentate phosphanyl- and arsanylboranes.

6.2 Results and Discussion

Herein, we report the first LB bridged bidentate phosphanylboranes LB·(BH₂PRR')₂ (**VI**, **2a-c**). In addition, we could extend this approach to synthesize the first LB bridged bidentate arsinoborane LB·(BH₂AsPh₂)₂ (**3**). The donor strength as well as the sterical hinderence of the bidentate LB has an essential effect on the stability of these bidentate pnictogenylboranes. We show that these compounds are suitable ligands to form dimeric and polymeric Au(I) complexes and are well suited to build up oligomeric group 13/15 compounds.

As Me₃N is useful as LB to stabilize pnictogenylboranes, the nearest related bidentate amine, tmeda (tetramethylethyldiamine), was chosen as starting material for the synthesis of bidentate pnictogenylboranes. Through iodination of tmeda·(BH₃)₂,^[16] tmeda·(BH₂I)₂ (**1**) is received in almost quantitative yield. The metathesis of **1** with two equivalents of NaPH₂ in thf leads to the parent compound of a LB bridged bidentate phosphanylborane, tmeda·(BH₂PH₂)₂ (**2a**, Scheme 1). **2a** is stable in solution and well soluble in polar solvents like thf and CH₂Cl₂. The reaction of **1** with substituted phosphanides NaPRR' (R = R' = Ph; R = H, R' = *t*Bu) yields the corresponding phosphanylboranes tmeda·(BH₂PPh₂)₂ (**2b**) and tmeda·(BH₂*t*BuPH)₂ (**2c**) (Scheme 1). Depending on the substituents on the P atom, the reactions of **2a-c** proceed up to 35% yield according to ³¹P NMR spectroscopy of the reaction mixtures due to side reactions.^[17]

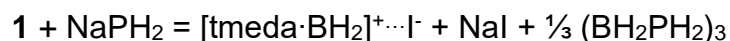


Scheme 1: Synthesis of compounds **2a – c** and **3**. Isolated yields are given in parentheses.

Compound **2b** is moderately soluble in toluene, whereas **2c** is already well soluble in *n*-hexane. The ³¹P NMR spectra and the ¹¹B NMR spectra of **2a-c** are comparable with the Me₃N stabilized phosphanylboranes.^[13c,18] As compound **2c** possesses two stereocenters at the P atoms, for the H₃C groups of the tmeda moiety three singulettts in a 1:1:2 ratio at δ = 1.95-1.99 ppm in the ¹H NMR spectrum can be observed. Whereas the two signals at δ = 1.98 ppm and δ = 1.99 ppm corresponds to the diastereotopic H₃C groups of the R,R' and S,S' pair of enantiomers, the broad singulett at δ = 1.95 is assigned to the H₃C groups of the meso compound. In addition, a broad multipllett at δ = 2.87 ppm can be attributed to the H₂C groups of tmeda unit.

Whereas **2a** and **2b** are stable in solution, **2c** decomposes fast in solution.^[19] Compared to monomeric phosphanylboranes^[13c,18] (55-70%), the yields of **2a-c** are rather low. An explanation is the formation of the five-membered ring [tmeda·BH₂]⁺ and polymeric/oligomeric phosphinoborane as competitive reaction. The formation of

molecular and ionic complexes of tmeda with group 13 Lewis acids EX_3 was examined both experimentally and computationally.^[20] It was shown that the electronegativity of the substituents X in EX_3 plays a decisive role on the ionic/molecular structure. The ionic form $[tmedaEX_2]^+ [EX_4]^-$ is preferred in case of Al and Ga halides, while the molecular complex $tmeda \cdot (BH_3)_2$ is favored in case of BH_3 . DFT computations^[21] show, that in the gas phase spontaneous ionization of $tmeda \cdot (BH_3)_2$ and $tmeda \cdot (BH_2I)_2$ into the ion pairs $[tmedaBH_2]^+ \cdots [BH_4]^-$ and $[tmedaBH_2]^+ \cdots [BH_2I_2]^-$ is endothermic by 133 and 43 kJ mol^{-1} , respectively. The reaction of **1** with $NaPH_2$ leading to the formation of **2a** according to Scheme 1 is exothermic; the first ($-103.2 \text{ kJ mol}^{-1}$) and the second ($-102.4 \text{ kJ mol}^{-1}$) step differ less than 1 kJ mol^{-1} . Note that the alternative reaction with formation of the five-membered cycle $[tmeda \cdot BH_2]^+$ and the oligomer $(BH_2PH_2)_3$



is even slightly more exothermic ($-106.2 \text{ kJ mol}^{-1}$). Thus, both reaction pathways are energetically similar and can proceed simultaneously, lowering the yield of **2a**.

We tried hard to use the synthetic pathway described in Scheme 1 for the synthesis of the bidentate parent arsanylborane $tmeda \cdot (BH_2AsH_2)_2$. Unfortunately, all attempts failed so far, due to the bad solubility and instability of $KAsH_2$, and only decomposition products could be observed.^[22] Therefore, we targeted the synthesis of a bidentate substituted arsanylborane. The reaction of **1** with two equivalents $KAsPh_2$ leads to $tmeda \cdot (BH_2AsPh_2)_2$ (**3**). The compound is well soluble in toluene. Due to the phenylsubstituents in **3**, the signal in the ^{11}B NMR spectra is shifted downfield relative to $\text{Me}_3\text{N} \cdot \text{BH}_2\text{AsH}_2$.^[13d]

To the best of our knowledge, compounds **2-3** are the first neutral bidentate pnictogenylboranes.

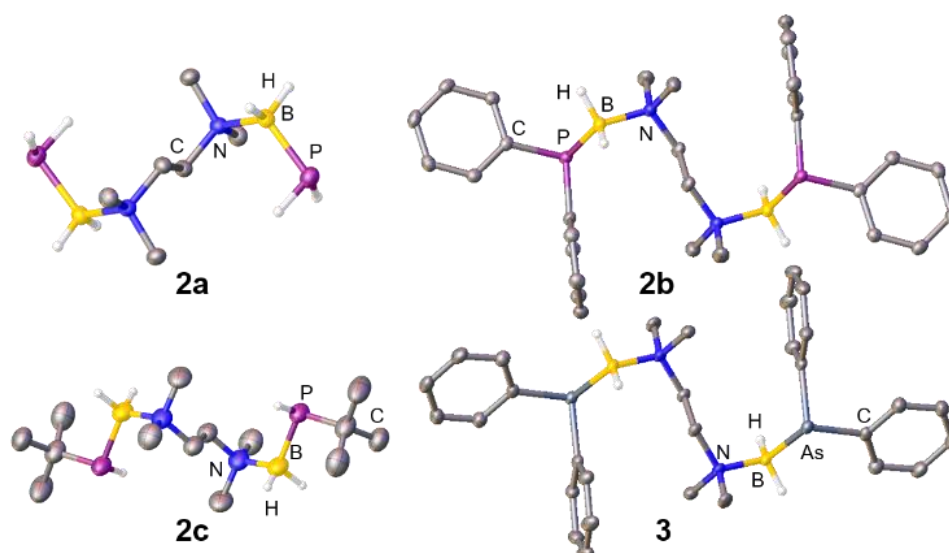
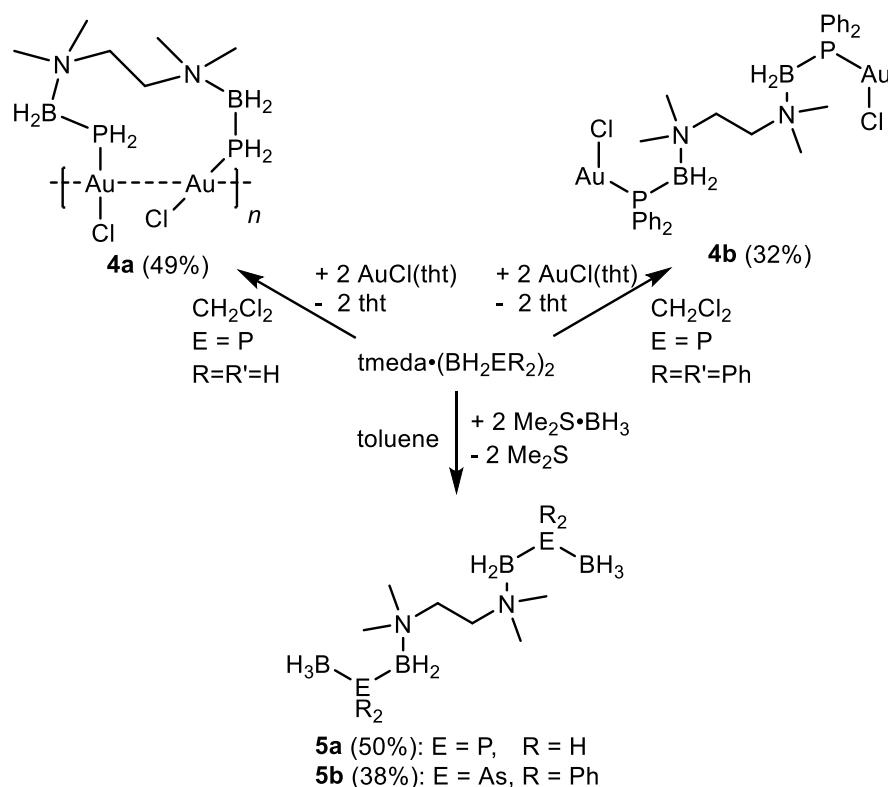


Figure 2: Molecular structures of **2** - **3** in the solid state. Hydrogen atoms bonded to carbon atoms are omitted for clarity. Thermal ellipsoids are drawn with 50% probability. Selected bond lengths [Å] and angles [°]: **2a**: P-B 1.965(2), B-N 1.627(2), P-B-N 116.95(11); **2b**: P-B 1.9840(18), B-N 1.640(2), P-B-N 109.85(10); **2c**: P-B 1.986(3)-1.990(12), B-N 1.632(3), P-B-N 109.0-109.39(15); **3**: As-B 2.087(3)-2.089(11), B-N 1.636(4)-1.642(11); As-B-N 108.77(19)-109.3(7).

The solid state structures of **2a**, **2b**, **2c** and **3** were determined by single crystal X-ray diffraction (Figure 2). The E-B (E = P, As) and the B-N bond lengths are comparable to single bonds. The molecular structure of **2-3** show a synclinal arrangement along the B-N axis. The parent compound **2a** adopts an antiperiplanar arrangement along the P-B axis, in contrast to the phenylsubstituted compounds **2b** and **3**, which show a synperiplanar configuration along the E-B bond. Similar to **2a**, **2c** adopts an antiperiplanar arrangement along the P-B axis, which leads to two N-B-P-C zigzag-chains.

The bond lengths and angles in the solid state structures of **2a-c** are comparable to the monomeric Me_3N stabilized phosphanylboranes.^[13c,18] In comparison to $\text{Me}_3\text{N}\cdot\text{BH}_2\text{PH}_2$,^[13c] the P-B bond length in **2a** is slightly shorter and the P-B-N angle is slightly tightened. Due to the substituents on the P atoms in **2b** and **2c**, respectively, the P-B-N angle is smaller as in **2a**. The P-B/B-N bond lengths in **2b** are slightly elongated in comparison to $\text{Me}_3\text{N}\cdot\text{BH}_2\text{PPh}_2$ (B-N 1.619(3) Å; P-B 1.975(2) Å), whereas the P-B-N angle in **2b** is smaller compared to the monomer^[18] (112.4(2)°). The angles and bond lengths in **2c** are nearly identical to the corresponding ones found in $\text{Me}_3\text{N}\cdot\text{BH}_2\text{tBuPH}$.^[18] The molecular structures of **2b** and **3** are similar. Compared to $\text{Me}_3\text{N}\cdot\text{BH}_2\text{AsH}_2$,^[13d] the B-N/As-B bond lengths are assimilable to **3**, whereas a contraction of the N-B-As angle (117.1(2)°) is observed, due to the influence of the phenylsubstituents.



Scheme 2: Synthesis of compounds **4** - **5**. Isolated yields are given in parentheses.

The reaction of the pnictogenylboranes **2a** and **2b**, respectively, with two equivalents AuCl(tht) (Scheme 2) yields the coordination compounds $\text{tmeda} \cdot (\text{BH}_2\text{PH}_2\text{AuCl})_2$ (**4a**) and $\text{tmeda} \cdot (\text{BH}_2\text{PPh}_2\text{AuCl})_2$ (**4b**). In contrast to **4b**, which is well soluble in all polar solvents, the parent compound **4a** reveals poor solubility after crystallization. In comparison to **2a/b**, the resonance signals in the NMR spectra of **4a** and **4b** are shifted downfield, due to the coordination to Au(I) .^[15] Whereas the hydrogen substituted parent phosphanylborane forms a polymeric structure with aurophilic interactions of the Au atoms in **4a**, the steric bulk of the phenylsubstituents in **4b** avoid such interactions and a dinuclear structure is formed (Figure 3). The gold atoms in **4a** show shorter intra- (3.230 Å), as well as longer intermolecular (3.360 Å) interactions.^[10] However, only the intramolecular $\text{Au} \cdots \text{Au}$ distances are shorter than the sum of van der Waals radii (3.32 Å).^[23]

All bond lengths in **4a** and **4b** are in the range of single bonds. The B-P-Au angle in **4b** (120.60(16)°) is slightly tightened compared to **4a** (123.9(4)°). In both cases, the B-P axis adopt a synclinal arrangement, however, due to the influence of the phenylsubstituents on the phosphorus atom in **4b**, the molecular structure is linear, which is comparable to **2b** and **3**, instead of the U-shaped structure formed in **4a**. Although, intra- as well as intermolecular interactions are present in the solid state of

4a, no luminescence properties were found. Therefore, we targeted the synthesis of cationic complexes with two pnictogenylboranes coordinated to Au(I). The reaction of **4a** with a second equivalent of **2a** in the presence of AlCl_3 leads to a fluorescent powder ($\lambda = 254 \text{ nm}$). Unfortunately, due to the bad solubility, further characterization of the product was not possible.

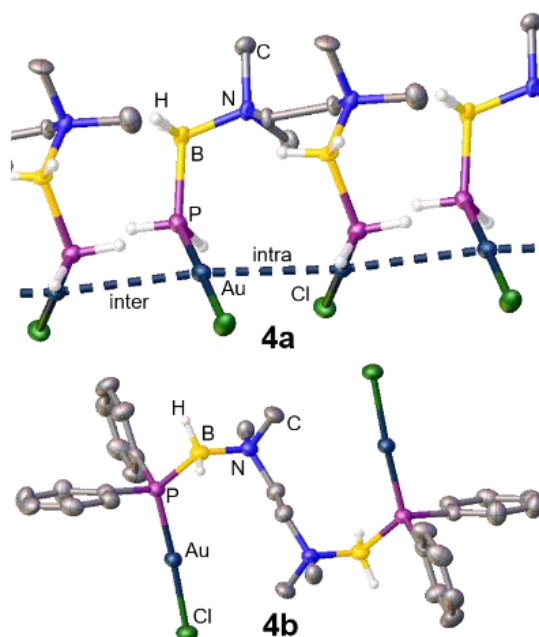
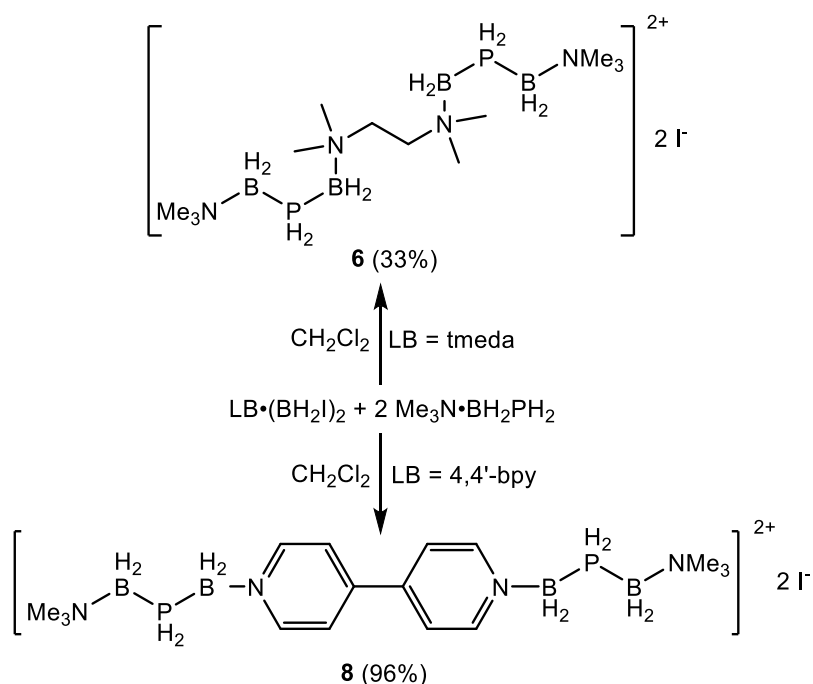


Figure 3: Molecular structure of **4a** and **4b** in the solid state. Hydrogen atoms bonded to carbon atoms are omitted for clarity. Thermal ellipsoids are drawn with 50% probability.

As a first step towards the construction of organic pnictogen-boron based frameworks, we further investigated the coordination behavior towards BH_3 . The reactions of either **2a** or **3** with two equivalents of $\text{Me}_2\text{S} \cdot \text{BH}_3$ in toluene leads to $\text{tmeda} \cdot (\text{BH}_2\text{P}(\text{Ph})_2\text{BH}_3)_2$ (**5a**) or $\text{tmeda} \cdot (\text{BH}_2\text{As}(\text{Ph})_2\text{BH}_3)_2$ (**5b**, Scheme 2), respectively. Compound **5a** is the first neutral parent compound containing two, only hydrogen substituted B-P-B chains and **5b** is the first neutral compound containing two B-As-B chains. The resonance of the P atoms in the ^{31}P NMR spectrum of **5a** ($\delta = -117.4 \text{ ppm}$) shows an expected downfield shift and a substantial broadening upon coordination to the boron moiety.^[12c,13c] In contrast, the resonance of the B atoms in the ^{11}B NMR spectrum of **5a** reveal a highfield shift ($\delta = -11.81 \text{ ppm}$ and -40.54 ppm) compared to the starting material **2a**. In the ^{11}B NMR spectrum of **5b**, a highfield shift ($\delta = -7.23 \text{ ppm}$ and -34.71 ppm) compared to the starting material **3** is observed as well.



Scheme 3: Synthesis of compounds **6** and **8**. Isolated yields are given in parentheses.

In order to synthesize the first LB connected, ionic phosphanylborane [tmeda·(BH₂PH₂BH₂·NMe₃)₂] [I]₂ (**6**), we reacted **1** with two equivalents Me₃N·BH₂PH₂ (Scheme 3). Compounds **5a**, **5b** and **6** are well soluble in polar solvents like CH₂Cl₂ and CH₃CN. The dicationic part of **6** can be seen as ionic analogue of **5a**. The resonance signals in the ¹¹B NMR and ³¹P NMR spectra of **6** are similar to [(Me₃N·BH₂PH₂BH₂·NMe₃)⁺·I⁻]₂.^[12a]

As synthetic procedures in which **1** is used as starting material show low yields due to the flexibility of the LB and therefore occurrence of side reactions like cyclisation, we decided to introduce the more rigid LB 4,4'-bipyridene (4,4'-bpy). The reaction of 4,4'-bpy with two equivalents Me₂S·BH₃ in Et₂O, and further iodination in benzene leads 4,4'-bpy·(BH₂I)₂ (**7**) in nearly quantitative yield. To evaluate if **7** is a suitable starting material for the synthesis of the desired products, we reacted **7** with two equivalents of Me₃N·BH₂PH₂ to obtain [4,4'-bpy·(BH₂PH₂BH₂·NMe₃)₂] [I]₂ (**8**, Scheme 3). The chemical shifts of the resonance signals in the ¹¹B NMR and ³¹P NMR spectrum are comparable to **6**. In contrast to the flexible tmeda linker, which reveal side reactions by cyclisation, the more rigid linker 4,4'-bpy avoid these reactions. The synthesis of **8** shows nearly quantitative yield. However, all attempts to synthesize the neutral 4,4'-bpy·(BH₂PRR')₂ from **7** failed so far, probably due to the lower donor strength of the LB.

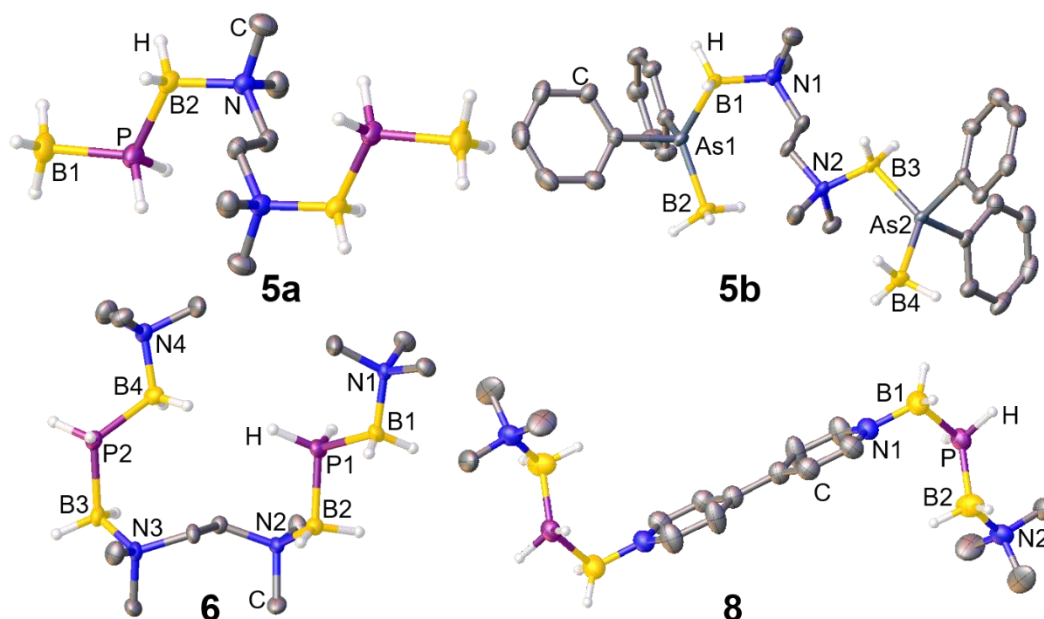


Figure 4: Molecular structures of **5** – **8** in the solid state. Counterions and hydrogen atoms bonded to carbon atoms are omitted for clarity. Thermal ellipsoids are drawn with 50% probability.

The E-B and B-N bond lengths of **5** – **8** are comparable to single bonds (Figure 4). The antiperiplanar arrangement of the B-P and B-N axis in **5a** leads to two B-P-B-N zigzag chains. Whereas an antiperiplanar environment along the B-N axis in **5b** is observed as well, the B-As bond presents a synclinal arrangement. A linear and a distorted U-shaped molecular structure are observed in the unit cell of **6**. Whereas the distorted U-shaped molecular structure results from the B2-N2-bond being in a synclinal arrangement and the B3-P2 axis showing an anticlinal orientation (Figure 4), the linear structure of **6** has a similar linear orientation as **5a** in the solid state. It is also noticeable, that the B1-P1-B2 angle in **6** ($116.6(2)^\circ$) is comparable to the B1-P-B2 angle in **5a** ($114.27(8)^\circ$), whereas the B3-P2-B4 angle in **6** is smaller ($108.0(2)^\circ$). This results presumably from packing effects. The B2-P bond in **8** has an antiperiplanar configuration, in contrast, the P-B1 bond adopts a synclinal arrangement.

6.3 Conclusion

In summary, we were able to synthesize the novel bidentate phosphanylboranes $\text{tmeda} \cdot (\text{BH}_2\text{PRR}')_2$ (**2a**: $\text{R} = \text{R}' = \text{H}$; **2b**: $\text{R} = \text{R}' = \text{Ph}$; **2c**: $\text{R} = \text{tBu}$, $\text{R}' = \text{H}$). These compounds are the first LB bridged phosphanylboranes and are interesting bidentate ligands due to their extended polarity inside the molecule compared to common

bidentate phosphine ligands. Moreover, by coordination to Au(I) centers, we were able to synthesize either dinuclear (**4b**) or polynuclear (**4a**) Au(I) complexes. Whereas **4b** shows no aurophilic interaction due to the sterical hindrance of the phenylsubstituents on the P atom, **4a** evoke intra- as well as intermolecular aurophilic interactions. This synthetic approach was further extended to the heavier homologue As to build the first bridged bidentate arsanylborane **3**. By coordination towards $\text{Me}_2\text{S}\cdot\text{BH}_3$, we were able to synthesize neutral group 13/15 oligomers **5a** and **5b**, as a first step to organic boron-pnictogen based networks. In addition, we could show that the iodinated compounds $\text{LB}\cdot(\text{BH}_2\text{I})_2$ (**1**, **7**) are useable starting materials to establish the first dicationic chains of group 13/15 elements (**6**, **8**). DFT calculations reveal the challenges of transferring the synthetic strategies of monodentate pnictogenylboranes to bidentate ones. The introduction of isopropyl-substituents on the nitrogen atoms of the bidentate LB should prevent a ring closure as well as ensure a higher solubility of the products. First approaches with the rigid *N,N,N',N'*-tetraisopropylethylenediamine (tipeda)^[24] are very promising and are currently under investigation.

6.4 References

- [1] a) J. Horstmann, M. Hyseni, A. Mix, B. Neumann, H.-G. Stammer, N. W. Mitzel, *Angew. Chem. Int. Ed.* **2017**, *56*, 6107-6111; *Angew. Chem.* **2017**, *129*, 6203-6207; b) Y. Liu, Y.-H. Yu, Y.-F. Liu, G.-F. Hou, X.-D. Wang, B. Wen, J.-S. Gao, *Z. Anorg. Allg. Chem.* **2013**, *639*, 193–196; c) S. Prusty, K. Yazaki, M. Yoshizawa, D. K. Chand, *Chem. Eur. J.* **2017**, *23*, 12456-12461; d) H. Jin Jang, S. L. Hopkins, M. A. Siegler, S. Bonnet, *Dalton Trans.* **2017**, *46*, 9969-9980; f) H. Clavier, J.-C. Guillemin, M. Mauduit, *Chirality* **2007**, *19*, 471-476; g) M.-C. Lagunasa, R. A. Gossage, W. J. J. Smeets, A. L. Spek, G. van Koten, *Eur. J. Inorg. Chem.* **1998**, 163-168.
- [2] a) M. E. Moussa, B. Attenberger, E. V. Peresyphkina, M. Fleischmann, G. Balázs, M. Scheer, *Chem. Commun.* **2016**, *52*, 10004--10007 b) D. Xiao, L. H. Do, *Organometallics* **2018**, *37*, 254–260; c) P. Milbeo, L. Moulart, C. Didierjean, E. Aubert, J. Martinez, M. Calmes, *Eur. J. Org. Chem.* **2018**, 178–187; d) T. N. Sevastianova, M. Bodensteiner, A. F. Maulieva, E. I. Davydova, A. V. Virovets, E. V. Peresyphkina, G. Balázs, C. Graßl, M. Seidl, M. Scheer, G. Frenking, E. A.

- Berezovskaya, I. V. Kazakov, O. V. Khoroshilova, A. Y. Timoshkin, *Dalton Trans.* **2015**, *44*, 20648-20658; e) C.-C. Wang, S.-Y. Ke, C.-W. Cheng, Y.-W. Wang, H.-S. Chiu, Y.-C. Ko, N.-K. Sun, M.-L. Ho, C.-K. Chang, Y.-C. Chuang, G.-H. Lee, *Polymers* **2017**, *9*, 644-661; f) A. S. Munn, S. Amabilino, T. W. Stevens, L. M. Daniels, G. J. Clarkson, F. Millange, M. J. Lennox, T. Düren, S. Bourelly, P. L. Llewellyn, R. I. Walton, *Cryst. Growth Des.* **2015**, *15*, 891-899; g) H. H. Karsch, P. A. Schlüter, M. Reisky, *Eur. J. Inorg. Chem.* **1998**, 433-436; j) N. C. Vieira, J. A. Pienkos, C. D. McMillen, A. R. Myers, A. P. Clay, P. S. Wagenknecht, *Dalton Trans.* **2017**, *46*, 15195-15199.
- [3] a) B. Attenberger, S. Welsch, M. Zabel, E. V. Peresypkina, M. Scheer, *Angew. Chem. Int. Ed.* **2011**, *50*, 11516-11519; *Angew. Chem.* **2011**, *123*, 11718 – 11722; b) B. Attenberger, E. V. Peresypkina, M. Scheer, *Inorg. Chem.* **2015**, *54*, 7021-7029; c) Y. Liu, Y.-H. Yu, Y.-F. Liu, G.-F. Hou, X.-D. Wang, B. Wen, J.-S. Gao, *Z. Anorg. Allg. Chem.* **2013**, *639*, (1), 193-196.
- [4] a) J. L. Kuiper, P. A. Shapley, C. M. Rayner, *Organometallics* **2004**, *23*, 3814-3818; b) P. Braunstein, M. A. Luke, A. Tiripicchio, M. Tiripicchio-Camellini, *Angew. Chem. Int. Ed.* **1987**, *26*, 768-770; *Angew. Chem.*, *99*, 802-803; c) H.-C. Böttcher, H. Schmidt, S. Tobisch, C. Wagner, *Z. Anorg. Allg. Chem.* **2003**, *629*, 686-692.
- [5] K. Nozaki, N. Sakai, T. Nanno, T. Higashijima, S. Mano, T. Horiuchi, H. Takaya, *J. Am. Chem. Soc.* **1997**, *119*, 4413-4423.
- [6] a) P. Binger, R. Milczarek, R. Mynott, M. Regitz, W. Ręsch, *Angew. Chem. Int. Ed.* **1986**, *25*, 644-645; *Angew. Chem.* **1986**, *98*, 645-646. b) P. B. Hitchcock, M. J. Maah, J. F. Nixon, *Chem. Commun.* **1986**, 737-738; c) E.-M. Rummel, G. Balász, V. Heintl, M. Scheer, *Angew. Chem. Int. Ed.* **2017**, *56*, 9592-9596; *Angew. Chem.* **2017**, *129*, 9720-9725; d) C. Jones, C. Schulten, A. Stasch, *Dalton Trans.* **2006**, 3733-3735; e) C. Rödl, R. Wolf, *Eur. J. Inorg. Chem.* **2016**, 736-742.
- [7] a) C. S. J. Callaghan, P. B. Hitchcock, J. F. Nixon, *J. Organomet. Chem.* **1999**, *584*, 87-93; b) C. Heindl, S. Reisinger, C. Schwarzmaier, L. Rummel, A. V. Virovets, E. Peresypkina, M. Scheer, *Eur. J. Inorg. Chem.* **2016**, 743-753.
- [8] a) K. Angermaier, E. Zeller, H. Schmidbaur, *J. Organomet. Chem.* **1994**, *472*, 371-376; b) a) P. D. Cookson, E. R. T. Tiekink, *Acta Cryst.* **1993**, *C49*, 1602-1603; c) C. A. Tolman, *Chem. Rev.* **1977**, *77*, 313-348; d) H. Schmidbaur, G.

- Weidenhiller, A. A. M. Aly, O. Steigelmann, G. Müller, *Z. Naturforsch.* **1989**, *44b*, 1503-1508.
- [9] J. R. Shakirova, E. V. Grachova, V. V. Sizov, G. L. Starova, I. O. Koshevoy, A. S. Melnikov, M. C. Gimeno, A. Lagunae, S. P. Tunik, *Dalton Trans.* **2017**, *46*, 2516–2523.
- [10] See as a review: H. Schmidbaur, A. Schier, *Chem. Soc. Rev.* **2012**, *41*, 370–412.
- [11] M. Streitberger, A. Schmied, E. Hey-Hawkins, *Inorg. Chem.* **2014**, *53*, 6794-6804.
- [12] a) C. Marquardt, C. Thoms, A. Stauber, G. Balázs, M. Bodensteiner, M. Scheer, *Angew. Chem. Int. Ed.* **2014**, *53*, 3727–3730; *Angew. Chem.* **2014**, *126*, 3801–3804; b) C. Marquardt, G. Balázs, J. Baumann, A. V. Virovets, M. Scheer, *Chem. Eur. J.* **2017**, *23*, 11423–11429; c) C. Marquardt, T. Kahoun, J. Baumann, A. Y. Timoshkin, M. Scheer, *Z. Anorg. Allg. Chem.* **2017**, *643*, 1326–1330; d) C. Marquardt, T. Kahoun, A. Stauber, G. Balázs, M. Bodensteiner, A. Y. Timoshkin, M. Scheer, *Angew. Chem. Int. Ed.* **2016**, *55*, 14828-14832; *Angew. Chem.* **2016**, *128*, 15048–15052.
- [13] a) A. C. Malcolm, K. J. Sabourin, R. McDonald, M. J. Ferguson, E. Rivard, *Inorg. Chem.* **2012**, *51*, 12905-12916; b) Z. Mo, A. Rit, J. Campos, E. L. Kolychev, S. Aldridge, *J. Am. Chem. Soc.* **2016**, *138*, 3306–3309; c) K.-C. Schwan, A. Y. Timoshkin, M. Zabel, M. Scheer, *Chem. Eur. J.* **2006**, *12*, 4900–4908; d) C. Marquardt, A. Adolf, A. Stauber, M. Bodensteiner, A. V. Virovets, A. Y. Timoshkin, M. Scheer, *Chem. Eur. J.* **2013**, *19*, 11887–11891.
- [14] a) U. Vogel, K.-C. Schwan, P. Hoemensch, M. Scheer, *Eur. J. Inorg. Chem.* **2005**, 1453-1458; b) C. Thoms, C. Marquardt, A. Y. Timoshkin, M. Bodensteiner, M. Scheer, *Angew. Chem. Int. Ed.* **2013**, *52*, 5150-5154; *Angew. Chem.* **2013**, *125*, 5254-5259; c) K.-C. Schwan, A. Adolf, M. Bodensteiner, M. Zabel, M. Scheer, *Z. Anorg. Allg. Chem.* **2008**, *634*, 1383-1387.
- [15] J. Braese, A. Schinabeck, M. Bodensteiner, H. Yersin, A. Y. Timoshkin, M. Scheer, *Chem. Eur. J.* 10.1002/chem.201802682.
- [16] N. E. Miller, E. L. Muetterties, *J. Am. Chem. Soc.* **1964**, *86*(6), 1033-1038.
- [17] In addition to [(tmeda·BH₂) I] the following decomposition/side products were observed in the NMR spectra of the reaction mixtures: **2a**) PH₃,

- (H₂PBH₂PH₂)Na; **2b**) HPPH₂, (Ph₂PBH₂)_n; **2c**) *t*BuPH₂, (*t*BuPHBH₂)_n; **3**) tmeda·(BH₃)₂.
- [18] C. Marquardt, T. Jurca, K.-C. Schwan, A. Stauber, A. V. Virovets, G. R. Whittell, I. Manners, M. Scheer, *Angew. Chem. Int. Ed.* **2015**, *54*, 13782–13786; *Angew. Chem.* **2015**, *127*, 13986–13991.
- [19] See Supporting Information: NMR spectroscopy tmeda·(BH₂*t*BuPH)₂.
- [20] C. Trinh, M. Bodensteiner, A. V. Virovets, E. V. Peresyphkina, M. Scheer, S. M. Matveev, A. Y. Timoshkin, *Polyhedron*, **2010**, *29*, 414–424.
- [21] See Supporting Information: Computational details.
- [22] Besides other decomposition products, which could not be further identified, tmeda·(BH₃)₂ was observed in the ¹¹B NMR spectra. However, no signal for tmeda·(BH₂AsH₂)₂ was observed in the expected range of LB stabilized arsanylboranates in the ¹¹B NMR spectra.
- [23] P. Pyykkö, M. Atsumi, *Chem. Eur. J.* **2009**, *15*, 12770 – 12779.
- [24] W. J. Marshall, V. V. Grushin, *Can. J. Chem.* **2005**, *83*, 640–645.

6.5 Supporting Information

Experimental section

Synthetic procedures

All manipulations were performed under an atmosphere of dry argon using standard glovebox and Schlenk techniques. All solvents are degassed and purified by standard procedures.

The compounds Me₃N·BH₂PH₂^[1], Me₃N·BH₂^[2], tmeda·(BH₃)₂^[3], Na*t*BuPH^[4], dioxane·KAsPh₂^[5] and (tht)AuCl^[6] were prepared according literature procedures. The synthesis of compound 4,4'-bpy·(BH₃)₂ was slightly modified.^[7] The compound Me₂S·BH₃ (Sigma-Aldrich) is commercially available.

The NMR spectra were recorded on either an Avance 400 spectrometer (¹H: 400.13 MHz, ³¹P:161.976 MHz, ¹¹B: 128.378 MHz, ¹³C{¹H}: 100.623 MHz, ²⁷Al: 104.261 MHz) with δ [ppm] referenced to external SiMe₄ (¹H, ¹³C), H₃PO₄ (³¹P), BF₃·Et₂O (¹¹B), CFC₃ (¹⁹F) or Al(NO₃)₃·9 H₂O (²⁷Al).

IR spectra were measured on a DIGILAB (FTS 800) FT-IR spectrometer and on a Thermo Scientific Nicolet iS5. All mass spectra were recorded on a Finnigan MAT 95 (FDMS and EI-MS) and a Jeol AccuTOF GCX (LIFDI).

The C, H, N analyses were measured on an Elementar Vario EL III apparatus.

Synthesis of $\text{tmeda} \cdot (\text{BH}_2\text{I})_2$ (**1**)

10.15 g (40 mmol) Iodine is added to a suspension of 5.73 g (39.5 mmol) $\text{tmeda} \cdot (\text{BH}_3)_2$ in Et_2O . The color turns brown and a development of gas is observed. After three days all volatiles of the bleached suspension are removed *in vacuo*. The off-white solid is washed two times with 40 mL *n*-hexane and dried *in vacuo*.

Yield: 13.56 g (86%, powder).

$^1\text{H-NMR}$ (C_6D_6): $\delta[\text{ppm}] = 2.90$ (m, br, 4 H, BH_2), 2.83 (s, 4 H, CH_2 tmeda), 1.94 (s, 12 H, CH_3 tmeda).

$^{11}\text{B}\{^1\text{H}\}\text{-NMR}$ (C_6D_6): $\delta[\text{ppm}] = -12.07$ (s, br).

$^{11}\text{B-NMR}$ (C_6D_6): $\delta[\text{ppm}] = -12.07$ (t, br, $^1J_{\text{BH}} = 120$ Hz).

Synthesis of $\text{tmeda} \cdot (\text{BH}_2\text{PH}_2)_2$ (**2a**)

To a suspension of 396 mg (1 mmol) **1** in 15 mL thf a suspension of 130 mg (2.2 mmol) NaPH_2 is added at -80°C . The suspension is either sonicated for 2 h or allowed to reach room temperature for 18 h. All volatiles are removed *in vacuo* and the remaining white solid is washed with 10 mL *n*-hexane. The solid is suspended in 30 mL toluene at 50°C and filtrated. The volume of the clear solution is reduced *in vacuo* to about 15 mL. **2a** crystallizes as colorless needles by storing the solution at -30°C .

Yield: 45 mg (22%, crystalline).

$^1\text{H-NMR}$ (C_6D_6): $\delta[\text{ppm}] = 1.45$ (dm, $^1J_{\text{HP}} = 189$ Hz, 4 H, PH_2), 1.79 (s, 12 H, CH_3), 2.38 (m, br, 4H, BH_2), 2.63 (s, 4 H, CH_2).

$^{11}\text{B}\{^1\text{H}\}\text{-NMR}$ (C_6D_6): $\delta[\text{ppm}] = -9.12$ (s, br, $\omega_{1/2} = 260$ Hz, BH_2).

$^{11}\text{B-NMR}$ (C_6D_6): $\delta[\text{ppm}] = -9.12$ (t, br, $^1J_{\text{BH}} = 108$ Hz, BH_2).

$^{31}\text{P}\{^1\text{H}\}\text{-NMR}$ (C_6D_6): $\delta[\text{ppm}] = -217.5$ (d, br, $^1J_{\text{PB}} = 30$ Hz, PH_2).

$^{31}\text{P-NMR}$ (C_6D_6): $\delta[\text{ppm}] = -217.5$ (td, br, $^1J_{\text{PB}} = 30$ Hz, $^1J_{\text{PH}} = 189$ Hz, PH_2).

EI-MS (CH₂Cl₂):	cation: <i>m/z</i> : 207 (2) (M ⁺), 175 (2) ((H ₂ B·TMEDA·BH ₂ PH ₂) ⁺), 129 (25) ((TMEDA·BH ₂) ⁺), 116 (8) (TMEDA ⁺), 58 (100) ((Me ₂ N=CH ₂) ⁺).
EA:	calculated for C ₆ H ₂₄ B ₂ N ₂ P ₂ : C 34.58%; H 11.62%, N 13.45% found: C 34.29%; H 11.37%; N 13.11%.
IR (KBr):	$\tilde{\nu}$ [cm ⁻¹] = 3445(vw), 2997(w, C-H), 2942(w, C-H), 2392(vs, B-H), 2280(vs, P-H), 1475(s), 1400(m), 1307(m), 1244(m), 1140(s), 1113(s), 1092(s), 1053(s), 1023(s), 990(m), 871(s), 788(m), 691(m), 588(m).

Synthesis of tmeda·(BH₂PPh₂)₂ (**2b**)

To a solution 198 mg (0.5 mmol) **1** in 15 mL thf 1.1 mL of a 1M solution of NaPPh₂ in thf is added at -80°C. After allowing the clear red solution to reach room temperature over 18 h, all volatiles are removed *in vacuo*. The remaining solid is suspended in 25 mL toluene and filtrated. The volume of the clear colorless solution is reduced *in vacuo* to 5mL and stored at -30°C for 24 h. The solvent is decanted and the microcrystalline solid is dried *in vacuo*. **2b** crystallizes as colorless blocks by storing a saturated solution of CH₂Cl₂ at -30°C.

Yield:	83 mg (32%, microcrystalline).
¹H-NMR (C₆D₆):	δ [ppm] = 1.90 (s, 12 H, CH ₃), 2.71 (s, br, $\omega_{1/2}$ = 175 Hz, 4 H, BH ₂), 2.78 (s, 4 H, CH ₂), 7.00-7.20 (m, 12 H, m/p-H Ph), 7.78 (m, 8 H, o-H Ph).
¹¹B{¹H}-NMR (C₆D₆):	δ [ppm] = -3.86 (s, br, $\omega_{1/2}$ = 590 Hz, BH ₂).
¹¹B-NMR (C₆D₆):	δ [ppm] = -3.86 (s, br, $\omega_{1/2}$ = 602 Hz, BH ₂).
¹³C-NMR (C₆D₆):	δ [ppm] = 51.56 (d, ² J _{CC} =11.17 Hz, CH ₃ tmeda), 56.79 (d, ² J _{CC} =11.17 Hz, CH ₂ tmeda), 126.67 (s, <i>p</i> -C ₆ H ₅), 128.01 (d, ³ J _{CP} =24.02 Hz, <i>m</i> -C ₆ H ₅), 134.88 (d, ² J _{CP} =16 Hz, <i>o</i> -C ₆ H ₅), 143.13 (d, ¹ J _{CP} =11 Hz, <i>i</i> -C ₆ H ₅).
³¹P{¹H}-NMR (C₆D₆):	δ [ppm] = -42.1 (s, br, $\omega_{1/2}$ = 45 Hz, PPh ₂).
³¹P-NMR (C₆D₆):	δ [ppm] = -42.1 (s, br, $\omega_{1/2}$ = 52 Hz, PPh ₂).
EI-MS (CH₂Cl₂):	cation: <i>m/z</i> : 641 (100) ((M+tmeda·BH ₂) ⁺), 512 (15) (M ⁺), 129 (100) ((tmeda·BH ₂) ⁺).

EA:	calculated for $C_6H_{24}B_2N_2P_2$: C 70.27% H 7.87% N 5.47% found: C 70.00% H 7.80% N 5.36%.
IR (KBr):	$\tilde{\nu}$ [cm^{-1}] = 3066 (vw, C_{arom-H}), 3049 (vw, C_{arom-H}), 3013 (vw, C_{arom-H}), 2991 (vw, $C_{methyl-H}$), 2938 (vw), 2381 (vs, B-H), 2343 (m, B-H), 1772 (vw), 1733 (vw), 1717 (w), 1699 (vw), 1684 (vw), 1674 (vw), 1669 (w), 1652 (m), 1646 (m), 1635 (m), 1623 (vw), 1616 (m), 1576 (m), 1569 (w), 1558 (vw), 1540 (m), 1521 (vw), 1506 (vw), 1496 (vw), 1475 (vs), 1456 (s), 1430 (s), 1400 (vw), 1386 (vw), 1301 (vw), 1243 (vw), 1194 (vw), 1141 (m), 1106 (w), 1079 (m), 1061 (s), 1019 (s), 989 (w), 862 (m), 793 (w), 760 (m), 733 (vs), 703 (vs), 693 (vs), 668 (w), 641 (w), 516 (m).

Synthesis of $tmeda \cdot (BH_2tBuPH)_2$ (**2c**)

To a suspension of 396 mg (1 mmol) **1** in 20 mL thf 10 mL of a fresh synthesized solution of Na^+tBuPH^- (2 mmol) in thf is added at $-80^\circ C$. The suspension is allowed to reach room temperature over 18 h. All volatiles are removed and the remaining white solid is suspended in 30 mL *n*-hexane. After filtration the volume of the clear solution is reduced to 15 mL and stored at $-30^\circ C$. **2c** crystallizes as colorless blocks. Due to the similar solubility of side/decomposition products and the thermal instability of **2c**, further purification was not possible.

Yield:	120 mg (69% purity according ^{31}P NMR spectra; 26%).
1H-NMR (C_6D_6):	δ [ppm] = 1.46 (d, $^3J_{HP}=11$ Hz, 18 H, $C(CH_3)_3$), 1.95 (s, br, 6H, CH_3 tmeda, meso), 1.98 (s, 3H, CH_3 tmeda, R,R' and S,S'), 1.99 (s, 3H, CH_3 tmeda, R,R' and S,S'), 2.17 (s, br, $\omega_{1/2} = 200$ Hz, 4H, BH_2), 2.46 (dt, $^1J_{HP} = 198$ Hz, $^3J_{HH} = 7$ Hz, 2H, PH), 2.87 (m, 4H, CH_2 tmeda).
$^{11}B\{^1H\}$-NMR (C_6D_6):	δ [ppm] = -8.12 (s, br, BH_2).
^{11}B-NMR (C_6D_6):	δ [ppm] = -8.12 (m, br, BH_2).
$^{31}P\{^1H\}$-NMR (C_6D_6):	δ [ppm] = -70.9 (d, br, $^1J_{PB} = 81$ Hz, PH).
^{31}P-NMR (C_6D_6):	δ [ppm] = -70.9 (m, br, $^1J_{PB} = 81$ Hz, $^1J_{PH} = 198$ Hz, PH).

ES-MS (CH₂Cl₂): cation: m/z : 525 [(M+(^tBuPHBH₂)₂)⁺],
 423 [(M+(^tBuPHBH₂))⁺], 321 [M⁺],
 219 [(tmeda·BH₂^tBuPH)⁺].

The crystallization of **2c** succeeded once. The IR spectrum and the EA were measured from this small amount of crystalline material (about 5 mg). As presented later on, the NMR spectra of the bulk phase shows impurities and decomposition products, which could not be further separated.

EA: calculated for C₁₄H₄₀B₂N₂P₂:
 C 52.45% H 12.59% N 8.47%
 found: C 51.99% H 12.22% N 7.92%.

IR (KBr): $\tilde{\nu}$ [cm⁻¹] = 2989 (w, C-H), 2930 (s, C-H), 2888 (m), 2850 (m), 2426 (m, B-H), 2395 (s, B-H), 2359 (s, B-H), 2325 (m), 2262 (m, P-H), 2241 (m, P-H), 1733 (vw), 1717 (vw), 1699 (vw), 1684 (vw), 1652 (vw), 1646 (w), 1635 (vw), 1558 (w), 1540 (w), 1521 (w), 1506 (w), 1471 (s), 1456 (s), 1436 (m), 1418 (vw), 1404 (vw), 1357 (m), 1300 (w), 1198 (vw), 1163 (w), 1145 (m), 1111 (m), 1067 (s), 1025 (m), 995 (w), 860 (m), 800 (vw), 780 (w).

Synthesis of tmeda·(BH₂AsPh₂)₂ (**3**)

To a suspension of 198 mg (0.5 mmol) **1** in 10 mL thf a solution of 340 mg (1.06 mmol) KAsPh₂·(dioxin)_{0.65} in 10 mL thf is added at -80°C. The solution is allowed to reach room temperature over 18 h and changes the color from deep red to colorless. All volatiles are removed *in vacuo* and the remaining white solid is washed with 10 mL *n*-hexane. The solid is suspended in 25 mL toluene and filtrated. The volume of the clear solution is reduced *in vacuo* to about 12 mL and stored at -30°C. **3** crystallizes as colorless blocks.

Yield: 53 mg (18%, crystalline).

¹H-NMR (C₆D₆): δ [ppm] = 1.84 (s, 12H, CH₃ tmeda), 2.67 (s, 4H, CH₂ tmeda), 2.69 (m, 4H, BH₂), 7.06 (m, 4H, *p*-C₆H₅), 7.15 (m, 8H, *m*-C₆H₅), 7.83 (d, 8H, ³J_{H,H} = 8 Hz, *o*-C₆H₅).

¹¹B{¹H}-NMR (C₆D₆): δ [ppm] = -2.90 (s, br).

¹¹B-NMR (C₆D₆): δ [ppm] = -2.90 (s, br, $\omega_{1/2}$ = 870 Hz).

$^{13}\text{C}\{^1\text{H}\}$-NMR ($\text{C}_6\text{D}_6$):	$\delta[\text{ppm}] = 52.08$ (s, CH_3 tmeda), 57.56 (s, CH_2 tmeda), 126.86 (s, $p\text{-C}_6\text{H}_5$), 128.35 (s, $m\text{-C}_6\text{H}_5$), 135.27 (s, $o\text{-C}_6\text{H}_5$), 143.24 (s, $i\text{-C}_6\text{H}_5$).
LIFDI-MS (toluene):	cation: m/z : 600 (M^+).
EA:	calculated for $\text{C}_{30}\text{H}_{46}\text{N}_2\text{B}_2\text{As}_2$: C 59.78%; H 7.03%; N 4.65% found: C 60.23%; H 6.55%; N 4.51%.
IR (KBr):	$\tilde{\nu} [\text{cm}^{-1}] = 3063$ (vw, C-H _{arom}), 3048 (w, C-H _{arom}), 2989 (vw, C-H _{alkyl}), 2399 (m, B-H), 2377 (m, B-H), 2342 (w), 1636 (vw), 1576 (w), 1477 (m), 1470 (m), 1456 (w), 1428 (w), 1401 (vw), 1300 (vw), 1242 (vw), 1150 (w), 1137 (w), 1104 (w), 1077 (w), 1051 (s), 1017 (m), 985 (w), 864 (w), 792 (w), 748 (m), 731 (s), 714 (s), 693 (w), 591 (vw), 487 (m), 452 (vw).

Synthesis of tmeda·($\text{BH}_2\text{PH}_2\text{AuCl}$)₂ (4a**)**

To a solution of 15 mg (0.07 mmol) **2a** in 10 mL CH_2Cl_2 at -80°C a solution of 48 mg (0.15 mmol) $\text{AuCl}(\text{tht})$ in 5 mL CH_2Cl_2 at -80°C is added. The solution is stirred for 30 min at -80°C and subsequently allowed to reach room temperature. All volatiles are removed *in vacuo* and the remaining white solid is washed with 10 mL *n*-hexane. The solid is suspended in 5 mL CH_2Cl_2 and filtrated. **4a** crystallizes as colorless needles by layering a saturated CH_2Cl_2 solution with threefold *n*-hexane. The crystalline material is badly soluble.

Yield:	23mg (49%, crystalline).
^1H-NMR (C_6D_6):	$\delta[\text{ppm}] = 2.09$ (m, br, 4H, BH_2 , $^1J_{\text{HB}} = 120\text{Hz}$), 2.99 (s, 12 H, CH_3), 3.83 (d, 4H, PH_2 , $^1J_{\text{HP}} = 352\text{Hz}$), 3.88 (s, 4H, CH_2).
$^{11}\text{B}\{^1\text{H}\}$-NMR ($\text{C}_6\text{D}_6$):	$\delta[\text{ppm}] = -11.47$ (m, br, BH_2).
^{11}B-NMR (C_6D_6):	$\delta[\text{ppm}] = -11.47$ (m, br, BH_2).
$^{31}\text{P}\{^1\text{H}\}$-NMR ($\text{C}_6\text{D}_6$):	$\delta[\text{ppm}] = -144.7$ (s, br, PH_2).
^{31}P-NMR (C_6D_6):	$\delta[\text{ppm}] = -144.7$ (m, br, PH_2).
IR (KBr):	$\tilde{\nu} [\text{cm}^{-1}] = 3057$ (w), 3012 (w), 2961 (w, C-H), 2938 (w, C-H), 2422 (s, B-H), 2405 (s, B-H), 2364 (m, P-H), 2343 (m, P-H),

2307 (m, P-H), 1581 (w), 1570 (w), 1475(vs), 1466 (m), 1431 (vs), 1403 (s), 1309 (s), 1262 (s), 1240 (m), 1190 (m), 1181 (m), 1151 (m), 1139 (s), 1094 (s), 1072 (vs), 1021 (vs), 999 (s), 982 (m), 870 (s), 854 (m), 801 (s), 789 (s), 765 (s), 743 (s), 700 (vs), 637 (s), 550 (w), 514 (s), 472 (m), 455 (s), 426 (m).

Synthesis of tmeda·(BH₂PPh₂AuCl)₂ (**4b**)

To a solution of 36 mg (0.07 mmol) **2b** in 30 mL CH₂Cl₂ at -80°C a solution of 45 mg (0.14 mmol) AuCl(tht) in 30 mL CH₂Cl₂ at -80°C is added. The solution is stirred for 30 min at -80°C and subsequently allowed to reach room temperature. All volatiles are removed *in vacuo* and the remaining white solid is washed with 10 mL *n*-hexane. The solid is suspended in 10 mL CH₂Cl₂ and filtrated. **4b** crystallizes as colorless needles by layering a saturated CH₂Cl₂ solution with threefold *n*-hexane. In addition, some black powder precipitates, presumably Au(0).

Yield:	22 mg (32%, crystalline).
¹H-NMR (CD₂Cl₂):	δ[ppm] = 2.68 (br, 4H, BH ₂), 2.78 (d, 12H, CH ₃ , ³ J _{HB} = 1.5 Hz), 3.70 (s, 4H, CH ₂), 7.35-7.41 (m, 12H, m/p-H C ₆ H ₅), 7.72-7.80 (m, 8H, o-H C ₆ H ₅).
¹¹B{¹H}-NMR (CD₂Cl₂):	δ[ppm] = -7.44 (s, br, ω _{1/2} = 590 Hz, BH ₂).
¹¹B-NMR (CD₂Cl₂):	δ[ppm] = -7.44 (s, br, ω _{1/2} = 602 Hz, BH ₂).
¹³C-NMR (CD₂Cl₂):	δ[ppm] = 53.41 (s, CH ₃ tmeda), 57.89 (d, ² J _{CC} = 6.5 Hz, CH ₂ tmeda), 129.11(d, ³ J _{CP} = 10.32 Hz, <i>m</i> -C ₆ H ₅), 130.59 (d, ⁴ J _{CP} = 2.73 Hz, <i>p</i> -C ₆ H ₅), 133.25 (d, ¹ J _{CP} = 50.34 Hz, <i>i</i> -C ₆ H ₅), 134.86 (d, ² J _{CP} = 11.48 Hz, <i>o</i> -C ₆ H ₅).
³¹P{¹H}-NMR (CD₂Cl₂):	δ[ppm] = -7.33 (s, br, ω _{1/2} = 465 Hz, PPh ₂).
³¹P-NMR (CD₂Cl₂):	δ[ppm] = -7.33 (s, br, ω _{1/2} = 535 Hz, PPh ₂).
FD-MS (CH₂Cl₂):	<i>m/z</i> (rel. Int. %): 976 (M ⁺), 941 ([M] ⁺ -Cl), 709 ([M] ⁺ -AuCl ₂).
EA:	calculated for [C ₃₀ H ₃₆ Au ₂ Cl ₂ B ₂ N ₂ P ₂](Au) _{0.45} : C: 33.81%; H: 3.79%; N: 2.63% found: C: 33.83%; H: 3.81%; N: 2.41%.
IR (KBr):	$\tilde{\nu}$ [cm ⁻¹] = 3054 (w, C-H _{arom}), 3009 (w, C-H _{alkyl}), 2465 (m, B-H), 2396 (m, B-H), 2360 (m), 2332 (m), 1733 (w), 1699

(m), 1683 (m), 1652 (w), 1635 (vw), 1506 (w), 1476 (s), 1457 (vs), 1435 (vs), 1265 (w), 1141 (w), 1116 (w), 1065 (vs), 1025 (w), 879 (w), 786 (w), 735 (vs), 690 (vs), 643 (vw), 520 (s), 484 (m).

Synthesis of $\text{tmeda} \cdot (\text{BH}_2\text{PH}_2\text{BH}_3)_2$ (**5a**)

To a solution of 35 mg (0.17 mmol) **2a** in 10 mL toluene 0.2 mL of a 2M $\text{Me}_2\text{S} \cdot \text{BH}_3$ in toluene is added at -80°C . The solution is allowed to reach room temperature over 10 h. All volatiles are removed *in vacuo*. **5a** crystallizes by storing a saturated solution of CH_2Cl_2 at -30°C .

Yield: 20 mg (50%, powder).

^1H – NMR (CDCl_3): $\delta[\text{ppm}] = 0.71$ (q, br, $^1J_{\text{HB}} = 95$ Hz, 6H, BH_3), 2.20 (m, br, 4H, BH_2), 2.84 (d, $^4J_{\text{HP}} = 1.87$ Hz, 12H, CH_3), 3.36 (dm, $^1J_{\text{HP}} = 333$ Hz, 4H, PH_2) 3.49 (s, 4H, CH_2).

$^{11}\text{B}\{^1\text{H}\}$ – NMR (CDCl_3): $\delta[\text{ppm}] = -40.54$ (d, $^1J_{\text{BP}} = 42$ Hz, BH_3), -11.81 (d, $^1J_{\text{BP}} = 70\text{Hz}$, BH_2).

^{11}B – NMR (CDCl_3): $\delta[\text{ppm}] = -40.54$ (qd, $^1J_{\text{BP}} = 42$ Hz $^1J_{\text{BH}} = 95\text{Hz}$, BH_3), -11.82 (m, BH_2).

$^{31}\text{P}\{^1\text{H}\}$ – NMR (CDCl_3): $\delta[\text{ppm}] = -117.4$ (s, br, PH_2).

^{31}P – NMR (CDCl_3): $\delta[\text{ppm}] = -117.4$ (t, br, $^1J_{\text{PH}} = 333\text{Hz}$, PH_2).

EI-MS (toluene): m/z (rel. Int. %): 221 (25) ($(\text{PH}_2\text{BH}_2 \cdot \text{tmeda} \cdot \text{BH}_2\text{PH}_2\text{BH}_3)^+$), 175 (10) ($(\text{tmeda} \cdot \text{BH}_2\text{PH}_2\text{BH}_3)^+$), 129 (100) ($(\text{tmeda} \cdot \text{BH}_2)^+$), 58 (40) ($(\text{Me}_2\text{N}=\text{CH}_2)^+$).

Synthesis of $\text{tmeda} \cdot (\text{BH}_2\text{AsPh}_2\text{BH}_3)_2$ (**5b**)

To a solution of 40 mg (0.066 mmol) **3** in 7 mL thf 0.02 mL (0.2 mmol) $\text{Me}_2\text{S} \cdot \text{BH}_3$ is added at -80°C . A white solid precipitates. The solution is stirred over 18 h and all volatiles are removed *in vacuo*. The remaining solid is washed with 10 mL *n*-hexane and dissolved in 5 mL CH_2Cl_2 . After filtration over diatomaceous earth the volume of the solution is reduced *in vacuo* to about 1 mL. **5b** crystallizes by storing a saturated solution of CH_2Cl_2 at -30°C as colorless blocks. Due to an impurity/decomposition

product (tmeda·(BH₃)₂) with similar solubility, it was not possible to achieve analytical purity.

Yield:	18 mg (crystalline, 88% purity according to ¹ H and ¹¹ B NMR spectra, 38%).
¹H-NMR (CD₂Cl₂):	δ[ppm] = 1.26 (q, br, ¹ J _{HB} = 111 Hz, 6H, BH ₃), 2.65 (s, 12H, CH ₃), 2.67 (m, br, 4H, BH ₂), 3.35 (s, 4 H, CH ₂), 7.31 (m, 12H, <i>p</i> - and <i>m</i> -C ₆ H ₅), 7.66 (m, 8H, <i>o</i> -C ₆ H ₅).
¹¹B{¹H}-NMR (CD₂Cl₂):	δ[ppm] = -7.23 (s, br, ω _{1/2} = 326 Hz, BH ₂), -34.71 (s, br, ω _{1/2} = 263 Hz, BH ₃).
¹¹B-NMR (CD₂Cl₂):	δ[ppm] = -7.23 (s, br, ω _{1/2} = 449 Hz, BH ₂), -34.71 (q, br, ¹ J _{BH} = 111 Hz, BH ₃).
FD-MS (CH₂Cl₂):	<i>m/z</i> : 614 [((Ph ₂ AsBH ₂)·tmeda·(BH ₂ AsPh ₂ BH ₃)) ⁺], 129 (100) ((tmeda·BH ₂) ⁺).
EA:	calculated for C ₃₀ H ₄₆ As ₂ B ₄ N ₂ C: 57.30%, H: 7.38%, N: 4.46%. found: C: 57.26%, H: 7.51%, N: 4.53%.
IR (KBr):	$\tilde{\nu}$ [cm ⁻¹] = 3062 (vw, C-H _{arom.}), 3043 (vw, C-H _{arom.}), 3001 (vw, C-H _{alkyl}), 2948 (vw, C-H _{alkyl}), 2919 (vw), 2849 (vw), 2453 (w, B-H), 2437 (m, B-H), 2389 (s, B-H), 2348 (m, B-H), 2295 (w), 2274 (w), 1733 (vw), 1699 (vw), 1652 (vw), 1581 (vw), 1558 (vw), 1540 (vw), 1506 (vw), 1475 (m), 1434 (s), 1352 (w), 1307 (w), 1240 (vw), 1164 (w), 1087 (w), 1048 (vs), 1023 (m), 999 (w), 976 (vw), 878 (w), 854 (w), 796 (w), 748 (m), 739 (m), 696 (m), 664 (vw), 604 (vw), 485 (w), 452 (w), 418 (vw).

Synthesis of [tmeda·(BH₂PH₂BH₂·NMe₃)]₂ (**6**)

To a suspension of 198 mg (0.5 mmol) of **1** in 25 mL CH₂Cl₂ 2mL (1mmol) of a solution of Me₃N·BH₂PH₂ in toluene is added at -30°C. The suspension is stirred for 10h and is allowed to reach room temperature. All volatiles are removed *in vacuo*. The remaining white solid is washed three times with 10mL toluene. **6** crystallizes by storing a saturated solution of acetonitrile at 3°C as colorless plates and needles.

Yield:	100 mg (33%, crystalline).
$^1\text{H-NMR}$ (CD_3CN):	$\delta[\text{ppm}] = 2.06$ (m, 8H, BH_2), 2.76 (d, 18H, $\text{N}(\text{CH}_3)_3$, $^4J_{\text{HP}} = 1.5\text{Hz}$), 2.84 (s, 12H, CH_3 tmeda), 3.40 (s, 4H, CH_2 tmeda), 3.92 (dm, 4H, PH_2 , $^1J_{\text{HP}} = 350\text{ Hz}$).
$^{11}\text{B}\{^1\text{H}\}\text{-NMR}$ (CD_3CN):	$\delta[\text{ppm}] = -11.19$ (m, br, $\text{Me}_3\text{N}\cdot\text{BH}_2$), -12.14 (m, br, tmeda $\cdot(\text{BH}_2)_2$).
$^{11}\text{B-NMR}$ (CD_3CN):	$\delta[\text{ppm}] = -11.19$ (m, br, $\text{Me}_3\text{N}\cdot\text{BH}_2$), -12.14 (m, br, tmeda $\cdot(\text{BH}_2)_2$).
$^{31}\text{P}\{^1\text{H}\}\text{-NMR}$ (CD_3CN):	$\delta[\text{ppm}] = -135.7$ (s, br, PH_2).
$^{31}\text{P-NMR}$ (CD_3CN):	$\delta[\text{ppm}] = -135.7$ (t, br, PH_2 , $^1J_{\text{PH}} = 350\text{ Hz}$).
ES-MS (MeCN):	cation: m/z : 1084 ($[[\text{tmeda}\cdot(\text{BH}_2\text{PH}_2\text{BH}_2\cdot\text{NMe}_3)]^{2+}]_2 [\text{I}^-]_3$), 2 (%), 479 ($[\text{tmeda}\cdot(\text{BH}_2\text{PH}_2\text{BH}_2\cdot\text{NMe}_3)]^{2+} [\text{I}^-]$), 20 (%), 176 ($[\text{tmeda}\cdot(\text{BH}_2\text{PH}_2\text{BH}_2\cdot\text{NMe}_3)]^{2+}$), 100 (%).
EA:	calculated for $\text{C}_{12}\text{H}_{34}\text{B}_4\text{I}_2\text{N}_2\text{P}_2$: C 23.76%; H 7.65%; N 9.24% found: C 23.80%; H 7.53%; N 9.16%.
IR (KBr):	$\tilde{\nu} [\text{cm}^{-1}] = 3500(\text{m})$, 3440(m), 2997(s, CH), 2950(m, CH), 2813(w), 2446(vs, BH), 2416(vs, BH), 2305(s, PH), 2041(vw), 1773(vw), 1613(vw), 1469(vs), 1414(s), 1355(vw), 1318(m), 1244(s), 1200(w), 1156(s), 1130(vs), 1106(vs), 1055(s), 1018(s), 975 (s), 870 (vs), 845(vs), 812(vs), 785(vs), 714(s), 671 (w), 617(w), 503(w), 474(vw), 420(vw).

Synthesis of 4,4'-bpy $\cdot(\text{BH}_3)_2$

To a solution of 790 mg (5.05 mmol) 4,4'-bpy in 60 mL Et_2O 7.5 mL of a 2M solution of $\text{Me}_2\text{S}\cdot\text{BH}_3$ in toluene is added at 0°C . A purple precipitate is observed. All volatiles are removed *in vacuo*. The remaining solid is washed with 20mL *n*-hexane and dried *in vacuo*.

Yield:	920 mg (99%, powder).
$^1\text{H-NMR}$ (CDCl_3):	$\delta[\text{ppm}] = 2.69$ (m, br, 6H, BH_3), 7.76 (m, 4H, $\alpha\text{-H}$ 4,4'-bpy), 8.81 (d, 4H, $^2J_{\text{H,H}} = 6\text{Hz}$, $m\text{-H}$ 4,4'-bpy).

$^{11}\text{B}\{^1\text{H}\}$ -NMR (CDCl_3): $\delta[\text{ppm}] = -12.05$ (s, br).

^{11}B -NMR (CDCl_3): $\delta[\text{ppm}] = -12.05$ (s, br, $\omega_{1/2} = 515\text{Hz}$).

Synthesis of $4,4'\text{-bpy}\cdot(\text{BH}_2\text{I})_2$ (**7**)

To a suspension of 184 mg (1 mmol) $4,4'\text{-bpy}\cdot(\text{BH}_3)_2$ in 25 mL benzene 253 mg (1 mmol) I_2 is added. A gas evolution is observed and the suspension turns brown. After stirring for 18 h, the color is changed to orange. The solvent is decanted. The remaining orange solid is washed with 35 mL *n*-hexane and dried *in vacuo*.

Yield: 360 mg (82%, powder).

^1H -NMR (CDCl_3): $\delta[\text{ppm}] = 3.25$ (m, 4H, BH_2), 8.41 (m, 4H, *o*-H $4,4'\text{-bpy}$), 8.93 (m, 4H, *m*-H $4,4'\text{-bpy}$).

$^{11}\text{B}\{^1\text{H}\}$ -NMR (CDCl_3): $\delta[\text{ppm}] = -12.10$ (s, br).

^{11}B -NMR (CDCl_3): $\delta[\text{ppm}] = -12.10$ (s, br, $\omega_{1/2} = 550\text{ Hz}$).

Synthesis of $[4,4'\text{-bpy}\cdot(\text{BH}_2\text{PH}_2\text{BH}_2\cdot\text{NMe}_3)_2][\text{I}]_2$ (**8**)

To a solution of 218 mg (0.5 mmol) of **7** in 20 mL CH_2Cl_2 2 mL of a 2M solution of $\text{Me}_3\text{N}\cdot\text{BH}_2\text{PH}_2$ in toluene is added at -80°C . After allowing the solution to reach room temperature overnight, the color changed from orange to deep red. The solution is filtrated over diatomaceous earth and the remaining solid is washed with 10 mL CH_2Cl_2 . The volume of the solution is reduced *in vacuo* to 15 mL. The solution is dropped into 60 mL *n*-hexane at -80°C . The solvent is decanted and the precipitate is washed with 20 mL *n*-hexane and dried *in vacuo*. **8** crystallizes by layering a saturated solution of CH_2Cl_2 with threefold *n*-hexane as orange plates.

Yield: 310 mg (96%, powder).

^1H -NMR (CD_3CN): $\delta[\text{ppm}] = 2.06$ (m, 4H, $\text{Me}_3\text{N}\cdot\text{BH}_2$), 2.75 (d, 18 H, $\text{N}(\text{CH}_3)_3$, $^4J_{\text{HP}} = 1.5\text{ Hz}$), 3.03 (m, 4H, $\text{bipy}\cdot\text{BH}_2$), 3.83 (dm, 4H, PH_2 , $^1J_{\text{HP}} = 351\text{ Hz}$, $^2J_{\text{H,B}} = 7.7\text{ Hz}$), 8.22 (m, 4H, *o*-H $4,4'\text{-bpy}$), 8.83 (m, 4H, *m*-H $4,4'\text{-bpy}$).

$^{11}\text{B}\{^1\text{H}\}$ -NMR (CD_3CN): $\delta[\text{ppm}] = -11.19$ (d, br, $^1J_{\text{B,P}} = 57\text{ Hz}$, $\text{Me}_3\text{N}\cdot\text{BH}_2$), -13.50 (m, br, $4,4'\text{-bpy}\cdot(\text{BH}_2)_2$).

^{11}B -NMR (CD_3CN): $\delta[\text{ppm}] = -11.19$ (m, br, $^1J_{\text{B,P}} = 57\text{ Hz}$, $^1J_{\text{B,H}} = 105\text{ Hz}$, $\text{Me}_3\text{N}\cdot\text{BH}_2$), -13.50 (m, br, $4,4'\text{-bpy}\cdot(\text{BH}_2)_2$).

$^{13}\text{C}\{^1\text{H}\}$-NMR ($\text{CD}_3\text{CN}$):	$\delta[\text{ppm}] = 54.38$ (d, $^2J_{\text{C,B}} = 5.8\text{ Hz}$, $\text{N}(\underline{\text{C}}\text{H}_3)_3$), 126.67 (d, $^2J_{\text{C,C}} = 1.4\text{ Hz}$, $\alpha\text{-C } 4,4'\text{-bpy}$), 149.10 (d, $^2J_{\text{C,C}} = 2.1\text{ Hz}$, $\beta\text{-C } 4,4'\text{-bpy}$), 150.06 (d, $^2J_{\text{C,C}} = 4.3\text{ Hz}$, $\gamma\text{-C } 4,4'\text{-bpy}$).
$^{31}\text{P}\{^1\text{H}\}$-NMR ($\text{CD}_3\text{CN}$):	$\delta[\text{ppm}] = -121.5$ (s, br, $\underline{\text{P}}\text{H}_2$).
^{31}P-NMR (CD_3CN):	$\delta[\text{ppm}] = -121.5$ (t, br, $\underline{\text{P}}\text{H}_2$, $^1J_{\text{PH}} = 339\text{ Hz}$).
ES-MS (MeCN):	cation: m/z : 519 ($[\text{4,4'}\text{-bpy} \cdot (\text{BH}_2\text{PH}_2\text{BH}_2 \cdot \text{NMe}_3)]^{2+} [\text{I}^-]$, 8 %), 274 ($[\text{4,4'}\text{-bpy} \cdot (\text{BH}_2\text{PH}_2\text{BH}_2 \cdot \text{NMe}_3)]^+$, 100%), 195 ($[\text{4,4'}\text{-bpy} \cdot (\text{BH}_2\text{PH}_2\text{BH}_2 \cdot \text{NMe}_3)_2]^{2+}$, 40 %).
EA:	calculated for $\text{C}_{16}\text{H}_{38}\text{B}_4\text{I}_2\text{N}_4\text{P}_2(\text{CH}_2\text{Cl}_2)_{1.5}$: C 27.20%; H 5.35%; N 7.26% found: C 27.23%; H 7.21%; N 7.21%.
IR (KBr):	$\tilde{\nu} [\text{cm}^{-1}] = 3019$ (w, C-H _{arom}), 2961 (w, C-H _{methyl}), 2444 (vs, B-H), 2411 (vs, B-H), 2303 (s, P-H), 1626 (vs, C=N), 1539 (m), 1482 (m), 1469 (m), 1424 (s), 1276 (vw), 1242 (m), 1160 (s), 1128 (m), 1071 (vs), 974 (m), 850 (m), 726 (m), 692 (vw).

X-ray Diffraction analysis

The X-ray diffraction experiments were performed on either an Agilent Gemini R Ultra diffractometer with Cu- $K\alpha$ radiation ($\lambda = 1.54178\text{ \AA}$) (**2a**, **8**), a SuperNova diffractometer with microfocus Cu-source and Atlas CCD-detector (**2b**, **4a**) or a GV50 diffractometer with TitanS2 detector (**2c**, **3**, **4b**, **5a**, **5b**, **6**) from Rigaku Oxford Diffraction (formerly Agilent Technologies) applying Cu- $K\alpha$ radiation ($\lambda = 1.54178\text{ \AA}$). The measurements were performed at 123 K. Crystallographic data together with the details of the experiments are given below. Absorption corrections were applied semi-empirically from equivalent reflections or analytically (SCALE3/ABSPACK algorithm implemented in CrysAlisPro software by Rigaku Oxford Diffraction).^[8]

Details of crystal structure solution and refinement

All structures were solved using SIR97^[9], SHELXT^[10] and OLEX.^[11] Least square refinements against F^2 in anisotropic approximation were done using SHELXL.^[8] All crystals of **2c** and **5a** showed twinning, they were refined applying hklf5 refinement.

Crystal structures***tmeda*·(BH₂PH₂)₂**

2a crystallizes as colorless needles in the triclinic space group $P\bar{1}$ by storing a saturated CH₂Cl₂ solution at -30°C. **Figure S1** shows the structure of **2a** in the solid state.

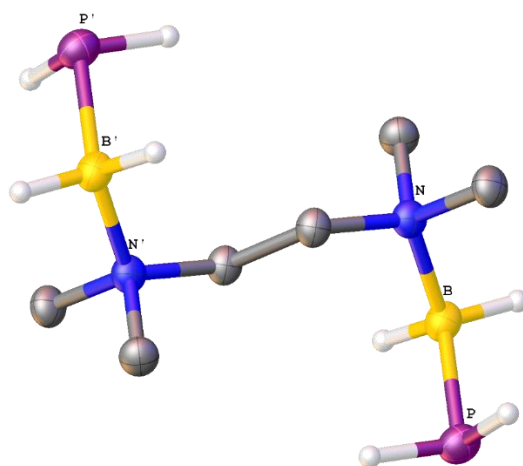


Figure S1: Molecular structure of **2a** in the solid state. Hydrogen atoms bonded to carbon are omitted for clarity. Thermal ellipsoids are drawn with 50% probability. Selected bond lengths [Å] and angles [°]: P-B 1.965(2), B-N 1.627(2), N-B-P 116.95(11).

***tmeda*·(BH₂PPh₂)₂**

2b crystallizes as colorless blocks in the triclinic space group $P\bar{1}$ by storing a saturated CH₂Cl₂ solution at -30°C with two molecules CH₂Cl₂ within the unit cell. **Figure S2** shows the structure of **2b** in the solid state.

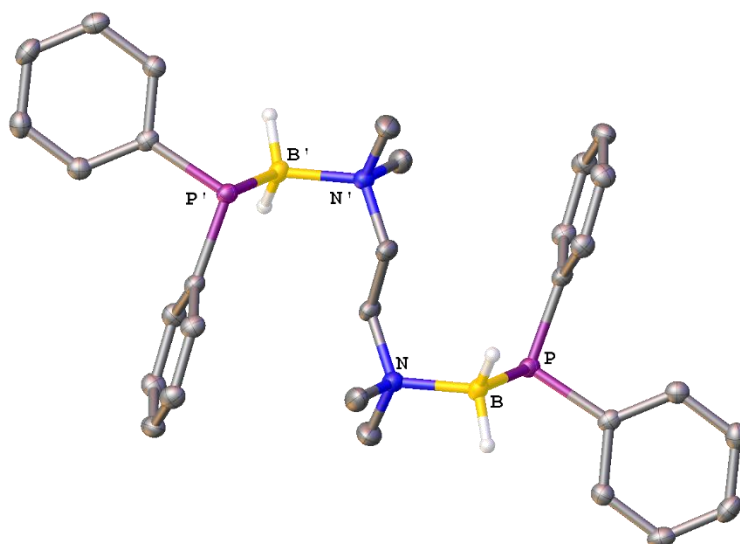


Figure S2: Molecular structure of **2b** in the solid state. Hydrogen atoms bonded to carbon are omitted for clarity. Thermal ellipsoids are drawn with 50% probability. Selected bond lengths [Å] and angles [°]: N-B 1.640(2), B-P 1.9840(18), N-B-P 109.85(10).

***tmeda*·(*BH₂tBuPH*)₂**

2c crystallizes as colorless needles in the monoclinic space group *P*2₁/*c* by storing a saturated *n*-hexane solution at -30°C. **Figure S3** and **Figure S4** show the molecular structure of **2c** in solid state. The structure solution shows distortion.

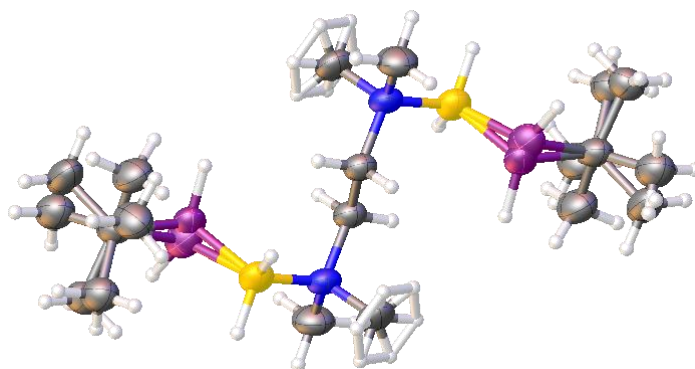


Figure S3: Distorted molecular structure of **2c** in solid state.

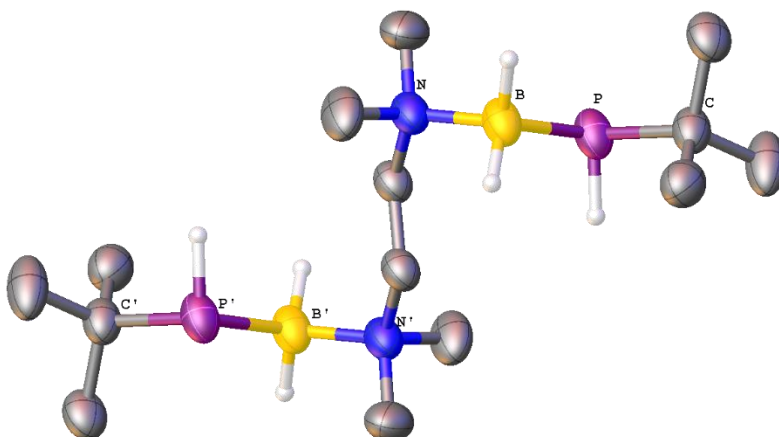


Figure S4: Molecular structure of **2c** in the solid state. Hydrogen atoms bonded to carbon are omitted for clarity. Thermal ellipsoids are drawn with 50% probability. Selected bond lengths [Å] and angles [°]: N-B 1.632(3), B-P 1.986(3)-1.990(12), P-C 1.873(3)-1.894(12), N-B-P 109.0(4)-109.39(15).

***tmeda*·(*BH*₂*AsPh*₂)₂**

3 crystallizes as colorless blocks in the triclinic space group *P*2₁/*c* by storing a saturated solution toluene at -30°C. **Figure S5** and **Figure S6** show the molecular structure of **3** in the solid state. The structure solution shows distortion.

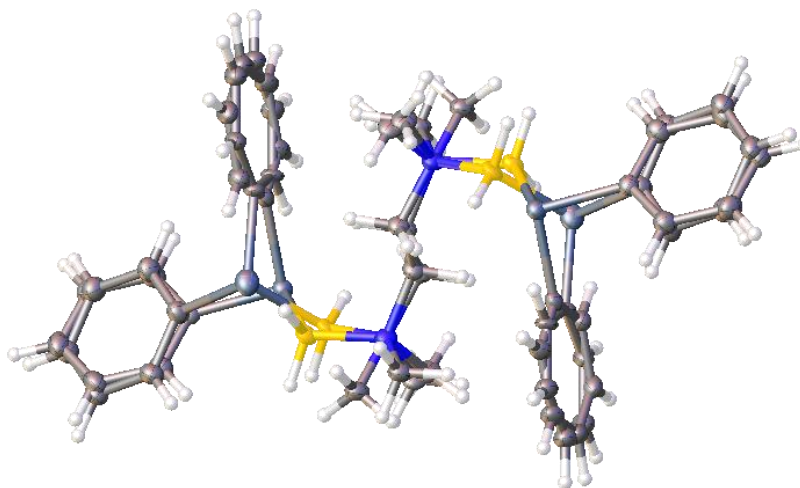


Figure S5: Distorted molecular structure of **3** in solid state.

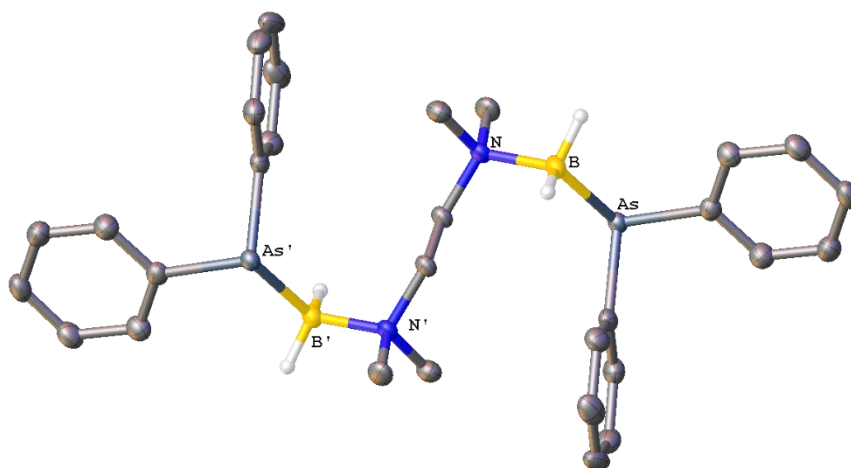


Figure S6: Molecular structure of **3** in the solid state. Hydrogen atoms bonded to carbon are omitted for clarity. Thermal ellipsoids are drawn with 50% probability. Selected bond lengths [Å] and angles [°]: As-B 2.087(3)-2.089(11), N-B 1.636(4)-1.642(11), N-B-As 108.78(17)-109.3(7).

***tmeda*·(BH₂PH₂AuCl)₂**

4a crystallizes as colorless blocks in the monoclinic space group *P*2₁ by layering a saturated CH₂Cl₂ solution with threefold *n*-hexane. **Figure S7** shows the structure of **4a** in the solid state.

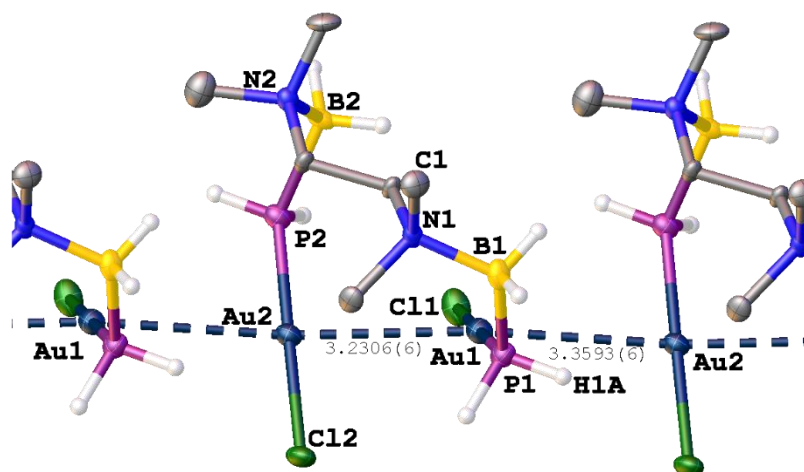


Figure S7: Solid state structure of **4a**. Hydrogen atoms bonded to carbon are omitted for clarity. Thermal ellipsoids are drawn with 50% probability. Selected bond lengths [Å] and angles [°]: N1-B1 1.604(15), B1-P1 1.970(14), P1-Au1 2.244(3), Au1-Au2_{intra} 3.231(1), Au1-Au2_{inter} 3.359(1), N1-B1-P1 113.8(8), P1-Au1-Cl1 179.4(1), P1-Au1-Au2-P2 127.2(1).

***tmeda*·(BH₂PPh₂AuCl)₂**

4b crystallizes as colorless rods in the monoclinic space group *P*2₁/*c* by layering a saturated CH₂Cl₂ solution with threefold *n*-hexane. **Figure S8** shows the structure of **4b** in the solid state.

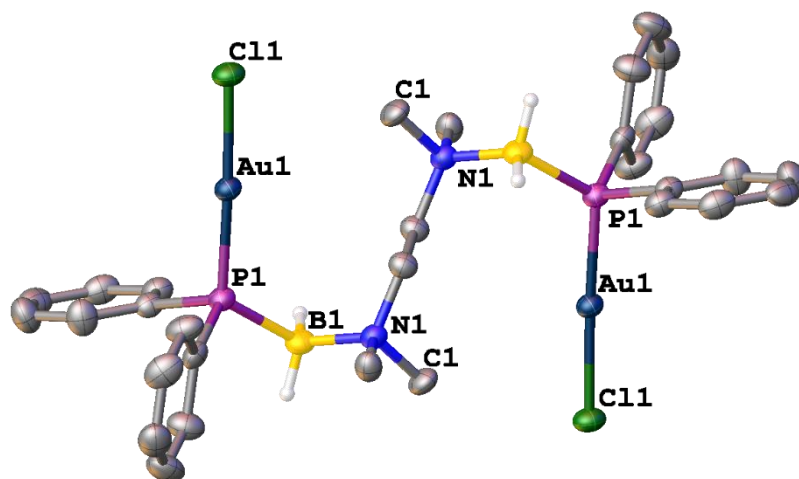


Figure S8: Molecular structure of **4b** in the solid state. Hydrogen atoms bonded to carbon are omitted for clarity. Thermal ellipsoids are drawn with 50% probability. Selected bond lengths [Å] and angles [°]: N-B 1.607(7), B-P 1.973(6), P-Au 2.247(1), N-B-P 115.4(3), P-Au-Cl 176.7(1).

***tmeda*·(BH₂PH₂BH₃)₂**

5a crystallizes as colorless blocks by storing a saturated CH₂Cl₂ solution at -30°C in the monoclinic space group *P*2₁/*c*. The structure was refined with HKLF5-data as twin with a BASF 0.487(2). **Figure S9** shows the structure of **5a** in the solid state.

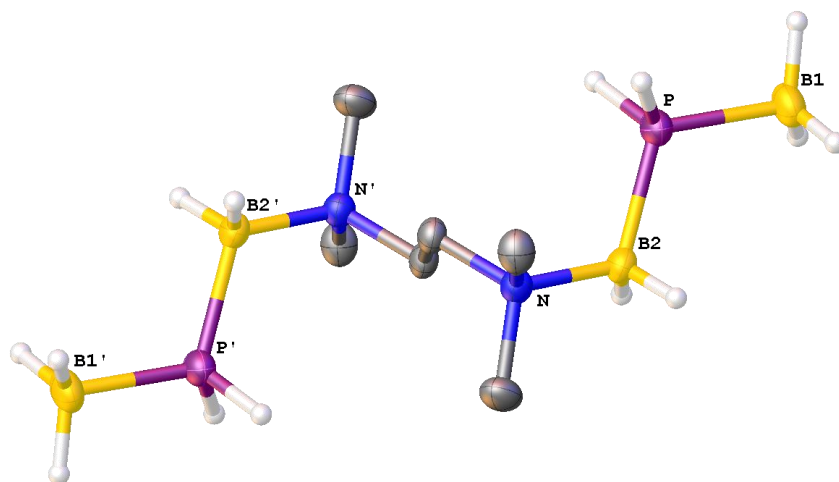


Figure S9: Molecular structure of **5a** in the solid state. Hydrogen atoms bonded to carbon are omitted for clarity. Thermal ellipsoids are drawn with 50% probability. Selected bond lengths [Å] and angles [°]: B1-P 1.940(2), P-B2 1.946(2), B2-N 1.613(2), B1-P-B2 114.27(8), P-B2-N 115.26(10).

***tmeda*·(BH₂AsPh₂BH₃)₂**

5b crystallizes as colorless blocks in the monoclinic space group $P2_1/n$ by storing a saturated CH₂Cl₂ solution at -30°C within a molecule toluene (occupancy 0.38) and CH₂Cl₂ (occupancy 0.12) in the unit cell. **Figure S10** shows the molecular structure of **5b** in solid state.

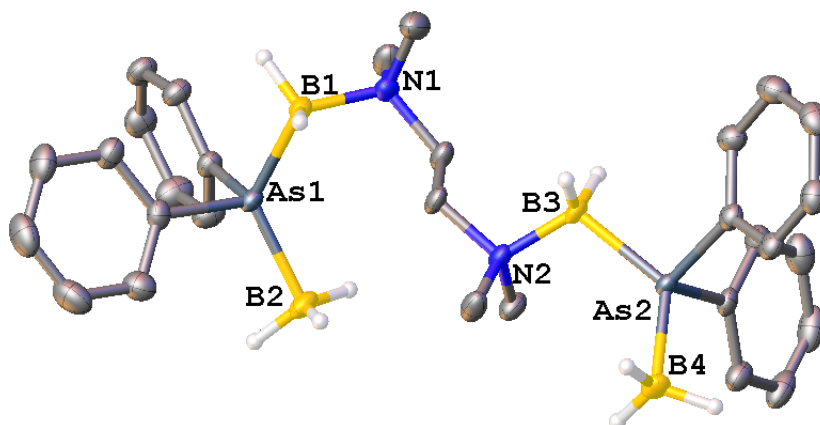


Figure S10: Molecular structure of **5b** in the solid state. Solvent molecules and hydrogen atoms bonded to carbon are omitted for clarity. Thermal ellipsoids are drawn with 50% probability. Selected bond lengths [Å] and angles [°]: N1-B1 1.611(4), B1-As1 2.087 (3), As1-B2 2.063(3), N2-B3 1.601(4), B3-As2 2.087(3), As2-B4 2.058 (3),

N1-B1-As1 113.88(18), B1-As1-B2 124.67(12), N2-B3-As2 112.44(17), B3-As2-B4 124.71(13).

[tmeda·(BH₂PH₂BH₂·NMe₃)₂][I]₂

6 crystallizes as colorless needles and plates in the triclinic space group $P\bar{1}$ by storing a saturated acetonitrile solution at 3°C within one molecule CH₃CN in the unit cell. **Figure S11** and **Figure S12** show the structure of **6** in the solid state. **6** exhibits a linear, as well as a U-shaped molecular structure in solid state.

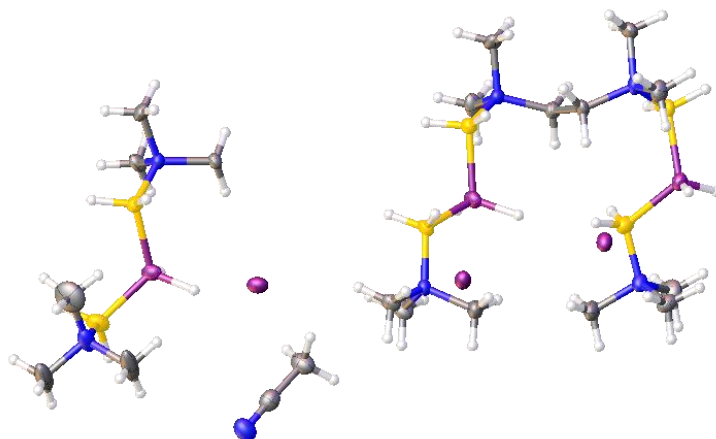


Figure S11: Molecular structure of **6** in solid state.

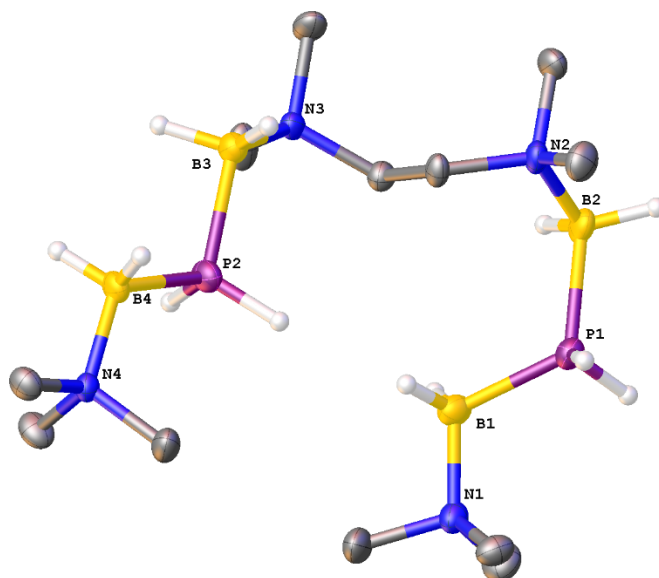


Figure S12: Molecular structure of **6** in the solid state. Counterions, solvent molecules and hydrogen atoms bonded to carbon are omitted for clarity. Thermal ellipsoids are drawn with 50% probability. Selected bond lengths [Å] and angles [°]: B1-P1 1.950(5), P1-B2 1.970(5), B3-P2 1.962(5), P2-B4 1.960(5), B1-P1-B2 116.6(2), B3-P2-B4 107.949, N1-B1-P1 115.0(3), N3-B3-P2 114.50(3).

[4,4'-bpy-(BH₂PH₂BH₂-NMe₃)₂] [I]₂

8 crystallizes as orange plates in the triclinic space group $P\bar{1}$ by layering a saturated CH₂Cl₂ solution with threefold *n*-hexane within one molecule CH₂Cl₂ in the unit cell. **Figure S13** and **Figure S14** show the structure of **8** in the solid state. The structure solution shows distortion.

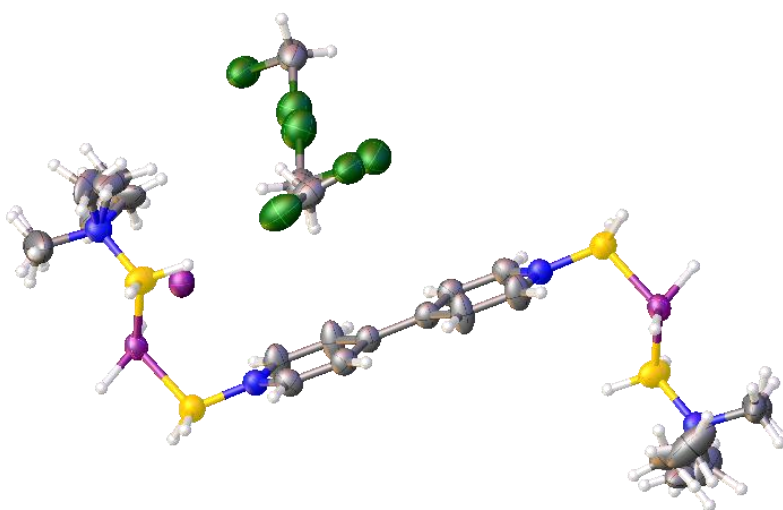


Figure S13: Distorted molecular structure of **8** in solid state.

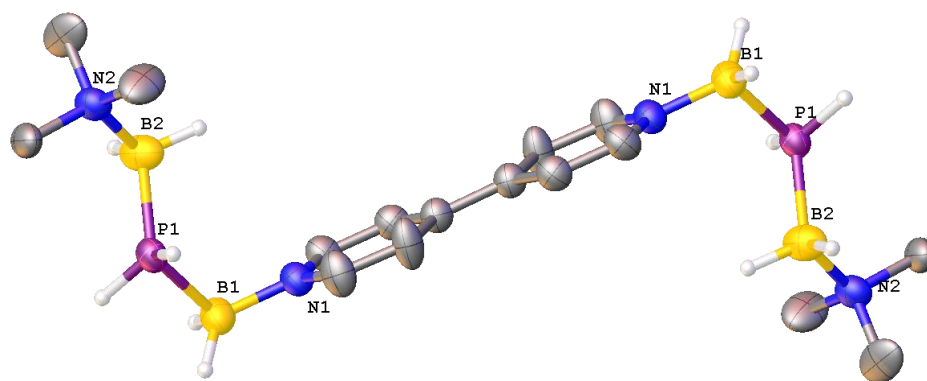


Figure S14: Molecular structure of **8** in the solid state. Counterions, solvent molecules and hydrogen atoms bonded to carbon are omitted for clarity. Thermal ellipsoids are drawn with 50% probability. Selected bond lengths [Å] and angles [°]: N-B 1.583(6)-1.593(6), B-P 1.938(6)-1.950(5), N1-B1-P1 109.1(3), B1-P1-B2 116.2(2).

Crystallographic Information**Table S1:** Crystallographic Data for compounds **2a**, **2b** and **2c**

	2a	2b	2c
Empirical formula	C ₆ H ₂₄ B ₂ N ₂ P ₂	C ₃₂ H ₄₄ B ₂ Cl ₄ N ₂ P ₂	C ₁₄ H ₄₀ B ₂ N ₂ P ₂
Formula weight	207.83	682.05	320.04
Crystal	colorless plate	colorless plate	Colorless block
Crystal size/mm ³	0.1817*0.1495*0.1297	0.098*0.064*0.035	0.349*0.204*0.138
Temperature/K	123	123	123
Crystal system	triclinic	triclinic	monoclinic
Space group	<i>P</i> $\bar{1}$	<i>P</i> $\bar{1}$	<i>P</i> 2 ₁ / <i>c</i>
Unit cell dimensions	<i>a</i> = 5.5178(4) Å	<i>a</i> = 9.4484(3) Å	<i>a</i> = 6.5964(5))
	<i>b</i> = 7.2575(6) Å	<i>b</i> = 9.9252(3) Å	<i>b</i> = 13.4102(9)
	<i>c</i> = 8.8580(6) Å	<i>c</i> = 10.0211(3) Å	<i>c</i> = 12.3472(7)
	α = 110.807(7)	α = 87.349(2)	α = 90
	β = 94.172(6)	β = 72.979(2)	β = 96.329(5)
	γ = 106.683(7)	γ = 80.015(2))	γ = 90
Volume <i>V</i>	311.53(4) Å ³	884.96(4) Å ³	1085.56(13)
Formula units <i>Z</i>	1	1	2
Absorption coefficient μ	2.807 mm ⁻¹	4.074 mm ⁻¹	1.747 mm ⁻¹
Density ρ_{calc}	1.445 g/cm ³	1.280 g/cm ³	0.979 g/cm ⁻³
<i>F</i> (000)	950	358.0	356
Theta range $\theta_{\text{min}}/\theta_{\text{max}}$	5.45 / 66.77	4.52 / 73.78	9.77 / 149.466
Absorption correction	analytical	multi-scan	multi-scan
Index ranges	-6 ≤ <i>h</i> ≤ 6	-11 ≤ <i>h</i> ≤ 11	-8 ≤ <i>h</i> ≤ 5
	-8 ≤ <i>k</i> ≤ 8	-12 ≤ <i>k</i> ≤ 12	-15 ≤ <i>k</i> ≤ 16
	-10 ≤ <i>l</i> ≤ 10	-12 ≤ <i>l</i> ≤ 12	-15 ≤ <i>l</i> ≤ 14
Reflections collected	7363 / 1109 (<i>R</i> _{int} = 0.0436)	14487/ 3506 (<i>R</i> _{int} = 0.0388)	7224/2179 (<i>R</i> _{int} = 0.0307)
Independent reflections	1018	3230	2179
Completeness to full θ	0.946	0.990	0.976
Transmission <i>T</i> _{min} / <i>T</i> _{max}	0.703 / 0.776	0.85601 / 1.00000	0.852/ 1.00000
Data/restraints/parameters	1109/4/73	3506/2/192	6600/6/216
Goodness-of-fit on <i>F</i> ²	1.082	1.042	1.077
Final <i>R</i> -values [<i>I</i> ≥ 2σ (<i>I</i>)]	<i>R</i> ₁ = 0.0336,	<i>R</i> ₁ = 0.0400,	<i>R</i> ₁ = 0.0533
	<i>wR</i> ₂ = 0.0851	<i>wR</i> ₂ = 0.1054	<i>wR</i> ₂ = 0.1489
Final <i>R</i> -values [all data]	<i>R</i> ₁ = 0.0372,	<i>R</i> ₁ = 0.0433,	<i>R</i> ₁ = 0.0575
	<i>wR</i> ₂ = 0.0883	<i>wR</i> ₂ = 0.1094	<i>wR</i> ₂ = 0.1540
Largest difference hole and peak $\Delta\rho$	-0.23,	-0.32,	-0.30
	0.30	0.51	0.27

Table S2: Crystallographic data for compounds **3**, **4a** and **4b**

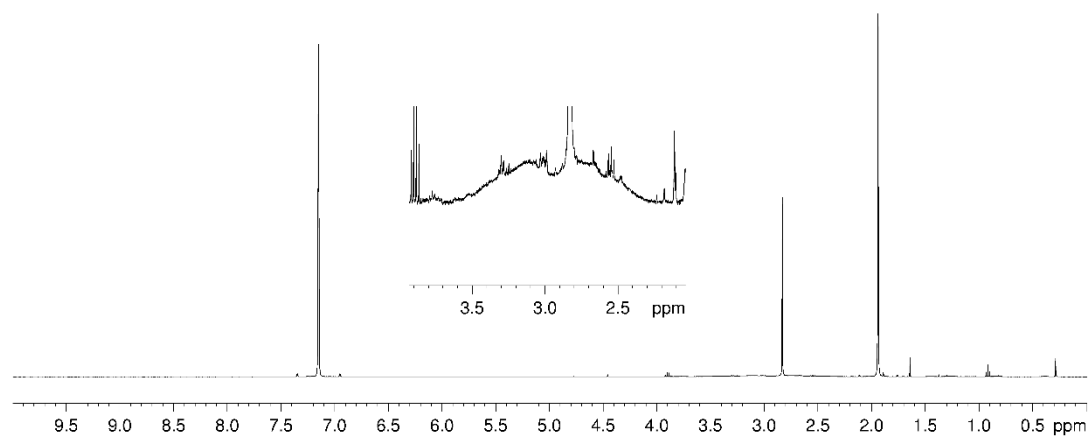
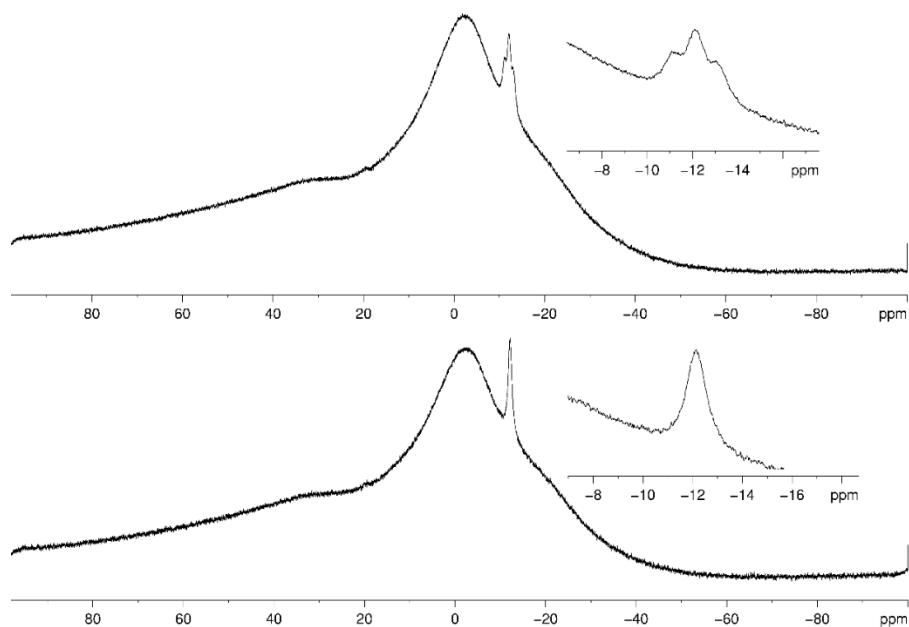
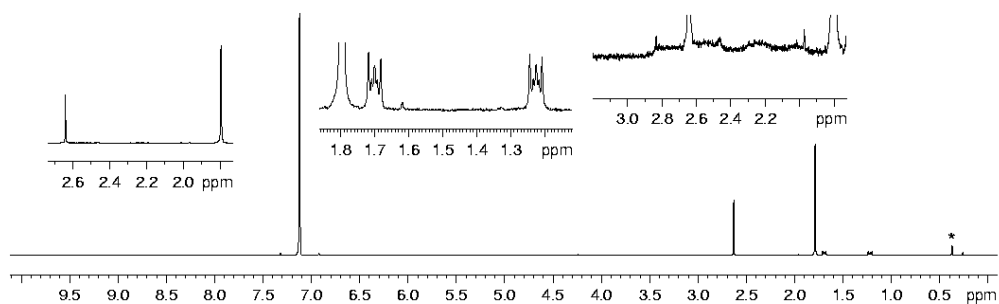
	3	4a	4b
Empirical formula	C ₁₅ H ₂₀ AsBN	C ₆ H ₂₄ Au ₂ B ₂ Cl ₂ N ₂ P ₂	C ₃₀ H ₄₀ Au ₂ B ₂ Cl ₂ N ₂ P ₂
Formula weight	300.05	672.66	977.03
Crystal	colorless block	clear colourless block	clear colourless rod
Crystal size/mm ³	0.077*0.074*0.035	0.08*0.07*0.06	0.18*0.10*0.06
Temperature/K	123	123	131
Crystal system	monoclinic	monoclinic	monoclinic
Space group	<i>P</i> 2 ₁ / <i>c</i>	<i>P</i> 2 ₁	<i>P</i> 2 ₁ / <i>c</i>
Unit cell dimensions	<i>a</i> = 9.0995(3) Å	<i>a</i> = 6.5803(3)	<i>a</i> = 14.6355(3)
	<i>b</i> = 5.8807(2) Å	<i>b</i> = 15.5749(5)	<i>b</i> = 13.9285(2)
	<i>c</i> = 26.9732(8) Å	<i>c</i> = 8.2257(3)	<i>c</i> = 8.18960(10)
	α = 90	α = 90	90
	β = 97.424(3)	β = 100.338(4)	90.229(2)
Volume <i>V</i>	γ = 90	γ = 90	90
	1431.27(8) Å ³	829.35(6)	1669.44(5)
Formula units <i>Z</i>	4	2	2
Absorption coefficient μ	3.037 mm ⁻¹	37.384 mm ⁻¹	18.832 mm ⁻¹
Density ρ_{calc}	1.397 g/cm ³	2.694 g/cm ³	1.944 g/cm ³
<i>F</i> (000)	402.0	612.0	932.0
Theta range $\theta_{\text{min}}/\theta_{\text{max}}$	6.61 / 148.54	5.467 / 74.245	4.382 / 74.796
Absorption correction	gaussian	gaussian	gaussian
Index ranges	-10 ≤ <i>h</i> ≤ 10	-8 ≤ <i>h</i> ≤ 6	-13 ≤ <i>h</i> ≤ 17
	-5 ≤ <i>k</i> ≤ 6	-19 ≤ <i>k</i> ≤ 19	-16 ≤ <i>k</i> ≤ 17
	-30 ≤ <i>l</i> ≤ 33	-9 ≤ <i>l</i> ≤ 10	-10 ≤ <i>l</i> ≤ 8
Reflections collected	4614 / 2747 (<i>R</i> _{int} = 0.0265)	3280 / 2216 (<i>R</i> _{int} = 0.0293)	7595 / 3256 (<i>R</i> _{int} = 0.0361)
Independent reflections	2747	2141	2990
Completeness to full θ	0.990	0.996	0.987
Transmission <i>T</i> _{min} / <i>T</i> _{max}	0.103 / 0.564	0.131 / 0.285	0.154 / 0.458
Data/restraints/parameters	2747/0/182	2216/1/168	3256/0/191
Goodness-of-fit on <i>F</i> ²	1.140	1.042	1.029
Final <i>R</i> -values [<i>I</i> ≥ 2 σ (<i>I</i>)]	<i>R</i> ₁ = 0.0331,	<i>R</i> ₁ = 0.0278	<i>R</i> ₁ = 0.02948
	<i>wR</i> ₂ = 0.0741	<i>wR</i> ₂ = 0.0654	<i>wR</i> ₂ = 0.0760
Final <i>R</i> -values [all data]	<i>R</i> ₁ = 0.0383,	<i>R</i> ₁ = 0.0289	<i>R</i> ₁ = 0.0323
	<i>wR</i> ₂ = 0.0762	<i>wR</i> ₂ = 0.0669	<i>wR</i> ₂ = 0.0785
Largest difference hole and peak $\Delta\rho$	-0.41,	-1.511	-1.463
	0.45	1.204	1.096

Table S3: Crystallographic data for compounds **5a**, **5b** and **6**

	5a	5b	6
Empirical formula	C ₆ H ₃₀ B ₄ N ₂ P ₂	C _{32.78} H _{49.28} As ₂ B ₄ Cl _{0.24} N ₂	C ₄₀ H ₁₄₄ B ₁₂ I ₆ N ₁₄ P ₆
Formula weight	235.50	672.97	1898.63
Crystal	Colorless block	Colorless block	colorless plate
Crystal size/mm ³	0.2136*0.103*0.075	0.19*0.13*0.09	0.1547*0.0657*0.0387
Temperature/K	123	123	123
Crystal system	monoclinic	Monoclinic	triclinic
Space group	<i>P</i> 2 ₁ / <i>c</i>	<i>P</i> 2 ₁ / <i>c</i>	<i>P</i> $\bar{1}$
Unit cell dimensions	<i>a</i> = 8.1121(4) Å <i>b</i> = 11.3287(4) Å <i>c</i> = 9.0700(5) Å α = 90° β = 112.047(7)° γ = 90°	<i>a</i> = 9.7341(2) <i>b</i> = 27.5085(4) <i>c</i> = 13.5745(3) α = 90° β = 105.446(2)° γ = 90°	<i>a</i> = 9.6291(3) Å <i>b</i> = 14.3377(4) Å <i>c</i> = 16.6833(4) Å α = 76.693(2)° β = 86.631(2)° γ = 76.751(2)°
Volume <i>V</i>	772.57(7) Å ³	3503.57(12) Å ³	2181.75(10) Å ³
Formula units <i>Z</i>	2	4	1
Absorption coefficient μ	2.286 mm ⁻¹	2.691 mm ⁻¹	18.063 mm ⁻¹
Density ρ_{calc}	1.012 g/cm ³	1.276 g/cm ³	1.445 g/cm ³
<i>F</i> (000)	260.0	1400	950
Theta range $\theta_{\text{min}}/\theta_{\text{max}}$	5.88 / 74.43	3.741 / 74.885	2.72 / 73.92
Absorption correction	analytical	Gaussian	gaussian
Index ranges	-9 ≤ <i>h</i> ≤ 10 -14 ≤ <i>k</i> ≤ 14 -11 ≤ <i>l</i> ≤ 11	-11 ≤ <i>h</i> ≤ 12 -24 ≤ <i>k</i> ≤ 33 -116 ≤ <i>l</i> ≤ 15	-10 ≤ <i>h</i> ≤ 11 -17 ≤ <i>k</i> ≤ 17 -20 ≤ <i>l</i> ≤ 15
Reflections collected	2538 / 2384 (<i>R</i> _{int} = 0.0623)	11830 / 6865 (<i>R</i> _{int} = 0.0326)	13055 / 8324 (<i>R</i> _{int} = 0.0544)
Independent reflections	2384	6865	7307
Completeness to full θ	0.998	0.955	0.943
Transmission <i>T</i> _{min} / <i>T</i> _{max}	0.577 / 0.762	0.801 / 1.000	0.134 / 0.587
Data/restraints/parameters	2538/7/94	6865/90/478	8324/15/464
Goodness-of-fit on <i>F</i> ²	1.091	1.043	1.037
Final <i>R</i> -values [<i>I</i> ≥ 2 σ (<i>I</i>)]	<i>R</i> ₁ = 0.0463, <i>wR</i> ₂ = 0.1348	<i>R</i> ₁ = 0.0440, <i>wR</i> ₂ = 0.1027	<i>R</i> ₁ = 0.0393, <i>wR</i> ₂ = 0.0967
Final <i>R</i> -values [all data]	<i>R</i> ₁ = 0.0478, <i>wR</i> ₂ = 0.1371	<i>R</i> ₁ = 0.0388, <i>wR</i> ₂ = 0.0995	<i>R</i> ₁ = 0.0451, <i>wR</i> ₂ = 0.1048
Largest difference hole and peak $\Delta\rho$	-0.48, 0.48	-1.005 0.552	-1.08, 1.40

Table S4: Crystallographic data of compound **8**

	8
Empirical formula	C ₁₈ H ₄₂ B ₄ Cl ₄ I ₂ N ₄ P ₂
Formula weight	815.33
Crystal	orange plate
Crystal size/mm ³	0.2449*0.1911*0.0483
Temperature/K	123
Crystal system	triclinic
Space group	$P\bar{1}$
Unit cell dimensions	$a = 8.0565(4)\text{\AA}$ $b = 10.3386(6)\text{\AA}$ $c = 11.4216(6)\text{\AA}$ $\alpha = 89.397(4)$ $\beta = 70.094(5)$ $\gamma = 77.457(5)$
Volume V	871.07(9) Å ³
Formula units Z	1
Absorption coefficient μ	17.981 mm ⁻¹
Density ρ_{calc}	1.554 g/cm ³
$F(000)$	402.0
Theta range $\theta_{\text{min}}/\theta_{\text{max}}$	8.252 / 133.394
Absorption correction	analytical
Index ranges	$-9 \leq h \leq 9$ $-12 \leq k \leq 12$ $-9 \leq l \leq 13$
Reflections collected	6506 / 3061 ($R_{\text{int}} = 0.0400$)
Independent reflections	3061
Completeness to full θ	0.990
Transmission $T_{\text{min}}/T_{\text{max}}$	0.103 / 0.564
Data/restraints/parameters	3061/17/240
Goodness-of-fit on F^2	1.038
Final R-values [$I \geq 2\sigma(I)$]	$R_1 = 0.0397$, $wR_2 = 0.1021$
Final R-values [all data]	$R_1 = 0.0409$, $wR_2 = 0.1042$
Largest difference hole and peak $\Delta\rho$	-0.70, 1.29

NMR spectroscopy***tmeda*·(BH₂I)₂****Figure S15:** ¹H NMR spectrum of **1** in C₆D₆.**Figure S16:** ¹¹B (top) and ¹¹B{¹H} (bottom) NMR spectrum of **1** in C₆D₆.***tmeda*·(BH₂PH₂)₂****Figure S17:** ¹H NMR spectrum of **2a** in C₆D₆ (* = H-grease).

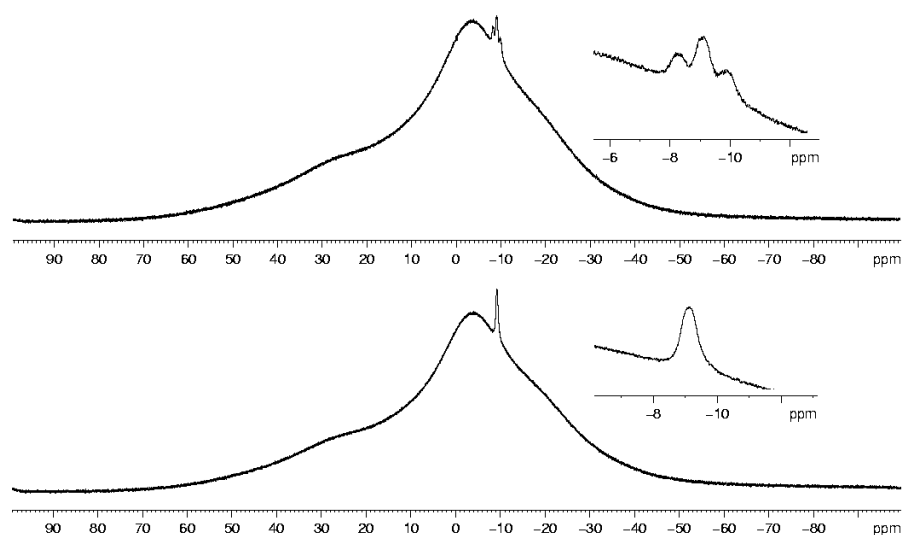


Figure S18: ^{11}B (top) and $^{11}\text{B}\{^1\text{H}\}$ (bottom) NMR spectrum of **2a** in C_6D_6 .

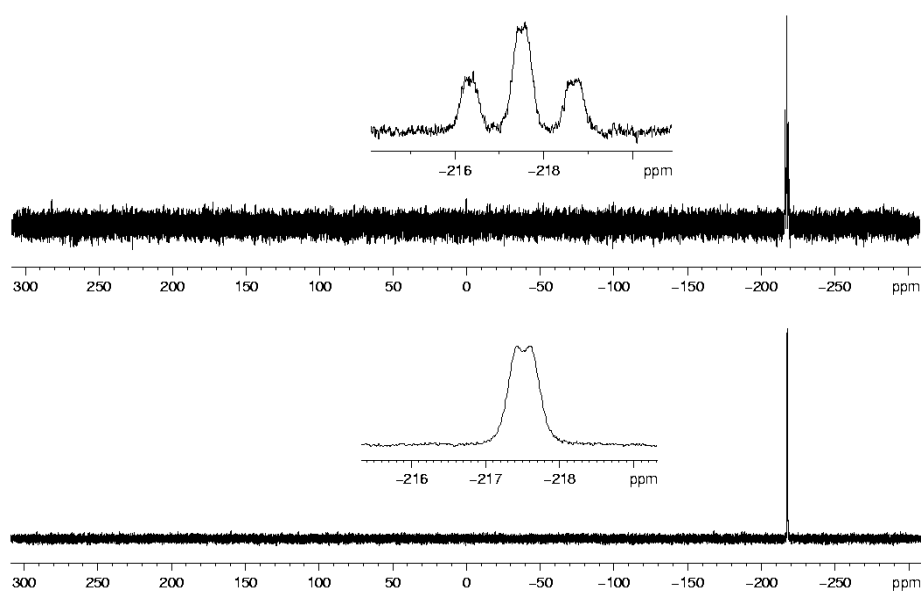


Figure S19: ^{31}P (top) and $^{31}\text{P}\{^1\text{H}\}$ (bottom) NMR spectrum of **2a** in C_6D_6 .

tmeda·(BH_2PPh_2)₂

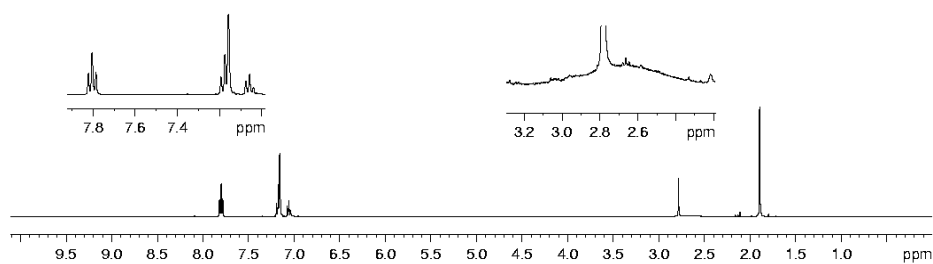


Figure S20: ^1H NMR spectrum of **2b** in C_6D_6 .

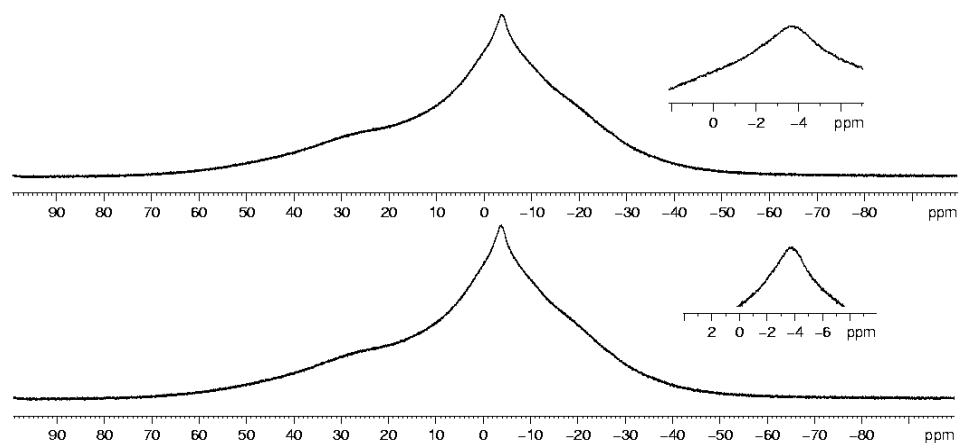


Figure S21: ^{11}B (top) and $^{11}\text{B}\{^1\text{H}\}$ NMR spectra of **2b** in C_6D_6 .

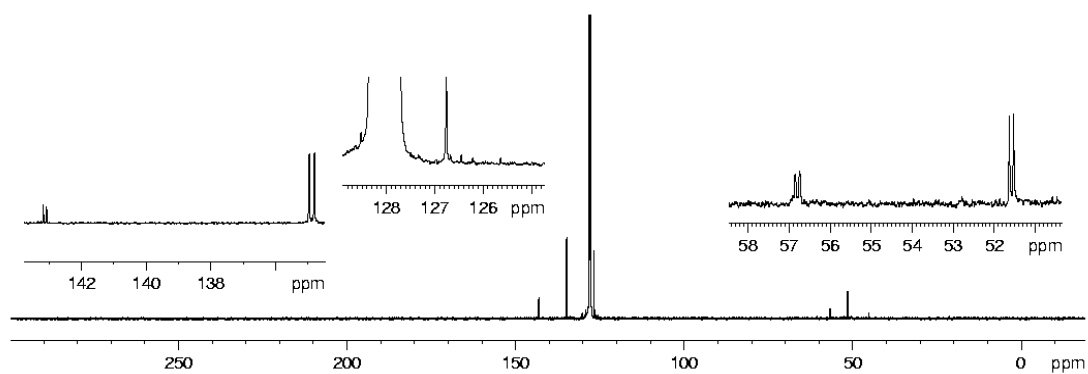


Figure S22: $^{13}\text{C}\{^1\text{H}\}$ NMR spectrum of **2b** in C_6D_6 .

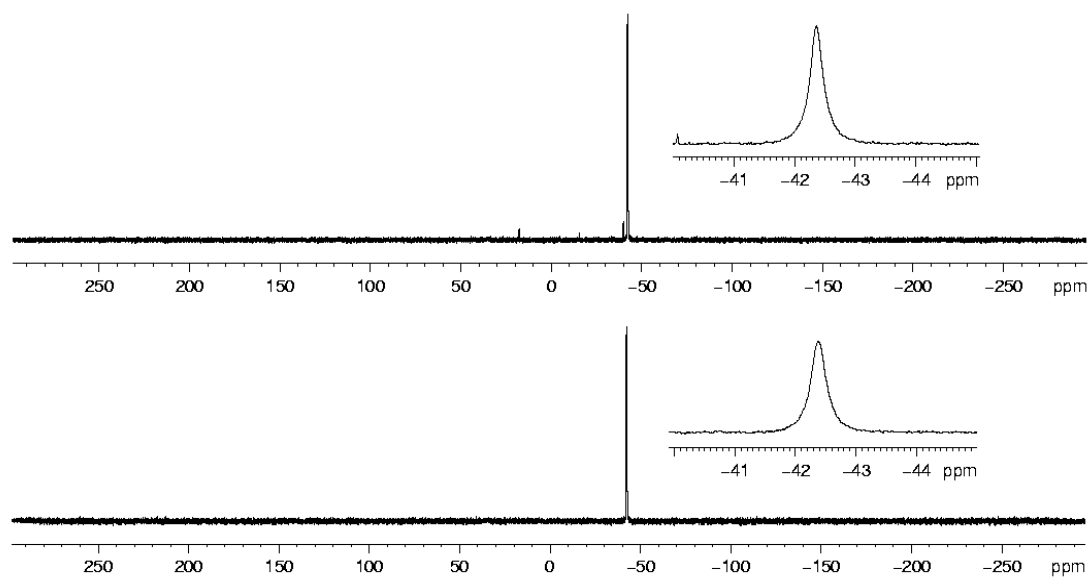


Figure S23: ^{31}P (top) and $^{31}\text{P}\{^1\text{H}\}$ NMR spectra of **2b** in C_6D_6 .

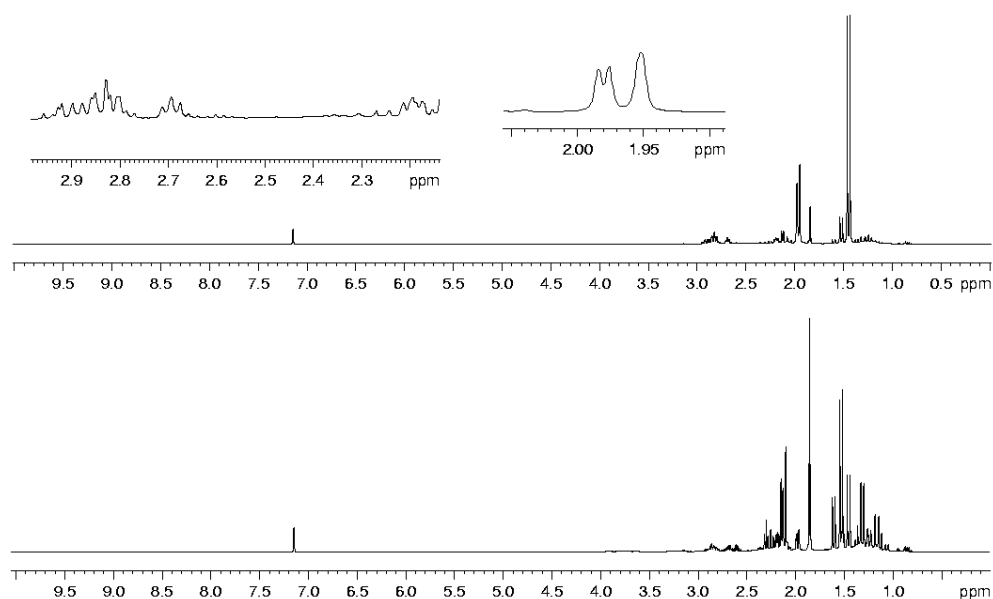
tmeda·(*BH₂tBuPH*)₂

Figure S24: ¹H NMR spectra of **2c** in C₆D₆ measured immediately after dissolving (top) and after 15 h (bottom).

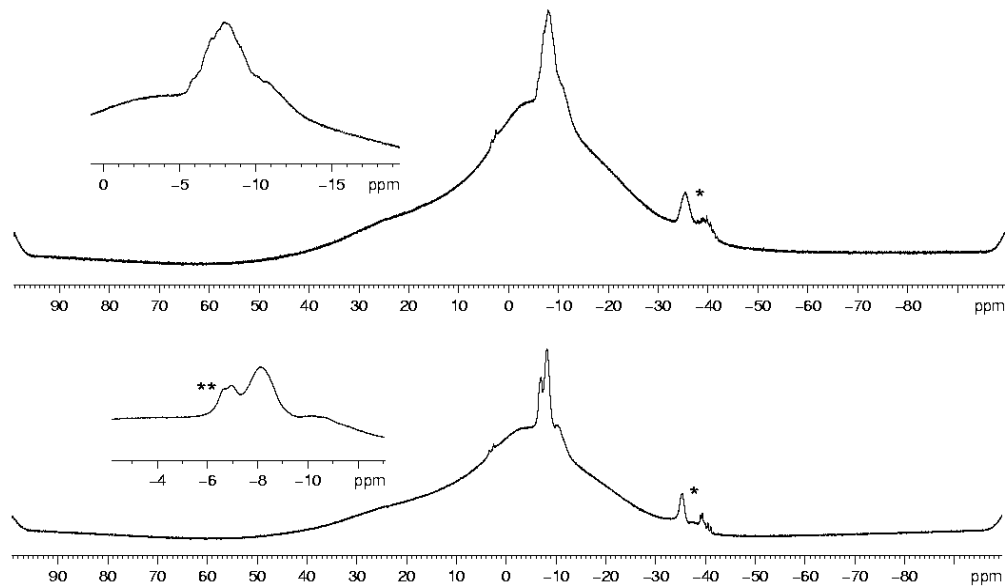


Figure S25: ¹¹B (top) and ¹¹B{¹H} (bottom) NMR spectra of **2c** in C₆D₆ (* = (*t*BuPHBH₂)_n; ** = unknown impurity).

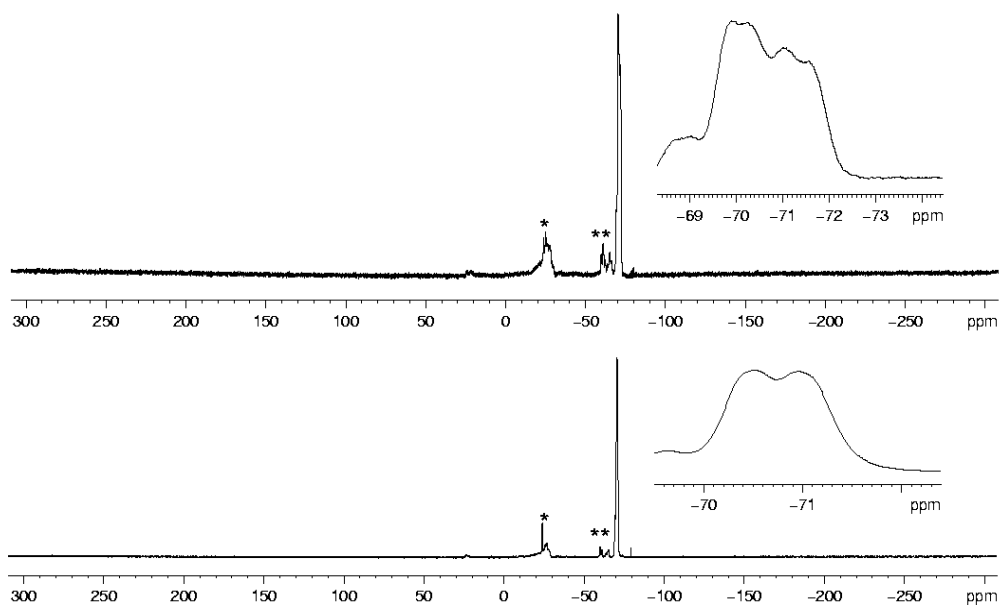


Figure S26: ^{31}P (top) and $^{31}\text{P}\{^1\text{H}\}$ (bottom) NMR spectra of **2c** in C_6D_6 (* = $(^i\text{BuPHBH}_2)$, ** = unknown impurity).

***tmeda*·(BH_2AsPh_2)₂**

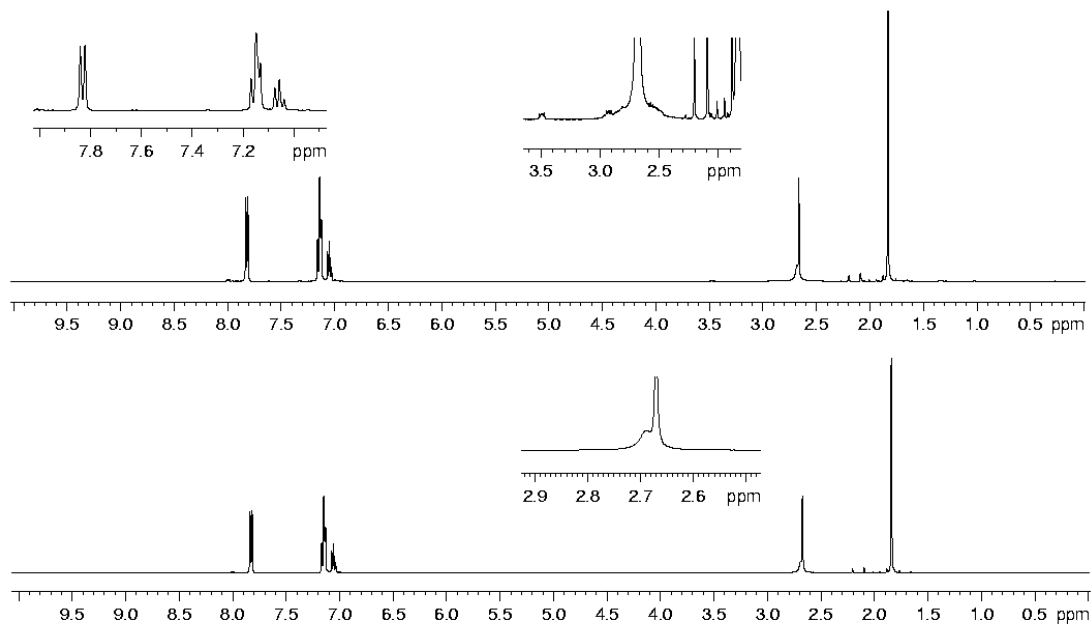


Figure S27: ^1H (top) and $^1\text{H}\{^{11}\text{B}\}$ NMR spectrum of **3** in C_6D_6 .

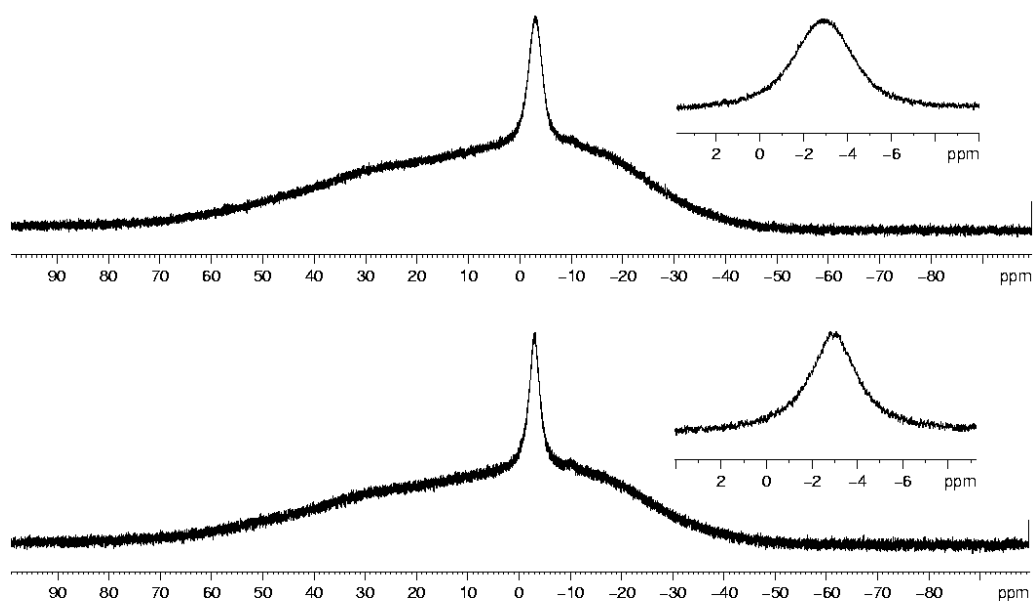


Figure S28: ^{11}B (top) and $^{11}\text{B}\{^1\text{H}\}$ (bottom) NMR spectrum of **3** in C_6D_6 .

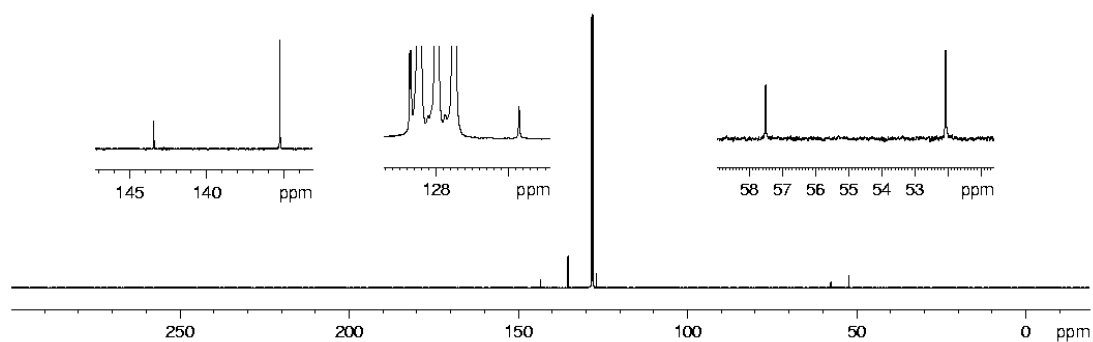


Figure S29: $^{13}\text{C}\{^1\text{H}\}$ NMR spectrum of **3** in C_6D_6 .

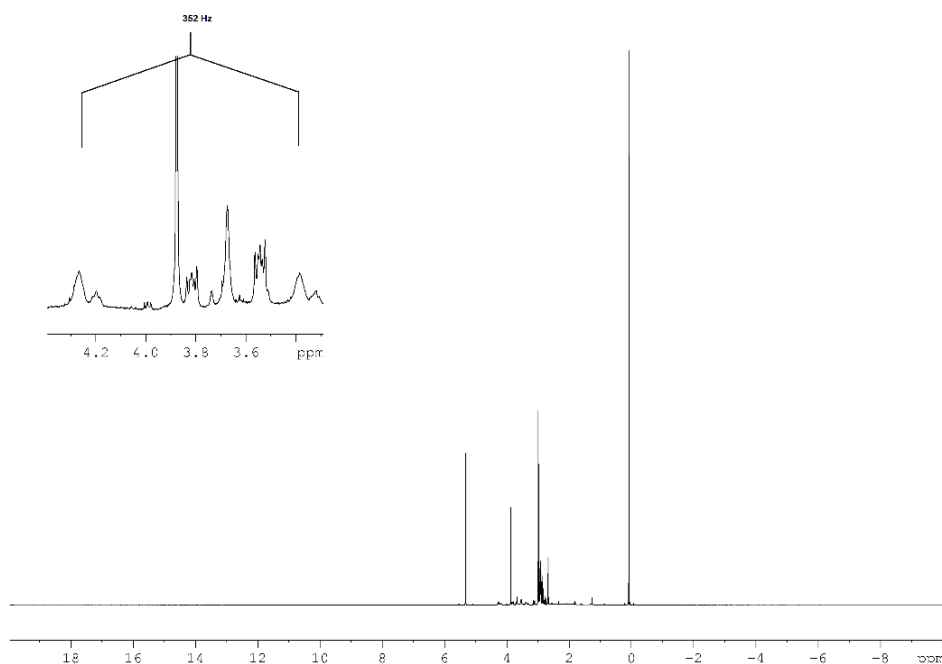
tmeda·(*BH*₂*PH*₂*AuCl*)₂

Figure S30: ¹H NMR spectrum of **4a** in CD₂Cl₂. The poor solubility of the crystalline material of **4a** does not allow NMR spectra without impurities.

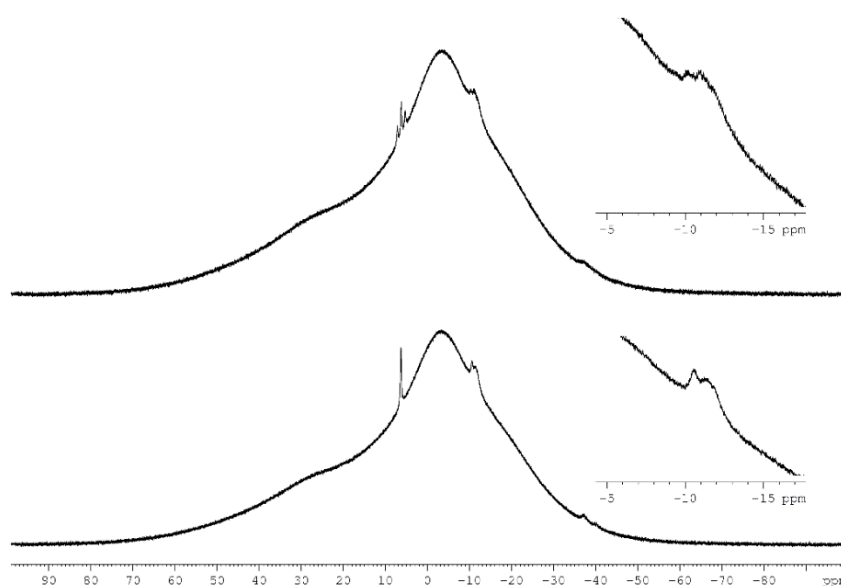


Figure S31: ¹¹B (top) and ¹¹B{¹H} (bottom) NMR spectrum of **4a** in CD₂Cl₂. The poor solubility of the crystalline material of **4a** does not allow NMR spectra without impurities.

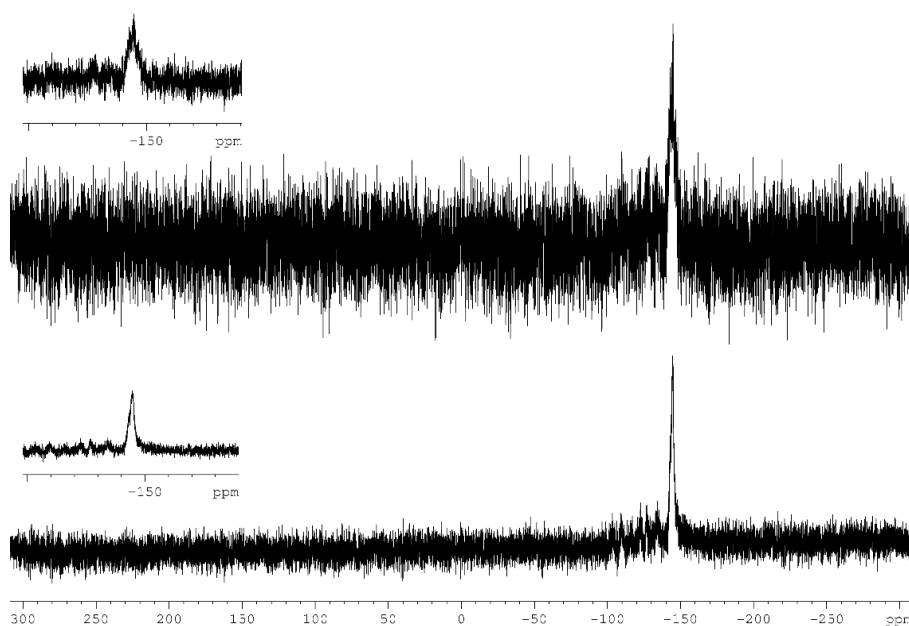


Figure S32: ^{31}P (top) and $^{31}\text{P}\{^1\text{H}\}$ (bottom) NMR spectrum of **4a** in CD_2Cl_2 . The poor solubility of the crystalline material of **4a** does not allow NMR spectra without impurities.

***tmeda*·($\text{BH}_2\text{PPh}_2\text{AuCl}$)₂**

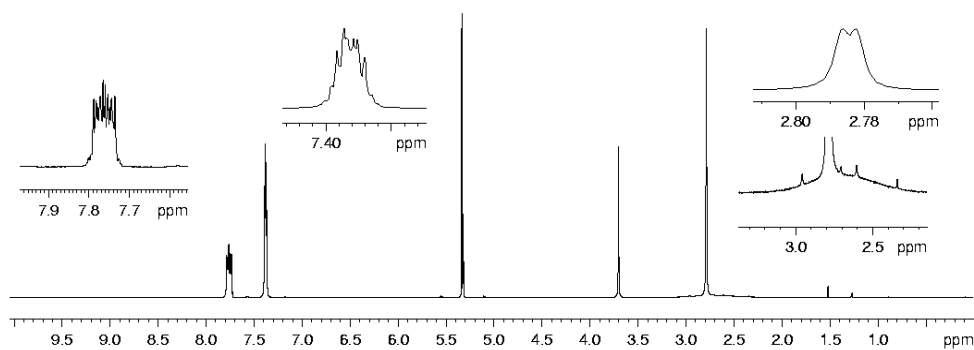


Figure S33: ^1H NMR spectrum of **4b** in CD_2Cl_2 .

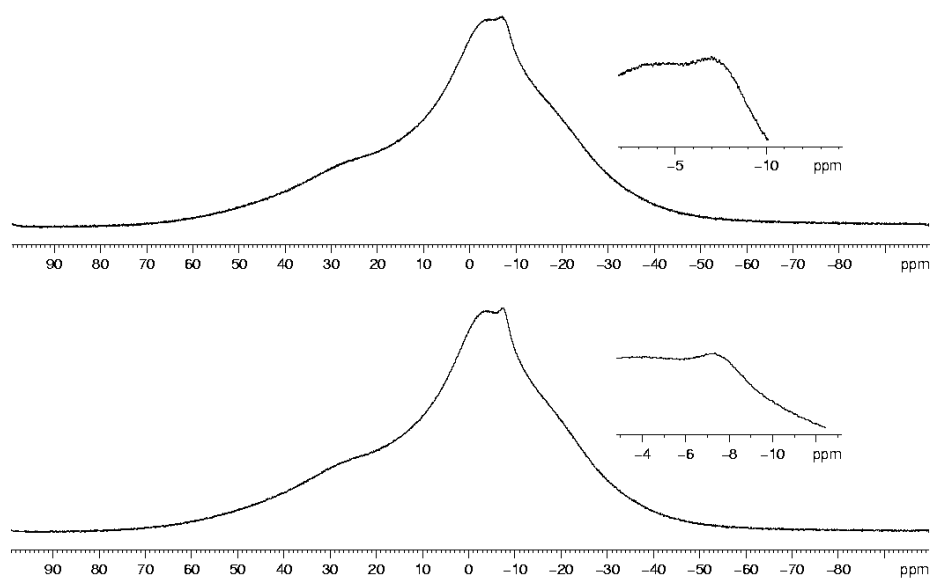


Figure S34: ^{11}B (top) and $^{11}\text{B}\{^1\text{H}\}$ (bottom) NMR spectra of **4b** in CD_2Cl_2 .

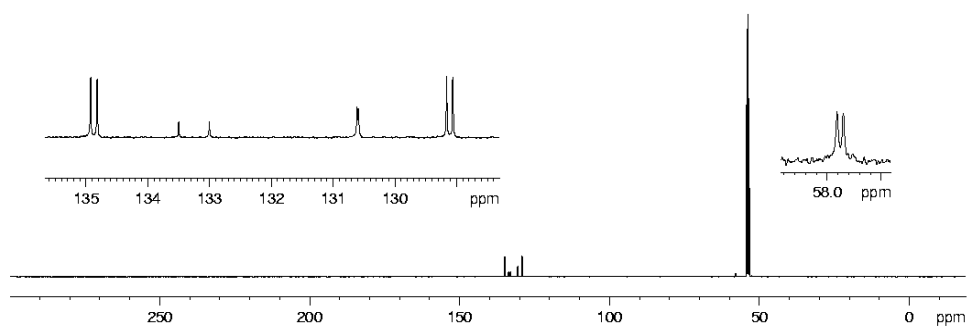


Figure S35: $^{13}\text{C}\{^1\text{H}\}$ NMR spectra of **4b** in CD_2Cl_2 .

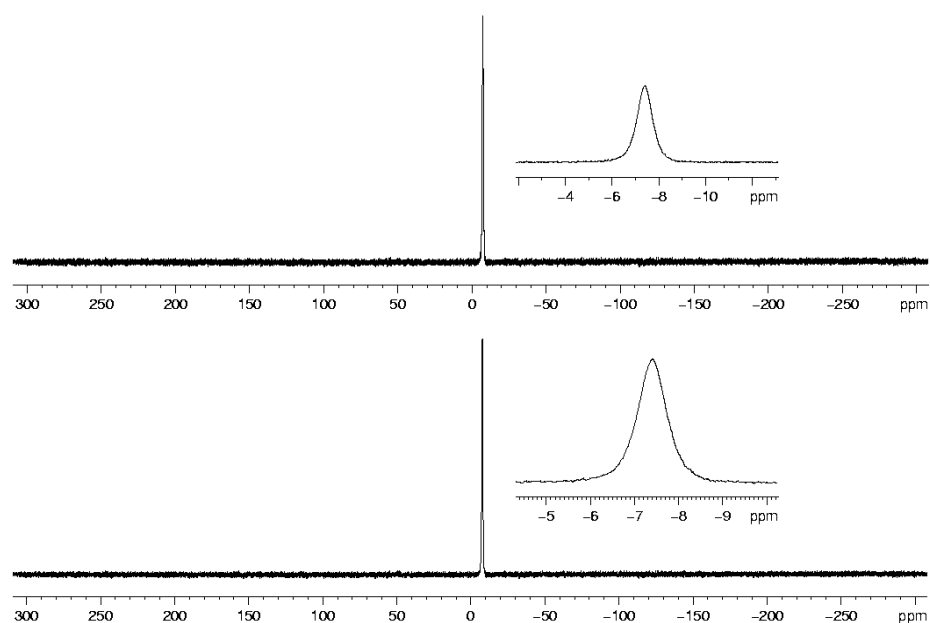
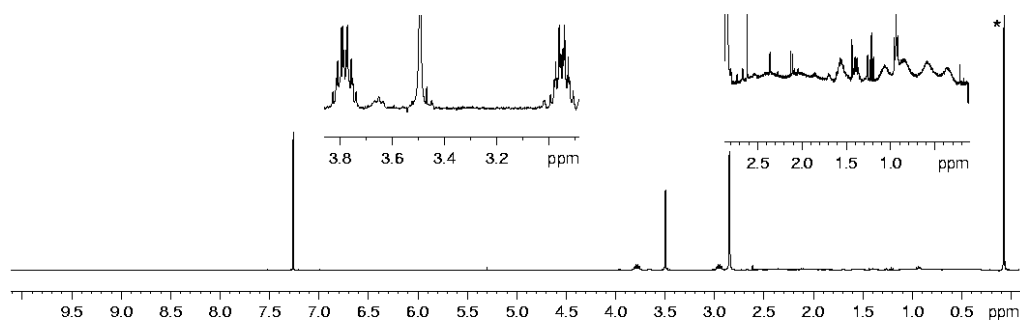
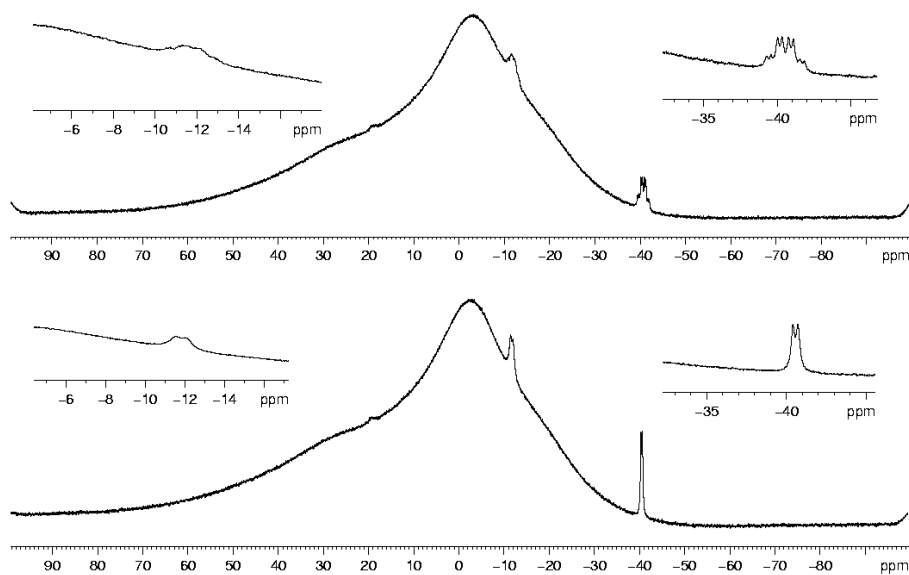
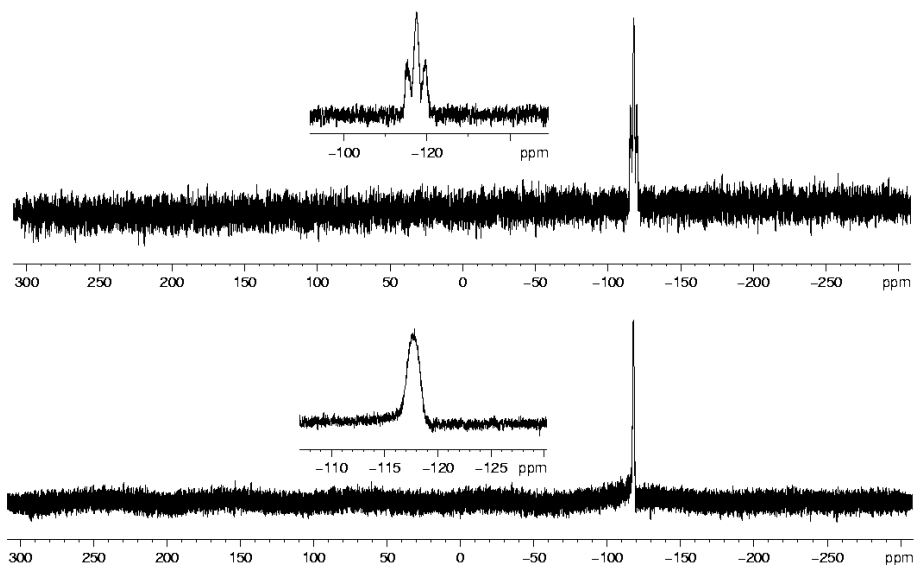


Figure S36: ^{31}P (top) and $^{31}\text{P}\{^1\text{H}\}$ (bottom) NMR spectra of **4b** in CD_2Cl_2 .

tmeda·($BH_2PH_2BH_3$)₂**Figure S37:** 1H NMR spectrum of **5a** in $CDCl_3$ (* = H-grease).**Figure S38:** ^{11}B NMR (top) and $^{11}B\{^1H\}$ NMR (bottom) spectra of **5a** in $CDCl_3$.**Figure S39:** ^{31}P NMR (top) and $^{31}P\{^1H\}$ NMR (bottom) spectra of **5a** in $CDCl_3$.

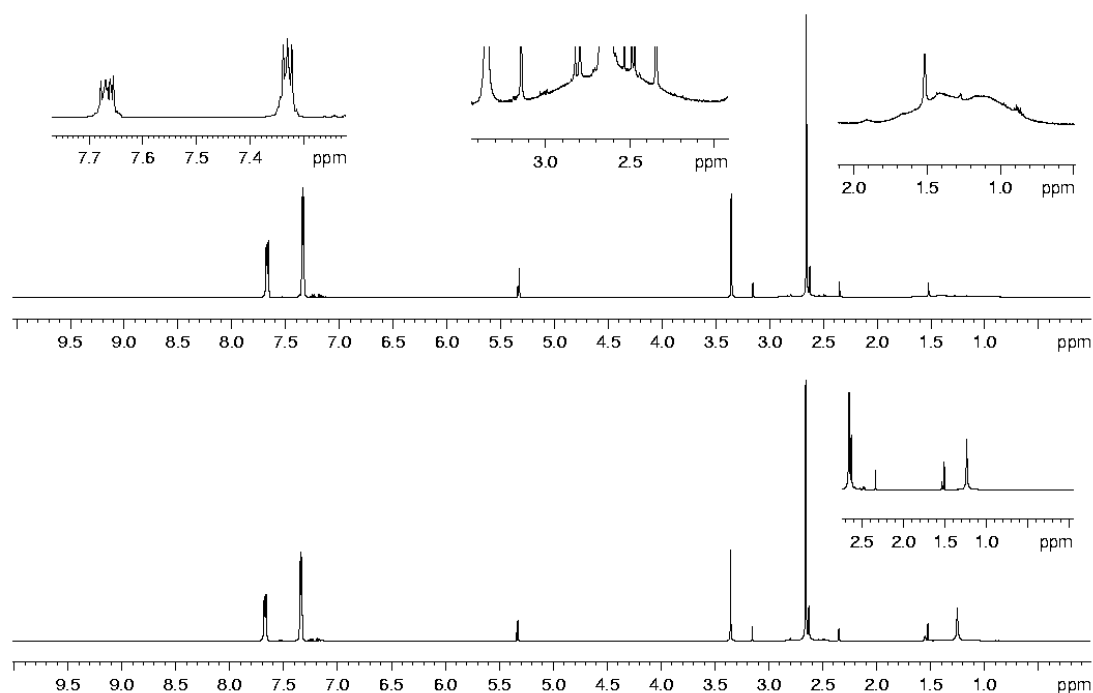
tmeda·(*BH*₂AsPh₂*BH*₃)₂

Figure S40: ^1H (top) and $^1\text{H}\{^{11}\text{B}\}$ NMR spectrum of **5b** in CD_2Cl_2 .

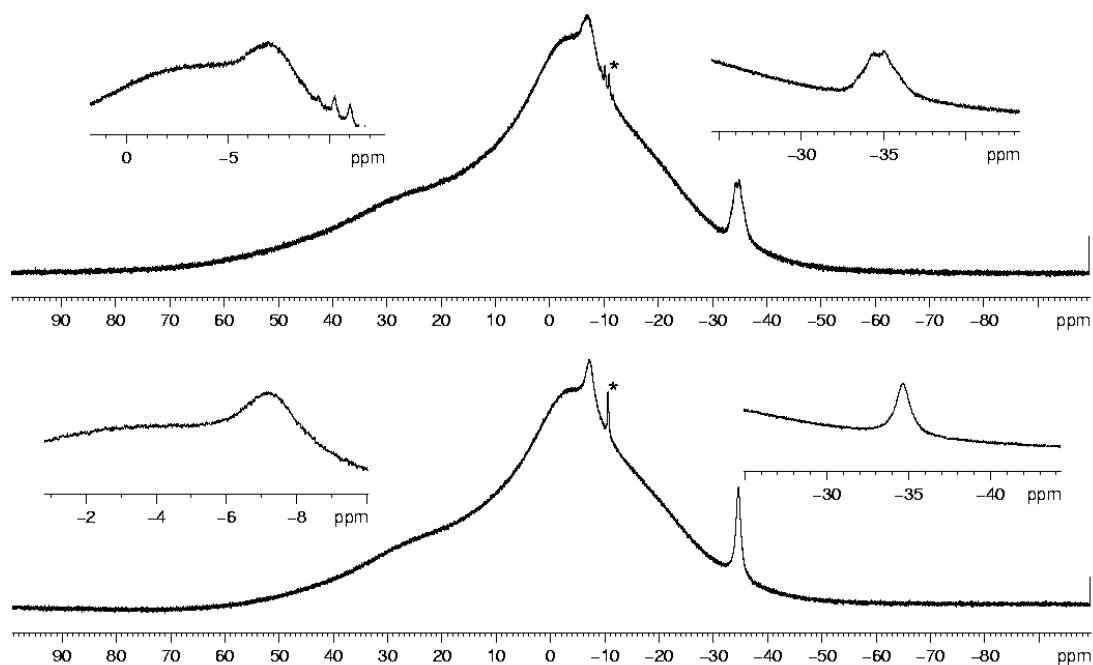


Figure S41: ^{11}B (top) and $^{11}\text{B}\{^1\text{H}\}$ NMR spectrum of **5b** in CD_2Cl_2 (impurity: * = *tmeda*·(*BH*₃)₂).

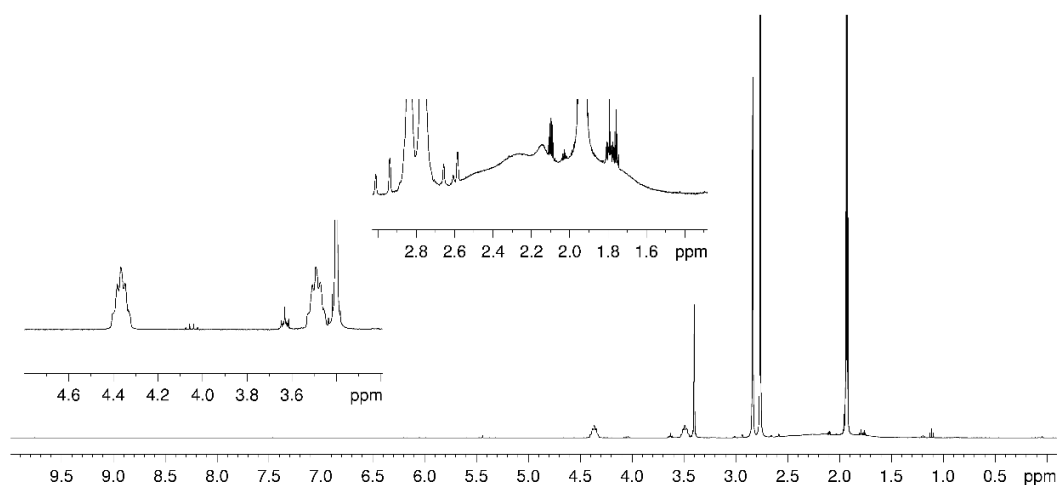


Figure S41: ¹H NMR spectrum of **6** in CD₃CN.

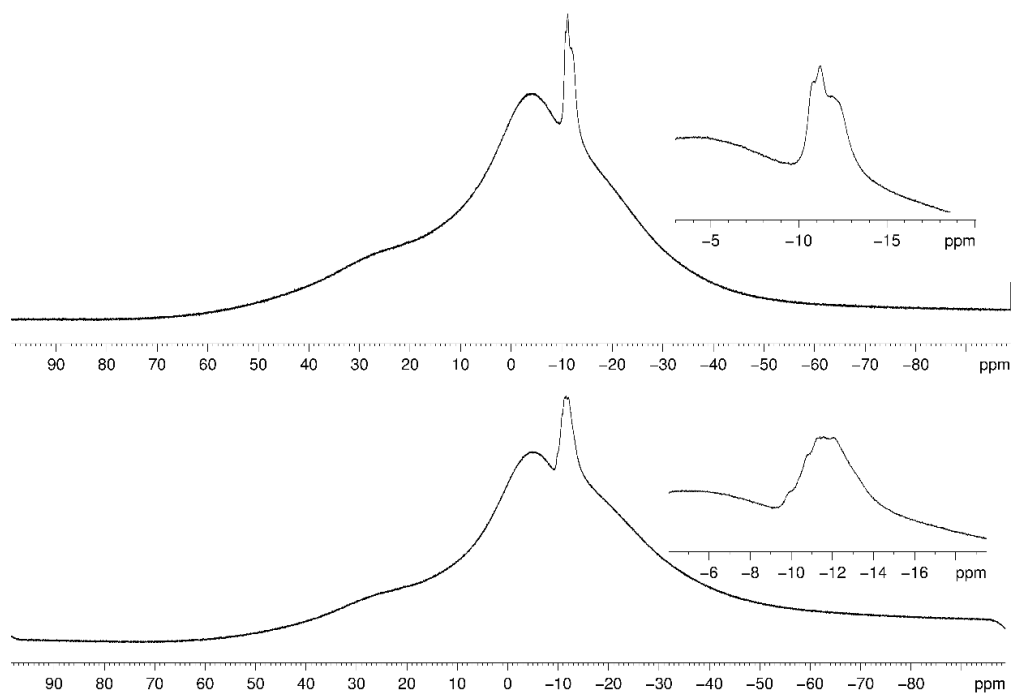


Figure S42: ¹¹B (top) and ¹¹B{¹H} (bottom) NMR spectrum of **6** in CD₃CN.

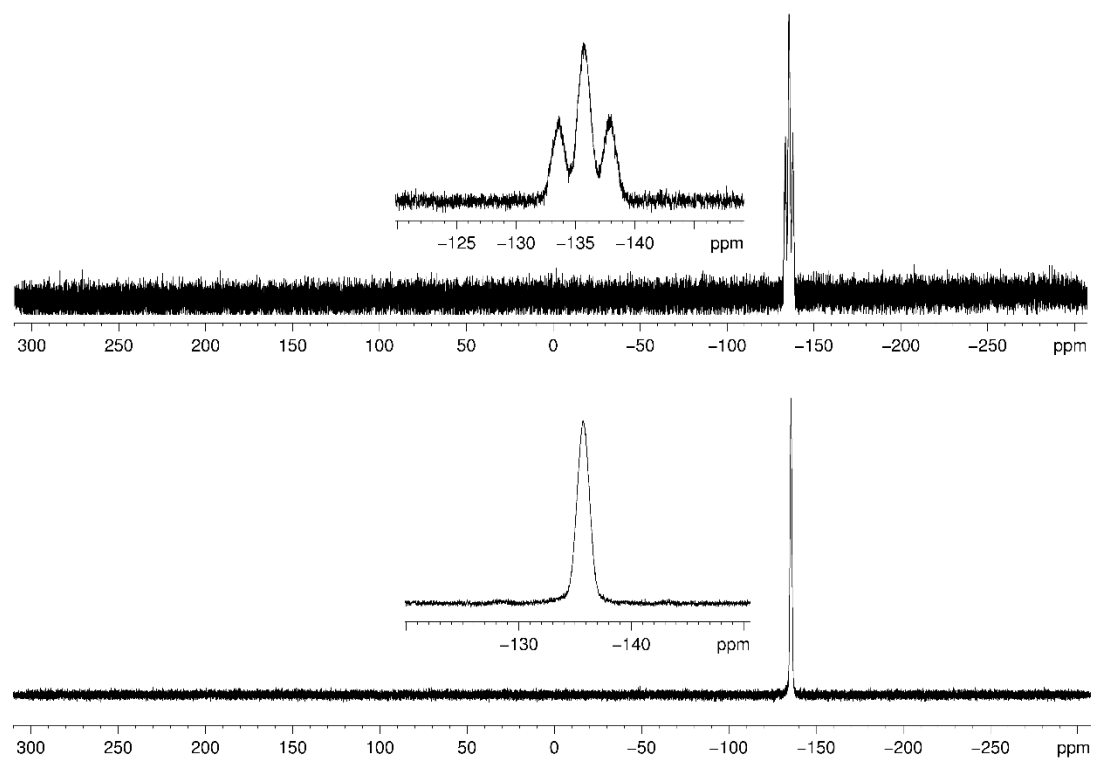


Figure S43: ^{31}P (top) and $^{31}\text{P}\{^1\text{H}\}$ (bottom) NMR spectrum of **6** in CD_3CN .

4,4'-bpy·(BH_2I)₂

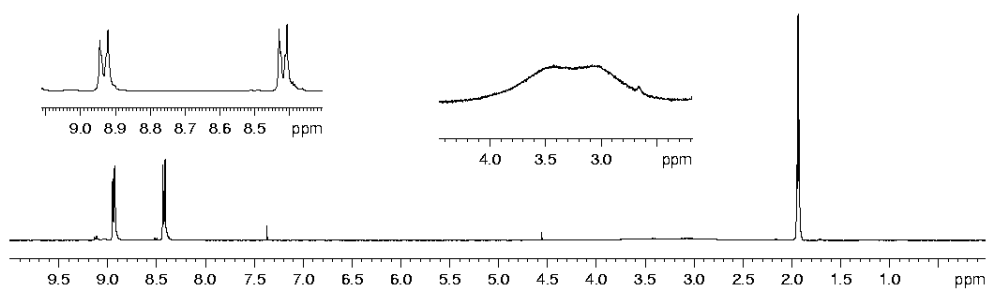


Figure S44: ^1H -NMR spectrum of **7** in CD_3CN .

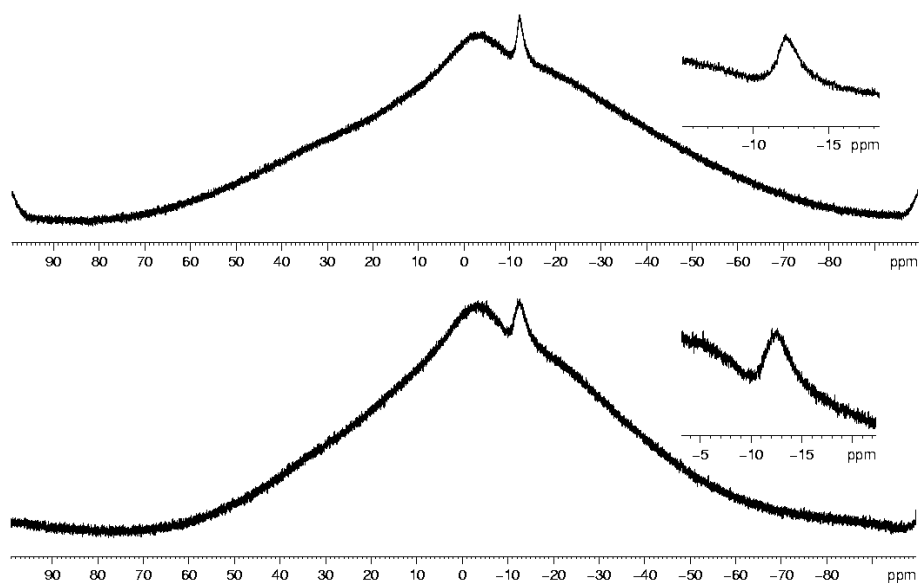


Figure S45: ^{11}B (top) and $^{11}\text{B}\{^1\text{H}\}$ (bottom) NMR spectrum of **7** in CD_3CN .

[4,4'-bpy-(BH₂PH₂BH₂-NMe₃)₂][I]₂

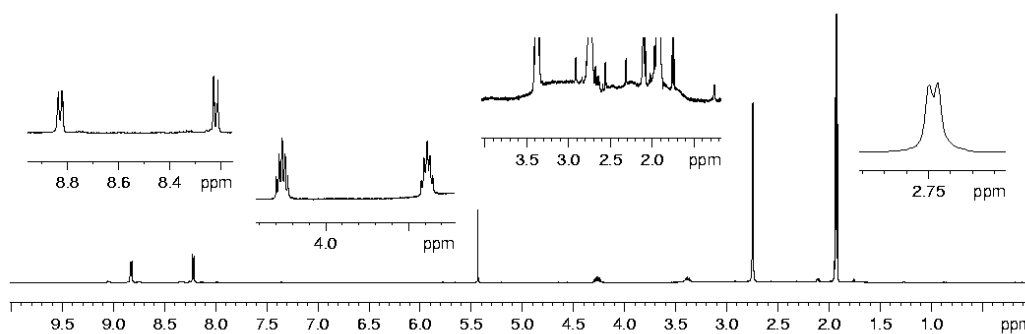


Figure S46: ^1H NMR spectrum of **8** in CD_3CN .

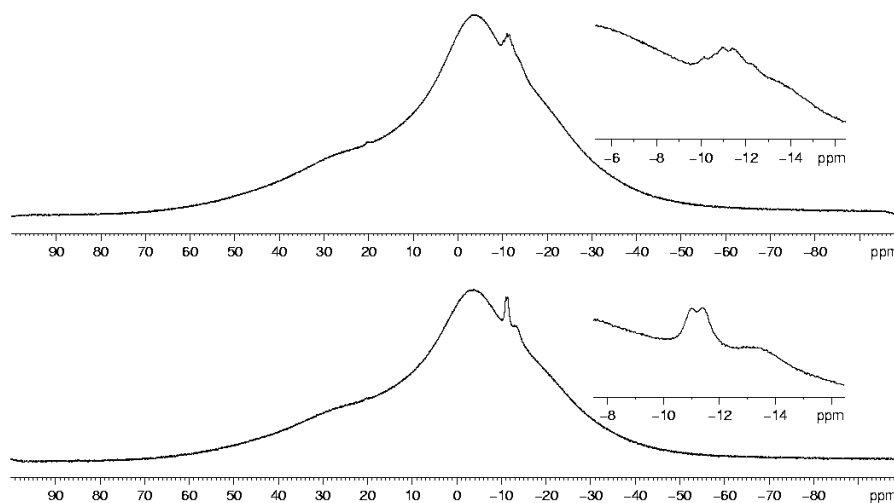


Figure S47: ^{11}B (top) and $^{11}\text{B}\{^1\text{H}\}$ (bottom) NMR spectrum of **8** in CD_3CN .

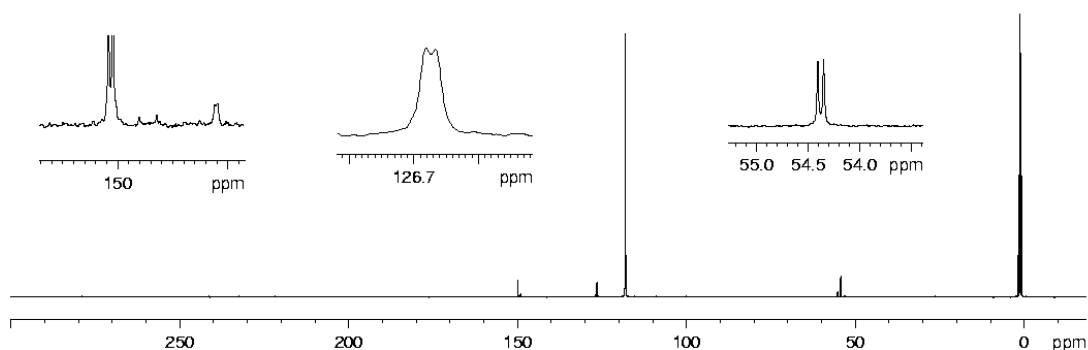


Figure S48: ^{13}C NMR spectrum of **8** in CD_3CN .

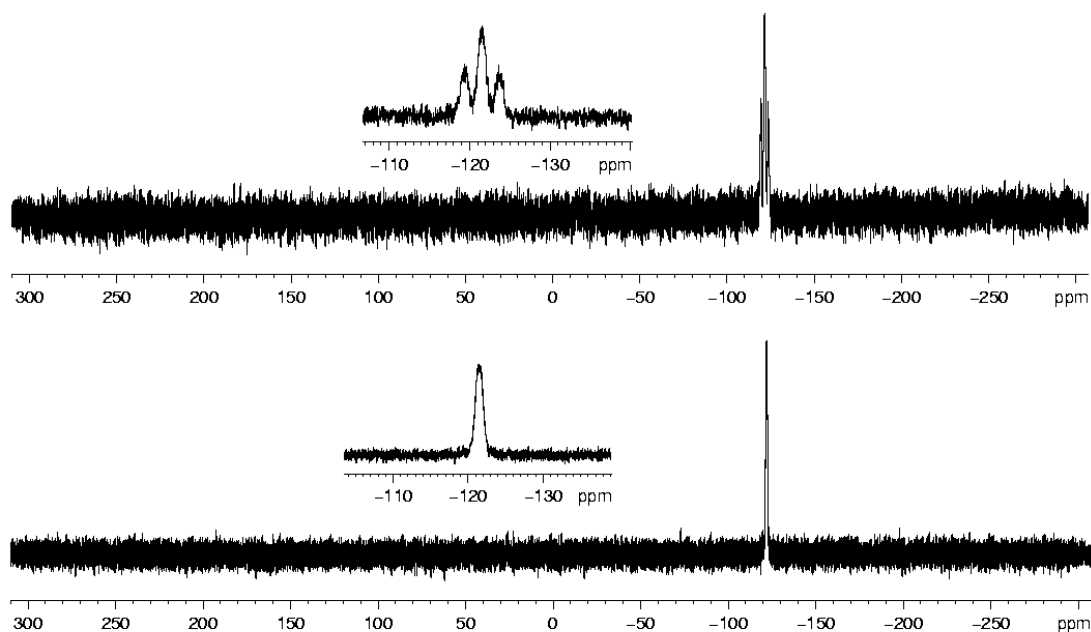


Figure S49: ^{31}P (top) and $^{31}\text{P}\{^1\text{H}\}$ (bottom) NMR spectrum of **8** in CD_3CN .

Computational details

The geometries of the compounds have been fully optimized with gradient-corrected density functional theory (DFT) in form of Becke's three-parameter hybrid method B3LYP^[12] with all electron def2-SVPD basis set (ECP for I).^[13] Gaussian 09 program package^[14] was used throughout. All structures correspond to minima on their respective potential energy surfaces. Basis sets were obtained from the EMSL basis set exchange database.^[15]

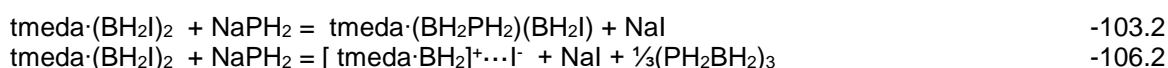
Short discussion

The complex of chelating bidentate coordination of tmeda with BH_2^+ is by circa 200 kJ mol^{-1} more stable than with monodentate coordination. Thus $[\text{tmeda} \cdot \text{BH}_2]^+$ cation is quite stable. The subsequent addition of two Lewis acids (LA) to tmeda with formation of molecular complexes of 1:1 and 1:2 composition (both feature non-chelating coordination of tmeda) expectedly decrease by 6-17 kJ mol^{-1} from first to second LA (Table S4). However, the first and second I^- abstraction from $\text{tmeda} \cdot (\text{BH}_2\text{I})_2$ using NaPH_2 differ less than 1 kJ mol^{-1} (-103.2 and -102.4 for the first and second, respectively).

Table S5. Standard enthalpies of addition of first and second LA to tmen (kJ mol^{-1}) and first and second I^- abstraction enthalpies from $\text{tmeda} \cdot (\text{BH}_2\text{I})_2$ with NaPH_2 . All data are for the gas phase species. B3LYP/def2-SVPD (ECP on I) level of theory.

LA	first	second
BH_3	-128.7	-122.4
BH_2I	-124.2	-107.7
BH_2PH_2	-95.4	-85.2
I^- abstraction with NaPH_2	-103.2	-102.4

The ionization of the molecular complex $\text{tmeda} \cdot (\text{BH}_2\text{I})_2$ into $[\text{tmeda} \cdot \text{BH}_2]^+ \cdots [\text{BH}_2\text{I}_2]^-$ ion pair is endothermic by 43.3 kJ mol^{-1} . However, the $[\text{BH}_2\text{I}_2]^-$ anion is predicted to exothermically react with NaPH_2 yielding $(\text{PH}_2\text{BH}_2)_n$ oligomer, modeled by $(\text{PH}_2\text{BH}_2)_3$ trimer. Comparison of the reaction enthalpies of $\text{tmeda} \cdot (\text{BH}_2\text{I})_2$ indicates, that reaction with 2 equivalents of NaPH_2 with formation of molecular $\text{tmeda} \cdot (\text{BH}_2\text{PH}_2)_2$ and NaI is exothermic by -205.6 kJ mol^{-1} , while reaction of 2 equivalents NaPH_2 with formation of $\text{tmeda} \cdot \text{BH}_2\text{PH}_2$, NaI and $\frac{1}{3}(\text{PH}_2\text{BH}_2)_3$ is more exothermic, -233.0 kJ mol^{-1} (Table S5). Reactions of $\text{tmeda} \cdot (\text{BH}_2\text{I})_2$ with one equivalent of NaPH_2 with formation of molecular and ionic species are exothermic and similar in standard enthalpy ΔH°_{298} (kJ mol^{-1}):



This may explain the observed side products upon reaction of $\text{tmeda} \cdot (\text{BH}_2\text{I})_2$ with NaPH_2 .

Table S6. Standard enthalpies of gas phase reaction of $\text{tmeda} \cdot (\text{BH}_2\text{I})_2$ (kJ mol^{-1}). B3LYP/def2-SVPD (ECP on I) level of theory. Symbol \cdots indicates ion pair.

Process	ΔH°_{298}
$\text{tmeda} \cdot (\text{BH}_2\text{I})_2 + \text{NaPH}_2 = \text{tmeda} \cdot (\text{BH}_2\text{PH}_2)(\text{BH}_2\text{I}) + \text{NaI}$	-103.2
$\text{tmeda} \cdot (\text{BH}_2\text{PH}_2)(\text{BH}_2\text{I}) + \text{NaPH}_2 = \text{tmeda} \cdot (\text{BH}_2\text{PH}_2)_2 + \text{NaI}$	-102.4
$\text{tmeda} \cdot (\text{BH}_2\text{I})_2 + 2\text{NaPH}_2 = \text{tmeda} \cdot (\text{BH}_2\text{PH}_2)_2 + 2\text{NaI}$	-205.6

$\text{tmeda} \cdot (\text{BH}_2\text{I})_2 = \text{tmeda} + \text{B}_2\text{H}_4\text{I}_2$	148.4
$\text{tmeda} \cdot (\text{BH}_2\text{I})_2 = [\text{tmeda} \cdot \text{BH}_2]^+ \cdots \text{I}^- + \text{BH}_2\text{I}$	134.8
$\text{tmeda} \cdot (\text{BH}_2\text{I})_2 = [\text{tmeda} \cdot \text{BH}_2]^+ \cdots [\text{BH}_2\text{I}_2]^-$	43.3
$\text{tmeda} \cdot (\text{BH}_2\text{I})_2 + \text{NaPH}_2 = [\text{tmeda} \cdot \text{BH}_2]^+ \cdots \text{I}^- + \text{NaI} + \frac{1}{3}(\text{PH}_2\text{BH}_2)_3$	-106.2
$\text{tmeda} \cdot (\text{BH}_2\text{I})_2 + 2\text{NaPH}_2 = \text{tmeda} \cdot \text{BH}_2\text{PH}_2 + 2\text{NaI} + \frac{1}{3}(\text{PH}_2\text{BH}_2)_3$	-233.0
$[\text{BH}_2\text{I}_2]^- + \text{NaPH}_2 = \frac{1}{3}(\text{PH}_2\text{BH}_2)_3 + \text{NaI} + \text{I}^-$	-127.4
$[\text{tmeda} \cdot \text{BH}_2]^+ \cdots [\text{BH}_2\text{I}_2]^- + 2\text{NaPH}_2 = \text{tmeda} \cdot \text{BH}_2\text{PH}_2 + 2\text{NaI} + \frac{1}{3}(\text{PH}_2\text{BH}_2)_3$	-276.4

Table S7. Reaction energies ΔE°_0 , standard enthalpies ΔH°_{298} , Gibbs energies ΔG°_{298} (kJ mol^{-1}) and standard entropies ΔS°_{298} ($\text{J mol}^{-1} \text{K}^{-1}$) for the considered gas phase processes. B3LYP/def2-SVPD (ECP on I) level of theory. Data are given for the most stable isomers in the gas phase.

Process	ΔE°_0	ΔH°_{298}	ΔS°_{298}	ΔG°_{298}
$\text{tmeda} + \text{BH}_2^+ = \text{tmeda} \cdot \text{BH}_2^+$ monodentate	-500.0	-483.1	-139.2	-441.6
$\text{tmeda} + \text{BH}_2^+ = [\text{BH}_2\text{tmen}]^+$ bidentate	-710.5	-682.7	-198.4	-623.6
$\text{tmen} + \text{BH}_3 = \text{tmeda} \cdot \text{BH}_3$	-144.8	-128.7	-158.0	-81.6
$\text{tmeda} \cdot \text{BH}_3 + \text{BH}_3 = \text{tmeda} \cdot (\text{BH}_3)_2$	-138.4	-122.4	-168.6	-72.1
$\text{tmeda} + \text{B}_2\text{H}_6 = \text{tmeda} \cdot (\text{BH}_3)_2$	-108.5	-95.1	-181.8	-40.8
$\text{tmen} + \text{BH}_2\text{I} = \text{tmeda} \cdot \text{BH}_2\text{I}$	-140.3	-124.2	-174.5	-72.2
$\text{tmeda} \cdot \text{BH}_2\text{I} + \text{BH}_2\text{I} = \text{tmeda} \cdot (\text{BH}_2\text{I})_2$	-123.0	-107.7	-181.8	-53.5
$\text{tmeda} + \text{B}_2\text{H}_4\text{I}_2 = \text{tmeda} \cdot (\text{BH}_2\text{I})_2$	-166.7	-148.4	-192.3	-91.1
$\text{tmeda} + \text{BH}_2\text{PH}_2 = \text{tmeda} \cdot \text{BH}_2\text{PH}_2$	-109.8	-95.4	-174.2	-43.5
$\text{tmeda} \cdot \text{BH}_2\text{PH}_2 + \text{BH}_2\text{PH}_2 = \text{tmeda} \cdot (\text{BH}_2\text{PH}_2)_2$	-99.6	-85.2	-194.7	-27.2
$\text{tmeda} \cdot \text{BH}_2\text{PH}_2 + \text{BH}_2\text{I} = \text{tmeda} \cdot (\text{BH}_2\text{PH}_2)(\text{BH}_2\text{I})$	-126.9	-111.3	-176.3	-58.7
$\text{tmeda} \cdot \text{BH}_2\text{I} + \text{BH}_2\text{PH}_2 = \text{tmeda} \cdot (\text{BH}_2\text{PH}_2)(\text{BH}_2\text{I})$	-96.5	-82.5	-175.9	-30.0
$\text{tmeda} \cdot (\text{BH}_2\text{I})_2 + 2\text{NaPH}_2 = \text{tmeda} \cdot (\text{BH}_2\text{PH}_2)_2 + 2\text{NaI}$	-214.0	-205.6	-46.4	-191.8
$\text{tmeda} \cdot (\text{BH}_2\text{I})_2 + \text{NaPH}_2 = \text{tmeda} \cdot (\text{BH}_2\text{PH}_2)(\text{BH}_2\text{I}) + \text{NaI}$	-107.4	-103.2	-11.0	-99.9
$\text{tmeda} \cdot (\text{BH}_2\text{PH}_2)(\text{BH}_2\text{I}) + \text{NaPH}_2 = \text{tmeda} \cdot (\text{BH}_2\text{PH}_2)_2 + \text{NaI}$	-106.7	-102.4	-35.4	-91.9
$\text{tmeda} \cdot (\text{BH}_2\text{I})_2 = [\text{tmeda} \cdot \text{BH}_2]^+ \cdots \text{I}^- + \text{BH}_2\text{I}$	143.1	134.8	155.5	88.5
$\text{tmeda} \cdot (\text{BH}_2\text{I})_2 + \text{NaPH}_2 = [\text{tmeda} \cdot \text{BH}_2]^+ \cdots \text{I}^- + \text{NaI} + \frac{1}{3}(\text{PH}_2\text{BH}_2)_3$	-111.2	-106.2	11.7	-109.7
$\text{tmeda} \cdot (\text{BH}_3)_2 = [\text{tmeda} \cdot \text{BH}_2]^+ \cdots [\text{BH}_4]^-$	136.9	132.6	7.6	130.3
$\text{tmeda} \cdot (\text{BH}_3)_2 = \text{tmeda} + \text{B}_2\text{H}_6$	108.5	95.1	181.8	40.8
$\text{tmeda} + \text{B}_2\text{H}_6 = [\text{tmeda} \cdot \text{BH}_2]^+ \cdots [\text{BH}_4]^-$	28.4	37.5	-174.2	89.5
$\text{tmeda} \cdot (\text{BH}_2\text{I})_2 = [\text{tmeda} \cdot \text{BH}_2]^+ \cdots [\text{BH}_2\text{I}_2]^-$	43.8	43.3	3.3	42.4
$\text{tmeda} \cdot (\text{BH}_2\text{I})_2 = \text{tmeda} + \text{B}_2\text{H}_4\text{I}_2$	166.7	148.4	192.3	91.1
$\text{tmeda} + \text{B}_2\text{H}_4\text{I}_2 = [\text{tmeda} \cdot \text{BH}_2]^+ \cdots [\text{BH}_2\text{I}_2]^-$	-122.9	-105.1	-188.9	-48.7
$[\text{BH}_2\text{I}_2]^- + \text{NaPH}_2 = \frac{1}{3}(\text{PH}_2\text{BH}_2)_3 + \text{NaI} + \text{I}^-$	-138.7	-127.4	-39.6	-115.6
$[\text{tmeda} \cdot \text{BH}_2]^+ \cdots [\text{BH}_2\text{I}_2]^- + 2\text{NaPH}_2 = \text{tmeda} \cdot \text{BH}_2\text{PH}_2 + 2\text{NaI} + \frac{1}{3}(\text{PH}_2\text{BH}_2)_3$	-278.6	-276.4	18.0	-281.7
$\text{tmeda} \cdot (\text{BH}_2\text{I})_2 + 2\text{NaPH}_2 = \text{tmeda} \cdot \text{BH}_2\text{PH}_2 + 2\text{NaI} + \frac{1}{3}(\text{PH}_2\text{BH}_2)_3$	-234.8	-233.0	21.4	-239.4

Table S8. Total energies E^0_0 , sum of electronic and thermal enthalpies H^0_{298} (Hartree) and standard entropies S^0_{298} (cal mol⁻¹K⁻¹). B3LYP/def2-SVPD (ECP on I) level of theory.

Compound	Point group	E^0_0	H^0_{298}	S^0_{298}
BH ₃	D _{3h}	-26.5920766	-26.562181	45.055
BH ₂ ⁺	D _{∞h}	-25.6077061	-25.587151	41.516
[BH ₄] ⁻	T _d	-27.2451821	-27.207941	45.298
B ₂ H ₆	D _{2h}	-53.2506989	-53.183802	55.511
BH ₂ I	C _{2v}	-323.831667	-323.807537	60.752
cis-B ₂ H ₄ I ₂	C _{2v}	-647.6998001	-647.646597	81.833
trans-B ₂ H ₄ I ₂	C _{2h}	-647.7001351	-647.646885	82.285
[BH ₂ I ₂] ⁻	C _{2v}	-621.7692381	-621.742007	76.254
I ⁻		-297.8935536	-297.891193	40.428
NaI	C _{∞v}	-460.1191828	-460.114828	59.579
NaPH ₂	C _s	-504.7158883	-504.695553	63.77
PH ₂ ⁻	C _{2v}	-342.4475193	-342.430938	49.501
BH ₂ PH ₂	C _s	-368.4793894	-368.437191	60.898
(PH ₂ BH ₂) ₃	C _{3v}	-1105.575711	-1105.440237	91.658
NMe ₃	C _{3v}	-174.3602413	-174.234491	69.505
PH ₂ BH ₂ I ⁻	C _s	-666.403285	-666.358458	76.502
PH ₂ BH ₂ NMe ₃	C _s	-542.882077	-542.708753	89.78
tmeda	C _{2h}	-347.5148435	-347.282348	99.608
BH ₂ tmeda ⁺ monodentate	C _s	-373.3129793	-373.053502	107.861
[BH ₂ tmeda] ⁺ bidentate	C ₂	-373.3931484	-373.129539	93.66
[BH ₂ tmeda] ⁺ [BH ₂ I ₂] ⁻ ion pair	C ₁	-995.2617735	-994.96925	136.735
[BH ₂ tmeda] ⁺ [BH ₄] ⁻ ion pair	C ₁	-400.7547143	-400.451865	113.477
[BH ₂ tmeda] ⁺ I ⁻ ion pair	C ₁	-671.3922932	-671.126864	112.365
tmeda·(BH ₃)	C _s	-374.162072	-373.893562	106.911
tmeda·(BH ₃) ₂	C _{2h}	-400.8068501	-400.502353	111.668
tmeda·(BH ₂ I)	C _s	-671.3999343	-671.137194	118.646
tmeda·(BH ₂ I) ₂	C ₁	-995.2784575	-994.98576	135.942
tmeda·(BH ₂ PH ₂)	C _s	-716.0360553	-715.755879	118.876
tmeda·(BH ₂ PH ₂) ₂	C ₂	-1084.553395	-1084.22553	133.236
tmeda·(BH ₂ I)(BH ₂ PH ₂)	C _s	-1039.916067	-1039.605801	137.496

Cartesian coordinates of the optimized geometry can be obtained from the provided DVD.

References

- [1] C. Marquardt, A. Adolf, A. Stauber, M. Bodensteiner, A. V. Virovets, A. Y. Timoshkin, M. Scheer, *Chem. Eur. J.* **2013**, 19, 11887 – 11891.
- [2] C. Marquardt, C. Thoms, A. Stauber, G. Balazs, M. Bodensteiner, M. Scheer, *Angew. Chem. Int. Ed.* **2014**, 53, 3727–3730.

- [3] A. R. Gatti, T. Wartik, *Inorg. Chem.* **1966**, Vol. 5, Nr. 2, February, 329 – 330.
- [4] C. Marquardt, T. Jurca, K.-C. Schwan, A. Stauber, A. V. Virovets, G. R. Whittell, I. Manners, M. Scheer, *Angew. Chem. Int. Ed.* **2015**, *54*, 13782–13786; *Angew. Chem.* **2015**, *127*, 13986-13991.
- [5] A. Tzschach, W. Lange, *Chem. Ber.* **1962**, *95*, 1360-1366.
- [6] R. Uson, A. Laguna, M. Laguna, D. A. Briggs, H. H. Murray, J. P. Fackler, (Tetrahydrothiophene)Gold(I) or Gold(III) Complexes, in *Inorganic Syntheses*, Vol. 26 (ed H. D. Kaesz), **1989**, John Wiley & Sons, Inc., Hoboken, NJ, USA.
- [7] P. C. Keller, R. L. Marks, J. V. Rund, *Polyhedron*, **1983**, *2*, 595-602.
- [8] Agilent Technologies **2006-2011**, CrysAlisPro Software system, different versions, Agilent Technologies UK Ltd, Oxford, UK.
- [9] A. Altomare, M. C. Burla, M. Camalli, G. L. Cascarano, C. Giacovazzo, A. Guagliardi, A. G. G. Moliterni, G. Polidori, R. Spagna, *J. Appl. Cryst.* (1999) *32*, 115-119.
- [10] G. M. Sheldrick, *Acta Cryst.* **2008**, *A64*, 112–122.
- [11] O.V. Dolomanov, L. J. Bourhis, R. J. Gildea, J. A. K. Howard, H. Puschmann, OLEX2: A complete structure solution, refinement and analysis program, **2009**. *J. Appl. Cryst.*, *42*, 339-341.
- [12] a) A.D. Becke, *J. Chem. Phys.* **1993**, *98*, 5648. b) C. Lee, W. Yang, R.G. Parr, *Phys. Rev. B.* **1988**, *37*, 785.
- [13] a) D. Rappoport, F. Furche, *J. Chem. Phys.* **2010**, *133*, 134105; b). F. Weigend, R. Ahlrichs, *Phys.Chem.Chem.Phys.*, **2005**, *7*, 3297-3305; c) D. Andrae, U. Haeussermann, M. Dolg, H. Stoll, H. Preuss, *Theor.Chim.Acta*, **1990**, *77*, 123-141; d) K. A. Peterson, D. Figgen, E. Goll, H. Stoll, M. Dolg, *J. Chem. Phys.* **2003**, *119*, 11113-11123.
- [14] M. J. Frisch, G. W. Trucks, H. B. Schlegel, G. E. Scuseria, M. A. Robb, J. R. Cheeseman, G. Scalmani, V. Barone, B. Mennucci, G. A. Petersson, H. Nakatsuji, M. Caricato, X. Li, H. P. Hratchian, A. F. Izmaylov, J. Bloino, G. Zheng, J. L. Sonnenberg, M. Hada, M. Ehara, K. Toyota, R. Fukuda, J. Hasegawa, M. Ishida, T. Nakajima, Y. Honda, O. Kitao, H. Nakai, T. Vreven, J. A. Montgomery, Jr., J. E. Peralta, F. Ogliaro, M. Bearpark, J. J. Heyd, E. Brothers, K. N. Kudin, V. N. Staroverov, T. Keith, R. Kobayashi, J. Normand, K. Raghavachari, A. Rendell, J. C. Burant, S. S. Iyengar, J. Tomasi, M. Cossi, N. Rega, J. M. Millam, M. Klene, J. E. Knox, J. B. Cross, V. Bakken, C. Adamo, J.

Jaramillo, R. Gomperts, R. E. Stratmann, O. Yazyev, A. J. Austin, R. Cammi, C. Pomelli, J. W. Ochterski, R. L. Martin, K. Morokuma, V. G. Zakrzewski, G. A. Voth, P. Salvador, J. J. Dannenberg, S. Dapprich, A. D. Daniels, O. Farkas, J. B. Foresman, J. V. Ortiz, J. Cioslowski, and D. J. Fox, Gaussian 09, Revision E.01, Gaussian, Inc., Wallingford CT, **2013**.

- [15] (a) D. Feller, *J. Comp. Chem.* **1996**, *17*, 1571-1586; (b) K. L. Schuchardt, B. T. Didier, T. Elsethagen, L. Sun, V. Gurumoorthi, J. Chase, J. Li, T. L. Windus, *J. Chem. Inf. Model.* **2007**, *47*, 1045-1052.

6.6 Author contributions

The synthesis and characterization of compounds **1**, **2a**, **2b**, **2c**, **5a** and **6** were already performed during the Master thesis of Oliver Hegen.

Compounds **3**, **5b**, **7** and **8** were synthesized and characterized by Oliver Hegen.

Compounds **4a** and **4b** were first synthesized by Jens Braese and characterized through multinuclear NMR measurements and single crystal X-ray diffraction.

Compound **4b** was further characterized by Oliver Hegen.

All DFT computations were performed by Prof. Dr. Aleksey Timoshkin.

The manuscript (including Supporting Information, figures, schemes and graphical abstract) was written by Oliver Hegen.

7 Thesis Treasury

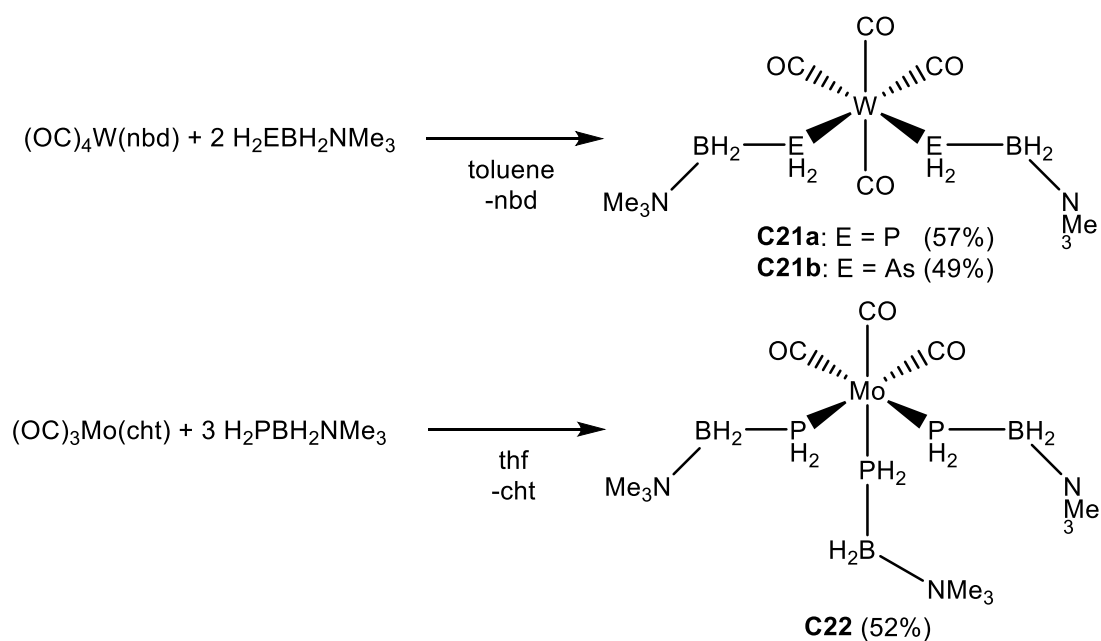
This chapter includes preliminary results, which will be included in future publications. Some of the obtained compounds could not be characterized completely so far, but all necessary data for the synthesis of the described compounds will be presented herein.

7.1 Systematical Coordination of Pnictogenylboranes towards Transition Metal Lewis Acids

To selectively build up networks, it is required to break down the overall phenomenon to a bottom-up approach. In Chapter 6, a strategy was developed to access Lewis base (LB) bridged pnictogenylboranes $(RR'EBH_2)_2tmeda$ ($E = P, As$; $R = R' = H, Ph$; $R = H, R' = tBu$) and first investigations were performed to use these compounds as linking units to connect between transition metals. At least two free coordination sites on a Lewis acid (LA) are necessary to link two pnictogenylboranes. Therefore the labile ligands norbornadiene (= nbd, C_7H_8) and cycloheptatriene (= cht, C_7H_8) were employed to simultaneously get access to either two (nbd) or three (cht) coordination sites. The reaction behavior of the transition metal complexes $(OC)_4W(nbd)$ and $(OC)_3Mo(cht)$ towards the parent pnictogenylboranes $H_2PBH_2NMe_3$ and $H_2AsBH_2NMe_3$ were investigated.

The reaction of $(OC)_4W(nbd)$ with two equivalents $H_2EBH_2NMe_3$ leads to $(OC)_4W(EH_2BH_2NMe_3)_2$ in moderate yields (**C21a**: $E = P$, **C21b**: $E = As$, **Scheme 1**). The reactions proceed selectively, nearly quantitatively according ^{11}B and ^{31}P NMR spectroscopic measurements and are accompanied by a color change from yellow to brown. A broad multiplett arises at $\delta = -170.34$ ppm ($^1J_{PB} = 32$ Hz) in the $^{31}P\{^1H\}$ NMR spectrum of **C21a**, which shows further splitting in the ^{31}P NMR spectrum ($^1J_{PH} = 280$ Hz). In the ^{11}B NMR spectrum, a broad multiplet is observed at $\delta = -7.52$ ppm ($^1J_{BP} = 32$ Hz, $^1J_{BH} = 130$ Hz). In comparison to the starting material the signal of the PH_2 -moieties shifts highfield to $\delta = 2.82$ ppm, whereas the signal of the BH_2 -moieties is shifted downfield to $\delta = 2.34$ ppm in the 1H NMR spectrum.^[1] A similar behaviour is observed for **C21b**. The signal generated by the AsH_2 -moieties shifts highfield to $\delta = 1.51$ ppm and the signal assigned to the BH_2 -groups shifts downfield to $\delta = 2.51$ ppm compared to the starting material.^[2] In the $^{11}B\{^1H\}$ NMR spectrum of **C21b** a

singlet arises at $\delta = -7.36$ ppm, which shows further splitting into a triplet in the ^{11}B NMR spectrum ($^1J_{\text{BH}} = 112$ Hz).



Scheme 1: Synthesis of **C21a**, **C21b** and **C22**. Isolated yields are given in parentheses.

The molecular structures in solid state of **C21a** and **C21b** were determined by single crystal X-ray diffraction analysis (**Figure 1**). The pnictogenylboranes are located at the two coordination sites in *cis*-position of the $\text{W}(\text{CO})_4$ fragment. All bonds are in the range of single bonds. The B-E axis adopt an antiperiplanar arrangement, whereas a synclinal arrangement is presented along the E-W axis. $\angle (\text{E1-W-E2})$ (E = P: $85.44(2)^\circ$, E = As: $84.56(3)^\circ$) is slightly smaller than in a perfect octahedron (90°). This results probably from packing effects.

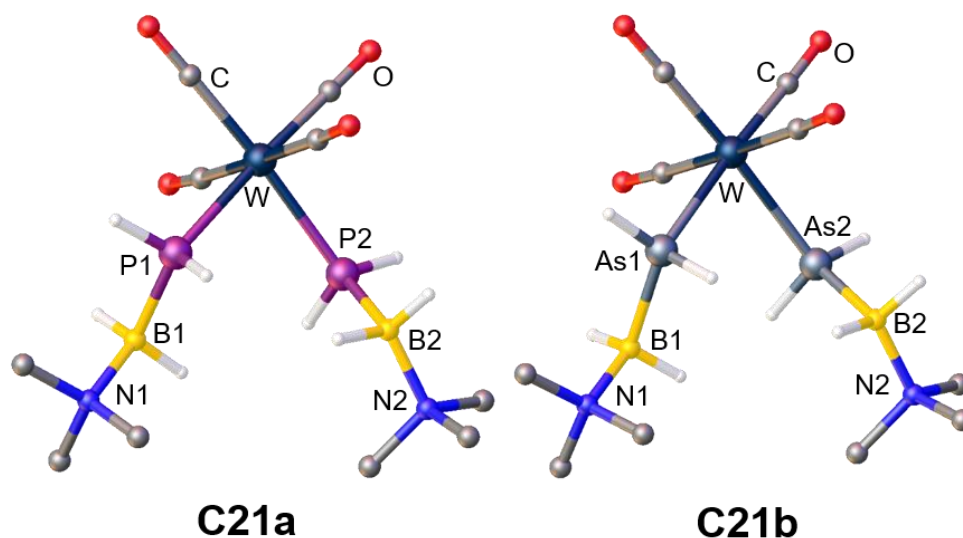


Figure 1: Molecular structures of **C21a** (left) and **C21b** (right) in solid state. Hydrogen atoms bound to Carbon are omitted for clarity. Thermal ellipsoids are drawn with 50% probability.

$(OC)_3Mo(PH_2BH_2NMe_3)_3$ (**C22**, **Figure 2**) was first reported and completely characterized by C. Thoms as a side product of the reaction of $[CpMo(CO)_3H]$ with $PH_2BH_2NMe_3$ in about 15% yield.^[3] In comparison, the reaction of $(OC)_3Mo(cht)$ with three equivalents $H_2PBH_2NMe_3$ leads to **C22** in moderate yields. The ^{31}P NMR spectrum of the reaction solution shows nearly quantitative conversion. However, due to further washing steps, the isolated yield is only moderate. A reaction of the As derivative $H_2AsBH_2NMe_3$ with $(OC)_3Mo(cht)$ was not observed according to NMR spectroscopy due to the lesser donor strength of As.

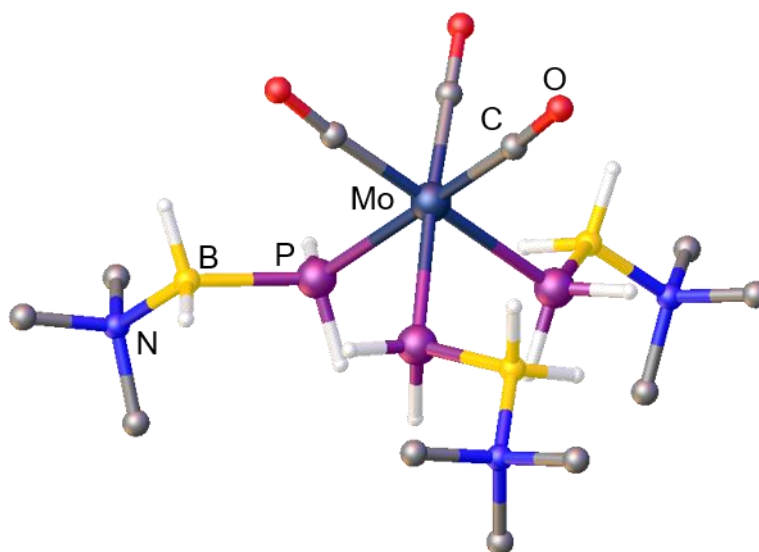


Figure 2: Molecular structure of **C22** in solid state. Hydrogen atoms bound to Carbon are omitted for clarity. Thermal ellipsoids are drawn with 50% probability.

Experimental section:**Synthesis of (OC)₄W(PH₂BH₂NMe₃)₂ (C21a):**

To a solution of 194 mg (OC)₄W(nbd) (0.5 mmol) in 20 mL toluene 2 mL of a 0.5 M solution of PH₂BH₂NMe₃ (1 mmol) in toluene is added at room temperature. After some minutes a color change from yellow to brown is observed and a yellowish solid precipitates. The reaction solution is stirred over 20 h. The supernatant is decanted. The solid is washed with 10 mL *n*-hexane and dried *in vacuo*. **C21a** crystallizes as yellow needles upon storing a saturated solution in CH₂Cl₂ at - 28°C.

Yield:	72 mg (57%, powder, M = 506 g/mol).
¹H NMR (CDCl₃):	δ [ppm] = 2.34 (m, 4H, ¹ J _{BH} = 130 Hz, PH ₂ B <u>H</u> ₂), 2.76 (s, 18H, N(CH ₃) ₃), 2.82 (m, 4H, ¹ J _{PH} = 280 Hz, P <u>H</u> ₂ BH ₂).
¹¹B NMR (CDCl₃):	δ [ppm] = - 7.52 (m, br, ¹ J _{BP} = 32 Hz, ¹ J _{BH} = 130 Hz, PH ₂ <u>B</u> H ₂).
¹¹B{¹H} NMR (CDCl₃):	δ [ppm] = - 7.52 (m, br, ¹ J _{BP} = 32 Hz, PH ₂ <u>B</u> H ₂).
³¹P NMR (CDCl₃):	δ [ppm] = - 170.34 (m, ¹ J _{PB} = 32 Hz, ¹ J _{PH} = 280 Hz, P <u>H</u> ₂ BH ₂).
³¹P{¹H} NMR (CDCl₃):	δ [ppm] = - 170.34 (m, ¹ J _{PB} = 32 Hz, <u>P</u> H ₂ BH ₂).
LIFDI MS (CH₂Cl₂):	<i>m/z</i> : 504 [M] ⁺ .
EA:	calculated for C ₁₀ H ₂₆ B ₂ N ₂ O ₄ WP ₂ C: 23.75 %; H: 5.18 %; N: 5.54 % found: C: 23.99 %; H: 5.13 %; N: 5.43 %.
IR (KBr):	$\tilde{\nu}$ [cm ⁻¹] = 3011 (vw, C-H), 2922 (w, C-H), 2847 (vw), 2402 (vw, P-H), 2360 (s, B-H), 2341 (s, B-H), 2002 (m), 1870 (s, C-O), 1825 (s, C-O), 1733 (w), 1717 (w), 1700 (w), 1684 (w), 1684 (w), 1652 (w), 1635 (w), 1558 (w), 1540 (w), 1521 (w), 1506 (w), 1457 (w, CH), 1258 (w), 1124 (w), 1089 (w), 1056 (w), 867 (w), 790 (w), 668 (w), 580 (w).

Synthesis of (OC)₄W(AsH₂BH₂NMe₃)₂ (C21b):

To a solution of 194 mg (OC)₄W(nbd) (0.5 mmol) in 20 mL toluene 1 mL of a 1 M solution of AsH₂BH₂NMe₃ (1mmol) in toluene is added at room temperature. After 30 min a color change from yellow to brown is observed and a yellowish solid precipitates. After stirring over 20 h the supernatant is decanted. The solid is washed

with 20 mL *n*-hexane and dried *in vacuo*. **C21b** crystallizes as yellow needles upon storing a saturated solution in CH₂Cl₂ at - 28°C.

Yield: m = 72 mg (49%, powder, M = 594 g/mol).

¹H NMR (CDCl₃): δ [ppm] = 1.51 (m, 4H, AsH₂BH₂), 2.51 (m, 4H, ¹J_{BH} = 112 Hz, AsH₂BH₂), 2.81 (s, 9H, N(CH₃)₃).

¹¹B NMR(CDCl₃): δ [ppm] = - 7.36 (t, ¹J_{BH} = 112 Hz, AsH₂BH₂).

¹¹B{¹H} NMR(CDCl₃): δ [ppm] = - 7.36 (s, AsH₂BH₂).

¹³C{¹H} NMR(CDCl₃): δ [ppm] = 53.65 (s, N(CH₃)₃), 204.26 (s, ¹J_{CW} = 63 Hz, C=O), 209.58 (s, ¹J_{CW} = 83 Hz, C=O).

LIFDI MS (CH₂Cl₂): *m/z*: 592 [M]⁺.

EA: calculated for C₁₀H₂₆As₂N₂O₄WP₂
C: 20.23 %; H: 4.41 %; N: 4.71 %
found: C: 20.52 %; H: 4.49 %; N: 4.54 %.

IR (KBr): $\tilde{\nu}$ [cm⁻¹] = 2955 (vw, C-H), 2911 (vw, C-H), 2845 (vw), 2359 (m, B-H), 2330 (m, B-H), 2114 (vw, As-H), 2001 (vw), 1868 (vs, C=O), 1824 (vs, C=O), 1771 (vw), 1733 (w), 1716 (w), 1699 (w), 1683 (m), 1669 (w), 1652 (w), 1635 (w), 1575 (vw), 1558 (m), 1540 (w), 1521 (w), 1506 (m), 1472 (w), 1456 (m), 1436 (w), 1414 (w), 1116 (w), 1068 (w), 845 (w), 687 (w), 668 (w), 419 (w).

Synthesis of (OC)₃Mo(PH₂BH₂NMe₃)₃ (**C22**):

To a solution of 82 mg (OC)₃Mo(cho) (0.3 mmol) in thf 2 mL of a 0.5 M solution of PH₂BH₂NMe₃ (1 mmol) in toluene is added at room temperature. The color changed immediately from deep red to orange after addition. The solution is stirred over 20 h and an orange solid precipitates. The solvent is removed *in vacuo* and the remaining solid is washed with two times 10 mL toluene. **C22** crystallizes as colorless prisms by layering a saturated solution in thf with four times of the volume *n*-hexane. NMR (CD₂Cl₂), IR (KBr), MS (FD), EA and X-ray diffraction analysis data is presented in the Dissertation of C. Thoms, Regensburg 2012, who synthesized this compound first by reaction of [CpMo(CO)₃H] with PH₂BH₂NMe₃.

Yield: 83 mg (52%, powder; M = 497 g/mol).

¹H NMR (thf-d⁸): δ [ppm] = 2.22 (m, 6H, ¹J_{PH} = 265 Hz, PH₂BH₂), 2.25 (m, 6H, PH₂BH₂), 2.77 (s, 27H, N(CH₃)₃).

^{11}B NMR (thf- d^8):	δ [ppm] = - 7.95 (m, br, PH_2BH_2).
$^{11}\text{B}\{^1\text{H}\}$ NMR (thf- d^8):	δ [ppm] = - 7.95 (s, br, PH_2BH_2).
^{31}P NMR (thf- d^8):	δ [ppm] = - 135.19 (t, br, $^1J_{\text{PH}} = 265$ Hz, PH_2BH_2).
$^{31}\text{P}\{^1\text{H}\}$ NMR (thf- d^8):	δ [ppm] = - 135.19 (s, br, PH_2BH_2).

Crystallographic Data:

All structures were solved using SHELXT^[4] and OLEX.^[5] Least square refinements against F^2 in anisotropic approximation were done using SHELXL.^[4] The hydrogen positions of the methyl groups were located geometrically and refined riding on the carbon atoms. **C21a**, **C21b** and **C22** were measured on a SuperNova with an Atlas detector. Gaussian absorption correction was applied for **C21a** and **C22**, analytical absorption correction for **C21b**. Hydrogen atoms belonging to BH_2 , PH_2 and AsH_2 groups were located from the difference Fourier map and refined without constraints (**C21a**, **C21b**, **C22**).

C21a crystallizes by storing a saturated solution in CH_2Cl_2 at -28°C as yellow needles in the monoclinic space group $P2_1/n$. **Figure 3** shows the molecular structure in solid state.

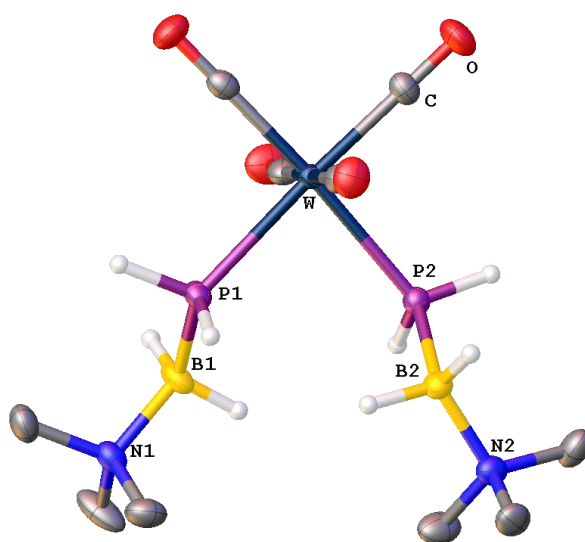


Figure 3: Molecular structure of **C21a** in the solid state. Thermal ellipsoids are drawn with 50% probability. Hydrogen atoms bound to Carbon are omitted for clarity. Selected bond lengths [Å] and angles [°]: P-B = 1.951(4) - 1.962(3), P-W = 2.5363(7) - 2.5408(7); P1-W-P2 = 85.44(2); N-B-P = 115.4(2) - 115.7(2).

C21b crystallizes by storing a saturated solution in CH_2Cl_2 at -28°C as colorless blocks in the monoclinic space group $P2_1/n$. **Figure 4** shows the molecular structure in solid state. All crystals of **C21b** showed twinning and were refined applying hklf5 refinement.

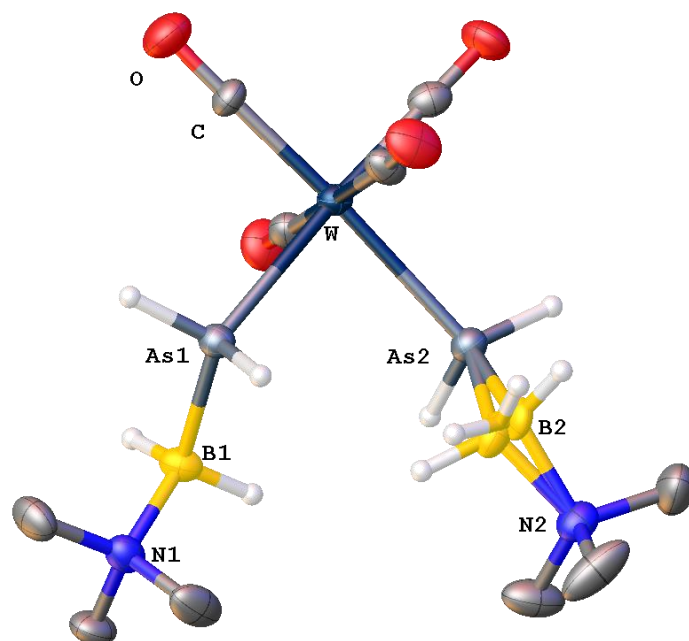


Figure 4: Molecular structure of **C21b** in the solid state. Thermal ellipsoids are drawn with 50% probability. Hydrogen atoms bound to Carbon are omitted for clarity. Selected bond lengths [Å] and angles [°]: As-B = 2.064(17) - 2.072(9), As-W = 2.6353(9) - 2.6337(9); As1-W-As2 = 84.56(3); N-B-As = 114.5(14) - 115.0(6).

Table 1: Crystallographic Data of **C21a/b**.

	C21a	C21b
Formula	C ₁₀ H ₂₆ B ₂ N ₂ O ₄ P ₂ W	C ₁₀ H ₂₆ As ₂ B ₂ N ₂ O ₄ W
$D_{calc.}/\text{g cm}^{-3}$	1.720	1.964
μ/mm^{-1}	12.621	14.431
Formula Weight	505.74	593.64
Colour	clear yellow	colourless
Shape	block	block
Size/mm ³	0.29×0.11×0.08	0.30×0.09×0.06
T/K	123.00(10)	123.00(10)
Crystal System	monoclinic	monoclinic
Space Group	$P2_1/n$	$P2_1/n$
$a/\text{\AA}$	9.5756(2)	9.7332(2)
$b/\text{\AA}$	11.9386(3)	12.0019(3)
$c/\text{\AA}$	17.0963(5)	17.1944(5)
$\alpha/^\circ$	90	90
$\beta/^\circ$	92.201(2)	91.403(3)
$\gamma/^\circ$	90	90
$V/\text{\AA}^3$	1952.99(9)	2007.99(9)
Z	4	4
Z'	1	1
Wavelength $\lambda/\text{\AA}$	1.54184	1.54184
Radiation type	CuK α	CuK α
$\theta_{min}/^\circ$	4.518	4.493
$\theta_{max}/^\circ$	73.788	73.728
Measured Refl.	6618	7066
Independent Refl.	3758	7066
Reflections Used	3572	6278
R_{int}	0.0158	/
Parameters	228	218
Restraints	0	8
Largest Peak	0.548	1.827
Deepest Hole	-0.950	-1.717
GooF	1.115	1.043
wR_2 (all data)	0.0522	0.1648
wR_2	0.0514	0.1608
R_1 (all data)	0.0212	0.0672
R_1	0.0197	0.0630

7.2 Synthesis of alkyl-substituted Lewis base stabilized phosphanylboranes

Monomeric pnictogenyltrialanes, $R_2EE'R'_2$ (E = pnictogen; E' = triele; R = H, alkyl, aryl; R' = H, alkyl, aryl) are highly reactive compounds due to the lone pair on the pnictogen atom and the vacant p-orbital on the triele atom. These unstable compounds, can be either handled under cryogenic conditions, like the parent azaborane $[H_2N=BH_2]$ ^[6], or be stabilized by appropriate electronical^[7] or sterical^[8] moieties/substituents under ambient conditions. In contrast the parent azaborane, the free parent phosphanylborane $[H_2P-BH_2]$ was not observed experimentally, yet. However, an isolation was achieved by donor-acceptor stabilization through the combination of a LB/LA.^[7] The synthetic pathway could be further improved to an only LB stabilization and was subsequently expanded to heavier homologues, the arsanylborane^[9] and stibanylborane.^[10]

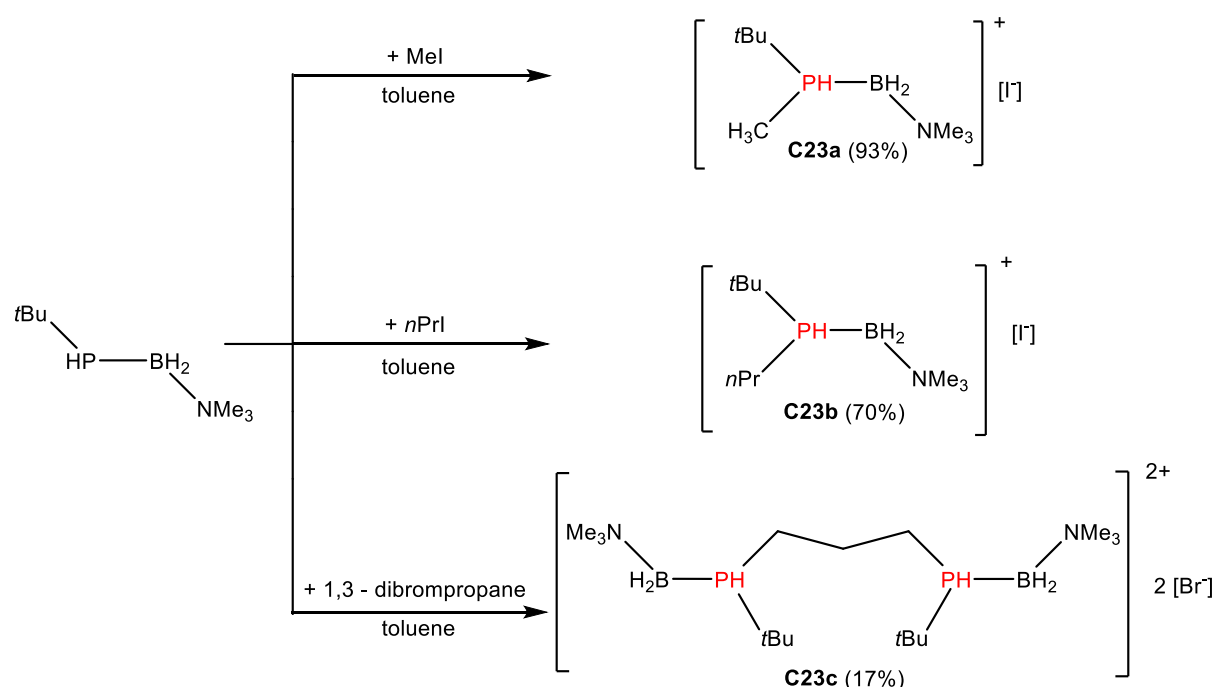
Thermal activation of phosphanylboranes, $R_2PBH_2NMe_3$, leads to an elimination of the LB and a head-to-tail polymerization occurs. Depending on the substituents on the P atom, the molecular weight differs significantly, resulting in either oligomeric material, like $[Ph_2P-BH_2]_n$ ($n < 6$), or in high molecular weight polymers, such as $[tBuPH-BH_2]_n$ ($n = 1900 - 2150$).^[11] Through introduction of a second alkyl substituent on the P atom, the donor strength as well as the sterical demand should be further increased. This might lead to a different polymerization behavior, resulting in different chain lengths and tacticity. Besides the well-established salt metathesis route, *Stauber* described another synthetic pathway to monoalkylated phosphanylboranes. By reaction of alkylhalides with $H_2PBH_2NMe_3$, the corresponding phosphonium salts are accessible in good yields. These can further be deprotonated with LiN/Pr_2 resulting in monoalkylated phosphanylboranes like $MePHBH_2NMe_3$.^[12] So far, there are no examples for LB stabilized phosphanylboranes with two alkyl-substituents on the P atom.

The reaction of $tBuPHBH_2NMe_3$ with different alkylhalides (MeI; nPr I; 1,3-dibromopropane) leads to the corresponding phosphonium salts (**Scheme 2**). The reactions to $(tBuMePHBH_2NMe_3)I$ (**C23a**) and $(tBuPrPHBH_2NMe_3)I$ (**C23b**) proceed selectively and in good yields according to ^{31}P NMR spectroscopy. Contrary, in the ^{31}P and ^{11}B NMR spectra of the reaction solution of $\{(Me_3NH_2BHPtBu)nPr(tBuPHBH_2NMe_3)\}(Br)_2\}$ (**C23c**) unknown side products are

observed, lowering the overall yield to about 40%. The resonance signals of the P atoms appear downfield shifted compared to the starting material, whereas the signals for the BH₂-moiety shifts to highfield (**Table 2**).

Table 2: ¹¹B and ³¹P NMR signals for **C23-C24**.

Compound	³¹ P NMR shift	¹¹ B NMR shift
C23a	δ = -15.70 ppm	δ = -10.30 ppm
C23b	δ = -7.35 ppm	δ = -11.05 ppm
C23c	δ = -10.35 ppm	δ = -10.87 ppm
C24	δ = -53.38 ppm	δ = -1.58 ppm



Scheme 2: Syntheses of compounds **C23a**, **C23b** and **C23c**. Isolated yields are given in parentheses.

It is noteworthy, that all phosphonium salts exhibit stereocenters on the phosphorus atoms. However, only for **C23c** different signals in the ¹³C{¹H} NMR spectrum, provoked by the different stereoisomers (*R,R'*; *S,S'*; *meso*), are observed. The molecular structures in solid state of **C23a-c** were determined by single crystal X-ray diffraction analysis. The molecular structure of **C23a** shows the *S* stereoisomer, whereas both *R* and *S* stereoisomers are observed for **C23b**. All bond lengths are in the range of single bonds. The B-P bond length in (**C23a**) amounts to 1.968(4) Å and the P exhibits a tetrahedral environment ∠(C1-P-C2) = 109.7(2)°; **Figure 5**. Although substituted by the sterically more hindered *n*Pr-group, this is also observed for (**C23b**)

(P-B = 1.953(5) Å, $\angle(\text{C1-P-C2}) = 108.7(2)^\circ$). However, the B-P axis in **C23a** shows an antiperiplanar arrangement, whereas in **C23b** an anticlinal arrangement is observed (**Figure 5**). The molecular structure of **C23c** shows only the meso form. An anticlinal arrangement is presented along the B-P axis and the tetrahedral environment on the P atom is slightly distorted ($\angle(\text{C-P-C}) = 104.6(9) - 104.8(10)^\circ$; **Figure 5**).

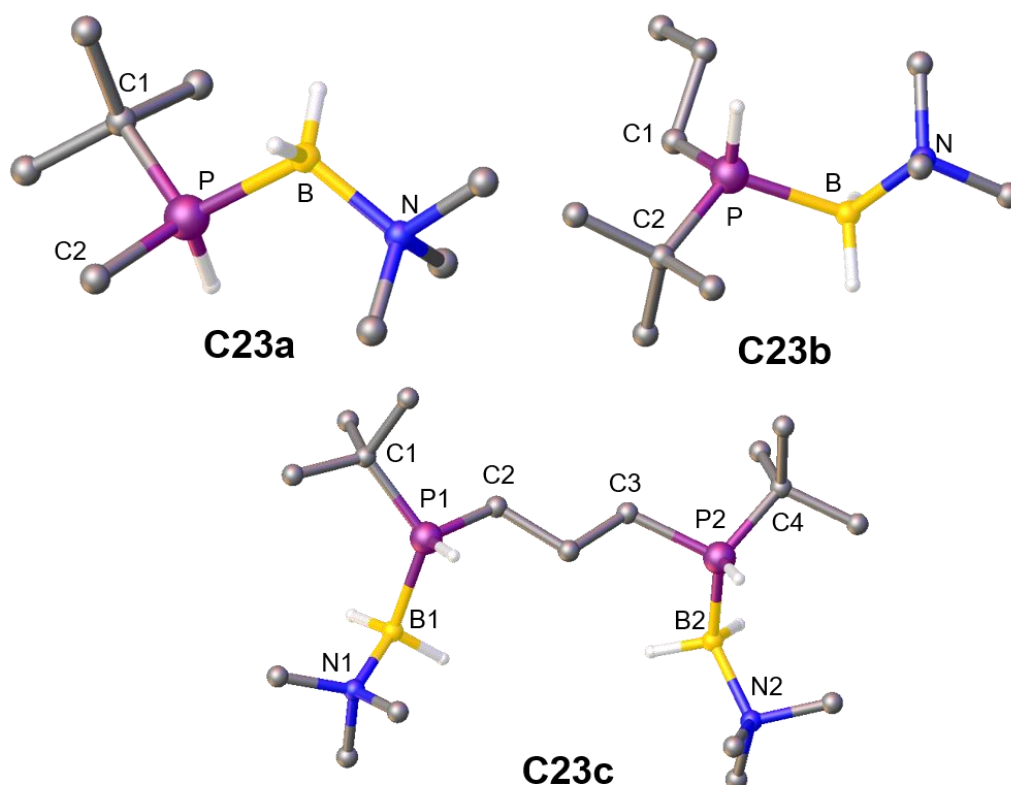
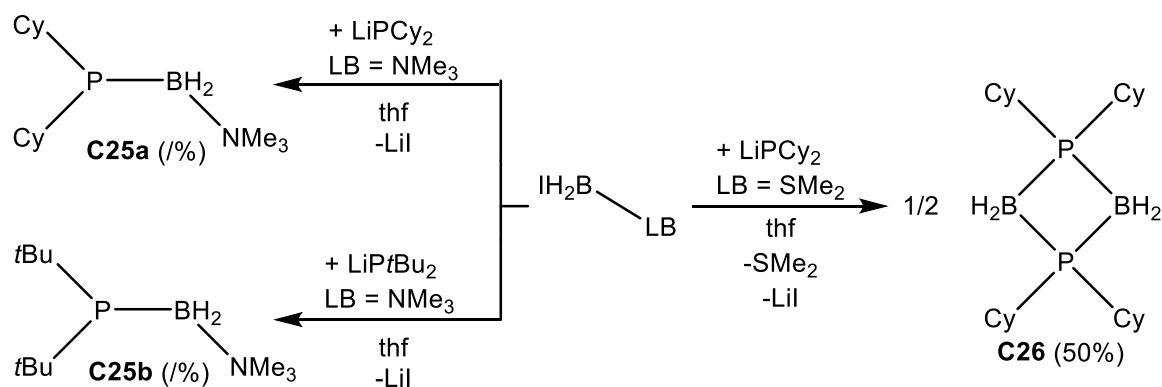


Figure 5: Molecular structure of **C23a** (top left), **C23b** (top right) and **C23c** (bottom) in solid state. Hydrogen atoms bound to carbon and counter-anions are omitted for clarity. Thermal ellipsoids are drawn with 50% probability.

Deprotonation of **C23a** with KH in CH₃CN at -40°C leads *t*BuPMeBH₂NMe₃ (**C24**). The reaction proceeds quantitatively according to ¹¹B and ³¹P NMR spectroscopy, however, due to the very good solubility of smallest impurities and **C24**, crystallization is necessary lowering the yield. **C23b** and **C23c** can be deprotonated by KH as well, but only **C24** is included in this thesis, as it was characterized completely. In accordance to previous results,^[9] the signal of the P atom is highfield shifted to $\delta = -53.38$ ppm through deprotonation and the resonance of the boron atom is downfield shifted to $\delta = -1.58$ ppm. The molecular structure in the solid state (**Figure 6**) reveals an antiperiplanar arrangement along the B-P bond and a P-B bond length of P-B = 2.003(2) Å.

The reaction of IBH_2NMe_3 with LiPCy_2 ^[12] (Cy = cyclohexyl-) or LiP^tBu_2 ^[13] yields the LB stabilized phosphanylboranes $\text{Cy}_2\text{PBH}_2\text{NMe}_3$ (**C25a**) and $^t\text{Bu}_2\text{PBH}_2\text{NMe}_3$ (**C25b**), respectively (**Scheme 3**). The synthesis of **C25b** proceeds in about 55 % yield according to ^{31}P NMR spectroscopy, whereas only 30% yield are observed in the ^{31}P NMR spectrum of the reaction solution **C25a**. As side products, the corresponding phosphines, HPCy_2 and HP^tBu_2 , respectively, could be identified in the ^{31}P NMR spectra. Due to the similar solubility of **C25a/b** and the phosphines, it was not possible to isolate the pure compounds.



Scheme 3: Syntheses of compounds **C25a**, **C25b** and **C26**. Isolated yields are given in parentheses.

However, both compounds were characterized by single crystal X-ray diffraction analysis. Additionally, the molecular structure of the decomposition product $^t\text{Bu}_2\text{PBH}_2^t\text{Bu}_2\text{PBH}_2\text{NMe}_3$ (**C25c**), was determined. **C25a** presents an anticlinal arrangement along the P-B axis (P-B = 1.983(3) Å) with $\angle(\text{N-B-P}) = 111.00(16)^\circ$ and $\angle(\text{C1-P-C2}) = 102.52(10)^\circ$ (**Figure 6**). A similar geometrical orientation is observed for **C25b** in solid state (**Figure 6**). The substituents along the P-B bond show also an anticlinal orientation with P-B = 1.987(3) Å. Whereas the N-B-P angle is quite similar compared to **C25a** (N-B-P = 111.72(17)°), the C1-P-C1' angle differs (C1-P-C1' = 109.952). In accordance with previous results (Chapter 3, $(\text{H}_2\text{PBH}_2)_2\text{NMe}_3$), the decomposition product **C25c** can be seen as an intermediate and is probably the first step to an oligomeric material. The molecular structure of **C25c** in solid state reveals an antiperiplanar arrangement along the P1-B1 axis and a synperiplanar orientation along the B1-P1 and B2-P2 bond resulting in a snap-off zigzag structure (**Figure 6**). All bonds are in the range of single bonds, however, the B-P bond lengths are slightly elongated (B-P = 2.004(3) – 2.009(3) Å) compared to **C25b**.

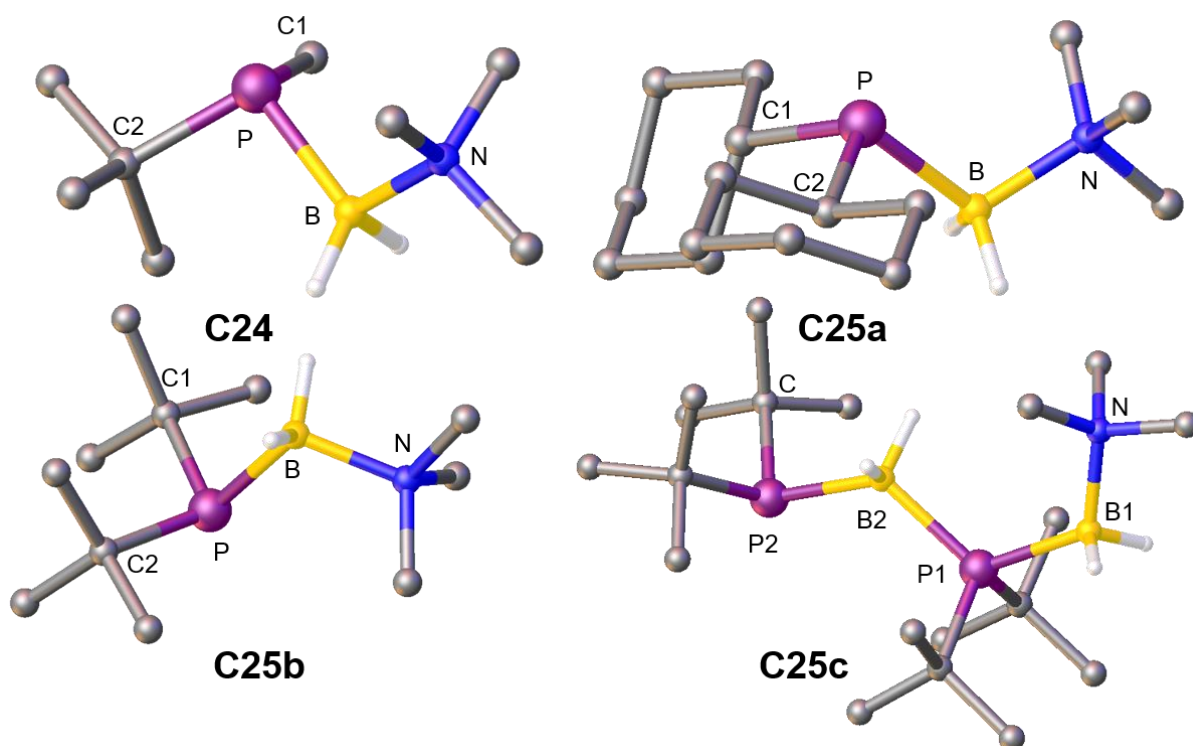


Figure 6: Molecular structures of **C24** (top left), **C25a** (top right), **C25b** (bottom left) and **C25c** (bottom right). Hydrogen atoms are omitted for clarity. Thermal ellipsoids are drawn with 50% probability.

The reaction of IBH_2SMe_2 with LiPCy_2 ^[12] in thf leads to $(\text{Cy}_2\text{PBH}_2)_2$ (**C26**) in moderate yields. This compound features a four-membered ring motif. The reaction mechanism probably includes the formation of $\text{Cy}_2\text{PBH}_2\text{SMe}_2$ as an intermediate, which undergoes dimerization and elimination of the weak LB SMe_2 . The resonance signals of the B and P nuclei are broadened in the ^{11}B and ^{31}P NMR spectra, respectively. The resonance signal of the P atoms appear at $\delta = -10.88$ ppm ($\omega_{1/2} = 483$ Hz) in the $^{31}\text{P}\{^1\text{H}\}$ NMR spectrum, which is further broadened in the ^{31}P NMR spectrum ($\omega_{1/2} = 530$ Hz). The signal of the B atoms is observed in the typical range of oligomeric or polymeric material^[10] at $\delta = -32.57$ ppm. The signals of the cyclohexyl-substituents arise at $\delta = 1.06 - 2.36$ ppm and the signals of the BH_2 -moieties at $\delta = 1.90$ ppm as broad multiplett in the ^1H NMR spectrum.

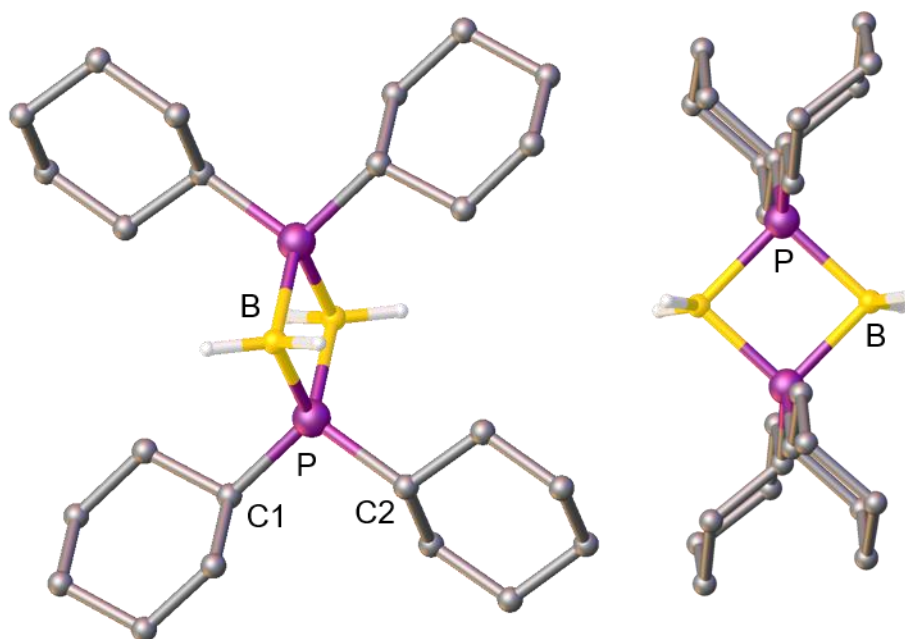


Figure 7: Molecular structures of **C26** in solid state. Hydrogen atoms bound to Carbon are omitted for clarity. Thermal ellipsoids are drawn with 50% probability.

The molecular structure of **C26** was determined by single crystal X-ray diffraction analysis (**Figure 7**). The P-B bond distance B-P = 1.9874(16) Å corresponds to a P-B single bond. The slightly distorted square-planar conformation shows a P-B-P angle with P-B-P = 88.144° and B-P-B angle with B-P-P = 91.856°. The P-P distance P-P = 2.766 Å and the B-B distance B-B = 2.858 Å are below the van der Waals radii ($\Sigma r(\text{P})^{\text{vdW}} = 3.60 \text{ Å}^{[14]}$; $r(\text{B})^{\text{vdW}} = 3.84 \text{ Å}^{[15]}$). Most likely, interactions between the P and B atoms take place, however, calculations still have to be done. In addition, by irradiation with UV-light ($\lambda = 366 \text{ nm}$) **C26** shows slightly blue luminescence as a solid as well as in solution. Further, green luminescence was observed by irradiation ($\lambda = 366 \text{ nm}$) of the starting material LiPCy₂. However, luminescent measurements still have to be conducted to get further insights into the electronic properties of this unique compound.

Experimental Section:

Synthesis of [(*t*BuMePHBH₂NMe₃)(I)] (**C23a**):

To a solution of 365 mg *t*BuPHBH₂NMe₃ (2.28 mmol) in 15 mL toluene 0.3 mL MeI (3.32 mmol) is added at room temperature. A white solid precipitates immediately. The solution is stirred for 20 h. The supernatant is decanted and the remaining solid is washed with 30 mL *n*-hexane. **C23a** crystallizes as colorless blocks upon layering a thf/MeCN solution (5:1) with three times of the volume of *n*-hexane.

Yield:	640 mg (93%, powder, M = 303 g/mol).
^1H NMR (CD_3CN):	δ [ppm] = 1.24 (d, 9H, $^3J_{\text{HP}} = 16$ Hz, $\text{C}(\text{CH}_3)_3$), 1.58 (dd, 3H, $^2J_{\text{HP}} = 12$ Hz, $^3J_{\text{HH}} = 6$ Hz, CH_3), 2.15 (m, 2H, BH_2), 2.83 (s, 9H, $\text{N}(\text{CH}_3)_3$), 5.47 (m, 1H, $^1J_{\text{PH}} = 396$ Hz, $^3J_{\text{HH}} = 6$ Hz, PH).
^{11}B NMR (CD_3CN):	δ [ppm] = - 10.30 (dt, $^1J_{\text{BP}} = 78$ Hz, $^1J_{\text{BH}} = 113$ Hz).
$^{11}\text{B}\{^1\text{H}\}$ NMR (CD_3CN):	δ [ppm] = - 10.30 (d, $^1J_{\text{BP}} = 78$ Hz).
$^{13}\text{C}\{^1\text{H}\}$ NMR (CD_3CN):	δ [ppm] = 26.24 (s, CH_3), 26.25 (s, $\text{C}(\underline{\text{C}}\text{H}_3)_3$), 27.71 (d, $^1J_{\text{CP}} = 40$ Hz, $\underline{\text{C}}(\text{CH}_3)_3$), 54.98 (d, $^3J_{\text{CP}} = 6$ Hz, $\text{N}(\text{CH}_3)_3$).
^{31}P NMR (CD_3CN):	δ [ppm] = - 15.70 (q, $^1J_{\text{PB}} = 78$ Hz).
$^{31}\text{P}\{^1\text{H}\}$ NMR (CD_3CN):	δ [ppm] = - 15.70 (m, br, $^1J_{\text{PH}} = 396$ Hz).
ES-MS (CH_3CN):	m/z (cation): 176 [$(t\text{BuMePHBH}_2\text{NMe}_3)^+$].
EA:	calculated for $\text{C}_8\text{H}_{24}\text{BPNI}$ C: 31.71%, H: 7.98%, N: 4.62%. found: C: 31.92%, H: 7.67%, N: 4.59%.
IR (KBr):	$\tilde{\nu}$ [cm^{-1}] = 2963 (m, C-H), 2949 (m, C-H), 2918 (w), 2863 (m), 2460 (m, P-H), 2414 (m), 2323 (m, B-H), 1481 (m), 1412 (w), 1375 (vw), 1298 (w), 1249 (w), 1192 (vw), 1165 (vw), 1142 (s), 1092 (m), 1034 (w), 1015 (w), 987 (vw), 945 (vw), 911 (w), 876 (w), 856 (m), 821 (w), 755 (vw), 702 (vw).

Synthesis of [$(t\text{BuPrPHBH}_2\text{NMe}_3)(\text{I})$] (**C23b**):

To a solution of 400 mg $t\text{BuPHBH}_2\text{NMe}_3$ (2.5 mmol) in 20 mL toluene 0.3 mL $n\text{PrI}$ (3 mmol) is added at room temperature. The solution is stirred for 20 h. All volatiles are removed *in vacuo* and the remaining solid is washed with 15 mL n -hexane. **C23b** crystallizes as colorless prisms upon layering a thf/MeCN solution (5:1) with three times of the volume of n -hexane.

Yield:	630 mg (70%, powder, M = 429 g/mol).
^1H NMR (CD_3CN):	δ [ppm] = 1.07 (td, 3H, $^3J_{\text{HH}} = 7$ Hz, $^4J_{\text{HH}} = 1$ Hz, CH_3), 1.27 (d, 9H, $^3J_{\text{HP}} = 16$ Hz, $\text{C}(\text{CH}_3)_3$), 1.57-2.13 (m, 4H, CH_2), 2.40 (m, 2H, BH_2), 2.81 (d, 9H, $^4J_{\text{HP}} = 1$ Hz, $\text{N}(\text{CH}_3)_3$), 5.29 (m, 1H, $^1J_{\text{PH}} = 380$ Hz, $^3J_{\text{HH}} = 3$ Hz, PH).
^{11}B NMR (CD_3CN):	δ [ppm] = - 11.05 (dt, $^1J_{\text{BP}} = 73$ Hz, $^1J_{\text{BH}} = 110$ Hz).
$^{11}\text{B}\{^1\text{H}\}$ NMR (CD_3CN):	δ [ppm] = - 11.05 (d, $^1J_{\text{BP}} = 73$ Hz).

$^{13}\text{C}\{^1\text{H}\}$ NMR (CD_3CN):	δ [ppm] = 14.74 (d, $^2J_{\text{CP}} = 14$ Hz, CH_2), 18.02 (d, $^1J_{\text{CP}} = 35$ Hz, $\text{H}_2\text{C-P}$), 18.28 (d, $^3J_{\text{CP}} = 4$ Hz, CH_3), 25.84 (d, $^2J_{\text{CP}} = 1$ Hz, $\text{C}(\underline{\text{CH}}_3)_3$), 27.75 (d, $^1J_{\text{CP}} = 38$ Hz, $\underline{\text{C}}(\text{CH}_3)_3$), 54.09 (d, $^3J_{\text{CP}} = 6$ Hz), $\text{N}(\text{CH}_3)_3$.
^{31}P NMR (CD_3CN):	δ [ppm] = - 7.35 (q, $^1J_{\text{PB}} = 73$ Hz).
$^{31}\text{P}\{^1\text{H}\}$ NMR (CD_3CN):	δ [ppm] = - 7.35 (m, br, $^1J_{\text{PH}} = 380$ Hz).
ES-MS (CH_3CN):	m/z (cation): 535 [$\{(\text{tBuPrPHBH}_2\text{NMe}_3)_2(\text{I})\}^+$], 204 [$(\text{tBuPrPHBH}_2\text{NMe}_3)^+$].
EA:	calculated for $\text{C}_{10}\text{H}_{28}\text{BPNI}$ C: 36.28%, H: 8.52%, N: 4.23%. found: C: 36.05%, H: 8.33%, N: 3.99%.
IR (KBr):	$\tilde{\nu}$ [cm^{-1}] = 2994(w, C-H), 2958 (s, C-H), 2870 (m), 2736 (vw), 2452 (m, P-H), 2399 (w), 2286 (m, B-H), 1473 (s), 1417 (w), 1373 (w), 1247 (w), 1196 (vw), 1162 (w), 1138 (s), 1096 (m), 1054 (m), 1029 (w), 978 (w), 910 (vw), 861 (s), 820 (w), 771 (vw), 719 (vw).

Synthesis of [$\{(\text{Me}_3\text{NH}_2\text{BHP}(\text{tBu})n\text{Pr}(\text{tBuPHBH}_2\text{NMe}_3)\}(\text{Br})_2$] (**C23c**):

To a solution of 240 mg $\text{tBuPHBH}_2\text{NMe}_3$ (1.5 mmol) in 15 mL toluene 0.075 mL (0.75 mmol) $\text{C}_3\text{H}_6\text{Br}_2$ is added at room temperature. The solution is stirred for 3 d and a white solid precipitates. All volatiles are removed *in vacuo* and the remaining solid is washed with 15 mL toluene. **C23c** crystallizes as colorless plates upon layering a saturated CH_2Cl solution with four times of the volume of *n*-hexane.

Yield:	65 mg (17%, powder, $M = 621$ g/mol).
^1H NMR (CD_3CN):	δ [ppm] = 1.29 (d, 18H, $^3J_{\text{HP}} = 16$ Hz, $\text{C}(\text{CH}_3)_3$), 2.01-2.41 (m, 6H, CH_2), 2.27-2.61 (m, 4H, BH_2), 2.89 (s, 9H, $\text{N}(\text{CH}_3)_3$), 6.41 (m, 1H, $^1J_{\text{PH}} = 390$ Hz, PH).
^{11}B NMR (CD_3CN):	δ [ppm] = - 10.87 (s, br, $\omega_{1/2} = 505$ Hz).
$^{11}\text{B}\{^1\text{H}\}$ NMR (CD_3CN):	δ [ppm] = - 10.87 (s, br, $\omega_{1/2} = 648$ Hz).
$^{13}\text{C}\{^1\text{H}\}$ NMR (CD_3CN):	δ [ppm] = 18.60 (d, $^1J_{\text{CP}} = 35$ Hz, $\text{H}_2\text{C-P}$), 21.81 (t, $^3J_{\text{CP}} = 3$ Hz, CH_2), 26.84 (d, $^2J_{\text{CP}} = 1$ Hz, $\text{C}(\underline{\text{CH}}_3)_3$), 28.79 (d, $^1J_{\text{CP}} = 38$ Hz, $\underline{\text{C}}(\text{CH}_3)_3$), 55.12 (d, $^3J_{\text{CP}} = 6$ Hz), $\text{N}(\text{CH}_3)_3$.
^{31}P NMR (CD_3CN):	δ [ppm] = - 10.35 (m, br, $^1J_{\text{PB}} = 70$ Hz).
$^{31}\text{P}\{^1\text{H}\}$ NMR (CD_3CN):	δ [ppm] = - 10.35 (m, br, $^1J_{\text{PH}} = 390$ Hz).

EI-MS (CH ₃ CN):	<i>m/z</i>	(cation):
	443	[{(Me ₃ NH ₂ BHP <i>t</i> Bu) <i>n</i> Pr(<i>t</i> BuPHBH ₂ NMe ₃)Br)} ⁺],
	363	[{(Me ₃ NH ₂ BP <i>t</i> Bu) <i>n</i> Pr(<i>t</i> BuPHBH ₂ NMe ₃)Br)} ⁺],
	182	[(Me ₃ NH ₂ BHP <i>t</i> Bu) <i>n</i> Pr(<i>t</i> BuPHBH ₂ NMe ₃) ²⁺].

Synthesis of *t*BuMePBH₂NMe₃ (**C24**):

To a solution of 909 mg **C23a** (3 mmol) in 25 mL CH₃CN 120 mg (3 mmol) KH is added as a solid at -40°C. The solution is stirred at -40°C until all solid disappears. All volatiles are removed *in vacuo* and the remaining white solid is dissolved in 20 mL *n*-hexane. After filtration over diatomaceous earth the solvent is removed *in vacuo*. **C24** crystallizes as colorless blocks upon storing a saturated solution in *n*-hexane at -30°C.

Yield: 287 mg (55%, crystalline, M = 175 g/mol).

¹H NMR (C₆D₆): δ [ppm] = 1.34 (s, br, 3H, CH₃), 1.41 (d, 9H, ³J_{HP} = 11 Hz, C(CH₃)₃), 1.95 (s, 9H, N(CH₃)₃), 2.45 (m, 2H, BH₂).

¹¹B NMR (C₆D₆): δ [ppm] = - 1.58 (dt, ¹J_{BP} = 53 Hz, ¹J_{BH} = 102 Hz).

¹¹B{¹H} NMR (C₆D₆): δ [ppm] = - 1.58 (d, ¹J_{BP} = 53 Hz).

¹³C{¹H} NMR (C₆D₆): δ [ppm] = 8.40 (s, ¹J_{CP} = 17 Hz, CH₃), 26.80 (d, ²J_{CP} = 5 Hz, C(CH₃)₃), 29.41 (d, ²J_{CP} = 5 Hz, C(CH₃)₃), 52.05 (d, ³J_{CP} = 12 Hz, N(CH₃)₃).

³¹P NMR (C₆D₆): δ [ppm] = - 53.38 (m, br.).

³¹P{¹H} NMR (C₆D₆): δ [ppm] = - 53.38 (q, br, ¹J_{PB} = 53 Hz).

LIFDI-MS (toluene): *m/z* (cation): 524 [{Me₃N(H₂BPMet*t*Bu)₄}⁺], 408 [{Me₃N(H₂BPMet*t*Bu)₃}⁺].

EA: calculated for C₈H₂₃BPN

C: 54.80%, H: 13.23%, N: 7.99%.

found: C: 54.66%, H: 12.90%, N: 7.90%.

IR (KBr): $\tilde{\nu}$ [cm⁻¹] = 2941 (m, C-H), 2897 (m, C-H), 2854 (m), 2374 (m, B-H), 2288 (w), 2187 (vw), 1653 (vw), 1485 (m), 1460 (m), 1422 (w), 1400 (w), 1383 (w), 1356 (w), 1253 (w), 1187 (vw), 1152 (w), 1123 (m), 1069 (s), 1014 (w, vw), 954 (vw), 884 (vw), 868 (vw), 842 (s), 817 (w), 681 (w), 637 (vw), 581 (vw), 472 (vw).

Synthesis of $\text{Cy}_2\text{PBH}_2\text{NMe}_3$ (**C25a**):

To a solution of 120 mg (0.59 mmol) LiPCy_2 in 10 mL thf a solution of 100 mg (0.5 mmol) IBH_2NMe_3 in 10 mL thf is added at -80°C . The color of the solution changed from yellow to colorless and the solution is allowed to reach room temperature over 18 h. All volatiles are removed *in vacuo*. The remaining solid is suspended in 10 mL *n*-hexane and filtrated over diatomaceous earth. The volume is reduced to 3 mL. **C25a** crystallizes as colorless plates upon storing a saturated solution of *n*-hexane at -30°C . Due to the similar solubility of decomposition products, it was not possible to obtain the pure **C25a**.

^{11}B NMR (C_6D_6 ; capillary in thf): δ [ppm] = - 4.25 (m, br, $\omega_{1/2}$ = 350 Hz).

$^{11}\text{B}\{^1\text{H}\}$ NMR (C_6D_6 ; capillary in thf): δ [ppm] = - 4.25 (s, br, $\omega_{1/2}$ = 200 Hz).

^{31}P NMR (C_6D_6 ; capillary in thf): δ [ppm] = - 37.29 (m, br).

Synthesis of $t\text{Bu}_2\text{PBH}_2\text{NMe}_3$ (**C25b**):

To a solution of 304 mg (2 mmol) $\text{Li}t\text{Bu}_2\text{P}$ in 10 mL thf a solution of 388 mg (1.95 mmol) IBH_2NMe_3 in 10 mL thf is added at -80°C . The color of the solution changed from yellow to colorless and the solution is allowed to reach room temperature over 18 h. All volatiles are removed *in vacuo*. The remaining white solid is suspended in 45 mL *n*-pentane and filtrated over diatomaceous earth. **C25b** crystallizes as colorless blocks upon storing a saturated solution in *n*-pentane at -30°C . Due to the similar solubility of decomposition products, it was not possible to obtain pure **C25b**. As decomposition product, $(t\text{Bu}_2\text{PBH}_2)_2\text{NMe}_3$ (**C25c**), could be structurally characterized. **C25c** crystallizes as colorless plates.

^1H NMR (C_6D_6): δ [ppm] = 1.21 (m, br, 2H, BH_2), 1.50 (d, 18H, $^3J_{\text{HP}}$ = 11 Hz, $\text{C}(\text{CH}_3)_3$), 1.96 (s, 9H, $\text{N}(\text{CH}_3)_3$).

^{11}B NMR (C_6D_6): δ [ppm] = - 4.18 (dt, $^1J_{\text{BP}}$ = 60 Hz, $^1J_{\text{BH}}$ = 106 Hz).

$^{11}\text{B}\{^1\text{H}\}$ NMR (C_6D_6): δ [ppm] = - 4.18 (d, $^1J_{\text{BP}}$ = 60 Hz).

^{31}P NMR (C_6D_6): δ [ppm] = 8.92 (m, br).

$^{31}\text{P}\{^1\text{H}\}$ NMR (C_6D_6): δ [ppm] = 8.92 (q, br, $^1J_{\text{PB}}$ = 60 Hz).

Synthesis of $(\text{Cy}_2\text{PBH}_2)_2$ (**C26**):

To a solution of 204 mg (1 mmol) LiPCy_2 in 10 mL thf 1 mL of a 1 M solution of IBH_2SMe_2 in toluene is added at -80°C . The solution is allowed to reach room temperature over 18 h and the color changes from yellow to colorless. All volatiles are

removed *in vacuo* and the remaining white solid is dried for 60 min. The solid is suspended in 20 mL *n*-hexane and filtrated over diatomaceous earth. All volatiles are removed and the remaining solid is dried under vacuum. **C26** crystallizes as colorless needles upon storing a saturated solution in toluene at -30°C.

Yield:	104 mg (50%).
¹H NMR (C ₆ D ₆):	δ [ppm] = 1.06-2.36 (m, 44H, Cy), 1.90 (m, 4H, BH ₂).
¹¹B NMR (C ₆ D ₆):	δ [ppm] = - 32.57 (m, br, ω _{1/2} = 605 Hz).
¹¹B{¹H} NMR (C ₆ D ₆):	δ [ppm] = - 32.57 (m, br, ω _{1/2} = 434 Hz).
³¹P NMR (C ₆ D ₆):	δ [ppm] = - 10.88 (m, br, ω _{1/2} = 530 Hz).
³¹P{¹H} NMR (C ₆ D ₆):	δ [ppm] = - 10.88 (m, br, ω _{1/2} = 483 Hz).
LIFDI-MS (toluene):	<i>m/z</i> (cation): 420 [((Cy ₂ PBH ₂) ₂) ⁺].
EA:	calculated for C ₂₄ H ₄₈ B ₂ P ₂
	C: 68.51%, H: 11.24%.
	found: C: 68.04%, H: 11.24%.

Crystallographic Data:

All structures were solved using SHELXT^[3] and OLEX.^[4] Least square refinements against *F*² in anisotropic approximation were done using SHELXL.^[3] The hydrogen positions of the methyl groups were located geometrically and refined riding on the carbon atoms. **C23a**, **C23b**, were measured on a SuperNova with an Atlas detector. **C23c**, **C24**, **C25a**, **C25b** were measured on a GV50 with TitanS2 detector. **C25c** and **C26** were measured on a Gemini ultra with an AtlasS2 detector. Gaussian absorption correction was applied for **C23a**, **C23b**, **C23c**, **C24**, **C25a**, **C25b**, **C25c** and analytical absorption correction for **C26**. All crystals of **C23c** showed twinning.

C23a crystallizes upon layering a thf/MeCN solution (5:1) with three times of the volume of *n*-hexane in the monoclinic space group *P*₂₁/*n* as colorless blocks. **Figure 8** shows the molecular structure of **C23a** in solid state

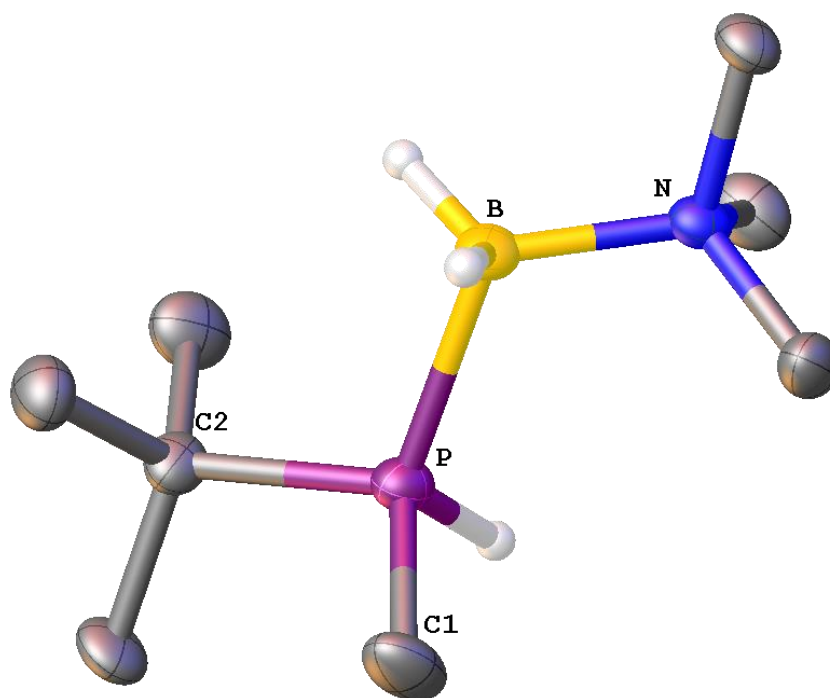


Figure 8: Molecular structure of **C23a** in the solid state. Thermal ellipsoids are drawn with 50% probability. Hydrogen atoms bound to carbon and counter-anions are omitted for clarity. Selected bond lengths [Å] and angles [°]: N-B = 1.593(5), B-P = 1.968(4), C1-P = 1.804(4), C2-P = 1.833(4), N-B-P = 112.4(3), C1-P-C2 = 109.7(2).

C23b crystallizes upon layering a thf/MeCN solution (5:1) with three times of the volume of *n*-hexane as clear colorless prisms in the triclinic space group $P\bar{1}$ with two molecules inside the unit cell. **Figure 9** shows the molecular structure in solid state.

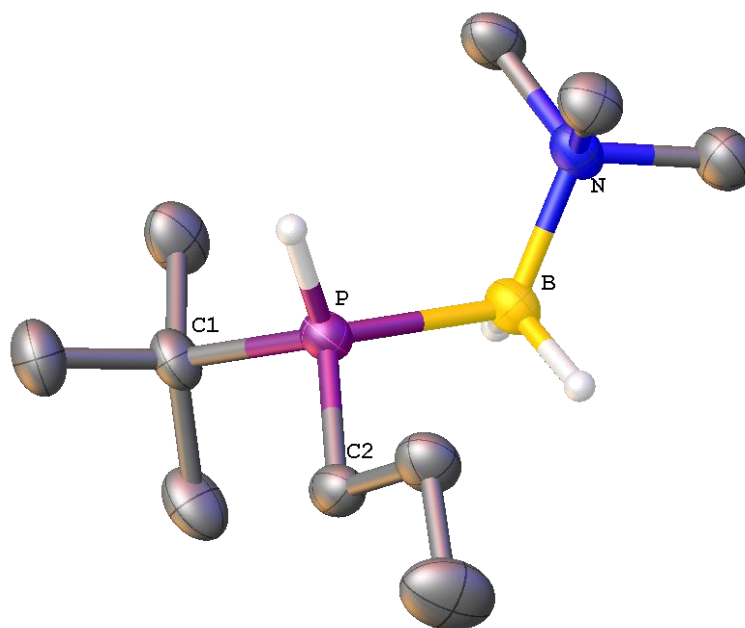


Figure 9: Molecular structure of **C23b** in the solid state. Thermal ellipsoids are drawn with 50% probability. Hydrogen atoms bound to carbon and counter-anions are omitted for clarity. Selected bond lengths [Å] and angles [°]: N-B = 1.604(6), P-B = 1.953(5), C1-P = 1.847(4), C2-P = 1.814(4), N-B-P = 114.1(3), C1-P-C2 = 108.7(2).

C23c crystallizes upon layering a saturated CH_2Cl solution with four times of the volume of *n*-hexane as clear colorless plates in the orthorhombic space group *Pna*2₁. All crystals of **C23c** showed twinning. **Figure 10** shows the molecular structure in solid state.

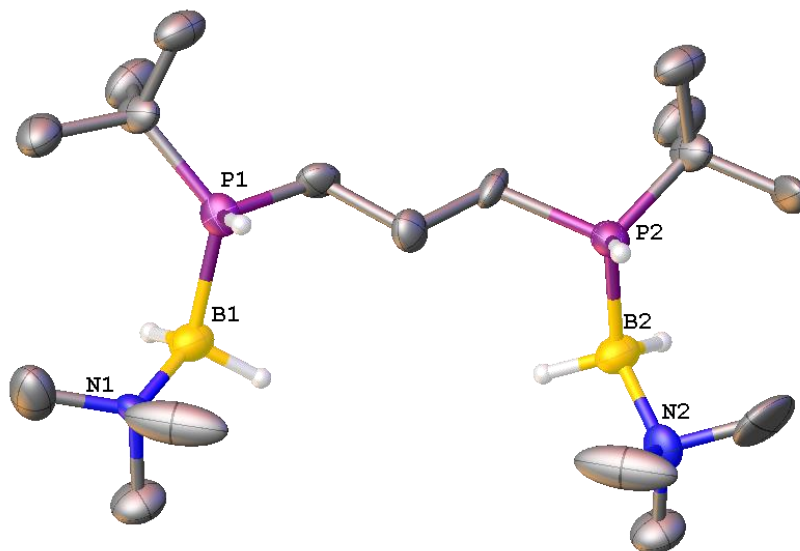


Figure 10: Molecular structure of **C23c** in the solid state. Thermal ellipsoids are drawn with 50% probability. Hydrogen atoms bound to carbon and counter-anions are omitted for clarity. Selected bond lengths [Å] and angles [°]: N-B = 1.56(3)-1.69(4), P-B = 1.91(2)-2.01(2), C-P = 1.70(3)-1.86(2), N-B-P = 116.6(15)-118.2(15), C-P-C = 104.6(9)-104.8(10).

C24 crystallizes upon storing a saturated solution in *n*-hexane at - 30°C as colorless blocks in the orthorhombic space group *Pnma*. **Figure 11** shows the molecular structure in solid state.

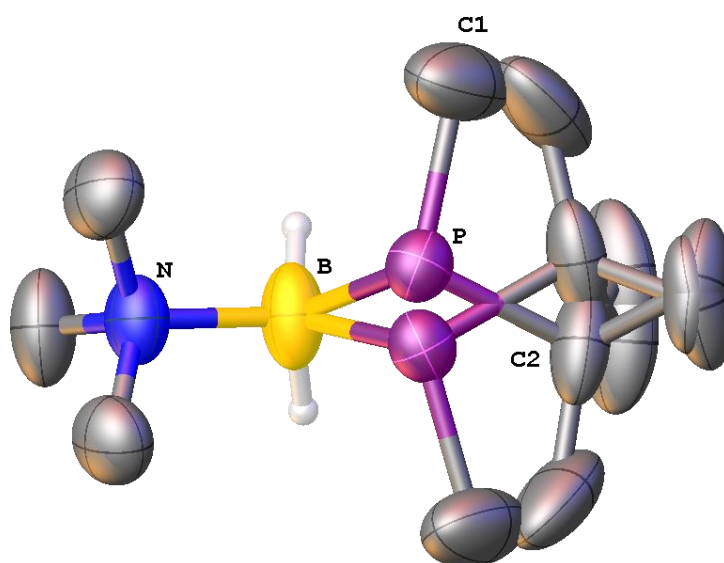


Figure 11: Molecular structure of **C24** in the solid state. Thermal ellipsoids are drawn with 50% probability. Hydrogen atoms bound to carbon are omitted for clarity. Selected bond lengths [Å] and angles [°]: N-B = 1.626(2), B-P = 2.003(2), C1-P = 1.850(4), C2-P = 1.855(2), N-B-P = 109.37(11), C1-P-C2 = 102.5(2).

C25a crystallizes upon storing a saturated solution in *n*-hexane at - 30°C as clear colorless plates in the monoclinic space group $P2_1/n$. **Figure 12** shows the molecular structure in solid state.

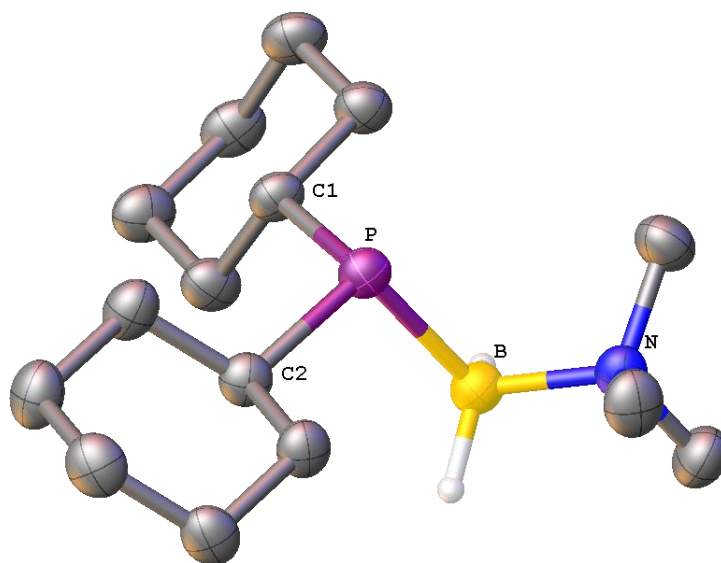


Figure 12: Molecular structure of **C25a** in the solid state. Thermal ellipsoids are drawn with 50% probability. Hydrogen atoms bound to carbon are omitted for clarity. Selected bond lengths [Å] and angles [°]: N-B = 1.644(3), B-P = 1.983(3), C1-P = 1.878(2), C2-P = 1.875(2), N-B-P = 111.00(16), C1-P-C2 = 102.52(10).

C25b crystallizes upon storing a saturated solution in *n*-pentane at - 30°C as colorless blocks in the orthorhombic space group $Cmc2_1$. **Figure 13** shows the molecular structure in solid state. Furthermore, as decomposition product, $(t\text{Bu}_2\text{PBH}_2)_2\text{NMe}_3$ (**C25c**), could be structurally characterized. **C25c** crystallizes as clear colorless plates in the monoclinic space group $P2_1/c$. **Figure 14** shows the molecular structure in solid state.

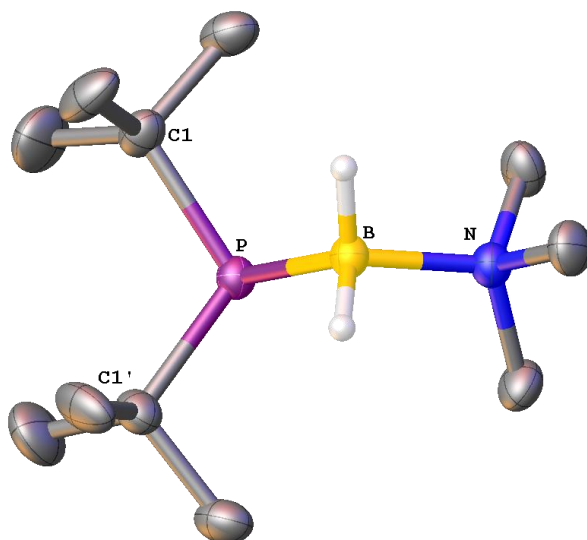


Figure 13: Molecular structure of **C25b** in the solid state. Thermal ellipsoids are drawn with 50% probability. Hydrogen atoms bound to carbon are omitted for clarity. Selected bond lengths [Å] and angles [°]: N-B = 1.636(6), B-P = 1.987(3), C1-P = 1.900(2), N-B-P = 111.72(17), C1-P-C1' = 109.952.

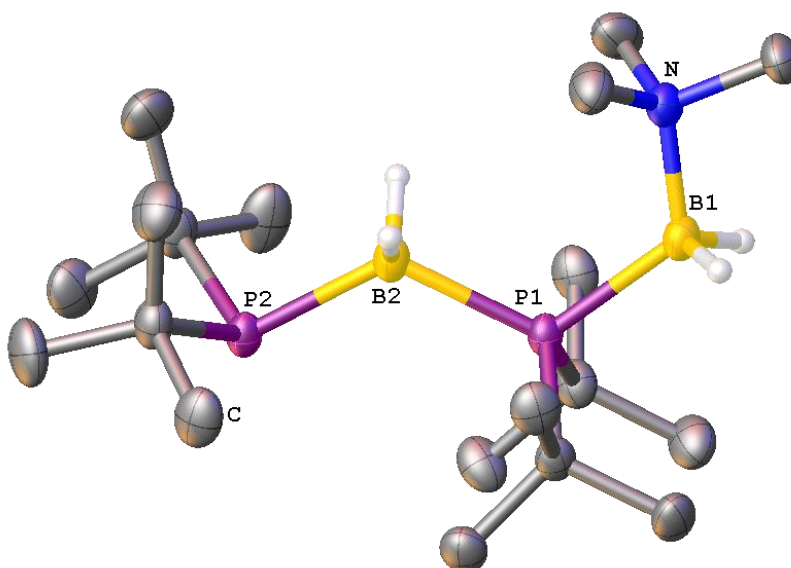


Figure 14: Molecular structure of **C25c** in the solid state. Thermal ellipsoids are drawn with 50% probability. Hydrogen atoms bound to carbon are omitted for clarity. Selected bond lengths [Å] and angles [°]: N-B = 1.612(4), B1-P1 = 2.008(3), P1-B2 = 2.009(3), B2-P2 = 2.004(3), N-B-P = 120.05(17), B1-P1-B2 = 116.13(12), P1-B2-P2 = 123.47(15).

C26 crystallizes upon storing a saturated solution in toluene at -30°C as colorless needles in the triclinic space group $P\bar{1}$. **Figure 15** shows the molecular structure in solid state.

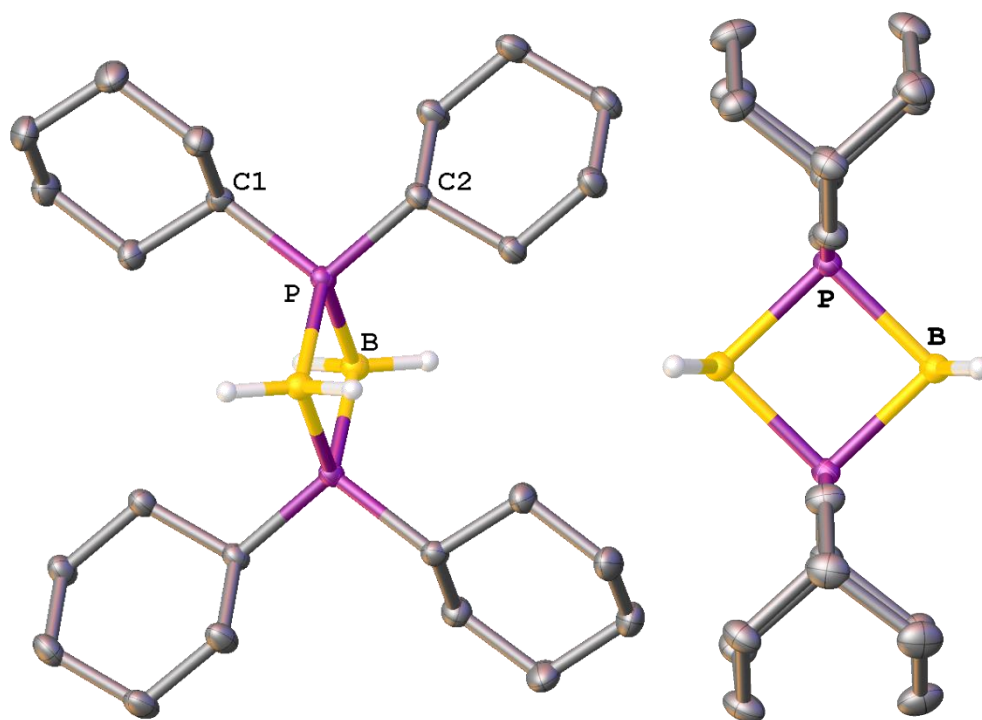


Figure 15: Molecular structure of **C25c** in the solid state. Thermal ellipsoids are drawn with 50% probability. Hydrogen atoms bound to carbon are omitted for clarity. Selected bond lengths [Å] and angles [°]: B-P = 1.9874(16), P-C = 1.8526(14)-1.8556(14), P-P = 2.766, B-B = 2.858, P-B-P = 88.144, B-P-B = 91.856.

Table 3: Crystallographic Data of **C23-C24**.

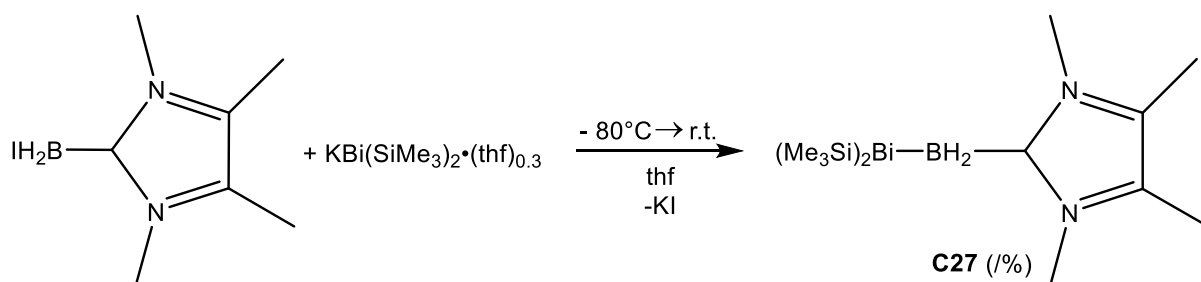
	C23a	C23b	C23c	C24
Formula	C ₈ H ₂₄ BNP	C ₂₀ H ₅₆ B ₂ I ₂ N ₂ P ₂	C ₁₇ H ₄₈ B ₂ Br ₂ N ₂ P ₂	C ₈ H ₂₃ BNP
$D_{\text{calc.}} / \text{g cm}^{-3}$	1.451	1.333	1.295	0.940
μ / mm^{-1}	18.903	15.940	4.966	1.561
Formula Weight	302.96	662.02	523.95	175.05
Colour	clear colorless	clear colorless	clear colorless	clear colorless
Shape	block	prism	plate	block
Size/mm ³	0.12×0.09×0.09	0.50×0.07×0.06	0.45×0.29×0.11	0.29×0.19×0.11
T/K	123.02(10)	123.00(10)	123.00(10)	123.01(13)
Crystal System	monoclinic	triclinic	orthorhombic	orthorhombic
Flack parameter	/	/	0.47(12)	/
Space Group	$P2_1/n$	$P\bar{1}$	$Pna2_1$	$Pnma$
$a/\text{\AA}$	6.8599(4)	10.7645(5)	18.7502(4)	10.5145(3)
$b/\text{\AA}$	13.3194(7)	12.6677(6)	9.92696(18)	10.8435(3)
$c/\text{\AA}$	15.4507(8)	12.8529(5)	7.21638(16)	10.8533(3)
α°	90	82.546(4)	90	90
β°	100.813(5)	84.823(3)	90	90
γ°	90	71.841(4)	90	90
$V/\text{\AA}^3$	1386.66(13)	1648.96(13)	1343.20(5)	1237.43(6)
Z	4	2	2	4
Z'	1	1	0.5	0.5
Wavelength/ \AA	1.54184	1.54184	1.54184	1.54184
Radiation type	CuK α	CuK α	CuK α	CuK α
$\theta_{\text{min}}^\circ$	4.417	3.694	4.717	5.768
$\theta_{\text{max}}^\circ$	73.454	74.078	73.740	74.169
Measured Refl.	5385	11605	4258	4667
Independent Refl.	2707	6371	2130	1299
Reflections Used	2402	5935	1986	1203
R_{int}	0.0320	0.0348	0.0310	0.0192
Parameters	125	291	192	98
Restraints	0	0	79	6
Largest Peak	1.247	2.396	1.236	0.217
Deepest Hole	-0.696	-1.546	-0.477	-0.147
GooF	1.126	1.052	1.109	1.069
wR_2 (all data)	0.0746	0.1115	0.1482	0.1507
wR_2	0.0679	0.1089	0.1456	0.1467
R_1 (all data)	0.0391	0.0453	0.0517	0.0482
R_1	0.0319	0.0424	0.0499	0.0465

Table 4: Crystallographic Data of **C25-C26**.

	C25a	C25b	C25c	C26
Formula	C ₁₅ H ₃₃ BNP	C ₁₁ H ₂₉ BNP	C ₁₉ H ₄₉ B ₂ NP ₂	C ₂₄ H ₄₈ B ₂ P ₂
$D_{\text{calc.}}/\text{g cm}^{-3}$	1.063	1.003	1.010	1.108
μ/mm^{-1}	1.299	1.419	1.583	1.594
Formula Weight	269.20	217.13	375.15	420.18
Colour	Clear colorless	clear colorless	clear colorless	clear colorless
Shape	plate	block	plate	needle
Size/mm ³	0.057×0.083×0.122	0.34×0.12×0.09	0.22×0.09×0.05	0.23×0.07×0.06
T/K	123	122.99(10)	123.0(3)	123
Crystal System	monoclinic	orthorhombic	monoclinic	triclinic
Flack parameter	/	-0.02(3)	/	/
Hooft parameter	/	-0.013(16)	/	/
Space Group	$P2_1/n$	$Cmc2_1$	$P2_1/c$	$P\bar{1}$
$a/\text{\AA}$	10.1968(6)	13.5421(7)	11.1560(3)	7.3788(5)
$b/\text{\AA}$	9.7119(6)	9.7505(5)	15.1823(6)	8.4655(5)
$c/\text{\AA}$	17.0604(12)	10.8930(5)	15.5711(4)	10.4949(6)
α°	90	90	90	91.866(5)
β°	95.370(6)	90	110.771(3)	103.402(5)
γ°	90	90	90	98.330(5)
$V/\text{\AA}^3$	1682.08(19)	1438.33(12)	2465.91(15)	629.49(7)
Z	4	4	4	1
Z'	1	0.5	1	0.5
Wavelength/ \AA	1.5418	1.54184	1.54184	1.54184
Radiation type	CuK α	CuK α	CuK α	CuK α
$\theta_{\text{min}}^\circ$	9.722	5.591	4.207	4.341
$\theta_{\text{max}}^\circ$	148.318	74.102	66.656	65.933
Measured Refl.	9294	3175	19393	4783
Independent Refl.	3325	1316	4331	2174
Reflections Used	2614	1266	3307	1933
R_{int}	0.0660	0.0236	0.0685	0.0266
Parameters	174	79	248	135
Restraints	0	2	0	0
Largest Peak	0.77	0.355	0.345	0.381
Deepest Hole	-0.28	-0.197	-0.266	-0.212
GooF	1.027	1.091	1.031	1.041
wR_2 (all data)	0.1493	0.0764	0.1226	0.0817
wR_2	0.1627	0.0746	0.1104	0.0791
R_1 (all data)	0.0762	0.0303	0.0727	0.0385
R_1	0.0611	0.0288	0.0502	0.0329

7.3 Synthesis of a LB stabilized Bismutylborane

In 2015, our group reported on the synthesis of the first LB stabilized stibanylborane R_2SbBH_2-LB .^[9] A salt metathesis route, enabled the access to the substituted $(Me_3Si)_2SbBH_2-LB$ as well as the parent H_2SbBH_2-LB stibanylborane (LB: NHC^{Me} , NMe_3) by methanolysis. Using the weak LB NMe_3 , it was possible to determine the molecular structure of the parent compound in solid state. In contrast, the use of the much stronger LB NHC^{Me} , results in $H_2SbBH_2NHC^{Me}$ with about 20% yield. *Marquardt* described in 2015 the synthesis of the first bismuthanylborane $(Me_3Si)_2BiBH_2-dmap$, whereas a successful reaction with NMe_3 as LB was not observed.^[16] Therefore, LBs with a similar or higher donor strength as *dmap* might enable a successful synthesis of the bismuthanylborane $(Me_3Si)_2BiBH_2-LB$ (LB = NEt_3 , NHC^{dipp} , NHC^{Me}). The reaction of $KBi(SiMe_3)_2 \cdot (thf)_{0.3}$ and IBH_2NHC^{Me} yields the silylated bismuthanylborane $(Me_3Si)_2BiBH_2NHC^{Me}$ (**C27**, **Scheme 4**).



Scheme 4: Synthesis of **C27**.

The reaction proceeds selectively and in nearly quantitative according ^{11}B NMR spectroscopic measurements. Besides **C27**, a black precipitate is formed during the reaction, probably elementary Bi, which could not be further separated, due to the good solubility of **C27**. Therefore, all attempts to isolate **C27** failed so far. However, it was possible to determine the molecular structure of **C27** in solid state. The substituents along the Bi-B bond ($d(Bi - Bi) = 2.442(7) \text{ \AA}$) adopt a synperiplanar arrangement (**Figure 16**). In the $^{11}B\{^1H\}$ NMR spectrum a broad singlet appears at $\delta = -39.52$ ppm, which reveals further splitting into a triplet ($^1J_{BH} = 111$ Hz) in the ^{11}B NMR spectrum. Besides the used NHC^{Me} , further experiments were performed with other LBs (NEt_3 , NHC^{dipp}), but the corresponding bismuthanylboranes $(Me_3Si)_2BiBH_2LB$ were not be observed in the ^{11}B NMR spectra, probably due to the lesser donor strength of these LBs compared to NHC^{Me} .^[17] To get further insight into the requirements on a LB to

stabilize bismuthanylboranes, additional reactions including other NHCs and CAACs (Cyclic (Alkyl)(Amino) Carbenes) still have to be made.

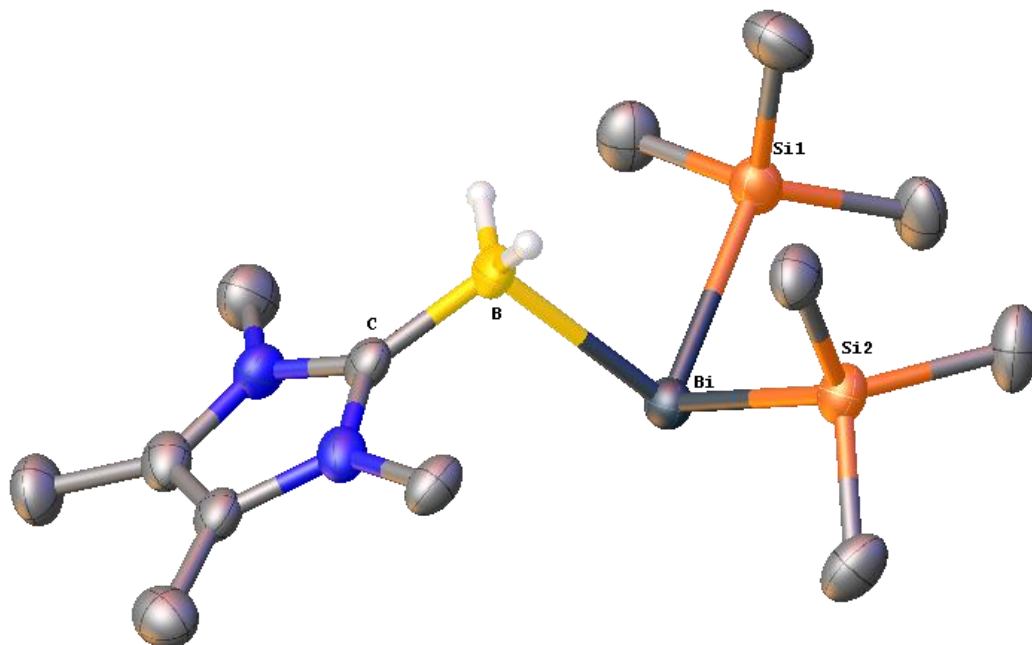


Figure 16: Molecular structure of **C22** in the solid state. Thermal ellipsoids are drawn with 50% probability. Hydrogen atoms bound to carbon are omitted for clarity. Selected bond lengths [Å] and angles [°]: B-Bi = 2.442(7), C-B = 1.569(9), C-B-Bi = 107.2(4), Si-Bi-Si = 94.57(6).

Experimental Section:

Synthesis of $(\text{Me}_3\text{Si})_2\text{BiBH}_2\text{NHC}^{\text{Me}}$ (**C27**):

To a solution of 264 mg (1 mmol) $\text{IBH}_2\text{NHC}^{\text{Me}}$ in 10 mL thf a solution of 416 mg $\text{KBi}(\text{SiMe}_3)_2(\text{thf})_{0.3}$ in 10 mL thf is added at -80°C . The solution is allowed to reach room temperature over 18 h and a black solid precipitates. All volatiles are removed *in vacuo* and the remaining solid is suspended in 20 mL *n*-hexane. The solution is filtrated and reduced to 3 mL. **C27** crystallizes as yellow blocks upon storing a saturated solution in *n*-hexane at -30°C . Due decomposition products, which could not be separated, it was not possible to isolate pure **C27**.

^{11}B NMR (C_6D_6 , capillary in thf): δ [ppm] = - 39.52 (t, br, $^1J_{\text{BH}}$ = 111 Hz).

$^{11}\text{B}\{^1\text{H}\}$ NMR (C_6D_6 , capillary in thf): δ [ppm] = - 39.52 (s, br).

Crystallographic Data:

All structures were solved using SHELXT^[3] and OLEX.^[4] Least square refinements against F^2 in anisotropic approximation were done using SHELXL.^[3] The hydrogen

positions of the methyl groups were located geometrically and refined riding on the carbon atoms. **C27** was measured on a GV50 with TitanS2 detector. Gaussian absorption correction was applied for **C27**.

C27 crystallizes upon storing a saturated solution in *n*-hexane at - 30°C as yellow blocks in the triclinic space group $P\bar{1}$. **Figure 16** shows the molecular structure in solid state.

Table 5: Crystallographic Data of **C27**.

C27	
Formula	C ₁₃ H ₃₂ BBiN ₂ Si ₂
$D_{calc.}/\text{g cm}^{-3}$	1.568
μ/mm^{-1}	17.605
Formula Weight	492.37
Colour	clear light yellow
Shape	block
Size/mm ³	0.19×0.13×0.12
T/K	123.00(10)
Crystal System	triclinic
Space Group	$P\bar{1}$
$a/\text{\AA}$	9.5403(4)
$b/\text{\AA}$	9.8557(6)
$c/\text{\AA}$	12.1971(4)
$\alpha/^\circ$	97.044(4)
$\beta/^\circ$	108.604(4)
$\gamma/^\circ$	101.577(4)
$V/\text{\AA}^3$	1043.07(9)
Z	2
Z'	1
Wavelength/ \AA	1.54184
Radiation type	CuK α
$\theta_{min}/^\circ$	3.904
$\theta_{max}/^\circ$	74.073
Measured Refl.	6314
Independent Refl.	3974
Reflections Used	3703
R_{int}	0.0365
Parameters	190
Restraints	0
Largest Peak	1.572
Deepest Hole	-2.289
GooF	1.050
wR_2 (all data)	0.0919
wR_2	0.0891
R_1 (all data)	0.0377
R_1	0.0350

7.4 Literature

- [1] K.-C. Schwan, A. Y. Timoshkin, M. Zabel, M. Scheer, *Chem. Eur. J.* **2006**, *12*, 4900–4908.
- [2] C. Marquardt, A. Adolf, A. Stauber, M. Bodensteiner, A. V. Virovets, A. Y. Timoshkin, M. Scheer, *Chem. Eur. J.* **2013**, *19*, 11887–11891.
- [3] C. Thoms, *Dissertation*, **2012**, Universität Regensburg.
- [4] G. M. Sheldrick, *Acta Cryst.* **2008**, *A64*, 112–122.
- [5] O.V. Dolomanov, L. J. Bourhis, R. J. Gildea, J. A. K. Howard, H. Puschmann, OLEX2: A complete structure solution, refinement and analysis program, **2009**. *J. Appl. Cryst.*, *42*, 339–341.
- [6] C. T. Kwon, H. A. McGee, Jr., *Inorg. Chem.* **1970**, *9*, 2458–2461.
- [7] U. Vogel, P. Hoemensch, K.-C. Schwan, A. Y. Timoshkin, M. Scheer, *Chem. Eur. J.* **2003**, *9*, 515–519.
- [8] R. T. Paine, H. Nöth, *Chem. Rev.* **1995**, *95*, 343–379.
- [9] C. Marquardt, A. Adolf, A. Stauber, M. Bodensteiner, A. V. Virovets, A. Y. Timoshkin, M. Scheer, *Chem. Eur. J.* **2013**, *19*, 11887–11891.
- [10] C. Marquardt, O. Hegen, M. Hautmann, G. Balázs, M. Bodensteiner, A. V. Virovets, A. Y. Timoshkin, M. Scheer, *Angew. Chem. Int. Ed.* **2015**, *54*, 13122–13125; *Angew. Chem.* **2015**, *127*, 13315–13318.
- [11] C. Marquardt, T. Jurca, K.-C. Schwan, A. Stauber, A. V. Virovets, G. R. Whittell, I. Manners, M. Scheer, *Angew. Chem. Int. Ed.* **2015**, *54*, 13782–13786; *Angew. Chem.* **2015**, *127*, 13986–13991.
- [12] A. Stauber, T. Jurca, C. Marquardt, M. Fleischmann, M. Seidl, G. R. Whittell, I. Manners, M. Scheer, *Eur. J. Inorg. Chem.* **2016**, 2684–2687.
- [13] E. C. Y. Tam, N. A. Maynard, D. C. Apperley, J. D. Smith, M. P. Coles, J. R. Fulton, *Inorg. Chem.* **2012**, *51*, 9403–9415.
- [14] R. Gilbert-Wilson, L. D. Field, M. M. Bhadbhade, *Inorg. Chem.* **2012**, *51*, 3239–3246.
- [15] A. Bondi: *J. Phys. Chem.*, 1964, *68*, 3, 441–451.
- [16] M. Mantina, A. C. Chamberlin, R. Valero, C. J. Cramer, D. G. Truhlar, *J. Phys. Chem.* 2009, *113*, 19, 5806–5812.
- [17] C. Marquardt, *Dissertation*, **2015**, Universität Regensburg.
- [18] See as a review for NHCs: D. Bourissou, O. Guerret, F. P. Gabbai, G. Bertrand, *Chem. Rev.* **2000**, *100*, 39–91.

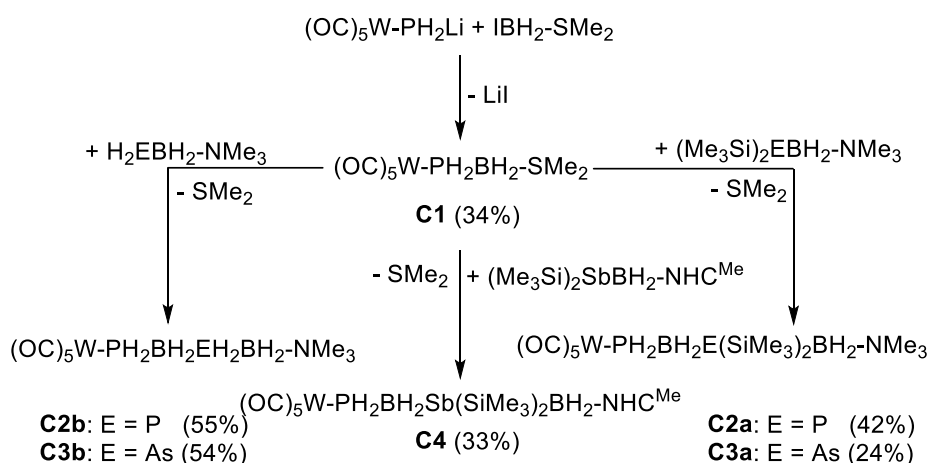
8 Conclusion

Mixed Pnictogenylboranes

Whereas longer, only hydrogen substituted anionic and cationic chain-like group 13/15 compounds are known, the quest for longer, only hydrogen substituted, neutral group 13/15 chain-like compounds was still open. First attempts were made by *C. Marquardt* and were reported in his dissertation. He succeeded in the synthesis of a dimeric, only hydrogen substituted phosphanylborane, $\text{H}_2\text{PBH}_2\text{PH}_2\text{BH}_2\text{-NMe}_3$, which turned out to be highly reactive, even at low temperatures. Therefore, a synthetic pathway was developed including a cooperative LA/LB stabilization, which is sufficient to work with these compounds at ambient conditions (**Scheme 1**).

The LA/LB stabilized phosphanylborane $(\text{OC})_5\text{W-PH}_2\text{BH}_2\text{-SMe}_2$ (**C1**) was synthesized through salt metathesis of $\text{IBH}_2\text{-SMe}_2$ and $\text{LiPH}_2\text{-W(CO)}_5$ (**Scheme 1**). By replacement of the weak LB SMe_2 with different phosphanylboranes, it was possible to synthesize the dimeric phosphanylboranes $(\text{OC})_5\text{W-PH}_2\text{BH}_2\text{-P(SiMe}_3)_2\text{BH}_2\text{-NMe}_3$ (**C2a**) and $(\text{OC})_5\text{W-PH}_2\text{BH}_2\text{-PH}_2\text{BH}_2\text{-NMe}_3$ (**C2b**). Furthermore, DFT calculations showed that heavier pnictogenylboranes should also be strong enough to substitute SMe_2 in **C1**. The reactions of LB stabilized arsanylboranes and stibanylboranes with **C1** resulted in the mixed pnictogenylboranes $(\text{OC})_5\text{W-PH}_2\text{BH}_2\text{-AsR}_2\text{BH}_2\text{-NMe}_3$ (**C3a**: $\text{R} = \text{H}$; **C3b**: $\text{R} = \text{SiMe}_3$) $(\text{OC})_5\text{W-PH}_2\text{BH}_2\text{-Sb(SiMe}_3)_2\text{BH}_2\text{-NHC}^{\text{Me}}$ (**C4**; $\text{NHC}^{\text{Me}} = 1,3,4,5\text{-tetramethylimidazolyldiene}$).

These compounds are the first neutral representatives containing P-B-E-B chains ($\text{E} = \text{As, Sb}$) and can be considered as a starting point into group 13/15 copolymers.



Scheme 1: Synthesis of compounds **C1-C4**. All reactions were performed in toluene for 18 h (**C2a**, **C2b**, **C3a**) or 3h (**C3b**, **C4**) at room temperature (isolated yields in parentheses).

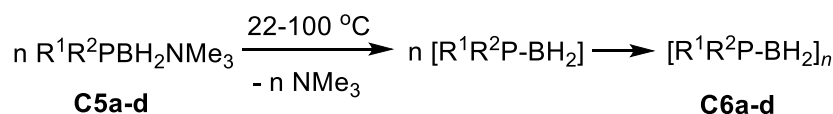
Depolymerization of Phosphanylboranes

Thermal treatment of Me₃N stabilized phosphanylboranes lead to the corresponding oligomeric/polymeric phosphanylboranes (**Scheme 2**, top). The reversible process, cleavage of these polymers was not investigated in detail so far. A systematical study of this process under different conditions was performed, which means various LBs and different substituted poly(phosphanylboranes).

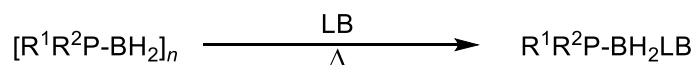
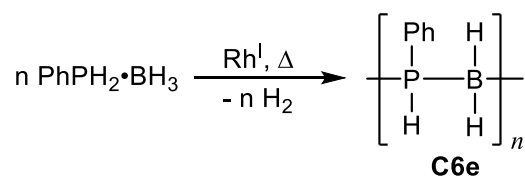
DFT calculations were performed on the model reaction



The favorability of the reaction depends not only on the donor strength of the LB, but also on the substituents on the P atoms. Whereas NMe₃ and DMAP are not predicted to cleave poly(phosphanylboranes) exothermically, all reactions with the strong LB NHC^{Me} are energetically favored and therefore a cleavage should be observed. In comparison, the weaker NHC^{dipp} (1,3-bis(2,6-diisopropylphenyl)imidazolin-2-ylidene) is predicted to cleave poly(phosphanylboranes) only the dihydrogen-substituted and the monophenyl-substituted poly(phosphanylborane) exothermically.



a: R¹ = R² = H; **b:** R¹ = R² = Ph; **c:** R¹ = ^tBu, R² = H; **d:** R¹ = Me, R² = H



R / LB	DMAP	NHC ^{Me}	NHC ^{dipp}
C6a: R ¹ = R ² = H	-	C8a (5%)	C9a (65%)
C6b: R ¹ = R ² = Ph	-	-	-
C6c: R ¹ = ^t Bu, R ² = H	-	C8c (29%)*	-
C6e: R ¹ = Ph, R ² = H	C7e (25%)	C8e (21%)*	-

Scheme 2. Top: Polymerization of phosphanylboranes by either LB elimination for **C6a-c** and dehydrocoupling for **C6d** (Rh^I = [Rh(1,5-cod)2][OTf]). Bottom: Depolymerization of poly(phosphinoboranes) (yields according to ³¹P NMR spectra in parentheses, * = isolated yields).

Experimentally, no cleavage was observed for DMAP with **C6a-c**. Only in case of **C6e** about 25% cleavage using an excess of DMAP in boiling toluene. Presumably, an

excess DMAP shifts the equilibrium to the formation of PhPHBH₂-DMAP **C7e** (**Scheme 2**, bottom).

In case of the stronger LB NHC^{dipp}, the monomeric H₂PBH₂-NHC^{dipp} (**C9a**) is formed by cleavage of **C6a** in about 65% yield according to the ³¹P NMR spectrum, whereas no monomeric PhPHBH₂-NHC^{dipp} could be obtained. In agreement with the calculations, no cleavage was observed for **C6b** and **C6c**. It can be assumed, that the big substituents on the NHC prevent a cleavage of the substituted poly(phosphanylboranes) **C6b**, **C6c** and **C6e**.

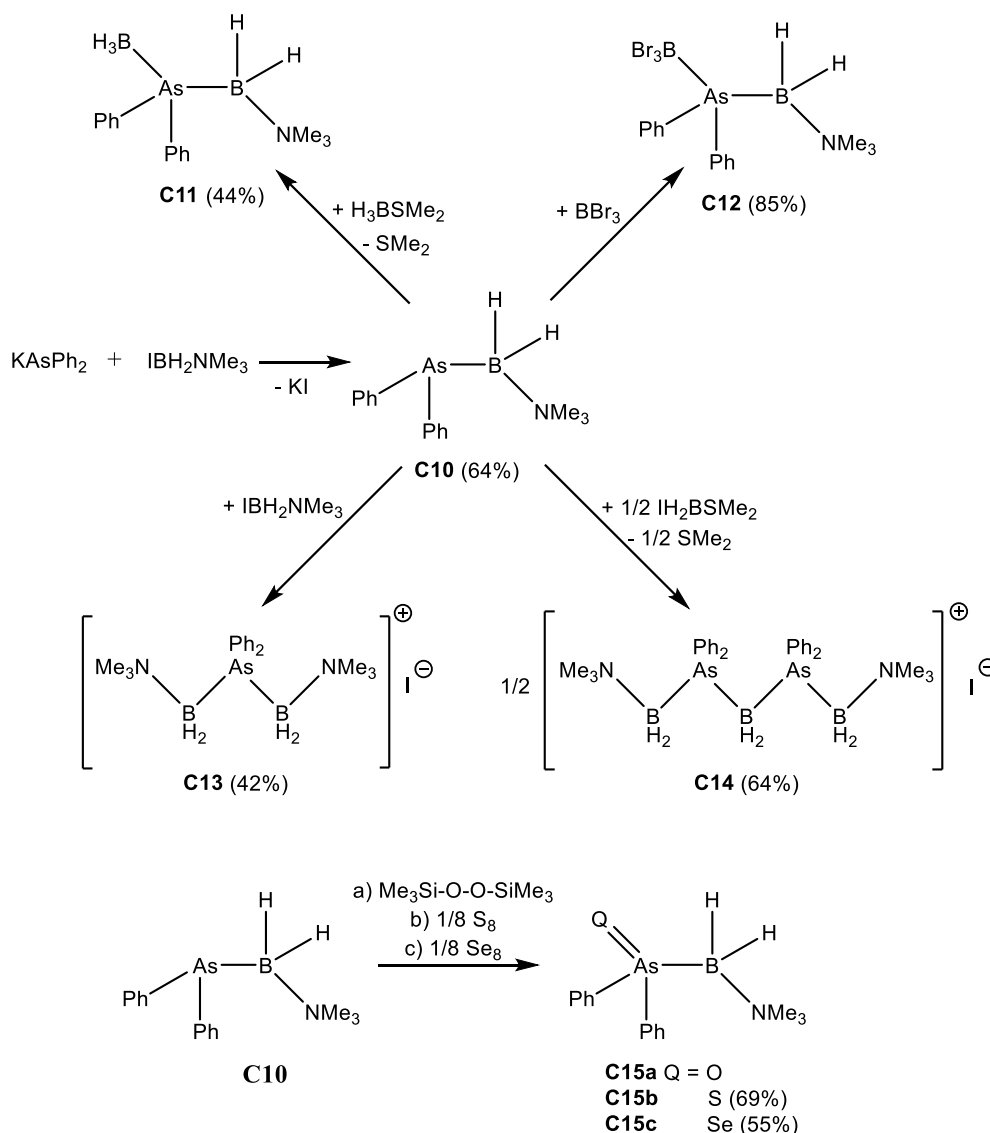
The scission of all investigated polymers with the stronger LB NHC^{Me} is predicted to be exergonic by DFT calculations. In contrast to the polymer **C6c**, which is cleaved smoothly (72h, 45°C, toluene) in about 80% yield (isolated yield 29%) and the polymer **C6d**, for which a cleavage of over 70% (isolated yield 21%) is observed after 30min in boiling thf, only 5% conversion to H₂PBH₂-NHC^{Me} is monitored for the polymer **C6a** after 72h in boiling toluene. Due to its steric shielding of two substituents on the phosphorus, the oligomer **C6b** could not be cleaved at all.

We could show that the depolymerization process depends not only on the donor strength, size and thermal stability of the LB, but also on the solubility and the substitution pattern of the poly(phosphanylboranes).

Substituted Arsanylboranes

Since the synthesis of the first LA/LB stabilized phosphanylborane (OC)₅W-PH₂BH₂-NMe₃, a variety of different substituted derivatives were synthesized. In contrast, for arsanylboranes, only the parent compound H₂AsBH₂-NMe₃ and the substituted derivative (Me₃Si)₂AsBH₂-NMe₃ are known. In the presented work, a new synthetic strategy was developed to get access to the diphenylsubstituted arsanylborane Ph₂AsBH₂-NMe₃ (**C10**, **Scheme 3**) in good yields. Even if arsanylboranes are far more reactive as their phosphorus derivatives, the compound shows higher thermal stability than Ph₂PBH₂-NMe₃. However, the reaction behavior towards main group LAs like H₃B-SMe₂ and BBr₃ is similar resulting in H₃B-Ph₂AsBH₂-NMe₃ (**C11**) and Br₃B-Ph₂AsBH₂-NMe₃ (**C12**, **Scheme 3**), respectively. Further, through coordination towards BH₂⁺ building blocks, cationic oligomers containing As-B chains were synthesized and fully characterized (**C13**, **C14**). In contrast to the parent compound, where all attempts for chemical oxidation lead to decomposition, the reactions of **C10** with bis(trimethylsilyl)peroxide, S₈ or Se_{grey}, respectively, yield the corresponding

oxidized arsanylboranes. Whereas $\text{Ph}_2\text{As}(\text{O})\text{BH}_2\text{-NMe}_3$ (**C15a**) could not be isolated, but unambiguously identified by mass spectrometry, multinuclear NMR and IR spectroscopy, respectively, $\text{Ph}_2\text{As}(\text{S})\text{BH}_2\text{-NMe}_3$ (**C15b**) and $\text{Ph}_2\text{As}(\text{Se})\text{BH}_2\text{-NMe}_3$ (**C15c**) were isolated in good yields and characterized completely.



Scheme 3: Synthesis of compounds **C10**–**C15** (isolated yields in parentheses).

All attempts for elimination of NMe_3 in **C10** to induce a head-to-tail polymerization failed. Therefore an alternative synthesis of such compound with a much weaker LB was developed. The salt metathesis of KAsPh_2 with $\text{IBH}_2\text{-SMe}_2$ yields the arsanylborane $\text{Ph}_2\text{AsBH}_2\text{-SMe}_2$ (**C16**). As expected, **C16** is highly reactive and decomposes even at low temperatures to form most likely the trimer $[\text{Ph}_2\text{AsBH}_2]_3$.

These results emphasize the similarities between the substituted phosphanyl- and arsanylboranes in their coordination behavior towards BH_3 , BBr_3 and $\text{IBH}_2\text{-LB}$ ($\text{LB} = \text{NMe}_3$, SMe_2) to build up either neutral (**C11**, **C12**) or cationic (**C13**, **C14**) oligomeric compounds, respectively. However, there are indeed several differences. Regarding their chemical oxidation, $\text{Ph}_2\text{PBH}_2\text{-NMe}_3$ can be oxidized with Te, whereas no reaction of **C10** with Te was observed. Furthermore, **C10** is thermally more stable than $\text{Ph}_2\text{PBH}_2\text{-NMe}_3$. At higher temperatures, only decomposition of **C10** could be observed and no elimination of the LB followed by a head-to-tail polymerization as in the case of $\text{Ph}_2\text{PBH}_2\text{-NMe}_3$.

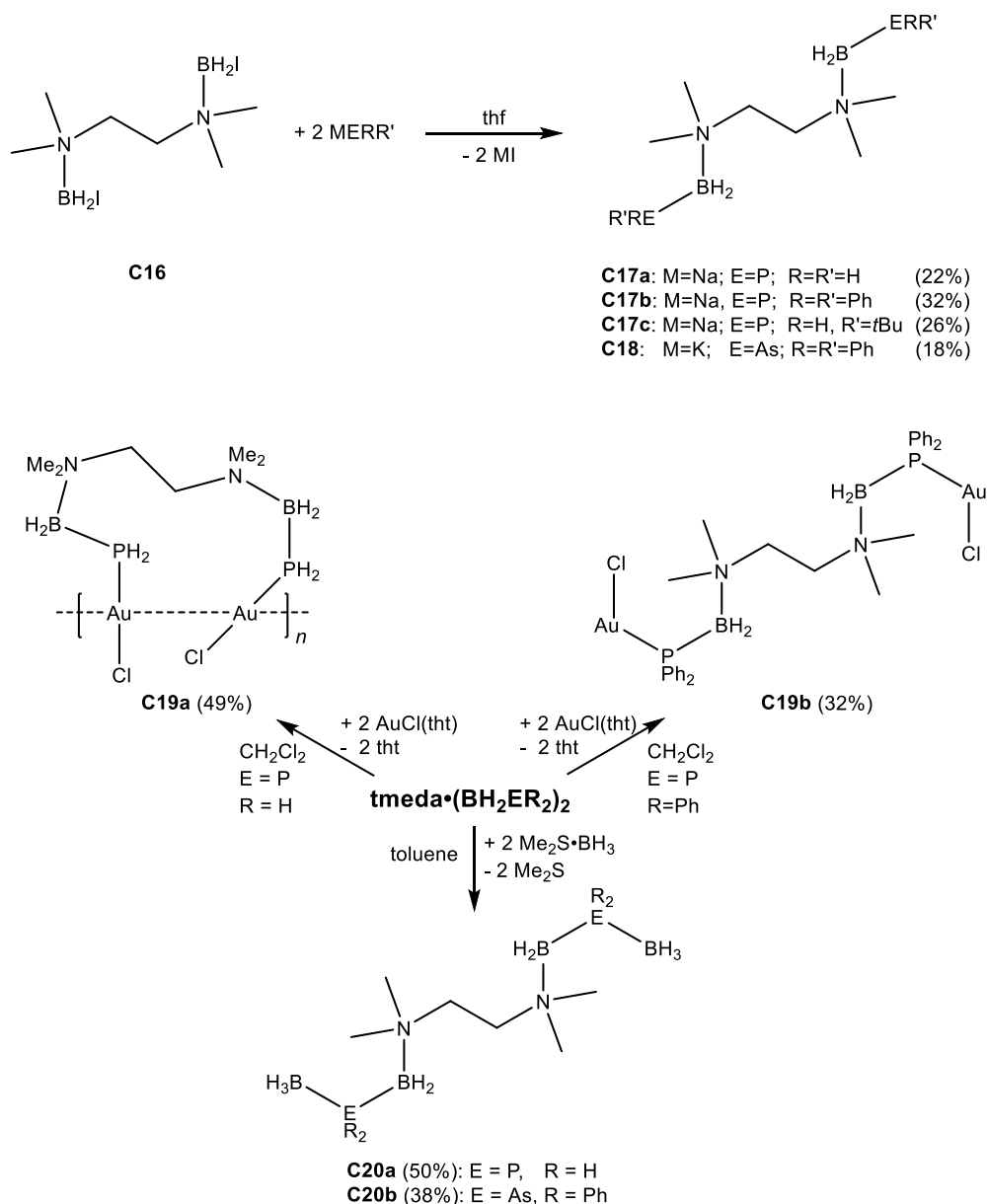
Bidentate Phosphanyl- and Arsanylboranes

The possibilities to build up discrete oligomeric units from LB stabilized phosphanyl-/arsanylboranes $\text{R}_2\text{EBH}_2\text{-NMe}_3$ are restricted due to only one pnictogen donor site. It was shown, that the use of a bidentate instead of a monodentate LB to stabilize pnictogenylboranes lead to an extension of the established chemistry. The reaction of $\text{tmeda}\cdot(\text{BH}_2\text{I})_2$ (tmeda = tetramethylethylenediamine) with NaPRR' ($\text{R} = \text{R}' = \text{H}$, Ph ; $\text{R} = \text{H}$, $\text{R}' = t\text{Bu}$) results in the corresponding bidentate phosphanylboranes $\text{tmeda}\cdot(\text{H}_2\text{BPRR}')_2$ (**C17a-c**, **Scheme 4**). Moreover, it was possible to transfer this synthesis towards arsanylboranes, resulting in the formation of the first bidentate arsanylborane $\text{tmeda}\cdot(\text{H}_2\text{BAsPh}_2)_2$ (**C18**). In accordance with DFT calculations, the low yields can be explained by a competitive cyclisation reaction:



This competitive reaction includes the formation of the cationic five-membered ring $(\text{tmeda}\cdot\text{BH}_2)^+$, which was observed regularly in these reactions by X-ray diffraction analysis, and poly(phosphanylborane), which could also be identified by NMR spectroscopy.

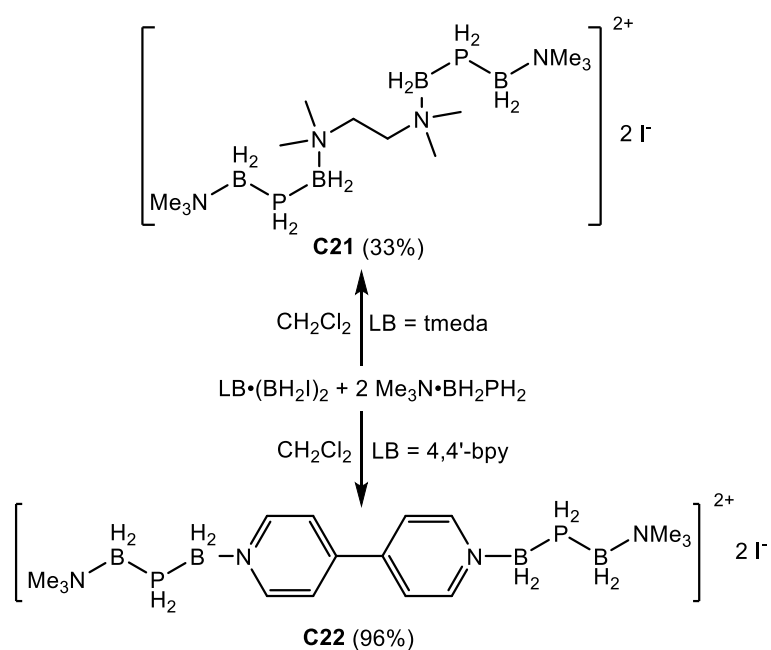
However, first steps to build up organic boron-pnictogen networks were successful. The reaction of **C17a** and **C18** with $\text{H}_3\text{B-SMe}_2$ yields $\text{tmeda}\cdot(\text{H}_2\text{BPH}_2\text{BH}_3)_2$ (**C20a**) and $\text{tmeda}\cdot(\text{BH}_2\text{AsPh}_2\text{BH}_3)_2$ (**C20b**), respectively. In addition, the reaction of **C17a** with $\text{IBH}_2\text{-NMe}_3$ yields $[\text{tmeda}\cdot(\text{H}_2\text{BPH}_2\text{BH}_2\text{-NMe}_3)_2]^{2+}$ (**C21**, **Scheme 5**), the cationic analogue of **C20a**.



Scheme 4. Synthesis of **C16-C20** (isolated yields in parentheses).

Moreover the coordination of **C17a** and **C17b** towards Au(I) centers lead to either dinuclear (**C19b**) or polynuclear molecules (**C19a**), depending on the substituents on the phosphorus atom.

To exclude the competitive reaction, the formation of the five-membered ring tmeda-(BH₂)⁺, we switched to a sterically more hindered LB, 4,4'-bipyridine (4,4'-bipy). First results, like the formation of the cationic [4,4'-bipy-(H₂BPH₂BH₂-NMe₃)₂]²⁺ (**C22**, **Scheme 5**) were very promising and result in high yields. However, the formation of 4,4'-bipy-(H₂BPH₂)₂ by salt metathesis could not be observed, due to the insufficient donor strength of the LB.



Scheme 5. Synthesis of **C21** and **C22** (isolated yields in parentheses).

Nevertheless, bidentate pnictogenylboranes have shown to be very promising starting materials to build up organic boron-pnictogen oligomers and they are interesting ligands for transition metal complexes as well.

9 Appendices

9.1 Alphabetic List of Abbreviations

Å	Angstroem, $1\text{Å} = 1 \times 10^{-10} \text{ m}$
°C	degree Celsius
br(NMR)	broad
btmsa	bis(trimethylsilyl)acetylene
CAAC	Cyclic (Alkyl)(Amino) Carbenes
cht	cycloheptatriene, C_7H_8
cod	cycloocta-1,5-diene
Cp	cyclopentadienyl, C_5H_5
Cy	cyclohexyl-, C_6H_{11}
d(NMR)	doublet
DLS	Dynamic light scattering
E°_0	reaction energy
H°_{296}	standard reaction enthalpy
S°_{296}	standard reaction entropy
G°_{296}	standard gibbs reaction energy
δ	chemical shift
Da	Dalton
DFT	density functional theory
Dipp	2,6-diisopropylphenyl
dmap	4-Dimethylaminopyridine
e^-	electron
EI MS	electron impact mass spectrometry
ESI MS	electron spray ionization mass spectrometry
FAI	$[\text{FAI}\{\text{OC}_6\text{F}_{10}(\text{C}_6\text{F}_5)\}_3]$
FD MS	field desorption ionization mass spectrometry
FLP	frustrated Lewis pair
GPC	Gel permeation chromatography
Hz	Hertz
<i>i</i> Pr	<i>iso</i> -propyl, C_3H_7
IR	infrared spectroscopy

$J(\text{NMR})$	coupling constant
LA	Lewis acid
LB	Lewis base
M	molecular ion peak
M_n	number-average molar mass
m/z	mass to charge ratio
Me	methyl, CH_3
Mes	mesityl, 2,4,6-trimethylphenyl
MOCVD	metalorganic chemical vapor deposition
NHC	N-heterocyclic carbene
NMR	nuclear magnetic resonance
NPA	Natural Population analysis
ν	frequency/wavenumber
$\omega_{1/2}$	half width
Ph	phenyl, C_6H_5
PPA	poly(aminoborane)
PPB	poly(phosphinoborane)
ppm	parts per million
$q(\text{NMR})$	quartet
R	organic substituent
r	radius
r.t.	room temperature
s(IR)	strong
s(NMR)	singlet
<i>t</i> Bu	<i>tert-butyl</i> , C_4H_9
t(NMR)	triplet
thf	tetrahydrofuran, $\text{C}_4\text{H}_8\text{O}$
vdW	van der Waals
VE	valence electron
VT	Various Temperature
w(IR)	weak

9.2 Acknowledgments

Finally special thanks got to:

- Prof. Dr. Manfred Scheer for giving me the opportunity to work on this very interesting project, providing excellent working conditions and the freedom to pursue my own ideas in the lab.
- Dr. Gábor Balász for spending so much time on discussing, always giving helpful advice, accurate proof-reading and the input for my research. Without him, nothing of this would have been possible.
- Prof. Dr. Alexey Timoshkin for the interesting discussions and for the ton of DFT calculations, helping to understand the presented chemistry
- Prof. Dr. Ian Manners and co-workers for the really nice time during my research stay at the School of Chemistry in Bristol, UK.
- Dr. Alexander V. Virovets and Dr. Eugenia Peresyphkina for the help with X-ray structure analyses.
- All staff and co-workers of the Central Analytical Services of the University of Regensburg
- Dr. Michael Seidl for all his help with X-ray structure problems
- The staff of the glass blowing, electronics and mechanics facilities of the University of Regensburg
- My current and former lab colleagues (Tobi, Jens, Matthias, Felix) for the really awesome and funny time
- Dr. Christian Marquardt for all his help and friendship
- All present and former members of the Scheer group. It was a pleasant working with you all =)
- Especially to my family and all my friends, who never stopped believing in me and my skills, and supported me during this time
- YOU